UNIVERSITY OF VENDA,
THOHOYANDOU, LIMPOPO PROVINCE,
SOUTH AFRICA

University of Venda

SCHOOL OF MATHEMATICAL AND NATURAL SCIENCES
DEPARTMENT OF CHEMISTRY

AB INITIO AND DFT COMPUTATIONAL STUDY OF MYRISTININ A AND A STRUCTURALLY-RELATED MOLECULE

BY

NEANI TSHILANDE, STUDENT NUMBER: 11630094

This thesis is submitted in fulfilment of the requirements for the degree of Masters in Chemistry.

SUPERVISOR: PROF. LILIANA MAMMINO

Department of Chemistry, University of Venda,

Thohoyandou, South Africa

CO-SUPERVISOR: Dr. CATERINA GHIO

Institute for Physico-Chemical processes,

Molecular Modelling Lab, Pisa, Italy

March, 2019

Declaration

I, Neani Tshilande hereby declare that the thesis for the award of Masters a degree submitted by me has never previously been submitted for a higher degree or diploma at this or any other University. And that to the best of my knowledge and belief, the thesis contains no material previously published or written by another person except where due reference is made in the thesis itself.

Signature…… Date: March 2019

ABSTRACT

The computational study of biologically active molecules is particularly important for drug development because it provides crucial information about the properties of a molecule, which determine its biological activities. The current work considers the results of a computational study of myristinin A and a structurally-related molecule (2-(4-hydroxyphenyl)-4-[2,4,6-trihydroxy-3-(9tetradecenoyl)phenyl]-3,4-dihydro-2H-benzopyran-7-ol, here denoted as DBPO). The two compounds pertain to the class of acylphloroglucinols. They were firstly isolated from *Horsfieldia amygdaline,* and they exhibit a variety of biological activities, including potent anti-inflammatory activity, potent DNA-damaging activity and DNA-polymerase ß inhibition. Their molecular structures differ only by the acyl chain. Both molecules have a bulky substituent meta to the acyl group consisting of a ring system (2-(4-hydroxyphenyl)-3,4-dihydro-2H-chromen-7-ol). The DBPO molecule can exist as *cis* and *trans* isomers in relation to the double bond present in the R chain, and both isomers are here investigated individually. The OHs *ortho* to the acyl group can form an intramolecular hydrogen bond (referred to as the first IHB) with the sp^2 O atom of the acyl group. The phenol OHs neighbouring the substituent ring system can form O–H···π interaction with the aromatic rings of the substituent, if suitable oriented.

This study focuses on the identification of the stable conformers of these molecules (considering all the possible geometries obtainable by rotations about relevant single bonds), and of the factors stabilising the conformers. Full-optimisation calculations were performed *in vacuo* and also in three conveniently selected solvents. The results show that the dominant stabilising factors are the first IHB and the O–H···π interactions. Other factors which have significant influence on conformational preferences are the orientation of the ring systems of the substituent, the orientation of the OHs on substituent, the mutual orientation of the OHs of the phloroglucinol moiety and also the orientation of the acyl chain. The results in solution are consistent with the findings of other acylphloroglucinols, for instance, the narrowing of the energy gaps and the increase of the dipole moment with the increase of solvent polarity.

Acronyms

ACS	:	Apparent Surface Charge
AM1	:	Austin Model 1
BO	:	Born-Oppenheimer
BSSE	:	Basis set superposition error
CHA	:	Chemical Hamiltonian Approach
CHPC	:	Centre for High Performance Computing
COX-1	:	Cyclooxygenases-1
COX-2	:	Cyclooxygenases-2
CP	:	Counterpoise
CPCM	:	Conductor-like PCM
$cPLA_2$	:	cytosolic PLA_2
DFT	:	Density Functional Theory
DPCM	:	Dielectric-PCM
GR	:	Glucocorticoid-receptors
GTOs	:	Gaussian type orbitals
HF	:	Hartree-Fock
HOMO	:	Highest Occupied Molecular Orbital
IEFPCM	:	Integral equation formalism–PCM
IHB	:	Intramolecular Hydrogen Bond
$iPLA_2$	:	Ca^{2+}-independent PLA_2
LCAO	:	Linear Combination of Atomic Orbitals
LTs	:	Leukotrienes
LUMO	:	Lowest Occupied Molecular Orbital
MINDO	:	Modified Intermediate Neglect of Differential Overlap
MP1	:	Møller-Plesset first perturbation theory
MP2	:	Møller-Plesset second perturbation theory
MP3	:	Møller-Plesset third perturbation theory
MP4	:	Møller-Plesset forth perturbation theory
MOs	:	Molecular Orbitals
NSAIDs	:	Nonsteroidal anti-inflammatory drugs
SCF	:	Self-Consistent Filed
SCIPCM	:	Self-consistent isodensity-PCM

STOs	:	Slater Type Orbitals
$sPLA_2$	:	secretory or secreted PLA_2
PCM	:	Polarizable Continuum Model
PES	:	Potential energy surface
PGs	:	Prostaglandins
PM3	:	Parameterized Model number 3
PM6	:	Parameterized Model number 6
PLA_2	:	Phospholipase A_2
ZPE	:	Zero Point Energy

List of figures

List of tables

TABLE OF CONTENTS

CHAPTER 1

INTRODUCTION

This chapter provides information about the problem statement, aim, and motivation for this study, and also about the organisation of the material in this thesis.

1.1. Background information

Anti-inflammatory drugs are drugs which are used for the relief of pain, fever and inflammations [1]. Many of them are based on molecules isolated from plants, in extracts used in traditional medicine in various continents (for example, aspirin, extracted from willow trees, which was used in traditional medicine in Europe). However, a common dose use of these drugs can also lead to increased risk of gastrointestinal ulceration, perforation and haemorrhage [2]. Therefore, the search for new drugs with fewer side effects is necessary.

Since the biological activity of a compound depends on its molecular properties, it is important to gain detailed information about the molecular properties of a biologically active compound, to better understand how it acts and for the design of derivative molecules with more potent activity [3]. This information is mainly obtained through computational studies. Modern drug development makes extensive use of the information about molecular properties.

This work focuses on the computational study of two anti-inflammatory compounds pertaining to the class of acylphloroglucinols (fig 1.1) [3]: myristinin A (1-{2,4,6-Trihydroxy-3-[(2S,4R)-7-hydroxy-2-(4-hydroxyphenyl)-3,4-dihydro-2H-chromen-4-yl]phenyl}-1-dodecanone) and (2-(4-hydroxyphenyl)-4-[2,4,6-trihydroxy-3-(9-tetradecenoyl)phenyl]-3,4-dihydro-2H-benzopyran-7-ol), which will be denoted as DBPO in the rest of this work. Their structures are shown in fig 1.2. The two molecules differ only by the R chain in the acyl group. The R chain in myristinin A is a long alkane chain, whereas the R chain in the DBPO molecule, also long, contains a C=C double bond; this gives rise to *cis* and *trans* geometric isomers, which are both considered in this work.

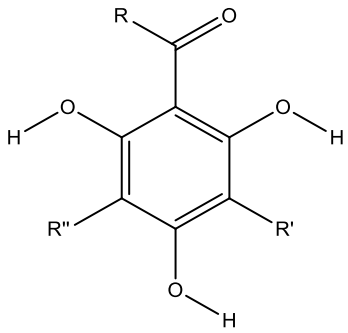

Figure 1.1. General structure of acylphloroglucinols.

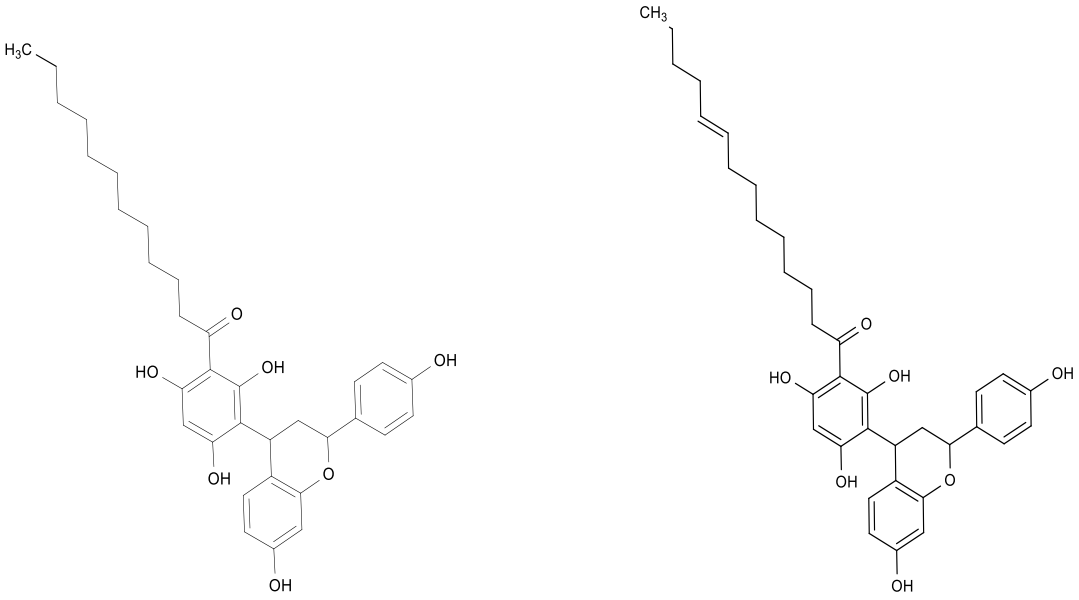

myristinin A **_trans_-DBPO isomer**

Figure 1.2. Structures of myristinin A and *trans*-DBPO.

1.2. Objectives of the study

The current study has the following objectives:

- Identifying the stable conformations of these molecules, considering all the possible geometries obtainable by rotations about relevant single bonds.
- Identifying the conformers' stabilising factors.

- Identifying the other computable properties of these molecules, such as dipole moments, HOMO-LUMO energy difference and vibrational frequencies (harmonic approximation).
- Investigating the effect of different solvents with different polarities on the conformational preferences and the other properties of the considered molecules.

To this purpose *ab initio* (HF and MP2) and DFT calculations have been performed on the selected molecules.

1.3. Motivations for the study

1.3.1. Motivation from a biological-activity point of view

As already mentioned, the anti-inflammatory compounds currently in use have some undesirable side effects, such as an increase in the risk of gastrointestinal disorders or an increase in the risk of cardiovascular complications. Therefore, the search for new drugs with fewer side effects is important. This study considers compounds which exhibit anti-inflammatory activity. They are non-steroidal compounds and have different structures from the ones which are currently in use or whose use has been discontinued.

1.3.2. Motivation from a computational point of view

This work falls within a broad computational study of acylphloroglucinols carried out at the University of Venda [4-20]. The computational study of the myristinin A and DBPO molecules is interesting, because their structure is substantially different from the structures of the monomeric acylphloroglucinols which have already been investigated [4-20], as the substituent at C3 is a ring system of different nature (2-(4-hydroxyphenyl)-3,4-dihydro-2H-chromen-7-ol). Furthermore, myristinin A and DBPO are the first anti-inflammatory acylphloroglucinols to be studied computationally.

The information that is obtained from this study is relevant as information about the properties of the myristinin A and DBPO molecules. It is also important because it enables comparisons with the results of the computational studies of other acylphloroglucinols, with different molecular structures and different biological activities. The selection of computational methods and of the solvents for the calculations in solution corresponds to the selection in the study of other acylphloroglucinols, to make comparisons meaningful.

1.4. Organisation of the material

The present work contains seven chapters:

Chapter 1 provides the background information for this study such as the importance of anti-inflammatory drugs, the importance of the search for new anti-inflammatory drugs with fewer side effects than the current ones, as well as the objectives and the motivations of this study.

Chapter 2 provides the theoretical background of computational approaches to the study of molecules, paying particular attention to the computational methods utilised in the current study and to the molecular properties considered here.

Chapter 3 provides a literature review on acylphloroglucinols, which is the class of compounds to which these molecules belong, and also information related to the selected molecules themselves.

Chapter 4 motivates selection of the computational methods utilised in this work and also describes the way in which the inputs were prepared.

Chapter 5 to 7 report the results obtained and analyse them. Chapter 5 presents the result of the computational study of myristinin A *in vacuo* and in solution. Chapter 6 presents the result of the computational study of *cis*-DBPO *in vacuo* and in solution. Chapter 7 presents the result of the computational study of *trans*-DBPO *in vacuo* and in solution.

Chapter 8 provides an overall discussion of the results obtained.

CHAPTER 2

THEORETICAL BACKGROUND

The computational study of molecules provides information about the energy, geometry (bond lengths, bond angles, and dihedral angles), dipole moments, molecular orbitals and other molecular properties. This study is particularly important for biologically active molecules, that is, molecules that can exert an activity in living organisms. It is important because biological activities depend on the molecular properties and, therefore, we need to know these properties to better understand the activities.

2.1. The description of molecules

A molecule is an electrically neutral grouping of two or more atoms held together by chemical bonds [21-25]. The atoms in a molecule are arranged in a sequence that is typical to each molecule. Their arrangement is three-dimensional in space [26]. The structure (sequence of atom) of a molecule is determined experimentally through spectroscopic techniques. Each molecule can take many geometries and each geometry is defined by its parameters, namely, bond lengths, bond angles and dihedral angles.

The bond length is the average distance between the centres of the nuclei of two bonded atoms and is expressed in Angstrom (Å, $1Å=10^{-10}$ m) or picometer (pm, $1pm=10^{-9}$ m). For example, the bond length in the H_2 molecule (at the left hand side of fig 2.1), is the distance between the nuclei of the two H atoms (H1 and H2) depicted as a black line.

A bond angle (θ) is the average angle between two consecutive bonds, i.e., the angle identified by three subsequently bonded atoms and is defined for molecules consisting of three or more atoms. For example, the bond angle in the water molecule (in the centre of fig 2.1) is ∠H2–O1–H3, i.e., the angle between the O1–H2 and O1–H3 bonds. For molecules with many atoms, bond angles are defined for each set of three consecutively bonded atoms.

The dihedral angle (torsion angle) is defined for groups of four atoms subsequently bonded in a chain, and is the angle between the plane formed by the first three atoms and the plane formed by the last three atoms. For molecules with many atoms, dihedral angles are defined for each set of

four consecutively bonded atoms. For example, in the ethane molecule (at the right hand side of fig 2.1) one can consider, for example, the four atoms in the H2–C1–C5–H6 sequence (showed by the red line in fig 2.1). The dihedral angle formed by these atoms can be defined as the angle between the C5–H6 and C1–H2 bonds when they are projected into the plane bisecting the C1–C5 bond (the green lines are the projections of the C5–H6 and C1–H2 bonds into the bisecting plane). The sign of the dihedral angle (denoted by ω in fig 2.1) depends on whether one choses to view the bisecting plane from the C5–H6 side or the C1–H2 side. Other dihedral angles in the ethane molecule are H2–C1–C5–H6, H2–C1–C5–H7, H2–C1–C5–H8, H3–C1–C5–H6, H3–C1–C5–H7, H3–C1–C5–H8, H4–C1–C5–H6, H4–C1–C5–H7, H4–C1–C5–H8.

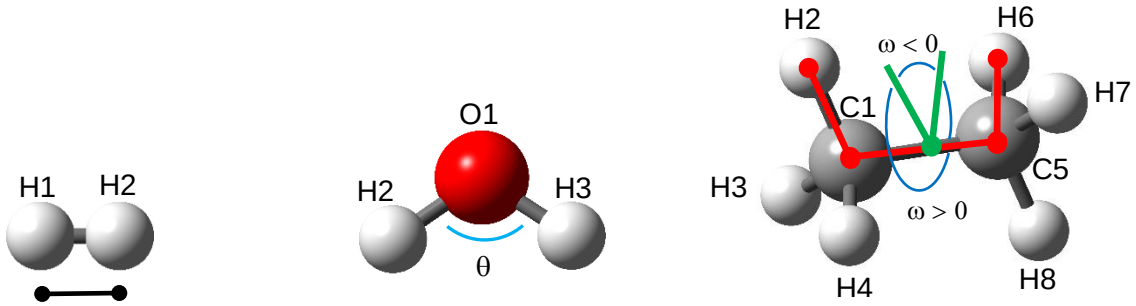

Figure 2.1. An illustration of the parameters that define the geometry of a molecule.

A molecule can change from one geometry to another by rotation around a single bond. Some of these geometries correspond to minima on the potential energy surface. A potential energy surface (PES) is the relationship – mathematical or graphical – between the energy of a molecule and its geometry [27]; it can be obtained by changing parameters such as bond angles or dihedral angles by specific amounts. The geometries corresponding to the minima on the PES are called conformers. A search for these conformers is referred to as conformational search.

Bond lengths, bond angles and dihedral angles are called the internal coordinates of a molecule. The geometry of a molecule can also be described by specifying the position of each atom through its Cartesian coordinates x, y and z. This is the form usually used in calculation inputs.

For a molecule with N atoms, there are $3N - 6$ internal coordinate (degrees of freedom). Since each of them could in principle be varied to find the PES, then the PES would have one coordinate for the energy and $3N - 6$ coordinates for the variation of the molecule's internal coordinates.

However, since we are able to represent only diagrams in two or three dimensions, we can only change one coordinate at a time and get a 2-dimension PES or two coordinates at a time and get a 3-dimension PES. In order to obtain the PES, we minimise the energy with respect to a coordinate; this means that the first derivative of the energy with respect to that selected coordinate must be equal to zero. In this way, stationary points are obtained. The stationary points can be of three types: they may correspond to a minimum, or to a saddle point, or to a maximum. The ones corresponding to a minimum represent equilibrium geometries. The first order saddle points correspond to transition states (the transition from one geometry to another or the transition state during a chemical reaction if one is considering how the energy changes during a reaction). Figure 2.2 represents a sample PES for a reaction involving one reactant and two products.

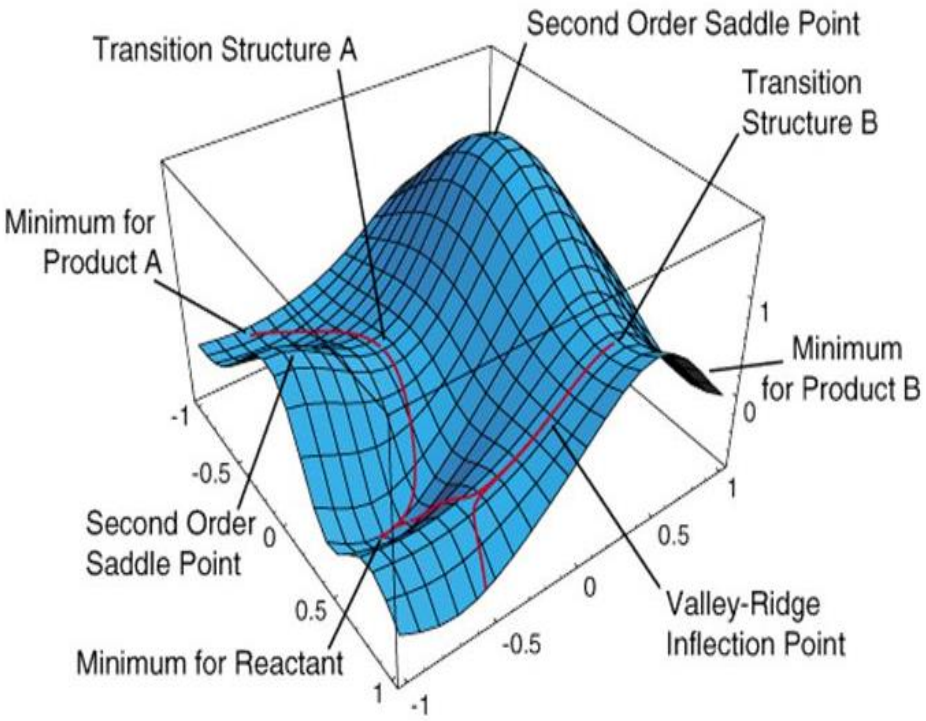

Figure 2.2. Features of the PES for a reaction involving one reactant and two products.

2.2. Methods for the computational study of molecules

Different methods have been developed for the computational study of molecules and they are grouped into two main groups: electronic structure methods and molecular mechanics. Electronic structure methods are the methods which describe the molecule as a system made of nuclei and electrons [29]. These methods are based on the solution of the Schrödinger equation of the considered molecule and can be classified as *ab initio* or semi-empirical according to the way in which the integrals appearing during the solution process are calculated. Molecular mechanics describes the molecule as a system made of *balls* and *sticks*, and utilises a classical mechanics approach. Since this work utilises electronic structure methods, the next paragraphs will focus on those methods.

2.2.1. The Schrödinger equation

All electronic structure methods pertain to quantum mechanics. In quantum mechanics, the description of the molecule is found by solving the Schrödinger equation [30-32]. The general Schrödinger equation is,

$$\hat{H}\,\psi_i = E_i\psi_i \qquad (1)$$

Where $\hat{H}$ is the Hamiltonian operator, i.e., the energy operator.

ψ_i is the total wavefunction of the i^{th} state

E_i is the corresponding energy value (eigenvalue)

The Hamiltonian operator contains all the energy terms needed to describe a system. It comprises the two types of energy involved, namely, the kinetic energy and the potential energy. The meaning of equation (1) is that the Hamiltonian operator acts upon the wavefunction of the system and returns both the wavefunction and the energy (eigenvalue) of the system.

2.2.2. The Born-Oppenheimer Approximation

The Hamiltonian for a molecule with M atoms is given by the following equation:

$$\hat{H} = -\sum_i^N \frac{\hbar^2}{2m_e} \nabla_i^2 - \sum_k^M \frac{\hbar^2}{2m_k} \nabla_k^2 - \sum_i^N \cdot \sum_k^M \frac{e^2 Z_k}{r_{ik}} + \sum_{i<j}^M \frac{e^2}{r_{ij}} + \sum_{k<l}^M \frac{e^2 Z_k Z_l}{r_{kl}} \quad (2)$$

where the subscripts *i* and *j* refer to the electrons while *k* and *l* refer to the nuclei

ħ is the Planck's constant

m_e is the mass of the electron

m_k is the mass of nucleus *k*

e is the charge of the electron

N is the number of electrons

M is the number of nuclei

Z_k is an atomic number of the nucleus *k*

Z_l is an atomic number of the nucleus *l*

r_{jk} is the distance between electron *i* and nucleus *k*

r_{ij} is the distance between electrons *i* and *j*

r_{kl} is the distance between nuclei *k* and *l*

∇^2 is the Laplacian operator

The first two terms represent the kinetic energies of the *N* electrons and *M* nuclei respectively. The last three terms represent the contribution to the potential energies: the third term accounts for the potential energy which arises from the attractive electrostatic interaction between each electron and each of the nuclei; the fourth and fifth terms account for the potential energy from repulsive electron-electron and nucleus-nucleus interactions respectively [33].

∇^2 is the Laplacian operator, used to express the kinetic energy of a particle. Since the position of the particle is described by three coordinate (x, y and z), the Laplacian operator of that particle is expressed by the following equation,

$$\nabla^2 = \left(\frac{\partial^2}{\partial x^2} + \frac{\partial^2}{\partial y^2} + \frac{\partial^2}{\partial z^2}\right) \quad (3)$$

Equation (2) contains all the terms for a complete description of a molecule. On the other hand, it becomes more difficult to solve the equation if we consider all the electrons and all the nuclei. Including the motion of the nuclei and their mutual repulsion complicates the solution. In the Born-Oppenheimer approximation [34], the motion of the nuclei is neglected and, in this way, also the nucleus-nucleus repulsion can be neglected. This is justifiable because a nucleus is thousands times heavier than an electron [34-36], and this means that electrons move much faster than the nuclei.

Within this approximation, the Hamiltonian operator is the electronic operator and is given by,

$$\hat{H}_{el} = -\sum_i^N \frac{\hbar^2}{2m_e} \nabla_i^2 - \sum_i^N \cdot \sum_k^M \frac{e^2 Z_k}{r_{ik}} + \sum_{i<j}^N \frac{e^2}{r_{ij}} \quad (4)$$

In practice, the approximation means that one considers a set of fixed nuclei and solves the Schrödinger equation for the electrons of that arrangement. Then, one might consider a different nuclei arrangement and solve the Schrödinger equation for the electrons in that arrangement.

The use of $\hat{H}_{el}$ to solve the Schrödinger equation yields the electronic wavefunction (Ψ_{elec}) and the electronic energy (E_{elec}). The PES as defined in section 2.1 refers to the electronic energy.

Since the nuclei are treated as fixed, the electronic wavefunction depends on the fixed nuclear coordinates and the three Cartesian coordinates of each electron; therefore, it depends on the spatial coordinates of the electrons (as the only coordinates that can vary) and on the spins of the electrons. Electrons are fermions [37]. Therefore, they must abide by the weak condition of Pauli Exclusion Principle which states that no two fermions can occupy the same quantum state [38-39]. This corresponds to the strong condition of the Pauli Exclusion Principle, which states that the n-electron wavefunction must be antisymmetric; this means that an ‘‘exchange’’ in the spatial coordinates of two particles must result in a change of the sign of the wavefunction [40].

2.2.3. The variational principle

The exact solutions of the Schrödinger equation can be determined only for one-electron systems such as H_2^+. For many-electron systems, approximation methods are needed to solve the Schrödinger equation. Many of these methods are based on the variational principle, which states that the expectation value of the Hamiltonian for a trial wavefunction, Ψ_{trial}, is always greater than or equal to the actual ground state energy, E_0 [41].

2.2.4. *Ab initio* electronic structure methods

Ab initio electronic structure methods are the methods which are derived from theoretical principles and do not include experimental values [42]. The term *ab initio* means "from the beginning" [43], and indicates that the solution of the Schrödinger equation is based on theoretical principles only, and all integrals are solved analytically. The most common *ab initio* methods are the Hartree-Fock (HF) method and the Møller-Plesset perturbation theory (MP).

2.2.4.1. The Hartree Fock (HF) method

The Hartree Fock (HF) method is one of the most common types of *ab initio* methods. The method uses a Self-Consistent-Field (SCF) procedure to solve the secular equations resulting from the application of the variational principle [44-45]. SCF procedures can be used for the study of both atoms and molecules, although with different implementation algorithms [45].

The bases of the method can be explained in a simpler way by considering the application to atoms. HF considers the average potential that an electron perceives due to the charges of all the other N-1 electrons and the nucleus (where N is the total number of electrons in the system considered) [44-46]. The first step of this procedure utilises a first guess of the potential, which takes into account the average electronic repulsion and uses it to write the Hamiltonian operator and the Schrödinger equation. By separating the variables, N identical equations are obtained, each of them depending on the coordinates of one electron. These equations are solved. Their solutions give the total wavefunction which is used to estimate the charge distribution; this, in turn, is used to determine the average potential [44-46]. The new potential thus obtained is then compared with the one used at the beginning of the procedure and, if there is a significant difference, the procedure is repeated. The procedure is repeated again and again until the difference between the potential which is obtained at the end of a cycle and the potential that was obtained at the end of the previous cycle is less than a pre-fixed value called the cut-off value [44-46]. At this point, the procedure is regarded as having converged and the wavefunction and energy values obtained are considered the wavefunction and energy of the system. Since the HF method replaces the electron-electron interaction by an average potential, the energy value obtained accounts for 99% of the total energy [47-48]. The remaining 1% is the electron correlation energy, which is important for the description of some molecular properties and chemical phenomena [47-48]. The electron correlation energy is defined as the energy difference between the exact energy and the energy obtained from the Hartree Fock solution [49]. The HF method does not take into account electron correlation, except for what is related to Pauli's exclusion principle.

The case of a molecule is more complex because a molecule has more than one nucleus. Thus, the potential does not have a spherical symmetry. Most calculations are carried out within the Born–Oppenheimer approximation, which considers a fixed arrangement of nuclei (separation of nuclear motion and electronic motion, section 2.2.2). For the molecular system, the eigenfunctions from equation (4) are referred as the molecular orbitals (MOs). Thus, all wavefunctions are electronic wavefunctions. A one-electron wavefunction is denoted by ψ_{el} and Ψ_{el} is used for a many-electron wavefunctions. The energy of an electron in a particular molecular orbital is the pure electronic eigenvalue that is associated with that molecular orbital.

2.2.4.2. Slater Determinant

The wavefunction used within the variational principle (Ψ_{trial}) can be expressed in many ways. The N electron wavefunction Ψ_0 can be written as a product of N one-electron wavefunctions, $\chi_i(\vec{x}_i)$ (spin orbitals), which gives the Hartree product. The spin orbitals consist of a spatial orbital component $\phi(\vec{r})$, (where $\vec{r}$ is a vector of coordinates which relates to the position of the electron) and a spin component, σ:

$$\chi(\vec{x}_i) = \phi(\vec{r})\sigma \tag{5}$$

The spin component represents the α and β spins of the electrons. Even though the Hartree product seems to appear to be a good approximation of Ψ_0, it does not meet the requirements on the wavefunction concerning physical observables. The fact that the electrons are indistinguishable from one another is violated by the association of each spin orbital with a specific electron. The Hartree product also does not meet the antisymmetry requirement [33], since it is not antisymmetric upon the interchange of electrons. Expressing the wavefunction as a Slater determinant Φ_{SD} [50] responds to the antisymmetry requirement.

$$\Phi_{SD} = \frac{1}{\sqrt{N!}} \begin{bmatrix} \chi_1(\vec{x}_1) & \chi_2(\vec{x}_1) & \cdots & \chi_N(\vec{x}_1) \\ \chi_1(\vec{x}_2) & \chi_2(\vec{x}_2) & \cdots & \chi_N(\vec{x}_2) \\ \vdots & \vdots & \ddots & \vdots \\ \chi_1(\vec{x}_N) & \chi_2(\vec{x}_N) & \cdots & \chi_N(\vec{x}_N) \end{bmatrix} \tag{6}$$

where $\frac{1}{\sqrt{N!}}$ is the normalisation coefficient, which makes sure that Φ_{SD} is normalised.

χ is a spin orbital

N is the total number of electrons

The Hartree Fock approximation utilises a single Slater determinant to represent the electronic (total) wavefunction. The Hartree Fock procedure can be used to obtain a set of MOs that accounts for the lowest energy E_{HF}. This energy can be obtained after applying the variation principle, whereby the spin orbitals of the Slater determinant are varied in a self-consistent way to obtain the lowest energy, and it is expressed as,

$$E_{HF} = \langle \Phi_{SD} | \hat{H} | \Phi_{SD} \rangle = \sum_i^N \langle i | \hat{h} | i \rangle + \frac{1}{2} \sum_i^N \sum_j^N (ii|jj) + (ij|ji) \quad (7)$$

where $(ii|jj) = \iint |\chi_i(\vec{x}_1)|^2 \frac{1}{r_{12}} |\chi_i(\vec{x}_2)|^2 d\vec{x}_1 d\vec{x}_2$ (7a)

$$(ij|ji) = \iint \chi_i(\vec{x}_1) \chi_j^* (\vec{x}_1) \frac{1}{r_{12}} \chi_j(\vec{x}_2) \chi_i^* (\vec{x}_2) d\vec{x}_1 d\vec{x}_2 \quad (7b)$$

The first term on the right hand side of eqn (7) accounts for one-electron integrals including the kinetic energy and the electron-nucleus attraction term; the $(ii|jj)$ term {which is further expanded in equation (7a)} represents the Coulomb integrals, that describe the repulsive interaction between all pairs of electrons; the $(ij|ji)$ term {which is expressed in equation (7b)} represents the exchange integrals, which originate from the antisymmetry rule whereby two electrons can swap orbitals [33].

2.2.4.3. The LCAO Approximation

Since molecules are made of atoms, molecular orbitals can be expressed through atomic orbitals. This can be achieved by using a Linear Combination of Atomic Orbitals (LCAO) approximation [41, 44, 51];

$$\psi = \sum_i C_i \chi_i \quad (8)$$

where C_i are the molecular orbital coefficients

χ_i are the atomic orbitals

Using the actual atomic orbitals (the expression of the atomic orbitals obtained from the solution of the Schrödinger equation for the atoms) has proved a bit complicated for the solution of some

integrals. So other functions have been introduced to express the atomic orbitals. The set of the χ_i functions utilised in the expansion of equation (8) is called basis set [52]. The C_i coefficients can be determined numerically by substituting equation (8) into the Schrödinger equation of the molecule considered and applying the variational principle (section 2.2.3.) [41, 44]. The calculation procedure leads to the Roothaan equations [44], which can be written in the form:

$$FC=SC\varepsilon \quad (9)$$

where F is the Fock matrix that depends on the coefficients C_i, C is the matrix of the coefficients C_i, S is the matrix of the overlaps of the basis functions and ε is the matrix of the orbital energies.

2.2.4.3.1. Basis sets

As already mentioned, a basis set is a set of atomic orbitals that is used in the formation of molecular orbitals (eqn. 8). Identifying a basis set that gives good results and is computationally affordable is the main concern in computational studies [53].

The atomic orbitals which contribute to the formation of molecular orbitals are the following;

- the orbitals of the inner, closed shells (core orbitals)
- the orbitals of the valence shell (valence orbitals)
- the orbitals that are not occupied in the ground state (virtual orbitals)

When choosing the basis set, one must choose the type of orbitals that will give good results with an affordable computational effort [53]. The following subsections discuss the most commonly used basis sets.

2.2.4.3.1.1. Functions used in the expansion of the molecular orbital

The χ_i functions used in the expansion of a molecular orbital (eqn. 8) could be the atomic orbitals themselves. These orbitals are centred on the nuclei and, altogether, yield a spherical symmetry for the isolated atom. However, they are not suitable to describe the changes in the spherical electron distribution of individual atoms caused by the neighbouring atoms in a molecule. Moreover, the mathematical form of atomic orbitals is not convenient for the solution of some integrals. Other types of atom-centred basis functions were proposed. The first ones were the Slater type orbitals (STOs) [54, 55]. The problem with STOs is that, most of the time, they are impractical for quantum chemical calculations, as some of the integrals are difficult or even impossible to solve [45]. In most

systems, numerical solutions are required. In recent times, the most used basis sets are those based on Gaussian functions, i.e., Gaussian type orbitals (GTOs) [35], whose integrals are analytical.

2.2.4.3.1.2. Minimal basis set.

A minimal basis set is a basis set which contains only the functions that are needed to accommodate all the electrons present in an atom [35, 44, 56]. For example, this corresponds to one (1s) function for the hydrogen and helium atoms, a set of 5 functions (1s, 2s, $2p_x$, $2p_y$, $2p_z$) for lithium to neon, a set of 9 functions (1s, 2s, $2p_x$ $2p_y$, $2p_z$, 3s, $3p_x$, $3p_y$, $3p_z$) for sodium to argon etc.

2.2.4.3.1.3. Split-Valence Basis Sets

Split-Valence Basis Sets are basis sets providing two sets of basis functions, namely inner and outer functions. These basis sets express core atomic orbitals by one set of functions, while valence atomic orbitals are split into arbitrarily many functions [57]. The following are the simplest split-valence basis sets: 3-21G, 4-31G, and 6-31G, where the first number is the number of functions used to express each of the core orbitals, and the two numbers before the G are the number of gaussian functions in the two parts into which each valence orbital is split.

2.2.4.3.1.4. Polarisation basis sets

Polarisation is the distortion of the shape of the atomic orbital in the formation of the molecule. Therefore, polarisation basis sets are the ones which account for the problem rising from the fact that atomic functions are centred on the nuclei of individual atoms. These basis sets include the basis functions with higher angular momentum quantum number than the occupied orbitals of the atomic ground state [58]. For example, they include d-type functions where the valence orbitals are of s and p types, and p-type functions when the valence orbital is of s type [58]. These diffuse orbitals in basis sets are denoted by *; for example, the basis set 6-31G with added polarisation functions for the heavy atoms becomes 6-31G*, which can also be written as 6-31G(d); if polarisation functions are added also for H atoms, the basis set is denoted as 6-31G**, which can also be written as 6-31G(d,p).

2.2.4.3.1.5. Diffusion basis sets

Diffuse basis sets are basis sets with added diffuse functions. They are mostly used in calculations involving anions, molecules with lone pairs, excited states and transition states [59]. The presence

of diffuse function is denoted by +; for example, the basis set 6-31G* with added diffuse function for the heavy atoms becomes 6-31+G*.

2.2.4.4. The Møller-Plesset (MP) perturbation theory

The Møller-Plesset perturbation theory (MP) is one of the approaches which use a perturbation on the Hartree-Fock solutions to decrease the error that was introduced in the Hartree-Fock procedure when the two-electron integrals were replaced by a one electron potential [60-62]. The two-electron integrals are restored. The perturbation theory starts from the uncorrelated HF wavefunction and adds a correction term to take into account the electron correlation [60-62]. This Hamiltonian is written as the sum of the unperturbed Hamiltonian operator ($\hat{H}_o$) and a perturbation operator ($\hat{H}'$) which adds the correction corresponding to the contribution by the dynamic electron correlation (the correlation of the electrons' motions) [60-63]. The perturbed Hamiltonian operator can be written in the form:

$$\hat{H} = \hat{H}_o + \lambda\hat{H}' \qquad (10)$$

where $\hat{H}$ is the perturbed Hamiltonian operator

$\hat{H}_o$ is the 'zeroth-order' Hamiltonian (the HF solution)

λ is the Lagrange multiplier, which determines the strength of the perturbation

$\hat{H}'$ is the first order Hamiltonian perturbation

The application of the approach proposed by Møller and Plesset is called by the acronym MPn, where n stands for the order in which the perturbation expansion is shortened. Expanding the operator up to the first order (referred as MP1) gives the Hartree-Fock solution, which does not go beyond the HF level for estimating the energy [60-63]. Including the second order correction (as in eqn (10)) leads to a method called MP2 [63]. Analytical first and second derivatives are available for the geometry optimisation procedure for this level of theory; therefore, MP2 can be easily utilised for exploring PESs. Just like all other orders of MPn, MP2 is size consistent and not variational and it is currently the less costly method for including a high proportion of the electron correlation, yielding better results. Including the third order perturbation leads to a method called MP3 [60-63] and including the fourth order perturbation leads to a method called MP4 [60-63]. As for the latter two orders, they are used in practice, but limited to very small size molecules because of their computational demands; another problem is that there are no analytical derivatives available for these orders [60].

2.2.5. Density Functional Theory (DFT) method

Similarly to HF, the DFT method describes the electronic structure and properties of a molecular system by solving the Schrödinger equation. Unlike HF, which focuses on the wavefunction, DFT focuses on the electron density (ρ). The electron density is a measure of the probability of an electron being present at a particular point in space and is a scalar quantity. A functional is defined in mathematics as a function of a function. DFT is referred as 'functional theory' because it considers the energy as a function of the electron density (E (ρ)), which, in turn, is a function of the position [ρ(r)]; thus, the energy is a function of a function, and is expressed as,

$$E = E\,[\rho(\vec{r})] \tag{10}$$

In 1964, Hohenberg and Kohn developed two DFT fundamental theorems [39, 41, 44, 65]. The first theorem was based on the idea that an external potential (V_{ext}) that originate from the position of the nuclei in a molecule is a distinct functional of the electron density, (ρ(r)) [39, 41, 44, 65]. This means that two different external potentials can only yield different ground state electron densities [39, 41, 44, 65]. Therefore, the Hamiltonian, $\hat{H}$, is a distinct functional of the electron density:

$$\hat{H} = \hat{T} + \hat{V}_{ee} + \hat{V}_{ext} \tag{11}$$

where $\hat{T}$ is the kinetic energy of the non-interacting electrons

$\hat{V}_{ee}$ is the external potential related to the classical electron-electron repulsion

$\hat{V}_{ext}$ is the external potential related to the nuclear-electron interaction

Hence, the ground state energy generated from the ground state electron density can be expressed by

$$E_0 = E\,[\rho(r)] \tag{12}$$

The components of eqn (11) can be re-written as functional of ρ(r),

$$E_0\,[\rho_0] = T\,[\rho_0] + E_{ee}\,[\rho_0] + E_{ne}\,[\rho_0] \tag{13}$$

T [ρ_0] and E_{ee} [ρ_0] depend on the electron density and are called "system independent", while E_{ne} [ρ_0] accounts for the potential energy generated from the nuclei-electron attraction and is dependent on the nuclei (it is, thus, system dependent). The energy functional (eqn.13) can be further divided into specific components as shown by the following equation

$$E[\rho(r)] = T_{ni}[\rho(r)] + V_{ne}[\rho(r)] + V_{ee}[\rho(r)] + \Delta T[\rho(r)] + \Delta V_{ee}[\rho(r)] \quad (14)$$

where, T_{ni} [ρ(r)] refers to the kinetic energy of the non-interacting electrons

V_{ne} [ρ(r)] refers to the nuclear-electron interaction

V_{ee} [ρ(r)] refers to the classical electron-electron repulsion

ΔT [ρ(r)] refers to the correction to the kinetic energy generated from the interacting nature of the electrons

ΔV_{ee} [ρ(r)] accounts for all non-classical corrections to the electron-electron repulsion energy

In equation (14), the first three terms account for the system independent contributions, and collectively form the Hohenberg-Kohn functional, F_{HK} [ρ_0]. The latter two terms, account for the system dependent contributions.

The Hohenberg-Kohn first theorem accounts for the ground state energy, E_0, generated from the F_{HK} [ρ_0], when the ground state electron density is specified. After some time, Hohenberg and Kohn developed a second theorem that was now accounting not only for ground state electron density, but also for any guess electron density, ρ_{trial}. The second theorem applies the variational principle to the fundamental concept of DFT [39, 41, 44, 65]. Thus, a ρ_{trial} related to an external potential yields an energy value which is higher than that of the ground state energy:

$$E[\rho_{trial}] = T[\rho_{trial}] + E_{ee}[\rho_{trial}] + E_{ne}[\rho_{trial}] \geq E_0 \quad (15)$$

However, the expression of the kinetic energy from Hohenberg-Kohn functional was not well established which caused the application of DFT within the Hohenberg-Kohn approximation to fail [33]. In 1965, Kohn and Sham developed another expression of the kinetic energy:

$$T_{HF} = \langle \chi_i | \nabla^2 | \chi_i \rangle \quad (16)$$

where χ_i are the spin orbitals.

This expression was obtained after they discovered the correspondence of the Slater determinant, which is an approximation to the N-electron wavefunction, with the true wavefunction for a system of non-interacting electrons from the HF approximation [33].

Thus, the ground state wavefunction can be expressed by a Slater determinant, Θ_s.

$$\Theta_{s=}\frac{1}{\sqrt{N!}}\begin{bmatrix}\varphi_1(\vec{x}_1) & \varphi_2(\vec{x}_1) & \cdots & \varphi_N(\vec{x}_1)\\ \varphi_1(\vec{x}_2) & \varphi_2(\vec{x}_2) & \cdots & \varphi_N(\vec{x}_2)\\ \vdots & \vdots & \ddots & \vdots\\ \varphi_1(\vec{x}_N) & \varphi_2(\vec{x}_N) & \cdots & \varphi_N(\vec{x}_N)\end{bmatrix} \quad (17)$$

Similarly to the HF theory, the Kohn-Sham (KS) orbitals [44], φ_i, are similar to those in equation (6), and are also related to the eigenvalue, ε_i, through the following eigenvalue equation

$$\hat{f}^{KS}\,\varphi_i = \varepsilon_i\varphi_i \quad (18)$$

where, $\hat{f}^{KS}$ is the Kohn-Sham operator, which can be expressed as

$$\hat{f}^{KS} = \frac{1}{2}\nabla^2 + V_S(\vec{r}) \quad (19)$$

where, $V_S(\vec{r})$, is the effective potential.

Therefore, within the Kohn-Sham approach, the Hohenberg-Kohn function is written as

$$E_{DFT}[\rho] = T_s[\rho] + E_{ne}[\rho] + J[\rho] + E_{xc}[\rho] \quad (20)$$

$T_s[\rho]$ is the kinetic energy of the non-interacting electrons, $E_{ne}[\rho]$ is the potential nucleus-electron interaction potential energy, $J[\rho]$ is the electron-electron interaction potential energy, and $E_{xc}[\rho]$ is the exchange correlation energy which is calculated with an exchange-correlation functional. $E_{xc}[\rho]$ takes into account part of the electron correlation energy.

The exchange-correlation models which are currently available include local density models and non-local models. The local density models are models in which the functionals are based on the local spin density approximation [44, 66]. This approximation fails if the electron density is not close to homogenous [67]. Non-local models are gradient-corrected models which include generalised gradient approximation functionals (GGA) and hybrid functionals [39]. The GGA are functionals which involve the first derivative of electron density when calculating $E_{xc}[\rho]$). The most commonly used GGA are PBE [68] and B88 [69]. Hybrid functionals are the functionals which employ the "exact" Hartree-Fock exchange as a component, and include BP, BLYP and EDF1 functionals [70], with B3LYP [71] being the most popular one.

Density functional models are not *ab initio* or size consistent; they are variational. They are well-defined and yield unique results [72]. Another aspect to be observed is that the density functional approach is "exact", provided that the exact exchange/correlation functional is known. However, there is still on-going development on these functionals, to try and achieve an arbitrary level of accuracy. A variety of new functionals have been designed. However, it seems to be very difficult to achieve arbitrary accuracy [73].

2.2.6. Semi-empirical methods

Semi-empirical methods are the methods which introduce some experimental values in the solution procedure, for instance, in place of some multi-electron integrals. Semi-empirical methods are much faster than *ab initio* methods, but have limited accuracy. Semi-empirical methods include the Austin Model 1 (known as AM1 [74]), the Modified Intermediate Neglect of Differential Overlap (known as MINDO [75]) and the Parameterized Model series (PM3 [76], PM6) [77]).

2.3. Consideration of relevant molecular properties

2.3.1. Thermodynamic properties and frequency

A molecule can have three different forms of motions, translational, rotational and vibrational. The translational motion refers to the motion of the whole molecule in space and the rotational motion refers to the rotation of the molecule around the axes (x, y and z axes). The vibrational motions refer to the motions of atoms in the molecule and arise from the fact that the atoms are not fixed in space within a molecule. These motions contribute greatly to the energy of a molecular system [78, 79]. Thus, the expression of the energy, E, of a molecule can be written as

$$E = \varepsilon^T+\varepsilon^R+\varepsilon^V+\varepsilon^E \quad (21)$$

where ε^T corresponds to the translation contribution

ε^R corresponds to the rotational contribution

ε^V corresponds to the vibrational contribution

ε^E is related to the electronic contribution

The summation of ε^T, ε^R, and ε^V give rise to the thermal energy of a given molecular system.

As already mentioned, each atom has 3 degrees of freedom in space (i.e., its three coordinates). In a molecule containing N atoms, the total number of degrees of freedom is 3N. Since the translational motion involves the entire molecule, there are 3 degrees of freedom corresponding to translational motion. For the rotational motion, a non-linear molecules has 3 degrees of freedom, a linear molecules has only 2 degrees of freedom. The remaining degrees of freedom correspond to vibrational motions. This means that the number of vibrational degrees of freedom is 3N - 6 for a non-linear molecule and 3N - 5 for a linear molecule. These vibrational motions are called normal vibrational modes of the molecule.

The vibrational motions of a molecule involve changes in its shape. The two main motions are stretching (changes in the inter-atomic distances along bond axes) and bending (changes in the angle between two bonds) [78]. The simplest way of describing these motions uses the harmonic oscillator model [44].

For a harmonic oscillator, vibrations are considered as harmonic (periodic) motions. The frequencies of the periodic motions of the atoms in a molecule are considered as the vibrational frequency of those motions. Finding the normal modes is one of the objectives of vibrational frequency calculations.

The harmonic oscillator has a parabolic potential:

$$V = \frac{1}{2}kx^2 \tag{22}$$

Thus, its Schrödinger equation is [81,82]

$$-\frac{h^2}{2m}\frac{\partial^2\psi}{\partial x^2} + \frac{1}{2}kx^2\psi = \mathrm{E}\psi \tag{23}$$

where m is the mass of the oscillating particle

x is the displacement along the x direction

k is the restoring force constant

The energy values from the solution of equation (23) are given by

$$E = (v + \frac{1}{2})h\omega \tag{24}$$

where v is the vibrational quantum number and ω is related to the force constant through the expression

$$\omega = \frac{1}{2\pi}\sqrt{\frac{k}{m}} \tag{25}$$

The separation between two neighbouring level is constant and equal to $h\omega$. The harmonic oscillator is a typical system having zero point energy. Putting v=o in eqn. 24 gives an energy value which is not equal to zero (is equal to $\frac{1}{2}h\omega$); this is the minimum energy value possible and it is not the bottom of the parabola. Thus, the zero point energy is the difference between the minimum energy possible and the bottom of the parabola.

The vibration of a bond corresponds to the harmonic approximation for the lower values of the quantum number v. When the values of v increase, the energy levels are closer than in the harmonic approximation. So the potential energy is better represented by use the Morse potential energy that has the bottom part very close to that of the harmonic oscillator and the upper part that is very different (fig.2.3). The harmonic approximation is the most commonly used in frequency calculations. If one needs highly precise values, one has to consider the deviations from this approximation and introduce anharmonicity corrections.

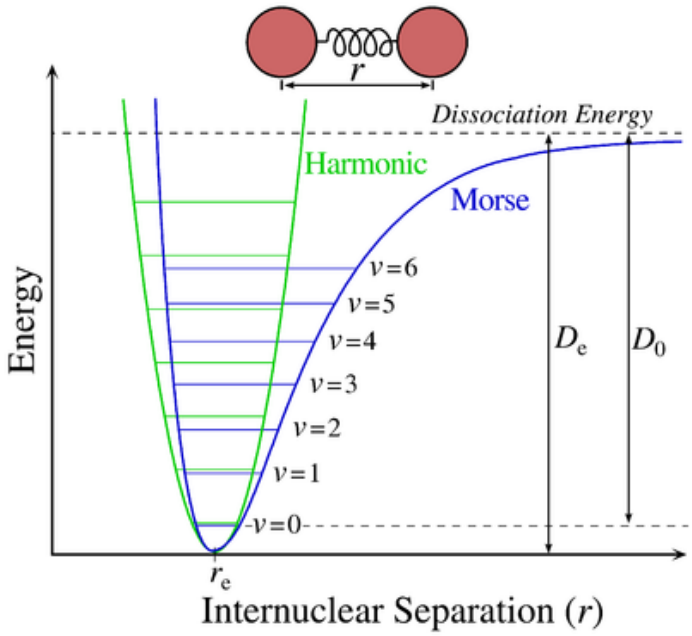

Figure 2.3. An illustration of the Morse potential (blue) and harmonic oscillator potential (green) energy curves [83].

The calculation of the vibrational frequencies is particularly important because of the type of information that it can provide. It enables one to know whether a stationary point identified by an optimisation calculation corresponds to a minimum on the potential energy surface (it corresponds to a minimum if there is no imaginary frequency, whereas, imaginary frequencies greater than zero always correspond to saddle points; when there is only one imaginary frequency, the saddle point corresponds to a transition state). The force constant, k, associated with the stretching frequency, determines the hardness of the molecule; it increases with the hardness of a molecule. The vibrational frequencies are also useful to have an idea of the strength of hydrogen bonds in terms of how the frequency of the donor group (for example OH for the molecules considered here) is lowered by the IHB. This lowering is called the red shift and it can give an indication of the hydrogen bond strength (a greater red shift indicates greater strength).

2.3.2. The molecular orbitals

By solving the Schrödinger equation for a molecule, one finds the expression of all the molecular orbitals, occupied and unoccupied. Using visualisation software, one can also visualise their shapes. The highest occupied molecular orbitals (HOMO) and the lowest unoccupied molecular orbitals (LUMO) are the ones with the greater interest for chemists and they are called the frontier molecular orbitals [84].

The concept of frontier molecular orbitals was firstly introduced by Woodward and Hoffmann to provide a fundamental key to get a picture of why some chemical reactions proceed easily, whereas others do not [85]. Later on, Fukui advanced similar ideas to simplify Woodward-Hoffmann rules for the analysis of chemical reactivity [86].The HOMO and LUMO orbitals are related to the chemical reactivity because chemical reactions involves formation and dissociation of bonds as well as oxidation and reduction, and all these phenomena involve redistribution of electrons [86]. The removal of electrons from the HOMO is related to the ionisation energy of the molecule; in many cases, the energy required is not much because the HOMO is the highest energy occupied orbital. The removal of electrons corresponds to the donation of electron density to form a bond or to do oxidation processes. The HOMO orbitals have nucleophile character.

When an electron is added to a molecule it will add to the LUMO, so this orbital is related to the reduction phenomenon and is also associated with the electron affinity. The LUMO orbitals have electrophile character. Woodward-Hoffmann formalisation indicated that symmetry plays a role in chemical reactivity [87]. In the cases where the HOMO or LUMO do not have the needed symmetry, the HOMO-1 orbital (i.e., the occupied molecular orbital immediately preceding the HOMO) or the LUMO+1 orbital (i.e., the unoccupied molecular orbital immediately following after the LUMO in terms of the energy) could be the ones that are involved in the reaction [87].

The HOMO–LUMO energy difference (gap) is important for the description of molecules, because it is related to relevant molecular properties including reactivity. The higher the HOMO–LUMO energy gap, the more stable a molecule becomes. Molecules with small HOMO–LUMO energy gap are more prone to undergo chemical reactions [88]. The shapes of the HOMO and LUMO give us information about the distribution of the electron density.

2.3.3. Hydrogen bonds

Nearly all acylphloroglucinols are characterised by an intramolecular hydrogen bond (IHB) between the sp^2 O of the acyl group and a neighbouring OH [10, 11]. Hydrogen bonds are given particular attention in chemistry because of their important roles for biological systems; for example they are responsible for the folding of proteins or for keeping together the two strands of the DNA, and have many other roles for biological systems. IHBs are interesting for drug development because they may be involved in the interactions between a drug and a biological target. For instance, when a drug enters the body, it interacts with a protein within the body. The drug–protein interaction may involve a variety of interactions, mostly non covalent such as hydrogen bonds, Van der Waals forces, dipole–ion interactions, and dipole–dipole forces. The presence of IHBs in a molecule may also have significant roles in some aspects of the biological activity mechanisms such as molecular recognition, selective binding and antitumor activity [15-16, 89-91].

H–bonds are usually given particular attention in conformational studies because they influence many properties of the molecule: its geometry, other molecular properties (above all physico-chemical properties [92]), interactions between solute and solvent when both are capable of forming it and also the arrangement of molecules in crystals [93].

H–bond is a strong type of dipole–dipole attraction which occurs when a hydrogen atom bonded to a strongly electronegative atom is present in the vicinity of another electronegative atom with a lone pair of electrons [94]. A hydrogen bond can generally be described or illustrated as A–H···B,
where,

- A–H is the proton donor. A can be either one of the small electronegative atoms (O, N, F) or in some cases, also C.
- B is the proton acceptor. B can be either one of the small electronegative atoms (O, N, F) or also a π-electron system.
- ··· represent the hydrogen bond.

Hydrogen bonds can have rather broad ranges of bond length and a broad range of strengths. The strength of the H–bond can be indicated by the following geometric measures: A···Y bond length, H···B distance and AĤB bond angle. Strong H–bonds are characterized by A···Y bond length of 1.2–1.5 Å, H···B distance of 2.2–2.5 Å, and AĤB bond angle of 170–180°, and their energy is ≥15 kcal/mol [95-98]. Moderate H–bonds are characterized by A···Y bond length of 1.5–2.2 Å, H···B distance of 2.5–3.2 Å, and AĤB bond angle of 130–150°, and their energy ranges between 4 and 15

kcal/mol [95-98]. Weaker H–bonds are characterized by A···Y bond length of 2.2–3.2 Å, H···B distance of 3.2–4.0 Å, and AĤB bond angle of 90–120°, and their energy ranges between 1 and 4 kcal/mol [95-98].

When an H–bond occurs between neighbouring molecules it is called intermolecular H-bond, and when it occurs within a molecule it is called intramolecular hydrogen bond. The two types are illustrated in fig. 2.5.

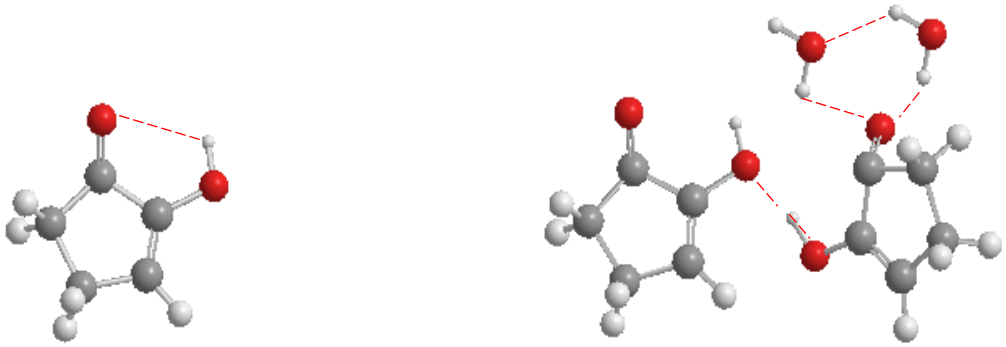

A B

Figure 2.5. Illustration of intramolecular (A) and intermolecular (B) hydrogen bonds.

One of the main roles of intramolecular hydrogen bonds is to stabilise conformers of a molecule in which they are present. Intermolecular hydrogen bonds are capable of stabilising the condensed phases of pure substances [99, 100]. They constitute the main interactions between solvent and solute molecules that are capable of forming them. In the cases when a molecule can form intramolecular H-bonds and a solvent can form H-bonds, there can be a competition between intra- and inter-H-bonds for the molecule. The outcome of the competition depends on the strength of the IHB and also on the geometry of the neighbouring part of the molecule. In many cases, the intramolecular hydrogen bonds that exist in the solid state have a tendency to persist also in solution, and when the temperature increases [101].

2.3.4. Dipole moment

The dipole moment (μ) is a quantity related to the presence of two opposite charges of q (q^+ and q^-) separated by a distance r (fig 2.6) [102] and has magnitude of:

$$\vec{\mu} = q\vec{r} \tag{26}$$

Nearly all molecules have non-zero dipole moment and the dipole moment is determined by the calculations performing geometry optimization. The value of the dipole moment helps in the determination of the polarity of a molecule (to know whether a molecule is non-polar or polar), which, in turn is relevant for other properties including solubility and some types of biological activities [103].

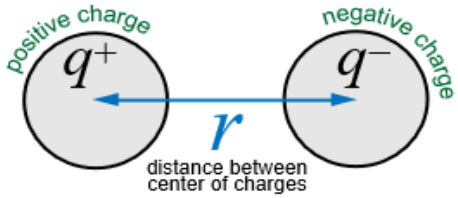

Figure 2.6. Illustration of the meaning of dipole moment [104].

2.4. The computational study of molecules in solution

2.4.1. The study of solvent effects

The study of the solvent effects on the properties of biologically active molecules is motivated by the fact that biological activities occur in some medium within living organisms [105]. The presence of a solvent has a significant influence on molecular properties such as bond lengths, energy level separation [106], stability of different conformers [107], dipole moments, etc. This study has considered the same solvents considered in previous studies on acylphloroglucinols, i.e., water, acetonitrile and chloroform [7, 11, 16]. These solvents have different polarities and different abilities to form hydrogen bonds; thus, they mimic different environments in which a molecule might be present in a living organism [105]. Water is always included as a solvent when studying a biologically active molecule, because water is the dominant component in living organisms [3].

Chloroform is known as a good model for non-polar media [105]. Acetonitrile is one of the most frequently used solvents both in computational studies and in experimental research [108].

Since most chemical reactions occur in a solution, especially in living organisms, a good computational method for modelling the solvent effect is required in order to accurately describe properties of molecules in solution as well as reaction barriers and energies in a chemical reaction [109-110]. There are two approaches for the description of solvent effects, considering the solvent either implicitly or explicitly [44, 111]. The implicit solvation models consider the solvent in a continuum and consider the interaction of a solute molecule with the surrounding continuum solvent [112]. Explicit solvation models consider a certain number of individual solvent molecules and how they interact with the solute molecule [111]. The two methods will be described more in detail in the next sections.

When a molecule enters into a solvent from the gas phase, its energy changes because of the interactions with the solvent. This change in energy is referred to as the free energy of solvation, ΔG_{solv}.

2.4.2. Implicit solvation models

The first implicit approach was developed by Born and Onsanger. The approach involves replacing a specific solvent–solute interaction by an average field, V_{int}. This term is introduced into the Hamiltonian in the Hartree-Fock approximation [44]. However, this approach is limited, since it does not provide much information about aspects such as hydrophilic effects and hydrogen bonds.

One of the most used implicit solvation model is the Polarizable Continuum Model (PCM) [113-119]. PCM exploits the apparent surface charge (ACS) approach [41, 44, 111, 117, 119]. In this model, the solvent is treated as a polarizable continuum characterised by a dielectric constant (ε) [41, 44, 111, 119]. The solute is viewed as embedded in a cavity surrounded by the solvent. The surface of the cavity is identified through superposition of interlocking atomic spheres with radii near the van der Waals radii of the given atoms [41, 44, 111, 119]; the intersection points are smoothed by ‘’rolling’’ a probe sphere of a size suitable for the given solvent on the surface of the interlocking spheres [41, 44, 111, 119].

The free energy of solvation is one of the significant aspects in the thermodynamic description of solutions, which plays a major role in chemical, biological and pharmaceutical science. In the PCM approach, the free energy of solvation is calculated as

$$\Delta G_{solv} = \Delta G_{el} + \Delta G_{dr} + \Delta G_{cav} \quad (27)$$

where, ΔG_{el} is the free energy change related to electrostatic interactions

ΔG_{dr} is the free energy change related to dispersion interactions

ΔG_{cav} is the free energy change corresponding to the formation of the cavity within the solvent system to host the solute molecule (cavitation energy).

ΔG_{dr} and ΔG_{cav} together form the non-electrostatic component of the free energy of solvation, $G_{non\text{-}el}$

$$\Delta G_{solv} = G_{el} + G_{non\text{-}el} \quad (28)$$

There are different types of PCM methods [113-119], such as dielectric PCM (DPCM) [45], conductor-like PCM (CPCM) [45, 120, 121], isodensity-PCM (IPCM) [129], self-consistent isodensity-PCM (SCIPCM) [129] and integral equation formalism–PCM (IEFPCM) [117, 118]. However, CPCM is one of the most used methods from the PCM family to calculate the free energy of solvation and is computationally efficient.

2.4.3. Explicit solvation models

The explicit solvation approach utilises molecular dynamics or MonteCarlo, and considers a solute molecule immersed in a cubic box containing a finite number of solvent molecules [44, 111]. With the use of Periodic Boundary Condition, a small number of particles begin to behave like a part of a bulk system [44, 111]. Thus, this approach takes into account the effects of bulk solvent together with solvent-solute and solvent-solvent interactions [44, 111]. The disadvantage of this approach is that it is computationally costly.

2.4.4. Adducts with explicit solvent molecules

If one wants to maintain purely quantum mechanical approaches like *ab initio* and DFT methods and consider the interactions between a solute molecule and solvent molecules, one may consider adducts of the solute molecule with a certain number of explicit solvent molecules [7, 10]. By using adducts with explicit solvent molecules, one can be able to understand the presence of

solute-solvent intermolecular hydrogen bonds and their effects on the solute molecular geometry and properties [7] as well as the outcomes of the competitions between intramolecular hydrogen bonds and intermolecular hydrogen bonds [7].

The calculation of the interaction energy between the solute and the solvent molecules ($\Delta E_{interaction}$) in an adduct with explicit solvent molecules needs to consider whether the solvent molecules are interacting with each other or not.

Considering an adduct with n solvent molecules and with negligible interactions between the solvent molecules, $\Delta E_{interaction}$ is given by:

$$\Delta E_{interaction} = E_{adduct} - E_F - nE_{solvent\ molecules} \quad (30)$$

where E_{adduct} is the energy of the adduct

E_F is the energy of the solute molecule

$nE_{solvent\ molecule}$ is the sum of the energies of the separated solvent molecules

When the solvent molecules around the central molecule are also interacting with each other, it is necessary to include the energy of these interactions. Water molecules can form H-bonds among/ between them. In the case of interacting water molecules, eqn. 30 becomes:

$$\Delta E_{interaction} = E_{adduct} - (E_{F(isolated)} + n\,E_{aq(isolated)}) - E_{aq\ aq} \quad (31)$$

where $n\,E_{aq\ (isolated)}$ is the energy of an isolated water molecule

$E_{F(isolated)}$ is the energy of the isolated solute molecule

$E_{aq\ aq}$ is the interaction energy among the water molecules in the adduct

Within this approach, a problem arises when the atoms of the interacting molecules approach each other, because their basis sets overlap [125, 126]. When the basis sets overlap, each atom ‘’borrows’’ basis set functions from nearby atoms; by doing so, it effectively improves its basis set and also its energy [125, 126]. When these atoms orientate closer to each other, they create a varying basis set against the interatomic distance [125, 126]. This effect is called the basis set superposition error (BSSE) [125, 126].

There are two methods which are currently in use to correct the BSSE, namely, the Chemical Hamiltonian Approach (CHA) [127] and the counterpoise (CP) [128] method. The CHA prevents the mixing of the basis sets by replacing the conventional Hamiltonian with one in which all the projector-containing terms that would allow mixing have been removed. The CP method utilises empty basis set functions (‘’ghost orbitals’’, basis set functions which have no electrons or protons) so that separate atoms can borrow functions of an empty basis set to improve their basis set. When this procedure is applied to all the atoms on the grid, BSSE gets corrected [128].

2.5. Importance of the computational study of biological active molecules

Biologically active molecules are molecules which have the capability to interact with one or more component(s) of the living tissue causing detectable changes (effects) [129]. Drugs are a typical example. Biologically active molecules of natural origin are a promising source of active molecular structures because it has already been confirmed that they exhibit a certain type of desired activity and they are known to be able to reach their targets within a living organisms [105]. The interest in biologically active molecules of natural origin utilised in traditional medicine in one or another culture is continuously increasing in the search for new drugs, in view of their being more compatible with living organisms and offering new molecular structures which may address the growing problem of drug resistance by several pathogens [130]. Since the current study considers biological active acylphloroglucinols, it is important to calculate their molecular properties in suitably-selected solvents.

CHAPTER 3

LITERATURE REVIEW

This chapter provides a literature review on acylphloroglucinols which is the class of compounds to which the molecules of interest belong to and also specific information about these molecules.

3.1. Acylphloroglucinols

Acylphloroglucinols are derivatives of phloroglucinol (1,3,5-trihydroxybenzene) which are characterised by the presence of a CRO group (acyl group, fig.1.1) [3, 15]. They are classified into monomeric, dimeric, trimeric, tetrameric and higher structure, and phlorotannins. Monomeric acylphloroglucinols are characterised by the presence of one phloroglucinol moiety. Dimeric acylphloroglucinols can be classified into two classes. Molecules of the first class are characterised by two acylphloroglucinol moieties joined through a methylene linkage; in the second class, the moieties are joined through the formation of a chroman ring [3]. Trimeric acylphloroglucinols contain three phloroglucinol units joined by methylene linkages [3]. Tetrameric and higher structures contain more than three phloroglucinol units joined by methylene linkages. Phlorotannins are characterised by phloroglucinol units linked to each other in various ways, such as ether linkage, phenyl linkage, ether and a phenyl linkage and a dibenzodioxin linkage [3].

Nearly all acylphloroglucinols are characterised by an intramolecular hydrogen bond (IHB) between the sp^2 O of the acyl group and a neighbouring OH [15]. The IHBs are interesting for drug development because they may be involved in the interactions between a drug and a biological target. Acylphloroglucinol are largely present in natural sources and exhibit a variety of biological activities that include antiviral, antifungal, antitumor, antioxidant, and antimalarial, antifeedant, antibacterial, spasmolytic among others [3]. Acylphloroglucinols are viewed as potential lead structures for the development of drugs against degenerative diseases as well as some anti-parasitic diseases [131]. All this makes acylphloroglucinols interesting in the search for medicinal remedies.

3.2. Computational studies of acylphloroglucinols.

Systematic conformational studies of several (over 100) acylphloroglucinols have been performed up to now [8]. The type of acylphloroglucinols that have been studied so far comprises

- monomeric acylphloroglucinols with different R in the CRO group and different open-chain R′ (fig 3.1) [4,6]
- dimeric acylphloroglucinols (fig.3.2) [8]
- monomeric acylphloroglucinols in which R′ contains a ring or a ring system (fig 3.3) [18-20]

Most of the performed studies aimed at identifying patterns for conformational preferences; thus, in order to single out the conformational aspects more closely related to the individuality of different structures, as these are expected to be more closely linked to the differences in the biological activities of different compounds [15]. The studies also aim to investigate patterns in the ways in which weaker intramolecular hydrogen bonds contribute to conformational stabilisation [16].

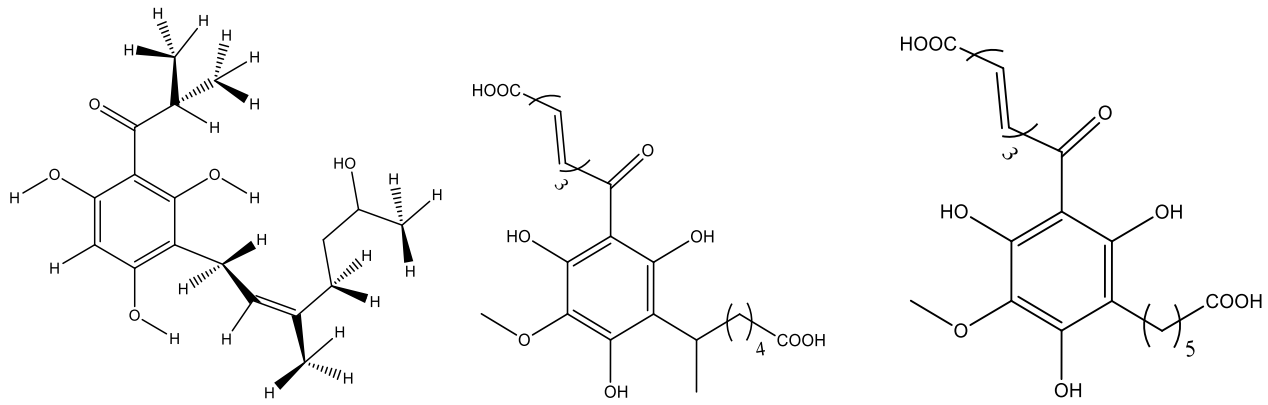

Caespitate Nodifloridin A Nodifloridin B

Figure 3.1. Examples of already studied monomeric acylphloroglucinols with different R in the CRO group and different open-chain R′.

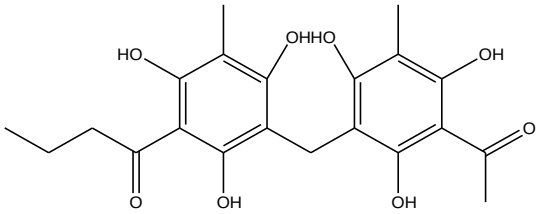

Abbreviatin AB

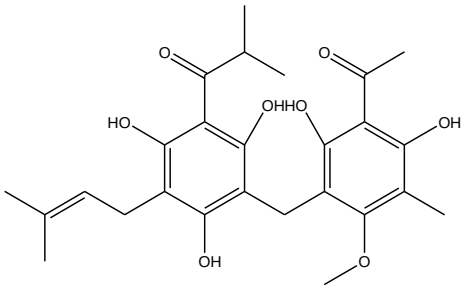

Isobutyryl mallotojaponin

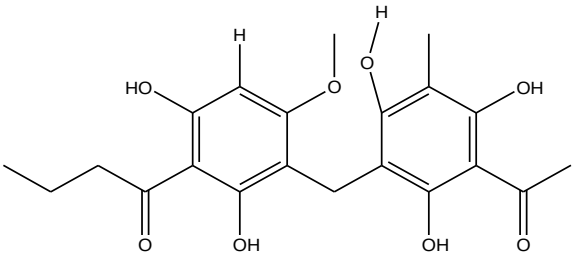

Phloraspins AB

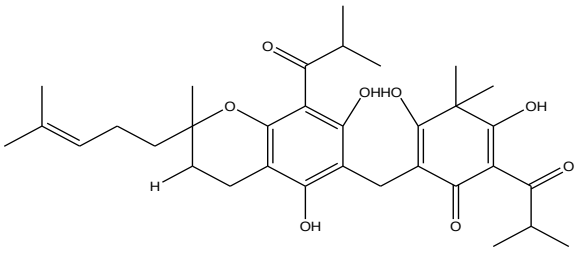

Sarothralens B

Figure 3.2. Examples of already studied dimeric acylphloroglucinols.

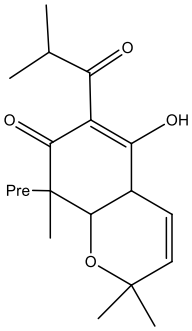

Hyperguinones B

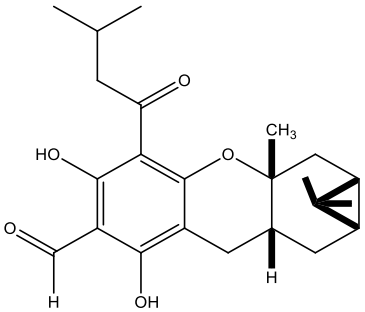

Euglobal G1

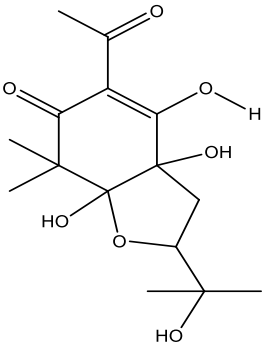

Furonewguinone B

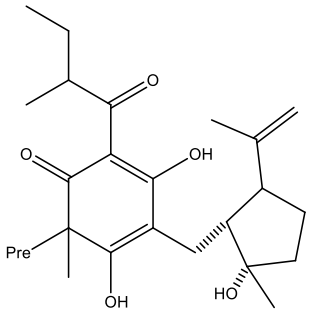

Chinesins I

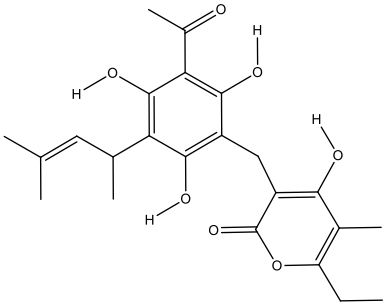

Arzanol

Figure 3.3. Examples of already studied monomeric acylphloroglucinols in which R′ contains a ring or a ring system.

3.1. The acylphloroglucinol molecules selected for this study.

The acylphloroglucinols selected for this study are myristinin A (1-{2,4,6-trihydroxy-3-[(2S,4R)-7-hydroxy-2-(4-hydroxyphenyl)-3,4-dihydro-2H-chromen-4-yl]phenyl}dodecan-1-one) as well as a structurally-related molecule (2-(4-hydroxyphenyl)-4-[2,4,6-trihydroxy-3-(9-tetradecenoyl)phenyl]-3,4-dihydro-2H-benzopyran-7-ol, here denoted as DBPO). These acylphloroglucinols are isolated from plants belonging to the *myristicaceae* family, namely, *Horsfieldia amygdaline, Knema glauca* and *Myristica cinnamomea*. *Horsfieldia amygdaline* is commonly found in the Thailand region and there are no reports on the traditional medical practice from this plant yet [132]. *Knema glauca* is commonly found in Asia, Africa, and Australia, and indigenous people from these continents use the bark and seeds to treat skin diseases and sore throat [133]. *Myristica cinnamomea* is commonly found in the regions of Sumatra, Peninsular Malaysia, Singapore and Borneo [134] and has been reported to be biologically active.

Studies on the *Horsfieldia amygdaline* plant show that the chroman in the myristinin A and DBPO molecules exhibits anti-inflammatory activity through direct inhibition of the enzyme phospholipase A_2 and with the inhibition of polymerase ß at low micro-molar concentrations [135-138]. They also exhibit biochemical activity both as potent DNA-damaging agents and as DNA-polymerase ß inhibitors, with the relaxation of supercoiled plasmid DNA at pico-molar concentrations [135-138].

3.2. Inflammatory processes and anti-inflammatory drugs

3.2.1. Mechanism of inflammatory processes

Inflammation is a reaction of living tissues towards injury [139], and it is a common phenomenon. It is caused by the release of chemical signals and migrating cells, such as prostaglandins (PGs), leukotrienes (LTs), histamine, bradykinins, etc. [140]. The classical local symptoms of inflammation are swelling, redness, heat, pain and loss of function [141, 142]. Figure 3.4 gives an overview of the processes that take place during inflammation events. When the living tissue is injured, the injury (stimulus) stimulates the phospholipase A_2 enzyme to turn the cell-membrane glycerophospholipids into arachidonic acid, which becomes a substrate for cyclooxygenases and lipoxygenases [139, 140]. Through the action of cyclooxygenases, arachidonic acid yields PGs that are precursor of the prostanoids (such as prostaglandins, prostacyclins and thromboxanes). Arachidonic acid also yields several LTs via the actions of lipoxygenases. PGs and LTs are the (intracellular) second messengers that prompt either anti- or pro-inflammatory response [143, 144].

Cyclooxygenase is an enzyme that is accountable for the synthesis of prostanoids. It consists of two isoforms, namely, cyclooxygenases-1 (COX-1) and cyclooxygenases-2 (COX-2), as shown in fig 3.5. The main difference between the two isoforms is that position 523 in COX-1 consists of the isoleucine amino acid, while the same position in COX-2 consists of the valine amino acid [145, 146].

This difference between the amino acids in position 523 influences whether the drug can access the pocket site of the enzyme or not. For example, aspirin gets hindered from accessing the hydrophobic side pocket in the COX-1 enzyme due to steric hindrance, while in COX-2, aspirin can access it [147]; this is because the size of isoleucine is bigger than that of valine. The consideration of this is a prerequisite for the production of selective inhibitor of COX-2 in a pharmaceutical industry [148, 149], because COX-2 can be deactivated without affecting the function of COX-1.

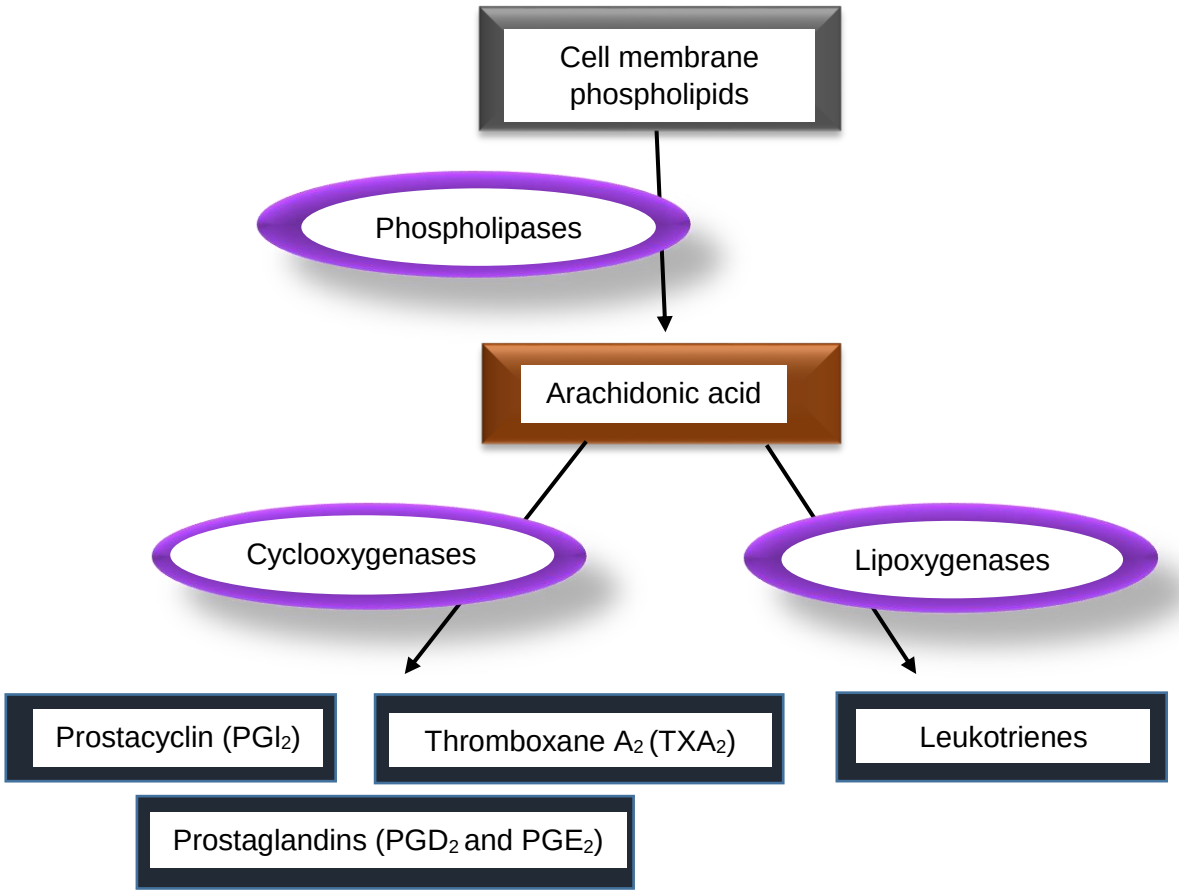

Figure 3.4. Illustration of an inflammation process.

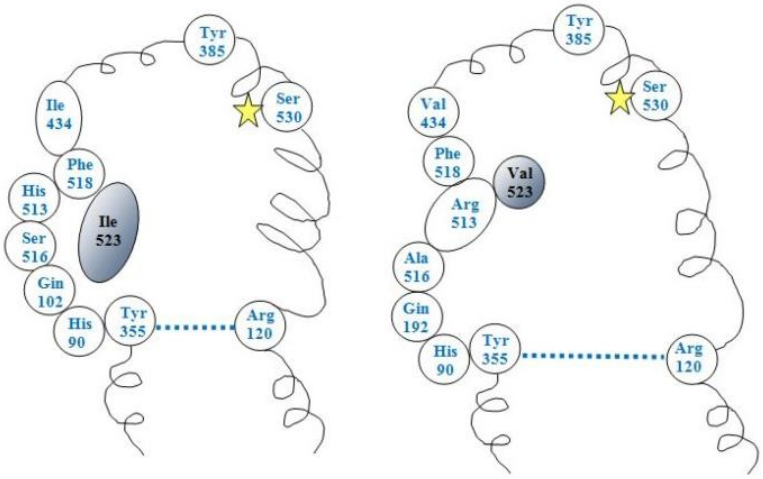

COX-1 COX-2

Figure 3.5. Structures of the cyclooxygenases isoforms [147].

COX-2 converts the dietary arachidonic acid into inflammatory prostaglandins which contribute to pain, swelling and heat: it is thus considered as ‘’inflammatory stimuli’’ [141, 142]. COX-1 functions in a different manner (physiological stimuli); it converts the arachidonic acid into what they call ‘’housekeeping’’ substances, since it yields platelet (regulate blood clotting), prostaglandin E_2 (responsible for kidney functioning), and prostaglandin I_2 (serves for gastric cytoprotection) [142, 145].

A high level of phospholipase A_2 enzymes has been determined in various inflammatory disorders such as rheumatoid arthritis, atherosclerosis, and also in cancer patient [150, 151]. Phospholipase A_2 enzymes are classified into three main distinctive isoforms which include cytosolic PLA_2 ($cPLA_2$), secretory or secreted PLA_2 ($sPLA_2$), and Ca^{2+}-independent PLA_2 ($iPLA_2$) [152, 153]. Each of these isoforms consists of number of isozyme that is classified based on nucleotide sequences and order of discovery [154].

Rheumatoid arthritis is caused by chronic inflammation in the joints, leading to pain and damage to joint cartilage and bone [155], and it has been determined that the $sPLA_2$-IIA ($sPLA_2$ isozyme) concentration in rheumatoid-arthritic synovial joints is significantly higher than in non-arthritic joints [156, 157]. Atherosclerosis is caused by the narrowing of the arteries due to the buildup of plaque on the artery walls. Studies show high concentrations of $sPLA_2$-IIA within the serum plasma of atherosclerotic patients compared to patients with no history of cardiovascular problems [158].

Cancer is a disease in which abnormal cells divide uncontrollably and destroy body tissue. In many cancerous tissues, over-expression of $sPLA_2$-IIA has been detected. $sPLA_2$-IIA can either promote or inhibit cell growth depending on the type of cells [159]. Therefore, since the phospholipase A_2 enzymes respond to inflammatory stimuli and maintain cell homeostasis by membrane remodeling during inflammation events, their role in the production of pro-inflammatory lipid mediators at the very beginning of the inflammation process makes these enzymes an important therapeutic target for the treatment of inflammatory disorders [160-162].

3.2.2. Anti-inflammatory compounds

Anti-inflammatory compounds are the compounds which are commonly used to treat health problems like pain, inflammation, rheumatoid arthritis and osteoarthritis [1]. There are two main classes of anti-inflammatory compounds currently in use, namely steroidal and non-steroidal. They will be briefly presented in the next subsections.

3.2.2.1. Non-steroidal anti-inflammatory drugs (NSAIDs).

Non-steroidal anti-inflammatory drugs are those compounds which produce their therapeutic activities through inhibition of cyclooxygenase enzymes [163, 164]. Since this enzyme catalyzes the synthesis of the prostanoids, its active site acts as the site of action of the NSAIDs, whereby these drugs (fig. 3.6) prevent the transformation of arachidonic acid into prostaglandin by binding the active sites of the COX [161, 165]. The major role of NSAIDs is to prevent or reduce the pain and inflammation. Examples of these drugs, which are currently in use, include aspirin, celecoxib (Cambia, Cataflam, Voltaren-XR, Zipsor, and Zorvolex), ibuprofen (Motrin, Advil), indomethacin, naproxen (Aleve, Anaprox, Naprelan, and Naprosym), oxaprozin, piroxicam [2]. The use of other NSAIDs (disflunisal etodoloc, ketorolac, nabumetone, salsalate, sulindac and tolmetin) has been discontinued, because of the severe side effects they share.

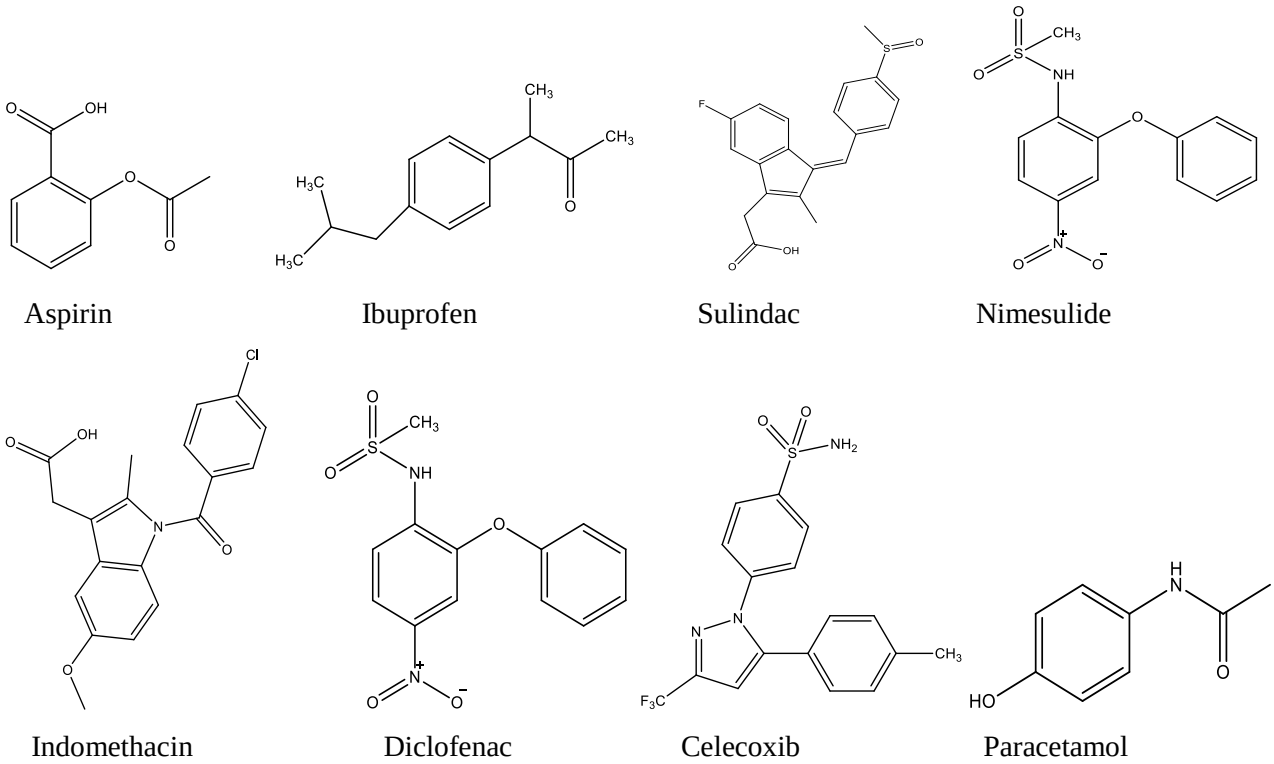

Figure 3.6. Examples of structure of non-steroidal anti-inflammatory drugs.

The use of NSAIDs results in severe health problems (fig 3.7.), due to the fact that they do not have selectivity characteristics towards the COX-1 and COX-2 enzymes [166-168]. When the COX-1 activity is inhibited, it leads to unregulated production of the stomach acid, ulcerations and gastrointestinal bleeding, thus disturbing the regulation of the physiological processes [166-168]. Figure 3.7 outlines the two types of effects of NSAIDs. The left-hand pathway corresponds to the inhibition of the formation of physiological stimuli prostaglandins (undesirable side effects); the right-hand pathway corresponds to the pharmacological action to reduce the inflammation and the pain.

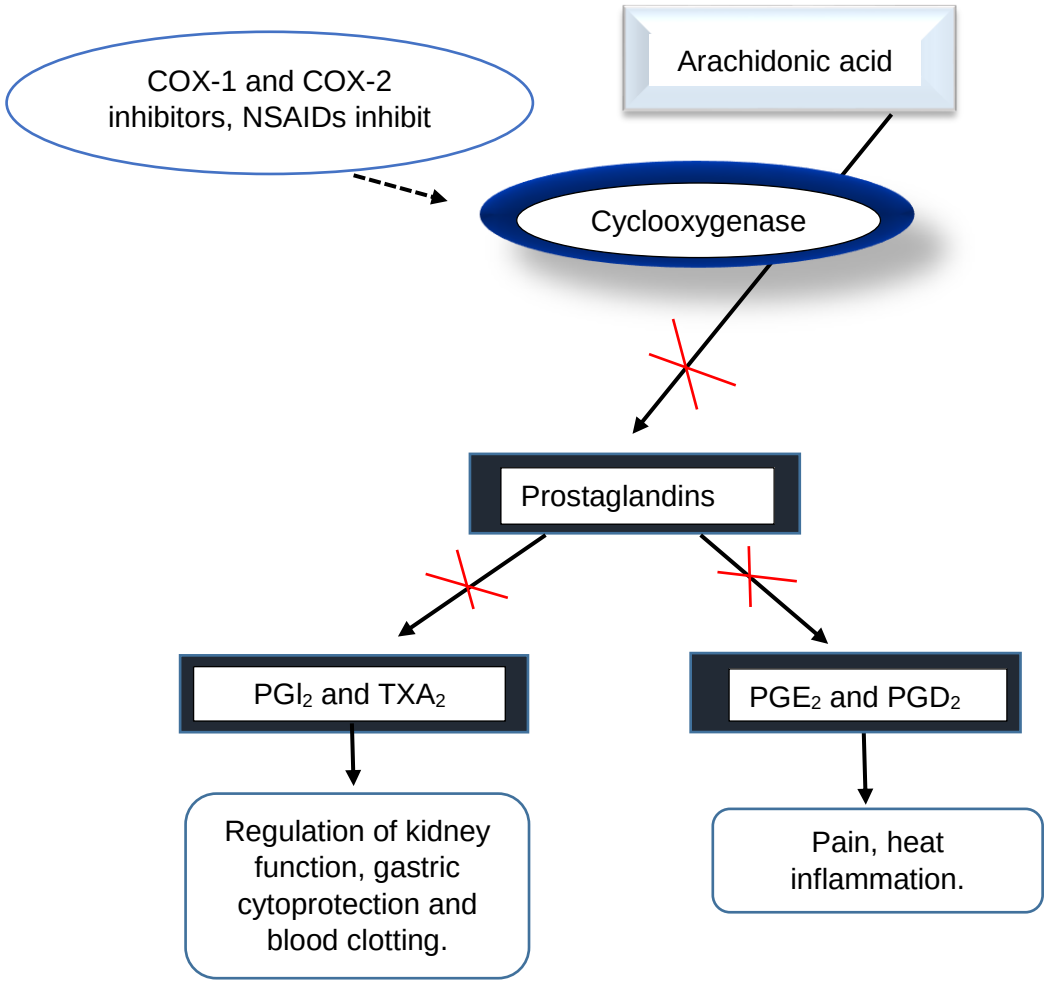

Figure 3.7. Effects of the use of NSAIDs.

3.2.2.2. Steroidal anti-inflammatory compounds

Steroidal compounds are hormones which play an important role in a physiological process occurring in a human body and are often called corticosteroids [169, 170]. They can either be naturally occurring in a body or man-made. They serve an important role in medicinal practice. They can be used to treat various disorders such as allergic, inflammatory and malignant disorders [169-171]. Corticosteroids that occur in nature are produced by the outermost adrenal gland known as cortex [172], and can be classified either as glucocorticoids or mineralocorticoids (fig 3.8).

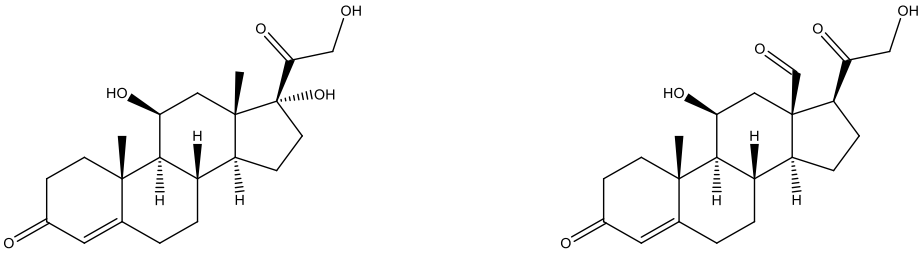

Glucocorticoids Mineralocorticoids

Figure 3.8. General structures of glucocorticoids and mineralocorticoids.

Glucocorticoids are responsible for physiological effects; they can suppress inflammation (anti-inflammatory) and immunity (immunosuppressive) and assist in the breakdown of fats, carbohydrates, and proteins [173-175]. They function by modulating gene expression, and accomplish this by binding to the receptors in the cytosol [173-175]. The receptors are called glucocorticoid-receptors (GR). Due to this binding, the receptors are able to enter the nucleus of the cell and bind the glucocorticoid-response element-receptor which influences gene expression. This binding can either cause the up-regulation of the anti-inflammatory genes or down-regulation of the pros-inflammatory genes [173-175]. Examples of glucocorticoids are hydrocortisone (Cortef), cortisone, ethamethasoneb (Celestone), prednisone (Prednisone Intensol), prednisolone (Orapred, Prelone), triamcinolone (Aristospan Intra-Articular, Aristospan Intralesional, Kenalog), Methylprednisolone (Medrol, Depo-Medrol, Solu-Medrol), dexamethasone (Dexamethasone Intensol, DexPak 10 Day, DexPak 13 Day, DexPak 6 Day) that regulate the balance of salt and water in the body. Mineralocorticoids (salt retaining) are corticosteroids that regulate bodily electrolyte and water balance [176]. Example is Fludrocortisone (Florinef).

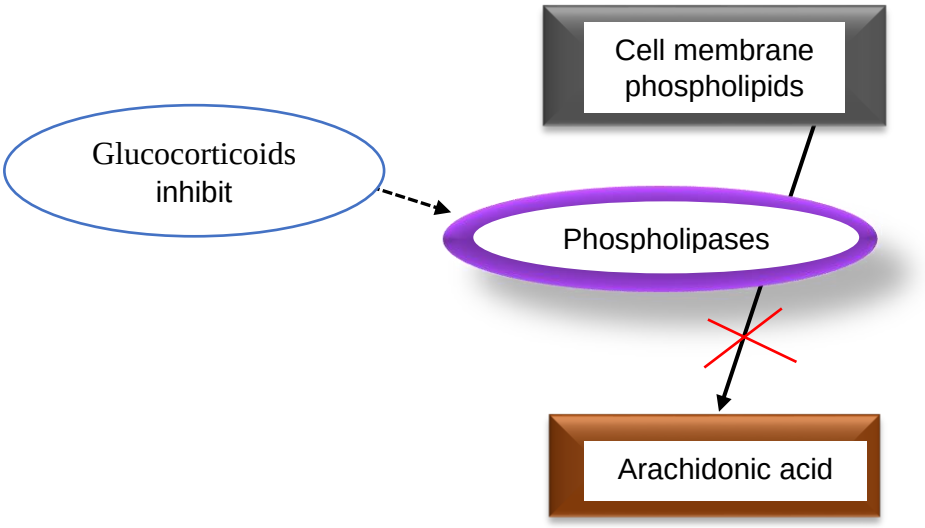

Figure 3.9. Glucocorticoids mechanism action.

Glucocorticoids (fig. 3.9) are divided into three subclasses, namely, systematic, inhaled and topical. Systematic glucocorticoids are glucocorticoids that are used to treat allergic and inflammatory disorders, to suppress autoimmune diseases and to replace hormones in case of adrenal deficiency [173-175]. Examples are prednisone, hydrocortisone and dexamethasone. Inhaled glucocorticoids are glucocorticoids that are used to treat asthma and chronic obstructive pulmonary diseases [177]. Examples are beclomethasone, budesonide and fluticasone. Topical glucocorticoids are glucocorticoids that are used to treat inflammatory skin diseases such as eczema and other skin flare-ups diseases [178]. Examples are hydrocortisone and betamethasone.

Glucocorticoids increase the glycogenesis (metabolic effect) from circulating fats and amino acids resulted from the catabolism/breakdown of muscles and fats [179]. This leads to the effects and side effects typical of each of the subclasses of glucocorticoids. Systematic glucocorticoids affect circulating monocytes and eosinophils, thus, suppressing their effects. Inhaled glucocorticoids, directly affect the respiratory tract, thus reducing mucosal inflammation, widening the airways and eliminating mucus secretion [180, 181]. Lastly, topical glucocorticoids show local effects, but the prolonged use of high doses might trigger systematic side effects [182].

Potential side effects of glucocorticoids include immunosuppression (increasing risk of infections), steroid-induced diabetes (due to increased glycogenesis), bone effects (steroid-induced

osteoporosis), muscles weakening (thin skinning and easy bruising), and mood alteration (depression, confusion, psychosis and insomnia) [179].

CHAPTER 4

COMPUTATIONAL DETAILS

This chapter gives an overview of the selection of the computational methods utilised in this work and also describes the way in which the inputs were prepared

4.1. Motivations for the selection of the computational methods

The selection of the computational methods for a particular study is based on finding the best compromise between the affordability of the computational cost and the accuracy of the results desired [53]. However, there is no general rule of determining the selection. The following aspects can be useful when one wants to determine the computational cost, the type of the theoretical method, the basis set, and the size of the molecule [183].

In view of the size (comparatively large size) of the molecules considered in this study, this study utilised *ab initio* method (which include the HF, MP2) and the DFT method, with non-too-large basis sets.

4.1.1. Calculations *in vacuo*

Hartree-Fock (HF) calculations were performed with full geometry optimisation (fully relaxed geometry), to identify stable conformations for each input geometry. The 6-31G(d,p) basis set was used, because it has already proved reliable for HF calculations on acylphloroglucinols [8]. This method is computationally less demanding than the others and can provide a good overview of conformational preferences and factors influencing them [14].

Møller-Plesset perturbation theory (MP2) calculations were performed on the HF results, with the same basis set (HF results constitute the “unperturbed” initial step for MP2 calculations). MP2 takes into account both the electron correlation and dispersion interactions. MP2 calculations were performed with full-optimisation. They were performed on conformers having lower energy from HF results.

For the DFT calculations, the B3LYP [71] functional was used with the 6-31+G(d,p) basis set. Previous studies on acylphloroglucinols as a class of compounds have shown that the presence of

diffuse functions on the heavy atoms is important for the quality of DFT/B3LYP results for acylphloroglucinols [14,16]. The use of diffuse and polarization functions is also important for a better description of IHBs.

After geometry optimization calculations, frequency calculations were performed only at HF/6–31G(d,p) level on conformers having lower energy from HF results. The keyword used for the basis set without diffuse functions is *Freq Test* for HF calculations. The results were scaled by 0.8992 (factor recommended for HF) [184].

4.1.2. Calculations in solution

Calculations in solution used conductor-like polarizable continuum model (CPCM). They were performed at the HF/6-31G(d,p) level with fully relaxed geometry. PCM re-optimization is important to identify conformational changes induced by the solvent [185].

4.2. Molecular properties considered in this study

The molecular properties which are considered in this study are outlined in the following paragraphs.

Relative energies: In the calculation of relative energies, the lowest energy conformer is taken as reference and ascribed energy zero, and the energy of the other conformers is compared with its energy. The relative energies provide information about which conformers are populated (i.e., correspond to a non-negligible number of molecules) and which ones are not (too few molecules take the geometry of these conformers and, therefore, these conformers do not contribute to the properties of the substance).

The parameters of the IHBs: The parameters of each IHB (H···O bond length, O···O distance, O-H···O bond angle) were calculated to obtain information about the strength of the given IHB.

Dipole moment: The value of the dipole moment was reported for each calculated conformer since it helps in the identification of whether a molecule is non-polar or polar.

Molecular orbitals: The energy difference between the HOMO and LUMO orbitals were determined for each calculated conformer. Their shapes were obtained from the checkpoint file.

Vibrational frequencies: Vibrational frequencies were calculated to determine whether the stationary points identified by optimisation calculations correspond to true minima; to determine the strength of the IHBs considering the red shifts caused by the IHB; and to obtain the zero-point energies.

Free energy of solvation: the free energy of solvation and its electrostatic component were determined from PCM calculations in solution.

4.3. Software used in this study

In this study two types of Gaussian software versions were used, namely, Gaussian 03 [186] and Gaussian 09 [187]. The reason for using two software versions is that only Gaussian 03 (running on desktop computers in the lab) was available at the beginning of the study. Later on, it became possible to use the Centre for High Performance Computing (CHPC) platform, where Gaussian 09 was installed. Gaussian 03 was used for the HF and DFT calculations *in vacuo*. Gaussian 09 was used for the MP2 calculations *in vacuo*, for all calculations in solution and for frequency calculations.
The GaussView [188] and Chem 3D [189] software were used for visualisation.

4.4. Preparation of inputs

A preliminary study on a model structure for myristinin A and the DBPO molecule had been performed, at HF level *in vacuo* to identify conformational preferences of the ring systems [190]. The model structure featured the ring systems while the long R chain was replaced by an ethyl group. This was sufficient to mimic the presence of an alkyl chain in the acyl group and its influence on the geometry features of the phloroglucinol moiety. The results obtained from this preliminary work have been used to investigate the two molecules individually, by considering the different geometries of their long chains in correspondence to each geometry identified for the ring systems.

Ninety-five different geometries of the ring systems were identified from the preliminary study. The R long chains have many single bonds and considering the rotation of each single bond would give a huge number of possible geometries. Combining the huge number of geometries identified for the R chain with the 95 geometries for the ring system, one would end up with a non-manageable number of possible conformers. On the other hand, when considering the biological active molecules, conformers of higher energy are not interesting because they do not influence the

biological activity of a molecule, since their population is very low. Therefore, it is more interesting to focus on low-energy conformers. The study was divided in two parts, each focusing on one pathway to identify low energy conformers.

The first part took into consideration that previous studies had shown that the geometry where the R chain is co-planar with the benzene ring and totally outstretched (not bent) is a stable one [11]. This geometry was chosen and was combined with each of the 95 geometries identified for the ring systems. Therefore, since this study entails 95 conformers, it was performed only *in vacuo*, while in solution it was carried out at the HF level because it is less expensive.

In the second part, the lowest energy conformer of the ring system was selected and the geometry of R was changed by rotating each of the single bonds in turn. Two types of rotations were made: by +90° or -90° (in which case the chain becomes perpendicular to the plane identified by the benzene ring, on one or the other side of the plane) and by 180° (in which case the chain remains on the plane, but with a bent geometry). In the former case, each bond can rotate by either +90° or -90°. For acylphloroglucinols, previous studies showed that molecules that have symmetrical geometries with respect to the plane of the benzene ring have the same energy [11]. In this perspective only the +90° or -90° rotation of each bond would have been necessary. However, it was opted to consider both rotations, to check whether they yield symmetrical outputs on optimisation, above all in view of possible influences by the large ring systems. In the case of the rotation by 180°, only one rotation is possible for each bond. Thus, the bonds denoted by 2, 4, 6, 8 and 10 can rotate by 180˚ to the side of R′ and those denoted by 3, 5, 7, and 9 can rotate by 180˚ to the other side with respect to R′. These rotations will be illustrated in fig. 5.3.

HF calculations were first performed on all these inputs *in vacuo* and in solution (for selected lower energy conformers). DFT and MP2 calculations were then performed *in vacuo* for the lower energy conformers.

The GaussView software was used to prepare inputs for the calculations *in vacuo*. The optimised geometries obtained from HF calculations were used as inputs for DFT and MP2 calculations. The optimised geometries obtained from calculations *in vacuo* were used for PCM calculations in solution.

4.5. Presentation of the results

The results obtained from Gaussian outputs are mostly given in atomic units. Therefore, energy values are in Hartrees, except the values of the free energy of solvation and its components,

obtained from PCM calculations, which are given in kcal/mol. All the energy values reported in this work are thus given in kcal/mol, for the sake of comparison with previous results. Since most of the energy values are given in Hartrees, they are multiplied by 627.509 (conversion factor to obtain values in kcal/mol). All energy values obtained through conversion will be in 3 decimal digits, whereas thermodynamic energy values are given in 2 decimal figures as in the output.

Bond lengths are given in angstroms with 3 decimal figures, bond angles are given in degrees with one decimal digit, and dipole moments are given in Debye with 3 decimal places.

For simplicity and better readability of the text in tables and figures, non-standard acronyms have been introduced. Acronyms denoting media are ‘vac’ (vacuum), ‘chlrf’ (chloroform), ‘actn’ (acetonitrile), and ‘aq’ (water). Acronyms used to denote the names of the considered molecules are myrin (myristinin A), *cis*-DBPO and *trans*-DBPO for the *cis* and *trans* isomers of (2-(4-hydroxy-phenyl)-4-[2,4,6-trihydroxy-3-(9-tetradecenoyl)phenyl]-3,4-dihydro-2H-benzopyran-7-ol).

The captions of tables and figures are placed at the top. The numbers of tables and figures are written in two digits form; the first digit represents the chapter number and the second one represents the table or figure number.

CHAPTER 5

COMPUTATIONAL STUDY OF THE MYRISTININ A MOLECULE *IN VACUO* AND IN SOLUTION

This chapter presents the results of the conformational study of the myristinin A molecule. The results are organised according to the two types of study performed, as explained in section 4.4. The first section (5.1) provides information relevant to both parts.

5.1. Naming of conformers

Conformers are denoted with acronyms providing information on their characteristics. The same letters which have been used to keep track of relevant geometry features of acylphloroglucinols [15–17] are currently used for the conformers of the molecules considered here, with some additional new letters for features specific to these molecules. On presenting the analysis of results, it is also important to mention each ring individually, thus, the rings are denoted by uppercase letters (A, B, D and E) as shown in fig. 5.1.

The following features are taken into consideration when naming the conformers: the O–H···O IHBs and O–H···π interactions; the orientation of O10–H16; the orientation of the ring system with respect to the A moiety; the orientation of O28–H29; the orientation of O36–H37; the position of C19 with respect to the plane identified by C9, C23, C22 and O21(important because ring D is not planar); the angle by which the specified single bond in R has been rotated in the input, with respect to the linear geometry, to generate new conformers in the second part of the study, as explained in section 4.4 (fig. 5.2 shows the numbers by which the single bonds are concisely denoted). Table 5.1 lists the symbols which are used to denote each of these geometry features.

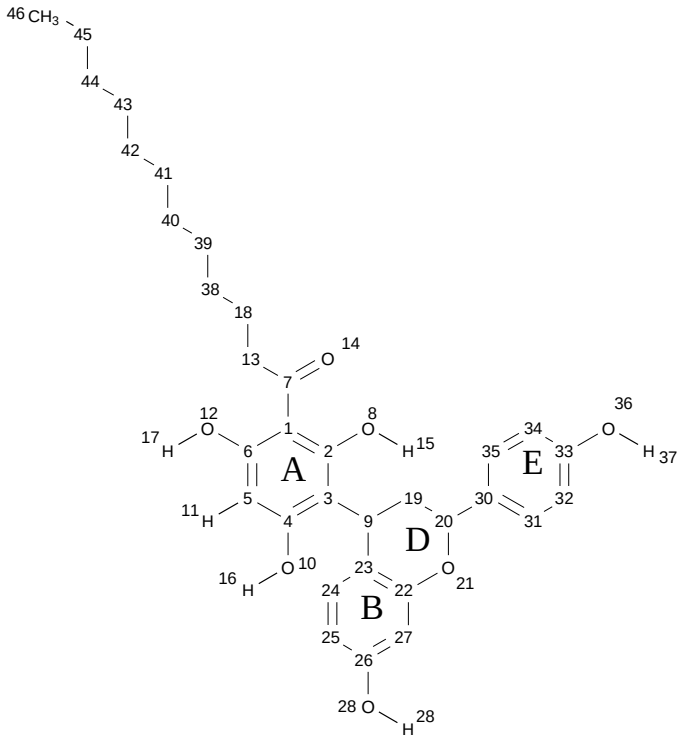

Figure 5.1. Structure of the myristinin A molecule and atom numbering utilised in this study.

The C atoms in the rings and in the acyl chain are represented by the numbers denoting their position (except the last C atom of the acyl chain) for better view of the structure. Only the H atoms attached to O atoms and to C5 atom are numbered individually, while the other H atoms are given the same number as the C atom to which they are attached and are not shown in the structure. The rings are denoted by uppercase letters (A, B, D and E).

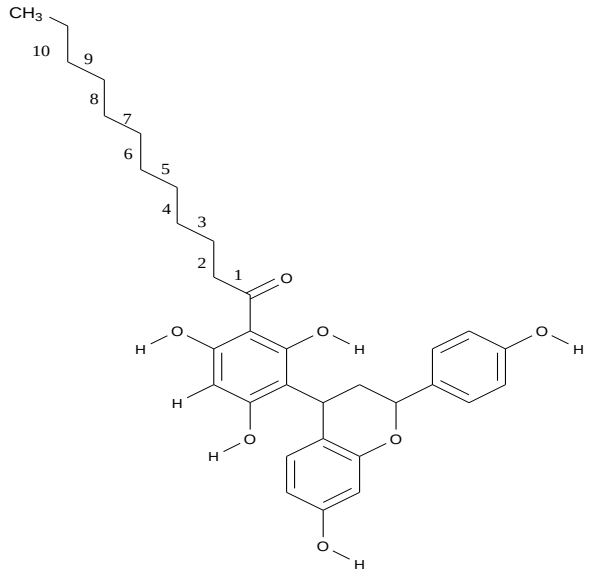

Bond number	Bond considered
1	C7–C13
2	C13–C18
3	C18–C38
4	C38–C39
5	C39–C40
6	C40–C41
7	C41–C42
8	C42–C43
9	C43–C44
10	C44–C45

Figure 5.2. Numbers concisely denoting the single bonds in the R chain of the myristinin A molecule. The numbers are shown for each bond in the chain (left) and their meaning is further stressed in the table on the right. The same numbering is used for the two DBPO isomers.

Table 5.1. Symbols which are used to denote the main geometry features of the conformers of myristinin A, *cis*-DBPO and *trans*-DBPO. The meaning of the symbols is also illustrated in fig. 5.3.

Symbol	Geometrical feature
d	the first IHB is on the same side as R′ (H15···O14)
s	the first IHB is on the other side with respect to R′(H17···O14)
r	the C3–C4–O10–H16 angle is close to 0º
w	the C3–C4–O10–H16 torsion angle is close to 180º
u	the *ortho* OH not engaged in the first IHB is oriented toward the acyl group
non-u	the *ortho* OH not engaged in the first IHB is oriented away from the acyl group
η	presence of O–H···π interaction between H16 and ring B
ε	presence of O–H···π interaction between H15 and ring B
a	C19 in ring D is above the plane identified by C9, C23, C22 and O21.
b	C19 in ring C is below the plane identified by C9, C23, C22 and O21.
p	the system of the B and D rings is ‘towards us’ and ring D ‘towards the back’ with reference to fig.5.1.
q	the system of the B and D rings is ‘towards the back’ and ring D ‘towards us’ with reference to fig.5.1.
e	O28–H29 is oriented to the side of C27
f	O28–H29 is oriented to the side of the phloroglucinol moiety
j	O36–H37 is oriented to the side of C34
k	O36–H37 is oriented to the side of the phloroglucinol moiety
y	at the input level, the bond specified by the number preceding the y has been rotated by -90˚ with respect to the linear geometry of R shown in fig. 5.1.
z	at the input level, the bond specified by the number preceding the z has been rotated by +90˚ with respect to the linear geometry of R shown in fig. 5.1.
x	at the input level, the bond specified by the number preceding the x has been rotated by 180˚ (to the side of R′) with respect to the linear geometry of R shown in fig. 5.1.
v	at the input level, the bond specified by the number preceding the v has been rotated by 180˚ (to the other side with respect to R′) with respect to the linear geometry of R shown in fig. 5.1.
1–10	numbers denoting the single bonds of R, as shown in fig.5.2.

Figure 5.3. The illustration of the meaning of the symbols.

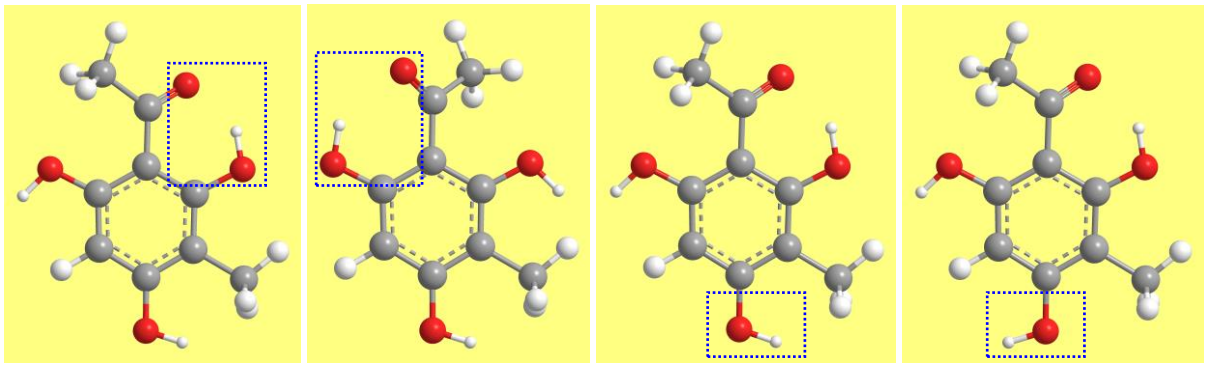

d — position of the first IHB

s

r — orientation of O10–H16

w

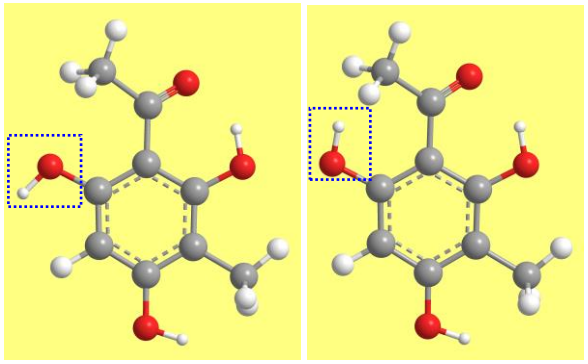

non-u

u

orientation of the OH *ortho* to CRO and not engaged in the first IHB

a) Features related to the acylphloroglucinol moiety
The features are illustrated using the simplest ACPL with R≠H and R′≠H

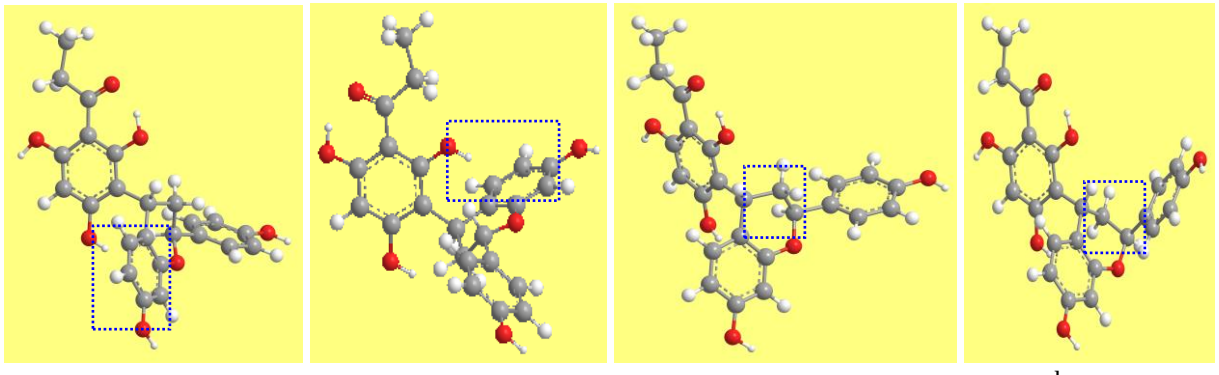

η — O–H···π interactions present

ε

a — position of C19 in ring D with respect to the plane identified by C9, C23, C22 and O21

b

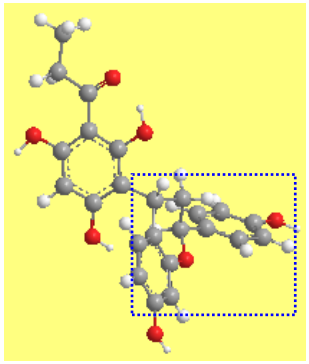
p

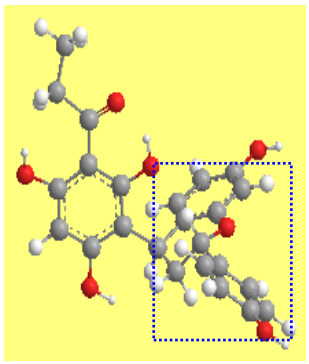
q

orientation of the BDE ring system with respect to the A moiety

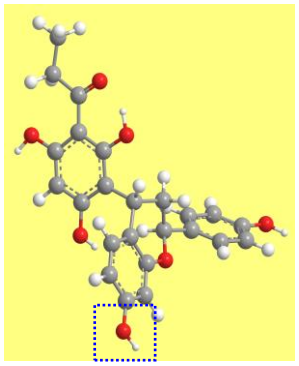
e

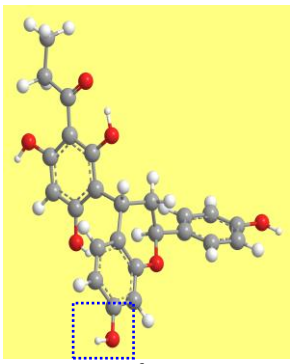
f

orientation of O28–H29

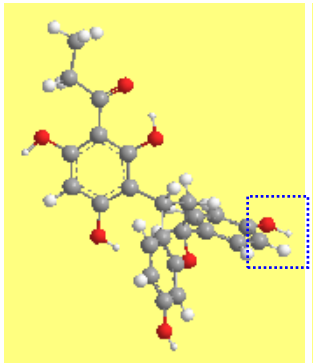
j

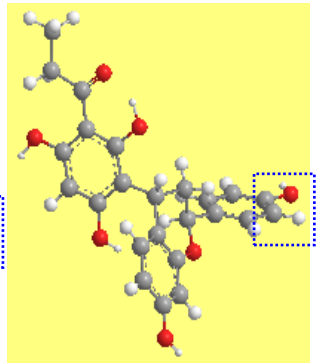
k

orientation of O36–H37

b) Features related to the ABCD ring system
The features are illustrated using the model structure MODL

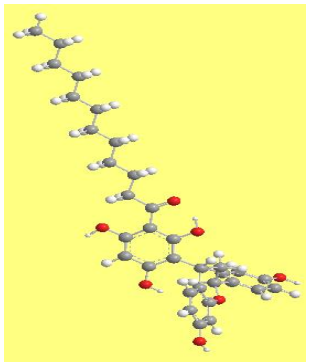
linear geometry

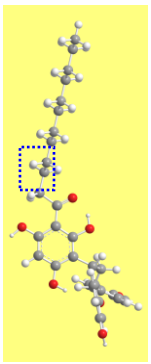
y

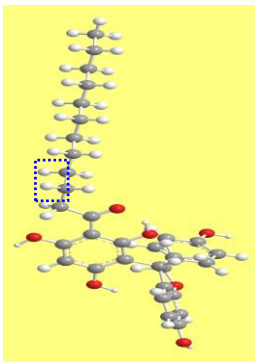
z

rotation of the single bond denoted as 3 by ±90°

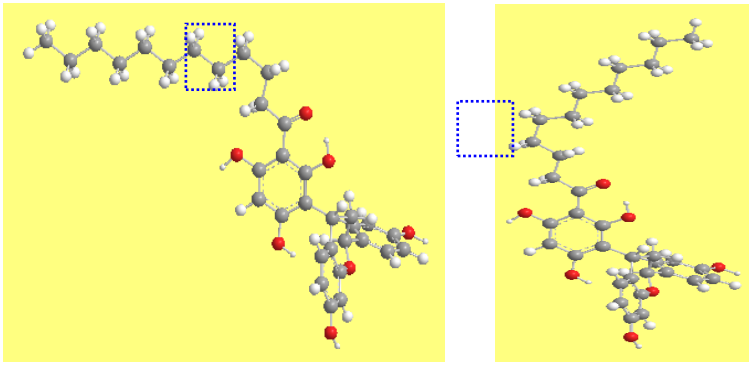

v x

rotation of a single bond in R by 180°

c) Features related to the geometry of the R chain at input level
The features are illustrated considering the rotation of the single bond denoted as 3

5.2. Results for conformers with the same geometry of R and different geometries of the ring system.

5.2.1. Results *in vacuo*

5.2.1.1. Relative energies of the conformers.

This part of the study considered 95 conformers, each of them corresponding to one of the identified geometries of the ring systems [190] (fig.5.5). Their geometries of the resulting conformers are shown in fig. 5.6 and their relative energies are reported in table 5.2.

Some trends are similar to those identified for other acylphloroglucinols [14, 16]. For example, the comparison of the relative energies of pairs of conformers differing only by the position of the first IHB (H15···O14 or H17···O14) shows that the d conformers have lower energy than the s conformers; the energy difference between them is in the 0.134–5.486 kcal/mol range.

Comparison of the relative energies of pairs of conformers differing only by the orientation of O10–H16 shows that the r conformer has lower energy than the w conformer when the r conformer has the O10–H16···π interaction between H16 and ring B (the difference is in the 0.217–4.667 kcal/mol range), and has higher energy than the w conformer when there is no O10–H16···π interaction between H16 and ring B, with some exceptions (the d-w-u-q-b-f-j / d-r-u-q-b-f-j, s-w-u-q-a-f-j / s-r-u-q-a-f-j, s-w-u-q-b-e-k / s-r-u-q-b-e-k and s-w-u-q-b-f-j / s-r-u-q-b-f-j pairs).

The comparison of the relative energies of pairs of conformers differing only by the orientation of the *ortho* phenol OH not engaged in the first IHB, shows that the u conformers always have higher energy than the corresponding non-u ones. Two situations are identified. When the non-u conformers do not have an O8–H15···π interaction between H15 and ring B, the difference is in the 1.124–5.463 kcal/mol range; this is consistent with the findings for other acylphloroglucinols [14, 16] and is due to steric hindrances between the H of the OH and the acyl group. When the non-u conformers have the O8–H15···π interaction between H15 and ring B, the difference is in the 5.798–7.577 kcal/mol range, because the O8–H15···π interaction stabilizes the non-u conformer and is lost in the u conformer.

The comparison of the relative energies of pairs of conformers differing by the orientation of the B, D and E ring system shows two types of trends. The p conformer has lower energy than the q

conformer when the q conformer does not have the O8–H15···π interaction between H15 and ring B; in this case, the energy difference is in the 0.052–5.731 kcal/mol range. The p conformer has higher energy than the q conformer when the q conformer has the O8–H15···π interaction between H15 and ring B; in this case, the energy difference is in the 0.188–7.053 kcal/mol range.

The comparison of the relative energies of pairs of conformers differing by the position of C19 in ring B with respect to the plane identified by the C9, C23, C22 and O21 atoms, which are co-planar in ring B, shows that the effect of this difference is smaller in comparison with the differences considered previously. Furthermore, the energy difference does not show a consistent pattern, because sometimes conformer *a* has lower energy than conformer *b* and other times it has higher energy. Similar observations apply for the e/f comparison and for the j/k comparison.

Table 5.3 reports the values of the relative energies corrected for ZPE and of the ZPE corrections, as well as the relative Gibbs free energies ($\Delta G_{corrected}$, sum of electronic and thermal free energies) and its correction, G_{corr}, for the conformers listed in table 5.5. The ZPE corrections for all the conformers are comparatively close. Their values range between 453.622 and 454.459 kcal/mol. The greater values of the ZPE corrections correspond to the conformers having higher energy, with some few exceptions. The relative energies corrected for ZPE and the uncorrected relative energies have the same trends, with some exceptions (Myrin-d-r-η-p-b-e-k, Myrin-d-r-η-p-b-e-j, Myrin-s-w-2-ε-q-b-e-j, Myrin-d-w-p-a-f-k, Myrin-d-w-q-a-e-j, Myrin-d-w-q-a-e-k, and Myrin-s-r-2-ε-q-a-f-k). Conformers with higher relative energy have higher relative Gibbs free energies as well as lower G_{corr}. The G_{corr} for all the conformers are comparatively close and their values range between 405.033 and 406.423 kcal/mol

5.2.1.2. Characteristics of intramolecular hydrogen bonds

Table 5.4 reports the parameters (H-O bond length, O···O distance, OĤO angle) of the first IHB of the calculated conformers of myristinin A. The comparison of the H···O length of pairs of conformers differing only by the position of the first IHB (H15···O14 or H17···O14) shows that the d conformers have shorter H···O length than the corresponding s conformers (this is consistent with the findings for other acylphloroglucinols [15-17]), and the length difference is in the 0.013-0.062 Å range. Considering the distance between the two oxygen atoms, the O14···O8 distance in the d conformers is shorter than the O14···O12 distance in the s conformers. Considering the OĤO bond

angles, d conformers have greater angle than the corresponding s conformers. All these values indicate that the H15···O14 first IHB is somewhat stronger than the H17···O14 first IHB.

The comparison of the H···O length for pairs of conformers differing only by the orientation of the *ortho* phenol OH not engaged in the first IHB shows that non-u conformers have shorter H···O length than the u conformers. The H···O length difference between them is in the 0.021-0.047 Å range. This is consistent with the findings for other acylphloroglucinols [15-17].

The comparison of the H···O length for pairs of conformers differing by the position of C19 in ring D with respect to the plane identified by the C9, C23, C22 and O21 atoms, shows a smaller H···O length difference than for previous comparisons. Thus, the position of C19 in ring D does not influence the characteristics of the first IHB significantly. Similarly, the orientation of O10–H16, the orientation of the R′ ring system with respect to the phloroglucinol moiety, and the orientation of O28–H29 and O36–H37 do not influence the characteristics of the first IHB significantly.

In the case of the OH···π interaction, it is not possible to define an H-bond length, because the acceptor π system is not a single atom. However, it is interesting to consider the distance between the H atom and the closest C atoms in the acceptor aromatic ring B. Table 5.5 reports the distance (Å) between the H atom and the closest C atom in ring B, for the conformers in which the O–H···π interaction is present. The distance (2.057–2.239 Å) is in the shorter range for this type of interaction, suggesting that the OH···π interaction in this molecule are strong.

Table 5.6 reports the values of the calculated vibrational frequencies (harmonic approximation) of the O–H bonds in the selected lower energy conformers of myristinin A *in vacuo*, at the HF level. Table 5.7 reports the red shift (lowering of the vibrational frequency of the donor due to the presence of the IHB) when the given OH is engaged in an O–H···O IHB or in O–H···π interaction (O8–H15, O10–H16 and O12–H17). The vibrational frequency of O8–H15 is lowered when it forms the first IHB with the sp^2 O of the acyl group and when it forms the O–H···π interactions with the B aromatic ring. The red shift of O8–H15 when it is engaged in the first IHB is greater than when it forms the O–H···π interaction. This shows that O–H···O IHBs are comparatively stronger than O–H···π interactions. The vibrational frequency of O12–H17 is lowered when it forms the first IHB with the sp^2 O of the acyl group. The red shift of O12–H17 when it is engaged in the first IHB is smaller than that of O8–H15 when it is engaged in the first IHB; this suggests that the H15···O14

IHB is somewhat stronger than the H17···O14 IHB, consistently with the differences in their lengths. The vibrational frequency of O10–H16 is lowered when it forms the O–H···π interactions with the B aromatic ring. The red shifts of O10–H16 and O8–H15 when they are engaged in the O–H···π interaction show that it is greater for O8–H15, suggesting that the O–H···π interaction is comparatively stronger for O8–H15 than for O10–H16. The orientation of O28–H29 and O36–H37 (which are never engaged in IHB) does not influence the lowering of the vibrational frequencies significantly.

5.2.1.3. Dipole moments of the conformers.

Table 5.8 reports the values of the dipole moment of the calculated conformers of myristinin A. The values range between 0.860 and 9.326 Debye. The dipole moment depends mostly on the orientation of the OHs groups [15–17]. It is also important to recall that the orientation of the phenol OHs in the phloroglucinol moiety is relevant for other properties, including the energies and has a significant influence on the dipole moment of the conformers. The orientation of these phenols OHs can be uniform or non-uniform, as shown in figure 5.4. When the orientation of the phenols OHs is uniform, the contributions to the dipole moment cancel each other. Conformers with uniform orientation of the phenol OHs in the phloroglucinol moiety are d-r and s-w, while all the others have non-uniform orientation. The analysis of the dipole moment shows that the conformers with uniform orientation of the phenol OHs in the phloroglucinol moiety have smaller dipole moment than conformers with non-uniform orientation. The orientation of the other two OHs (O28–H29 and O36–H37) also influences the dipole moment significantly.

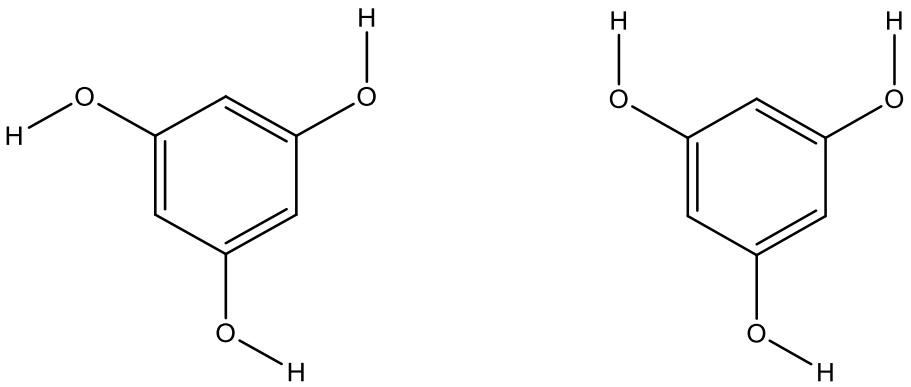

uniform non-uniform

Figure 5.4. Structures of phloroglucinol moiety showing uniform and non-uniform orientation of OHs.

The smallest dipole moment corresponds to the d-r-η-u-p-a-e-j conformer, in which the three OHs in the phloroglucinol moiety and the two OHs in the substituent ring system are oriented in a manner in which their total contribution becomes negligible. In this case, the orientation of the OHs in the phloroglucinol moiety is not uniform and, therefore, their total contribution to the dipole moment is not close to zero. On the other hand, O28–H29 and O36–H37 are oriented to the same side. Thus, it is reasonable to infer that the contributions from O28–H29 and O36–H37 and the contribution from the OH in the phloroglucinol moiety largely cancel each other. The highest dipole moment corresponds to the d-w-q-a-f-k conformer, where the OHs of the phloroglucinol moiety have non-uniform orientation and the contributions of O28–H29 and O36–H37 sum up to their contributions enhancing the dipole moment (O28–H29 and O36–H37 are both oriented towards the phloroglucinol moiety).

Differently from acylphloroglucinols with no additional OH, in the case of myristinin A, the u-conformers have smaller dipole moment than the corresponding non-u ones. Thus, d-r-u conformers have smaller dipole moment than d-r conformers, with a 0.16–2.59 Debye difference; d-w-u conformers have smaller dipole moment than d-w conformers, with a 0.54–2.37 Debye difference; s-r-u conformers have smaller dipole moment than s-r conformers, with a 0.07–3.80 Debye difference; s-w-u conformers have smaller dipole moment than s-w conformers, with a 0.70–3.54 Debye difference. This can be understood by considering the orientation of O10–H16 and the orientation of O28–H29 and O36–H37 in each of these conformers.

Like in the previous comparisons, it is also important to compare the dipole moments for pairs of conformers differing by specific characteristics. For pairs of conformers differing only by the orientation of O28–H29, the dipole moment depends on the orientation of O10–H16 with respect to R′. Thus, d-r-e conformers have higher dipole moment than d-r-f conformers, with a 0.30–3.50 Debye difference; d-w-e conformers have smaller dipole moment than d-w-f conformers, with a 0.01–1.80 Debye difference; s-r-e conformers have smaller dipole moment than s-r-f conformers, with a 0.07–2.04 Debye difference; s-w-e conformers have smaller dipole moment than s-w-f conformers, with a 0.04–3.10 Debye difference. This suggests that the mutual orientation of O28–H29 and O10–H16 influences the dipole moment significantly.

Comparisons of dipole moments for pairs of conformers differing only by the orientation of O36–H37 also show dependence on the orientation of O10–H16 with respect to R′. Thus, d-r-j

conformers have higher dipole moment than d-r-k conformers, with a 0.00–3.59 Debye difference; d-w-j conformers have smaller dipole moment than d-w-k conformers, with a 1.00–2.66 Debye difference; s-r-j conformers have smaller dipole moment than s-r-k conformers, with a 0.56–2.74 Debye difference; s-w-j conformers have smaller dipole moment than s-w-k conformers, with a 0.36–3.02 Debye difference. Just like in the previous comparison the orientation of the O36–H37 with respect to the orientation of O10–H16 influence the dipole moment significantly.

The comparison of the dipole moments of conformers differing only by orientation of the B–D–E ring system with respect to the phloroglucinol moiety does not show a consistent pattern, because sometimes p conformers have smaller dipole moment than q conformers and other times they have greater dipole moment. The difference is usually small. This suggests that the dipole moment of the conformers does not depend significantly on the orientation of the B–D–E ring system.

5.2.1.4. HOMO-LUMO energy gap of the conformers.

Table 5.9 reports the energy difference between the frontier orbitals (HOMO, highest occupied molecular orbital, and LUMO, lowest unoccupied molecular orbital). The values of the HOMO-LUMO energy gap of the calculated conformers range between 235.410 and 260.975 kcal/mol.

Comparison of the HOMO-LUMO energy gap of pairs of conformers differing only by the position of the first IHB (O14···H15 or O14···H17) shows that the d conformers have smaller HOMO-LUMO energy gap than the s conformers, with a 0.195–19.007 kcal/mol difference. The only exception is d-r-η-p-b-e-j, which has a greater HOMO-LUMO energy gap than s-r-η-p-b-e-j.

Comparison of the HOMO-LUMO energy gap of pairs of conformers differing only by the orientation of the *ortho* phenol OH not engaged in the first IHB shows two types of trends depending on the position of the first IHB with respect to R′. The non-u conformer has greater HOMO-LUMO energy gap than the u conformer for d-type conformers, and their energy gaps differ by 5.077–7.110 kcal/mol. The non-u conformer has greater HOMO-LUMO energy gap than the u conformer for the s-type conformers, and their gaps differ by 9.325–19.509 kcal/mol.

Comparison of the HOMO-LUMO energy gap of pairs of conformers with and without O10–H16···π interaction shows that the conformers with O10–H16···π interaction have greater HOMO-LUMO energy gap than the conformers without O10–H16···π interaction; the HOMO-LUMO energy gap difference is in the 6.928–14.257 kcal/mol range.

Comparisons of the HOMO-LUMO energy gap of conformers differing only by the orientation of the substituent at C3 with respect to the phloroglucinol moiety show two types of trends depending on the position of the first IHB with respect to R′. For d-conformers the p conformers have greater HOMO-LUMO energy gap than the q conformers when the q conformers with a 0.031–15.430 kcal/mol difference. For s-conformers, the p conformer has lower HOMO-LUMO energy gap than the q conformer with a 0.879 – 6.683 kcal/mol difference.

The comparison of HOMO-LUMO energy difference for pairs of conformers differing only by the orientation of O28–H29 shows a smaller HOMO-LUMO energy gap than for previous comparisons. Thus, the orientation of O28–H29 does not influence the HOMO-LUMO energy difference significantly. Similarly, the orientation of O36–H37 does not influence the HOMO-LUMO energy difference significantly.

Figure 5.6 shows the shapes of the HOMO and LUMO frontier orbitals for the conformers listed in table 5.2. The shapes of HOMO orbitals show greater electron concentration density in the phloroglucinol moiety and the other two ring system for all conformers with few exceptions for d-w, d-r-q and s-w-u conformers where the electron density in concentrated in the B–D rings. The shapes of LUMO orbitals show greater concentration of electrons in the phloroglucinol moiety.

5.3.1. Results in solution

5.3.1.1. Relative energies of the conformers

Calculations in solution were performed at the HF level on the lowest energy conformers listed in table 5.11, (conformers with relative energy ≤ 1.984 kcal/mol). Table 5.10 reports the relative energy of these conformers in different media (vacuum, chloroform, acetonitrile and water). The relative energies show that Myrin-d-r-η-p-a-e-j does not remain the most stable conformer in solution. The most stable conformer in solution is Myrin-d-r-η-p-a-e-k. The values of the relative energy also show that the conformers have lower energy in solution than *in vacuo*. The relative energy of the conformers slightly decreases with an increase in solvent polarity (taken as the chloroform–acetonitrile–water sequence), with the only exception of Myrin-d-r-η-p-a-e-j, where the trend is reversed.

Table 5.11 reports the free energy of solvation (solvent effect, ΔG_{solv}) and its electrostatic component (G_{el}) for the conformers of myristinin A calculated in part one. ΔG_{solv} is positive in

acetonitrile and negative in chloroform and water. The magnitude of ΔG_{solv} increases with the solvent-polarity. The ranges of the magnitude of ΔG_{solv} are 0.13–2.27, 5.38–7.52, and 13.24–16.25 kcal/mol in chloroform, acetonitrile and water respectively. Another interesting aspect is that Myrin-d-r-η-p-a-e-j has the smallest magnitude of ΔG_{solv} in chloroform and water, and the greatest in acetonitrile. The electrostatic component (G_{el}) of ΔG_{solv} has negative values in all three solvents and its magnitude is greater in water than in the other two solvents.

5.3.1.2. Characteristics of intramolecular hydrogen bonds

Table 5.12 reports the parameters of the first IHBs *in vacuo* and in the three solvents, for the conformers that have been calculated in solution. It is interesting to note that the H15···O14 bond has the same length in acetonitrile and water for all the d conformers (with the only exception of Myrin-d-r-η-p-b-e-k); for the s conformers the length of H17···O14 may be different for different conformers, but it is the same for the same conformer in acetonitrile and in water. For the d conformers, the bond length (Å) of H15···O14 is 1.651–1.652 *in vacuo*, 1.646–1.647 in chloroform, 1.644 in acetonitrile and 1.644 in water; for the s conformers, the bond length of H17···O14 is 1.651–1.652 *in vacuo*, 1.646–1.647 in chloroform, 1.676–1.681 in acetonitrile and 1.676–1.681 in water. Thus, the bond length of H15···O14 is smaller in chloroform than *in vacuo*, and smaller in acetonitrile or water than in chloroform. The values of the O···O distance are smaller in chloroform than *in vacuo*, and smaller in acetonitrile or water than in chloroform. The values of the O$\hat{H}$O bond angles increase with an increase in the medium polarity.

Table 5.13 reports the distance between the H atom and the closest C atom in the acceptor B aromatic ring (H15···C23 or H16···C23) for the O–H···π interactions of the calculated conformers of myristinin A in the media considered. The results show that the H15···C23 or H16···C23 distances slightly decrease from vacuum to chloroform to acetonitrile for the first four lowest energy conformer and slightly increases for higher energy conformers. The distances may be different for different conformers, but they have the same value for the same conformer in acetonitrile and in water. The H15···C23 distance in Myrin-s-w-ε-q-a-e-j remains the same in all media.

5.3.1.3. Dipole moments and HOMO-LUMO energy gap in different media

Table 5.14 reports the values of the dipole moments of the conformers of myristinin A calculated in different media. Dipole moment increases as the medium polarity increases. The value of the dipole moments ranges between 2.278–5.111, 2.696–6.258, 2.863–6.626, and 2.879–6.659 Debye *in vacuo*, chloroform acetonitrile and water respectively.

Table 5.15 reports the values of the HOMO-LUMO energy gap of the conformers of myristinin A calculated in different media. The HOMO-LUMO energy gap slightly decreases as the medium polarity increases. The value of the HOMO-LUMO energy gap ranges between 254.693–258.854, 254.411–256.871, 254.204–257.003, and 254.191–256.959 kcal/mol *in vacuo*, chloroform acetonitrile and water respectively. The minimum and maximum HOMO-LUMO energy gaps in solution occur for the same conformers despite the different permittivities of the solvents.

5.4. Results for conformers with different geometries of R and the same geometry of the ring system

5.4.1. Results *in vacuo*

5.4.1.1. Types of investigated conformers

This part consider the results of the study of conformers with different geometries of R associated with the best geometry of the phloroglucinol moiety and the B–D–E ring system identified from the study of a model structure considering of these units and R replaced by an ethyl (fig 5.4) [190]. The best identified geometry was d-r-η-p-a-e-j, this geometry has the following stabilising factors: presence of the first IHB on the same side of the R′ substituent; presence of the O10–H16···π interaction; orientation of the OH *ortho* to the acyl group and not engaged in the first IHB away from the COR group; orientation of the two fused rings (B and D) 'towards us' and ring E 'towards the back' with reference to fig.5.1; orientation of O28–H29 to the side of C27; orientation of O36–H37 to the side of C34; C19 in ring D being above the plane identified by C9, C23, C22 and O21.

Different geometries of the R chain were built by rotating each single bond in turn, as explained in section 4.4. This study involved 30 inputs and yielded 28 conformers, because some inputs with the R chain bent by 180° (remaining on the plane of the benzene ring A) optimized to conformers coinciding with those coming from inputs where R has been bent by -90° or +90°; for instance, the

input where C13–C18 had been rotated by 180° (to the side of R′) as gave the same output geometry when it had been rotated by -90°.

5.4.1.2. Relative energies of the conformers

Conformers corresponding to the ±90° and 180° rotations of all the single bonds in R were calculated at the HF/6-31G(d,p) level. The geometries of the optimized conformers are shown in figure 5.8 and their relative energies are reported in table 5.16. The lowest energy conformer is the same as for the first part of the study of myristinin A (table 5.2). The energy values show that the lowest energy conformer is the one in which the R chain is linear (outstretched) and on the plane defined by the benzene ring A. When the R chain is bent, the energy of the conformers where the relevant bond has been rotated by +90° or -90° is lower than the energy of the conformers where the same bond has been rotated by 180° or 180°, suggesting that the conformers where the R chain is bent out of the plane have better energy than conformers with the R chain bent on the plane identified by the benzene ring A. The energy values also confirm that conformers in which the R chain is symmetrical with respect to the plane defined by the benzene ring A are twofold degenerate (and this is in consistent with findings on other acylphloroglucinols [15–17]). This suggests that the ring system at C3 does not influence the optimisation of inputs with symmetrical R geometries towards non-symmetrical outputs.

Table 5.17 reports the values of the relative energies corrected for ZPE and of the ZPE corrections as well as the relative Gibbs free energies ($\Delta G_{corrected}$, sum of electronic and thermal free energy) and its correction, G_{corr}, for the conformers listed in table 5.10 at HF level. The ZPE corrections for all the conformers are comparatively close. Their values range between 454.103 and 454.318 kcal/mol. The greater values of the ZPE corrections correspond to the conformers having lower energy. The relative energies corrected for ZPE and the uncorrected relative energies have the same trends, with only two exceptions (Myrin-d-r-η-p-a-e-j-8z and Myrin-d-r-η-p-a-e-j-8y). Conformers with lower relative energy have lower relative Gibbs free energies. The values of G_{corr} are comparatively close.

DFT/B3LYP/6-31+G(d,p) and MP2/ 6-31G(d,p) calculations were performed on the conformers of this part having lower energy in the HF results. Table 5.24 reports the relative energies obtained from these calculations and compares them with the HF results. The relative energy (kcal/mol) of the highest energy conformer of this set is 1.054 / HF, 0.956 /DFT and 0.861 /MP2, showing a

narrowing of the energy range. Furthermore, the energy sequence of the conformers is not the same with the three methods. Thus, the lowest and highest energy conformers are not the same with the three methods, as it is, the lowest energy conformer at HF and DFT levels is Myrin-d-r-η-p-a-e-j, and at MP2 level, is Myrin-d-r-η-p-a-e-j-2z. The highest energy conformer at HF and DFT levels is Myrin-d-r-η-p-a-e-j-5y, and at MP2 level, is Myrin-d-r-η-p-a-e-j-10z.

5.4.1.3. Characteristics of intramolecular hydrogen bonds

Table 5.25 reports the parameters of the first IHB in the lowest energy conformers of myristinin A listed in table 5.16 *in vacuo*, at HF/6-31G(d,p), DFT/B3LYP/B3LYP/6-31+G(d,p) and MP2/ 6-32G(d,p) levels of theory. HF gave the longest bond lengths, DFT gave the shortest and MP2 gave intermediate values. This is consistent with the fact that HF underestimates the strength of H-bonds, and DFT overestimates it; the MP2 results can be considered as those closer to the actual values. The ranges of the bond lengths (Å) of H15···O14 are 1.644–1.654 /HF, 1.516–1.530 /DFT and 1.574–1.583 /MP2. These values indicate that the first IHB is comparatively strong. The values of the O···O distance are nearly close to 2.5 Å for all results obtained (2.503–2.510 /HF, 2.458–2.468 /DFT and 2.498–2.505 /MP2). The OĤO bond angles are estimated around 146° /HF, 151° /DFT and 151° MP2.

For the O–H···π interactions (table 5.26), the distance between the H atom and the closest C atom of the B aromatic ring is 2.128–2.129 Å /HF, 2.038–2.057 Å /DFT and 2.008–2.012 Å /MP2. By comparing the results of the three methods, one can see that MP2 optimizes to geometries with shorter IHBs; this is consistent with the fact that it takes into account also dispersion contributions. The parameters show a stronger IHB for Myrin-d-r-η-p-a-e-j-z and Myrin-d-r-η-p-a-e-j-y conformers.

Table 5.20 reports the values of the calculated vibrational frequency of the O–H bonds in selected conformers of myristinin A *in vacuo* at the HF level. The values of the calculated vibrational frequencies of the O–H bonds (O8–H15 and O10–H16) show the lowering of the frequency due to the presence of the IHBs, as already discussed in part 1. The values of the calculated vibrational frequency also show that the orientation of the R chain has a significant influence on the vibrational frequency of O8–H15 and O12–H17 and minor influence on the vibrational frequency of O51–H52, O28–H29 and O10–H16. When the R chain is bent at C13–C18 by +90° or -90°, the vibrational frequency of O8–H15 increases slightly and that of O12–H17 decreases slightly. When the R chain

is bent at C7–C13 by +90° or -90°, the vibrational frequency of O8–H15 decreases slightly and that of O12–H17 increases slightly.

Table 5.21 reports the red shifts (lowering of the vibrational frequency of the donor due to the presence of the IHBs) when the given OH is engaged in an O8–H15···O15 IHB or in O10–H16···π interaction with the B aromatic ring. The red shift of O8–H15 when it is engaged in the first IHB is greater than when it forms the O–H··· interaction. This is consistent with the fact that O–H···O IHBs are stronger than O–H···π interactions.

5.4.1.4. Dipole moments of the conformers

Table 5.27 reports the values of the dipole moments of the conformers calculated in this part, at HF/6-31G(d,p), DFT/B3LYP/B3LYP/6-31+G(d,p) and MP2/6-31G(d,p) levels of theory. There is no typical sequence in the values of the dipole moment in the results of the different methods utilised. Comparison of the values of the dipole moment obtained with the three different methods shows that DFT yields lower values with respect to other two methods, with only one exception (Myrin-d-r-η-p-a-e-j-4y). The values of the dipole moments range between 2.273 and 2.439 Debye in the HF results, between 2.144 and 2.511 Debye in the DFT results, and between 2.282 and 2.528 Debye in the MP2 results.

5.4.1.5. HOMO-LUMO energy gap of the conformers

Table 5.28 reports the values of the HOMO-LUMO energy gap of the calculated conformers of myristinin A *in vacuo,* at HF/6-31G(d,p), DFT/B3LYP/B3LYP/6-31+G(d,p) and MP2/6-31G(d,p) level of theory. The values of the HOMO-LUMO energy gap range between 255.446 and 257.479 kcal/mol in the HF results, between 2.711 and 2.999 kcal/mol in the DFT results, and between 247.678 and 249.134 kcal/mol in the MP2 results.

Comparisons of the three methods show a huge difference between the values HOMO-LUMO energy gap of the DFT and the other two methods (HF and MP2). For analyses purpose, one can consider the values of the HOMO-LUMO energy gap from the MP2 results, because this method gives the results which are close to the experimental ones. The highest values of HOMO-LUMO energy gap corresponds to the conformers which were obtained by bending the C38–C39, C40–C41 and C42–C43 bonds of the R chain by -90° or +90°. The smallest values of the HOMO-LUMO

energy gap correspond to the conformers in which the bond that was rotated is closer to the sp^2 O of the acyl group (for instance, the C13–C18 bond).

Figure 5.9 shows the shapes of the HOMO and LUMO frontier orbitals for the conformers listed in table 5.18 at HF level. The shapes of HOMO orbitals show a greater electron concentration density in the phloroglucinol moiety and B-D-E ring system. The shapes of LUMO orbitals show a greater electron concentration density in the phloroglucinol moiety.

5.5.2. Results in solution

5.5.2.1. Relative energies of the conformers

Calculations in solution were performed on the lowest energy conformers listed in table 5.16, at the HF level (conformers with relative energy ≤ 1.054 kcal/mol) in the three solvents consider. The dielectric constants of theses solvents are 4.81 for chloroform, 36.64 for acetonitrile and 78.54 for water.

Table 5.29 reports the relative energy of these conformers in different media (vacuum, chloroform, acetonitrile and water). Unlike in part one, the relative energies of the conformers show that Myrin-d-r-η-p-a-e-j remains the most stable conformer in solution, except in chloroform, where the most stable conformer is Myrin-d-r-η-p-a-e-j-10y. The values of the relative energy also show that the conformers have lower energy *in vacuo* than in solution. The relative energy of the conformers slightly increases with an increase in solvent polarity (taken as the chloroform–acetonitrile–water sequence), with the only exception of Myrin-d-r-η-p-a-e-j-1z, Myrin-d-r-η-p-a-e-j-1y, and Myrin-d-r-η-p-a-e-j-7y, for which the trend is reversed.

Table 5.30 reports the free energy of solvation (solvent effect, ΔG_{solv}) and its electrostatic component (G_{el}) for the conformers of myristinin A calculated in part two. Similarly to part one, ΔG_{solv} is positive in acetonitrile and negative in chloroform and water. The magnitude of ΔG_{solv} ranges between 0.13 and 2.01, 5.96 and 7.52, and 13.24 and 15.44 kcal/mol in chloroform, acetonitrile and water respectively. The magnitude of ΔG_{solv} increases with the solvent-polarity. Myrin-d-r-η-p-a-e-j has the smallest magnitude of ΔG_{solv} in chloroform and water, and greatest in acetonitrile. The electrostatic component (G_{el}) has negative values in all three solvents and its magnitude is greater in water than in the other two solvents.

5.5.2.2. Characteristics of intramolecular hydrogen bonds

Table 5.31 reports the parameters of the first IHB *in vacuo* and in the three solvents, for the conformers that have been calculated in solution. The range of the bond lengths (Å) of the H15···O14 is 1.644–1.654, 1.640–1.653, 1.638–1.651 and 1.638–1.651, respectively, *in vacuo*, chloroform acetonitrile and water. Thus, the value of the bond lengths of the H15···O14 decreases with an increase in the media polarity. The values of the O···O distance increases with an increase in the media polarity. The values of the OĤO bond angles increases with an increase in the media polarity.

Table 5.32 reports the distance (Å) between the H atom and the closest C atom (H16···C39) in the acceptor B aromatic ring for the O–H···π interactions of the calculated conformers of myristinin A in the media considered. There is no drastical change in the H16···C23 distance; however, there are some slight changes. The values of the H16···C23 distance range comparatively close to 2 in different media. Thus, the H16···C23 distance is smaller in chloroform than *in vacuo,* with some exceptions (Myrin-d-r-η-p-a-e-j-3z and Myrin-d-r-η-p-a-e-j-8y, where the trend is reversed; Myrin-d-r-η-p-a-e-j-4y, Myrin-d-r-η-p-a-e-j-9y and Myrin-d-r-η-p-a-e-j-5z, where the distance remains the same), and smaller in acetonitrile or water than in chloroform, with some few exceptions, where the distance remains the same.

5.5.2.3. Dipole moments and HOMO-LUMO energy gaps in different media

Table 5.33 reports the values of the dipole moments of the conformers of myristinin A calculated in different media. Dipole moment slightly increases as the medium polarity increases. The ranges of the values of the dipole moments are 2.272–2.439, 2.676–2.942, 2.842–3.137, and 2.858–3.155 Debye *in vacuo*, chloroform acetonitrile and water respectively.

Table 5.34 reports the values of the HOMO-LUMO energy gap of the conformers of myristinin A calculated in different media. The HOMO-LUMO energy gap slightly increases as the medium polarity increases. The ranges of the values of the HOMO-LUMO energy gaps are 255.446–257.505, 254.323– 256.871, 253.903–256.607, and 253.865–256.821 kcal/mol *in vacuo*, chloroform acetonitrile and water respectively.

5.6. Overview of the results

The results have been analysed separately for part one and part two because of the different approaches in the preparation of the inputs and in the considering geometry aspects. Since the molecule is the same, it is important to have an overall view of all the results. Using the criteria explained in section 4.4, a total of 123 conformers of myristinin A was calculated.

Table 5.35 reports the values of the relative energies for all the conformers of myristinin A *in vacuo*, at the HF level. The relative energies of the conformers having different geometries of R and the same geometry of the ring system account for most of the lower energy conformers. This is to be expected because these conformers have the best geometry of the ring systems. Thus, these results show that the influence of the geometry of R on the overall energy of the molecule is smaller than the influence of the ring systems; this is understandable by considering that the ring system contains the most important stabilising factors such as the first IHB and O–H···π interaction.

Table 5.36 reports the values of the parameters of the first IHB for all the conformers of myristinin A *in vacuo*, at the HF level. The values of the parameters of the first IHB of the conformers having different geometries of R and the same geometry of the ring system show that the influence of the geometry of R on the overall parameters of the first IHB of the molecule is smaller than the influence of the ring systems. Like for the energy, this is to be expected because these conformers have the best geometry for the ring systems as already mention in the previous comparison.

Table 5.37 reports the values of the distance between the H atom and the closest C atom in the acceptor aromatic B ring for all the conformers of myristinin A *in vacuo*, at the HF level. The values of the distance between the H atom and the closest C atom in the acceptor aromatic B ring of the conformers having different geometries of R and the same geometry of the ring system show that the geometry of R on the overall does influence the O–H···π interactions. Like for the energy, this is to be expected because these conformers have the best geometry for the ring systems as already mention in the previous comparison.

Table 5.38 reports the values of the dipole moments for all the conformers of myristinin A *in vacuo*, at the HF level. The values of the dipole moments of the conformers having different geometries of R and the same geometry of the ring system are all around 2 Debye; this is to be expected because these conformers have the same geometry of the ring systems, all the OHs are oriented in the same

way, and, therefore, it can be concluded that the orientation of the acyl chain does not significantly influence the values of the dipole moments.

Table 5.39 reports the values of the HOMO-LUMO energy gaps for all the conformers of myristinin A *in vacuo*, at the HF level. The HOMO-LUMO energy gaps of the conformers having different geometries of R and the same geometry of the ring system show that the influence of the geometry of R on the overall HOMO-LUMO energy gap of the molecule is smaller than the influence of the ring systems. Like for the energy, this is understandable by considering that the ring system contains the most important stabilising factors.

Figure 5.5. Examples of some calculated conformers of the model structure in order of increasing relative energy. HF/6-31G(d,p) results *in vacuo*.

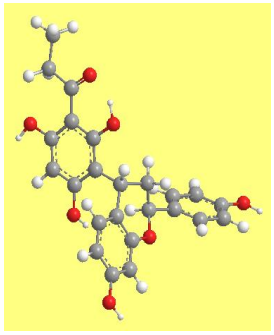
d-r-η-p-a-e-j

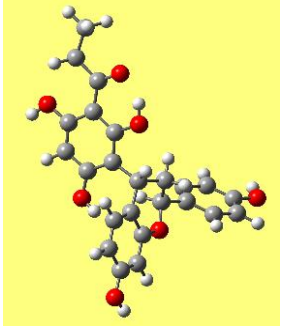
d-r-η-p-e-a-k

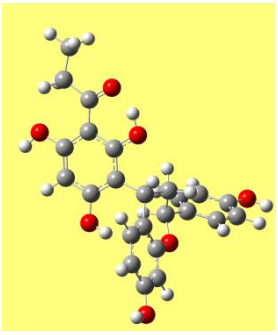
d-r-η-p-a-f-j

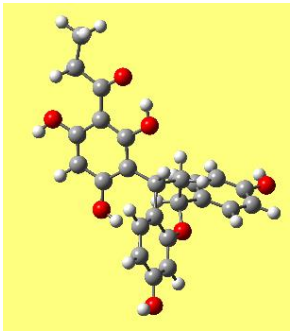
d-r-η-p-a-f-k

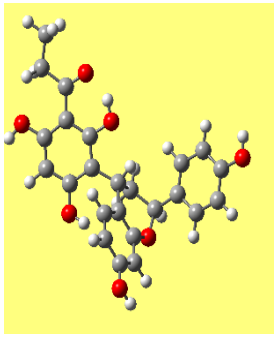
d-r-η-p-b-e-k

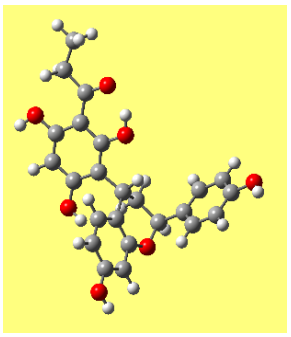
d-r-η-p-b-e-j

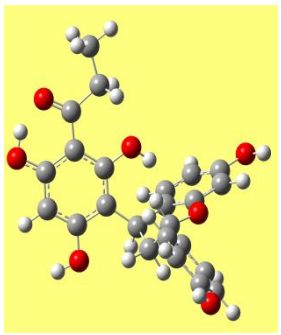
s-w-ε-q-a-e-k

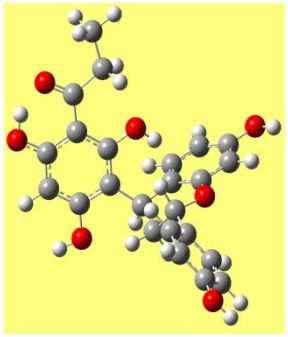
s-w-ε-q-a-e-j

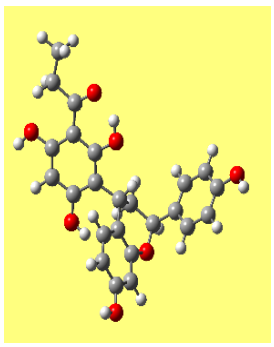
d-r-η-p-b-f-j

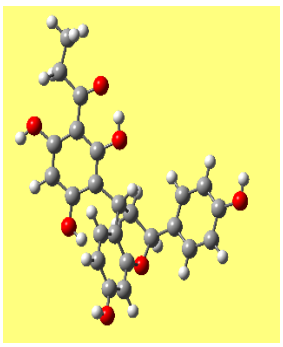
d-r-η-p-b-f-k

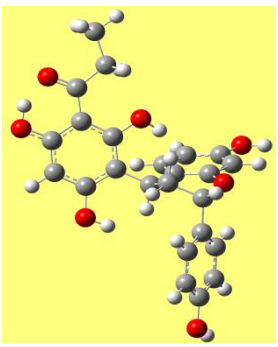
s-r-ε-q-b-e-j

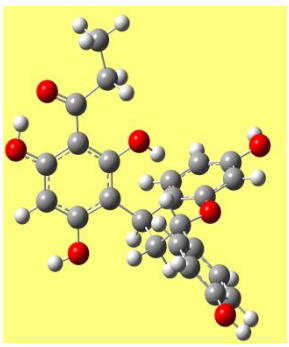
s-w-ε-q-a-f-j

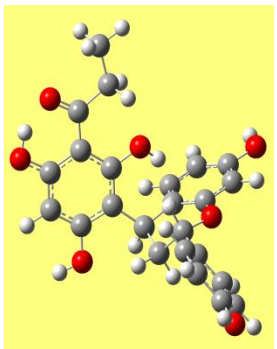
s-w-ε-q-a-f-k

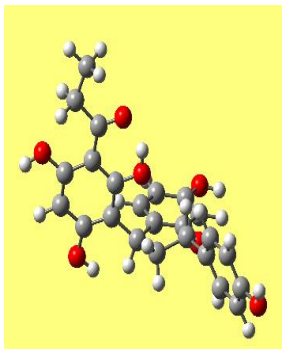
d-r-q-b-e-k

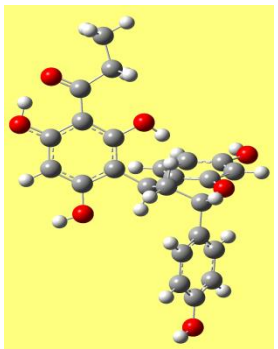
s-w-ε-q-b-f-k

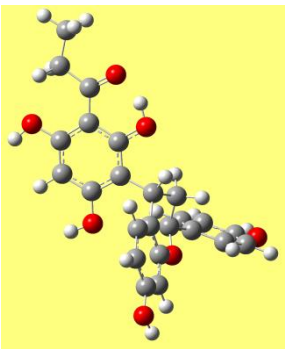
d-w-p-a-e-k

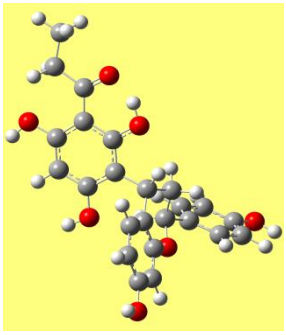
d-w-p-a-f-j

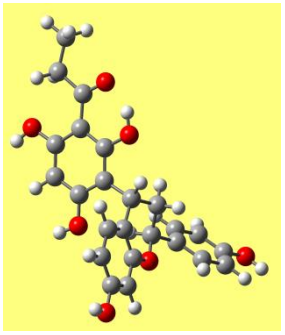
d-w-p-b-f-j

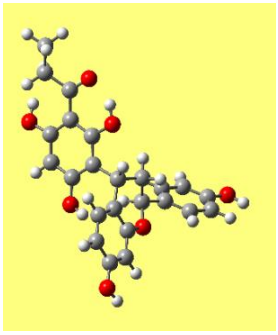
d-r-η-u-p-a-e-j

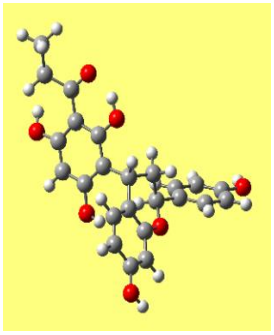
d-r-η-u-p-a-e-k

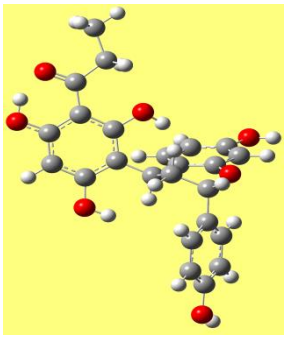
s-r-ε-q-b-e-j

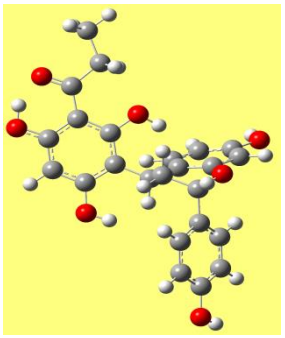
s-r-ε-q-b-f-j

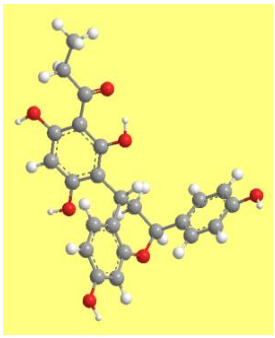
d-w-p-b-e-j

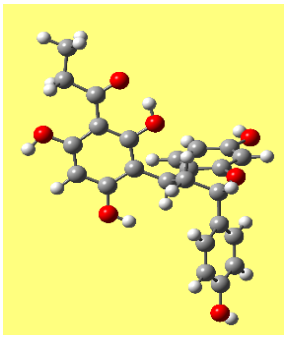
d-r-q-b-f-j

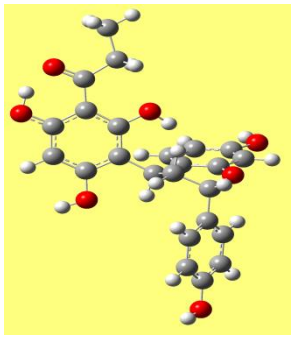
s-r-ε-q-b-f-k

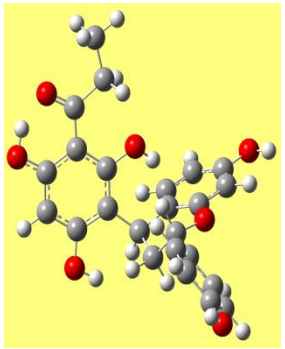
s-r-ε-q-a-e-k

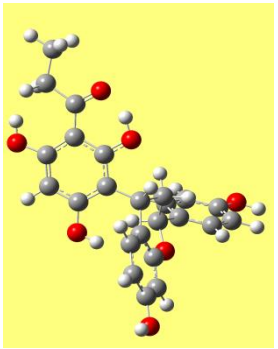
d-r-η-u-p-a-f-j

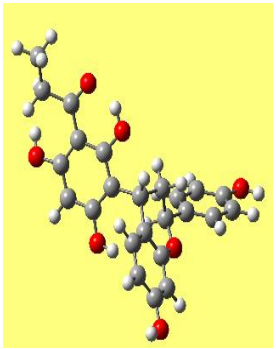
d-w-p-b-e-k

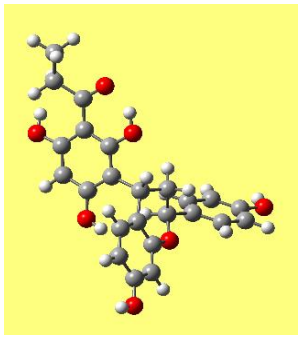
d-r-η-u-p-a-f-k

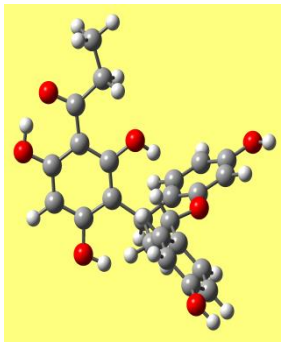
s-r-ε-q-a-e-j

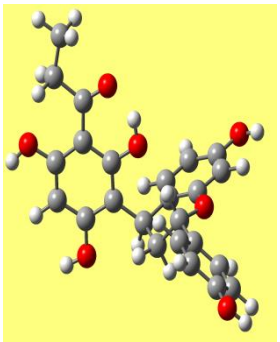
d-w-q-b-e-j

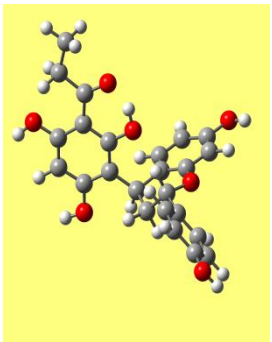
d-w-p-b-f-k

Figure 5.6. Optimized conformers of myristinin A having the same geometry of R and different geometries of the ring system.
HF/6-32G(d,p) results *in vacuo*. The conformers are arranged in order of increasing relative energy.

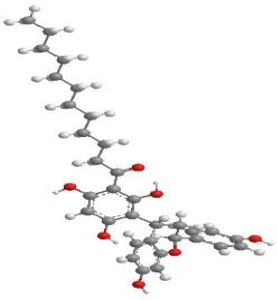
Myrin-d-r-η-p-a-e-j

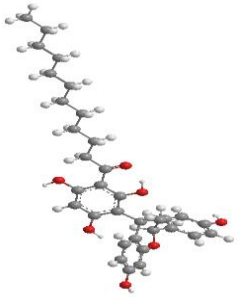
Myrin-d-r-η-p-e-a-k

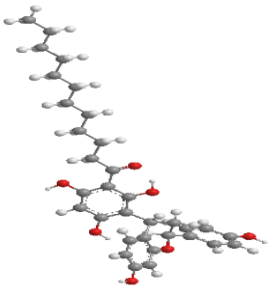
Myrin-d-r-η-p-a-f-j

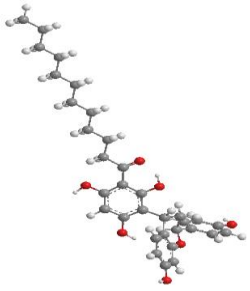
Myrin-d-r-η-p-a-f-k

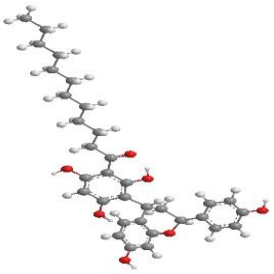
Myrin-d-r-η-p-b-e-k

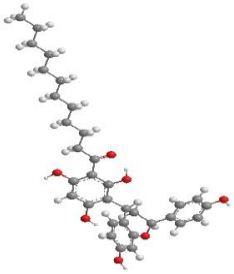
Myrin-d-r-η-p-b-e-j

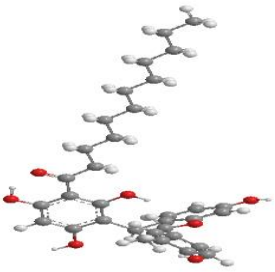
Myrin-s-w-ε-q-a-e-k

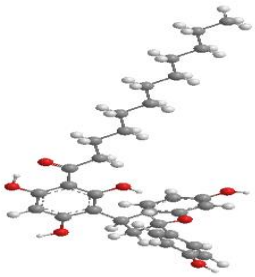
Myrin-s-w-ε-q-a-e-j

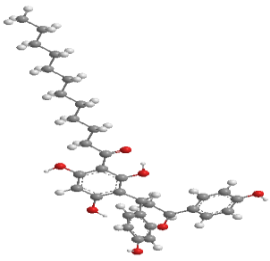
Myrin-d-r-η-p-b-f-j

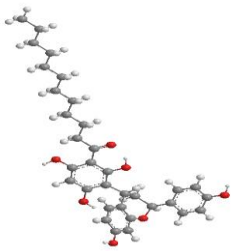
Myrin-d-r-η-p-b-f-k

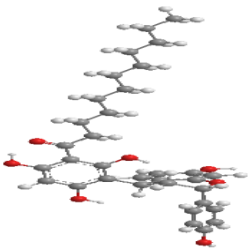
Myrin-s-r-ε-q-b-e-j

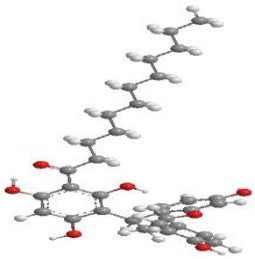
Myrin-s-w-ε-q-a-f-j

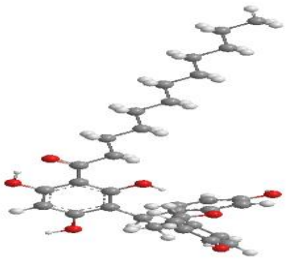
Myrin-s-w-ε-q-a-f-k

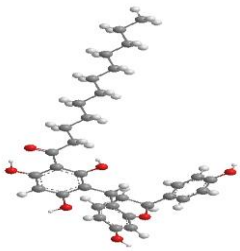
Myrin-s-w-u-p-b-e-k

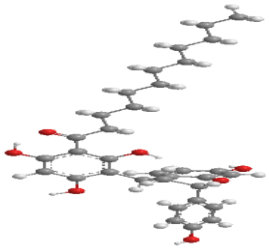
Myrin-s-w-ε-q-b-f-k

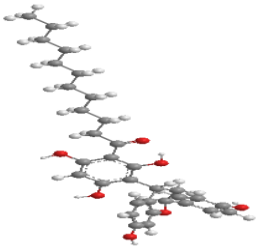
Myrin-d-w-p-a-e-k

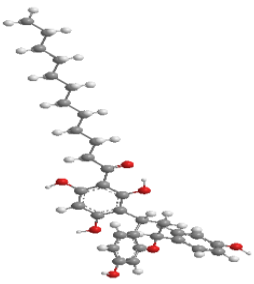
Myrin-d-w-p-a-f-j

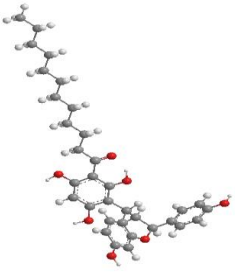
Myrin-d-w-p-b-f-j

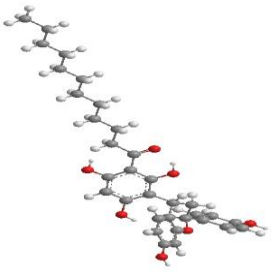
Myrin-d-r-η-u-p-a-e-j

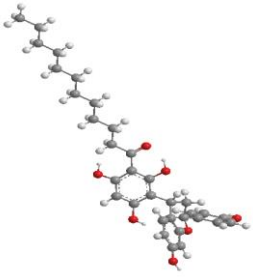
Myrin-d-r-η-u-p-a-e-k

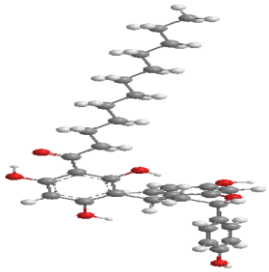

Myrin-s-r-ε-q-b-e-j

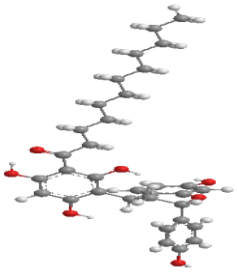

Myrin-s-r-ε-q-b-f-j

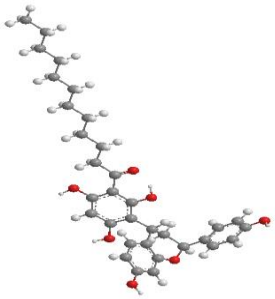

Myrin-d-w-p-b-e-j

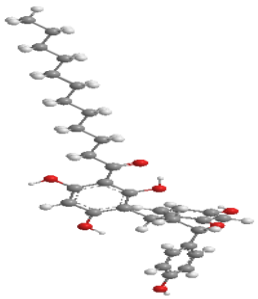

Myrin-d-r-q-b-f-j

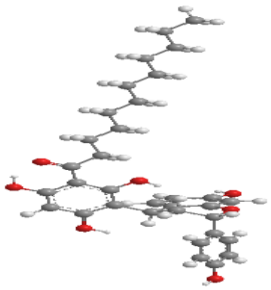

Myrin-s-r-ε-q-b-f-k

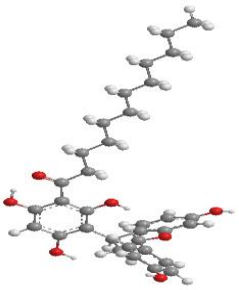

Myrin-s-r-ε-q-a-e-k

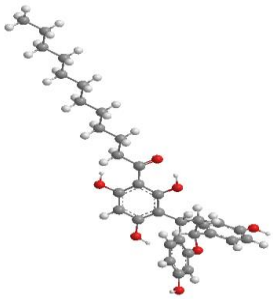

Myrin-d-r-η-u-p-a-f-j

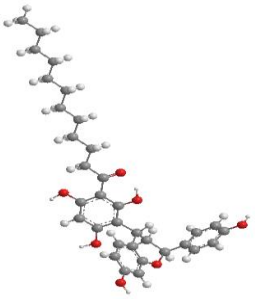

Myrin-d-w-p-b-e-k

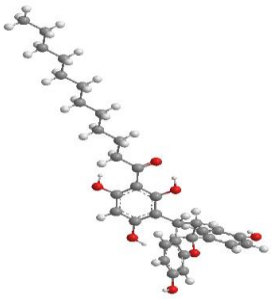

Myrin-d-r-η-u-p-a-f-k

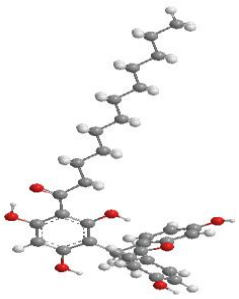

Myrin-s-r-ε-q-a-e-j

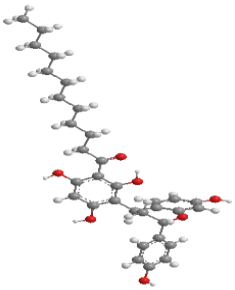

Myrin-d-w-q-b-e-j

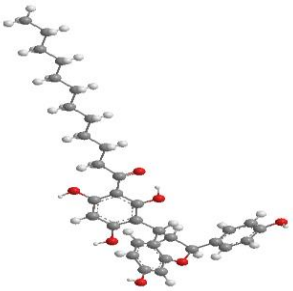

Myrin-d-w-p-b-f-k

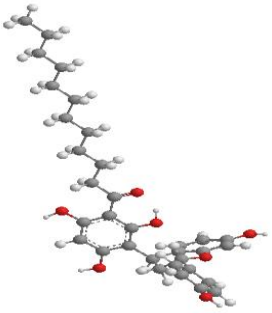

Myrin-d-w-q-a-e-j

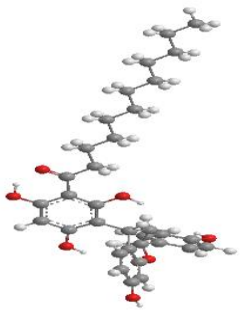

Myrin-s-r-η-p-e-a-k

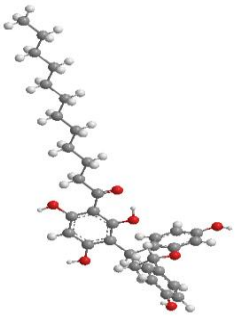

Myrin-d-w-q-a-e-k

Myrin-s-r-η-p-a-e-j

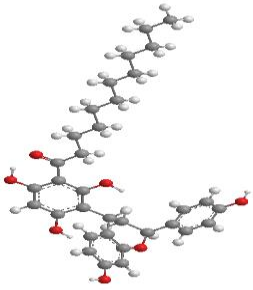

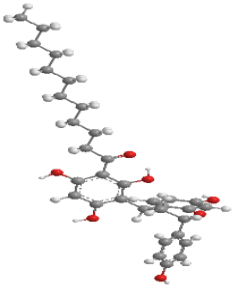

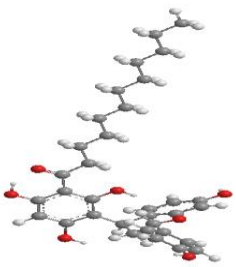

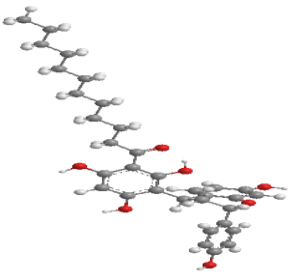

Myrin-s-r-η-p-b-f-k

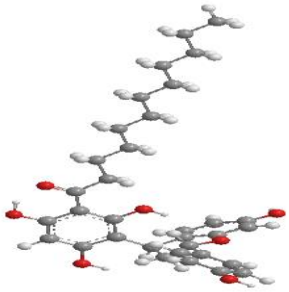

Myrin-d-w-q-b-f-j

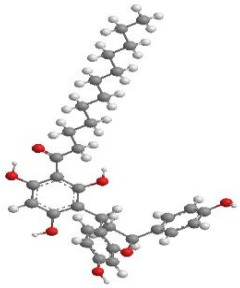

Myrin-s-r-ε-q-a-f-k

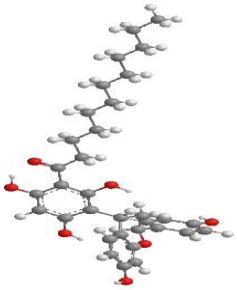

Myrin-d-w-q-b-e-k

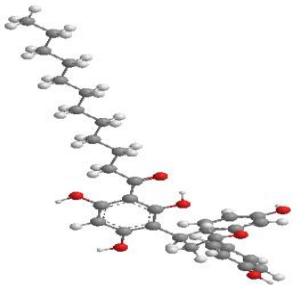

Myrin-s-r-ε-q-a-f-j

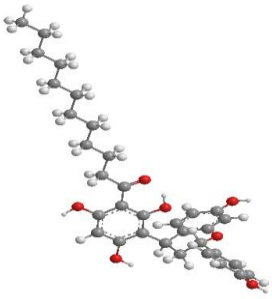

Myrin-s-w-p-b-f-j

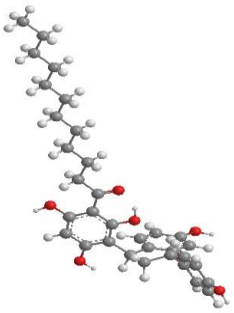

Myrin-s-r-η-p-a-f-k

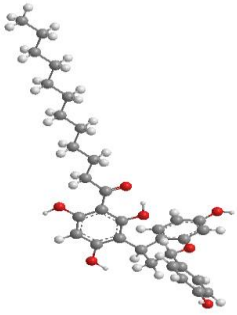

Myrin-d-w-q-a-f-j

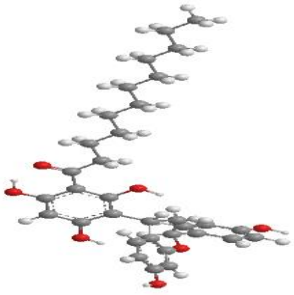

Myrin-d-r-q-a-e-j

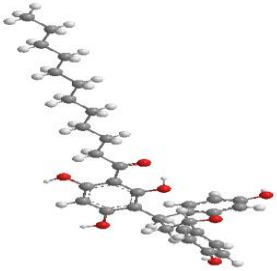

Myrin-d-r-q-b-e-j

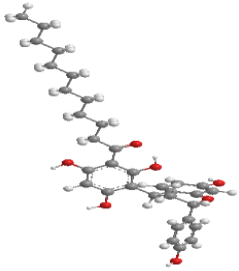

Myrin-d-r-q-a-e-k

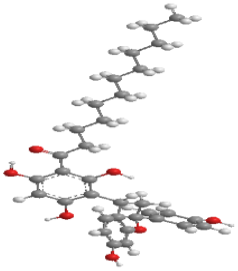

Myrin-s-r-η-p-a-f-j

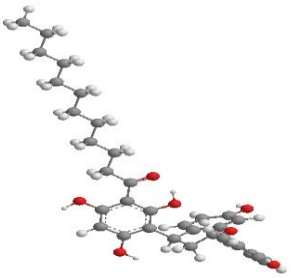

Myrin-d-w-q-a-f-k

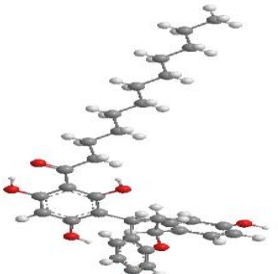

Myrin-d-w-q-b-f-k

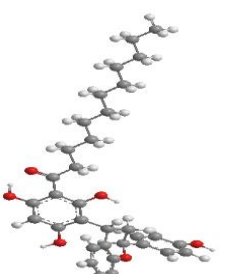

Myrin-s-w-p-a-e-j

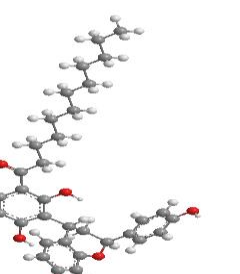

Myrin-d-r-q-a-f-k

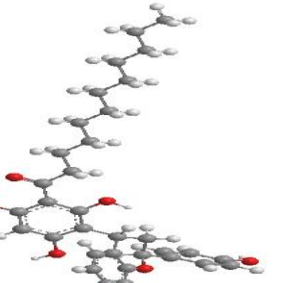

Myrin-s-r-η-u-p-a-e-j

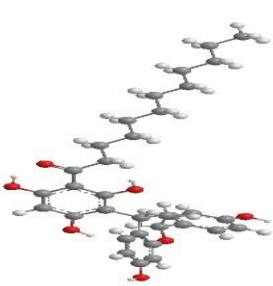

Myrin-s-w-p-a-f-j

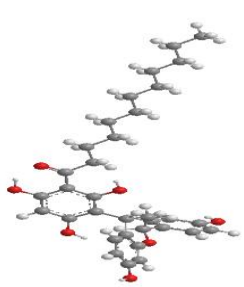

Myrin-s-r-η-p-b-e-j

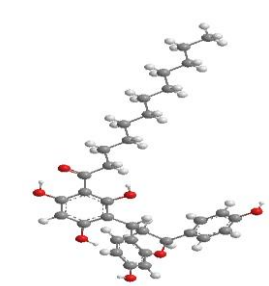

Myrin-s-w-p-a-f-k

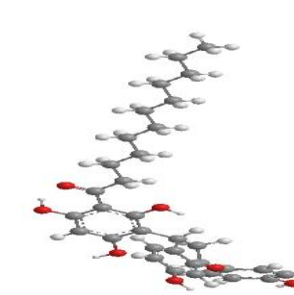

Myrin-s-r-η-u-p-a-f-j

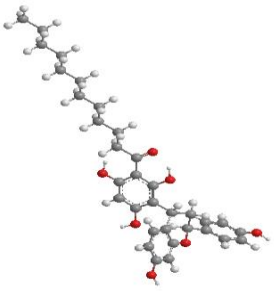

Myrin-s-r-η-u-p-a-f-k

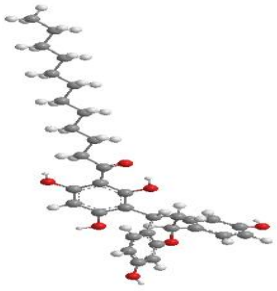

Myrin-s-r-η-u-p-b-f-k

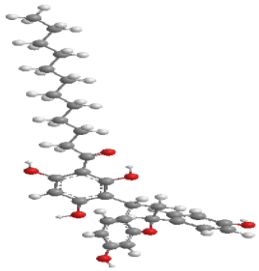

Myrin-s-w-p-e-a-k

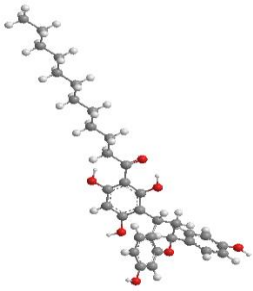

Myrin-d-w-u-p-a-e-j

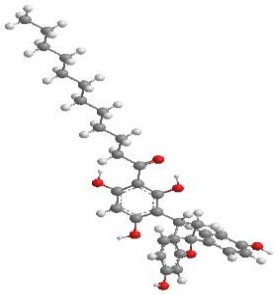

Myrin-d-w-u-p-e-a-k

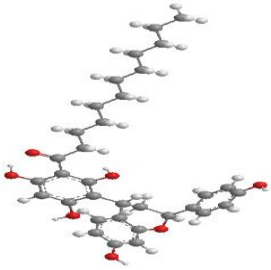

Myrin-d-w-u-p-b-e-k

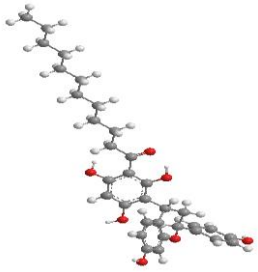

Myrin-d-w-u-p-a-f-j

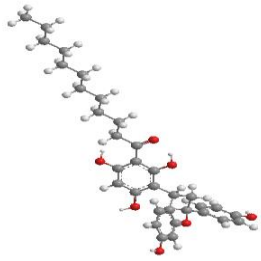

Myrin-d-w-u-p-b-f-j

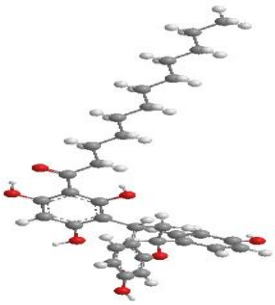

Myrin-s-w-u-p-b-e-j

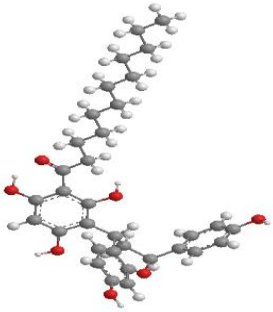

Myrin-d-w-u-p-a-f-k

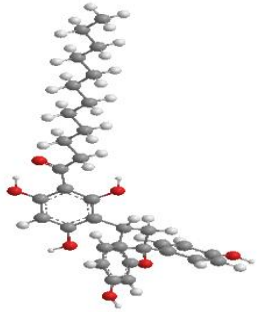

Myrin-d-w-u-p-b-f-k

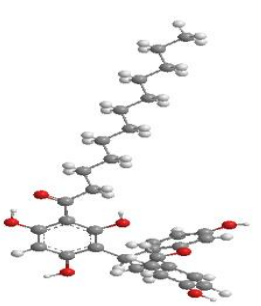

Myrin-s-w-u-p-e-a-k

Myrin-s-w-p-b-e-j

Myrin-s-w-u-p-a-e-j

Myrin-s-w-u-q-a-e-j

Myrin-s-w-u-q-b-e-j

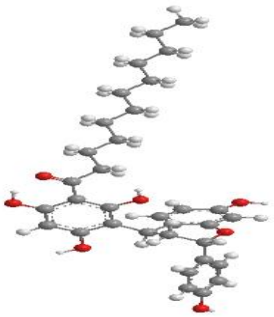

Myrin-d-w-u-q-b-e-j

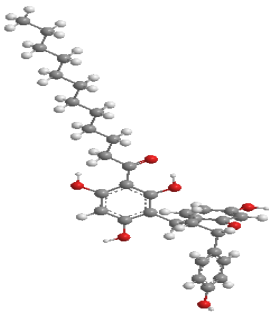

Myrin-d-w-u-q-a-e-j

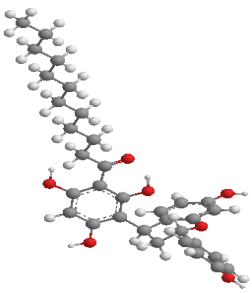

Myrin-s-w-u-p-b-f-j

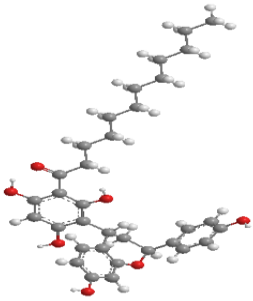

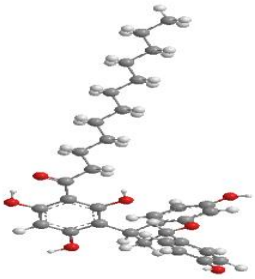

Myrin-s-w-u-q-a-e-k

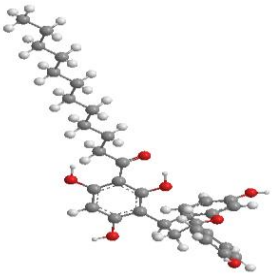

Myrin-d-w-u-q-a-e-k

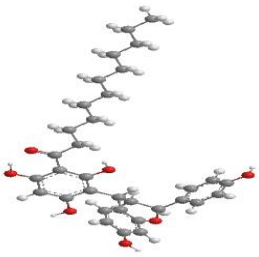

Myrin-s-w-u-p-b-e-k

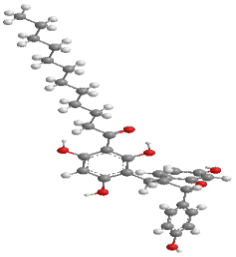

Myrin-d-w-u-q-b-f-j

Myrin-s-w-u-p-a-f-k

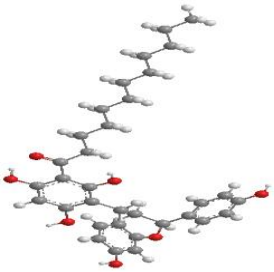

Myrin-s-w-u-p-b-f-k

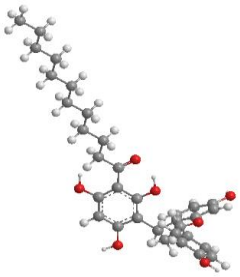

Myrin-d-w-u-q-a-f-j

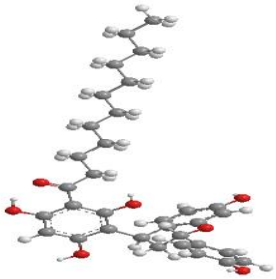

Myrin-s-w-u-q-a-f-k

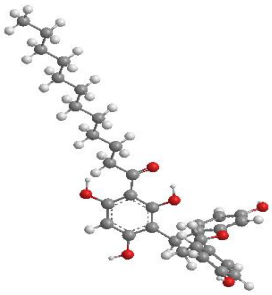

Myrin-d-w-u-q-a-f-k

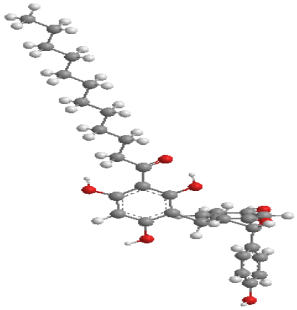

Myrin-d-w-u-q-b-f-k

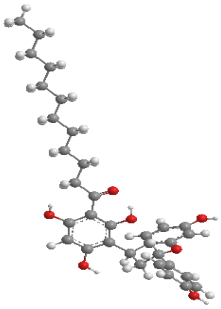

Myrin-d-r-u-q-a-e-j

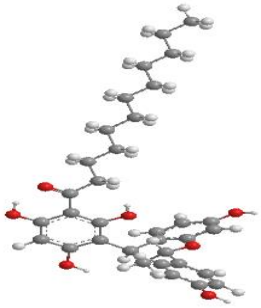

Myrin-s-r-u-q-b-e-j

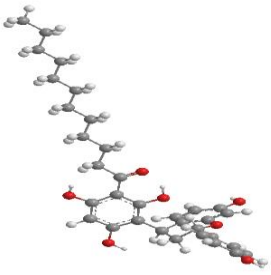

Myrin-d-r-u-q-a-f-j

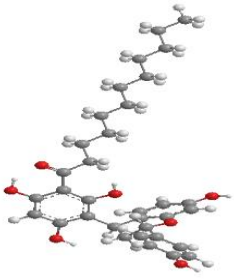

Myrin-s-r-u-q-a-e-j

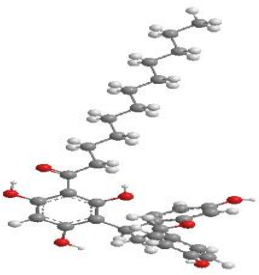

Myrin-s-r-u-q-a-e-k

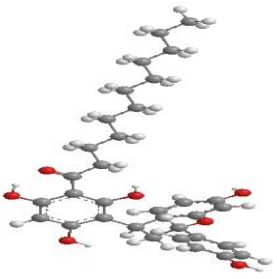

Myrin-s-r-u-q-a-f-j

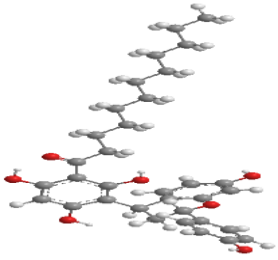

Myrin-s-r-u-q-a-f-k

Table 5.2. Relative energies of the calculated conformers of myristinin A having the same geometry of R and different geometries of the ring system.
HF/6-31G(d,p) results *in vacuo*. The conformers are arranged in order of increasing relative energy.
The absolute energy of the lowest energy conformer is -1797.0892235 hartree.

Conformer	Relative energy (kcal/mol)	Conformer	Relative energy (kcal/mol)
Myrin-d-r-η-p-a-e-j	0.000	Myrin-s-r-η-p-a-f-j	5.751
Myrin-d-r-η-p-a-e-k	0.013	Myrin-d-w-q-a-f-k	5.819
Myrin-d-r-η-p-a-f-j	0.423	Myrin-d-w-q-b-f-k	5.868
Myrin-d-r-η-p-a-f-k	0.495	Myrin-s-w-p-a-e-j	6.121
Myrin-d-r-η-p-b-e-k	1.004	Myrin-d-r-q-a-f-k	6.224
Myrin-d-r-η-p-b-e-j	1.010	Myrin-s-r-η-u-p-a-e-j	6.260
Myrin-s-w-ε-q-a-e-k	1.160	Myrin-s-w-p-a-f-j	6.427
Myrin-s-w-ε-q-a-e-j	1.207	Myrin-s-r-η-p-b-e-j	6.496
Myrin-d-r-η-p-b-f-j	1.212	Myrin-s-w-p-a-f-k	6.507
Myrin-d-r-η-p-b-f-k	1.244	Myrin-s-r-η-u-p-a-f-j	6.684
Myrin-s-w-ε-q-b-e-j	1.501	Myrin-s-r-η-u-p-a-f-k	6.701
Myrin-s-w-ε-q-a-f-j	1.646	Myrin-d-r-q-b-e-k	6.761
Myrin-s-w-ε-q-a-f-k	1.661	Myrin-s-r-η-u-p-b-e-k	6.919
Myrin-s-w-ε-q-b-e-k	1.752	Myrin-s-r-η-u-p-b-f-k	7.125
Myrin-s-w-ε-q-b-f-k	1.984	Myrin-s-w-p-e-a-k	7.141
Myrin-d-w-p-a-e-k	4.452	Myrin-d-w-u-p-a-e-j	7.704
Myrin-d-w-p-a-f-j	4.652	Myrin-d-w-u-p-a-e-k	7.828
Myrin-d-w-p-b-f-j	4.652	Myrin-d-w-u-p-b-e-k	7.828
Myrin-d-r-η-u-p-a-e-j	4.659	Myrin-d-w-u-p-a-f-j	8.048
Myrin-d-r-η-u-p-a-e-k	4.666	Myrin-d-w-u-p-b-f-j	8.048
Myrin-s-r-ε-q-b-e-j	4.707	Myrin-s-w-u-p-a-f-j	8.182
Myrin-s-r-ε-q-b-f-j	4.837	Myrin-s-w-u-p-b-e-j	8.221
Myrin-d-w-p-a-f-k	4.846	Myrin-d-w-u-p-a-f-k	8.233
Myrin-d-w-p-b-e-j	4.921	Myrin-d-w-u-p-b-f-k	8.233
Myrin-d-r-q-b-f-j	4.981	Myrin-s-w-u-p-e-a-k	8.267
Myrin-s-r-ε-q-b-f-k	5.030	Myrin-s-w-p-b-e-j	8.323
Myrin-s-r-ε-q-a-e-k	5.034	Myrin-s-w-u-p-a-e-j	8.327
Myrin-d-r-η-u-p-a-f-j	5.080	Myrin-s-w-u-q-a-e-j	8.396
Myrin-d-w-p-b-e-k	5.143	Myrin-s-w-u-q-b-e-j	8.402
Myrin-d-r-η-u-p-a-f-k	5.145	Myrin-d-w-u-q-b-e-j	8.416
Myrin-s-r-ε-q-a-e-j	5.158	Myrin-d-w-u-q-a-e-j	8.418
Myrin-d-w-q-b-e-j	5.165	Myrin-s-w-u-p-b-f-j	8.476
Myrin-d-w-p-b-f-k	5.203	Myrin-s-w-u-q-a-e-k	8.487

Myrin-d-w-q-a-e-j	5.206	Myrin-d-w-u-q-a-e-k	8.523
Myrin-s-r-η-p-e-a-k	5.220	Myrin-s-w-u-p-b-e-k	8.534
Myrin-s-r-3-p-b-e-k	5.243	Myrin-d-w-u-q-b-f-j	8.710
Myrin-d-w-q-a-e-k	5.284	Myrin-s-w-u-p-a-f-k	8.814
Myrin-s-r-η-p-a-e-j	5.353	Myrin-s-w-u-p-b-f-k	8.827
Myrin-s-r-η-p-b-f-k	5.383	Myrin-d-w-u-q-a-f-j	8.861
Myrin-d-w-q-b-f-j	5.461	Myrin-s-w-u-q-a-f-k	8.874
Myrin-d-r-q-b-f-k	5.485	Myrin-d-w-u-q-a-f-k	9.028
Myrin-s-r-ε-q-a-f-k	5.511	Myrin-d-w-u-q-b-f-k	9.092
Myrin-d-w-q-b-e-k	5.536	Myrin-d-r-u-q-a-e-j	10.103
Myrin-s-r-ε-q-a-f-j	5.572	Myrin-s-r-u-q-b-e-j	10.266
Myrin-s-w-p-b-f-j	5.581	Myrin-d-r-u-q-a-f-j	10.513
Myrin-s-r-η-p-a-f-k	5.679	Myrin-s-r-u-q-a-e-j	11.089
Myrin-d-w-q-a-f-j	5.679	Myrin-s-r-u-q-a-e-k	11.112
Myrin-d-r-q-a-e-j	5.716	Myrin-s-r-u-q-a-f-j	11.389
Myrin-d-r-q-b-e-j	5.733	Myrin-s-r-u-q-a-f-k	11.473
Myrin-d-r-q-a-e-k	5.743		

Table 5.3. Relative energy corrected for ZPE (sum of electronic and zero-point energies, $\Delta E_{corrected}$, kcal/mol), ZPE correction to the electronic energy (ZPE_{corr}, kcal/mol), relative Gibbs free energies (sum of electronic and thermal free energy, $\Delta G_{corrected}$) and its thermal correction (G_{corr}), for the conformers of myristinin A listed in table 5.4.

HF/6-31G(d,p) results in vacuo. The corrected energies and corresponding corrections are from harmonic-approximation frequency calculations. The conformers are listed in order of increasing uncorrected relative energy. The absolute values for the lower energy conformer are -1796.365514 hartree ($\Delta E_{corrected}$) and -1796.442006 hartree ($\Delta G_{corrected}$).

Conformer	$\Delta E_{corrected}$	ZPE_{corr}	$\Delta G_{corrected}$	G_{corr}
Myrin-d-r-η-p-a-e-j	0.000	454.135	0.000	406.134
Myrin-d-r-η-p-a-e-k	0.024	454.145	0.076	406.197
Myrin-d-r-η-p-a-f-j	0.341	454.052	0.305	406.017
Myrin-d-r-η-p-a-f-k	0.415	454.055	0.403	406.042
Myrin-d-r-η-p-b-e-k	1.329	454.459	1.444	406.574
Myrin-d-r-η-p-b-e-j	1.222	454.346	1.193	406.318
Myrin-s-w-ε-q-a-e-k	1.201	454.175	1.034	406.008
Myrin-s-w-ε-q-a-e-j	1.232	454.160	1.008	405.936
Myrin-d-r-η-p-b-f-j	1.381	454.304	1.274	406.198
Myrin-d-r-η-p-b-f-k	1.498	454.388	1.532	406.423
Myrin-s-w-ε-q-b-e-j	1.757	454.390	1.739	406.372
Myrin-s-w-ε-q-a-f-j	1.586	454.074	1.297	405.786
Myrin-s-w-ε-q-a-f-k	1.608	454.081	1.364	405.838
Myrin-s-w-u-q-b-e-k	1.980	454.363	1.872	406.256
Myrin-s-w-ε-q-b-f-k	2.163	454.314	2.009	406.160
Myrin-d-w-p-a-e-k	4.009	453.691	3.629	405.312
Myrin-d-w-p-a-f-j	4.155	453.637	3.756	405.238
Myrin-d-w-p-b-f-j	4.155	453.636	3.758	405.240
Myrin-d-r-η-u-p-a-e-j	4.634	454.109	4.585	406.061
Myrin-d-r-η-u-p-a-e-k	4.657	454.126	4.650	406.119
Myrin-s-r-ε-q-b-e-j	4.725	454.151	4.478	405.905

Myrin-s-r-ε-q-b-f-j	4.824	454.121	4.585	405.882
Myrin-d-w-p-a-f-k	4.334	453.622	3.923	405.211
Myrin-d-w-p-b-e-j	4.762	453.975	4.505	405.718
Myrin-d-r-q-b-f-j	4.817	453.971	4.671	405.825
Myrin-s-r-ε-q-b-f-k	4.981	454.085	4.653	405.757
Myrin-s-r-ε-q-a-e-k	4.899	454.000	4.617	405.718
Myrin-d-r-η-u-p-a-f-j	4.967	454.022	4.879	405.934
Myrin-d-w-p-b-e-k	4.971	453.963	4.598	405.590
Myrin-d-r-η-u-p-a-f-k	5.043	454.032	4.990	405.979
Myrin-s-r-ε-q-a-e-j	5.000	453.976	4.630	405.607
Myrin-d-w-q-b-e-j	5.018	453.987	4.850	405.819
Myrin-d-w-p-b-f-k	5.006	453.937	4.726	405.658
Myrin-d-w-q-a-e-j	4.792	453.720	4.202	405.130
Myrin-s-r-η-p-e-a-k	5.100	454.015	4.863	405.777
Myrin-s-r-η-p-b-e-k	5.219	454.111	4.869	405.761
Myrin-d-w-q-a-e-k	4.880	453.729	4.294	405.144
Myrin-s-r-η-p-a-e-j	5.208	453.989	4.906	405.687
Myrin-s-r-η-p -b-f-k	5.331	454.082	5.002	405.754
Myrin-d-w-q-b-f-j	5.264	453.938	5.075	405.749
Myrin-d-r-q-b-f-k	5.509	454.158	5.491	406.141
Myrin-s-r-ε-q-a-f-k	1.608	454.081	1.364	405.838
Myrin-d-w-q-b-e-k	5.346	453.945	5.101	405.700
Myrin-s-r-ε-q-a-f-j	5.331	453.894	4.855	405.418
Myrin-s-w-p-b-f-j	5.423	453.976	5.057	405.611
Myrin-s-r-η-p-a-f-k	5.471	453.926	5.179	405.635
Myrin-d-w-q-a-f-j	5.186	453.641	4.584	405.039
Myrin-d-r-q-a-e-j	5.331	453.750	4.897	405.316
Myrin-d-r-q-b-e-j	5.425	453.826	4.960	405.362
Myrin-d-r-q-a-e-k	5.368	453.760	4.953	405.345
Myrin-s-r-η-p-a-f-j	5.525	453.909	5.175	405.559
Myrin-d-w-q-a-f-k	5.327	453.642	4.717	405.033
Myrin-d-w-q-b-f-k	5.624	453.890	5.351	405.617

Table 5.4. Parameters of the first IHB of the calculated conformers of myristinin A having the same geometry of R and different geometries of the ring system.
HF/6-31G(d,p) results *in vacuo*. For d-type conformers, the first IHB is H15···O14; for s-type conformers, the first IHB is H17···O14. The conformers are arranged in order of increasing relative energy.

Conformer	Parameters of the first IHB		
	OH···O (Å)	O···O (Å)	OHO (°)
Myrin-d-r-η-p-a-e-j	1.652	2.508	146.4
Myrin-d-r-η-p-a-e-k	1.652	2.508	146.3
Myrin-d-r-η-p-a-f-j	1.652	2.508	146.4

Myrin-d-r-η-p-a-f-k	1.652	2.508	146.4
Myrin-d-r-η-p-b-e-k	1.651	2.508	146.6
Myrin-d-r-η-p-b-e-j	1.655	2.510	146.2
Myrin-s-w-ε-q-a-e-k	1.684	2.522	143.9
Myrin-s-w-ε-q-a-e-j	1.683	2.521	143.9
Myrin-d-r-η-p-b-f-j	1.655	2.510	146.2
Myrin-d-r-η-p-b-f-k	1.651	2.508	146.5
Myrin-s-w-ε-q-b-e-j	1.689	2.527	144.0
Myrin-s-w-ε-q-a-f-j	1.682	2.520	143.9
Myrin-s-w-ε-q-a-f-k	1.683	2.521	143.9
Myrin-s-w-ε-q-b-f-k	1.689	2.526	144.0
Myrin-d-w-p-a-e-k	1.656	2.511	146.2
Myrin-d-w-p-a-f-j	1.656	2.511	146.3
Myrin-d-w-p-b-f-j	1.655	2.510	146.3
Myrin-d-r-η-u-p-a-e-j	1.675	2.523	145.4
Myrin-d-r-η-u-p-a-e-k	1.676	2.524	145.4
Myrin-s-r-ε-q-b-e-j	1.695	2.531	143.9
Myrin-s-r-ε-q-b-f-j	1.694	2.531	143.9
Myrin-d-w-p-a-f-k	1.656	2.511	146.2
Myrin-d-w-p-b-e-j	1.659	2.512	146.1
Myrin-d-r-q-b-f-j	1.657	2.510	145.9
Myrin-s-r-ε-q-b-f-k	1.694	2.531	143.9
Myrin-s-r-ε-q-a-e-k	1.692	2.527	143.8
Myrin-d-r-η-u-p-a-f-j	1.675	2.522	145.4
Myrin-d-w-p-b-e-k	1.658	2.512	146.2
Myrin-d-r-η-u-p-a-f-k	1.676	2.523	145.4
Myrin-s-r-ε-q-a-e-j	1.690	2.526	143.8
Myrin-d-w-q-b-e-j	1.664	2.514	145.6
Myrin-d-w-p-b-f-k	1.659	2.513	146.1
Myrin-d-w-q-a-e-j	1.654	2.508	146.1
Myrin-s-r-η-p-e-a-k	1.697	2.532	143.8
Myrin-s-r-η-p-b-e-k	1.692	2.528	143.8
Myrin-d-w-q-a-e-k	1.654	2.508	146.1
Myrin-s-r-η-p-a-e-j	1.697	2.532	143.8
Myrin-s-r-η-p-b-f-k	1.691	2.527	143.8
Myrin-d-w-q-b-f-j	1.665	2.515	145.6
Myrin-d-r-q-b-f-k	1.659	2.511	145.8
Myrin-s-r-ε-q-a-f-k	1.689	2.526	143.8
Myrin-d-w-q-b-e-k	1.664	2.514	145.6
Myrin-s-r-ε-q-a-f-j	1.688	2.524	143.9
Myrin-s-w-p-b-f-j	1.683	2.521	143.9
Myrin-s-r-η-p-a-f-k	1.696	2.532	143.8
Myrin-d-w-q-a-f-j	1.655	2.508	146.0
Myrin-d-r-q-a-e-j	1.646	2.503	146.4
Myrin-d-r-q-b-e-j	1.646	2.504	146.5

Myrin-d-r-q-a-e-k	1.646	2.503	146.4
Myrin-s-r-η-p-a-f-j	1.696	2.531	143.8
Myrin-d-w-q-a-f-k	1.656	2.509	146.0
Myrin-d-w-q-b-f-k	1.665	2.515	145.6
Myrin-s-w-p-a-e-j	1.689	2.526	143.7
Myrin-d-r-q-a-f-k	1.648	2.504	146.3
Myrin-s-r-η-u-p-a-e-j	1.737	2.560	142.4
Myrin-s-w-p-a-f-j	1.689	2.526	143.8
Myrin-s-r-η-p-b-e-j	1.691	2.527	143.8
Myrin-s-w-p-a-f-k	1.689	2.526	143.8
Myrin-s-r-η-u-p-a-f-j	1.738	2.560	142.4
Myrin-s-r-η-u-p-a-f-k	1.737	2.559	142.5
Myrin-d-r-q-b-e-k	1.646	2.504	146.5
Myrin-s-r-η-u-p-b-e-k	1.730	2.555	142.6
Myrin-s-r-η-u-p-b-f-k	1.731	2.555	142.6
Myrin-s-w-p-e-a-k	1.685	2.522	143.8
Myrin-d-w-u-p-a-e-j	1.682	2.527	145.3
Myrin-d-w-u-p-a-e-k	1.681	2.526	145.2
Myrin-d-w-u-p-b-e-k	1.681	2.526	145.2
Myrin-d-w-u-p-a-f-j	1.682	2.527	145.3
Myrin-d-w-u-p-b-f-j	1.681	2.527	145.3
Myrin-d-w-u-p-a-f-k	1.682	2.528	145.3
Myrin-d-w-u-p-b-f-k	1.682	2.528	145.3
Myrin-s-w-u-p-e-a-k	1.730	2.553	142.4
Myrin-s-w-p-b-e-j	1.725	2.551	142.6
Myrin-s-w-u-p-a-e-j	1.730	2.554	142.5
Myrin-s-w-u-q-a-e-j	1.732	2.555	142.4
Myrin-s-w-u-q-b-e-j	1.729	2.554	142.6
Myrin-d-w-u-q-b-e-j	1.694	2.532	144.4
Myrin-d-w-u-q-a-e-j	1.686	2.527	144.7
Myrin-s-w-u-p-b-f-j	1.726	2.551	142.6
Myrin-s-w-u-q-a-e-k	1.732	2.556	142.4
Myrin-d-w-u-q-a-e-k	1.685	2.526	144.7
Myrin-s-w-u-p-b-e-k	1.725	2.550	142.6
Myrin-s-w-u-p-a-f-k	1.729	2.553	142.5
Myrin-s-w-u-p-b-f-k	1.726	2.551	142.6
Myrin-d-w-u-q-a-f-j	1.689	2.529	144.5
Myrin-s-w-u-q-a-f-k	1.731	2.555	142.5
Myrin-d-w-u-q-a-f-k	1.688	2.528	144.5
Myrin-d-w-u-q-b-f-k	1.696	2.534	144.3
Myrin-d-r-u-q-a-e-j	1.676	2.524	145.5
Myrin-s-r-u-q-b-e-j	1.739	2.561	142.4
Myrin-d-r-u-q-a-f-j	1.677	2.523	145.4
Myrin-s-r-u-q-a-e-j	1.739	2.561	142.4
Myrin-s-r-u-q-a-e-k	1.740	2.562	142.4

Myrin-s-r-u-q-a-f-j	1.737	2.560	142.4
Myrin-s-r-u-q-a-f-k	1.738	2.560	142.4

Table 5.5 Distance between the H atom and the closest C atom in the acceptor aromatic ring for the O–H···π interactions of the calculated conformers of myristinin A having the same geometry of R and different geometries of the ring system.
HF/6-31G(d,p) results *in vacuo*. The conformers are arranged in order of increasing relative energy. For p-type conformers, the distance considered is H16···C23; for q-type conformers, the distance considered is H15···C23.

Conformer	H15···C23 or H16···C23 (Å)	Conformer	H15···C23 or H16···C23 (Å)
Myrin-d-r-η-p-a-e-j	2.128	Myrin-s-r-ε-q-b-f-k	2.171
Myrin-d-r-η-p-a-e-k	2.127	Myrin-s-r-ε-q-a-e-k	2.057
Myrin-d-r-η-p-a-f-j	2.131	Myrin-d-r-η-u-p-a-f-j	2.131
Myrin-d-r-η-p-a-f-k	2.130	Myrin-d-r-η-u-p-a-f-k	2.130
Myrin-d-r-η-p-b-e-k	2.213	Myrin-s-r-ε-q-a-e-j	2.058
Myrin-d-r-η-p-b-e-j	2.236	Myrin-s-r-η-p-e-a-k	2.109
Myrin-s-w-ε-q-a-e-k	2.074	Myrin-s-r-η-p-b-e-k	2.220
Myrin-s-w-ε-q-a-e-j	2.074	Myrin-s-r-η-p-a-e-j	2.109
Myrin-d-r-η-p-b-f-j	2.239	Myrin-s-r-η-p-b-f-k	2.221
Myrin-d-r-η-p-b-f-k	2.219	Myrin-s-r-ε-q-a-f-k	2.059
Myrin-s-w-ε-q-b-e-j	2.185	Myrin-s-r-ε-q-a-f-j	2.060
Myrin-s-w-ε-q-a-f-j	2.076	Myrin-s-r-η-p-a-f-k	2.111
Myrin-s-w-ε-q-a-f-k	2.075	Myrin-s-r-η-p-a-f-j	2.112
Myrin-s-w-ε-q-b-f-k	2.187	Myrin-s-r-η-u-p-a-e-j	2.121
Myrin-d-r-η-u-p-a-e-j	2.128	Myrin-s-r-η-u-p-a-f-j	2.122
Myrin-d-r-η-u-p-a-e-k	2.128	Myrin-s-r-η-u-p-a-f-k	2.123
Myrin-s-r-ε-q-b-e-j	2.165	Myrin-s-r-η-u-p-b-e-k	2.237
Myrin-s-r-ε-q-b-f-j	2.169	Myrin-s-r-η-u-p-b-f-k	2.240

Table 5.6. Vibrational frequencies (harmonic approximation) of the O–H bonds of the lower energy conformers of myristinin A having the same geometry of R and different geometries of the ring system.

HF/6-31G(d,p) results *in vacuo*. The frequency values have been scaled by 0.8992, as recommended for HF/6-31G(d,p) calculations [184]. The conformers are arranged in order of increasing relative energy.

Conformer	Vibrational frequencies (cm^{-1})				
	O8–H15	O10–H16	O12–H17	O44–H50	O51–H52
Myrin-d-r-η-p-a-e-j	3397.26	3704.41	3762.01	3769.59	3773.51
Myrin-d-r-η-p-a-e-k	3397.63	3702.76	3762.06	3769.34	3773.30
Myrin-d-r-η-p-a-f-j	3397.05	3707.49	3761.97	3772.94	3773.45
Myrin-d-r-η-p-a-f-k	3397.87	3705.90	3762.02	3773.03	3773.54
Myrin-d-r-η-p-b-e-k	3399.88	3703.12	3762.23	3770.87	3773.29
Myrin-d-r-η-p-b-e-j	3410.45	3709.01	3762.57	3770.54	3772.99
Myrin-s-w-ε-q-a-e-k	3682.96	3764.20	3460.45	3768.80	3772.85
Myrin-s-w-ε-q-a-e-j	3684.84	3764.10	3459.81	3769.05	3773.38
Myrin-d-r-η-p-b-f-j	3410.79	3710.26	3762.55	3772.66	3772.99
Myrin-d-r-η-p-b-f-k	3401.29	3705.23	3762.25	3772.69	3772.99
Myrin-s-w-ε-q-b-e-j	3695.37	3765.93	3466.51	3770.03	3773.37
Myrin-s-w-ε-q-a-f-j	3688.12	3764.10	3458.21	3772.49	3773.29
Myrin-s-w-ε-q-a-f-k	3686.24	3764.20	3459.27	3772.58	3773.08
Myrin-s-w-u-q-b-e-k	3693.60	3766.12	3465.93	3769.94	3773.91
Myrin-s-w-ε-q-b-f-k	3694.94	3766.09	3466.06	3772.17	3774.01
Myrin-d-w-p-a-e-k	3415.31	3770.84	3765.98	3772.69	3774.20
Myrin-d-w-p-a-f-j	3414.24	3770.99	3765.89	3773.73	3775.19
Myrin-d-w-p-b-f-j	3414.24	3770.99	3765.89	3775.19	3773.73
Myrin-d-r-η-u-p-a-e-j	3456.02	3707.73	3824.57	3769.60	3773.55
Myrin-d-r-η-u-p-a-e-k	3457.90	3706.01	3825.28	3769.37	3773.29
Myrin-s-r-ε-q-b-e-j	3701.86	3807.55	3486.86	3769.19	3771.57
Myrin-s-r-ε-q-b-f-j	3486.67	3806.53	3486.67	3770.89	3771.51
Myrin-d-w-p-a-f-k	3415.30	3771.08	3765.92	3775.26	3774.42
Myrin-d-w-p-b-e-j	3425.62	3772.01	3766.46	3773.02	3773.37
Myrin-d-r-q-b-f-j	3409.45	3762.18	3789.99	3774.40	3772.12
Myrin-s-r-ε-q-b-f-k	3701.58	3806.76	3486.31	3770.98	3772.53
Myrin-s-r-ε-q-a-e-k	3696.58	3815.75	3482.05	3767.81	3772.10
Myrin-d-r-η-u-p-a-f-j	3455.10	3710.80	3824.02	3772.94	3773.47
Myrin-d-w-p-b-e-k	3425.14	3771.95	3766.36	3773.02	3774.58
Myrin-d-r-η-u-p-a-f-k	3456.99	3709.09	3824.75	3773.04	3773.50
Myrin-s-r-ε-q-a-e-j	3698.13	3816.19	3480.39	3768.06	3772.98
Myrin-d-w-q-b-e-j	3430.99	3774.28	3766.53	3773.21	3773.03
Myrin-d-w-p-b-f-k	3426.72	3772.19	3766.46	3775.10	3773.35
Myrin-d-w-q-a-e-j	3412.54	3772.81	3766.62	3773.00	3774.07
Myrin-s-r-η-p-e-a-k	3815.81	3725.35	3491.71	3768.09	3772.06
Myrin-s-r-η-p-b-e-k	3806.84	3722.94	3483.47	3769.31	3772.67
Myrin-d-w-q-a-e-k	3413.47	3772.70	3766.58	3772.95	3774.13

Myrin-s-r-η-p-a-e-j	3816.35	3727.04	3491.19	3768.33	3773.02
Myrin-s-r-η-p -b-f-k	3805.90	3724.40	3481.89	3771.07	3772.71
Myrin-d-w-q-b-f-j	3433.23	3774.28	3766.50	3775.44	3773.01
Myrin-d-r-q-b-f-k	3416.27	3789.81	3762.08	3774.37	3772.12
Myrin-s-r-ε-q-a-f-k	3699.13	3815.62	3479.54	3771.54	3772.34
Myrin-d-w-q-b-e-k	3431.14	3774.38	3766.61	3773.12	3775.02
Myrin-s-r-ε-q-a-f-j	3700.71	3815.95	3477.63	3771.42	3772.88
Myrin-s-w-p-b-f-j	3796.09	3764.20	3459.24	3773.72	3771.84
Myrin-s-r-η-p-a-f-k	3815.88	3727.88	3490.98	3771.69	3772.30
Myrin-d-w-q-a-f-j	3415.85	3772.81	3766.68	3773.97	3775.89
Myrin-d-r-q-a-e-j	3389.21	3798.56	3762.26	3772.31	3773.66
Myrin-d-r-q-b-e-j	3383.46	3794.50	3762.03	3772.11	3773.93
Myrin-d-r-q-a-e-k	3416.27	3789.81	3762.08	3774.37	3772.12
Myrin-s-r-η-p-a-f-j	3816.38	3729.61	3490.60	3771.60	3772.93
Myrin-d-w-q-a-f-k	3416.28	3772.91	3766.63	3775.98	3774.33
Myrin-d-w-q-b-f-k	3432.76	3774.42	3766.59	3775.53	3775.10

Table 5.7. Red shift of the vibrational frequencies of the O8–H15, O10–H16 and O12–H17 bonds in the conformers of myristinin A listed in table 5.5, when they are engaged in IHBs (O8–H15···O14, O12–H17···O14 and O10–H16···π).
HF/6-31G(d,p) results *in vacuo*.

Conformer	Red shift (cm^{-1})		
	O8–H15	O10–H16	O12–H17
Myrin-d-r-η-p-a-e-j	413.20	80.25	
Myrin-d-r-η-p-a-e-k	412.83	81.90	
Myrin-d-r-η-p-a-f-j	413.41	77.17	
Myrin-d-r-η-p-a-f-k	412.59	78.76	
Myrin-d-r-η-p-b-e-k	410.58	81.54	
Myrin-d-r-η-p-b-e-j	400.01	75.65	
Myrin-s-w-ε-q-a-e-k	127.50	20.46	310.72
Myrin-s-w-ε-q-a-e-j	125.62	20.56	311.36
Myrin-d-r-η-p-b-f-j	399.67	74.40	
Myrin-d-r-η-p-b-f-k	409.17	79.43	
Myrin-s-w-ε-q-b-e-j	115.09	18.73	304.66
Myrin-s-w-ε-q-a-f-j	122.34	20.56	312.96
Myrin-s-w-ε-q-a-f-k	124.22	20.46	311.90
Myrin-s-w-ε-q-b-e-k	116.86	18.54	305.24
Myrin-s-w-ε-q-b-f-k	115.52	18.57	305.11
Myrin-d-w-p-a-e-k	395.15		
Myrin-d-w-p-a-f-j	396.22		
Myrin-d-w-p-b-f-j	396.22		
Myrin-d-r-η-u-p-a-e-j	354.44	76.93	
Myrin-d-r-η-u-p-a-e-k	352.56	78.65	
Myrin-s-r-ε-q-b-e-j	108.60		284.31
Myrin-s-r-ε-q-b-f-j	323.79		284.50

Myrin-d-w-p-a-f-k	395.16		
Myrin-d-w-p-b-e-j	384.84		
Myrin-d-r-q-b-f-j	401.01		
Myrin-s-r-ε-q-b-f-k	108.88		284.86
Myrin-s-r-ε-q-a-e-k	113.88		289.12
Myrin-d-r-η-u-p-a-f-j	355.36	73.86	
Myrin-d-w-p-b-e-k	385.32		
Myrin-d-r-η-u-p-a-f-k	353.47	75.57	
Myrin-s-r-ε-q-a-e-j	112.33		290.78
Myrin-d-w-q-b-e-j	379.47		
Myrin-d-w-p-b-f-k	383.74		
Myrin-d-w-q-a-e-j	397.92		
Myrin-s-r-η-p-e-a-k		59.31	279.46
Myrin-s-r-η-p-b-e-k		61.72	287.70
Myrin-d-w-q-a-e-k	396.99		
Myrin-s-r-η-p-a-e-j		57.62	279.98
Myrin-s-r-η-p-b-f-k		60.26	289.28
Myrin-d-w-q-b-f-j	377.23		
Myrin-d-r-q-b-f-k	394.19		
Myrin-s-r-ε-q-a-f-k	111.33		291.63
Myrin-d-w-q-b-e-k	379.32		
Myrin-s-r-ε-q-a-f-j	109.75		293.54
Myrin-s-w-p-b-f-j			311.93
Myrin-s-r-η-p-a-f-k		56.78	280.19
Myrin-d-w-q-a-f-j	394.61		
Myrin-d-r-q-a-e-j	421.25		
Myrin-d-r-q-b-e-j	427.00		
Myrin-d-r-q-a-e-k	394.19		
Myrin-s-r-η-p-a-f-j		55.05	280.57
Myrin-d-w-q-a-f-k	394.18		
Myrin-d-w-q-b-f-k	377.70		

Table 5.8. Dipole moments of the calculated conformers of myristinin A having the same geometry of R and different geometries of the ring system.
HF/6-31G(d,p) results *in vacuo*. The conformers are arranged in order of increasing relative energy.

Conformer	Dipole moment (Debye)	Conformer	Dipole moment (Debye)
Myrin-d-r-η-p-a-e-j	2.278	Myrin-d-r-q-a-e-k	4.715
Myrin-d-r-η-p-a-e-k	3.695	Myrin-s-r-η-p-a-f-j	7.092
Myrin-d-r-η-p-a-f-j	2.873	Myrin-d-w-q-a-f-k	9.326
Myrin-d-r-η-p-a-f-k	4.092	Myrin-d-w-q-b-f-k	9.019
Myrin-d-r-η-p-b-e-k	2.468	Myrin-s-w-p-a-e-j	4.341
Myrin-d-r-η-p-b-e-j	2.643	Myrin-d-r-q-a-f-k	6.037
Myrin-s-w-ε-q-a-e-k	2.792	Myrin-s-r-η-u-p-a-e-j	5.623
Myrin-s-w-ε-q-a-e-j	5.111	Myrin-s-w-p-a-f-j	3.386
Myrin-d-r-η-p-b-f-j	3.475	Myrin-s-r-η-p-b-e-j	7.585
Myrin-d-r-η-p-b-f-k	3.697	Myrin-s-w-p-a-f-k	0.958
Myrin-s-w-ε-q-b-e-j	4.746	Myrin-s-r-η-u-p-a-f-j	5.619
Myrin-s-w-ε-q-a-f-j	4.964	Myrin-s-r-η-u-p-a-f-k	3.965
Myrin-s-w-ε-q-a-f-k	2.640	Myrin-d-r-q-b-e-k	3.609
Myrin-s-w-u-q-b-e-k	4.227	Myrin-s-r-η-u-p-b-e-k	5.182
Myrin-s-w-ε-q-b-f-k	2.906	Myrin-s-r-η-u-p-b-f-k	4.482
Myrin-d-w-p-a-e-k	7.121	Myrin-s-w-p-e-a-k	3.169
Myrin-d-w-p-a-f-j	5.378	Myrin-d-w-u-p-a-e-j	3.572
Myrin-d-w-p-b-f-j	5.377	Myrin-d-w-u-p-a-e-k	6.300
Myrin-s-w-u-p-a-e-j	2.222	Myrin-d-w-u-p-b-e-k	6.300
Myrin-d-r-η-u-p-a-e-j	0.860	Myrin-d-w-u-p-a-f-j	4.952
Myrin-d-r-η-u-p-a-e-k	2.852	Myrin-d-w-u-p-b-f-j	4.953
Myrin-s-r-ε-q-b-e-j	7.629	Myrin-s-w-u-p-b-e-j	1.641
Myrin-s-r-ε-q-b-f-j	6.089	Myrin-d-w-u-p-a-f-k	7.142
Myrin-d-w-p-a-f-k	7.395	Myrin-d-w-u-p-b-f-k	7.141
Myrin-d-w-p-b-e-j	5.510	Myrin-s-w-u-p-e-a-k	2.906
Myrin-d-r-q-b-f-j	4.715	Myrin-s-w-p-b-e-j	1.575
Myrin-s-r-ε-q-b-f-k	4.321	Myrin-s-w-u-q-a-e-j	1.214
Myrin-s-r-ε-q-a-e-k	5.339	Myrin-s-w-u-q-b-e-j	1.239
Myrin-d-r-η-u-p-a-f-j	2.759	Myrin-d-w-u-q-b-e-j	4.067
Myrin-d-w-p-b-e-k	6.548	Myrin-d-w-u-q-a-e-j	4.215
Myrin-d-r-η-u-p-a-f-k	3.956	Myrin-s-w-u-p-b-f-j	2.385
Myrin-s-r-ε-q-a-e-j	7.754	Myrin-s-w-u-q-a-e-k	2.070
Myrin-d-w-q-b-e-j	5.856	Myrin-d-w-u-q-a-e-k	6.530
Myrin-d-w-p-b-f-k	6.559	Myrin-s-w-u-p-b-e-k	3.383
Myrin-d-w-q-a-e-j	6.251	Myrin-d-w-u-q-b-f-j	6.246
Myrin-s-r-η-p-e-a-k	5.269	Myrin-s-w-u-p-a-f-k	3.842
Myrin-s-r-η-p-b-e-k	6.633	Myrin-s-w-u-p-b-f-k	3.538
Myrin-d-w-q-a-e-k	7.703	Myrin-d-w-u-q-a-f-j	5.975
Myrin-s-r-η-p-a-e-j	7.718	Myrin-s-w-u-q-a-f-k	2.644
Myrin-s-r-η-p-b-f-k	4.877	Myrin-d-w-u-q-a-f-k	7.841
Myrin-d-w-q-b-f-j	7.831	Myrin-d-w-u-q-b-f-k	7.584
Myrin-d-r-q-b-f-k	4.738	Myrin-d-r-u-q-a-e-j	1.051
Myrin-s-r-ε-q-a-f-k	4.240	Myrin-s-r-u-q-b-e-j	4.530
Myrin-d-w-q-b-e-k	7.463	Myrin-d-r-q-a-f-j	5.058

Myrin-s-r-ε-q-a-f-j	6.978	Myrin-d-r-u-q-a-f-j	2.730
Myrin-s-w-p-b-f-j	2.483	Myrin-s-r-u-q-a-e-j	4.530
Myrin-s-r-η-p-a-f-k	4.414	Myrin-s-r-u-q-a-e-k	3.122
Myrin-d-w-q-a-f-j	8.066	Myrin-s-r-u-q-a-f-j	3.559
Myrin-d-r-q-a-e-j	3.511	Myrin-s-r-u-q-a-f-k	1.343
Myrin-d-r-q-b-e-j	3.340		

Table 5.9. HOMO-LUMO energy gap of the calculated conformers of myristinin A having the same geometry of R and different geometries of the ring system.
HF/6-31G(d,p) results *in vacuo*. The conformers are arranged in order of increasing relative energy.

Conformer	HOMO-LUMO energy gap (kcal/mol)	Conformer	HOMO-LUMO energy gap (kcal/mol)
Myrin-d-r-η-p-a-e-j	257.479	Myrin-s-r-η-p-a-f-j	259.977
Myrin-d-r-η-p-a-e-k	257.574	Myrin-d-w-q-a-f-k	241.710
Myrin-d-r-η-p-a-f-j	256.319	Myrin-d-w-q-b-f-k	242.846
Myrin-d-r-η-p-a-f-k	256.494	Myrin-s-w-p-a-e-j	252.215
Myrin-d-r-η-p-b-e-k	254.693	Myrin-d-r-q-a-f-k	247.797
Myrin-d-r-η-p-b-e-j	255.942	Myrin-s-r-η-u-p-a-e-j	251.537
Myrin-s-w-ε-q-a-e-k	258.854	Myrin-s-w-p-a-f-j	253.143
Myrin-s-w-ε-q-a-e-j	258.816	Myrin-s-r-η-p-b-e-j	260.328
Myrin-d-r-η-p-b-f-j	256.099	Myrin-s-w-p-a-f-k	252.679
Myrin-d-r-η-p-b-f-k	255.170	Myrin-s-r-η-u-p-a-f-j	250.840
Myrin-s-w-ε-q-b-e-j	258.678	Myrin-s-r-η-u-p-a-f-k	250.972
Myrin-s-w-ε-q-a-f-j	258.101	Myrin-d-r-q-b-e-k	248.751
Myrin-s-w-ε-q-a-f-k	258.207	Myrin-s-r-η-u-p-b-e-k	250.903
Myrin-s-w-u-q-b-e-k	258.345	Myrin-s-r-η-u-p-b-f-k	251.129
Myrin-s-w-ε-q-b-f-k	258.308	Myrin-s-w-p-e-a-k	253.043
Myrin-d-w-p-a-e-k	242.815	Myrin-d-w-u-p-a-e-j	237.594
Myrin-d-w-p-a-f-j	244.503	Myrin-d-w-u-p-a-e-k	236.916
Myrin-d-w-p-b-f-j	244.503	Myrin-d-w-u-p-b-e-k	236.922
Myrin-d-r-η-u-p-a-e-j	251.650	Myrin-d-w-u-p-a-f-j	238.742
Myrin-d-r-η-u-p-a-e-k	251.732	Myrin-d-w-u-p-b-f-j	238.742
Myrin-s-r-ε-q-b-e-j	260.868	Myrin-s-w-u-p-b-e-j	240.010
Myrin-s-r-ε-q-b-f-j	260.768	Myrin-d-w-u-p-a-f-k	238.202
Myrin-d-w-p-a-f-k	243.963	Myrin-d-w-u-p-b-f-k	238.196
Myrin-d-w-p-b-e-j	243.091	Myrin-s-w-u-p-e-a-k	238.723
Myrin-d-r-q-b-f-j	249.918	Myrin-s-w-p-b-e-j	239.702
Myrin-s-r-ε-q-b-f-k	260.705	Myrin-s-w-u-p-a-e-j	239.326
Myrin-s-r-ε-q-a-e-k	261.056	Myrin-s-w-u-q-a-e-j	240.229
Myrin-d-r-η-u-p-a-f-j	250.589	Myrin-s-w-u-q-b-e-j	240.305
Myrin-d-w-p-b-e-k	242.426	Myrin-d-w-u-q-b-e-j	237.211
Myrin-d-r-η-u-p-a-f-k	250.771	Myrin-d-w-u-q-a-e-j	236.000
Myrin-s-r-ε-q-a-e-j	260.975	Myrin-s-w-u-p-b-f-j	240.876
Myrin-d-w-q-b-e-j	242.413	Myrin-s-w-u-q-a-e-k	239.658
Myrin-d-w-p-b-f-k	243.932	Myrin-d-w-u-q-a-e-k	235.410

Myrin-d-w-q-a-e-j	241.070	Myrin-s-w-u-p-b-e-k	239.439
Myrin-s-r-ɳ-p-e-a-k	260.498	Myrin-d-w-u-q-b-f-j	238.127
Myrin-s-r-ɳ-p-b-e-k	260.128	Myrin-s-w-u-p-a-f-k	239.878
Myrin-d-w-q-a-e-k	240.518	Myrin-s-w-u-p-b-f-k	240.298
Myrin-s-r-ɳ-p-a-e-j	260.435	Myrin-d-w-u-q-a-f-j	237.255
Myrin-s-r-ɳ-p-b-f-k	260.128	Myrin-s-w-u-q-a-f-k	240.807
Myrin-d-w-q-b-f-j	243.323	Myrin-d-w-u-q-a-f-k	236.652
Myrin-d-r-q-b-f-k	249.504	Myrin-d-w-u-q-b-f-k	237.644
Myrin-s-r-ε-q-a-f-k	260.586	Myrin-d-r-u-q-a-e-j	242.287
Myrin-d-w-q-b-e-k	241.936	Myrin-s-r-u-q-b-e-j	246.404
Myrin-s-r-ε-q-a-f-j	260.473	Myrin-d-r-q-a-f-j	248.362
Myrin-s-w-p-b-f-j	253.620	Myrin-d-r-u-q-a-f-j	243.492
Myrin-s-r-ɳ-p-a-f-k	260.077	Myrin-s-r-u-q-a-e-j	246.404
Myrin-d-w-q-a-f-j	242.275	Myrin-s-r-u-q-a-e-k	245.889
Myrin-d-r-q-a-e-j	247.144	Myrin-s-r-u-q-a-f-j	247.377
Myrin-d-r-q-b-e-j	249.203	Myrin-s-r-u-q-a-f-k	246.900
Myrin-d-r-q-a-e-k	246.592		

Figure 5.7. Shapes of the HOMO and LUMO molecular orbitals of the calculated conformers of myristinin A having the same geometry of R and different geometries of the ring system *in vacuo*.
HF/6-31G(d,p) results. The conformers are listed in order of increasing relative energy.

HOMO	LUMO	HOMO	LUMO
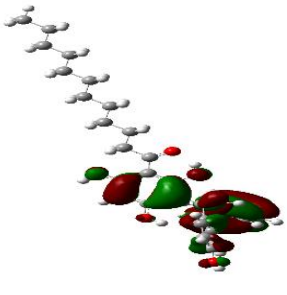	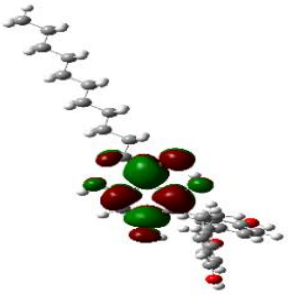		
Myrin-d-r-η-p-a-e-j		Myrin-s-r-η-p-a-f-j	
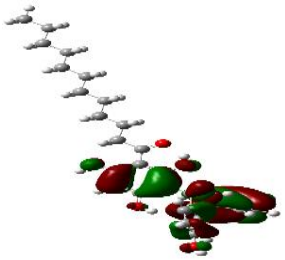	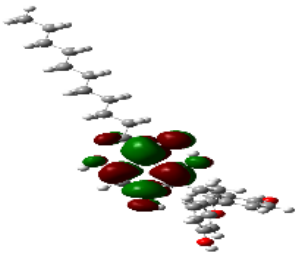	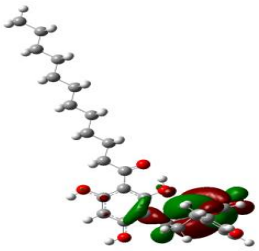	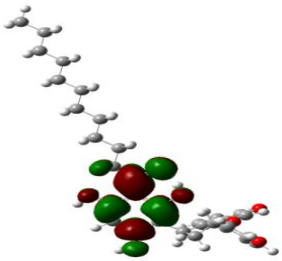
Myrin-d-r-η-p-a-e-k		Myrin-d-w-q-a-f-k	
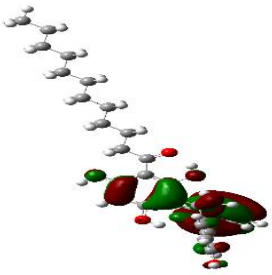	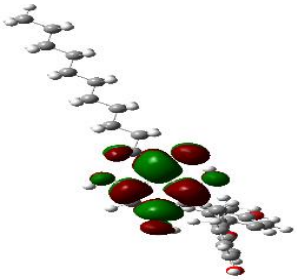	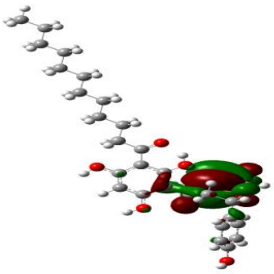	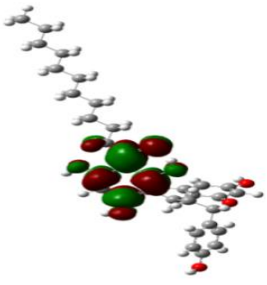
Myrin-d-r-η-p-a-f-j		Myrin-d-w-q-b-f-k	
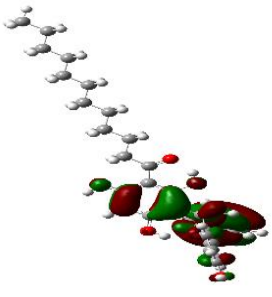	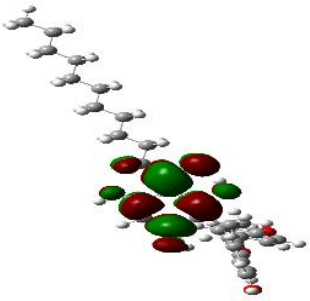		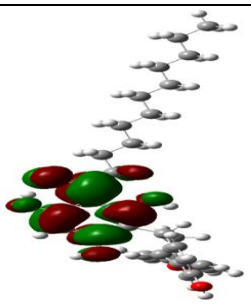
Myrin-d-r-η-p-a-f-k		Myrin-s-w-p-a-e-j	
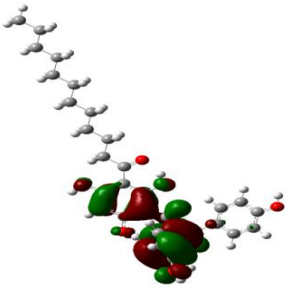	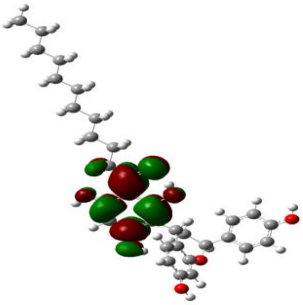	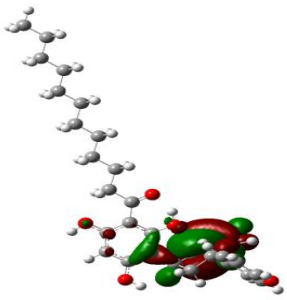	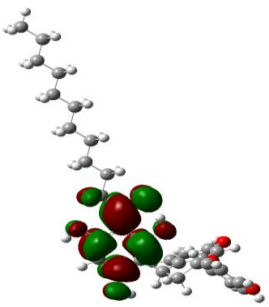

Myrin-d-r-η-p-b-e-k		Myrin-d-r-q-a-f-k	
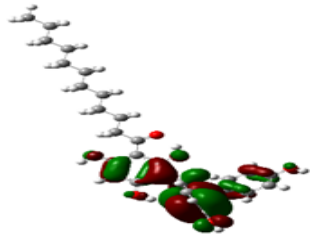	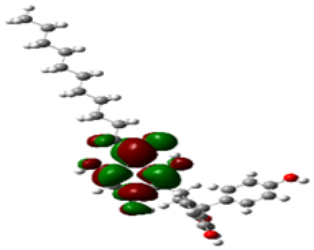	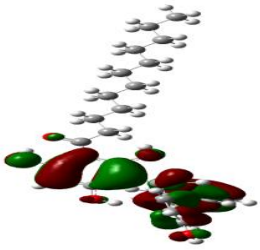	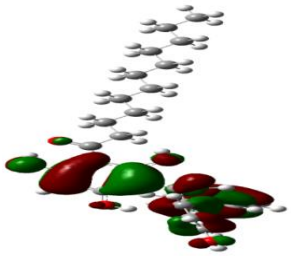
Myrin-d-r-η-p-b-e-j		Myrin-s-r-η-u-p-a-e-j	
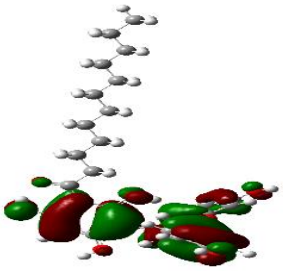	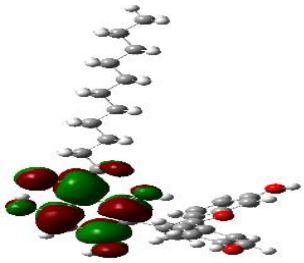	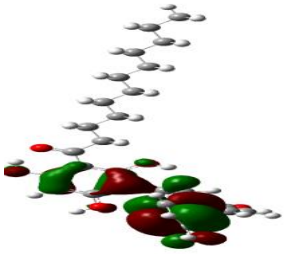	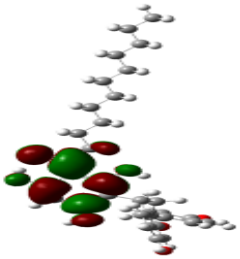
Myrin-s-w-ε-q-a-e-k		Myrin-s-w-p-a-f-j	
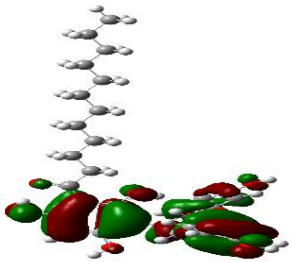	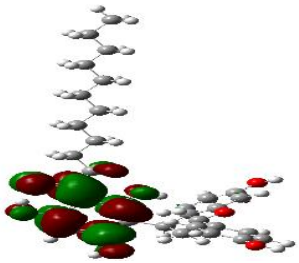	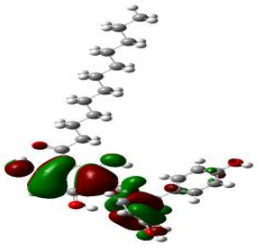	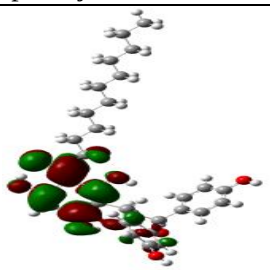
Myrin-s-w-ε-q-a-e-j		Myrin-s-r-η-p-b-e-j	
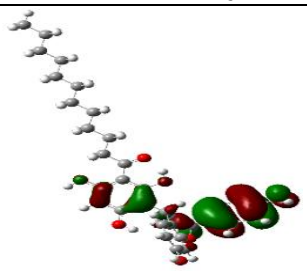	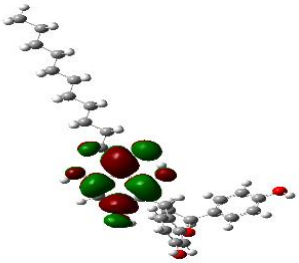	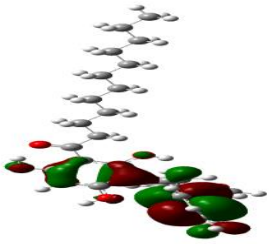	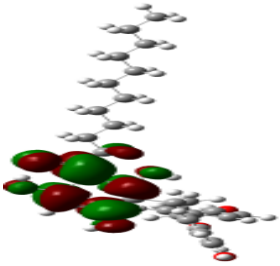
Myrin-d-r-η-p-b-f-j		Myrin-s-w-p-a-f-k	
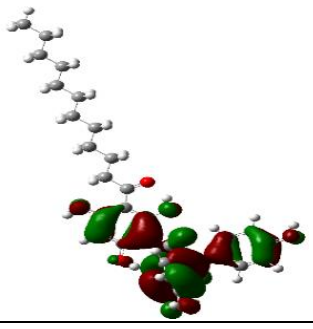	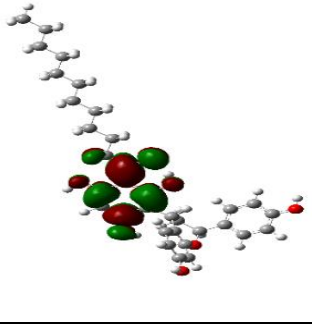		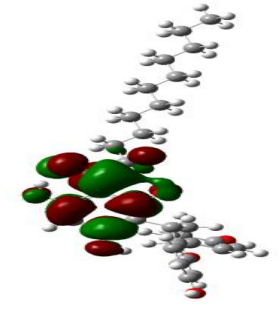
Myrin-d-r-η-p-b-f-k		Myrin-s-r-η-u-p-a-f-j	

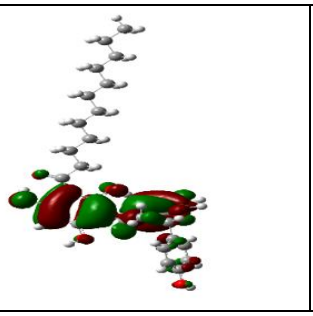 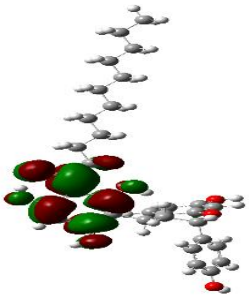	 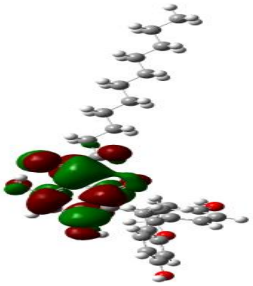
Myrin-s-w-ε-q-b-e-j	Myrin-s-r-η-u-p-a-f-k
 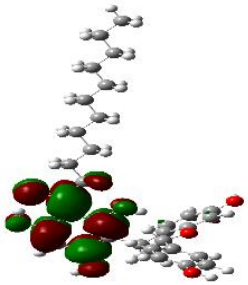	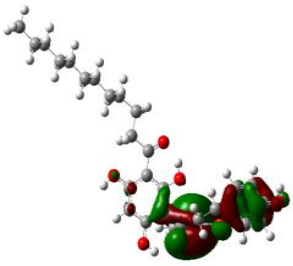 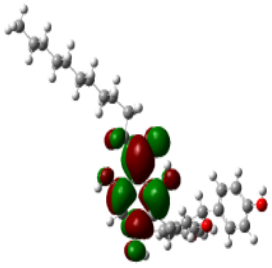
Myrin-s-w-ε-q-a-f-j	Myrin-d-r-q-b-e-k
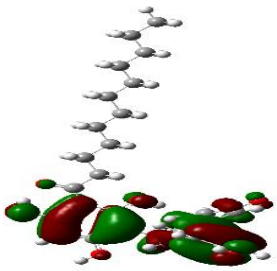 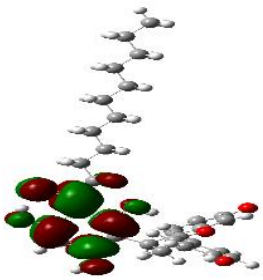	 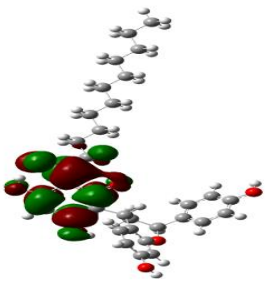
Myrin-s-w-ε-q-a-f-k	Myrin-s-r-η-u-p-b-e-k
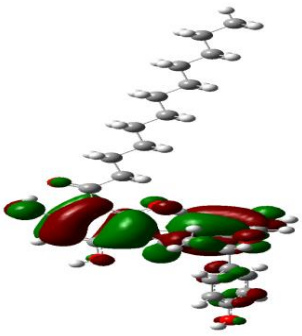 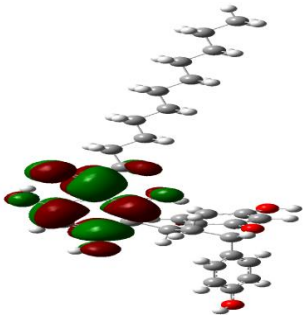	 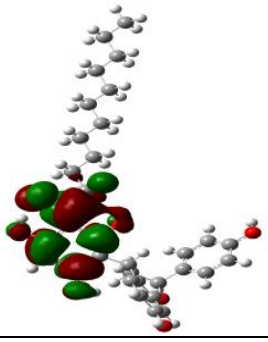
Myrin-s-w-ε-q-b-e-k	Myrin-s-r-η-u-p-b-f-k
 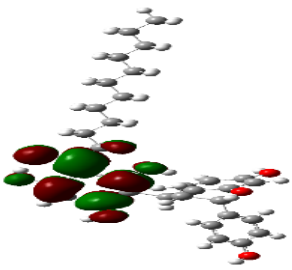	 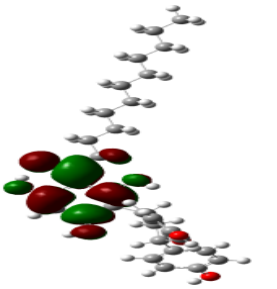
Myrin-s-w-ε-q-b-f-k	Myrin-s-w-p-e-a-k

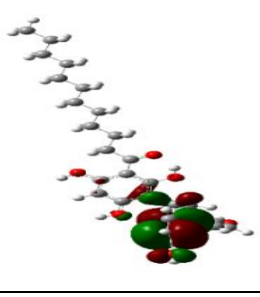 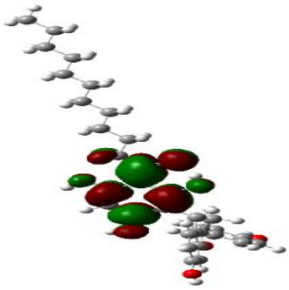	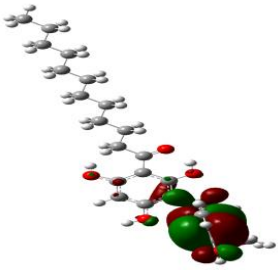 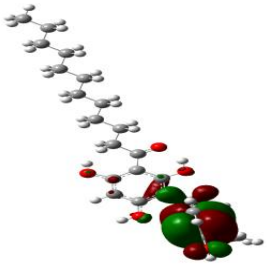
Myrin-d-w-p-a-e-k	Myrin-d-w-u-p-a-e-j
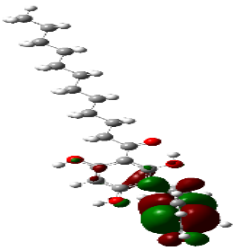 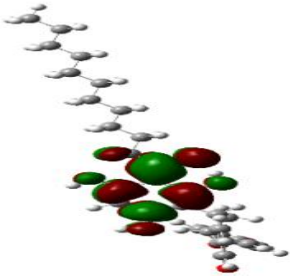	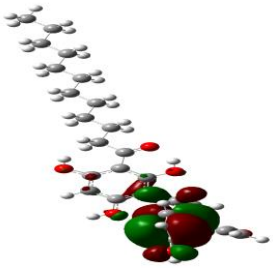 
Myrin-d-w-p-a-f-j	Myrin-d-w-u-p-a-e-k
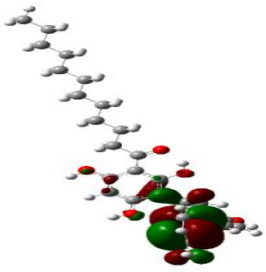 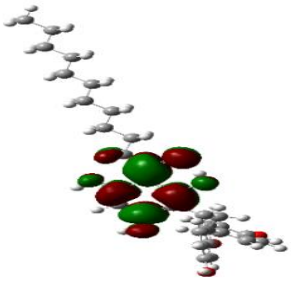	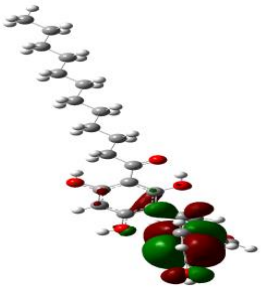 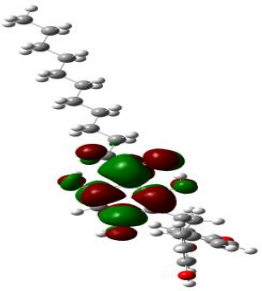
Myrin-d-w-p-b-f-j	Myrin-d-w-u-p-b-e-k
 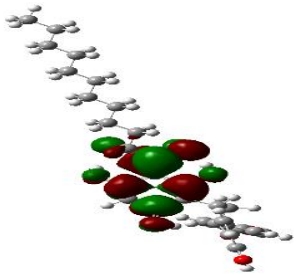	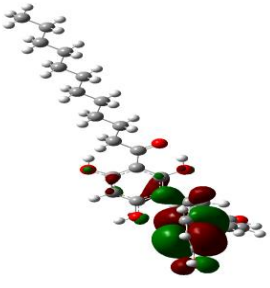 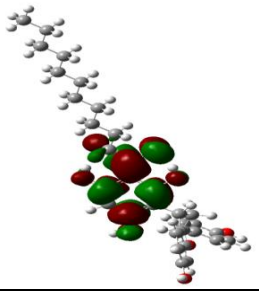
Myrin-d-r-η-u-p-a-e-j	Myrin-d-w-u-p-a-f-j
 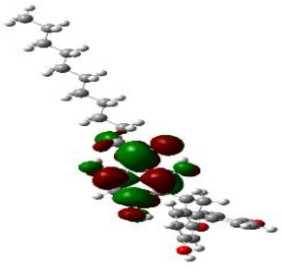	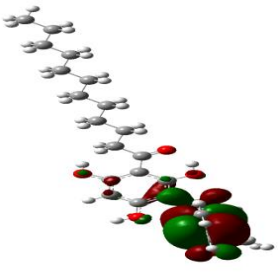 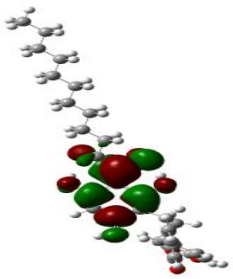
Myrin-d-r-η-u-p-a-e-k	Myrin-d-w-u-p-b-f-j

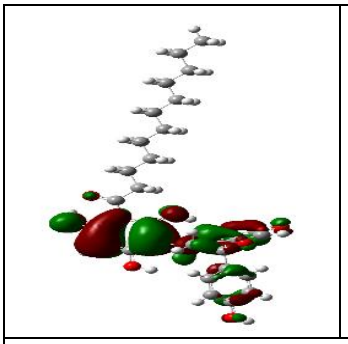	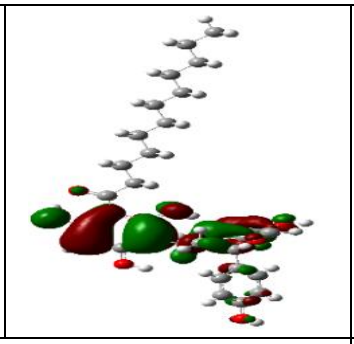
Myrin-s-r-ε-q-b-e-j	
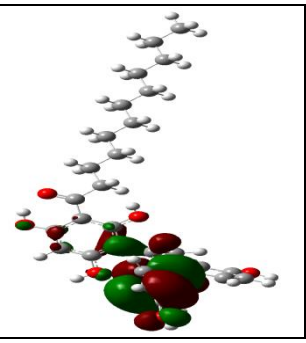	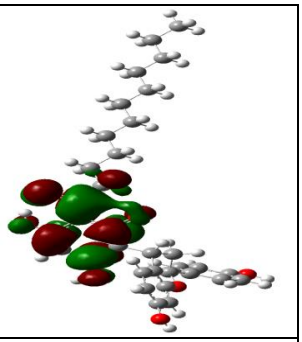
Myrin-s-w-u-p-a-f-j	
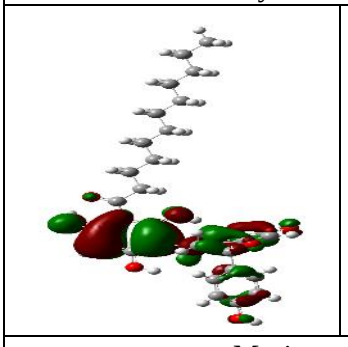	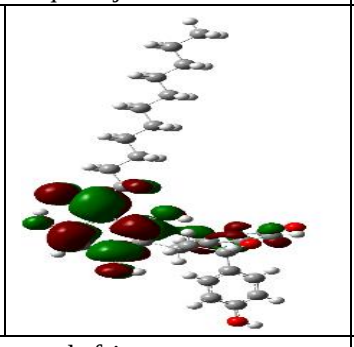
Myrin-s-r-ε-q-b-f-j	
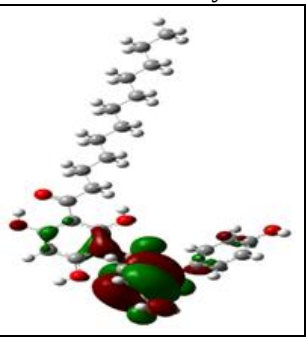	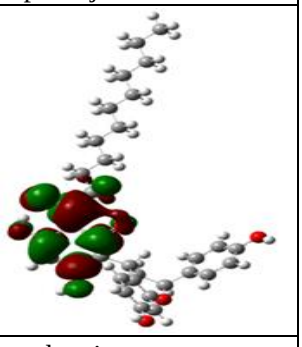
Myrin-s-w-u-p-b-e-j	
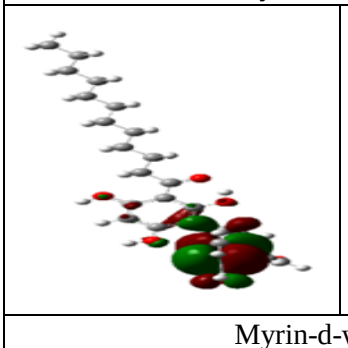	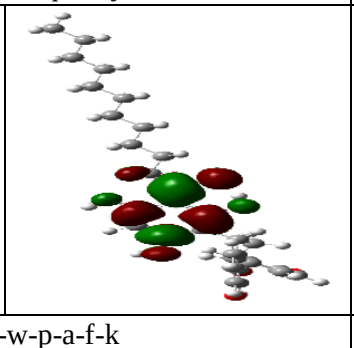
Myrin-d-w-p-a-f-k	
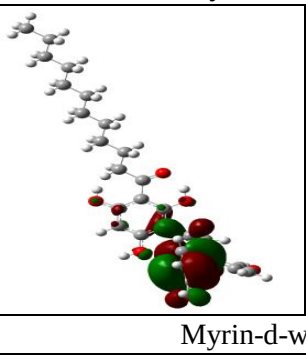	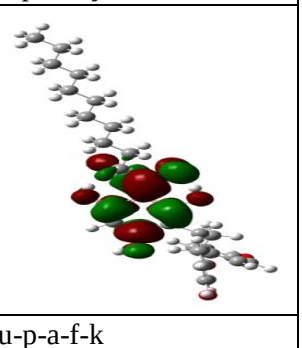
Myrin-d-w-u-p-a-f-k	
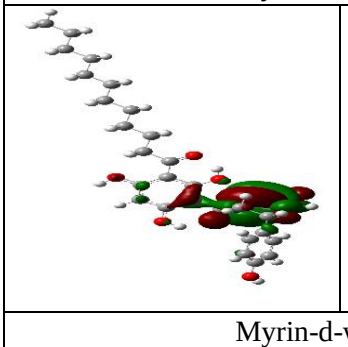	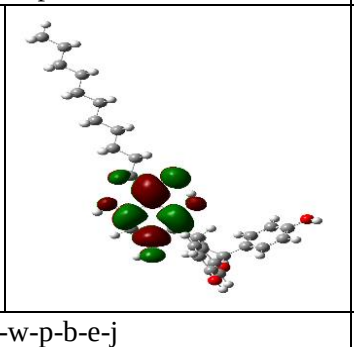
Myrin-d-w-p-b-e-j	
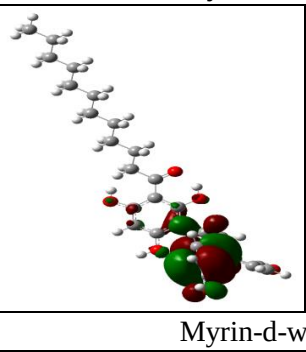	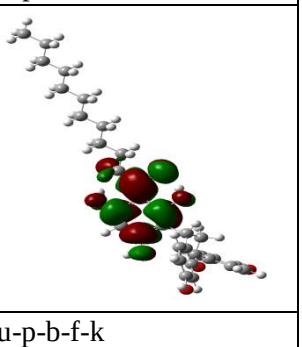
Myrin-d-w-u-p-b-f-k	
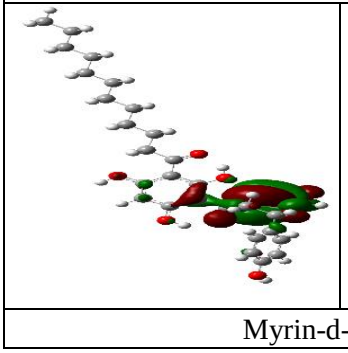	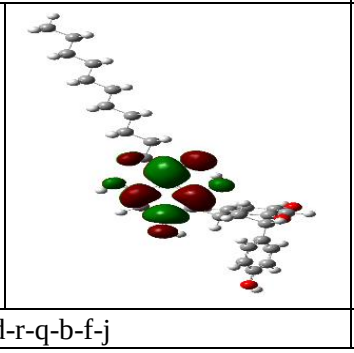
Myrin-d-r-q-b-f-j	
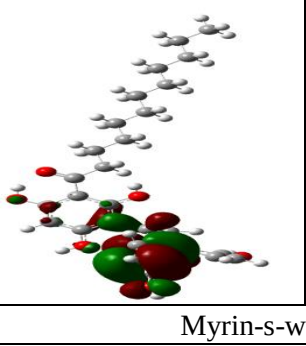	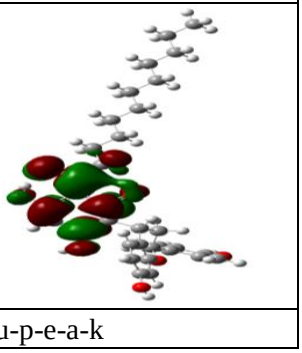
Myrin-s-w-u-p-e-a-k	

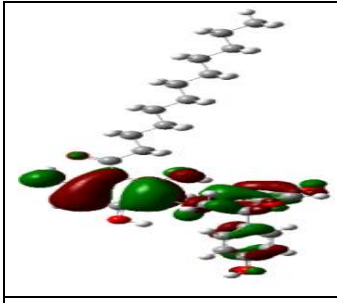	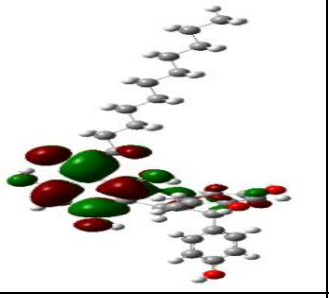
Myrin-s-r-ε-q-b-f-k	Myrin-s-w-p-b-e-j
	
Myrin-s-r-ε-q-a-e-k	Myrin-s-w-u-p-a-e-j
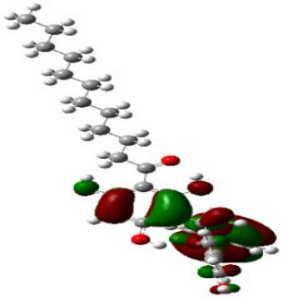	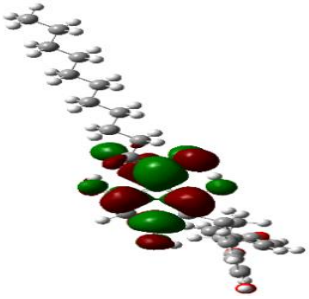
Myrin-d-r-η-u-p-a-f-j	Myrin-s-w-u-q-a-e-j
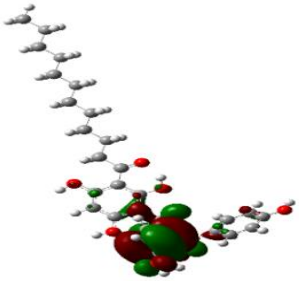	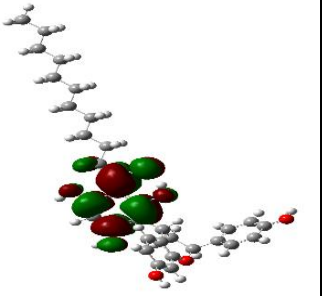
Myrin-d-w-p-b-e-k	Myrin-s-w-u-q-b-e-j
	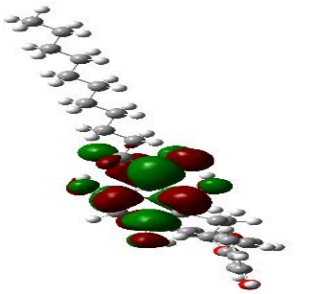
Myrin-d-r-η-u-p-a-f-k	Myrin-d-w-u-q-b-e-j

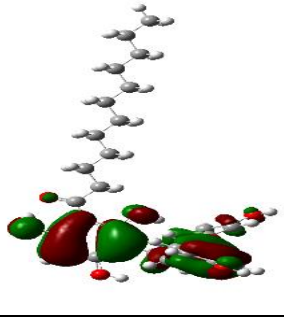	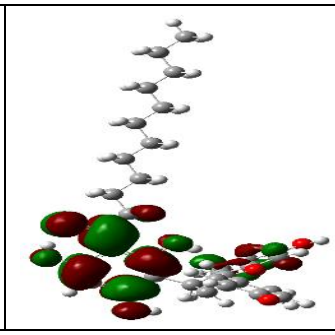
Myrin-s-r-ε-q-a-e-j	Myrin-d-w-u-q-a-e-j
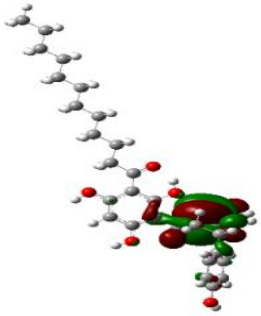	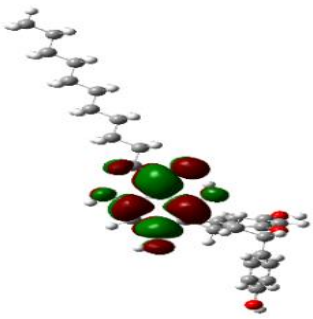
Myrin-d-w-q-b-e-j	Myrin-s-w-u-p-b-f-j
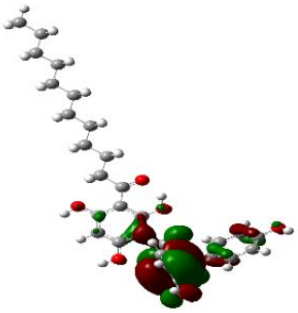	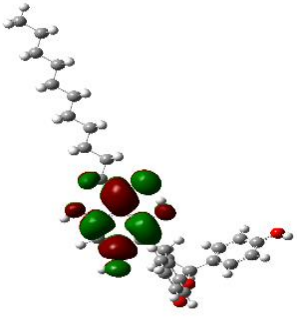
Myrin-d-w-p-b-f-k	Myrin-s-w-u-q-a-e-k
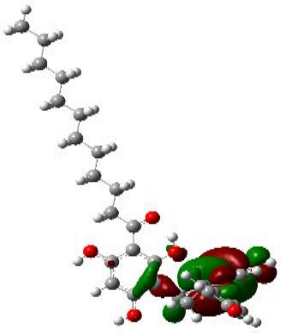	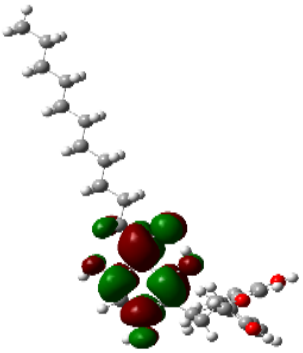
Myrin-d-w-q-a-e-j	Myrin-d-w-u-q-a-e-k
	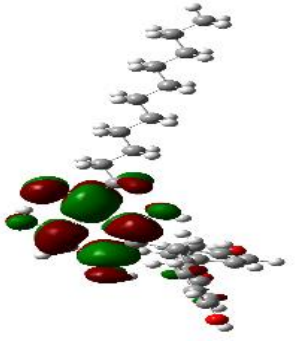
Myrin-s-r-η-p-e-a-k	Myrin-s-w-u-p-b-e-k

 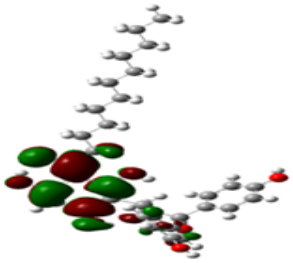	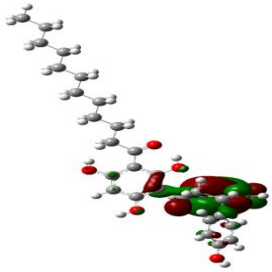 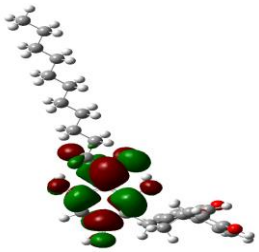
Myrin-s-r-η-p-b-e-k	Myrin-d-w-u-q-b-f-j
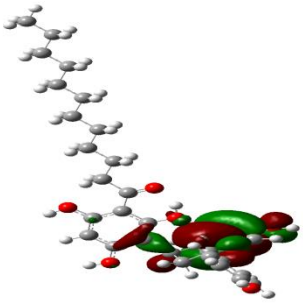 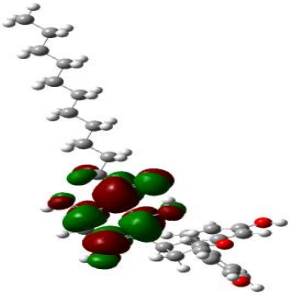	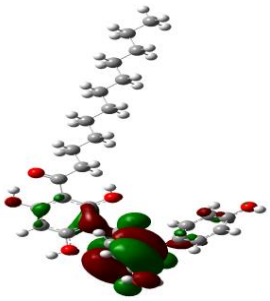 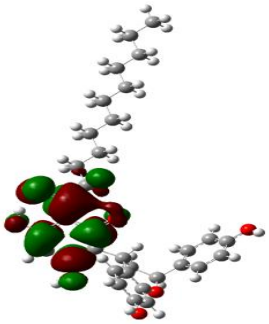
Myrin-d-w-q-a-e-k	Myrin-s-w-u-p-a-f-k
 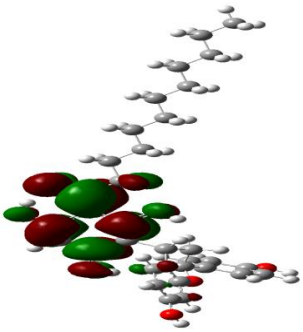	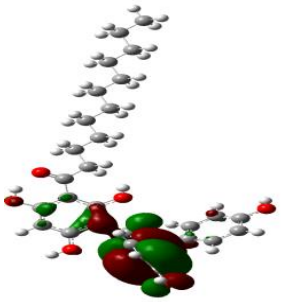 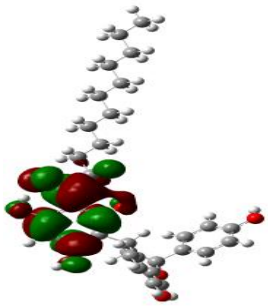
Myrin-s-r-η-p-a-e-j	Myrin-s-w-u-p-b-f-k
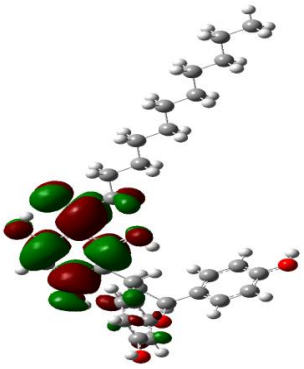 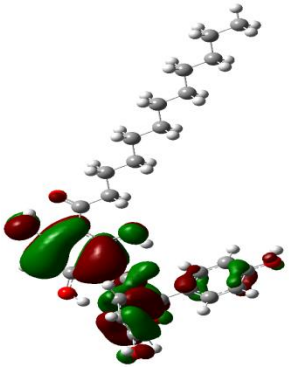	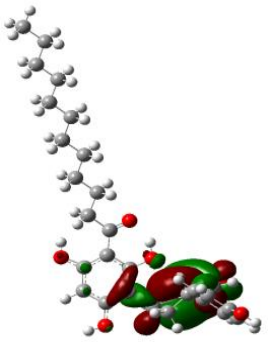 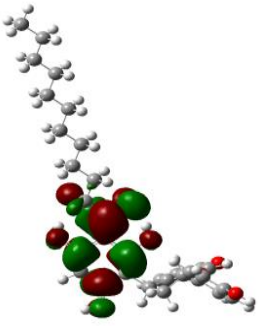
Myrin-s-r-η-p-b-f-k	Myrin-d-w-u-q-a-f-j
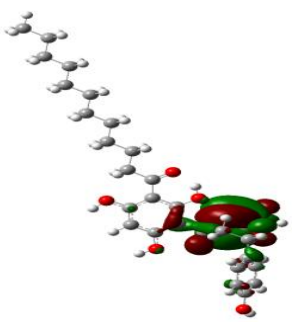 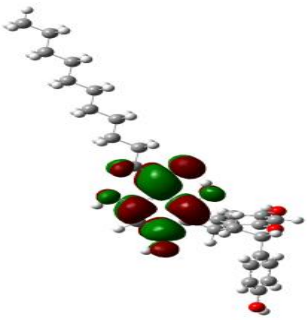	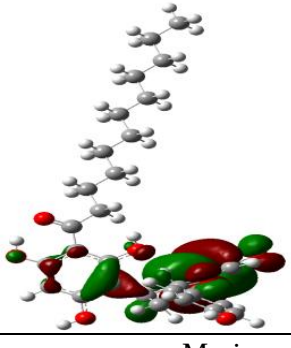 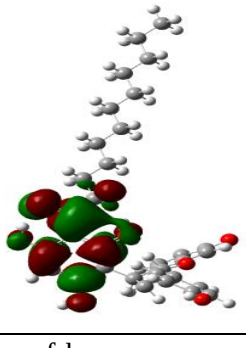
Myrin-d-w-q-b-f-j	Myrin-s-w-u-q-a-f-k

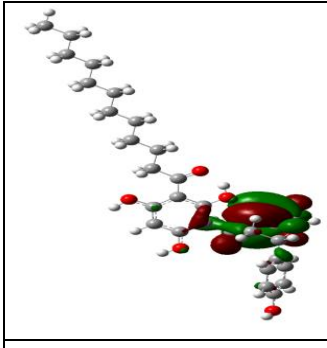 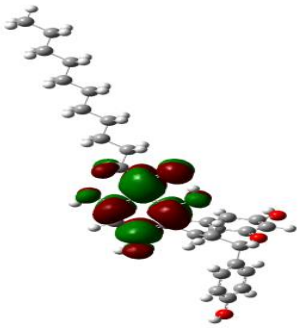	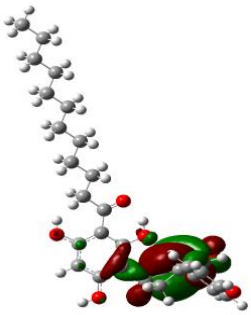 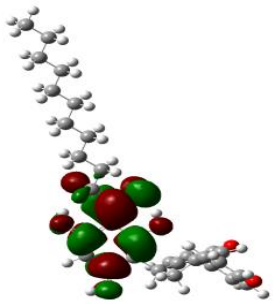
Myrin-d-r-q-b-f-k	Myrin-d-w-u-q-a-f-k
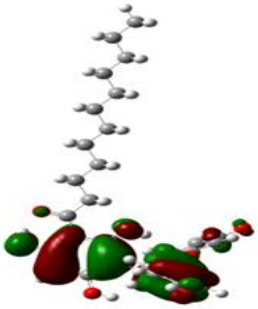 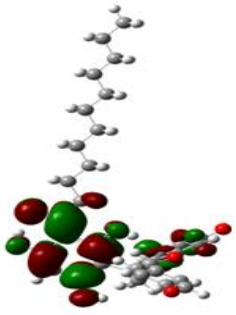	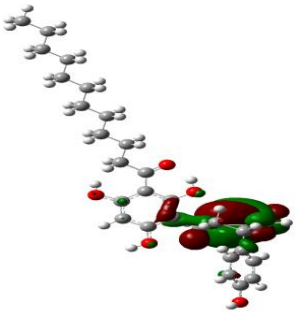 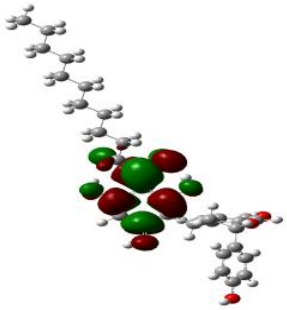
Myrin-s-r-ε-q-a-f-k	Myrin-d-w-u-q-b-f-k
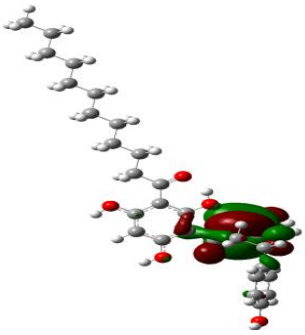 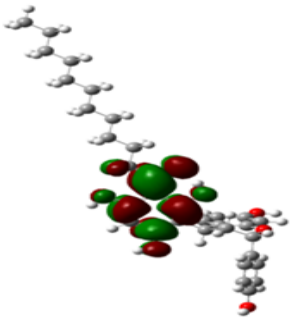	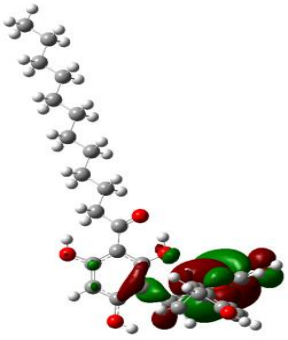 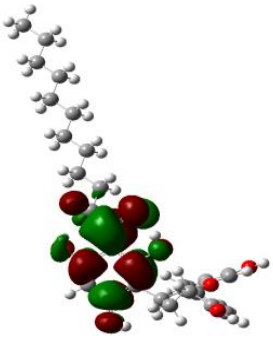
Myrin-d-w-q-b-e-k	Myrin-d-r-u-q-a-e-j
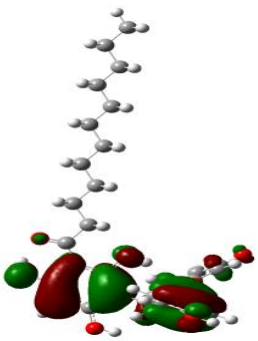 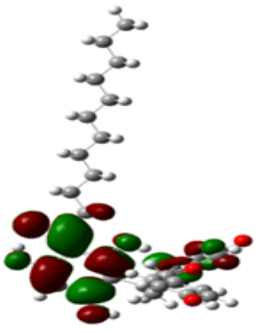	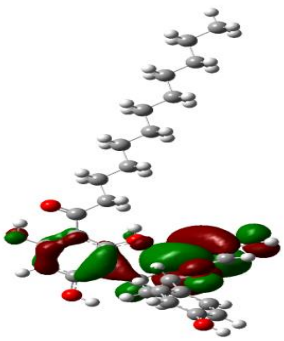 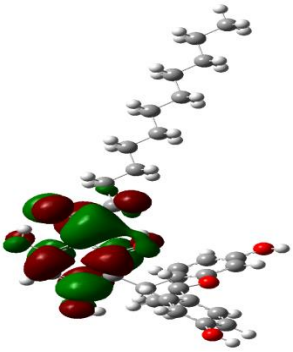
Myrin-s-r-ε-q-a-f-j	Myrin-s-r-u-q-b-e-j
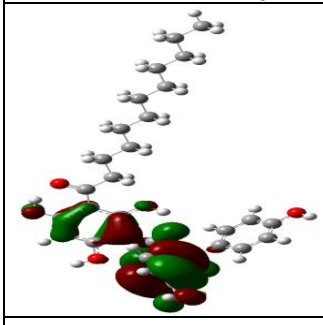 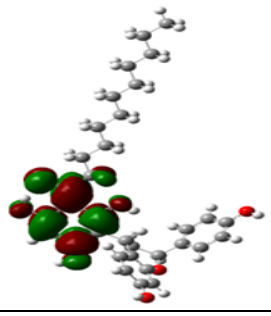	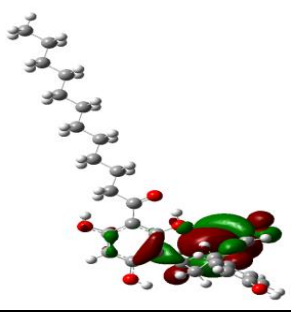 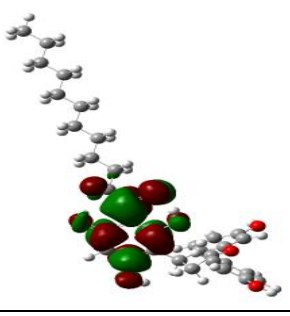
Myrin-s-w-p-b-f-j	Myrin-d-r-u-q-a-f-j

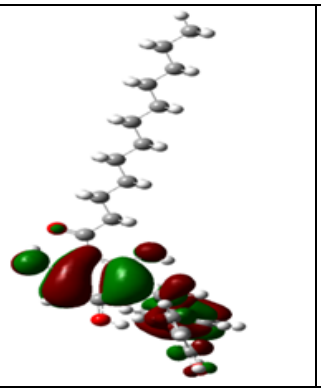 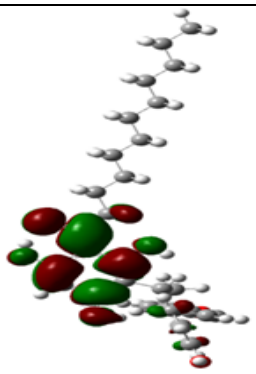	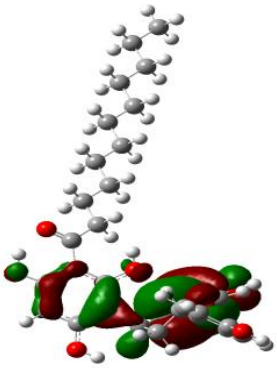 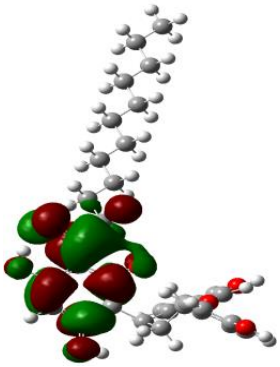
Myrin-s-r-η-p-a-f-k	Myrin-s-r-u-q-a-e-j
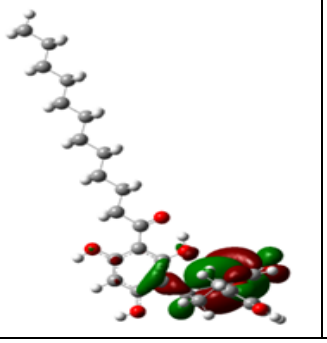 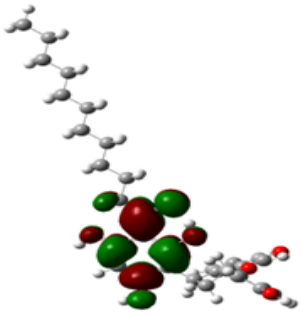	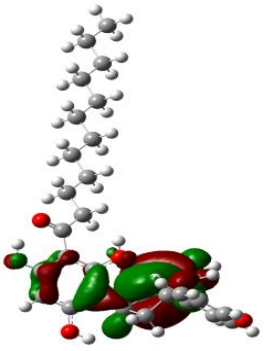 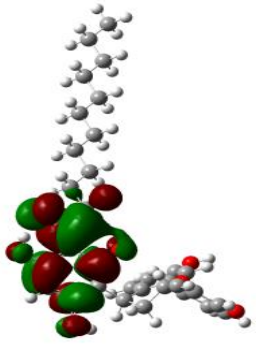
Myrin-d-w-q-a-f-j	Myrin-s-r-u-q-a-e-k
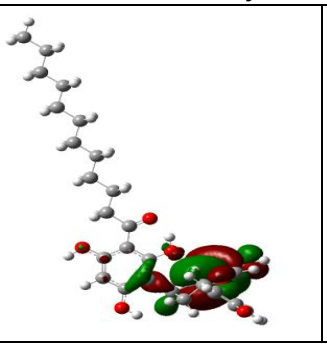 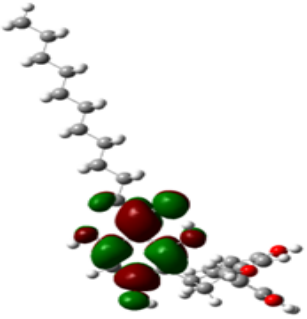	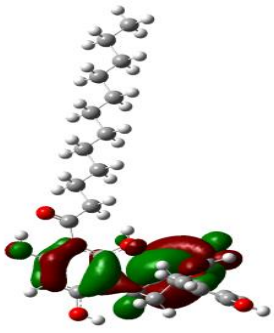 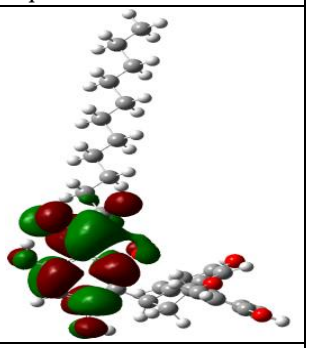
Myrin-d-r-q-a-e-j	Myrin-s-r-u-q-a-f-j
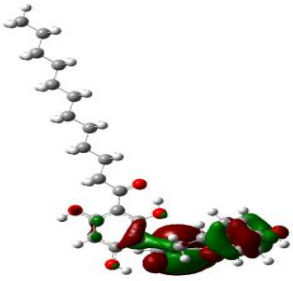 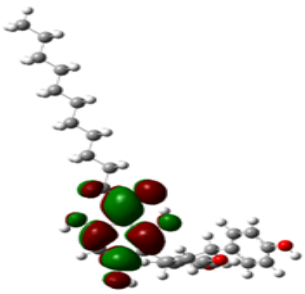	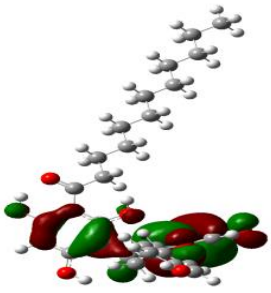 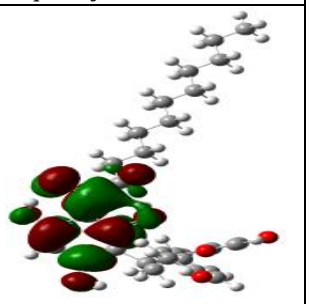
Myrin-d-r-q-b-e-j	Myrin-s-r-u-q-a-f-k
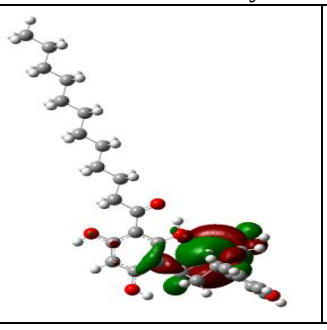 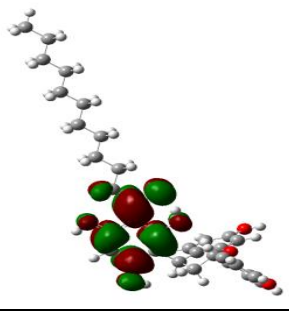	
Myrin-d-r-q-a-e-k	

Table 5.10. Relative energies of the calculated conformers of myristinin A having the same geometry of R and different geometries of the ring system *in vacuo* and in three solvents, chloroform, acetonitrile and water (respectively denoted as vac, chlrf, actn and aq in the column headings).
HF/6-31G(d,p) results are from full optimisation calculations. The conformers are listed in order of increasing relative energies in the HF results *in vacuo*.

Conformer	Relative energy (kcal/mol)			
	vac	chlrf	actn	aq
Myrin-d-r-η-p-a-e-j	0.000	0.016	0.031	0.033
Myrin-d-r-η-p-a-e-k	0.013	0.000	0.000	0.000
Myrin-d-r-η-p-a-f-j	0.423	0.233	0.160	0.153
Myrin-d-r-η-p-a-f-k	0.495	0.230	0.128	0.118
Myrin-d-r-η-p-b-e-k	1.004	0.776	0.661	0.650
Myrin-d-r-η-p-b-e-j	1.010	0.681	0.581	0.572
Myrin-s-w-ε-q-a-e-k	1.160	0.981	0.940	0.936
Myrin-s-w-ε-q-a-e-j	1.207	1.021	0.969	0.965
Myrin-d-r-η-p-b-f-j	1.212	0.793	0.655	0.642
Myrin-d-r-η-p-b-f-k	1.244	0.783	0.737	0.722
Myrin-s-w-ε-q-b-e-j	1.501	1.159	1.080	1.074
Myrin-s-w-ε-q-a-f-j	1.646	1.250	1.106	1.092
Myrin-s-w-ε-q-a-f-k	1.661	1.236	1.090	1.076
Myrin-s-w-ε-q-b-e-k	1.752	1.289	1.158	1.146
Myrin-s-w-ε-q-b-f-k	1.984	1.400	1.216	1.200

Table 5.11. The solvation free energy (ΔG_{solv}) and its electrostatic component (G_{el}) of the calculated conformers of myristinin A having the same geometry of R and different geometries of the ring system in three solvents chloroform, acetonitrile and water (respectively denoted as chlrf, actn, aq in the column headings).
HF/6-31G(d,p) results. The results in solution are from full optimisation calculations. Conformers are listed in order of increasing relative energies in the HF results *in vacuo*.

Conformer	(ΔG_{solv}) (kcal/mol)			(G_{el}) (kcal/mol)		
	chlrf	actn	aq	chlrf	actn	aq
Myrin-d-r-η-p-a-e-j	-0.13	7.52	-13.24	-8.03	-11.49	-26.49
Myrin-d-r-η-p-a-e-k	-2.08	5.86	-15.53	-7.99	-11.42	-26.64
Myrin-d-r-η-p-a-f-j	-2.22	5.64	-15.80	-8.13	-11.64	-26.90
Myrin-d-r-η-p-a-f-k	-2.27	5.54	-15.86	-8.18	-11.74	-26.96
Myrin-d-r-η-p-b-e-k	-2.13	5.53	-16.04	-8.33	-11.99	-27.62
Myrin-d-r-η-p-b-e-j	-2.17	5.58	-15.99	-8.31	-11.94	-27.57
Myrin-s-w-ε-q-a-e-k	-1.51	6.10	-15.19	-8.16	-11.74	-26.91
Myrin-s-w-ε-q-a-e-j	-1.51	6.05	-15.22	-8.15	-11.77	-26.93
Myrin-d-r-η-p-b-f-j	-2.24	5.45	-16.06	-8.38	-12.07	-27.63
Myrin-d-r-η-p-b-f-k	-2.25	5.38	-16.25	-8.39	-12.14	-27.83
Myrin-s-w-ε-q-b-e-j	-1.72	5.92	-15.44	-8.37	-12.01	-27.49
Myrin-s-w-ε-q-a-f-j	-1.69	5.75	-15.51	-8.34	-12.08	-27.23
Myrin-s-w-ε-q-a-f-k	-1.70	5.93	-15.32	-8.34	-12.07	-27.23
Myrin-s-w-ε-q-b-e-k	-1.81	5.65	-15.81	-8.46	-12.08	-27.74
Myrin-s-w-ε-q-b-f-k	-1.96	5.66	-15.93	-8.55	-12.20	-27.90

Table 5.12. Parameters of the first IHB of selected conformers of myristinin A having the same geometry of R and different geometries of the ring system, *in vacuo* and in three solvents, chloroform, acetonitrile and water (respectively denoted as vac, chlrf, actn, aq in the column headings).
HF/6-31G(d,p) results. The results *in vacuo* and in solution are from full optimisation calculations. Conformers are listed in order of increasing relative energies in the HF results *in vacuo*.

Conformer	Parameters of the first IHB			
	Media	O···H (Å)	O···O (Å)	OĤO (°)
Myrin-d-r-η-p-a-e-j	vac	1.652	2.508	146.4
	chlrf	1.646	2.506	146.9
	actn	1.644	2.506	147.1
	aq	1.644	2.507	147.1
Myrin-d-r-η-p-a-e-k	vac	1.652	2.508	146.3
	chlrf	1.646	2.506	147.1
	actn	1.644	2.506	146.9
	aq	1.644	2.506	147.1
Myrin-d-r-η-p-a-f-j	vac	1.652	2.508	146.4
	chlrf	1.646	2.506	146.9
	actn	1.644	2.505	147.1
	aq	1.644	2.505	147.2
Myrin-d-r-η-p-a-f-k	vac	1.652	2.508	146.4
	chlrf	1.646	2.506	146.9
	actn	1.644	2.505	147.1
	aq	1.644	2.505	147.2
Myrin-d-r-η-p-b-e-k	vac	1.651	2.508	146.6
	chlrf	1.647	2.507	147.0
	actn	1.644	2.505	147.2
	aq	1.643	2.505	147.2
Myrin-d-r-η-p-b-e-j	vac	1.655	2.510	146.2
	chlrf	1.647	2.507	146.9
	actn	1.644	2.506	147.2
	aq	1.644	2.505	147.2
Myrin-s-w-ε-q-a-e-k	vac	1.684	2.522	143.9
	chlrf	1.681	2.522	144.4
	actn	1.681	2.523	144.6
	aq	1.681	2.523	144.6
Myrin-s-w-ε-q-a-e-j	vac	1.683	2.521	143.9
	chlrf	1.677	2.520	144.5
	actn	1.675	2.519	144.8
	aq	1.675	2.519	144.8
Myrin-d-r-η-p-b-f-j	vac	1.655	2.510	146.2
	chlrf	1.647	2.507	146.9
	actn	1.644	2.506	147.2
	aq	1.644	2.506	147.2
Myrin-d-r-η-p-b-f-k	vac	1.651	2.508	146.5
	chlrf	1.647	2.507	146.9
	actn	1.644	2.506	147.2
	aq	1.644	2.506	147.2
Myrin-s-w-ε-q-b-e-j	vac	1.689	2.527	144.0

	chlrf	1.682	2.524	144.6
	actn	1.679	2.523	144.8
	aq	1.679	2.523	144.9
Myrin-s-w-ε-q-a-f-j	vac	1.682	2.520	143.9
	chlrf	1.678	2.520	144.5
	actn	1.676	2.520	144.7
	aq	1.676	2.520	144.8
Myrin-s-w-ε-q-a-f-k	vac	1.683	2.521	143.9
	chlrf	1.680	2.522	144.5
	actn	1.681	2.524	144.6
	aq	1.681	2.524	144.6
Myrin-s-w-ε-q-b-e-k	vac	1.689	2.526	144.0
	chlrf	1.682	2.524	144.6
	actn	1.679	2.523	144.8
	aq	1.679	2.523	144.8
Myrin-s-w-ε-q-b-f-k	vac	1.689	2.526	144.0
	chlrf	1.682	2.525	144.6
	actn	1.680	2.524	144.8
	aq	1.680	2.524	144.8

Table 5.13. Distance between the H atom and the closest C atom in the acceptor aromatic B ring for the O–H···π interactions in selected conformers of myristinin A having the same geometry of R and different geometries of the ring system *in vacuo* and in three solvents chloroform, acetonitrile and water (respectively denoted as vac, chlrf, actn, aq in the column headings).
HF/6-31G(d,p) results. The results *in vacuo* and in solution are from full optimisation calculations. Conformers are listed in order of increasing relative energies in the HF results *in vacuo*.

Conformer	H16···C23 distance considered (Å)			
	vac	chlrf	actn	aq
Myrin-d-r-η-p-a-e-j	2.128	2.125	2.124	2.124
Myrin-d-r-η-p-a-e-k	2.127	2.125	2.124	2.124
Myrin-d-r-η-p-a-f-j	2.131	2.129	2.127	2.127
Myrin-d-r-η-p-a-f-k	2.130	2.128	2.127	2.127
Myrin-d-r-η-p-b-e-k	2.213	2.254	2.263	2.264
Myrin-d-r-η-p-b-e-j	2.236	2.256	2.263	2.263
Myrin-s-w-ε-q-a-e-k	2.074	2.075	2.076	2.076
Myrin-s-w-ε-q-a-e-j	2.074	2.074	2.074	2.074
Myrin-d-r-η-p-b-f-j	2.239	2.258	2.263	2.263
Myrin-d-r-η-p-b-f-k	2.219	2.249	2.262	2.263
Myrin-s-w-ε-q-b-e-j	2.185	2.197	2.200	2.200
Myrin-s-w-ε-q-a-f-j	2.076	2.075	2.074	2.074
Myrin-s-w-ε-q-a-f-k	2.075	2.075	2.077	2.077
Myrin-s-w-ε-q-b-e-k	2.187	2.196	2.200	2.200
Myrin-s-w-ε-q-b-f-k	2.187	2.199	2.204	2.204

Table 5.14. Dipole moment of the calculated conformers of myristinin A having the same geometry of R and different geometries of the ring system *in vacuo* and in three solvents chloroform, acetonitrile and water (respectively denoted as vac, chlrf, actn, aq in the column headings).
HF/6-31G(d,p) results. The results *in vacuo* and in solution are from full optimisation calculations. Conformers are listed in order of increasing relative energies in the HF results *in vacuo*.

Conformer	Dipole moment (Debye)			
	vac	chlrf	actn	aq
Myrin-d-r-η-p-a-e-j	2.278	2.696	2.863	2.879
Myrin-d-r-η-p-a-e-k	3.695	4.891	5.292	5.329
Myrin-d-r-η-p-a-f-j	2.873	3.582	3.830	3.853
Myrin-d-r-η-p-a-f-k	4.092	5.399	5.840	5.880
Myrin-d-r-η-p-b-e-k	2.468	4.158	4.616	4.658
Myrin-d-r-η-p-b-e-j	2.643	3.515	3.835	3.865
Myrin-s-w-ε-q-a-e-k	2.792	3.322	3.455	3.468
Myrin-s-w-ε-q-a-e-j	5.111	6.258	6.626	6.659
Myrin-d-r-η-p-b-f-j	3.475	4.636	5.035	5.072
Myrin-d-r-η-p-b-f-k	3.697	4.678	5.391	5.433
Myrin-s-w-ε-q-b-e-j	4.746	5.707	6.016	6.044
Myrin-s-w-ε-q-a-f-j	4.964	6.160	6.550	6.585
Myrin-s-w-ε-q-a-f-k	2.640	3.193	3.440	3.461
Myrin-s-w-ε-q-b-e-k	4.227	5.113	5.401	5.426
Myrin-s-w-ε-q-b-f-k	2.906	3.310	3.433	3.444

Table 5.15. HOMO-LUMO energy gap of the calculated conformers of myristinin having the same geometry of R and different geometries of the ring system *in vacuo* and in three solvents chloroform, acetonitrile and water (respectively denoted as vac, chlrf, actn, aq in the column headings).
HF/6-31G(d,p) results. The results *in vacuo* and in solution are from full optimisation calculations. Conformers are listed in order of increasing relative energies in the HF results *in vacuo*.

Conformer	HOMO-LUMO energy gap (kcal/mol)			
	vac	chlrf	actn	aq
Myrin-d-r-η-p-a-e-j	257.479	256.871	256.582	256.557
Myrin-d-r-η-p-a-e-k	257.574	256.902	256.651	256.632
Myrin-d-r-η-p-a-f-j	256.319	256.557	256.475	256.457
Myrin-d-r-η-p-a-f-k	256.494	256.645	256.551	256.538
Myrin-d-r-η-p-b-e-k	254.693	254.411	254.204	254.191
Myrin-d-r-η-p-b-e-j	255.942	254.606	254.242	254.204
Myrin-s-w-ε-q-a-e-k	258.854	257.492	257.003	256.959
Myrin-s-w-ε-q-a-e-j	258.816	257.423	256.877	256.827
Myrin-d-r-η-p-b-f-j	256.099	255.108	254.744	254.712
Myrin-d-r-η-p-b-f-k	255.170	254.955	254.687	254.675
Myrin-s-w-ε-q-b-e-j	258.678	256.463	255.653	255.584
Myrin-s-w-ε-q-a-f-j	258.101	257.210	256.833	256.796
Myrin-s-w-ε-q-a-f-k	258.207	257.298	256.984	256.946
Myrin-s-w-ε-q-b-e-k	258.345	256.306	255.616	255.553
Myrin-s-w-ε-q-b-f-k	258.308	256.576	255.986	255.936

Figure 5.8. Optimized conformers of myristinin A having different geometries of R and the same geometry of the ring system *in vacuo*.
HF/6-31G(d,p) results. The conformers are listed in order of increasing relative energy.

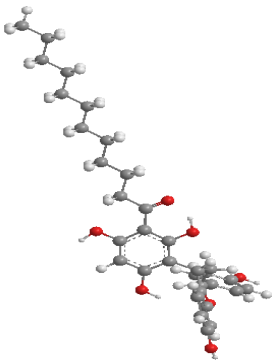

Myrin-d-r-η-p-a-e-j

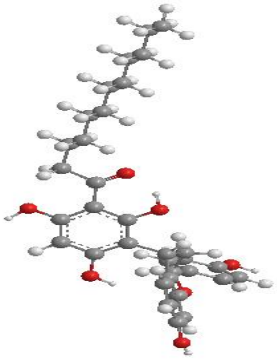

Myrin-d-r-η-p-a-e-j-2y

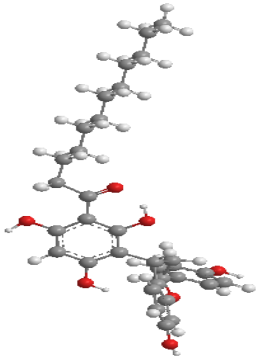

Myrin-d-r-η-p-a-e-j-2z

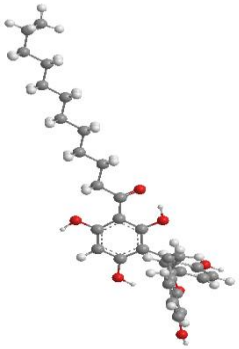

Myrin-d-r-η-p-a-e-j-10y

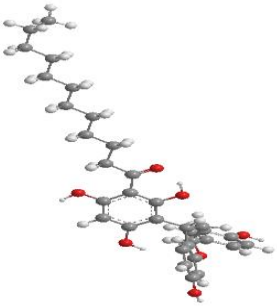

Myrin-d-r-η-p-a-e-j-10z

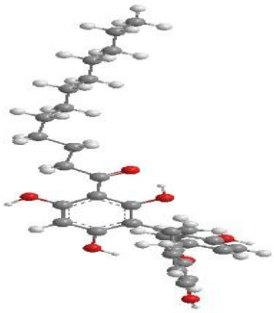

Myrin-d-r-η-p-a-e-j-4z

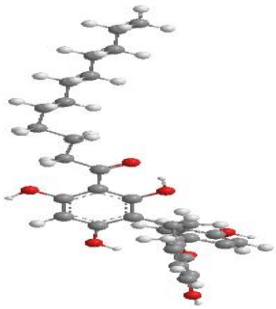

Myrin-d-r-η-p-a-e-j-4y

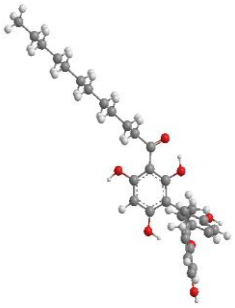

Myrin-d-r-η-p-a-e-j-1z

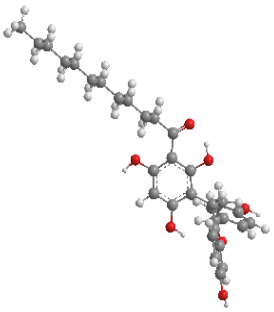

Myrin-d-r-η-p-a-e-j-1y

Myrin-d-r-η-p-a-e-j-6y

Myrin-d-r-η-p-a-e-j-6z

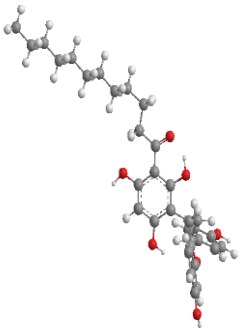

Myrin-d-r-η-p-a-e-j-3z

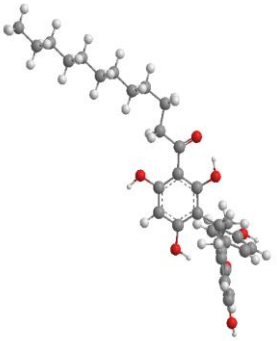

Myrin-d-r-η-p-a-e-j-3y

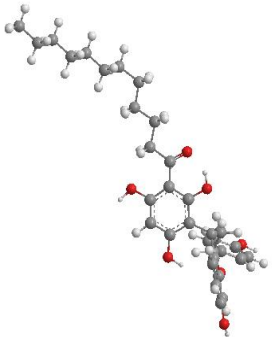

Myrin-d-r-η-p-a-e-j-8y

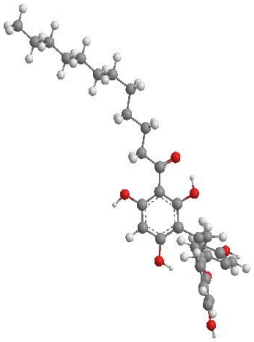

Myrin-d-r-η-p-a-e-j-8z

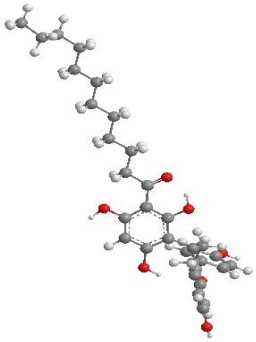

Myrin-d-r-η-p-a-e-j-9y

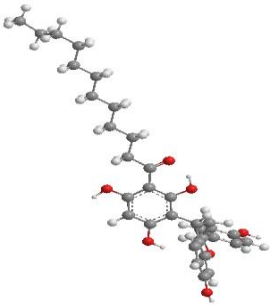

Myrin-d-r-η-p-a-e-j-9y

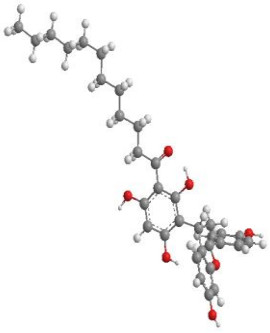

Myrin-d-r-η-p-a-e-j-7y

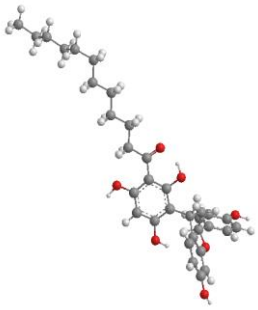

Myrin-d-r-η-p-a-e-j-7z

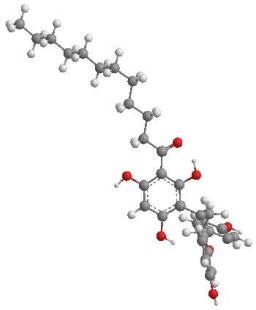

Myrin-d-r-η-p-a-e-j-5z

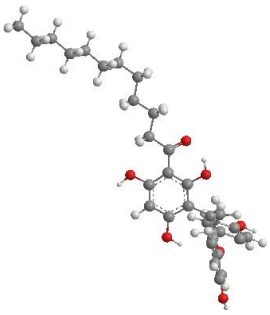

Myrin-d-r-η-p-a-e-j-5y

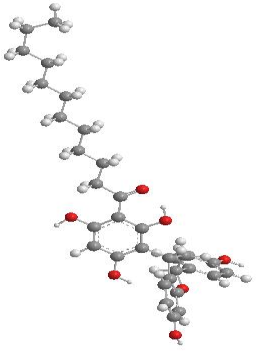

Myrin -d-r-η-p-a-e-j-10v

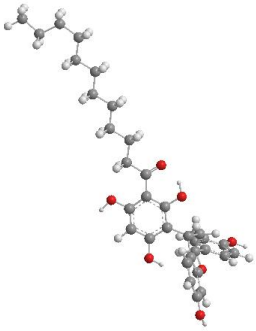

Myrin -d-r-η-p-a-e-j-9x

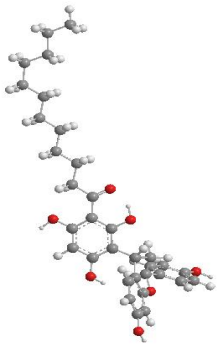

Myrin -d-r-η-p-a-e-j-8v

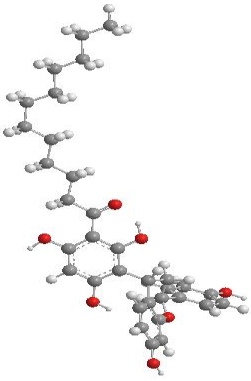

Myrin -d-r-η-p-a-e-j-6v

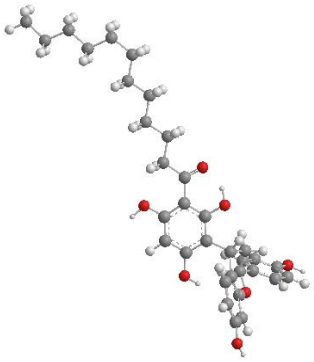

Myrin -d-r-η-p-a-e-j-7x

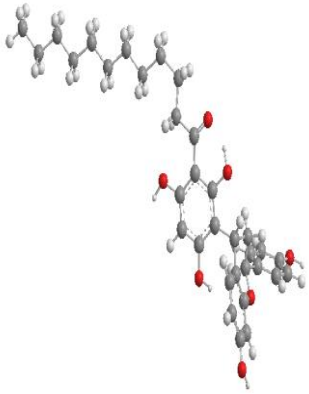

Myrin -d-r-η-p-a-e-j-3x

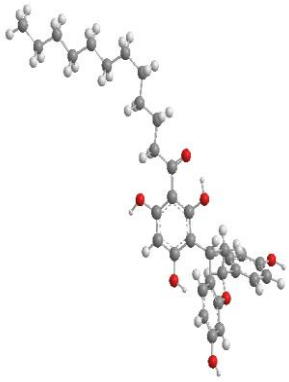

Myrin -d-r-η-p-a-e-j-5x

Table 5.16. Relative energies of the calculated conformers of myristinin A having different geometries of R and the same geometry of the ring system.
HF/6-31G(d,p) results. The conformers are arranged in order of increasing relative energy. The absolute energy of the lowest energy conformer is -1797.0892235 hartree.

Conformer	Relative energy (kcal/mol)
Myrin-d-r-η-p-a-e-j	0.000
Myrin-d-r-η-p-a-e-j-2y	0.513
Myrin-d-r-η-p-a-e-j-2z	0.525
Myrin-d-r-η-p-a-e-j-10y	0.999
Myrin-d-r-η-p-a-e-j-10z	0.999
Myrin-d-r-η-p-a-e-j-4z	1.007
Myrin-d-r-η-p-a-e-j-4y	1.007
Myrin-d-r-η-p-a-e-j-1z	1.026
Myrin-d-r-η-p-a-e-j-1y	1.031
Myrin-d-r-η-p-a-e-j-6y	1.038
Myrin-d-r-η-p-a-e-j-6z	1.038
Myrin-d-r-η-p-a-e-j-3z	1.042
Myrin-d-r-η-p-a-e-j-3y	1.044
Myrin-d-r-η-p-a-e-j-8y	1.043
Myrin-d-r-η-p-a-e-j-8z	1.043
Myrin-d-r-η-p-a-e-j-9y	1.047
Myrin-d-r-η-p-a-e-j-9z	1.047
Myrin-d-r-η-p-a-e-j-7y	1.049
Myrin-d-r-η-p-a-e-j-7z	1.049
Myrin-d-r-η-p-a-e-j-5z	1.054
Myrin-d-r-η-p-a-e-j-5y	1.054
Myrin-d-r-η-p-a-e-j-10v	6.297
Myrin-d-r-η-p-a-e-j-9x	6.365
Myrin-d-r-η-p-a-e-j-8v	6.383
Myrin-d-r-η-p-a-e-j-6v	6.384
Myrin-d-r-η-p-a-e-j-7x	6.390
Myrin-d-r-η-p-a-e-j-3x	6.536
Myrin-d-r-η-p-a-e-j-5x	6.392

Table 5.17. Relative energy corrected for ZPE (sum of electronic and zero-point energies, $\Delta E_{corrected}$, kcal/mol), ZPE correction to the electronic energy (ZPE_{corr}, kcal/mol), relative Gibbs free energies (sum of electronic and thermal free energy, $\Delta G_{corrected}$) and its thermal correction (G_{corr}), for the conformers of myristinin A having different geometries of R and the same geometry of the ring system.

Results from HF/6-31G(d,p) frequency calculations. Conformers are listed in order of increasing relative energies in the HF/6-31G(d,p) results *in vacuo*. The absolute energy of the lowest energy conformer is -1796.365514 hartree.

Conformer	$\Delta E_{corrected}$	ZPE_{corr}	$\Delta G_{corrected}$	G_{corr}
Myrin-d-r-η-p-a-e-j	0.000	454.135	0.000	406.134
Myrin-d-r-η-p-a-e-j-2y	0.697	454.318	0.810	406.431
Myrin-d-r-η-p-a-e-j-2z	0.709	454.318	0.805	406.414
Myrin-d-r-η-p-a-e-j-10y	1.114	454.250	1.071	406.207
Myrin-d-r-η-p-a-e-j-10z	1.114	454.250	1.070	406.206
Myrin-d-r-η-p-a-e-j-4z	2.373	454.183	3.877	407.688
Myrin-d-r-η-p-a-e-j-4y	2.849	454.143	3.586	406.881
Myrin-d-r-η-p-a-e-j-1z	1.402	454.511	1.192	406.301
Myrin-d-r-η-p-a-e-j-1y	1.406	454.510	1.184	406.288
Myrin-d-r-η-p-a-e-j-6y	3.382	454.128	6.213	408.960
Myrin-d-r-η-p-a-e-j-6z	2.698	454.131	5.692	409.125
Myrin-d-r-η-p-a-e-j-3z	3.741	454.145	6.675	409.081
Myrin-d-r-η-p-a-e-j-3y	3.603	454.145	3.863	406.406
Myrin-d-r-η-p-a-e-j-8y	2.858	454.120	5.546	408.809
Myrin-d-r-η-p-a-e-j-8z	3.043	454.117	5.537	408.612
Myrin-d-r-η-p-a-e-j-9y	3.468	454.119	5.893	408.545
Myrin-d-r-η-p-a-e-j-9z	3.016	454.103	5.304	408.391
Myrin-d-r-η-p-a-e-j-7y	2.518	454.139	3.376	406.997
Myrin-d-r-η-p-a-e-j-7z	3.387	454.126	6.111	408.850
Myrin-d-r-η-p-a-e-j-5z	3.569	454.124	6.265	408.820
Myrin-d-r-η-p-a-e-j-5y	3.742	454.123	6.568	408.949

Table 5.18. Parameters of the first IHB of the selected calculated conformers of myristinin A having different geometries of R and the same geometry of the ring system *in vacuo*.
HF/6-31G(d,p) results. The first IHB is H15···O14. The results are from full optimisation calculations. Conformers are listed in order of increasing relative energy in the HF results *in vacuo*.

Conformer	Parameters of the first IHB		
	OH···O (Å)	O···O (Å)	OHO (°)
Myrin-d-r-η-p-a-e-j	1.652	2.508	146.4
Myrin-d-r-η-p-a-e-j-2y	1.654	2.510	146.3
Myrin-d-r-η-p-a-e-j-2z	1.654	2.509	146.3
Myrin-d-r-η-p-a-e-j-10y	1.652	2.508	146.4
Myrin-d-r-η-p-a-e-j-10z	1.651	2.508	146.4
Myrin-d-r-η-p-a-e-j-4z	1.651	2.508	146.4
Myrin-d-r-η-p-a-e-j-4y	1.651	2.508	146.4
Myrin-d-r-η-p-a-e-j-1z	1.644	2.504	146.6
Myrin-d-r-η-p-a-e-j-1y	1.644	2.503	146.6
Myrin-d-r-η-p-a-e-j-6y	1.651	2.508	146.4
Myrin-d-r-η-p-a-e-j-6z	1.651	2.508	146.4
Myrin-d-r-η-p-a-e-j-3z	1.651	2.508	146.4
Myrin-d-r-η-p-a-e-j-3y	1.651	2.508	146.4
Myrin-d-r-η-p-a-e-j-8y	1.651	2.508	146.4
Myrin-d-r-η-p-a-e-j-8z	1.651	2.508	146.4
Myrin-d-r-η-p-a-e-j-9y	1.651	2.508	146.4
Myrin-d-r-η-p-a-e-j-9z	1.652	2.508	146.4
Myrin-d-r-η-p-a-e-j-7y	1.651	2.508	146.4
Myrin-d-r-η-p-a-e-j-7z	1.652	2.508	146.4
Myrin-d-r-η-p-a-e-j-5z	1.651	2.508	146.4
Myrin-d-r-η-p-a-e-j-5y	1.651	2.508	146.4
Myrin -d-r-η-p-a-e-j-10v	1.651	2.508	146.4
Myrin-d-r-η-p-a-e-j-9x	1.651	2.508	146.4
Myrin-d-r-η-p-a-e-j-8v	1.651	2.508	146.4
Myrin-d-r-η-p-a-e-j-6v	1.651	2.508	146.4
Myrin-d-r-η-p-a-e-j-7x	1.651	2.508	146.4
Myrin-d-r-η-p-a-e-j-3x	1.651	2.508	146.4
Myrin-d-r-η-p-a-e-j-5x	1.651	2.508	146.4

Table 5.19. The distance between the H atom and the closest C atom in the acceptor aromatic ring for the O–H···π interactions of the selected calculated conformers of myristinin A having different geometries of R and the same geometry of the ring system *in vacuo*.
HF/6-31G(d,p) results are from full optimisation. Conformers are listed in order of increasing relative energy in the HF results.

Conformer	H16···C23 distance considered (Å)	Conformer	H16···C23 distance considered (Å)
Myrin-d-r-η-p-a-e-j	2.128	Myrin-d-r-η-p-a-e-j-8z	2.128
Myrin-d-r-η-p-a-e-j-2y	2.129	Myrin-d-r-η-p-a-e-j-9y	2.128
Myrin-d-r-η-p-a-e-j-2z	2.127	Myrin-d-r-η-p-a-e-j-9z	2.128
Myrin-d-r-η-p-a-e-j-10y	2.128	Myrin-d-r-η-p-a-e-j-7y	2.128
Myrin-d-r-η-p-a-e-j-10z	2.128	Myrin-d-r-η-p-a-e-j-7z	2.128
Myrin-d-r-η-p-a-e-j-4z	2.128	Myrin-d-r-η-p-a-e-j-5z	2.128
Myrin-d-r-η-p-a-e-j-4y	2.128	Myrin-d-r-η-p-a-e-j-5y	2.128
Myrin-d-r-η-p-a-e-j-1z	2.129	Myrin -d-r-η-p-a-e-j-10v	2.128
Myrin-d-r-η-p-a-e-j-1y	2.128	Myrin-d-r-η-p-a-e-j-9x	2.128
Myrin-d-r-η-p-a-e-j-6y	2.128	Myrin-d-r-η-p-a-e-j-8v	2.128
Myrin-d-r-η-p-a-e-j-6z	2.128	Myrin-d-r-η-p-a-e-j-6v	2.128
Myrin-d-r-η-p-a-e-j-3z	2.128	Myrin-d-r-η-p-a-e-j-7x	2.128
Myrin-d-r-η-p-a-e-j-3y	2.128	Myrin-d-r-η-p-a-e-j-3x	2.128
Myrin-d-r-η-p-a-e-j-8y	2.128	Myrin-d-r-η-p-a-e-j-5x	2.128

Table 5.20. Vibrational frequency of the O–H bonds in the selected conformers of myristinin A having different geometries of R and the same geometry of the ring system.
HF/6-31G(d,p) results *in vacuo*. The frequency values have been scaled by 0.8992, as recommended for HF/6-31G(d,p) calculations [184]. The conformers are arranged in order of increasing relative energy.

Conformer	Vibrational frequencies (cm^{-1})				
	O8–H15	O10–H16	O12–H17	O44–H50	O51–H52
Myrin-d-r-η-p-a-e-j	3397.26	3704.41	3762.01	3769.59	3773.51
Myrin-d-r-η-p-a-e-j-2y	3403.46	3704.15	3761.92	3769.55	3773.52
Myrin-d-r-η-p-a-e-j-2z	3403.52	3704.10	3761.88	3769.55	3773.50
Myrin-d-r-η-p-a-e-j-10y	3396.80	3704.37	3762.01	3769.58	3773.50
Myrin-d-r-η-p-a-e-j-10z	3396.77	3704.39	3762.01	3769.58	3773.52
Myrin-d-r-η-p-a-e-j-4z	3396.84	3704.37	3762.02	3769.59	3773.51
Myrin-d-r-η-p-a-e-j-4y	3397.01	3704.37	3762.02	3769.57	3773.50
Myrin-d-r-η-p-a-e-j-1z	3374.53	3703.68	3763.13	3769.57	3773.52
Myrin-d-r-η-p-a-e-j-1y	3373.67	3703.64	3763.09	3769.56	3773.51
Myrin-d-r-η-p-a-e-j-6y	3396.89	3704.39	3761.99	3769.57	3773.52
Myrin-d-r-η-p-a-e-j-6z	3396.83	3704.39	3762.00	3769.59	3773.52
Myrin-d-r-η-p-a-e-j-3z	3396.49	3704.39	3762.02	3769.58	3773.51
Myrin-d-r-η-p-a-e-j-3y	3396.50	3704.40	3762.00	3769.58	3773.51

Myrin-d-r-η-p-a-e-j-8y	3396.76	3704.37	3762.00	3769.57	3773.51
Myrin-d-r-η-p-a-e-j-8z	3396.77	3704.37	3770.99	3769.57	3773.51
Myrin-d-r-η-p-a-e-j-9y	3396.85	3704.38	3762.00	3769.58	3773.51
Myrin-d-r-η-p-a-e-j-9z	3396.85	3704.38	3762.00	3769.58	3773.51
Myrin-d-r-η-p-a-e-j-7y	3397.31	3704.37	3762.02	3769.58	3773.50
Myrin-d-r-η-p-a-e-j-7z	3397.30	3704.37	3762.02	3769.58	3773.50
Myrin-d-r-η-p-a-e-j-5z	3396.77	3704.37	3762.01	3769.57	3773.50
Myrin-d-r-η-p-a-e-j-5y	3396.67	3704.38	3762.01	3769.56	3773.51

Table 5.21. Red shift of the vibrational frequency of the O–H bonds in the selected conformers of myristinin A having different geometries of R and the same geometry of the ring system.
HF/6-31G(d,p) results *in vacuo*.

Conformer	Red shift (vibrational, cm^{-1})	
	O8–H15	O10–H16
Myrin-d-r-η-p-a-e-j	413.20	80.25
Myrin-d-r-η-p-a-e-j-2y	407.00	80.51
Myrin-d-r-η-p-a-e-j-2z	406.94	80.56
Myrin-d-r-η-p-a-e-j-10y	413.66	80.29
Myrin-d-r-η-p-a-e-j-10z	413.69	80.27
Myrin-d-r-η-p-a-e-j-4z	413.62	80.29
Myrin-d-r-η-p-a-e-j-4y	413.45	80.29
Myrin-d-r-η-p-a-e-j-1z	435.93	80.98
Myrin-d-r-η-p-a-e-j-1y	436.79	81.02
Myrin-d-r-η-p-a-e-j-6y	413.57	80.27
Myrin-d-r-η-p-a-e-j-6z	413.63	80.27
Myrin-d-r-η-p-a-e-j-3z	413.97	80.27
Myrin-d-r-η-p-a-e-j-3y	413.96	80.26
Myrin-d-r-η-p-a-e-j-8y	413.70	80.29
Myrin-d-r-η-p-a-e-j-8z	413.69	80.29
Myrin-d-r-η-p-a-e-j-9y	413.61	80.28
Myrin-d-r-η-p-a-e-j-9z	413.61	80.28
Myrin-d-r-η-p-a-e-j-7y	413.15	80.29
Myrin-d-r-η-p-a-e-j-7z	413.16	80.29
Myrin-d-r-η-p-a-e-j-5z	413.69	80.29
Myrin-d-r-η-p-a-e-j-5y	413.79	80.28

Table 5.22. Dipole moment of the calculated conformers of myristinin A having different geometries of R and the same geometry of the ring system *in vacuo*.
HF/6-31G(d,p) results are from full optimisation. Conformers are listed in order of increasing relative energy in the HF results.

Conformer	Dipole moment (Debye)	Conformer	Dipole moment (Debye)
Myrin-d-r-η-p-a-e-j	2.278	Myrin-d-r-η-p-a-e-j-8z	2.297
Myrin-d-r-η-p-a-e-j-2y	2.403	Myrin-d-r-η-p-a-e-j-9y	2.294
Myrin-d-r-η-p-a-e-j-2z	2.403	Myrin-d-r-η-p-a-e-j-9z	2.296
Myrin-d-r-η-p-a-e-j-10y	2.300	Myrin-d-r-η-p-a-e-j-7y	2.288
Myrin-d-r-η-p-a-e-j-10z	2.291	Myrin-d-r-η-p-a-e-j-7z	2.290
Myrin-d-r-η-p-a-e-j-4z	2.312	Myrin-d-r-η-p-a-e-j-5z	2.285
Myrin-d-r-η-p-a-e-j-4y	2.323	Myrin-d-r-η-p-a-e-j-5y	2.282
Myrin-d-r-η-p-a-e-j-1z	2.439	Myrin -d-r-η-p-a-e-j-10v	2.295
Myrin-d-r-η-p-a-e-j-1y	2.411	Myrin-d-r-η-p-a-e-j-9x	2.312
Myrin-d-r-η-p-a-e-j-6y	2.309	Myrin-d-r-η-p-a-e-j-8v	2.304
Myrin-d-r-η-p-a-e-j-6z	2.300	Myrin-d-r-η-p-a-e-j-6v	2.309
Myrin-d-r-η-p-a-e-j-3z	2.275	Myrin-d-r-η-p-a-e-j-7x	2.304
Myrin-d-r-η-p-a-e-j-3y	2.273	Myrin-d-r-η-p-a-e-j-3x	2.287
Myrin-d-r-η-p-a-e-j-8y	2.307	Myrin-d-r-η-p-a-e-j-5x	2.297

Table 5.23. HOMO-LUMO energy gap of the calculated conformers of myristinin A having different geometries of R and the same geometry of the ring system *in vacuo*.
HF/6-31G(d,p) results are from full optimisation. Conformers are listed in order of increasing relative energy in the HF results.

Conformer	HOMO-LUMO energy gap (kcal/mol)	Conformer	HOMO-LUMO energy gap (kcal/mol)
Myrin-d-r-η-p-a-e-j	257.479	Myrin-d-r-η-p-a-e-j-8z	257.473
Myrin-d-r-η-p-a-e-j-2y	256.996	Myrin-d-r-η-p-a-e-j-9y	257.473
Myrin-d-r-η-p-a-e-j-2z	257.021	Myrin-d-r-η-p-a-e-j-9z	257.473
Myrin-d-r-η-p-a-e-j-10y	257.479	Myrin-d-r-η-p-a-e-j-7y	257.473
Myrin-d-r-η-p-a-e-j-10z	257.479	Myrin-d-r-η-p-a-e-j-7z	257.473
Myrin-d-r-η-p-a-e-j-4z	257.448	Myrin-d-r-η-p-a-e-j-5z	257.473
Myrin-d-r-η-p-a-e-j-4y	257.448	Myrin-d-r-η-p-a-e-j-5y	257.473
Myrin-d-r-η-p-a-e-j-1z	255.446	Myrin -d-r-η-p-a-e-j-10v	257.486
Myrin-d-r-η-p-a-e-j-1y	255.465	Myrin-d-r-η-p-a-e-j-9x	257.479
Myrin-d-r-η-p-a-e-j-6y	257.473	Myrin-d-r-η-p-a-e-j-8v	257.486
Myrin-d-r-η-p-a-e-j-6z	257.473	Myrin-d-r-η-p-a-e-j-6v	257.486
Myrin-d-r-η-p-a-e-j-3z	257.498	Myrin-d-r-η-p-a-e-j-7x	257.479
Myrin-d-r-η-p-a-e-j-3y	257.505	Myrin-d-r-η-p-a-e-j-3x	257.574
Myrin-d-r-η-p-a-e-j-8y	257.479	Myrin-d-r-η-p-a-e-j-5x	257.492

Table 5.24. Relative energies of the calculated conformers of myristinin A having different geometries of R and the same geometry of the ring system.
HF/6-31G(d,p), DFT/B3LYP/6-31+G(d,p) and MP2/ 6-31G(d,p) results *in vacuo*. The results are from full optimisation calculations. Conformers are listed in order of increasing relative energies in the HF results *in vacuo*. The absolute energies of the lowest-energy conformer is -1797.0892235, -1808.3341215 and -1802.8236804 hartree in the HF, DFT and MP2 results respectively.

Conformer	Relative energy (kcal/mol)		
	HF	DFT	MP2
Myrin-d-r-η-p-a-e-j	0.000	0.000	0.303
Myrin-d-r-η-p-a-e-j-2y	0.513	0.551	0.009
Myrin-d-r-η-p-a-e-j-2z	0.525	0.570	0.000
Myrin-d-r-η-p-a-e-j-10y	0.999	0.895	0.861
Myrin-d-r-η-p-a-e-j-10z	0.999	0.892	0.861
Myrin-d-r-η-p-a-e-j-4z	1.007	0.916	0.681
Myrin-d-r-η-p-a-e-j-4y	1.007	0.885	0.682
Myrin-d-r-η-p-a-e-j-1z	1.026	0.532	0.285
Myrin-d-r-η-p-a-e-j-1y	1.031	0.476	0.298
Myrin-d-r-η-p-a-e-j-6y	1.038	0.920	0.737
Myrin-d-r-η-p-a-e-j-6z	1.038	0.930	0.737
Myrin-d-r-η-p-a-e-j-3z	1.042	0.944	0.622
Myrin-d-r-η-p-a-e-j-3y	1.044	0.956	0.624
Myrin-d-r-η-p-a-e-j-8y	1.043	0.910	0.763
Myrin-d-r-η-p-a-e-j-8z	1.043	0.923	0.763
Myrin-d-r-η-p-a-e-j-9y	1.047	0.910	0.823
Myrin-d-r-η-p-a-e-j-9z	1.047	0.907	0.823
Myrin-d-r-η-p-a-e-j-7y	1.049	0.946	0.753
Myrin-d-r-η-p-a-e-j-7z	1.049	0.948	0.753
Myrin-d-r-η-p-a-e-j-5z	1.054	0.952	0.736
Myrin-d-r-η-p-a-e-j-5y	1.054	0.955	0.738

Table 5.25. Parameters of the first IHB of the selected calculated conformers of myristinin A having different geometries of R and the same geometry of the ring system.
HF/6-31G(d,p), DFT/B3LYP/6-31+G(d,p) and MP2/ 6-31G(d,p) results *in vacuo*. The first IHB is H15···O14. The results are from full optimisation calculations. Conformers are listed in order of increasing relative energies in the HF results *in vacuo*.

Conformer	Method	Parameters of the first IHB		
		OH···O (Å)	O···O (Å)	OHO (°)
Myrin-d-r-η-p-a-e-j	HF	1.652	2.508	146.4
	DFT	1.529	2.466	151.8
	MP2	1.584	2.505	151.4
Myrin-d-r-η-p-a-e-j-2y	HF	1.654	2.510	146.3
	DFT	1.530	2.466	151.7
	MP2	1.585	2.505	151.3
Myrin-d-r-η-p-a-e-j-2z	HF	1.654	2.509	146.3
	DFT	1.529	2.466	151.7
	MP2	1.585	2.505	151.3
Myrin-d-r-η-p-a-e-j-10y	HF	1.652	2.508	146.4
	DFT	1.529	2.466	151.8
	MP2	1.583	2.505	151.5
Myrin-d-r-η-p-a-e-j-10z	HF	1.651	2.508	146.4
	DFT	1.529	2.466	151.8
	MP2	1.583	2.505	151.5
Myrin-d-r-η-p-a-e-j-4z	HF	1.651	2.508	146.4
	DFT	1.530	2.467	151.8
	MP2	1.583	2.504	151.5
Myrin-d-r-η-p-a-e-j-4y	HF	1.651	2.508	146.4
	DFT	1.529	2.466	151.8
	MP2	1.583	2.504	151.5
Myrin-d-r-η-p-a-e-j-1z	HF	1.644	2.504	146.6
	DFT	1.517	2.459	152.1
	MP2	1.573	2.498	151.8
Myrin-d-r-η-p-a-e-j-1y	HF	1.644	2.503	146.6
	DFT	1.516	2.458	152.0
	MP2	1.574	2.498	151.8
Myrin-d-r-η-p-a-e-j-6y	HF	1.651	2.508	146.4
	DFT	1.530	2.467	151.8
	MP2	1.583	2.505	151.5
Myrin-d-r-η-p-a-e-j-6z	HF	1.651	2.508	146.4
	DFT	1.528	2.466	151.8
	MP2	1.583	2.504	151.5
Myrin-d-r-η-p-a-e-j-3z	HF	1.651	2.508	146.4
	DFT	1.528	2.465	151.8
	MP2	1.583	2.504	151.5
Myrin-d-r-η-p-a-e-j-3y	HF	1.651	2.508	146.4
	DFT	1.530	2.466	151.7
	MP2	1.583	2.504	151.5

Myrin-d-r-η-p-a-e-j-8y	HF	1.651	2.508	146.4
	DFT	1.529	2.466	151.8
	MP2	1.583	2.504	151.5
Myrin-d-r-η-p-a-e-j-8z	HF	1.651	2.508	146.4
	DFT	1.530	2.467	151.7
	MP2	1.583	2.504	151.5
Myrin-d-r-η-p-a-e-j-9y	HF	1.651	2.508	146.4
	DFT	1.528	2.466	151.8
	MP2	1.583	2.505	151.5
Myrin-d-r-η-p-a-e-j-9z	HF	1.652	2.508	146.4
	DFT	1.529	2.466	151.8
	MP2	1.583	2.504	151.5
Myrin-d-r-η-p-a-e-j-7y	HF	1.651	2.508	146.4
	DFT	1.530	2.467	151.7
	MP2	1.583	2.505	151.5
Myrin-d-r-η-p-a-e-j-7z	HF	1.652	2.508	146.4
	DFT	1.531	2.468	151.7
	MP2	1.583	2.505	151.5
Myrin-d-r-η-p-a-e-j-5z	HF	1.651	2.508	146.4
	DFT	1.530	2.467	151.8
	MP2	1.583	2.504	151.5
Myrin-d-r-η-p-a-e-j-5y	HF	1.651	2.508	146.4
	DFT	1.528	2.468	152.3
	MP2	1.583	2.504	151.5

Table 5.26. The distance between the H atom and the closest C atom in the acceptor aromatic 3ring for the O–H···π interactions of the selected calculated conformers of myristinin A having different geometries of R and the same geometry of the ring system *in vacuo*.
HF/6-31G(d,p), DFT/B3LYP/6-31+G(d,p) and MP2/ 6-31G(d,p) results are from full optimisation calculations. Conformers are listed in order of increasing relative energy in the HF results.

Conformer	H16···C23distance considered (Å)		
	HF	DFT	MP2
Myrin-d-r-η-p-a-e-j	2.128	2.055	2.008
Myrin-d-r-η-p-a-e-j-2y	2.129	2.052	2.011
Myrin-d-r-η-p-a-e-j-2z	2.127	2.055	2.007
Myrin-d-r-η-p-a-e-j-10y	2.128	2.055	2.008
Myrin-d-r-η-p-a-e-j-10z	2.128	2.055	2.008
Myrin-d-r-η-p-a-e-j-4z	2.128	2.052	2.008
Myrin-d-r-η-p-a-e-j-4y	2.128	2.055	2.008
Myrin-d-r-η-p-a-e-j-1z	2.129	2.053	2.008
Myrin-d-r-η-p-a-e-j-1y	2.128	2.055	2.012
Myrin-d-r-η-p-a-e-j-6y	2.128	2.056	2.008
Myrin-d-r-η-p-a-e-j-6z	2.128	2.057	2.008
Myrin-d-r-η-p-a-e-j-3z	2.128	2.056	2.008
Myrin-d-r-η-p-a-e-j-3y	2.128	2.054	2.008
Myrin-d-r-η-p-a-e-j-8y	2.128	2.057	2.008
Myrin-d-r-η-p-a-e-j-8z	2.128	2.057	2.008
Myrin-d-r-η-p-a-e-j-9y	2.128	2.054	2.008
Myrin-d-r-η-p-a-e-j-9z	2.128	2.052	2.008
Myrin-d-r-η-p-a-e-j-7y	2.128	2.057	2.008
Myrin-d-r-η-p-a-e-j-7z	2.128	2.052	2.008
Myrin-d-r-η-p-a-e-j-5z	2.128	2.057	2.008
Myrin-d-r-η-p-a-e-j-5y	2.128	2.038	2.008

Table 5.27. Dipole moment of the calculated conformers of myristinin A having different geometries of R and the same geometry of the ring system.
HF/6-31G(d,p), DFT/B3LYP/6-31+G(d,p) anf MP2/ 6-31G(d,p) results *in vacuo* are from full optimisation calculations. Conformers are listed in order of increasing relative energies in the HF results *in vacuo*.

Conformer	Dipole moment (Debye)		
	HF	DFT	MP2
Myrin-d-r-η-p-a-e-j	2.278	2.231	2.288
Myrin-d-r-η-p-a-e-j-2y	2.403	2.369	2.413
Myrin-d-r-η-p-a-e-j-2z	2.403	2.270	2.411
Myrin-d-r-η-p-a-e-j-10y	2.300	2.255	2.294
Myrin-d-r-η-p-a-e-j-10z	2.291	2.291	2.292
Myrin-d-r-η-p-a-e-j-4z	2.312	2.231	2.311

Myrin-d-r-η-p-a-e-j-4y	2.323	2.255	2.313
Myrin-d-r-η-p-a-e-j-1z	2.439	2.511	2.528
Myrin-d-r-η-p-a-e-j-1y	2.411	2.331	2.496
Myrin-d-r-η-p-a-e-j-6y	2.309	2.220	2.299
Myrin-d-r-η-p-a-e-j-6z	2.300	2.157	2.299
Myrin-d-r-η-p-a-e-j-3z	2.275	2.153	2.288
Myrin-d-r-η-p-a-e-j-3y	2.273	2.193	2.286
Myrin-d-r-η-p-a-e-j-8y	2.307	2.210	2.297
Myrin-d-r-η-p-a-e-j-8z	2.297	2.169	2.296
Myrin-d-r-η-p-a-e-j-9y	2.294	2.180	2.294
Myrin-d-r-η-p-a-e-j-9z	2.296	2.178	2.293
Myrin-d-r-η-p-a-e-j-7y	2.288	2.229	2.288
Myrin-d-r-η-p-a-e-j-7z	2.290	2.247	2.287
Myrin-d-r-η-p-a-e-j-5z	2.285	2.211	2.284
Myrin-d-r-η-p-a-e-j-5y	2.282	2.251	2.282

Table 5.28. HOMO-LUMO energy gap of the calculated conformers of myristinin A having different geometries of R and the same geometry of the ring system.
HF/6-31G(d,p), DFT/B3LYP/6-31+G(d,p) and MP2/ 6-31G(d,p) results *in vacuo*. The results are from full optimisation calculations. Conformers are listed in order of increasing relative energies in the HF results *in vacuo*.

Conformer	HOMO-LUMO energy gap (kcal/mol)		
	HF	DFT	MP2
Myrin-d-r-η-p-a-e-j	257.479	105.208	249.058
Myrin-d-r-η-p-a-e-j-2y	256.996	104.989	248.487
Myrin-d-r-η-p-a-e-j-2z	257.021	104.781	248.387
Myrin-d-r-η-p-a-e-j-10y	257.479	105.233	249.058
Myrin-d-r-η-p-a-e-j-10z	257.479	105.233	249.058
Myrin-d-r-η-p-a-e-j-4z	257.448	105.221	249.033
Myrin-d-r-η-p-a-e-j-4y	257.448	105.171	249.027
Myrin-d-r-η-p-a-e-j-1z	255.446	103.464	247.678
Myrin-d-r-η-p-a-e-j-1y	255.465	103.319	247.734
Myrin-d-r-η-p-a-e-j-6y	257.473	105.221	249.058
Myrin-d-r-η-p-a-e-j-6z	257.473	105.133	249.052
Myrin-d-r-η-p-a-e-j-3z	257.498	105.309	249.127
Myrin-d-r-η-p-a-e-j-3y	257.505	105.327	249.134
Myrin-d-r-η-p-a-e-j-8y	257.479	105.164	249.065
Myrin-d-r-η-p-a-e-j-8z	257.473	105.214	249.058
Myrin-d-r-η-p-a-e-j-9y	257.473	105.227	249.052
Myrin-d-r-η-p-a-e-j-9z	257.473	105.271	249.052
Myrin-d-r-η-p-a-e-j-7y	257.473	105.171	249.052
Myrin-d-r-η-p-a-e-j-7z	257.473	105.271	249.058
Myrin-d-r-η-p-a-e-j-5z	257.473	105.177	249.052
Myrin-d-r-η-p-a-e-j-5y	257.473	105.155	249.058

Figure 5.9. Shapes of the HOMO and LUMO molecular orbitals of the calculated conformers of myristinin A having different geometries of R and the same geometry of the ring system *in vacuo*.
HF/6-31G(d,p) results. The conformers are listed in order of increasing relative energy.

HOMO	LUMO	HOMO	LUMO
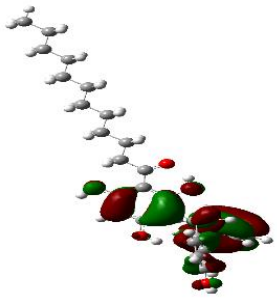	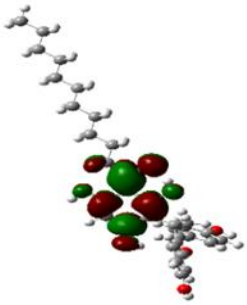	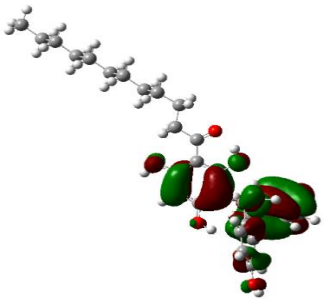	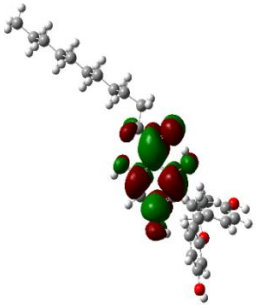
Myrin-d-r-η-p-a-e-j		Myrin-d-r-η-p-a-e-j-3z	
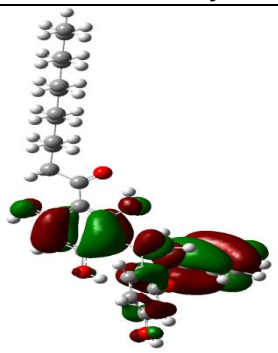	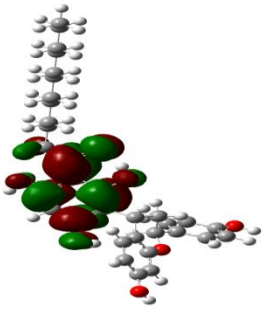	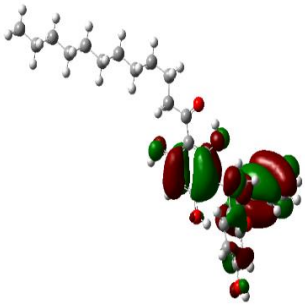	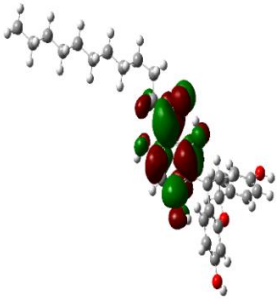
Myrin-d-r-η-p-a-e-j-2y		Myrin-d-r-η-p-a-e-j-3y	
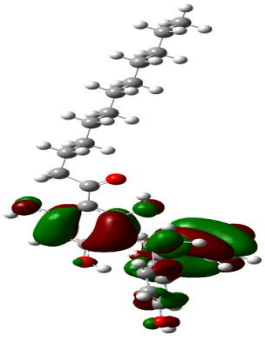	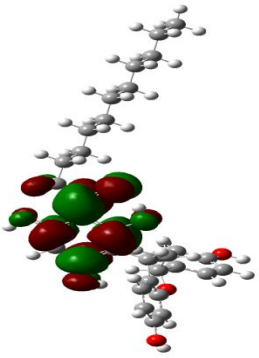	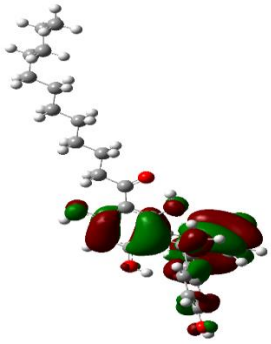	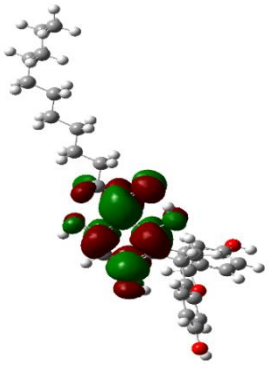
Myrin-d-r-η-p-a-e-j-2z		Myrin-d-r-η-p-a-e-j-8y	
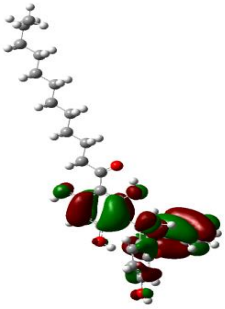	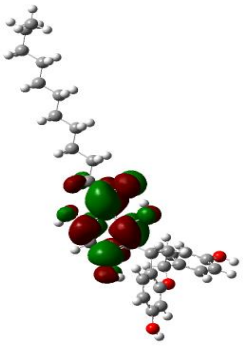	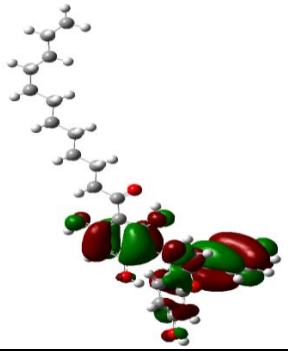	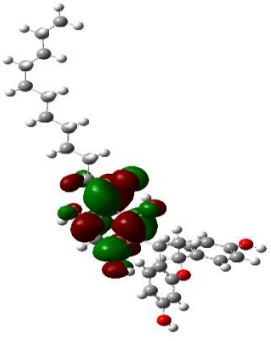
Myrin-d-r-η-p-a-e-j-10y		Myrin-d-r-η-p-a-e-j-8z	

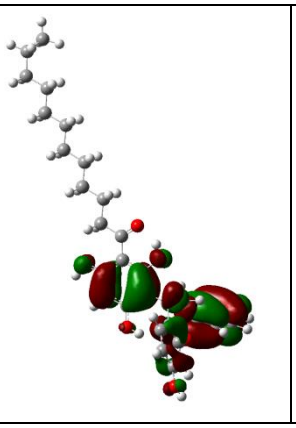	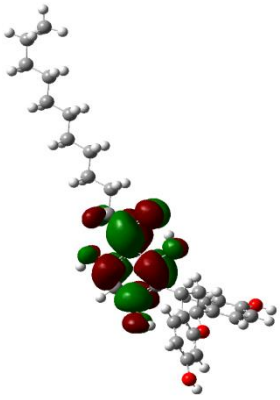
Myrin-d-r-η-p-a-e-j-10z	
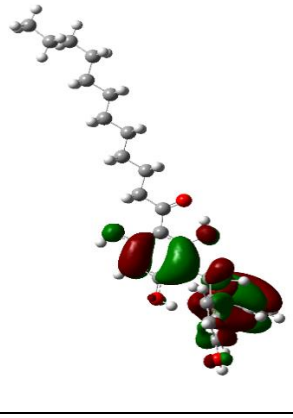	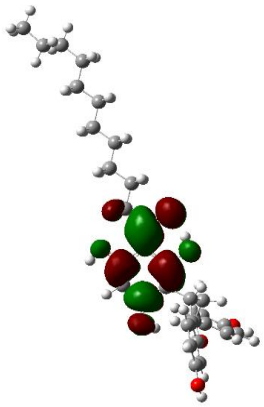
Myrin-d-r-η-p-a-e-j-9y	
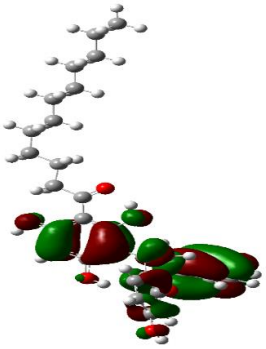	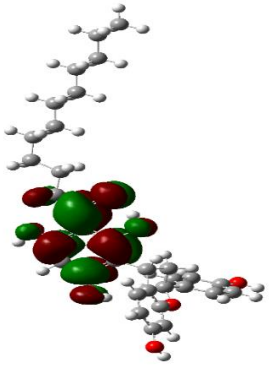
Myrin-d-r-η-p-a-e-j-4z	
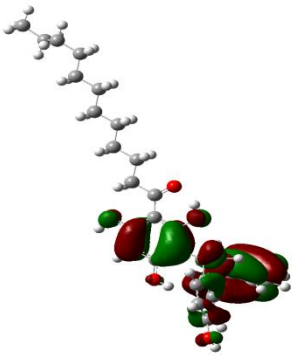	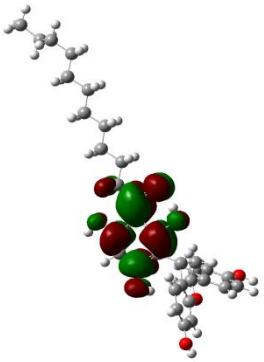
Myrin-d-r-η-p-a-e-j-9z	
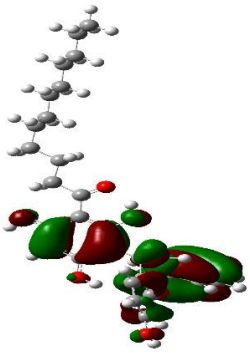	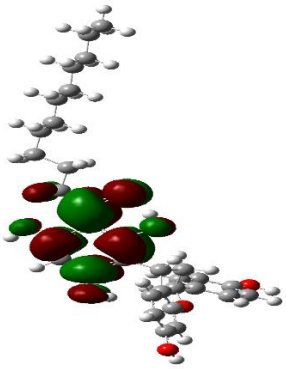
Myrin-d-r-η-p-a-e-j-4y	
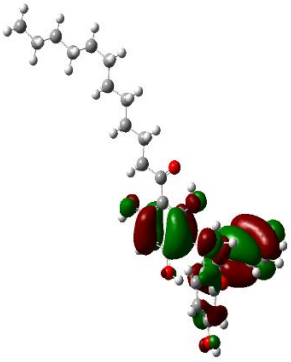	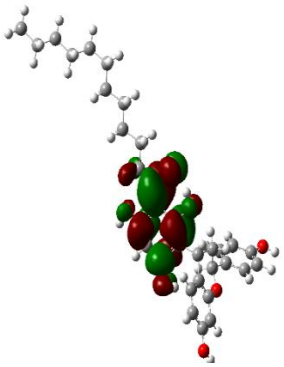
Myrin-d-r-η-p-a-e-j-7y	
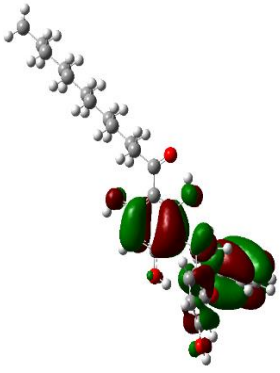	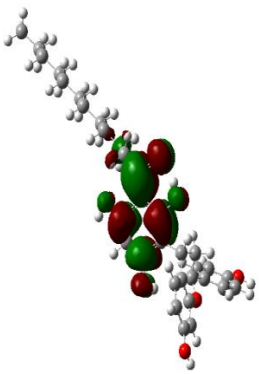
Myrin-d-r-η-p-a-e-j-1z	
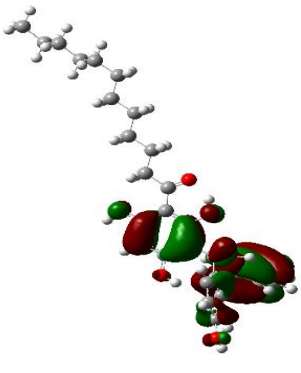	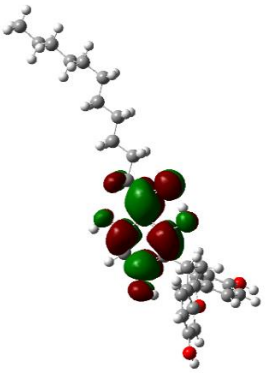
Myrin-d-r-η-p-a-e-j-7z	

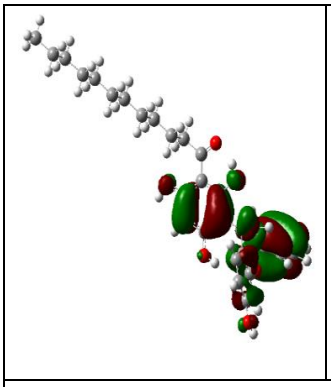 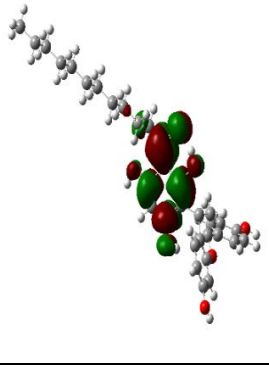	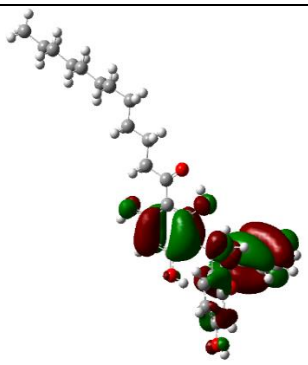 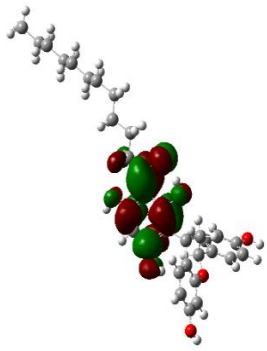
Myrin-d-r-η-p-a-e-j-1y	Myrin-d-r-η-p-a-e-j-5z
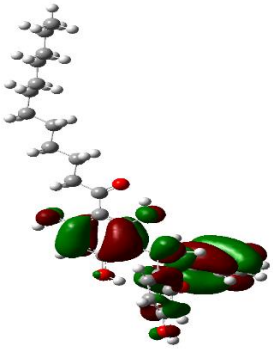 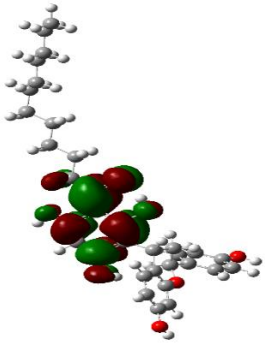	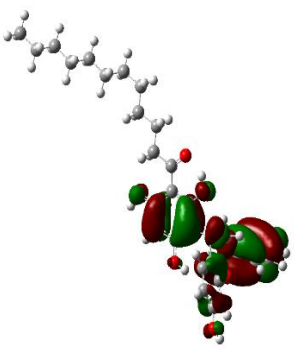 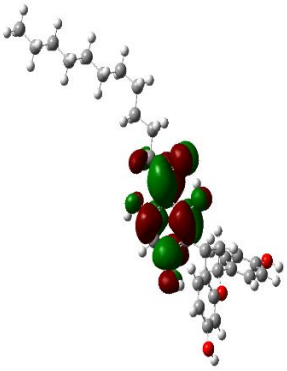
Myrin-d-r-η-p-a-e-j-6y	Myrin-d-r-η-p-a-e-j-5y
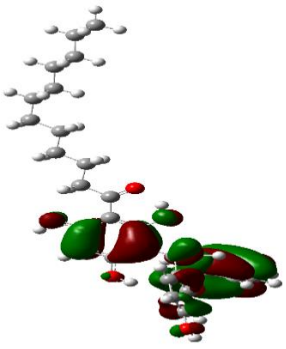 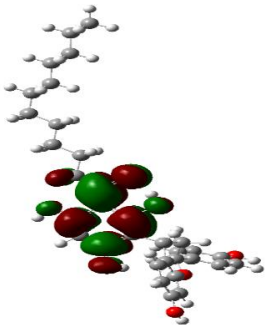	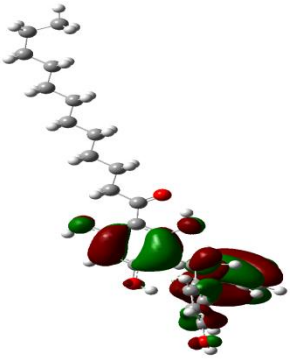 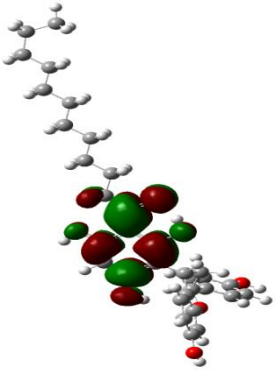
Myrin-d-r-η-p-a-e-j-6z	Myrin-d-r-η-p-a-e-j-10v
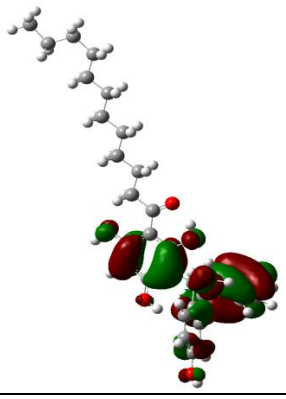 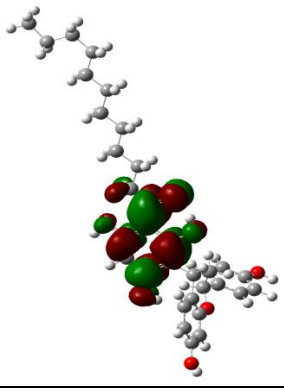	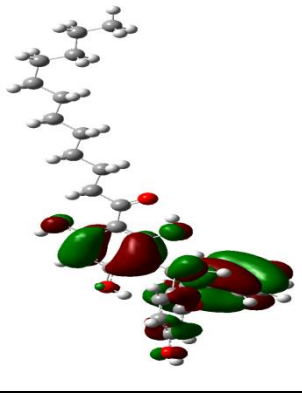 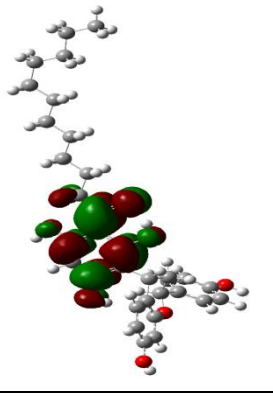
Myrin-d-r-η-p-a-e-j-9x	Myrin-d-r-η-p-a-e-j-8v

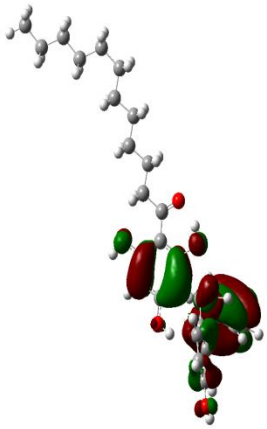	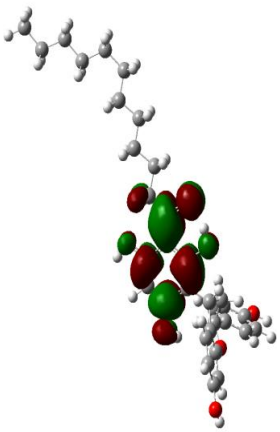	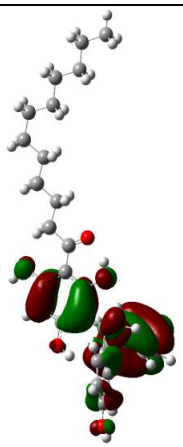	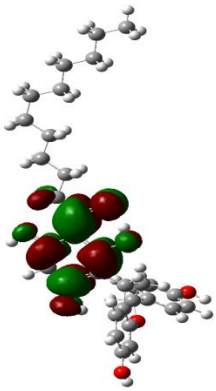
Myrin-d-r-η-p-a-e-j-7x		Myrin-d-r-η-p-a-e-j-6v	
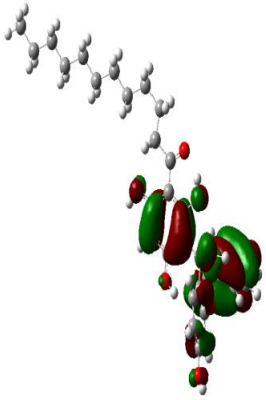	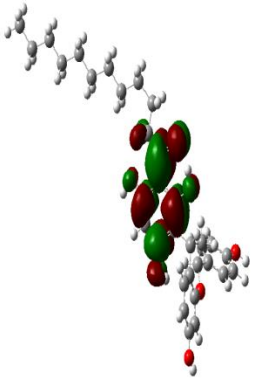	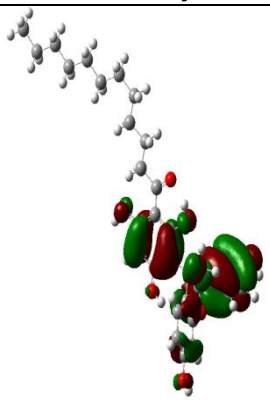	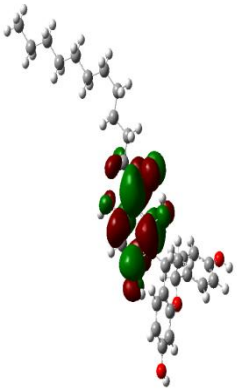
Myrin-d-r-η-p-a-e-j-3x		Myrin-d-r-η-p-a-e-j-5x	

Table 5.29. Relative energies of the calculated conformers of myristinin A having different geometries of R and the same geometry of the ring system *in vacuo* and in three solvents chloroform acetonitrile and water (respectively denoted as vac, chlrf, actn, aq in the column headings).
HF/6-31G(d,p) results. The results *in vacuo* and in solution are from full optimisation calculations. Conformers are listed in order of increasing relative energies in the HF results *in vacuo*. The absolute energies of the lowest-energy conformer (hartree) are -1797.0892235, -1797.1073376, -1797.1120259 and -1797.1124234 in vacuo, chloroform, acetonitrile and water respectively.

Conformer	Relative energy (kcal/mol)			
	vac	chlrf	actn	aq
Myrin-d-r-η-p-a-e-j	0.000	1.933	0.000	0.000
Myrin-d-r-η-p-a-e-j-2y	0.513	2.655	0.775	0.779
Myrin-d-r-η-p-a-e-j-2z	0.525	2.669	0.792	0.797
Myrin-d-r-η-p-a-e-j-10y	0.999	0.000	1.008	1.009
Myrin-d-r-η-p-a-e-j-10z	0.999	2.932	1.000	1.000
Myrin-d-r-η-p-a-e-j-4z	1.007	2.961	1.034	1.034
Myrin-d-r-η-p-a-e-j-4y	1.007	2.964	1.037	1.037
Myrin-d-r-η-p-a-e-j-1z	1.026	2.880	0.926	0.924
Myrin-d-r-η-p-a-e-j-1y	1.031	2.893	0.940	0.938
Myrin-d-r-η-p-a-e-j-6y	1.038	2.979	1.049	1.049
Myrin-d-r-η-p-a-e-j-6z	1.038	2.998	1.077	1.079
Myrin-d-r-η-p-a-e-j-3z	1.042	2.981	1.046	1.046
Myrin-d-r-η-p-a-e-j-3y	1.044	3.004	1.079	1.080
Myrin-d-r-η-p-a-e-j-8y	1.043	2.985	1.053	1.053
Myrin-d-r-η-p-a-e-j-8z	1.043	2.979	1.048	1.048
Myrin-d-r-η-p-a-e-j-9y	1.047	2.992	1.060	1.060
Myrin-d-r-η-p-a-e-j-9z	1.047	2.987	1.055	1.056
Myrin-d-r-η-p-a-e-j-7y	1.049	2.973	1.038	1.037
Myrin-d-r-η-p-a-e-j-7z	1.049	2.996	1.069	1.069
Myrin-d-r-η-p-a-e-j-5z	1.054	2.989	1.057	1.058
Myrin-d-r-η-p-a-e-j-5y	1.054	2.979	0.000	1.043

Table 5.30. The solvation free energy (ΔG_{solv}) and its electrostatic component (G_{el}) of the calculated conformers of myristinin A having different geometries of R and the same geometry of the ring system in three solvents chloroform, acetonitrile and water (respectively denoted as chlrf, actn, aq in the column headings).
HF/6-31G(d,p) results. The results in solution are from full optimisation calculations. Conformers are listed in order of increasing relative energies in the HF results *in vacuo*.

Conformer	(ΔG_{solv}) (kcal/mol)			(G_{el}) (kcal/mol)		
	chlrf	actn	aq	chlrf	actn	aq
Myrin-d-r-η-p-a-e-j	-0.13	7.52	-13.24	-8.03	-11.49	-26.49
Myrin-d-r-η-p-a-e-j-2y	-1.58	6.38	-14.82	-7.79	-11.15	-26.25
Myrin-d-r-η-p-a-e-j-2z	-1.47	6.41	-14.77	-7.78	-11.18	-26.26
Myrin-d-r-η-p-a-e-j-10y	-2.01	5.96	-15.44	-8.00	-11.38	-26.63
Myrin-d-r-η-p-a-e-j-10z	-1.96	5.98	-15.39	-7.96	-11.36	-26.58
Myrin-d-r-η-p-a-e-j-4z	-1.75	6.16	-15.12	-7.94	-11.35	-26.50

Myrin-d-r-η-p-a-e-j-4y	-1.77	6.15	-15.14	-7.94	-11.34	-26.50
Myrin-d-r-η-p-a-e-j-1z	-1.58	6.30	-15.39	-8.09	-11.53	-26.58
Myrin-d-r-η-p-a-e-j-1y	-1.62	6.24	-14.80	-8.09	-11.56	-26.56
Myrin-d-r-η-p-a-e-j-6y	-1.87	6.03	-15.31	-7.96	-11.39	-26.59
Myrin-d-r-η-p-a-e-j-6z	-1.85	6.03	-15.29	-7.95	-11.39	-26.58
Myrin-d-r-η-p-a-e-j-3z	-1.66	6.22	-15.04	-7.95	-11.37	-26.53
Myrin-d-r-η-p-a-e-j-3y	-1.69	6.19	-15.05	-7.95	-11.37	-26.52
Myrin-d-r-η-p-a-e-j-8y	-1.88	6.01	-15.29	-7.96	-11.41	-26.57
Myrin-d-r-η-p-a-e-j-8z	-1.89	6.03	-15.32	-7.97	-11.38	-26.61
Myrin-d-r-η-p-a-e-j-9y	-1.94	5.99	-15.36	-7.98	-11.40	-26.60
Myrin-d-r-η-p-a-e-j-9z	-1.92	6.00	-15.37	-7.96	-11.39	-26.62
Myrin-d-r-η-p-a-e-j-7y	-1.88	6.05	-15.34	-7.97	-11.37	-26.62
Myrin-d-r-η-p-a-e-j-7z	-1.86	6.06	-15.36	-7.96	-11.37	-26.65
Myrin-d-r-η-p-a-e-j-5z	-1.85	6.06	-15.30	-7.97	-11.38	-26.61
Myrin-d-r-η-p-a-e-j-5y	-1.86	6.14	-15.13	-7.97	-11.41	-26.56

Table 5.31. Parameters of the first IHB of the selected conformers of myristinin A having different geometries of R and the same geometry of the ring system *in vacuo* and in three solvents chloroform, acetonitrile and water (respectively denoted as vac, chlrf, actn, aq in the column headings).
HF/6-31G(d,p) results. The results *in vacuo* and in solution are from full optimisation calculations. Conformers are listed in order of increasing relative energies in the HF results *in vacuo*.

Conformer	Parameters of the first IHB			
	Media	O···H (Å)	O···O (Å)	OĤO (°)
Myrin-d-r-η-p-a-e-j	vac	1.652	2.508	146.4
	chlrf	1.646	2.506	146.9
	actn	1.644	2.506	147.1
	aq	1.644	2.507	147.1
Myrin-d-r-η-p-a-e-j-2y	vac	1.654	2.510	146.3
	chlrf	1.653	2.511	146.7
	actn	1.651	2.511	146.9
	aq	1.651	2.511	146.9
Myrin-d-r-η-p-a-e-j-2z	vac	1.654	2.509	146.3
	chlrf	1.652	2.510	146.7
	actn	1.651	2.510	146.9
	aq	1.650	2.510	146.9
Myrin-d-r-η-p-a-e-j-10y	vac	1.652	2.508	146.4
	chlrf	1.645	2.506	147.1
	actn	1.645	2.506	147.1
	aq	1.645	2.506	147.1
Myrin-d-r-η-p-a-e-j-10z	vac	1.651	2.508	146.4
	chlrf	1.646	2.506	146.9
	actn	1.645	2.506	147.1
	aq	1.644	2.506	147.1
Myrin-d-r-η-p-a-e-j-4z	vac	1.651	2.508	146.4

	chlrf	1.647	2.507	146.9
	actn	1.645	2.507	147.1
	aq	1.645	2.507	147.1
Myrin-d-r-η-p-a-e-j-4y	vac	1.651	2.508	146.4
	chlrf	1.646	2.506	146.9
	actn	1.644	2.505	147.1
	aq	1.643	2.505	147.2
Myrin-d-r-η-p-a-e-j-1z	vac	1.644	2.504	146.6
	chlrf	1.642	2.504	147.1
	actn	1.641	2.504	147.3
	aq	1.641	2.504	147.3
Myrin-d-r-η-p-a-e-j-1y	vac	1.644	2.503	146.6
	chlrf	1.640	2.502	147.1
	actn	1.638	2.502	147.3
	aq	1.638	2.502	147.4
Myrin-d-r-η-p-a-e-j-6y	vac	1.651	2.508	146.4
	chlrf	1.646	2.506	146.9
	actn	1.644	2.506	147.1
	aq	1.644	2.506	147.2
Myrin-d-r-η-p-a-e-j-6z	vac	1.651	2.508	146.4
	chlrf	1.646	2.507	146.9
	actn	1.645	2.506	147.1
	aq	1.644	2.506	147.2
Myrin-d-r-η-p-a-e-j-3z	vac	1.651	2.508	146.4
	chlrf	1.646	2.506	146.9
	actn	1.644	2.505	147.1
	aq	1.644	2.505	147.2
Myrin-d-r-η-p-a-e-j-3y	vac	1.651	2.508	146.4
	chlrf	1.646	2.506	146.9
	actn	1.644	2.505	147.1
	aq	1.644	2.505	147.2
Myrin-d-r-η-p-a-e-j-8y	vac	1.651	2.508	146.4
	chlrf	1.646	2.507	146.9
	actn	1.644	2.506	147.1
	aq	1.644	2.506	147.2
Myrin-d-r-η-p-a-e-j-8z	vac	1.651	2.508	146.4
	chlrf	1.646	2.507	146.9
	actn	1.645	2.506	147.1
	aq	1.644	2.506	147.2
Myrin-d-r-η-p-a-e-j-9y	vac	1.651	2.508	146.4
	chlrf	1.646	2.506	146.9
	actn	1.645	2.506	147.1
	aq	1.645	2.506	147.1
Myrin-d-r-η-p-a-e-j-9z	vac	1.652	2.508	146.4
	chlrf	1.646	2.506	146.9
	actn	1.644	2.505	147.1
	aq	1.644	2.505	147.1
Myrin-d-r-η-p-a-e-j-7y	vac	1.651	2.508	146.4
	chlrf	1.646	2.506	146.9
	actn	1.644	2.506	147.1
	aq	1.644	2.505	147.2

Myrin-d-r-η-p-a-e-j-7z	vac	1.652	2.508	146.4
	chlrf	1.646	2.506	146.9
	actn	1.644	2.506	147.1
	aq	1.644	2.506	147.2
Myrin-d-r-η-p-a-e-j-5z	vac	1.651	2.508	146.4
	chlrf	1.646	2.506	146.9
	actn	1.644	2.506	147.1
	aq	1.644	2.506	147.1
Myrin-d-r-η-p-a-e-j-5y	vac	1.651	2.508	146.4
	chlrf	1.646	2.506	146.9
	actn	1.644	2.506	147.1
	aq	1.644	2.506	147.2

Table 5.32. Distance between the H atom and the closest C atom in the acceptor aromatic ring for the O–H···π interactions in selected conformers of myristinin A having different geometries of R and the same geometry of the ring system *in vacuo* and in three solvents chloroform, acetonitrile and water (respectively denoted as vac, chlrf, actn, aq in the column headings).
HF/6-31G(d,p) results. The results *in vacuo* and in solution are from full optimisation calculations. Conformers are listed in order of increasing relative energies in the HF results *in vacuo*.

Conformer	H16···C23 distance considered (Å)			
	vac	chlrf	actn	aq
Myrin-d-r-η-p-a-e-j	2.128	2.125	2.124	2.124
Myrin-d-r-η-p-a-e-j-2y	2.129	2.127	2.126	2.126
Myrin-d-r-η-p-a-e-j-2z	2.127	2.127	2.126	2.126
Myrin-d-r-η-p-a-e-j-10y	2.128	2.124	2.124	2.124
Myrin-d-r-η-p-a-e-j-10z	2.128	2.125	2.124	2.124
Myrin-d-r-η-p-a-e-j-4z	2.128	2.124	2.123	2.123
Myrin-d-r-η-p-a-e-j-4y	2.128	2.128	2.127	2.127
Myrin-d-r-η-p-a-e-j-1z	2.129	2.127	2.126	2.126
Myrin-d-r-η-p-a-e-j-1y	2.128	2.125	2.124	2.124
Myrin-d-r-η-p-a-e-j-6y	2.128	2.127	2.126	2.126
Myrin-d-r-η-p-a-e-j-6z	2.128	2.126	2.126	2.126
Myrin-d-r-η-p-a-e-j-3z	2.128	2.129	2.129	2.129
Myrin-d-r-η-p-a-e-j-3y	2.128	2.126	2.126	2.126
Myrin-d-r-η-p-a-e-j-8y	2.128	2.129	2.128	2.128
Myrin-d-r-η-p-a-e-j-8z	2.128	2.125	2.124	2.124
Myrin-d-r-η-p-a-e-j-9y	2.128	2.128	2.128	2.128
Myrin-d-r-η-p-a-e-j-9z	2.128	2.126	2.125	2.125
Myrin-d-r-η-p-a-e-j-7y	2.128	2.126	2.125	2.125
Myrin-d-r-η-p-a-e-j-7z	2.128	2.126	2.126	2.126
Myrin-d-r-η-p-a-e-j-5z	2.128	2.128	2.127	2.127
Myrin-d-r-η-p-a-e-j-5y	2.128	2.126	2.125	2.125

Table 5.33. Dipole moment of the calculated conformers of myristinin A having different geometries of R and the same geometry of the ring system *in vacuo* and in three solvents chloroform, acetonitrile and water (respectively denoted as vac, chlrf, actn, aq in the column headings).
HF/6-31G(d,p) results. The results *in vacuo* and in solution are from full optimisation calculations. Conformers are listed in order of increasing relative energies in the HF results *in vacuo*.

Conformer	Dipole moment (Debye)			
	vac	chlrf	actn	aq
Myrin-d-r-η-p-a-e-j	2.278	2.696	2.863	2.879
Myrin-d-r-η-p-a-e-j-2y	2.403	2.756	2.903	2.917
Myrin-d-r-η-p-a-e-j-2z	2.403	2.783	2.940	2.955
Myrin-d-r-η-p-a-e-j-10y	2.300	2.909	2.909	2.925
Myrin-d-r-η-p-a-e-j-10z	2.291	2.721	2.891	2.907
Myrin-d-r-η-p-a-e-j-4z	2.312	2.757	2.922	2.937
Myrin-d-r-η-p-a-e-j-4y	2.323	2.726	2.876	2.892
Myrin-d-r-η-p-a-e-j-1z	2.439	2.943	3.137	3.156
Myrin-d-r-η-p-a-e-j-1y	2.411	2.918	3.098	3.114
Myrin-d-r-η-p-a-e-j-6y	2.309	2.718	2.880	2.895
Myrin-d-r-η-p-a-e-j-6z	2.300	2.736	2.889	2.905
Myrin-d-r-η-p-a-e-j-3z	2.275	2.676	2.843	2.858
Myrin-d-r-η-p-a-e-j-3y	2.273	2.735	2.886	2.899
Myrin-d-r-η-p-a-e-j-8y	2.307	2.726	2.884	2.899
Myrin-d-r-η-p-a-e-j-8z	2.297	2.740	2.921	2.937
Myrin-d-r-η-p-a-e-j-9y	2.294	2.740	2.906	2.922
Myrin-d-r-η-p-a-e-j-9z	2.296	2.710	2.873	2.888
Myrin-d-r-η-p-a-e-j-7y	2.288	2.727	2.898	2.914
Myrin-d-r-η-p-a-e-j-7z	2.290	2.745	2.903	2.918
Myrin-d-r-η-p-a-e-j-5z	2.285	2.705	2.872	2.888
Myrin-d-r-η-p-a-e-j-5y	2.282	2.714	2.883	2.899

Table 5.34. HOMO-LUMO energy gap of the calculated conformers of myristinin A having different geometries of R and the same geometry of the ring system *in vacuo* and in three solvents chloroform, acetonitrile and water (respectively denoted as vac, chlrf, actn, aq in the column headings).
HF/6-31G(d,p) results. The results *in vacuo* and in solution are from full optimisation calculations. Conformers are listed in order of increasing relative energies in the HF results *in vacuo*.

Conformer	HOMO-LUMO energy gap (kcal/mol)			
	vac	chlrf	actn	aq
Myrin-d-r-η-p-a-e-j	257.479	256.871	256.582	256.557
Myrin-d-r-η-p-a-e-j-2y	256.996	254.417	254.022	253.984
Myrin-d-r-η-p-a-e-j-2z	257.021	254.323	253.903	253.865
Myrin-d-r-η-p-a-e-j-10y	257.479	256.576	256.344	256.319
Myrin-d-r-η-p-a-e-j-10z	257.479	256.526	256.281	256.256
Myrin-d-r-η-p-a-e-j-4z	257.448	256.839	256.570	256.545
Myrin-d-r-η-p-a-e-j-4y	257.448	256.902	256.607	256.576

Myrin-d-r-η-p-a-e-j-1z	255.446	256.827	256.551	256.526
Myrin-d-r-η-p-a-e-j-1y	255.465	256.865	256.588	256.563
Myrin-d-r-η-p-a-e-j-6y	257.473	256.865	256.588	256.563
Myrin-d-r-η-p-a-e-j-6z	257.473	256.827	256.545	256.519
Myrin-d-r-η-p-a-e-j-3z	257.498	256.839	256.557	256.532
Myrin-d-r-η-p-a-e-j-3y	257.505	256.808	256.532	256.501
Myrin-d-r-η-p-a-e-j-8y	257.479	256.839	256.545	256.513
Myrin-d-r-η-p-a-e-j-8z	257.473	256.513	256.551	256.821
Myrin-d-r-η-p-a-e-j-9y	257.473	256.802	256.501	256.469
Myrin-d-r-η-p-a-e-j-9z	257.473	256.839	256.551	256.526
Myrin-d-r-η-p-a-e-j-7y	257.473	256.808	256.507	256.482
Myrin-d-r-η-p-a-e-j-7z	257.473	256.865	256.588	256.563
Myrin-d-r-η-p-a-e-j-5z	257.473	256.588	256.588	256.557
Myrin-d-r-η-p-a-e-j-5y	257.473	256.865	256.582	256.557

Table 5.35. Relative energies of all calculated conformers of myristinin A.
HF/6-31G(d,p) results *in vacuo*. The conformers are arranged in order of increasing relative energy.

Conformer	Relative energy (kcal/mol)	Conformer	Relative energy (kcal/mol)
Myrin-d-r-η-p-a-e-j	0.000	Myrin-s-w-p-b-f-j	5.581
Myrin-d-r-η-p-a-e-k	0.013	Myrin-s-r-η-p-a-f-k	5.679
Myrin-d-r-η-p-a-f-j	0.423	Myrin-d-w-q-a-f-j	5.679
Myrin-d-r-η-p-a-f-k	0.495	Myrin-d-r-q-a-e-j	5.716
Myrin-d-r-η-p-a-e-j-2y	0.513	Myrin-d-r-q-b-e-j	5.733
Myrin-d-r-η-p-a-e-j-2z	0.525	Myrin-d-r-q-a-e-k	5.743
Myrin-d-r-η-p-a-e-j-10y	0.999	Myrin-s-r-η-p-a-f-j	5.751
Myrin-d-r-η-p-a-e-j-10z	0.999	Myrin-d-w-q-a-f-k	5.819
Myrin-d-r-η-p-b-e-k	1.004	Myrin-d-w-q-b-f-k	5.868
Myrin-d-r-η-p-a-e-j-4z	1.007	Myrin-s-w-p-a-e-j	6.121
Myrin-d-r-η-p-a-e-j-4y	1.007	Myrin-d-r-q-a-f-k	6.224
Myrin-d-r-η-p-b-e-j	1.010	Myrin-s-r-η-u-p-a-e-j	6.260
Myrin-d-r-η-p-a-e-j-1z	1.026	Myrin -d-r-1-p-a-e-j-10v	6.297
Myrin-d-r-η-p-a-e-j-1y	1.031	Myrin -d-r-1-p-a-e-j-9x	6.365
Myrin-d-r-η-p-a-e-j-6y	1.038	Myrin -d-r-1-p-a-e-j-8v	6.383
Myrin-d-r-η-p-a-e-j-6z	1.038	Myrin -d-r-1-p-a-e-j-6v	6.384
Myrin-d-r-η-p-a-e-j-3z	1.042	Myrin -d-r-1-p-a-e-j-7x	6.390
Myrin-d-r-η-p-a-e-j-3y	1.044	Myrin -d-r-1-p-a-e-j-5x	6.392
Myrin-d-r-η-p-a-e-j-8y	1.043	Myrin-s-w-p-a-f-j	6.427
Myrin-d-r-η-p-a-e-j-8z	1.043	Myrin-s-r-η-p-b-e-j	6.496
Myrin-d-r-η-p-a-e-j-9y	1.047	Myrin-s-w-p-a-f-k	6.507
Myrin-d-r-η-p-a-e-j-9z	1.047	Myrin -d-r-1-p-a-e-j-3x	6.536
Myrin-d-r-η-p-a-e-j-7y	1.049	Myrin-s-r-η-u-p-a-f-j	6.684

Myrin-d-r-ɳ-p-a-e-j-7z	1.049	Myrin-s-r-ɳ-u-p-a-f-k	6.701
Myrin-d-r-ɳ-p-a-e-j-5z	1.054	Myrin-d-r-q-b-e-k	6.761
Myrin-d-r-ɳ-p-a-e-j-5y	1.054	Myrin-s-r-ɳ-u-p-b-e-k	6.919
Myrin-s-w-ɛ-q-a-e-j	1.207	Myrin-s-r-ɳ-u-p-b-f-k	7.125
Myrin-d-r-ɳ-p-b-f-j	1.212	Myrin-s-w-p-e-a-k	7.141
Myrin-d-r-ɳ-p-b-f-k	1.244	Myrin-d-w-u-p-a-e-j	7.704
Myrin-s-w-ɛ-q-b-e-j	1.501	Myrin-d-w-u-p-a-e-k	7.828
Myrin-s-w-ɛ-q-a-f-j	1.646	Myrin-d-w-u-p-b-e-k	7.828
Myrin-s-w-ɛ-q-a-f-k	1.661	Myrin-d-w-u-p-a-f-j	8.048
Myrin-s-w-ɛ-q-b-e-k	1.752	Myrin-d-w-u-p-b-f-j	8.048
Myrin-s-w-ɛ-q-b-f-k	1.984	Myrin-s-w-u-p-a-f-j	8.182
Myrin-d-w-p-a-e-k	4.452	Myrin-s-w-u-p-b-e-j	8.221
Myrin-d-w-p-a-f-j	4.652	Myrin-d-w-u-p-a-f-k	8.233
Myrin-d-w-p-b-f-j	4.652	Myrin-d-w-u-p-b-f-k	8.233
Myrin-d-r-ɳ-u-p-a-e-j	4.659	Myrin-s-w-u-p-e-a-k	8.267
Myrin-d-r-ɳ-u-p-a-e-k	4.666	Myrin-s-w-p-b-e-j	8.323
Myrin-s-r-ɛ-q-b-e-j	4.707	Myrin-s-w-u-p-a-e-j	8.327
Myrin-s-r-ɛ-q-b-f-j	4.837	Myrin-s-w-u-q-a-e-j	8.396
Myrin-d-w-p-a-f-k	4.846	Myrin-s-w-u-q-b-e-j	8.402
Myrin-d-w-p-b-e-j	4.921	Myrin-d-w-u-q-b-e-j	8.416
Myrin-d-r-q-b-f-j	4.981	Myrin-d-w-u-q-a-e-j	8.418
Myrin-s-r-ɛ-q-b-f-k	5.030	Myrin-s-w-u-p-b-f-j	8.476
Myrin-s-r-ɛ-q-a-e-k	5.034	Myrin-s-w-u-q-a-e-k	8.487
Myrin-d-r-ɳ-u-p-a-f-j	5.080	Myrin-d-w-u-q-a-e-k	8.523
Myrin-d-w-p-b-e-k	5.143	Myrin-s-w-u-p-b-e-k	8.534
Myrin-d-r-ɳ-u-p-a-f-k	5.145	Myrin-d-w-u-q-b-f-j	8.710
Myrin-s-r-ɛ-q-a-e-j	5.158	Myrin-s-w-u-p-a-f-k	8.814
Myrin-d-w-q-b-e-j	5.165	Myrin-s-w-u-p-b-f-k	8.827
Myrin-d-w-p-b-f-k	5.203	Myrin-d-w-u-q-a-f-j	8.861
Myrin-d-w-q-a-e-j	5.206	Myrin-s-w-u-q-a-f-k	8.874
Myrin-s-r-ɳ-p-e-a-k	5.220	Myrin-d-w-u-q-a-f-k	9.028
Myrin-s-r-ɳ-p-b-e-k	5.243	Myrin-d-w-u-q-b-f-k	9.092
Myrin-d-w-q-a-e-k	5.284	Myrin-d-r-u-q-a-e-j	10.103
Myrin-s-r-ɳ-p-a-e-j	5.353	Myrin-s-r-u-q-b-e-j	10.266
Myrin-s-r-ɳ-p-b-f-k	5.383	Myrin-d-r-q-a-f-j	10.412
Myrin-d-w-q-b-f-j	5.461	Myrin-d-r-u-q-a-f-j	10.513
Myrin-d-r-q-b-f-k	5.485	Myrin-s-r-u-q-a-e-j	11.089
Myrin-s-r-ɛ-q-a-f-k	5.511	Myrin-s-r-u-q-a-e-k	11.112
Myrin-d-w-q-b-e-k	5.536	Myrin-s-r-u-q-a-f-j	11.389
Myrin-s-r-ɛ-q-a-f-j	5.572	Myrin-s-r-u-q-a-f-k	11.473

Table 5.36. Parameters of the first IHB of all calculated conformers of myristinin A.
HF/6-31G(d,p) results *in vacuo*. For d-type conformers, the first IHB is H15···O14; for s-type conformers, the first IHB is H17···O14. The conformers are arranged in order of increasing relative energy.

Conformer	Parameters of the first IHB		
	OH···O (Å)	O···O (Å)	OHO (°)
Myrin-d-r-η-p-a-e-j	1.652	2.508	146.4
Myrin-d-r-η-p-a-e-k	1.652	2.508	146.3
Myrin-d-r-η-p-a-f-j	1.652	2.508	146.4
Myrin-d-r-η-p-a-f-k	1.652	2.508	146.4
Myrin-d-r-η-p-a-e-j-2y	1.654	2.510	146.3
Myrin-d-r-η-p-a-e-j-2z	1.654	2.509	146.3
Myrin-d-r-η-p-a-e-j-10y	1.652	2.508	146.4
Myrin-d-r-η-p-a-e-j-10z	1.651	2.508	146.4
Myrin-d-r-η -p-b-e-k	1.651	2.508	146.6
Myrin-d-r-η-p-a-e-j-4z	1.651	2.508	146.4
Myrin-d-r-η-p-a-e-j-4y	1.651	2.508	146.4
Myrin-d-r-η -p-b-e-j	1.655	2.510	146.2
Myrin-d-r-η-p-a-e-j-1z	1.644	2.504	146.6
Myrin-d-r-η-p-a-e-j-1y	1.644	2.503	146.6
Myrin-d-r-η-p-a-e-j-6y	1.651	2.508	146.4
Myrin-d-r-η-p-a-e-j-6z	1.651	2.508	146.4
Myrin-d-r-η-p-a-e-j-3z	1.651	2.508	146.4
Myrin-d-r-η-p-a-e-j-3y	1.651	2.508	146.4
Myrin-d-r-η-p-a-e-j-8y	1.651	2.508	146.4
Myrin-d-r-η-p-a-e-j-8z	1.651	2.508	146.4
Myrin-d-r-η-p-a-e-j-9y	1.651	2.508	146.4
Myrin-d-r-η-p-a-e-j-9z	1.652	2.508	146.4
Myrin-d-r-η-p-a-e-j-7y	1.651	2.508	146.4
Myrin-d-r-η-p-a-e-j-7z	1.652	2.508	146.4
Myrin-d-r-η-p-a-e-j-5z	1.651	2.508	146.4
Myrin-d-r-η-p-a-e-j-5y	1.651	2.508	146.4
Myrin-s-w-ε-q-a-e-j	1.683	2.521	143.9
Myrin-d-r-η-p-b-f-j	1.655	2.510	146.2
Myrin-d-r-η-p-b-f-k	1.651	2.508	146.5
Myrin-s-w-ε-q-b-e-j	1.689	2.527	144.0
Myrin-s-w-ε-q-a-f-j	1.682	2.520	143.9
Myrin-s-w-ε-q-a-f-k	1.683	2.521	143.9
Myrin-s-w-ε-q-b-f-k	1.689	2.526	144.0
Myrin-d-w-p-a-e-k	1.656	2.511	146.2
Myrin-d-w-p-a-f-j	1.656	2.511	146.3

Myrin-d-w-p-b-f-j	1.655	2.510	146.3
Myrin-d-r-η-u-p-a-e-j	1.675	2.523	145.4
Myrin-d-r-η-u-p-a-e-k	1.676	2.524	145.4
Myrin-s-r-ε-q-b-e-j	1.695	2.531	143.9
Myrin-s-r-ε-q-b-f-j	1.694	2.531	143.9
Myrin-d-w-p-a-f-k	1.656	2.511	146.2
Myrin-d-w-p-b-e-j	1.659	2.512	146.1
Myrin-d-r-q-b-f-j	1.657	2.510	145.9
Myrin-s-r-ε-q-b-f-k	1.694	2.531	143.9
Myrin-s-r-ε-q-a-e-k	1.692	2.527	143.8
Myrin-d-r-η-u-p-a-f-j	1.675	2.522	145.4
Myrin-d-w-p-b-e-k	1.658	2.512	146.2
Myrin-d-r-η-u-p-a-f-k	1.676	2.523	145.4
Myrin-s-r-ε-q-a-e-j	1.690	2.526	143.8
Myrin-d-w-q-b-e-j	1.664	2.514	145.6
Myrin-d-w-p-b-f-k	1.659	2.513	146.1
Myrin-d-w-q-a-e-j	1.654	2.508	146.1
Myrin-s-r-η-p-e-a-k	1.697	2.532	143.8
Myrin-s-r-η-p-b-e-k	1.692	2.528	143.8
Myrin-d-w-q-a-e-k	1.654	2.508	146.1
Myrin-s-r-η-p-a-e-j	1.697	2.532	143.8
Myrin-s-r-η-p-b-f-k	1.691	2.527	143.8
Myrin-d-w-q-b-f-j	1.665	2.515	145.6
Myrin-d-r-q-b-f-k	1.659	2.511	145.8
Myrin-s-r-ε-q-a-f-k	1.689	2.526	143.8
Myrin-d-w-q-b-e-k	1.664	2.514	145.6
Myrin-s-r-ε-q-a-f-j	1.688	2.524	143.9
Myrin-s-w-p-b-f-j	1.683	2.521	143.9
Myrin-s-r-η-p-a-f-k	1.696	2.532	143.8
Myrin-d-w-q-a-f-j	1.655	2.508	146.0
Myrin-d-r-q-a-e-j	1.646	2.503	146.4
Myrin-d-r-q-b-e-j	1.646	2.504	146.5
Myrin-d-r-q-a-e-k	1.646	2.503	146.4
Myrin-s-r-η-p-a-f-j	1.696	2.531	143.8
Myrin-d-w-q-a-f-k	1.656	2.509	146.0
Myrin-d-w-q-b-f-k	1.665	2.515	145.6
Myrin-s-w-p-a-e-j	1.689	2.526	143.7
Myrin-d-r-q-a-f-k	1.648	2.504	146.3
Myrin-s-r-η-u-p-a-e-j	1.737	2.560	142.4
Myrin -d-r-η-p-a-e-j-10v	1.651	2.508	146.4
Myrin-d-r-η-p-a-e-j-9x	1.651	2.508	146.4
Myrin-d-r-η-p-a-e-j-8v	1.651	2.508	146.4
Myrin-d-r-η-p-a-e-j-6v	1.651	2.508	146.4
Myrin-d-r-η-p-a-e-j-7x	1.651	2.508	146.4
Myrin-d-r-η-p-a-e-j-3x	1.651	2.508	146.4

Myrin-d-r-η-p-a-e-j-5x	1.651	2.508	146.4
Myrin-s-w-p-a-f-j	1.689	2.526	143.8
Myrin-s-r-η-p-b-e-j	1.691	2.527	143.8
Myrin-s-w-p-a-f-k	1.689	2.526	143.8
Myrin-s-r-η-u-p-a-f-j	1.738	2.560	142.4
Myrin-s-r-η-u-p-a-f-k	1.737	2.559	142.5
Myrin-d-r-q-b-e-k	1.646	2.504	146.5
Myrin-s-r-η-u-p-b-e-k	1.730	2.555	142.6
Myrin-s-r-η-u-p-b-f-k	1.731	2.555	142.6
Myrin-s-w-p-e-a-k	1.685	2.522	143.8
Myrin-d-w-u-p-a-e-j	1.682	2.527	145.3
Myrin-d-w-u-p-a-e-k	1.681	2.526	145.2
Myrin-d-w-u-p-b-e-k	1.681	2.526	145.2
Myrin-d-w-u-p-a-f-j	1.682	2.527	145.3
Myrin-d-w-u-p-b-f-j	1.681	2.527	145.3
Myrin-s-w-u-p-b-e-j	1.725	2.551	142.6
Myrin-d-w-u-p-a-f-k	1.682	2.528	145.3
Myrin-d-w-u-p-b-f-k	1.682	2.528	145.3
Myrin-s-w-u-p-e-a-k	1.730	2.553	142.4
Myrin-s-w-p-b-e-j	1.725	2.551	142.6
Myrin-s-w-u-p-a-e-j	1.730	2.554	142.5
Myrin-s-w-u-q-a-e-j	1.732	2.555	142.4
Myrin-s-w-u-q-b-e-j	1.729	2.554	142.6
Myrin-d-w-u-q-b-e-j	1.694	2.532	144.4
Myrin-d-w-u-q-a-e-j	1.686	2.527	144.7
Myrin-s-w-u-p-b-f-j	1.726	2.551	142.6
Myrin-s-w-u-q-a-e-k	1.732	2.556	142.4
Myrin-d-w-u-q-a-e-k	1.685	2.526	144.7
Myrin-s-w-u-p-b-e-k	1.725	2.550	142.6
Myrin-d-w-u-q-b-f-j	1.696	2.534	144.3
Myrin-s-w-u-p-a-f-k	1.729	2.553	142.5
Myrin-s-w-u-p-b-f-k	1.726	2.551	142.6
Myrin-d-w-u-q-a-f-j	1.689	2.529	144.5
Myrin-s-w-u-q-a-f-k	1.731	2.555	142.5
Myrin-d-w-u-q-a-f-k	1.688	2.528	144.5
Myrin-d-w-u-q-b-f-k	1.696	2.534	144.3
Myrin-d-r-u-q-a-e-j	1.676	2.524	145.5
Myrin-s-r-u-q-b-e-j	1.739	2.561	142.4
Myrin-d-r-q-a-f-j	1.648	2.504	146.3
Myrin-d-r-u-q-a-f-j	1.677	2.523	145.4
Myrin-s-r-u-q-a-e-j	1.739	2.561	142.4
Myrin-s-r-u-q-a-e-k	1.740	2.562	142.4
Myrin-s-r-u-q-a-f-j	1.737	2.560	142.4
Myrin-s-r-u-q-a-f-k	1.738	2.560	142.4

Table 5.37. Distance between the H atom and the closest C atom in the acceptor aromatic ring for the O–H···π interactions of all calculated conformers of myristinin A.
HF/6-31G(d,p) results *in vacuo*. The conformers are arranged in order of increasing relative energy. For p-type conformers, the distance considered is H16···C23; for q-type conformers, the distance considered is H15···C23.

Conformer	H15···C23 or H16···C23 (Å)	Conformer	H15···C23 or H16···C23 (Å)
Myrin-d-r-η -p-a-e-j	2.128	Myrin-s-w-ε-q-b-f-k	2.187
Myrin-d-r-η -p-a-e-k	2.127	Myrin-d-r-η-u-p-a-e-j	2.128
Myrin-d-r-η -p-a-f-j	2.131	Myrin-d-r-η-u-p-a-e-k	2.128
Myrin-d-r-η -p-a-f-k	2.130	Myrin-s-r-ε-q-b-e-j	2.165
Myrin-d-r-η-p-a-e-j-2y	2.129	Myrin-s-r-ε-q-b-f-j	2.169
Myrin-d-r-η-p-a-e-j-2z	2.127	Myrin-s-r-ε-q-b-f-k	2.171
Myrin-d-r-η-p-a-e-j-10y	2.128	Myrin-s-r-ε-q-a-e-k	2.057
Myrin-d-r-η-p-a-e-j-10z	2.128	Myrin-d-r-η-u-p-a-f-j	2.131
Myrin-d-r-η-p-b-e-k	2.213	Myrin-d-r-η-u-p-a-f-k	2.130
Myrin-d-r-η-p-a-e-j-4z	2.128	Myrin-s-r-ε-q-a-e-j	2.058
Myrin-d-r-η-p-a-e-j-4y	2.128	Myrin-s-r-η-p-e-a-k	2.109
Myrin-d-r-η -p-b-e-j	2.236	Myrin-s-r-η-p-b-e-k	2.220
Myrin-d-r-η-p-a-e-j-1z	2.129	Myrin-s-r-η-p-a-e-j	2.109
Myrin-d-r-η-p-a-e-j-1y	2.128	Myrin-s-r-η-p-b-f-k	2.221
Myrin-d-r-η-p-a-e-j-6y	2.128	Myrin-s-r-ε-q-a-f-k	2.059
Myrin-d-r-η-p-a-e-j-6z	2.128	Myrin-s-r-ε-q-a-f-j	2.060
Myrin-d-r-η-p-a-e-j-3z	2.128	Myrin-s-r-η-p-a-f-k	2.111
Myrin-d-r-η-p-a-e-j-3y	2.128	Myrin-s-r-η-p-a-f-j	2.112
Myrin-d-r-η-p-a-e-j-8y	2.128	Myrin-d-r-η-p-a-e-j-10v	2.128
Myrin-d-r-η-p-a-e-j-8z	2.128	Myrin-d-r-η-p-a-e-j-9x	2.128
Myrin-d-r-η-p-a-e-j-9y	2.128	Myrin-d-r-η-p-a-e-j-8v	2.128
Myrin-d-r-η-p-a-e-j-9z	2.128	Myrin-d-r-η-p-a-e-j-6v	2.128
Myrin-d-r-η-p-a-e-j-7y	2.128	Myrin-d-r-η-p-a-e-j-7x	2.128
Myrin-d-r-η-p-a-e-j-7z	2.128	Myrin-d-r-η-p-a-e-j-3x	2.128
Myrin-d-r-η-p-a-e-j-5z	2.128	Myrin-d-r-η-p-a-e-j-5x	2.128
Myrin-d-r-η-p-a-e-j-5y	2.128	Myrin-s-r-η-u-p-a-e-j	2.121
Myrin-d-r-η -p-b-f-j	2.239	Myrin-s-r-η-u-p-a-f-j	2.122
Myrin-d-r-η -p-b-f-k	2.219	Myrin-s-r-η-u-p-a-f-k	2.123
Myrin-s-w-ε-q-b-e-j	2.185	Myrin-s-r-η-u-p-b-e-k	2.237
Myrin-s-w-ε-q-a-f-j	2.076	Myrin-s-r-η-u-p -b-f-k	2.240
Myrin-s-w-ε-q-a-f-k	2.075		

Table 5.38. Dipole moments of the calculated conformers of myristinin A of all calculated conformers of myristinin A.
HF/6-31G(d,p) results *in vacuo*. The conformers are arranged in order of increasing relative energy.

Conformer	Dipole moment (Debye)	Conformer	Dipole moment (Debye)
Myrin-d-r-η-p-a-e-j	2.278	Myrin-s-r-ε-q-a-f-j	6.978
Myrin-d-r-η-p-a-e-k	3.695	Myrin-s-w-p-b-f-j	2.483
Myrin-d-r-η-p-a-f-j	2.873	Myrin-s-r-η-p-a-f-k	4.414
Myrin-d-r-η-p-a-f-k	4.092	Myrin-d-w-q-a-f-j	8.066
Myrin-d-r-η-p-a-e-j-2y	2.403	Myrin-d-r-q-a-e-j	3.511
Myrin-d-r-η-p-a-e-j-2z	2.403	Myrin-d-r-q-b-e-j	3.340
Myrin-d-r-η-p-a-e-j-10y	2.300	Myrin-d-r-q-a-e-k	4.715
Myrin-d-r-η-p-a-e-j-10z	2.291	Myrin-s-r-η-p-a-f-j	7.092
Myrin-d-r-η-p-b-e-k	2.468	Myrin-d-w-q-a-f-k	9.326
Myrin-d-r-η-p-a-e-j-4z	2.312	Myrin-d-w-q-b-f-k	9.019
Myrin-d-r-η-p-a-e-j-4y	2.323	Myrin-s-w-p-a-e-j	4.341
Myrin-d-r-η-p-b-e-j	2.643	Myrin-d-r-q-a-f-k	6.037
Myrin-d-r-η-p-a-e-j-1z	2.439	Myrin-s-r-η-u-p-a-e-j	5.623
Myrin-d-r-η-p-a-e-j-1y	2.411	Myrin -d-r-η-p-a-e-j-10v	2.295
Myrin-d-r-η-p-a-e-j-6y	2.309	Myrin-d-r-η-p-a-e-j-9x	2.312
Myrin-d-r-η-p-a-e-j-6z	2.300	Myrin-d-r-η-p-a-e-j-8v	2.304
Myrin-d-r-η-p-a-e-j-3z	2.275	Myrin-d-r-η-p-a-e-j-6v	2.309
Myrin-d-r-η-p-a-e-j-3y	2.273	Myrin-d-r-η-p-a-e-j-7x	2.304
Myrin-d-r-η-p-a-e-j-8y	2.307	Myrin-d-r-η-p-a-e-j-3x	2.287
Myrin-d-r-η-p-a-e-j-8z	2.297	Myrin-d-r-η-p-a-e-j-5x	2.297
Myrin-d-r-η-p-a-e-j-9y	2.294	Myrin-s-w-p-a-f-j	3.386
Myrin-d-r-η-p-a-e-j-9z	2.296	Myrin-s-r-η-p-b-e-j	7.585
Myrin-d-r-η-p-a-e-j-7y	2.288	Myrin-s-w-p-a-f-k	0.958
Myrin-d-r-η-p-a-e-j-7z	2.290	Myrin-s-r-η-u-p-a-f-j	5.619
Myrin-d-r-η-p-a-e-j-5z	2.285	Myrin-s-r-η-u-p-a-f-k	3.965
Myrin-d-r-η-p-a-e-j-5y	2.282	Myrin-d-r-q-b-e-k	3.609
Myrin-s-w-ε-q-a-e-k	2.792	Myrin-s-r-η-u-p-b-e-k	5.182
Myrin-s-w-ε-q-a-e-j	5.111	Myrin-s-r-η-u-p-b-f-k	4.482
Myrin-d-r-η-p-b-f-j	3.475	Myrin-s-w-p-e-a-k	3.169
Myrin-d-r-η-p-b-f-k	3.697	Myrin-d-w-u-p-a-e-j	3.572
Myrin-s-w-ε-q-b-e-j	4.746	Myrin-d-w-u-p-a-e-k	6.300
Myrin-s-w-ε-q-a-f-j	4.964	Myrin-d-w-u-p-b-e-k	6.300
Myrin-s-w-ε-q-a-f-k	2.640	Myrin-d-w-u-p-a-f-j	4.952
Myrin-s-w-u-q-b-e-k	4.227	Myrin-d-w-u-p-b-f-j	4.953
Myrin-s-w-ε-q-b-f-k	2.906	Myrin-s-w-u-p-b-e-j	1.641
Myrin-d-w-p-a-e-k	7.121	Myrin-d-w-u-p-a-f-k	7.142
Myrin-d-w-p-a-f-j	5.378	Myrin-d-w-u-p-b-f-k	7.141
Myrin-d-w-p-b-f-j	5.377	Myrin-s-w-u-p-e-a-k	2.906
Myrin-s-w-u-p-a-e-j	2.222	Myrin-s-w-p-b-e-j	1.575
Myrin-d-r-η-u-p-a-e-j	0.860	Myrin-s-w-u-q-a-e-j	1.214
Myrin-d-r-η-u-p-a-e-k	2.852	Myrin-s-w-u-q-b-e-j	1.239
Myrin-s-r-ε-q-b-e-j	7.629	Myrin-d-w-u-q-b-e-j	4.067
Myrin-s-r-ε-q-b-f-j	6.089	Myrin-d-w-u-q-a-e-j	4.215
Myrin-d-w-p-a-f-k	7.395	Myrin-s-w-u-p-b-f-j	2.385
Myrin-d-w-p-b-e-j	5.510	Myrin-s-w-u-q-a-e-k	2.070
Myrin-d-r-q-b-f-j	4.715	Myrin-d-w-u-q-a-e-k	6.530

Myrin-s-r-ε-q-b-f-k	4.321	Myrin-s-w-u-p-b-e-k	3.383
Myrin-s-r-ε-q-a-e-k	5.339	Myrin-d-w-u-q-b-f-j	6.246
Myrin-d-r-η-u-p-a-f-j	2.759	Myrin-s-w-u-p-a-f-k	3.842
Myrin-d-w-p-b-e-k	6.548	Myrin-s-w-u-p-b-f-k	3.538
Myrin-d-r-η-u-p-a-f-k	3.956	Myrin-d-w-u-q-a-f-j	5.975
Myrin-s-r-ε-q-a-e-j	7.754	Myrin-s-w-u-q-a-f-k	2.644
Myrin-d-w-q-b-e-j	5.856	Myrin-d-w-u-q-a-f-k	7.841
Myrin-d-w-p-b-f-k	6.559	Myrin-d-w-u-q-b-f-k	7.584
Myrin-d-w-q-a-e-j	6.251	Myrin-d-r-u-q-a-e-j	1.051
Myrin-s-r-η-p-e-a-k	5.269	Myrin-s-r-u-q-b-e-j	4.530
Myrin-s-r-η-p-b-e-k	6.633	Myrin-d-r-q-a-f-j	5.058
Myrin-d-w-q-a-e-k	7.703	Myrin-d-r-u-q-a-f-j	2.730
Myrin-s-r-η-p-a-e-j	7.718	Myrin-s-r-u-q-a-e-j	4.530
Myrin-s-r-η-p-b-f-k	4.877	Myrin-s-r-u-q-a-e-k	3.122
Myrin-d-w-q-b-f-j	7.831	Myrin-s-r-u-q-a-f-j	3.559
Myrin-d-r-q-b-f-k	4.738	Myrin-s-r-u-q-a-f-k	1.343
Myrin-s-r-ε-q-a-f-k	4.240		
Myrin-d-w-q-b-e-k	7.463		

Table 5.39. HOMO-LUMO energy gap of the calculated conformers of myristinin A of all calculated conformers of myristinin A.
HF/6-31G(d,p) results *in vacuo*. The conformers are arranged in order of increasing relative energy.

Conformer	HOMO-LUMO energy gap (kcal/mol)	Conformer	HOMO-LUMO energy gap (kcal/mol)
Myrin-d-r-η-p-a-e-j	257.479	Myrin-s-r-ε-q-a-f-k	260.586
Myrin-d-r-η-p-a-e-k	257.574	Myrin-d-w-q-b-e-k	241.936
Myrin-d-r-η-p-a-f-j	256.319	Myrin-s-r-ε-q-a-f-j	260.473
Myrin-d-r-η-p-a-f-k	256.494	Myrin-s-w-p-b-f-j	253.620
Myrin-d-r-η-p-a-e-j-2y	256.996	Myrin-s-r-η-p-a-f-k	260.077
Myrin-d-r-η-p-a-e-j-10z	257.479	Myrin-d-w-q-a-f-j	242.275
Myrin-d-r-η-p-b-e-k	254.693	Myrin-d-r-q-a-e-j	247.144
Myrin-d-r-η-p-a-e-j-4z	257.448	Myrin-d-r-q-b-e-j	249.203
Myrin-d-r-η-p-a-e-j-4y	257.448	Myrin-d-r-q-a-e-k	246.592
Myrin-d-r-η-p-b-e-j	255.942	Myrin-s-r-η-p-a-f-j	259.977
Myrin-d-r-η-p-a-e-j-1z	255.446	Myrin-d-w-q-a-f-k	241.710
Myrin-d-r-η-p-a-e-j-1y	255.465	Myrin-d-w-q-b-f-k	242.846
Myrin-d-r-η-p-a-e-j-6y	257.473	Myrin-s-w-p-a-e-j	252.215
Myrin-d-r-η-p-a-e-j-6z	257.473	Myrin-d-r-q-a-f-k	247.797
Myrin-d-r-η-p-a-e-j-3z	257.498	Myrin-s-r-η-u-p-a-e-j	251.537
Myrin-d-r-η-p-a-e-j-3y	257.505	Myrin-s-w-p-a-f-j	253.143
Myrin-d-r-η-p-a-e-j-8y	257.479	Myrin-s-w-p-a-f-k	252.679
Myrin-d-r-η-p-a-e-j-8z	257.473	Myrin-s-r-η-u-p-a-f-j	250.840
Myrin-d-r-η-p-a-e-j-9y	257.473	Myrin-s-r-η-u-p-a-f-k	250.972
Myrin-d-r-η-p-a-e-j-9z	257.473	Myrin-d-r-q-b-e-k	248.751
Myrin-d-r-η-p-a-e-j-7y	257.473	Myrin-s-r-η-u-p-b-e-k	250.903
Myrin-d-r-η-p-a-e-j-7z	257.473	Myrin-s-r-η-u-p-b-f-k	251.129

Myrin-d-r-η-p-a-e-j-5z	257.473	Myrin-s-w-p-e-a-k	253.043
Myrin-d-r-η-p-a-e-j-5y	257.473	Myrin-d-w-u-p-a-e-j	237.594
Myrin-s-w-ε-q-a-e-k	258.854	Myrin-d-w-u-p-a-e-k	236.916
Myrin-s-w-ε-q-a-e-j	258.816	Myrin-d-w-u-p-b-e-k	236.922
Myrin-d-r-η-p-b-f-j	256.099	Myrin-d-w-u-p-a-f-j	238.742
Myrin-d-r-η-p-b-f-k	255.170	Myrin-d-w-u-p-b-f-j	238.742
Myrin-s-w-ε-q-b-e-j	258.678	Myrin-s-w-u-p-b-e-j	240.010
Myrin-s-w-ε-q-a-f-j	258.101	Myrin-d-w-u-p-a-f-k	238.202
Myrin-s-w-ε-q-a-f-k	258.207	Myrin-d-w-u-p-b-f-k	238.196
Myrin-s-w-u-q-b-e-k	258.345	Myrin-s-w-u-p-e-a-k	238.723
Myrin-s-w-ε-q-b-f-k	258.308	Myrin-s-w-p-b-e-j	239.702
Myrin-d-w-p-a-e-k	242.815	Myrin-s-w-u-p-a-e-j	239.326
Myrin-d-w-p-a-f-j	244.503	Myrin-s-w-u-q-a-e-j	240.229
Myrin-d-w-p-b-f-j	244.503	Myrin-s-w-u-q-b-e-j	240.305
Myrin-d-r-η-u-p-a-e-j	251.650	Myrin-d-w-u-q-b-e-j	237.211
Myrin-d-r-η-u-p-a-e-k	251.732	Myrin-d-w-u-q-a-e-j	236.000
Myrin-s-r-ε-q-b-e-j	260.868	Myrin-s-w-u-p-b-f-j	240.876
Myrin-s-r-ε-q-b-f-j	260.768	Myrin-s-w-u-q-a-e-k	239.658
Myrin-d-w-p-a-f-k	243.963	Myrin-d-w-u-q-a-e-k	235.410
Myrin-d-w-p-b-e-j	243.091	Myrin-s-w-u-p-b-e-k	239.439
Myrin-d-r-q-b-f-j	249.918	Myrin-d-w-u-q-b-f-j	238.127
Myrin-s-r-ε-q-b-f-k	260.705	Myrin-s-w-u-p-a-f-k	239.878
Myrin-s-r-ε-q-a-e-k	261.056	Myrin-s-w-u-p-b-f-k	240.298
Myrin-d-r-η-u-p-a-f-j	250.589	Myrin-d-w-u-q-a-f-j	237.255
Myrin-d-w-p-b-e-k	242.426	Myrin-s-w-u-q-a-f-k	240.807
Myrin-d-r-η-u-p-a-f-k	250.771	Myrin-d-w-u-q-a-f-k	236.652
Myrin-s-r-ε-q-a-e-j	260.975	Myrin-d-w-u-q-b-f-k	237.644
Myrin-d-w-q-b-e-j	242.413	Myrin-d-r-u-q-a-e-j	242.287
Myrin-d-w-p-b-f-k	243.932	Myrin-s-r-u-q-b-e-j	246.404
Myrin-d-w-q-a-e-j	241.070	Myrin-d-r-q-a-f-j	248.362
Myrin-s-r-η-p-e-a-k	260.498	Myrin-d-r-u-q-a-f-j	243.492
Myrin-s-r-3-p-b-e-k	260.128	Myrin-s-r-u-q-a-e-j	246.404
Myrin-d-w-q-a-e-k	240.518	Myrin-s-r-u-q-a-e-k	245.889
Myrin-s-r-η-p-a-e-j	260.435	Myrin-s-r-u-q-a-f-j	247.377
Myrin-s-r-η-p-b-f-k	260.128	Myrin-s-r-u-q-a-f-k	246.900
Myrin-d-w-q-b-f-j	243.323		
Myrin-d-r-q-b-f-k	249.504		

CHAPTER 6

COMPUTATIONAL STUDY OF THE *CIS*-DBPO ISOMER *IN VACUO* AND IN SOLUTION

This chapter presents the results of the conformational study of the *cis*-DBPO isomer. The results are organised according to the two types of study, as explained in section 4.4.

6.1. Naming of conformers

Conformers are denoted with acronyms providing information on their characteristics. The same letters which are used to keep track of relevant geometry features of myristinin A (section 5.1) are also used for the conformers of *cis*- DBPO. Figure 6.1 shows the structure of the *cis*- DBPO isomer.

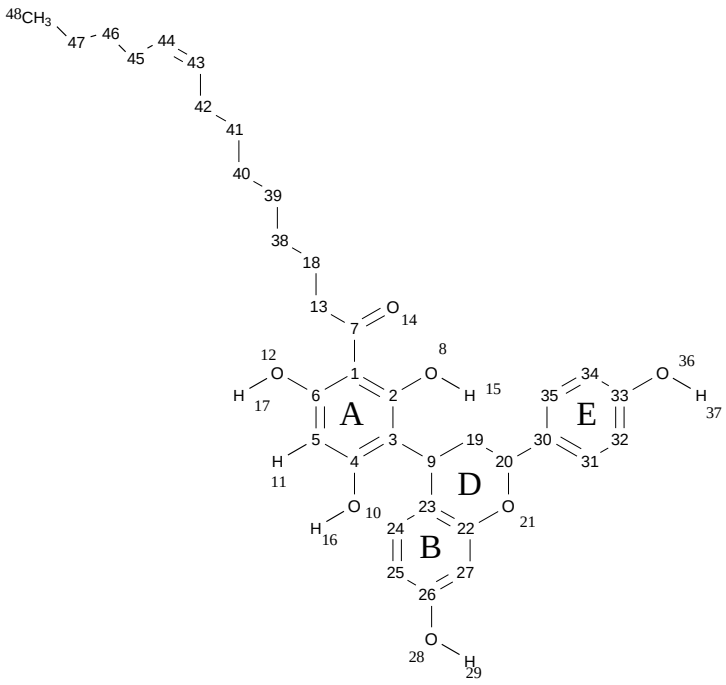

Figure 6.1. Structure of the *cis*-DBPO isomer and atom numbering utilised in this study.

The C atoms in the rings and in the acyl chain are represented by the numbers denoting their position (except the last C atom of the acyl chain) for better view of the structure. Only the H atoms attached to O atoms and to C5 atom are numbered individually, while the other H atoms are given the same number as the C atom to which they are attached and are not shown in the structure. The rings are denoted by uppercase letters (A, B, D and E).

6.2. Results for conformers with the same geometry of R and different geometries of the ring system.

6.2.1. Results *in vacuo*

6.2.1.1. Relative energies of the conformers

This part of the study considered 95 conformers, each of them corresponding to one of the identified geometries of the ring systems [190] (fig.5.3). Their geometries of the resulting conformers are shown in figure 6.2 and their relative energies are reported in table 6.1. The trends identified for *cis*-DBPO are similar to those of myristinin A (section 5.2). The d conformers have lower energy than the s conformers; when the r conformers have the O10–H16···π interaction between H16 and ring B, the r conformers have lower energy than the w conformers, and has higher energy than the w conformer when there is no O10–H16···π interaction between H16 and ring B; the u conformers always have higher energy than the corresponding non-u ones; the p conformer has lower energy than the q conformer when the q conformer does not have the O8–H15···π interaction between H15 and ring B and has higher energy than the q conformer when the q conformer has the O8–H15···π interaction between H15 and ring B. The following pairs of conformers, a/b, e/f and j/k shows no consistent pattern in the conformational preference.

6.2.1.2. Characteristics of intramolecular hydrogen bonds

Table 6.2 reports the parameters (H-O bond length, O···O distance, OĤO angle) of the first IHB of the calculated conformers of myristinin A. The trends identified from myristinin A hold for *cis*-DBPO. The comparison of the H···O length of pairs of conformers differing only by the position of the first IHB (H15···O14 or H17···O14) shows that the d conformers have shorter H···O length than the corresponding s conformers. Considering the distance between the two oxygen atoms, the O14···O8 distance in the d conformers is shorter than the O14···O12 distance in the s conformers. Considering the OĤO bond angles, d conformers have greater angle than the corresponding s conformers. All these values indicate that the H15···O14 first IHB is somewhat stronger than the H17···O14 first IHB.

It is also noted that non-u conformers have shorter H···O length than the u conformers. The orientation of O10–H16, O28–H29 and O36–H37, as well as the position of C19 in ring D do not influence the characteristics of the first IHB significantly.

As already mentioned earlier (section 5.2.1.2), in the case of the OH···π interaction, it is not possible to define an H-bond length, because the acceptor π system is not a single atom. However, it is interesting to consider the distance between the H atom and the closest C atoms in the acceptor ring B. Table 6.3 reports the distance (Å) between the H atom and the closest C atom in the acceptor aromatic ring, for the conformers in which the O–H···π interaction is present. The distance (2.058–2.240 Å) is in the shorter range for this type of interaction, suggesting that the OH···π interaction in this molecule are strong.

6.2.1.3. Dipole moments of the conformers

Table 6.4 reports the values of the dipole moments of the calculated conformers of the *cis*-DBPO isomer. The values of the dipole moments of the calculated conformers range between 0.648 and 9.417 Debye. The orientation of the phenol OHs has a significant influence on the dipole moment of the conformers of the *cis*-DBPO just like in case of myristinin A (section 5.2.1.3). The trends identified from myristinin A hold for *cis*-DBPO. The smallest dipole moment corresponds to the d-r-η-u-p-a-e-j conformer, in which the three OHs in the phloroglucinol moiety and the two OHs in the substituent ring system are oriented in a manner in which their contributions cancel. In this case, the orientation of the OHs in the phloroglucinol moiety is not uniform and, therefore, their total contribution to the dipole moment is not close to zero. On the other hand, O28–H29 and O36–H37 are oriented to the same side. Thus, it is reasonable to infer that the contributions from O28–H29 and O36–H37 and the contribution from the OH in the phloroglucinol moiety largely cancel each other. The highest dipole moment corresponds to the d-w-q-a-f-k conformer, where the OHs of the phloroglucinol moiety have non-uniform orientation and the contributions of O28–H29 and O36–H37 sum up to their contributions enhancing the dipole moment (O28–H29 and O36–H37 are both oriented towards the phloroglucinol moiety).

The u-conformers have smaller dipole moment than the corresponding non-u ones; d-r-u conformers have smaller dipole moment than d-r conformers; d-w-u conformers have smaller dipole moment than d-w conformers; s-r-u conformers have smaller dipole moment than s-r conformers; s-w-u conformers have smaller dipole moment than s-w conformers.

The d-r-e conformers have higher dipole moment than d-r-f conformers; d-w-e conformers have smaller dipole moment than d-w-f conformers; s-r-e conformers have smaller dipole moment than s-r-f conformers; s-w-e conformers have smaller dipole moment than s-w-f conformers. This

suggests that the mutual orientation of O28–H29 and O10–H16 influence the dipole moment significantly.

The d-r-j conformers have higher dipole moment than d-r-k conformers; d-w-j conformers have smaller dipole moment than d-w-k conformers; s-r-j conformers have smaller dipole moment than s-r-k conformers; s-w-j conformers have smaller dipole moment than s-w-k conformers. Just like in the previous comparison the orientation of the O36–H37 with respect to the orientation of O10–H16 influence the dipole moment significantly.

The comparison of the dipole moments of conformers differing only by orientation of the B–D–E ring system with respect to the phloroglucinol moiety does not show a consistent pattern, because sometimes p conformer lower dipole moment than q conformer and other times they higher dipole moment. The difference is usually small. This suggests that the dipole moment of the conformers does not depend significantly on the orientation of the B–D–E ring system.

6.2.1.4. HOMO-LUMO energy gap of the conformers

Table 6.5 reports the energy difference between the frontier orbitals (HOMO, highest occupied molecular orbital, and LUMO, lowest unoccupied molecular orbital). The values of the HOMO-LUMO energy gap of the calculated conformers range between 235.536 and 260.855 kcal/mol. The trends observed in section 5.2.1.4 are similar to the ones observed in *cis*-BPO. The d conformers have smaller HOMO-LUMO energy gap than the corresponding s conformers. The non-u conformers have greater HOMO-LUMO energy gap than the corresponding u conformer. The conformers with O10–H16···π interaction have greater HOMO-LUMO energy gap than the corresponding conformers without O10–H16···π interaction. For d-type conformers, the p conformers have greater HOMO-LUMO energy than the corresponding q conformers. For s-type conformers, the p conformers have smaller HOMO-LUMO energy gap than the q conformer. The orientation of O28–H29 and O36–H37 do not influence the HOMO-LUMO energy difference significantly.

Figure 6.3 shows the shapes of the HOMO and LUMO frontier orbitals for the conformers listed in table 6.1. The shapes of HOMO orbitals show greater electron concentration density in the phloroglucinol moiety and the other two ring system for all conformers with few exceptions for d-w, d-r-q and s-w-u conformers where the electron density in concentrated in the B–D rings. The shapes of LUMO orbitals show greater concentration of electrons in the phloroglucinol moiety.

6.3. Results for conformers with different geometries of R and the same geometry of the ring system.

6.3.1. Results *in vacuo*

6.3.1.1. Types of investigated conformers

This part consider the results of the study of conformers with different geometries of R associated with the best geometry of the phloroglucinol moiety and the B–D–E ring system identified from the study of a model structure considering of these units and R replaced by an ethyl (fig 5.4) [190]. The best identified geometry is d-r-η-p-a-e-j and its stabilising factors are already described in section 5.4.1.1.

Different geometries of the R chain were built by rotating each single bond in turn, as explained in section 4.4. This study involved 25 inputs and yielded 15 conformers, because all the inputs with the R chain bent by ±180° (remaining on the plane of the benzene ring A) optimized to conformers coinciding with those coming from inputs where R has been bent by -90° or +90°; for instance, the input where C13–C18 had been rotated by +180° (to the side of R′) as gave the same output geometry when it had been rotated by -90°.

6.3.1.2. Relative energies of the conformers

Conformers corresponding to the ±90° and ±180° rotations of all the single bonds in R were calculated at the HF/6-31G(d,p) level. The geometries of the optimized conformers are shown in figure 6.4 and their relative energies are reported in table 6.6. The lowest energy conformer is the same as for the first part of the study of *cis*-DBPO (table 6.1). When the R chain is bent, the energy of the conformers where the relevant bond has been rotated by +90 or -90 is the same as the energy of the conformers where the same bond has been rotated by +180 or -180, suggesting that the conformers where the R chain is bent out off the plane are the possible preferred ones than conformers with the R chain bent on the plane identified by the benzene ring A. When the R chain is bent, the energy of the conformers where the relevant bond is being rotated by +90 or -90 are nearly close, with some few exceptions, where the energies are not close, that is when the R chain is bent in the bond that is close to the double bond (C40–C41, C41–C42 and C42–C43). This suggests that the double bond on the long acyl chain does slightly affect the optimisation of input with symmetrical R.

Table 6.7 reports the values of the relative energies corrected for ZPE and of the ZPE corrections as well as the relative Gibbs free energies ($\Delta G_{corrected}$, sum of electronic and thermal free energy) and its correction, G_{corr}, for the conformers listed in table 6.6 at HF level. The ZPE corrections for all the conformers are comparatively close. Their values range between 476,816 and 477,196 kcal/mol. The greater values of the ZPE corrections correspond to the conformers having higher energy. The relative energies corrected for ZPE and the uncorrected relative energies have the same trends, with only three exceptions (DBPO-d-r-η-p-a-e-j-8y-c, DBPO-d-r-η-p-a-e-j-2z-c and DBPO-d-r-η-p-a-e-j-2y-c). Conformers with lower relative energy have lower relative Gibbs free energies. The values of G_{corr} are comparatively close.

DFT/B3LYP/6-31+G(d,p) and MP2/ 6-31G(d,p) calculations were performed on the conformers of this part having lower energy in the HF results. Table 6.13 reports the relative energies obtained from these calculations and compares them with the HF results. The relative energy (kcal/mol) of the highest energy conformer of this set is 1.008 / HF, 1.067 /DFT and 1.414 /MP2, showing a widening of the energy range. Furthermore, the energy sequence of the conformers is not the same with the three methods. Thus, the lowest and highest energy conformers are not the same with the three methods, as it is, the lowest energy conformer at HF and DFT levels is DBPO d-r-η-p-a-e-j, and at MP2 level, is DBPO-d-r-η-p-a-e-j-8y. The highest energy conformer at HF and MP2 levels is DBPO-d-r-η-p-a-e-j-7y, and at DFT level, is DBPO-d-r-η-p-a-e-j-4z.

6.3.1.3. Characteristics of intramolecular hydrogen bonds

Table 6.14 reports the parameters of the first IHB in the lowest energy conformers of *cis*-DBPO listed in table 6.6 *in vacuo*, at HF/6-31G(d,p), DFT/B3LYP/6-31+G(d,p) and MP2/6-32G(d,p) levels of theory. HF gave the longest bond lengths, DFT gave the shortest and MP2 gave intermediate values. This is consistent with the fact that HF underestimates the strength of H-bonds, and DFT overestimates it; the MP2 results can be considered as those closer to the actual values. The ranges of the bond lengths (Å) of H15···O14 are 1.638–1.652 /HF, 1.456–1.531 /DFT and 1.574–1.585 /MP2. These values indicate that the first IHB is comparatively strong. The values of the O···O distance are nearly close to 2.5 Å for all results obtained (2.502–2.509 /HF, 2.445–2.467 /DFT and 2.498–2.506 /MP2.). The OĤO bond angles are estimated around 147° /HF, 151° /DFT and 151° MP2.

For the O–H···π interactions (table 6.15), the distance (Å) between the H atom and the closest C atom of the B aromatic ring is 123–2.129 /HF, 1.998–2.057 /DFT and 2.007–2.011 /MP2. By

comparing the results of the three methods, one can see that MP2 optimizes to geometries with longer IHBs; this is consistent with the fact that it takes into account also dispersion contributions. The parameters show a stronger IHB for DBPO-d-r-η-p-a-e-j-2z-c and DBPO-d-r-η-p-a-e-j-2y-c conformers.

Table 6.10 reports the values of the calculated vibrational frequency of the O–H bonds in selected conformers of *cis*-DBPO *in vacuo* at the HF level. The values of the calculated vibrational frequency also show that the orientation of the R chain has a significant influence on the vibrational frequency of O8–H15 and O12–H17 and minor influence on the vibrational frequency of O51–H52, O28–H29 and O10–H16. When the R chain is bent at C13–C18 by +90° or -90°, the vibrational frequency of O8–H15 increases slightly and that of O12–H17 decreases slightly. When the R chain is bent at C7–C13 by +90° or -90°, the vibrational frequency of O8–H15 decreases slightly and that of O12–H17 increases slightly.

6.3.1.4. Dipole moments of the conformers

Table 6.16 reports the values of the dipole moments of the conformers calculated in this part, at HF/6-31G(d,p), DFT/B3LYP/B3LYP/6-31+G(d,p) and MP2/6-31G(d,p) levels of theory. There is no typical sequence in the values of the dipole moments in the results of the different methods utilised. Comparison of the values of the dipole moments obtained with the three different methods shows that DFT yields lower values with respect to other two methods. The values of the dipole moments range between 2.097 and 2.558 Debye in the HF results, between 1.946 and 2.663 Debye in the DFT results, and between 2.120 and 2.606 Debye in the MP2 results.

6.3.1.5. HOMO-LUMO energy gap of the conformers

Table 6.17 reports the values of the HOMO-LUMO energy gap of the calculated conformers of *cis*-DBPO *in vacuo*, at HF/6-31G(d,p), DFT/B3LYP/B3LYP/6-31+G(d,p) and MP2/6-31G(d,p) level of theory. The values of the HOMO-LUMO energy gap range between 255.359 and 257.511 kcal/mol in the HF results, between 2.604 and 3.006 kcal/mol in the DFT results, and between 247,565 and 249,083 kcal/mol in the MP2 results.

Comparisons of the three methods show a huge difference between the values HOMO-LUMO energy gap of the DFT and the other two methods (HF and MP2). For analyses purpose, one can consider the values of the HOMO-LUMO energy gap from the MP2 results, because this method gives the results which are close to the experimental ones. The highest values of HOMO-LUMO

energy gap corresponds to the conformers which were obtained by bending the C38–C39, C40–C41 and C42–C43 bonds of the R chain by -90° or +90°. The smallest values of the HOMO-LUMO energy gap correspond to the conformers in which the bond that was rotated is closer to the sp^2 O of the acyl group (for instance, the C13–C18 bond).

Figure 6.5 shows the shapes of the HOMO and LUMO frontier orbitals for the conformers listed in table 6.6. The shapes of HOMO orbitals show a greater electron concentration density in the phloroglucinol moiety and B-D-E ring system. The shapes of LUMO orbitals show a greater electron concentration density in the phloroglucinol moiety.

6.3.2. Results in solution

6.3.2.1. Relative energies of the conformers

Calculations in solution were performed on the conformers listed in 6.6, at the HF level. Table 6.18 reports the relative energy of these conformers in different media (vacuum, chloroform, acetonitrile and water). The relative energies of the conformers show that DBPO-d-r-η-p-a-e-j, remains the most stable conformer in solution. The values of the relative energy also show that the conformers have lower energy *in vacuo* than in solution. The relative energy of the conformers slightly increases with an increase in solvent polarity (taken as the chloroform–acetonitrile–water sequence).

Table 6.19 reports the free energy of solvation (solvent effect, ΔG_{solv}) and its electrostatic component (G_{el}) for the conformers of *cis*-DBPO calculated in part two. ΔG_{solv} is positive in acetonitrile and negative in chloroform and water. The magnitude of ΔG_{solv} ranges between 1.34 to 2.45, 6.00 to 6.80 and 14.82 to 16.32 kcal/mol in chloroform, acetonitrile and water respectively. The magnitude of ΔG_{solv} increases with the solvent-polarity. The electrostatic component (G_{el}) has negative values in all three solvents and its magnitude is greater in water than in the other two solvents.

6.3.2.2. Characteristics of intramolecular hydrogen bonds

Table 6.20 reports the parameters of the first IHB *in vacuo* and in the three solvents, for the conformers that have been calculated in solution. The range of the bond lengths (Å) of the H15···O14 is 1.644–1.654, 1.640–1.653, 1.638–1.651 and 1.638–1.651, respectively, *in vacuo*, chloroform, acetonitrile and water. Thus, the value of the bond lengths of the H15···O14 decreases

with an increase in the media polarity. The values of the O···O distance increases with an increase in the media polarity. The values of the OĤO bond angles increases with an increase in the media polarity.

Table 6.21 reports the distance (Å) between the H atom and the closest C atom (H16···C39) in the acceptor B aromatic ring for the O–H···π interactions of the calculated conformers of *cis*-DBPO in the media considered. There is no drastical change in the H16···C23 distance; however, there are some slight changes. The values of the H16···C23 distance range comparatively close to 2 in different media. Thus, the H16···C23 distance is smaller in chloroform than *in vacuo*, with some exceptions (DBPO-d-r-η-p-a-e-j, DBPO-d-r-η-p-a-e-j-3z, DBPO-d-r-η-p-a-e-j-6z and DBPO-d-r-η-p-a-e-j-6y), where the trend is reversed), and smaller in acetonitrile or water than in chloroform, with some few exceptions, where the distance remains the same.

6.3.2.3. Dipole moments and the HOMO-LUMO energy gap of the conformers

Table 6.22 reports the values of the dipole moments of the conformers of *cis*-DBPO calculated in different media. Dipole moment slightly increases as the medium polarity increases. The ranges of the values of the dipole moments are 2.097–2.607, 2.463–3.009, 2.596–3.253 and 2.609–3.272 Debye *in vacuo*, chloroform acetonitrile and water respectively.

Table 6.23 reports the values of the HOMO-LUMO energy gap of the conformers of *cis*-DBPO calculated in different media. The HOMO-LUMO energy gap slightly increases as the medium polarity increases. The ranges of the values of the HOMO-LUMO energy gaps are 255.359–257.511, 254.235–256.890, 254.016–256.626 and 253.984–256.607 kcal/mol *in vacuo*, chloroform acetonitrile and water respectively.

6.4. Overview of the results

The results have been analysed separately for part one and part two because of the different approaches in the preparation of the inputs and in the considering geometry aspects. Since the molecule is the same, it is important to have an overall view of all the results. Using the criteria explained in section 4.4, a total of 115 conformers of *cis*-DBPO was calculated.

Table 6.24 reports the values of the relative energies for all the conformers of *cis*-DBPO *in vacuo*, at the HF level. The relative energies of the conformers having different geometries of R and the same geometry of the ring system account for most of the lower energy conformers. This is to be expected because these conformers have the best geometry of the ring systems. Thus, these results show that the influence of the geometry of R on the overall energy of the molecule is smaller than the influence of the ring systems; this is understandable by considering that the ring system contains the most important stabilising factors such as the first IHB and O–H···π interaction. It is noticed that the acyl chain group and the ring systems somewhat do influence the conformational preferences and other molecular properties of *cis*-DBPO.

Table 6.25 reports the values of the parameters of the first IHB for all the conformers of *cis*-DBPO *in vacuo*, at the HF level. The values of the parameters of the first IHB of the conformers having different geometries of R and the same geometry of the ring system show that the influence of the geometry of R on the overall parameters of the first IHB of the molecule is smaller than the influence of the ring systems. Like for the energy, this is to be expected because these conformers have the best geometry for the ring systems as already mention in the previous comparison.

Table 6.26 reports the values of the distance between the H atom and the closest C atom in the acceptor aromatic B ring for all the conformers of *cis*-DBPO *in vacuo*, at the HF level. The values of the distance between the H atom and the closest C atom in the acceptor aromatic B ring of the conformers having different geometries of R and the same geometry of the ring system show that the geometry of R on the overall does influence the O–H···π interactions. Like for the energy, this is to be expected because these conformers have the best geometry for the ring systems as already mention in the previous comparison.

Table 6.27 reports the values of the dipole moments for all the conformers of *cis*-DBPO *in vacuo*, at the HF level. The values of the dipole moments of the conformers having different geometries of R and the same geometry of the ring system are all around 2 Debye; this is to be expected because

these conformers have the same geometry of the ring systems, all the OHs are oriented in the same way, and, therefore, it can be concluded that the orientation of the acyl chain does not significantly influence the values of the dipole moments.

Table 6.28 reports the values of the HOMO-LUMO energy gaps for all the conformers of *cis*-DBPO *in vacuo*, at the HF level. The HOMO-LUMO energy gaps of the conformers having different geometries of R and the same geometry of the ring system show that the influence of the geometry of R on the overall HOMO-LUMO energy gap of the molecule is smaller than the influence of the ring systems. Like for the energy, this is understandable by considering that the ring system contains the most important stabilising factors.

Figure 6.2. Optimized conformers of the *cis*- DBPO having the same geometry of R and different geometries of the ring system *in vacuo*.
HF/6-32G(d,p) results. The conformers are listed in order of increasing relative energy.

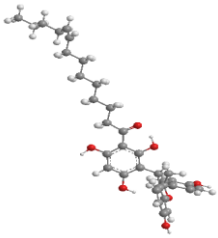

c-DBPO-d-r-η-p-a-e-j

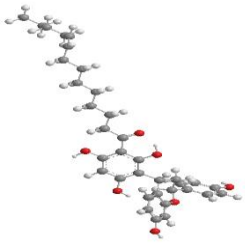

c-DBPO-d-r-η-p-e-a-k

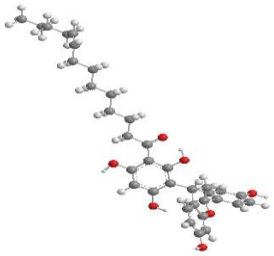

c-DBPO-d-r-η-p-a-f-j

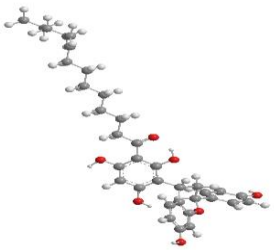

c-DBPO-d-r-η-p-a-f-k

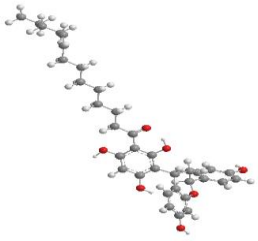

c-DBPO-d-r-η-p-b-e-k

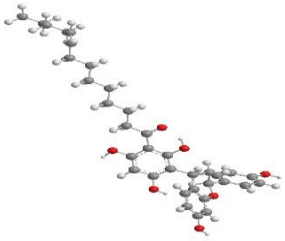

c-DBPO-d-r-η-p-b-e-j

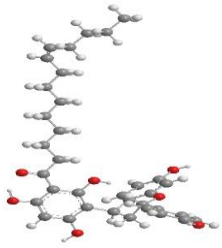

c-DBPO-s-w-ε-q-a-e-k

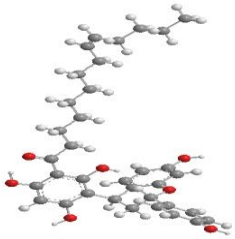

c-DBPO-s-w-ε-q-a-e-j

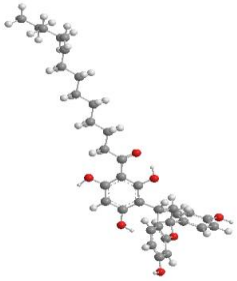

c-DBPO-d-r-η-p-b-f-j

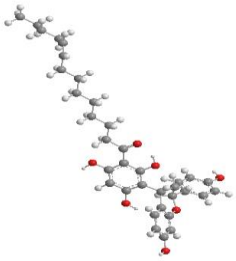

c-DBPO-d-r-η-p-b-f-k

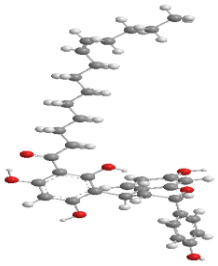

c-DBPO-s-w-ε-q-b-e-j

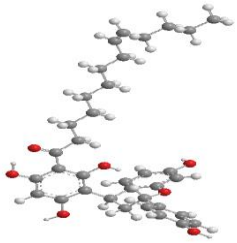

c-DBPO-s-w-ε-q-a-f-j

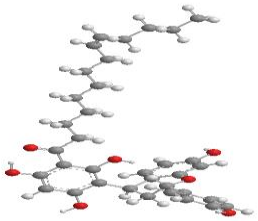

c-DBPO-s-w-ε-q-a-f-k

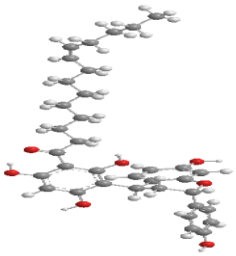

c-DBPO-s-w-u-q-b-e-k

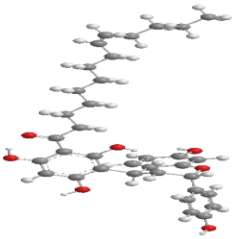

c-DBPO-s-w-ε-q-b-f-k

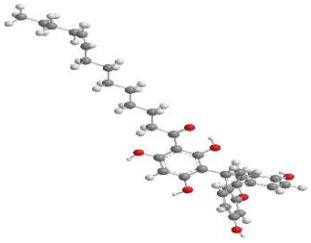

c-DBPO-d-w-p-e-a-k

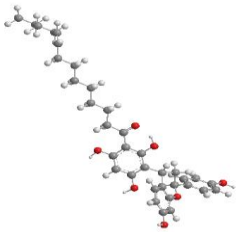

c-DBPO-d-w-p-a-f-j

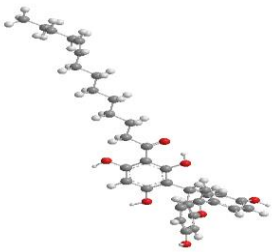

c-DBPO-d-w-p-b-f-j

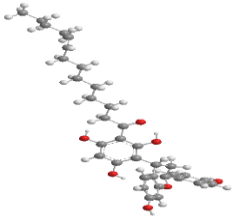

c-DBPO-d-r-η-u-p-a-e-j

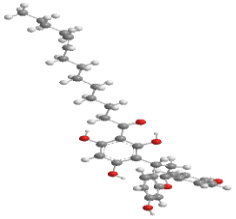

c-DBPO-d-r-η-u-p-e-a-k

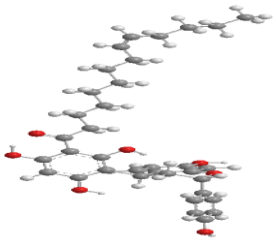

c-DBPO-s-r-ε-q-b-e-j

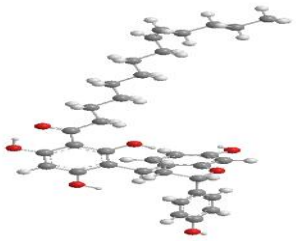

c-DBPO-s-r-ε-q-b-f-j

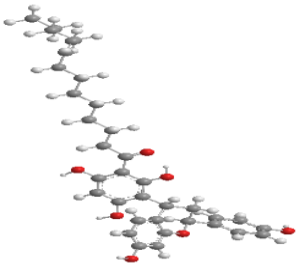

c-DBPO-d-w-p-a-f-k

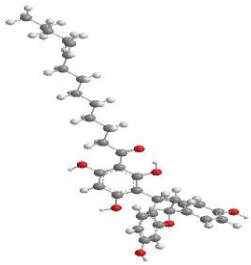

c-DBPO-d-w-p-b-e-j

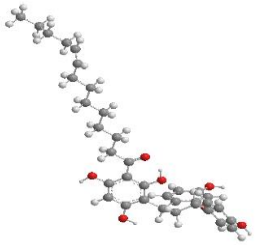

c-DBPO-d-r-q-b-f-j

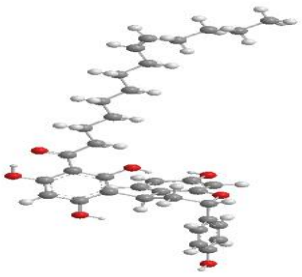

c-DBPO-s-r-ε-q-b-f-k

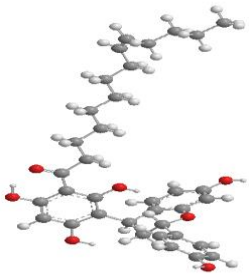

c-DBPO-s-r-ε-q-a-e-k

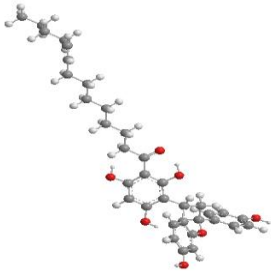

c-DBPO-d-r-η-u-p-a-f-j

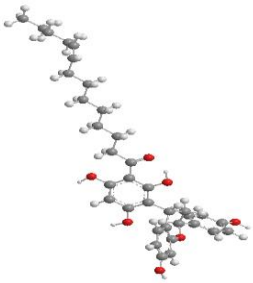

c-DBPO-d-w-p-b-e-k

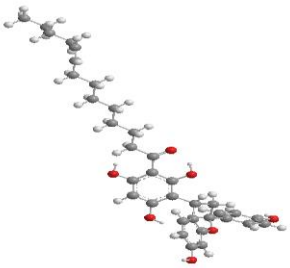

c-DBPO-d-r-η-u-p-a-f-k

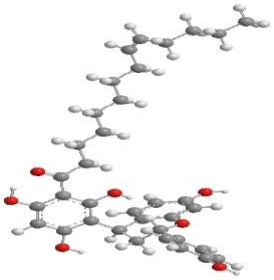

c-DBPO-s-r-ε-q-a-e-j

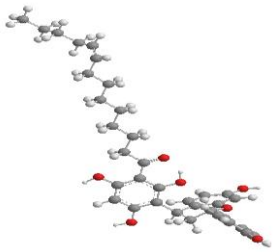

c-DBPO-d-w-q-b-e-j

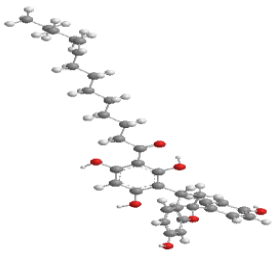

c-DBPO-d-w-p-b-f-k

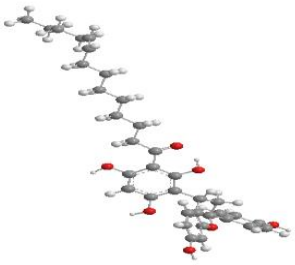

c-DBPO-d-w-p-a-e-j

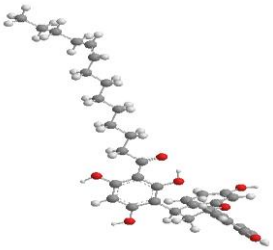

c-DBPO-d-w-q-a-e-j

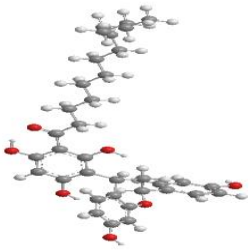

c-DBPO-s-r-η-p-e-a-k

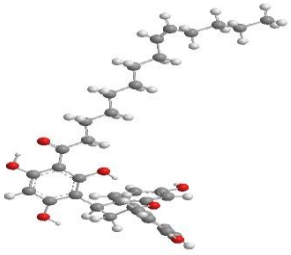

c-DBPO-s-r-3-p-b-e-k

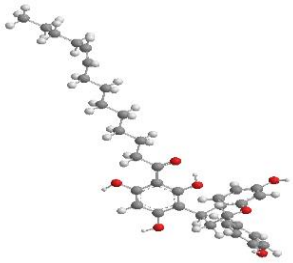

c-DBPO-d-w-q-a-e-k

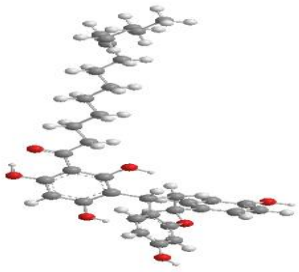

c-DBPO-s-r-η-p-a-e-j

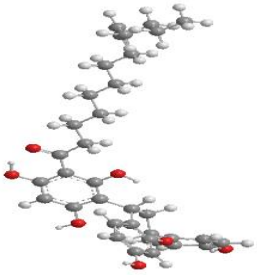

c-DBPO-s-r-η-p-b-f-k

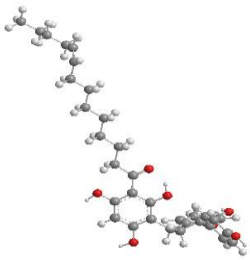

c-DBPO-d-w-q-b-f-j

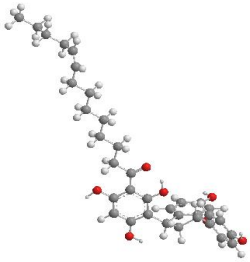

c-DBPO-d-r-q-b-f-k

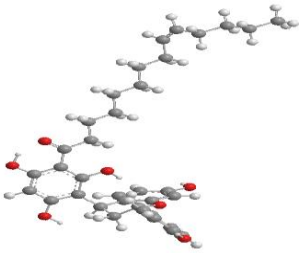

c-DBPO-s-r-ε-q-a-f-k

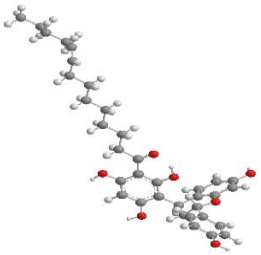

c-DBPO-d-w-q-b-e-k

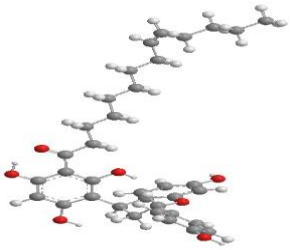

c-DBPO-s-r-ε-q-a-f-j

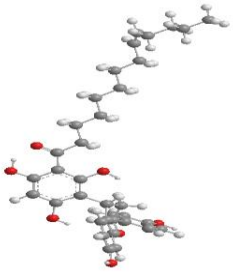

c-DBPO-s-w-p-b-f-j

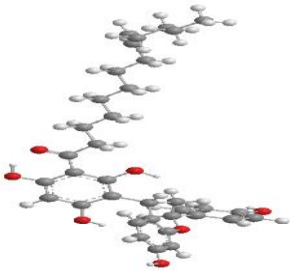

c-DBPO-s-r-η-p-a-f-k

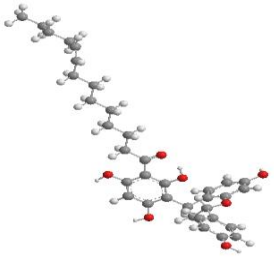

c-DBPO-d-w-q-a-f-j

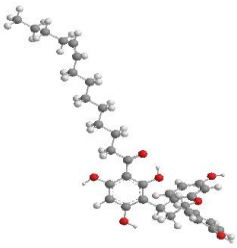

c-DBPO-d-r-q-a-e-j

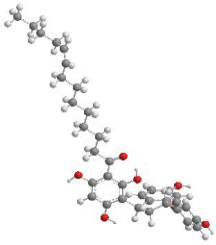

c-DBPO-d-r-q-b-e-j

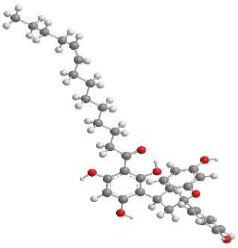

c-DBPO-d-r-q-a-e-k

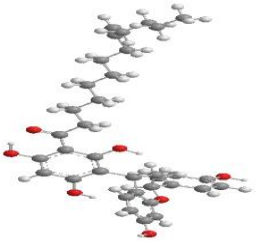

c-DBPO-s-r-η-p-a-f-j

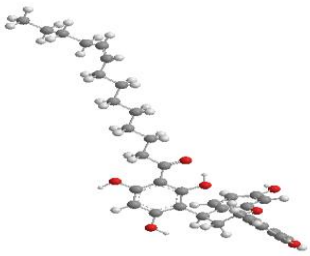

c-DBPO-d-w-q-a-f-k

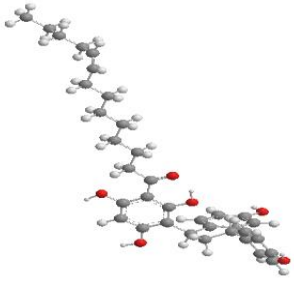

c-DBPO-d-w-q-b-f-k

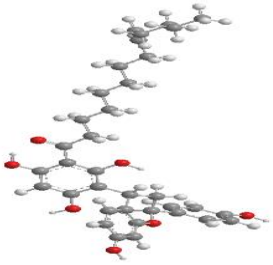

DB PO-s-w-p-a-e-j

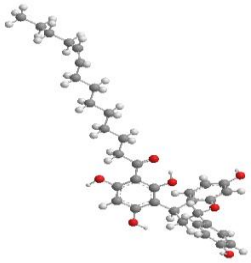

c-DBPO-d-r-q-a-f-k

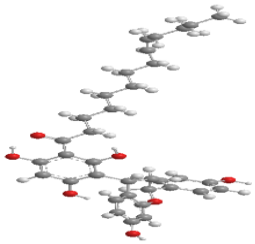

c-DBPO-s-r-η-u-p-a-e-j

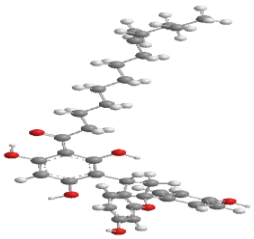

c-DBPO-s-w-p-a-f-j

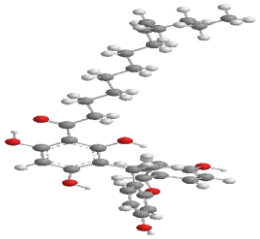

c-DBPO-s-r-η-p-b-e-j

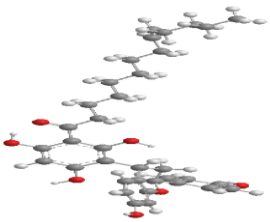

c-DBPO-s-w-p-a-f-k

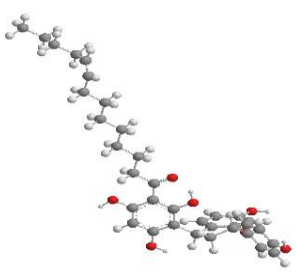

c-DBPO-s-r-η-u-p-a-f-j

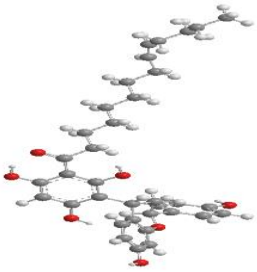

c-DBPO-s-r-η-u-p-a-f-k

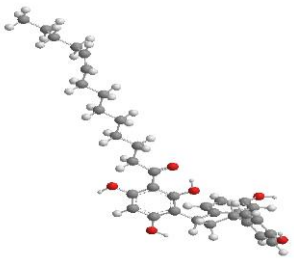

c-DBPO-d-r-q-b-e-k

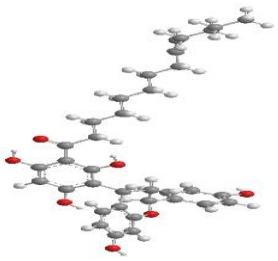

c-DBPO-s-r-η-u-p-b-e-k

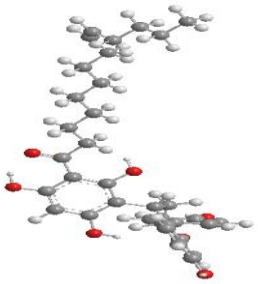

c-DBPO-s-r-η-u-p-b-f-k

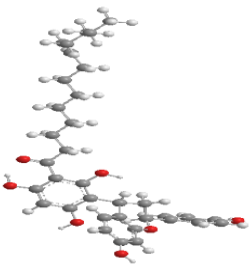

c-DBPO-s-w-p-e-a-k

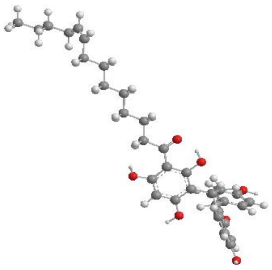

c-DBPO-d-w-u-p-a-e-j

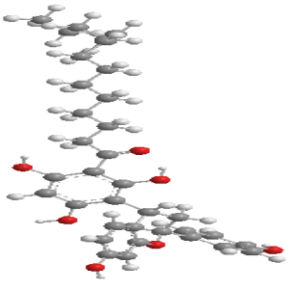

c-DBPO-d-w-u-p-e-a-k

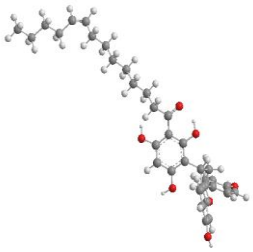

c-DBPO-d-w-u-p-b-e-k

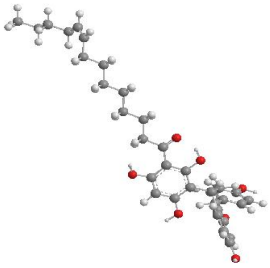

c-DBPO-d-w-u-p-a-f-j

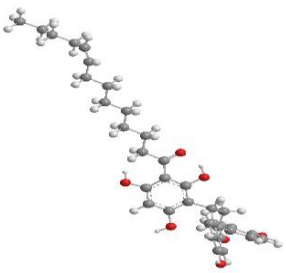

c-DBPO-d-w-u-p-b-f-j

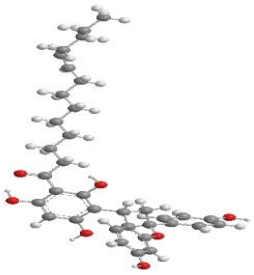

c-DBPO-s-w-u-p-a-f-j

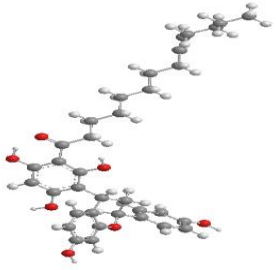

c-DBPO-s-w-u-p-b-e-j

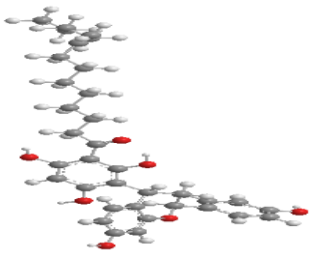

c-DBPO-d-w-u-p-a-f-k

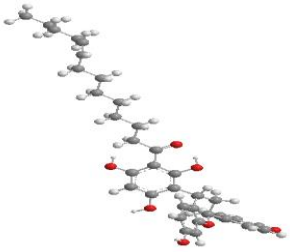

c-DBPO-d-w-u-p-b-f-k

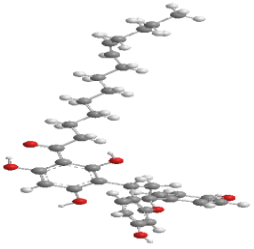

c-DBPO-s-w-u-p-e-a-k

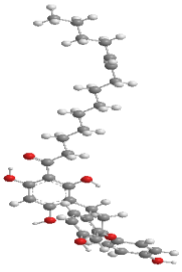

c-DBPO-s-w-p-b-e-j

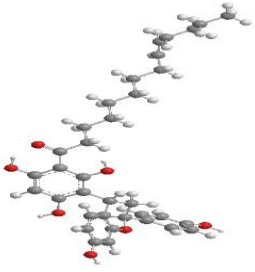

c-DBPO-s-w-u-p-a-e-j

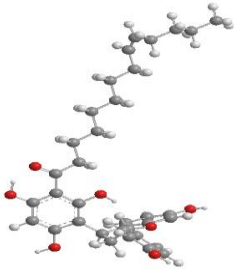

c-DBPO-s-w-u-q-a-e-j

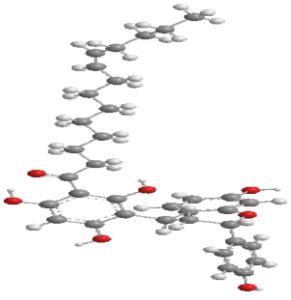

c-DBPO-s-w-u-q-b-e-j

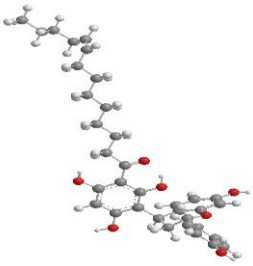

c-DBPO-d-w-u-q-b-e-j

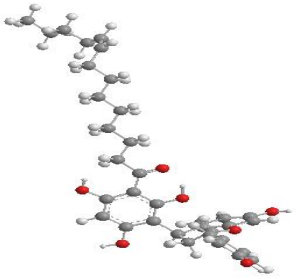

c-DBPO-d-w-u-q-a-e-j

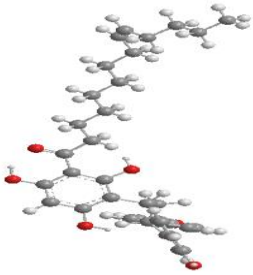

c-DBPO-s-w-u-p-b-f-j

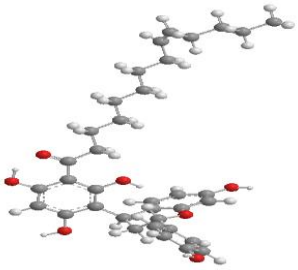

c-DBPO-s-w-u-q-a-e-k

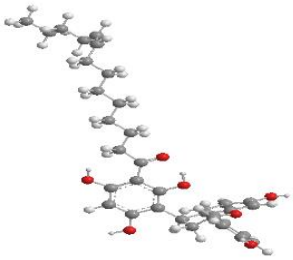

c-DBPO-d-w-u-q-a-e-k

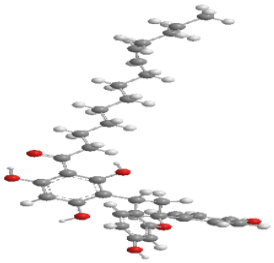

c-DBPO-s-w-u-p-b-e-k

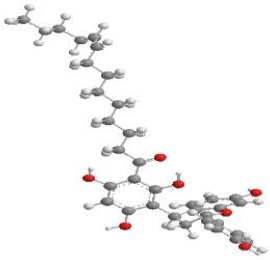

c-DBPO-d-w-u-q-b-f-j

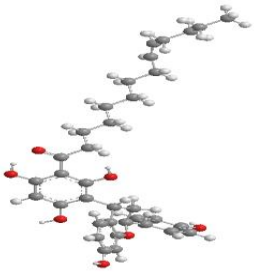

c-DBPO-s-w-u-p-a-f-k

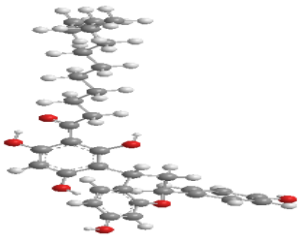

c-DBPO-s-w-u-p-b-f-k

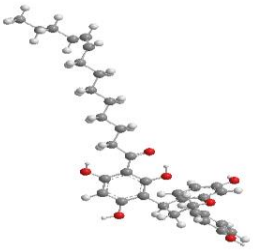

c-DBPO-d-w-u-q-a-f-j

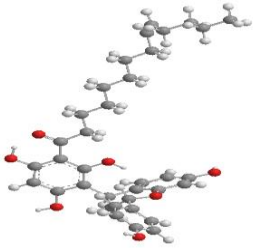

c-DBPO-s-w-u-q-a-f-k

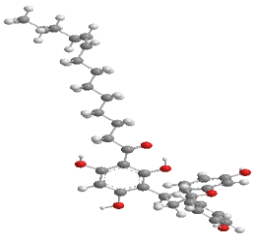

c-DBPO-d-w-u-q-a-f-k

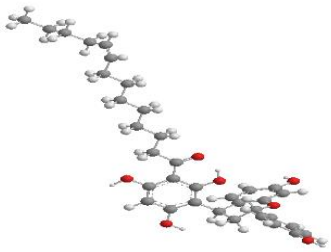

c-DBPO-d-w-u-q-b-f-k

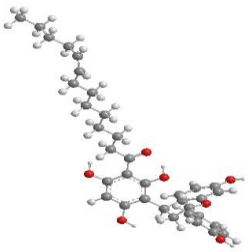

c-DBPO-d-r-u-q-a-e-j

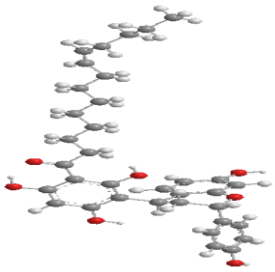

c-DBPO-s-r-u-q-b-e-j

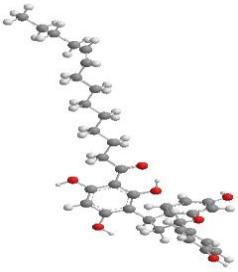

c-DBPO-d-r-q-a-f-j

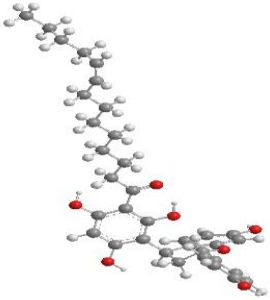

c-DBPO-d-r-u-q-a-f-j

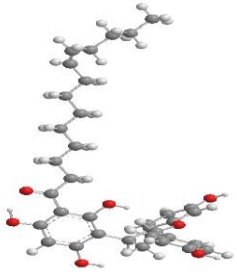

c-DBPO-s-r-u-q-a-e-j

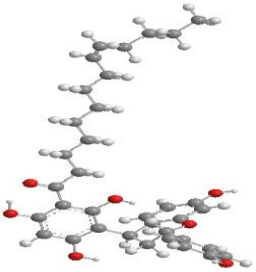

c-DBPO-s-r-u-q-a-e-k

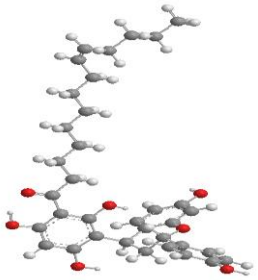

c-DBPO-s-r-u-q-a-f-j

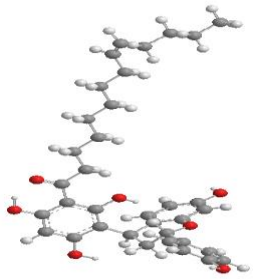

c-DBPO-s-r-u-q-a-f-k

Table 6.1. Relative energies of the calculated conformers of *cis*- c-DBPO having the same geometry of R and different geometries of the ring system.
HF/6-31G(d,p) results *in vacuo*. The conformers are listed in order of increasing relative energy. The absolute energy of the lowest energy conformer is -1873.9714609 hartree.

Conformer name	Relative energy kcal/mol	Conformer	Relative energy kcal/mol
c-DBPO-d-r-η-p-a-e-j	0.000	c-DBPO-d-w-q-a-f-k	5.827
c-DBPO-d-r-η-p-a-e-k	0.014	c-DBPO-d-w-q-b-f-j	5.853
c-DBPO-d-r-η-p-a-f-j	0.424	c-DBPO-d-w-q-b-f-k	5.936
c-DBPO-d-r-η-p-a-f-k	0.496	c-DBPO-d-r-q-b-f-j	6.116
c-DBPO-d-r-η-p-b-e-k	1.023	c-DBPO-s-w-p-a-e-j	6.122
c-DBPO-d-r-η-p-b-e-j	1.028	c-DBPO-d-r-q-b-f-k	6.149
c-DBPO-s-w-ε-q-a-e-k	1.154	c-DBPO-d-r-q-a-f-j	6.158
c-DBPO-s-w-ε-q-a-e-j	1.200	c-DBPO-d-r-q-a-f-k	6.228
c-DBPO-d-r-η-p-b-f-j	1.231	c-DBPO-s-r-η-u-p-b-e-k	6.236
c-DBPO-d-r-η-p-b-f-k	1.264	c-DBPO-s-r-η-u-p-a-e-j	6.281
c-DBPO-s-w-ε-q-b-e-j	1.496	c-DBPO-d-w-u-p-a-e-j	6.398
c-DBPO-s-w-ε-q-a-f-j	1.636	c-DBPO-s-w-p-a-f-j	6.429
c-DBPO-s-w-ε-q-a-f-k	1.652	c-DBPO-s-w-p-a-f-k	6.509
c-DBPO-s-w-ε-q-b-f-k	1.976	c-DBPO-s-w-u-p-b-f-j	6.615
c-DBPO-d-w-p-a-e-j	4.323	c-DBPO-s-r-η-u-p-a-f-j	6.705
c-DBPO-d-w-p-a-e-k	4.459	c-DBPO-s-r-η-u-p-a-f-k	6.722
c-DBPO-d-w-p-a-f-j	4.658	c-DBPO-s-w-p-b-e-j	7.079
c-DBPO-d-w-p-b-f-j	4.678	c-DBPO-s-w-p-e-a-k	7.159
c-DBPO-d-r-η-u-p-a-e-k	4.684	c-DBPO-s-r-η-u-p-b-f-k	7.172
c-DBPO-d-r-η-u-p-a-e-j	4.696	c-DBPO-s-r-η-p-b-f-k	7.459
c-DBPO-s-r-ε-q-b-e-j	4.705	c-DBPO-d-w-u-p-a-e-k	7.851
c-DBPO-s-r-ε-q-b-f-j	4.833	c-DBPO-d-w-u-p-b-e-k	7.875
c-DBPO-d-w-p-a-f-k	4.853	c-DBPO-d-w-u-p-a-f-j	8.070
c-DBPO-s-r-ε-q-b-f-k	5.026	c-DBPO-d-w-u-p-b-f-j	8.095
c-DBPO-s-r-ε-q-a-e-k	5.031	c-DBPO-d-w-u-p-a-f-k	8.256
c-DBPO-s-r-η-p-b-e-j	5.046	c-DBPO-d-w-u-p-b-f-k	8.258
c-DBPO-d-r-η-u-p-a-f-j	5.096	c-DBPO-s-w-u-p-e-a-k	8.285
c-DBPO-s-r-ε-q-a-e-j	5.155	c-DBPO-d-w-u-q-a-e-j	8.391
c-DBPO-d-r-η-u-p-a-f-k	5.163	c-DBPO-s-w-u-q-a-e-j	8.409
c-DBPO-d-w-p-b-e-k	5.166	c-DBPO-d-w-u-q-b-e-j	8.459
c-DBPO-d-w-q-b-e-j	5.188	c-DBPO-d-w-u-q-a-e-k	8.488
c-DBPO-s-r-η-p-e-a-k	5.222	c-DBPO-s-w-u-q-a-e-k	8.500
c-DBPO-d-w-p-b-f-k	5.228	c-DBPO-s-w-u-p-a-f-j	8.557
c-DBPO-s-r-η-p-b-e-k	5.265	c-DBPO-s-w-u-p-b-e-k	8.572
c-DBPO-d-w-q-a-e-k	5.291	c-DBPO-s-w-u-p-a-f-k	8.702
c-DBPO-s-r-η-p-a-e-j	5.355	c-DBPO-d-w-u-q-a-f-j	8.850
c-DBPO-s-r-ε-q-a-f-k	5.505	c-DBPO-s-w-u-p-b-f-k	8.867
c-DBPO-d-w-q-b-e-k	5.559	c-DBPO-s-w-u-q-a-f-k	8.884
c-DBPO-s-r-ε-q-a-f-j	5.565	c-DBPO-d-w-u-q-a-f-k	9.008
c-DBPO-s-w-p-b-f-j	5.596	c-DBPO-d-w-u-q-b-f-k	9.239
c-DBPO-s-r-η-p-a-f-k	5.682	c-DBPO-d-r-u-q-a-e-j	10.163
c-DBPO-d-w-q-a-f-j	5.687	c-DBPO-s-r-u-q-b-e-j	10.283
c-DBPO-d-r-q-a-e-j	5.718	c-DBPO-d-r-u-q-a-f-j	10.563
c-DBPO-d-r-q-b-e-k	5.719	c-DBPO-s-r-u-q-a-e-j	11.105
c-DBPO-d-r-q-b-e-j	5.736	c-DBPO-s-r-u-q-a-e-k	11.128
c-DBPO-d-r-q-a-e-k	5.745	c-DBPO-s-r-u-q-a-f-j	11.402

c-DBPO-s-r-η-p-a-f-j	5.754	c-DBPO-s-r-u-q-a-f-k	11.487

Table 6.2. Parameters of the first IHB of the calculated conformers of *cis*- c-DBPO having the same geometry of R and different geometries of the ring system.
HF/6-31G(d,p) results *in vacuo*. For conformers of d type, the first IHB is H15···O14; for conformers of s type, the first IHB is H17···O14. The conformers are listed in order of increasing relative energy.

Conformer	Parameters of the first IHB		
	OH···O (Å)	OH···O (Å)	OH···O (°)
c-DBPO-d-r-η-p-a-e-j	1.652	2.508	146.3
c-DBPO-d-r-η-p-a-e-k	1.652	2.508	146.3
c-DBPO-d-r-η-p-a-f-j	1.652	2.508	146.4
c-DBPO-d-r-η-p-a-f-k	1.652	2.508	146.3
c-DBPO-d-r-η-p-b-e-k	1.651	2.508	146.6
c-DBPO-d-r-η-p-b-e-j	1.656	2.510	146.2
c-DBPO-s-w-ε-q-a-e-k	1.684	2.522	143.9
c-DBPO-s-w-ε-q-a-e-j	1.684	2.521	143.9
c-DBPO-d-r-η-p-b-f-j	1.656	2.510	146.2
c-DBPO-d-r-η-p-b-f-k	1.651	2.509	146.5
c-DBPO-s-w-ε-q-b-e-j	1.689	2.527	144.0
c-DBPO-s-w-ε-q-a-f-j	1.682	2.520	143.9
c-DBPO-s-w-ε-q-a-f-k	1.683	2.521	143.9
c-DBPO-s-w-ε-q-b-f-k	1.689	2.526	144.0
c-DBPO-d-w-p-a-e-j	1.656	2.511	146.2
c-DBPO-d-w-p-a-e-k	1.656	2.511	146.2
c-DBPO-d-w-p-a-f-j	1.656	2.511	146.2
c-DBPO-d-w-p-b-f-j	1.656	2.511	146.2
c-DBPO-d-r-η-u-p-a-e-j	1.676	2.523	145.4
c-DBPO-d-r-η-u-p-a-e-k	1.676	2.524	145.4
c-DBPO-s-r-ε-q-b-e-j	1.695	2.531	143.9
c-DBPO-s-r-ε-q-b-f-j	1.694	2.531	143.9
c-DBPO-d-w-p-a-f-k	1.656	2.511	146.2
c-DBPO-s-r-ε-q-b-f-k	1.694	2.531	143.9
c-DBPO-s-r-ε-q-a-e-k	1.692	2.527	143.8
c-DBPO-s-r-η-p-b-e-j	1.692	2.528	143.8
c-DBPO-d-r-η-u-p-a-f-j	1.675	2.522	145.4
c-DBPO-d-w-p-b-e-k	1.658	2.512	146.2
c-DBPO-d-r-η-u-p-a-f-k	1.676	2.523	145.4
c-DBPO-s-r-ε-q-a-e-j	1.690	2.526	143.8
c-DBPO-d-w-q-b-e-j	1.664	2.514	145.6
c-DBPO-d-w-p-b-f-k	1.659	2.513	146.1
c-DBPO-d-w-q-a-e-j	1.654	2.508	146.1

c-DBPO-s-r-η-p-e-a-k	1.697	2.532	143.7
c-DBPO-s-r-η-p-b-e-k	1.692	2.528	143.8
c-DBPO-d-w-q-a-e-k	1.654	2.508	146.1
c-DBPO-s-r-η-p-a-e-j	1.697	2.532	143.7
c-DBPO-s-r-ε-q-a-f-k	1.689	2.526	143.8
c-DBPO-d-w-q-b-e-k	1.664	2.514	145.6
c-DBPO-s-r-ε-q-a-f-j	1.688	2.524	143.9
c-DBPO-s-w-p-b-f-j	1.683	2.521	143.9
c-DBPO-s-r-η-p-a-f-k	1.697	2.532	143.7
c-DBPO-d-w-q-a-f-j	1.655	2.509	146.0
c-DBPO-d-r-q-a-e-j	1.646	2.503	146.4
c-DBPO-d-r-q-b-e-k	1.647	2.505	146.5
c-DBPO-d-r-q-b-e-j	1.647	2.504	146.4
c-DBPO-d-r-q-a-e-k	1.646	2.503	146.4
c-DBPO-s-r-η-p-a-f-j	1.696	2.531	143.7
c-DBPO-d-w-q-a-f-k	1.656	2.509	146.0
c-DBPO-d-w-q-b-f-j	1.657	2.510	145.9
c-DBPO-d-w-q-b-f-k	1.657	2.511	146.0
c-DBPO-d-r-q-b-f-j	1.649	2.506	146.3
c-DBPO-s-w-p-a-e-j	1.689	2.526	143.7
c-DBPO-d-r-q-b-f-k	1.649	2.506	146.3
c-DBPO-d-r-q-a-f-j	1.648	2.504	146.3
c-DBPO-d-r-q-a-f-k	1.648	2.504	146.3
c-DBPO-s-r-η-u-p-b-e-k	1.736	2.559	142.5
c-DBPO-s-r-η-u-p-a-e-j	1.737	2.560	142.4
c-DBPO-d-w-u-p-a-e-j	1.714	2.546	143.4
c-DBPO-s-w-p-a-f-j	1.689	2.526	143.8
c-DBPO-s-w-p-a-f-k	1.689	2.526	143.8
c-DBPO-s-w-u-p-b-f-j	1.739	2.562	142.5
c-DBPO-s-r-η-u-p-a-f-j	1.738	2.560	142.4
c-DBPO-s-r-η-u-p-a-f-k	1.737	2.560	142.4
c-DBPO-s-w-p-b-e-j	1.686	2.523	143.7
c-DBPO-s-w-p-e-a-k	1.686	2.523	143.8
c-DBPO-s-r-η-u-p-b-f-k	1.731	2.555	142.6
c-DBPO-s-r-η-p-b-f-k	1.686	2.523	143.8
c-DBPO-d-w-u-p-a-e-k	1.681	2.526	145.2
c-DBPO-d-w-u-p-b-e-k	1.681	2.526	145.2
c-DBPO-d-w-u-p-a-f-j	1.682	2.527	145.2
c-DBPO-d-w-u-p-b-f-j	1.682	2.527	145.3
c-DBPO-d-w-u-p-a-f-k	1.682	2.527	145.2
c-DBPO-d-w-u-p-b-f-k	1.682	2.528	145.3
c-DBPO-s-w-u-p-e-a-k	1.731	2.554	142.4
c-DBPO-d-w-u-q-a-e-j	1.685	2.530	145.2
c-DBPO-s-w-u-q-a-e-j	1.732	2.556	142.4
c-DBPO-d-w-u-q-b-e-j	1.694	2.533	144.4
c-DBPO-d-w-u-q-a-e-k	1.686	2.530	145.2
c-DBPO-s-w-u-q-a-e-k	1.733	2.556	142.4
c-DBPO-s-w-u-p-a-f-j	1.731	2.554	142.4

c-DBPO-s-w-u-p-b-e-k	1.725	2.550	142.6
c-DBPO-s-w-u-p-a-f-k	1.731	2.554	142.4
c-DBPO-d-w-u-q-a-f-j	1.686	2.529	145.1
c-DBPO-s-w-u-p-b-f-k	1.726	2.551	142.6
c-DBPO-s-w-u-q-a-f-k	1.731	2.555	142.5
c-DBPO-d-w-u-q-a-f-k	1.687	2.530	145.1
c-DBPO-d-w-u-q-b-f-k	1.684	2.528	145.1
c-DBPO-d-r-u-q-a-e-j	1.676	2.520	145.0
c-DBPO-s-r-u-q-b-e-j	1.738	2.562	142.5
c-DBPO-d-r-u-q-a-f-j	1.679	2.522	144.8
c-DBPO-s-r-u-q-a-e-j	1.739	2.561	142.4
c-DBPO-s-r-u-q-a-e-k	1.740	2.562	142.4
c-DBPO-s-r-u-q-a-f-j	1.737	2.560	142.4
c-DBPO-s-r-u-q-a-f-k	1.738	2.561	142.4

Table 6.3. The distance between the H atom and the closest C atom in the acceptor aromatic ring for the O–H···π interactions of the calculated conformers of *cis*-DBPO having the same geometry of R and different geometries of the ring system *in vacuo*.
HF/6-31G(d,p) results. The conformers are arranged in order of increasing relative energy. For p-type conformers, the distance considered is H16···C23; for q-type conformers, the distance considered is H15···C23.

Conformer	H15···C23 or H16···C23 (Å)	Conformer	H15···C23 or H16···C23 (Å)
c-DBPO-d-r-η-p-a-e-j	2.127	c-DBPO-s-r-ε-q-b-f-k	2.171
c-DBPO-d-r-η-p-a-e-k	2.127	c-DBPO-s-r-η-p-b-e-j	2.216
c-DBPO-d-r-η-p-a-f-j	2.131	c-DBPO-d-r-η-u-p-a-f-j	2.130
c-DBPO-d-r-η-p-a-f-k	2.130	c-DBPO-d-r-η-u-p-a-f-k	2.130
c-DBPO-d-r-η-p-b-e-k	2.213	c-DBPO-s-r-ε-q-a-e-j	2.058
c-DBPO-d-r-η-p-b-e-j	2.236	c-DBPO-s-r-η-p-e-a-k	2.109
c-DBPO-s-w-ε-q-a-e-k	2.074	c-DBPO-s-r-η-p-b-e-k	2.220
c-DBPO-s-w-ε-q-a-e-j	2.074	c-DBPO-s-r-η-p-a-e-j	2.109
c-DBPO-d-r-η-p-b-f-j	2.239	c-DBPO-s-r-ε-q-a-f-k	2.059
c-DBPO-d-r-η-p-b-f-k	2.219	c-DBPO-s-r-ε-q-a-f-j	2.059
c-DBPO-s-w-ε-q-b-e-j	2.185	c-DBPO-s-r-η-p-a-f-k	2.111
c-DBPO-s-w-ε-q-a-f-j	2.076	c-DBPO-s-r-η-p-a-f-j	2.112
c-DBPO-s-w-ε-q-a-f-k	2.075	c-DBPO-s-r-η-u-p-b-e-k	2.121
c-DBPO-s-w-ε-q-b-f-k	2.187	c-DBPO-s-r-η-u-p-a-e-j	2.121
c-DBPO-d-r-η-u-p-a-e-j	2.128	c-DBPO-s-r-η-u-p-a-f-j	2.123
c-DBPO-d-r-η-u-p-a-e-k	2.128	c-DBPO-s-r-η-u-p-a-f-k	2.123
c-DBPO-s-r-ε-q-b-e-j	2.165	c-DBPO-s-r-η-u-p-b-f-k	2.240
c-DBPO-s-r-ε-q-b-f-j	2.169		

Table 6.4. Dipole moment of the calculated conformers of *cis*-DBPO having the same geometry of R and different geometries of the ring system.
HF/6-31G(d,p) results *in vacuo*. The conformers are listed in order of increasing relative energy.

Conformer	Dipole moment (Debye)	Conformer	Dipole moment (Debye)
c-DBPO-d-r-η-p-a-e-j	2.460	c-DBPO-d-w-q-a-f-k	7.228
c-DBPO-d-r-η-p-a-e-k	3.834	c-DBPO-d-w-q-b-f-j	0.892
c-DBPO-d-r-η-p-a-f-j	2.877	c-DBPO-d-w-q-b-f-k	9.417
c-DBPO-d-r-η-p-a-f-k	4.115	c-DBPO-d-r-q-b-f-j	5.606
c-DBPO-d-r-η-p-b-e-k	2.597	c-DBPO-s-w-p-a-e-j	9.149
c-DBPO-d-r-η-p-b-e-j	2.806	c-DBPO-d-r-q-b-f-k	8.498
c-DBPO-s-w-ε-q-a-e-k	2.993	c-DBPO-d-r-q-a-f-j	4.731
c-DBPO-s-w-ε-q-a-e-j	5.279	c-DBPO-d-r-q-a-f-k	4.463
c-DBPO-d-r-η-p-b-f-j	3.489	c-DBPO-s-r-η-u-p-b-e-k	3.571
c-DBPO-d-r-η-p-b-f-k	3.723	c-DBPO-s-r-η-u-p-a-e-j	6.137
c-DBPO-s-w-ε-q-b-e-j	4.900	c-DBPO-d-w-u-p-a-e-j	3.270
c-DBPO-s-w-ε-q-a-f-j	5.068	c-DBPO-s-w-p-a-f-j	5.700
c-DBPO-s-w-ε-q-a-f-k	2.723	c-DBPO-s-w-p-a-f-k	7.716
c-DBPO-s-w-ε-q-b-f-k	2.780	c-DBPO-s-w-u-p-b-f-j	4.223
c-DBPO-d-w-p-a-e-j	6.642	c-DBPO-s-r-η-u-p-a-f-j	0.995
c-DBPO-d-w-p-a-e-k	3.062	c-DBPO-s-r-η-u-p-a-f-k	5.749
c-DBPO-d-w-p-a-f-j	7.227	c-DBPO-s-w-p-b-e-j	2.727
c-DBPO-d-w-p-b-f-j	5.408	c-DBPO-s-w-p-e-a-k	4.389
c-DBPO-d-r-η-u-p-a-e-j	5.472	c-DBPO-s-r-η-u-p-b-f-k	3.845
c-DBPO-d-r-η-u-p-a-e-k	0.648	c-DBPO-s-r-η-p-b-f-k	7.838
c-DBPO-s-r-ε-q-b-e-j	2.946	c-DBPO-d-w-u-p-a-e-k	7.692
c-DBPO-s-r-ε-q-b-f-j	7.759	c-DBPO-d-w-u-p-b-e-k	6.327
c-DBPO-d-w-p-a-f-k	6.184	c-DBPO-d-w-u-p-a-f-j	6.268
c-DBPO-s-r-ε-q-b-f-k	5.408	c-DBPO-d-w-u-p-b-f-j	4.848
c-DBPO-s-r-ε-q-a-e-k	4.480	c-DBPO-d-w-u-p-a-f-k	1.686
c-DBPO-s-r-η-p-b-e-j	3.536	c-DBPO-d-w-u-p-b-f-k	7.098
c-DBPO-d-r-η-u-p-a-f-j	5.494	c-DBPO-s-w-u-p-e-a-k	7.160
c-DBPO-d-w-p-b-e-k	2.573	c-DBPO-d-w-u-q-a-e-j	4.116
c-DBPO-d-r-η-u-p-a-f-k	6.559	c-DBPO-s-w-u-q-a-e-j	2.284
c-DBPO-s-r-ε-q-a-e-j	3.896	c-DBPO-d-w-u-q-b-e-j	1.363
c-DBPO-d-w-q-b-e-j	7.897	c-DBPO-d-w-u-q-a-e-k	2.155
c-DBPO-d-w-p-b-f-k	5.980	c-DBPO-s-w-u-q-a-e-k	5.888
c-DBPO-d-w-q-a-e-j	5.040	c-DBPO-s-w-u-p-a-f-j	4.890
c-DBPO-s-r-η-p-e-a-k	6.363	c-DBPO-s-w-u-p-b-e-k	6.449
c-DBPO-s-r-η-p-b-e-k	5.365	c-DBPO-s-w-u-p-a-f-k	6.114
c-DBPO-d-w-q-a-e-k	6.769	c-DBPO-d-w-u-q-a-f-j	3.390
c-DBPO-s-r-η-p-a-e-j	7.756	c-DBPO-s-w-u-p-b-f-k	3.661
c-DBPO-s-r-ε-q-a-f-k	5.723	c-DBPO-s-w-u-q-a-f-k	6.114
c-DBPO-d-w-q-b-e-k	4.350	c-DBPO-d-w-u-q-a-f-k	2.491
c-DBPO-s-r-ε-q-a-f-j	5.723	c-DBPO-d-w-u-q-b-f-k	7.871
c-DBPO-s-w-p-b-f-j	7.085	c-DBPO-d-r-u-q-a-e-j	7.985

c-DBPO-s-r-η-p-a-f-k	2.551	c-DBPO-s-r-u-q-b-e-j	1.061
c-DBPO-d-w-q-a-f-j	4.531	c-DBPO-d-r-u-q-a-f-j	5.163
c-DBPO-d-r-q-a-e-j	8.205	c-DBPO-s-r-u-q-a-e-j	2.888
c-DBPO-d-r-q-b-e-k	4.035	c-DBPO-s-r-u-q-a-e-k	4.649
c-DBPO-d-r-q-b-e-j	3.641	c-DBPO-s-r-u-q-a-f-j	3.273
c-DBPO-d-r-q-a-e-k	3.463	c-DBPO-s-r-u-q-a-f-k	3.566
c-DBPO-s-r-η-p-a-f-j	4.755		

Table 6.5. HOMO-LUMO energy gap of the calculated conformers of *cis*-DBPO having the same geometry of R and different geometries of the ring system.
HF/6-31G(d,p) results *in vacuo*. The conformers are listed in order of increasing relative energy.

Conformer	HOMO-LUMO energy gap (kcal/mol)	Conformer	HOMO-LUMO energy gap (kcal/mol)
c-DBPO-d-r-η-p-a-e-j	257.410	c-DBPO-d-w-q-a-f-k	259.946
c-DBPO-d-r-η-p-a-e-k	257.517	c-DBPO-d-w-q-b-f-j	253.125
c-DBPO-d-r-η-p-a-f-j	256.250	c-DBPO-d-w-q-b-f-k	241.641
c-DBPO-d-r-η-p-a-f-k	256.425	c-DBPO-d-r-q-b-f-j	242.457
c-DBPO-d-r-η-p-b-e-k	254.612	c-DBPO-s-w-p-a-e-j	242.570
c-DBPO-d-r-η-p-b-e-j	255.867	c-DBPO-d-r-q-b-f-k	243.066
c-DBPO-s-w-ε-q-a-e-k	258.829	c-DBPO-d-r-q-a-f-j	246.523
c-DBPO-s-w-ε-q-a-e-j	258.785	c-DBPO-d-r-q-a-f-k	252.158
c-DBPO-d-r-η-p-b-f-j	255.992	c-DBPO-s-r-η-u-p-b-e-k	248.657
c-DBPO-d-r-η-p-b-f-k	256.049	c-DBPO-s-r-η-u-p-a-e-j	247.728
c-DBPO-s-w-ε-q-b-e-j	258.647	c-DBPO-d-w-u-p-a-e-j	252.987
c-DBPO-s-w-ε-q-a-f-j	258.069	c-DBPO-s-w-p-a-f-j	251.493
c-DBPO-s-w-ε-q-a-f-k	258.182	c-DBPO-s-w-p-a-f-k	260.297
c-DBPO-s-w-ε-q-b-f-k	239.796	c-DBPO-s-w-u-p-b-f-j	236.100
c-DBPO-d-w-p-a-e-j	243.844	c-DBPO-s-r-η-u-p-a-f-j	252.629
c-DBPO-d-w-p-a-e-k	258.276	c-DBPO-s-r-η-u-p-a-f-k	250.797
c-DBPO-d-w-p-a-f-j	242.739	c-DBPO-s-w-p-b-e-j	238.673
c-DBPO-d-w-p-b-f-j	244.427	c-DBPO-s-w-p-e-a-k	251.085
c-DBPO-d-r-η-u-p-a-e-j	244.415	c-DBPO-s-r-η-u-p-b-f-k	251.531
c-DBPO-d-r-η-u-p-a-e-k	251.581	c-DBPO-s-r-η-p-b-f-k	260.404
c-DBPO-s-r-ε-q-b-e-j	251.688	c-DBPO-d-w-u-p-a-e-k	258.691
c-DBPO-s-r-ε-q-b-f-j	260.855	c-DBPO-d-w-u-p-b-e-k	236.841
c-DBPO-d-w-p-a-f-k	260.743	c-DBPO-d-w-u-p-a-f-j	236.822
c-DBPO-s-r-ε-q-b-f-k	249.435	c-DBPO-d-w-u-p-b-f-j	238.560
c-DBPO-s-r-ε-q-a-e-k	260.680	c-DBPO-d-w-u-p-a-f-k	239.947
c-DBPO-s-r-η-p-b-e-j	253.099	c-DBPO-d-w-u-p-b-f-k	238.002
c-DBPO-d-r-η-u-p-a-f-j	261.025	c-DBPO-s-w-u-p-e-a-k	238.127

c-DBPO-d-w-p-b-e-k	250.527	c-DBPO-d-w-u-q-a-e-j	237.111
c-DBPO-d-r-η-u-p-a-f-k	242.338	c-DBPO-s-w-u-q-a-e-j	239.225
c-DBPO-s-r-ε-q-a-e-j	250.715	c-DBPO-d-w-u-q-b-e-j	240.267
c-DBPO-d-w-q-b-e-j	256.250	c-DBPO-d-w-u-q-a-e-k	239.602
c-DBPO-d-w-p-b-f-k	242.319	c-DBPO-s-w-u-q-a-e-k	250.571
c-DBPO-d-w-q-a-e-j	243.273	c-DBPO-s-w-u-p-a-f-j	238.648
c-DBPO-s-r-η-p-e-a-k	240.995	c-DBPO-s-w-u-p-b-e-k	235.536
c-DBPO-s-r-η-p-b-e-k	260.473	c-DBPO-s-w-u-p-a-f-k	237.318
c-DBPO-d-w-q-a-e-k	260.096	c-DBPO-d-w-u-q-a-f-j	240.236
c-DBPO-s-r-η-p-a-e-j	240.449	c-DBPO-s-w-u-p-b-f-k	239.796
c-DBPO-s-r-ε-q-a-f-k	249.096	c-DBPO-s-w-u-q-a-f-k	237.318
c-DBPO-d-w-q-b-e-k	260.561	c-DBPO-d-w-u-q-a-f-k	240.775
c-DBPO-s-r-ε-q-a-f-j	241.842	c-DBPO-d-w-u-q-b-f-k	236.747
c-DBPO-s-w-p-b-f-j	260.454	c-DBPO-d-r-u-q-a-e-j	237.424
c-DBPO-s-r-η-p-a-f-k	253.558	c-DBPO-s-r-u-q-b-e-j	241.961
c-DBPO-d-w-q-a-f-j	260.052	c-DBPO-d-r-u-q-a-f-j	248.312
c-DBPO-d-r-q-a-e-j	242.206	c-DBPO-s-r-u-q-a-e-j	243.204
c-DBPO-d-r-q-b-e-k	250.928	c-DBPO-s-r-u-q-a-e-k	246.379
c-DBPO-d-r-q-b-e-j	247.075	c-DBPO-s-r-u-q-a-f-j	245.858
c-DBPO-d-r-q-a-e-k	249.134	c-DBPO-s-r-u-q-a-f-k	247.345
c-DBPO-s-r-η-p-a-f-j	246.529		

Figure 6.3. Shapes of the HOMO and LUMO molecular orbitals of the calculated conformers of *cis*-DBPO having the same geometry of R and different geometries of the ring system *in vacuo*.
HF/6-31G(d,p) results. The conformers are not listed in order of increasing relative energy.

HOMO	LUMO	HOMO	LUMO
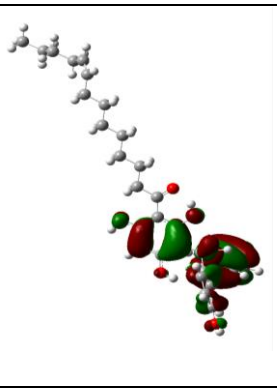	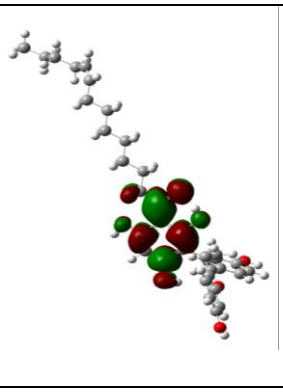		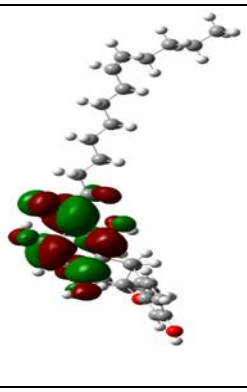
c-DBPO-d-r-η-p-a-e-j		c-DBPO-s-w-p-a-e-j	
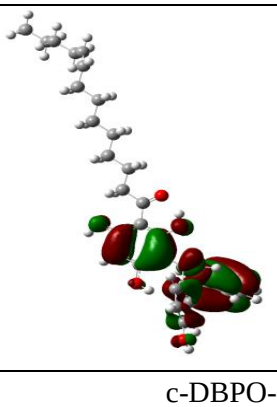	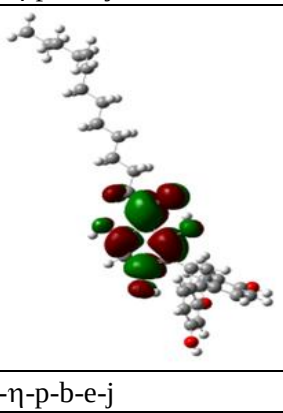	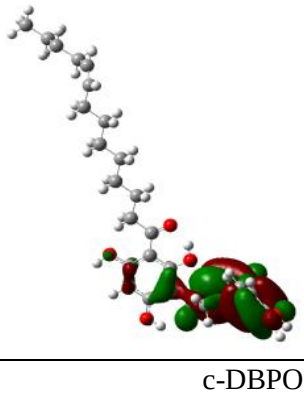	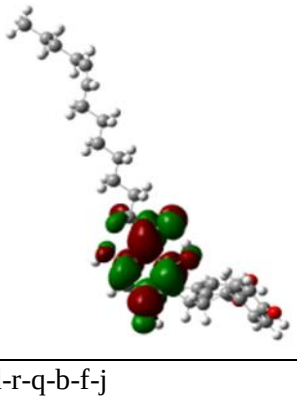
c-DBPO-d-r-η-p-b-e-j		c-DBPO-d-r-q-b-f-j	
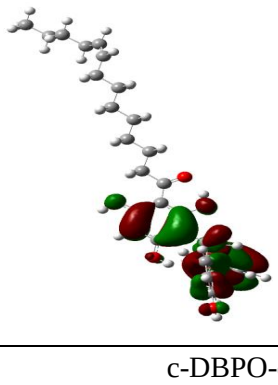	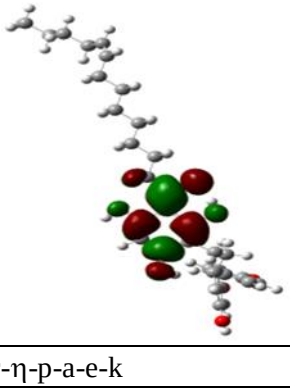	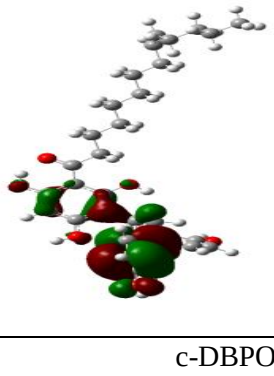	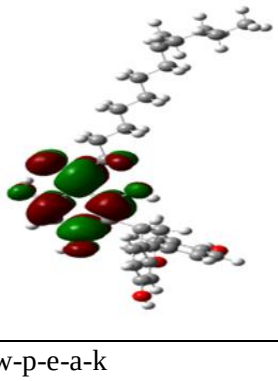
c-DBPO-d-r-η-p-a-e-k		c-DBPO-s-w-p-e-a-k	
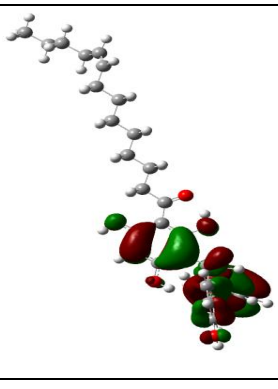	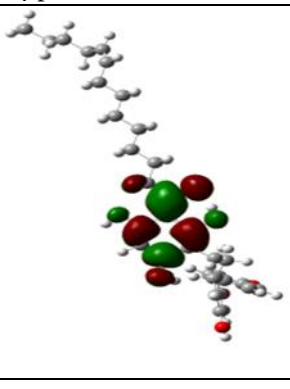	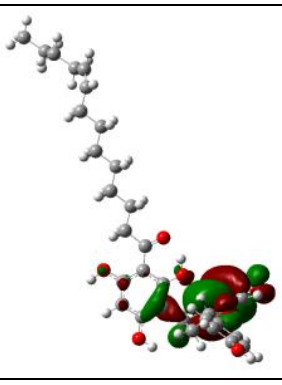	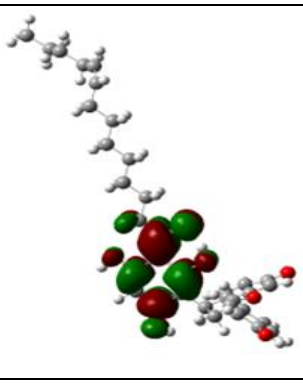
c-DBPO-d-r-η-p-b-e-k		c-DBPO-d-r-q-a-f-j	

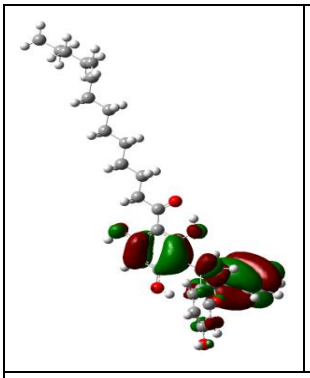 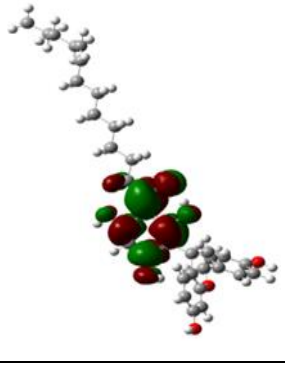	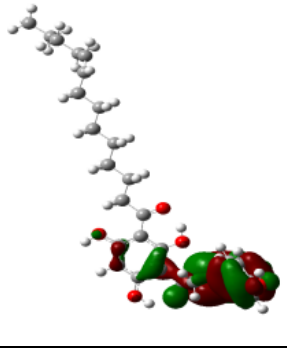 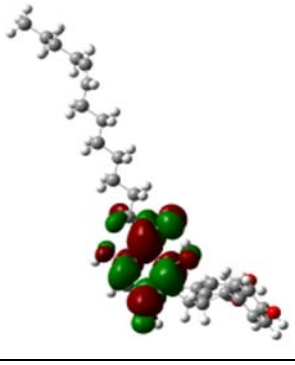
c-DBPO-d-r-η-p-a-f-j	c-DBPO-d-r-q-b-f-k
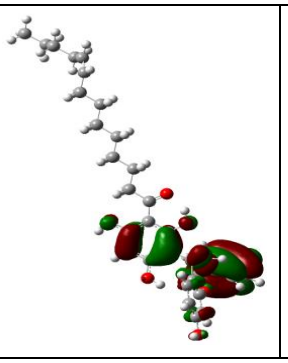 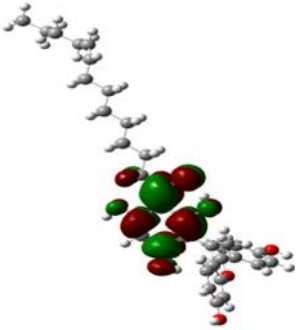	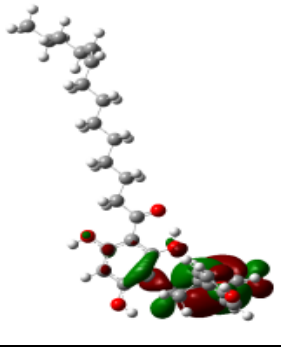 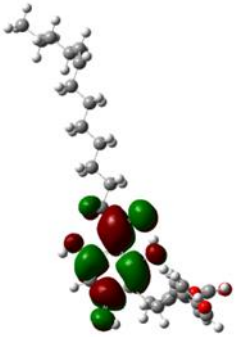
c-DBPO-d-r-η-p-b-f-j	c-DBPO-d-r-q-a-f-k
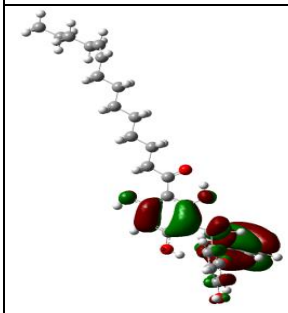 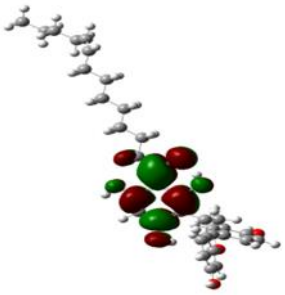	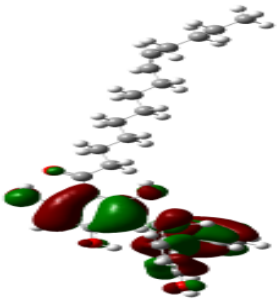 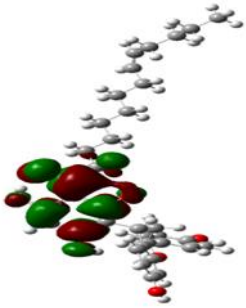
c-DBPO-d-r-η-p-a-f-k	c-DBPO-s-r-η-u-p-a-e-j
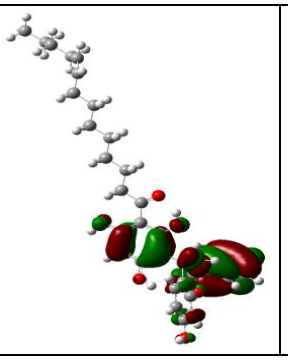 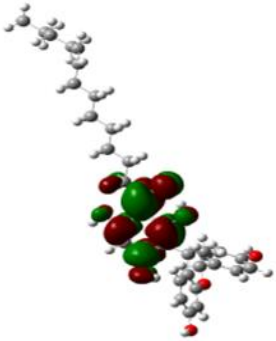	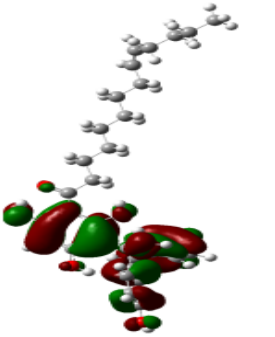 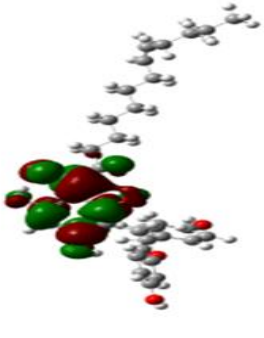
c-DBPO-d-r-η-p-b-f-k	c-DBPO-s-r-η-u-p-b-e-k
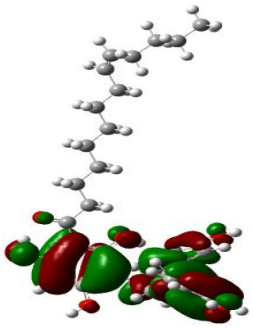 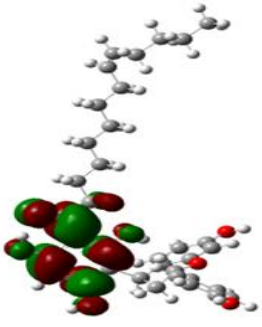	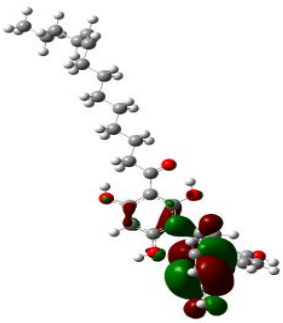 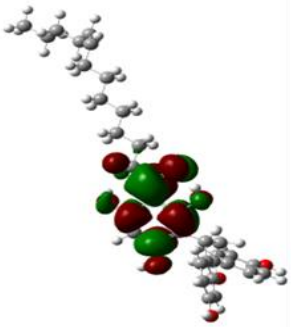
c-DBPO-s-w-ε-q-a-e-k	c-DBPO-d-w- u-p-a-e-j

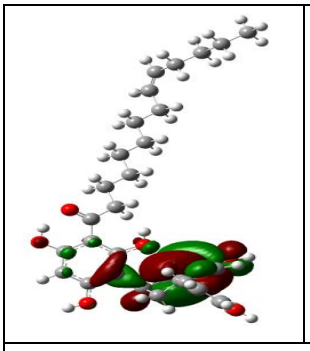 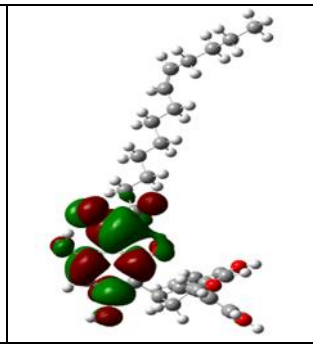	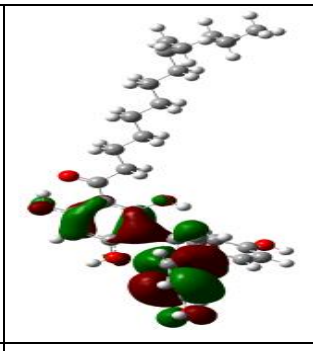 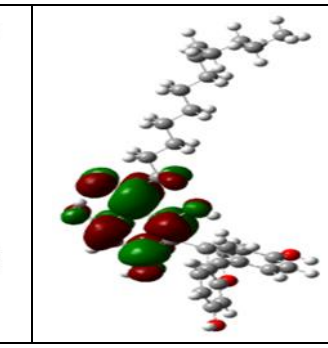
c-DBPO-s-w-u-q-a-e-k	c-DBPO-s-w-p-a-f-j
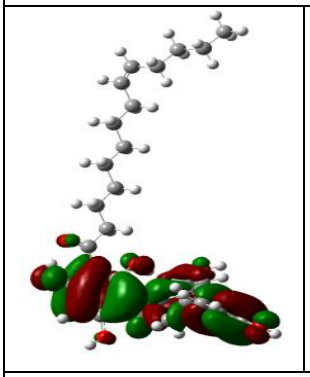 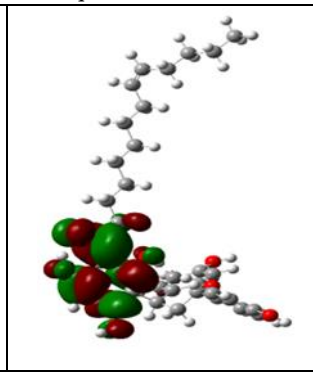	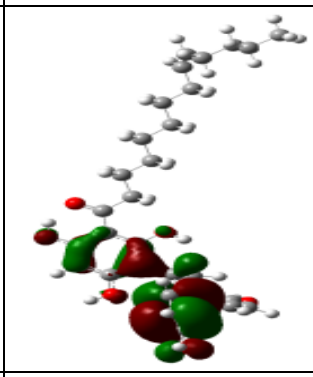 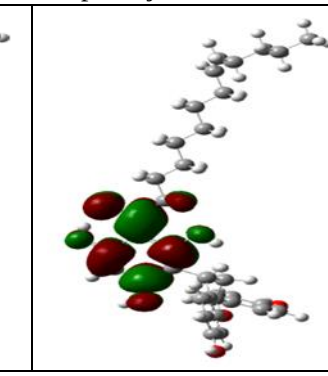
c-DBPO-s-w-ε-q-a-e-j	c-DBPO-s-w-p-a-f-k
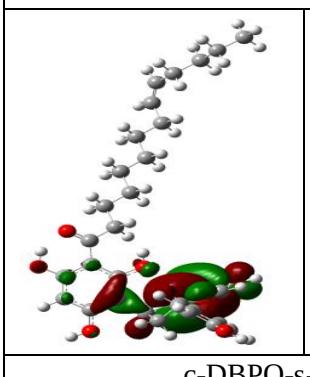 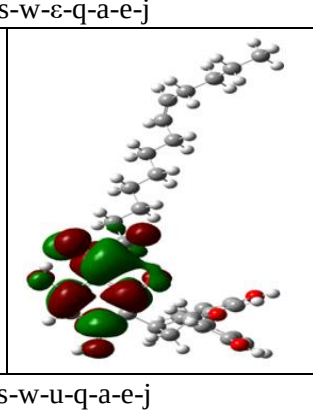	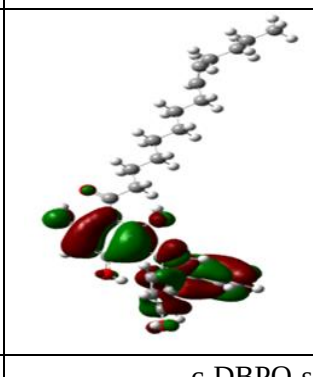 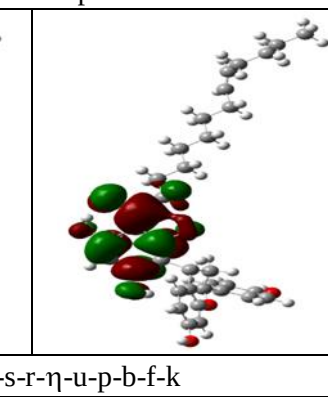
c-DBPO-s-w-u-q-a-e-j	c-DBPO-s-r-η-u-p-b-f-k
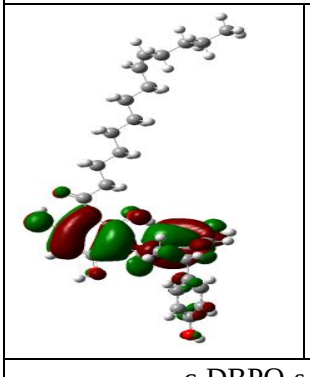 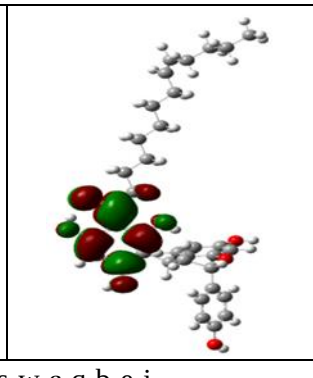	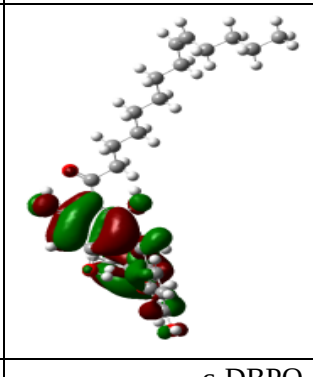 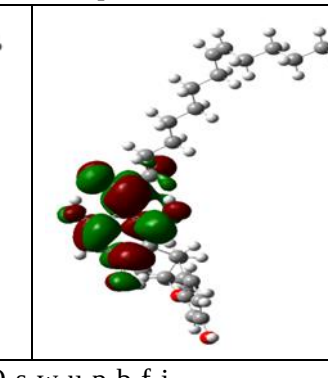
c-DBPO-s-w-ε-q-b-e-j	c-DBPO-s-w-u-p-b-f-j
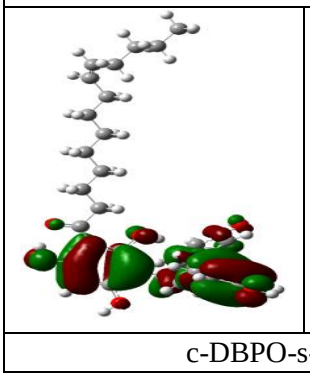 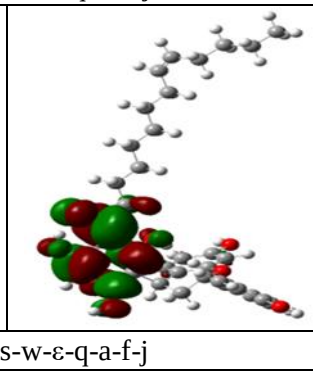	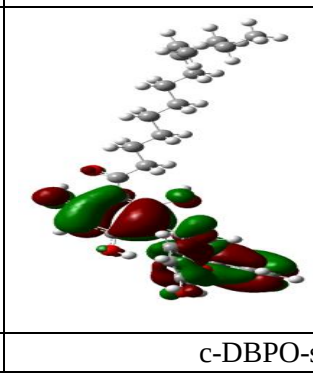 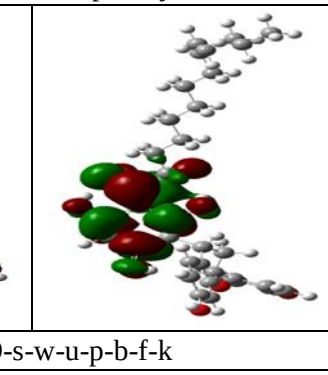
c-DBPO-s-w-ε-q-a-f-j	c-DBPO-s-w-u-p-b-f-k

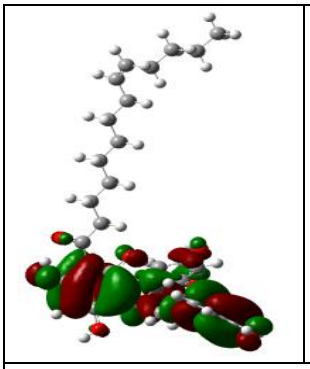	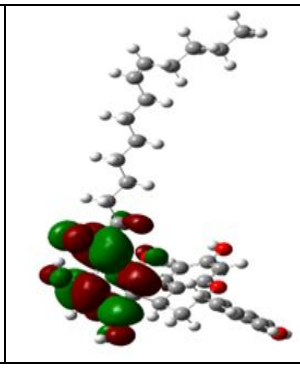
c-DBPO-s-w-ε-q-a-f-k	c-DBPO-s-r-η-u-p-a-f-j
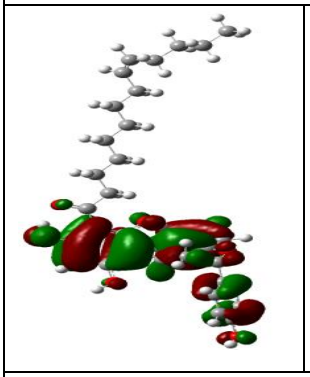	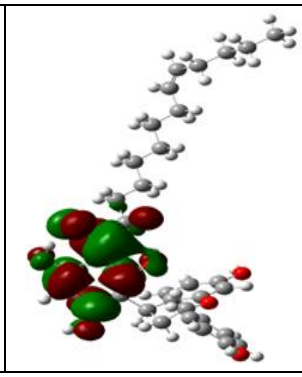
c-DBPO-s-w-u-q-a-f-k	c-DBPO-s-w-p-b-e-j
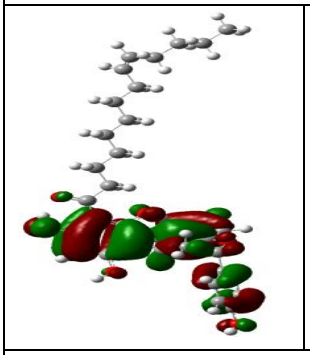	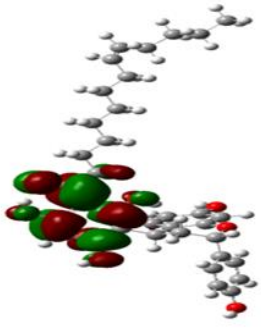
c-DBPO-s-w-ε-q-b-f-k	c-DBPO-s-r-η-u-p-a-f-k
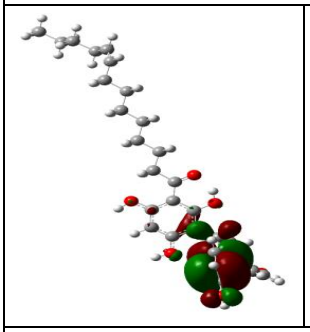	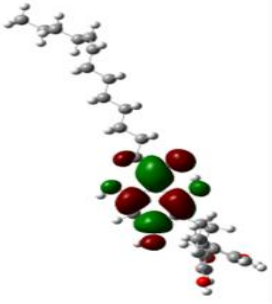
c-DBPO-d-w-p-a-e-j	c-DBPO-s-r-η-p-b-f-k
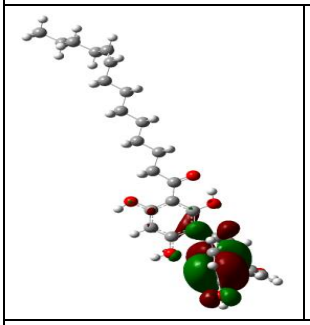	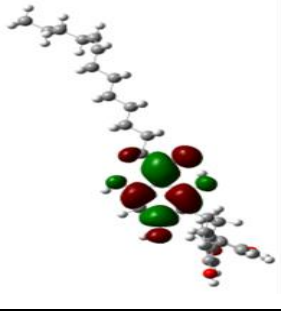
c-DBPO-d-w-p-b-e-j	c-DBPO-d-w-u-p-a-e-k

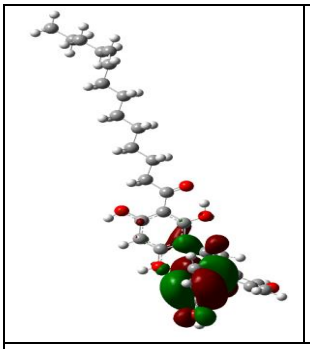 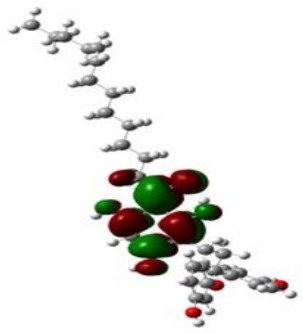	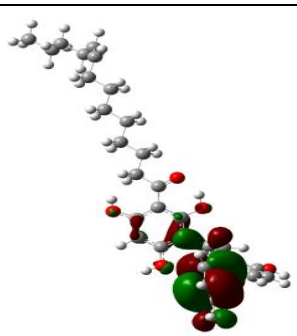 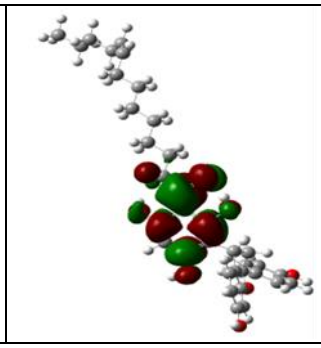
c-DBPO-d-w-p-a-e-k	c-DBPO-d-w-u-p-a-f-j
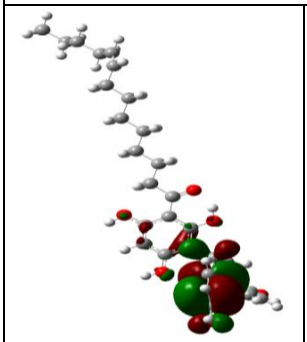 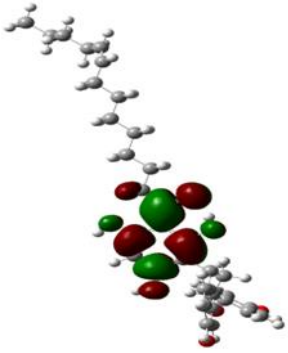	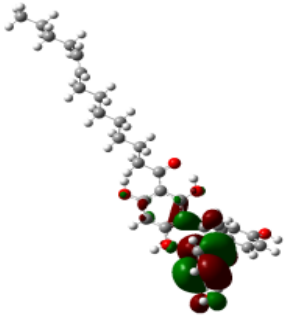 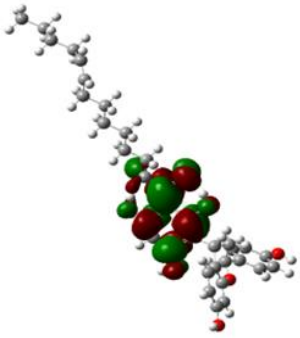
c-DBPO-d-w-p-a-f-j	c-DBPO-d-w-u-p-b-f-j
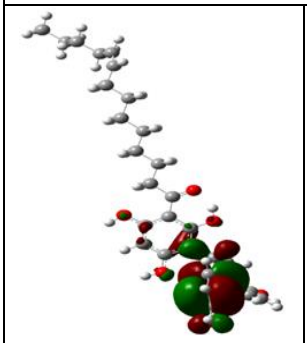 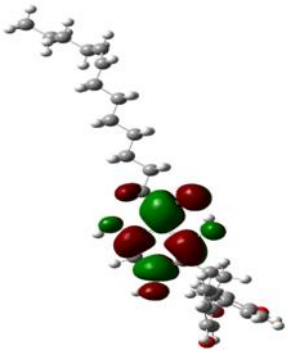	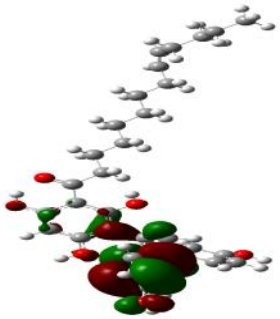 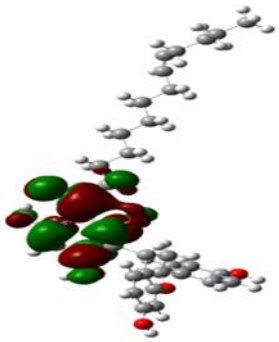
c-DBPO-d-w-p-b-f-j	c-DBPO-s-w-u-p-a-e-j
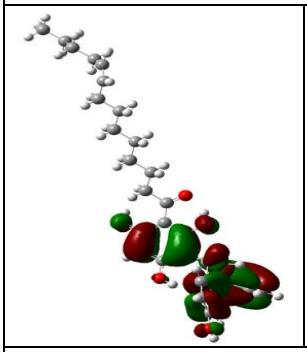 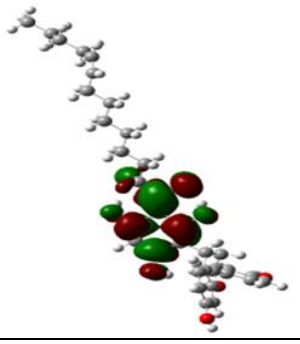	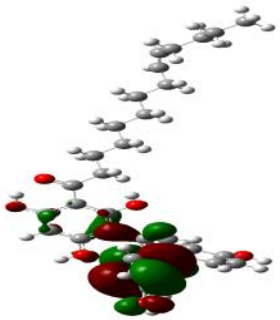 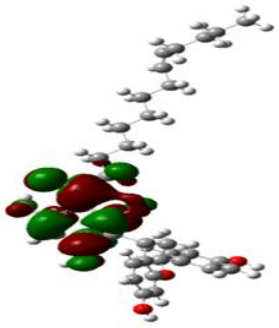
c-DBPO-d-r-η-u-p-a-e-k	c-DBPO-s-w-u-p-b-e-j
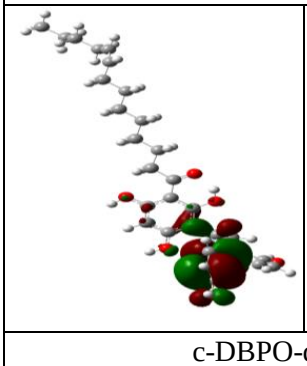 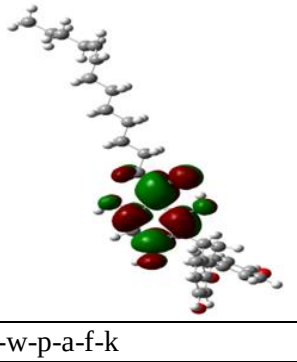	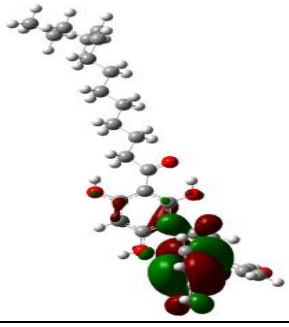 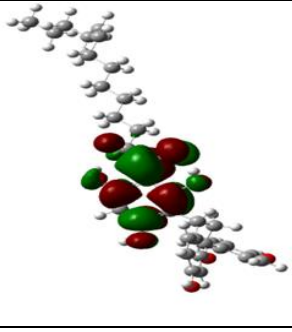
c-DBPO-d-w-p-a-f-k	c-DBPO-d-w-u-p-a-f-k

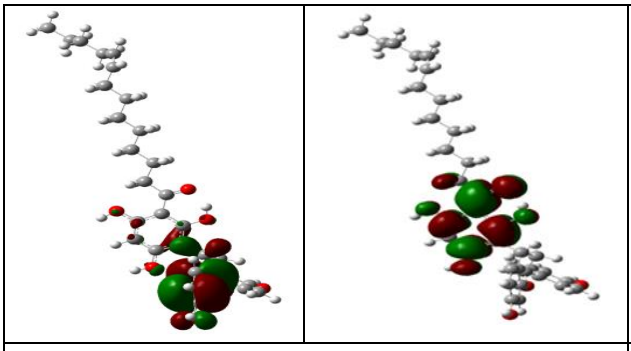	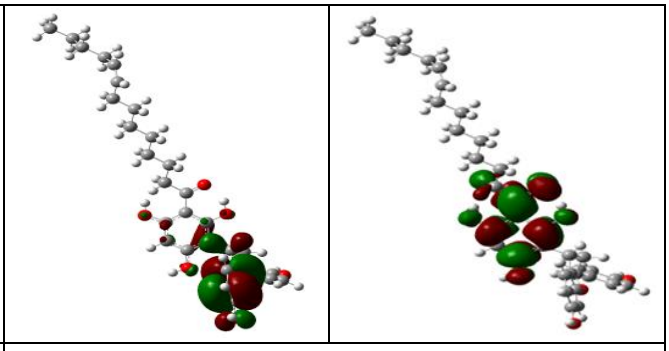
c-DBPO-d-w-p-b-f-k	c-DBPO-d-w-u-p-b-f-k
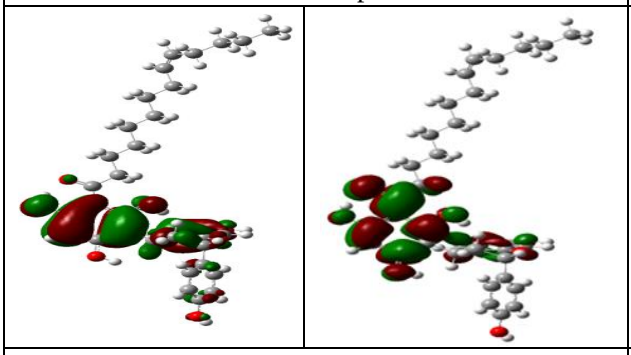	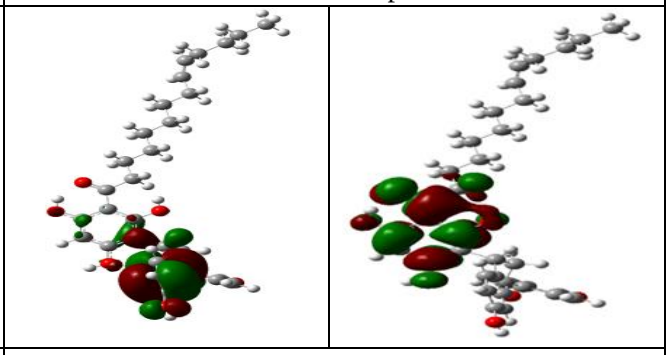
c-DBPO-s-r-ε-q-b-e-j	c-DBPO-s-w-u-p-e-a-k
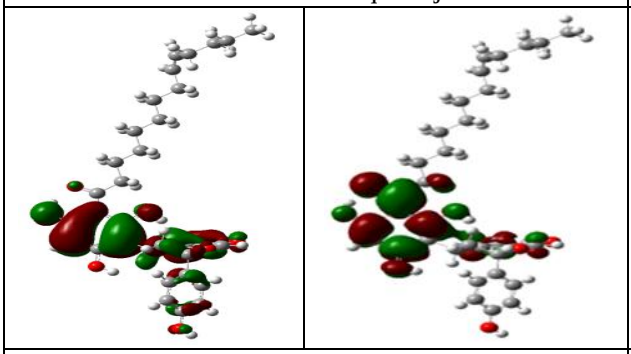	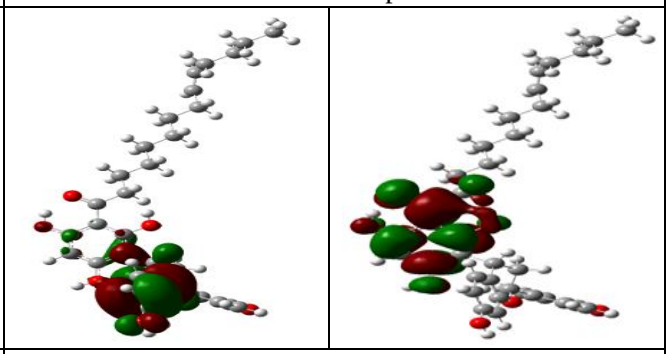
c-DBPO-s-r-ε-q-b-f-j	c-DBPO-s-w-u-p-b-e-k
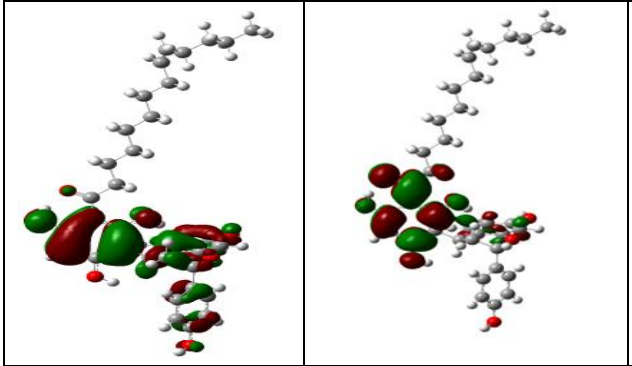	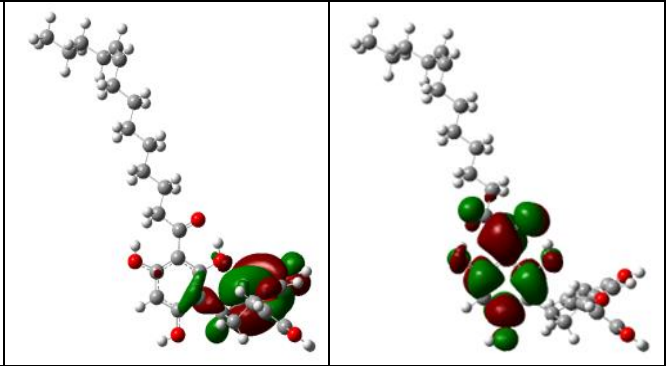
c-DBPO-s-r-ε-q-b-f-k	c-DBPO-d-w-u-q-a-e-j
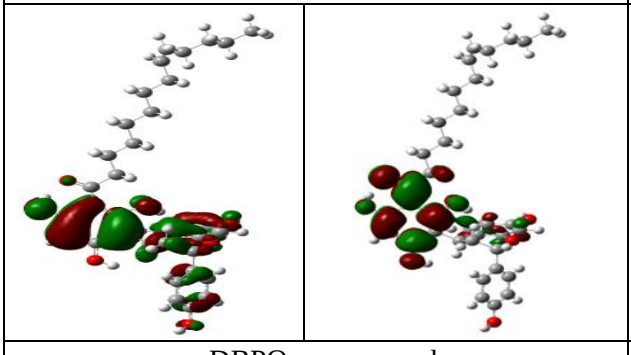	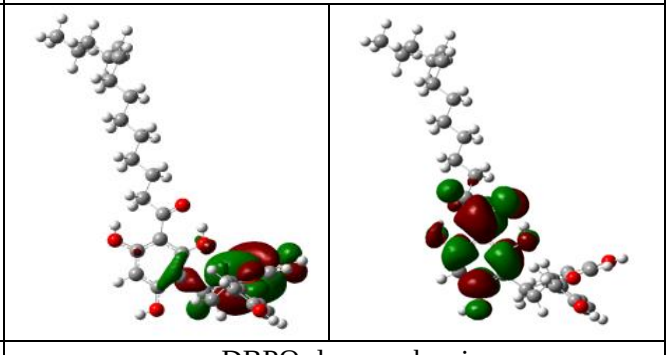
c-DBPO-s-r-ε-q-a-e-k	c-DBPO-d-w-u-q-b-e-j

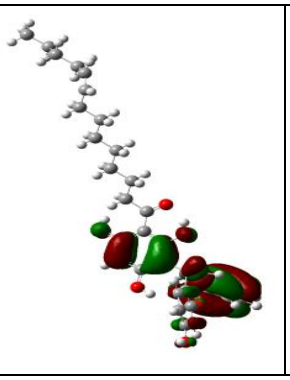 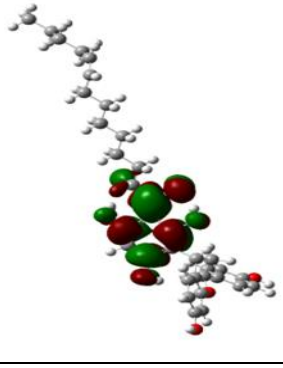	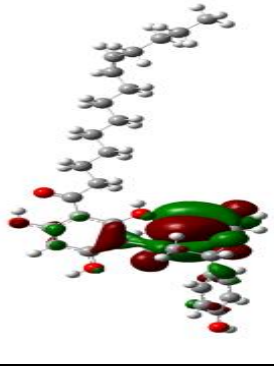 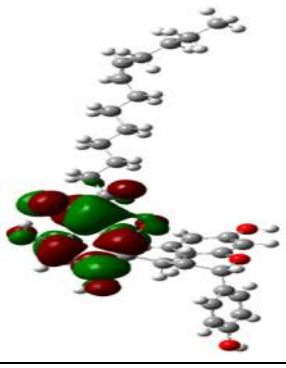
c-DBPO-d-r-η-u-p-a-f-j	c-DBPO-s-w-u-q-b-e-j
 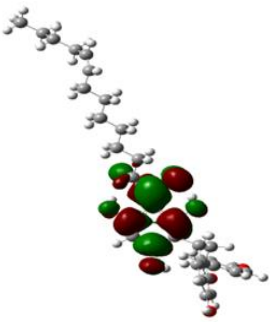	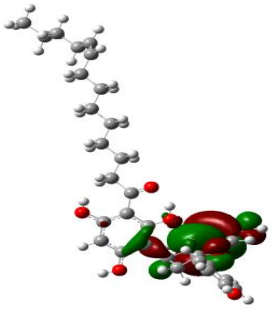 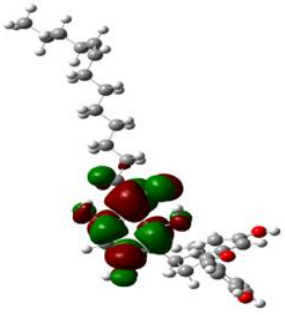
c-DBPO-d-r-η-u-p-a-f-k	c-DBPO-d-w-u-q-a-e-k
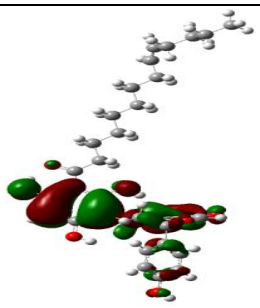 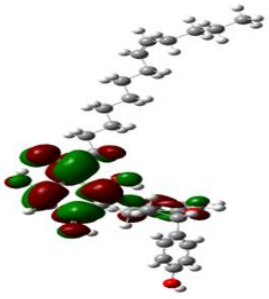	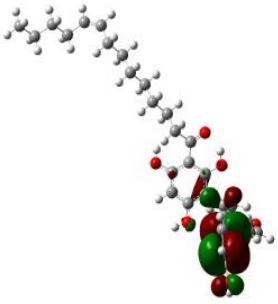 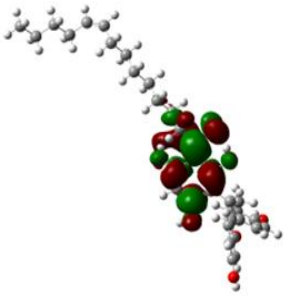
c-DBPO-s-r-ε-q-a-e-j	c-DBPO-d-w-u-p-b-e-k
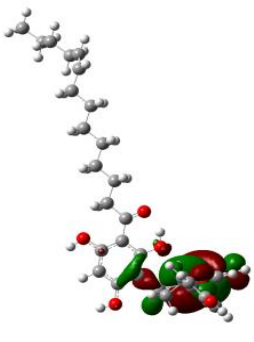 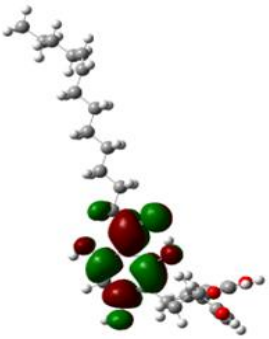	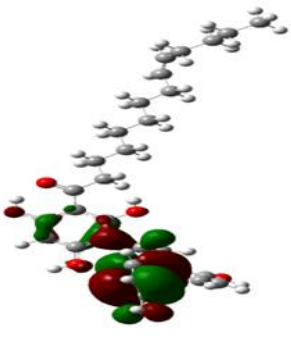 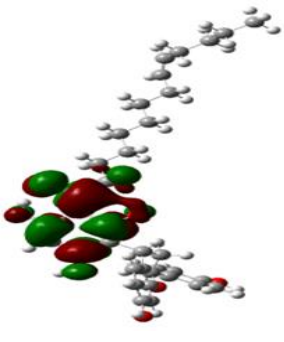
c-DBPO-d-w-q-a-e-j	c-DBPO-s-w-u-p-a-f-j
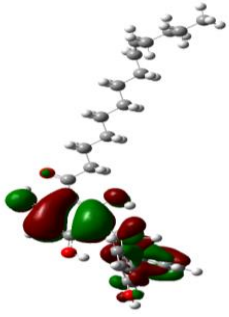 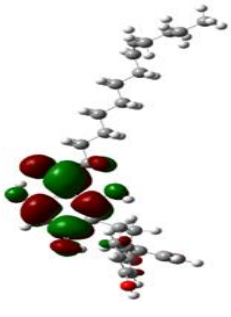	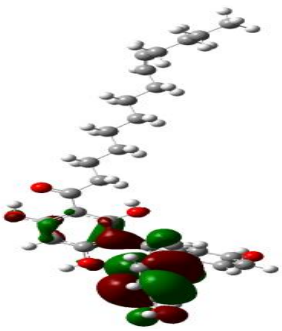 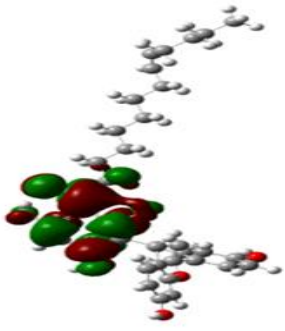
c-DBPO-s-r-η-p-e-a-k	c-DBPO-s-w-u-p-a-f-k

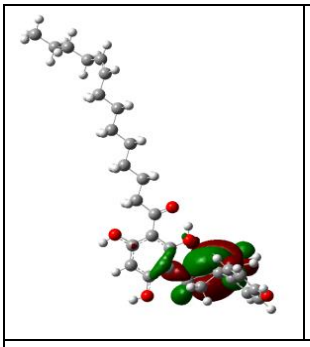	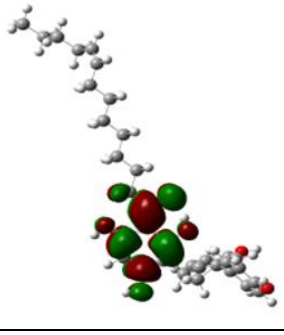
c-DBPO-d-w-q-a-e-k	
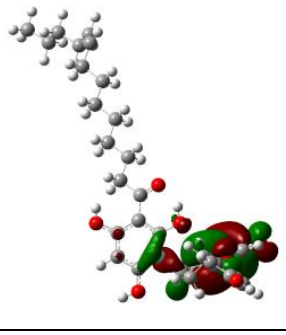	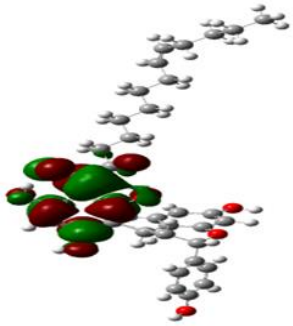
c-DBPO-s-w-u-q-b-e-k	
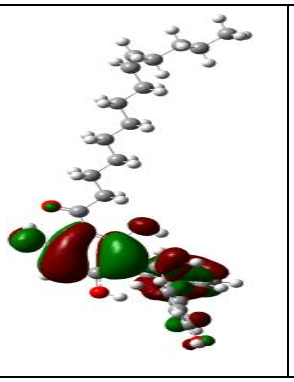	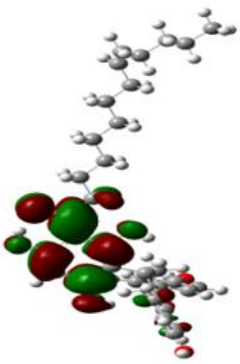
c-DBPO-s-r-η-p-a-e-j	
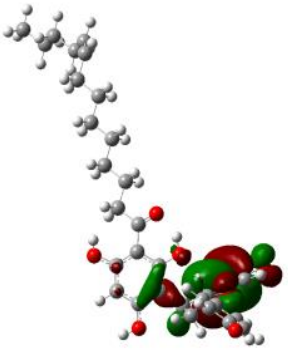	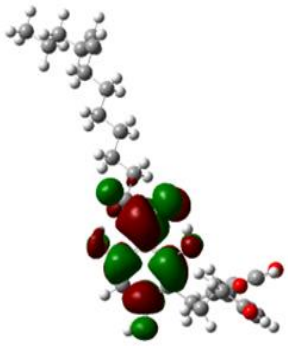
c-DBPO-d-w-u-q-a-f-j	
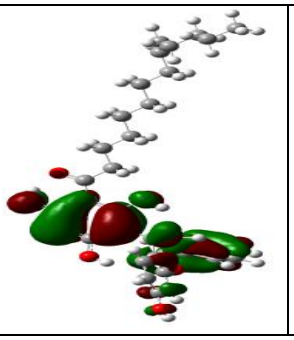	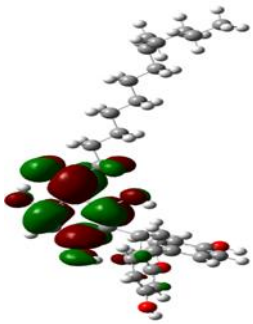
c-DBPO-s-r-η-p-b-e-j	
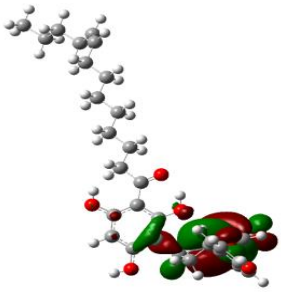	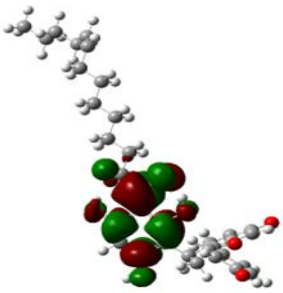
c-DBPO-d-w-u-q-b-f-j	
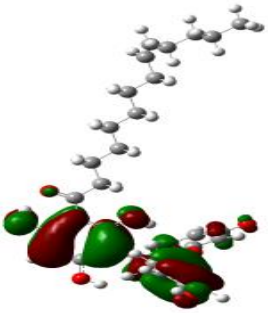	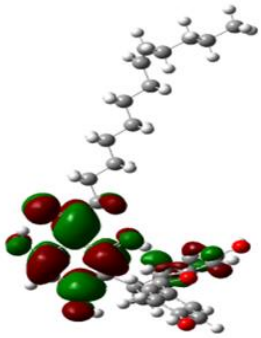
c-DBPO-s-r-ε-q-a-f-k	
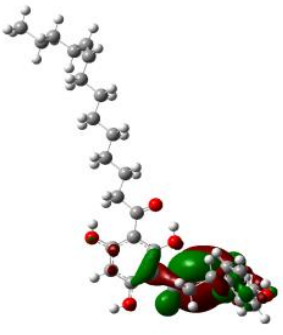	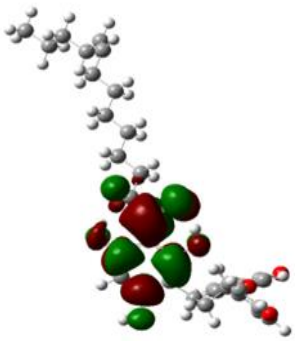
c-DBPO-d-w-u-q-a-f-k	
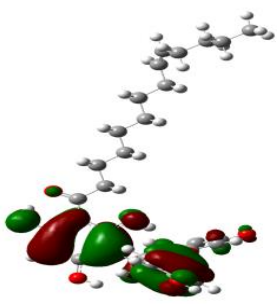	
c-DBPO-s-r-ε-q-a-f-j	
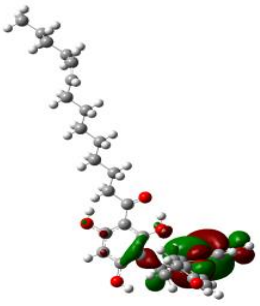	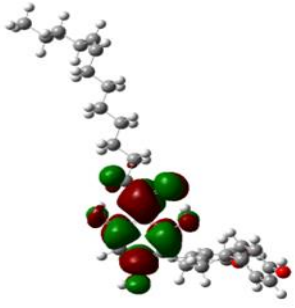
c-DBPO-d-w-u-q-b-f-k	

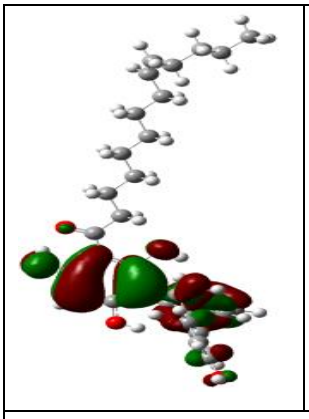 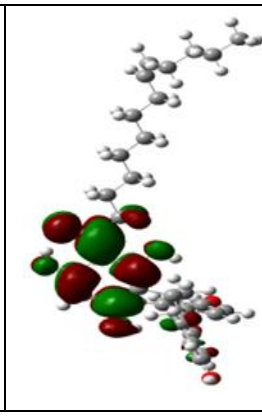	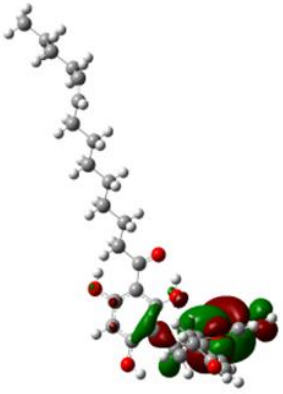 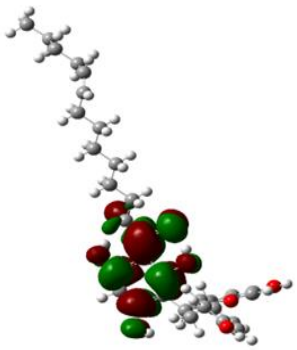
c-DBPO-s-r-η-p-a-f-k	c-DBPO-d-r-u-q-a-e-j
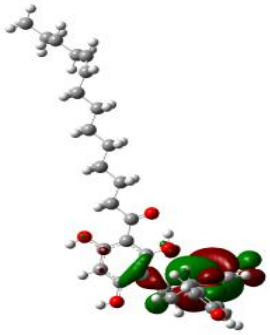 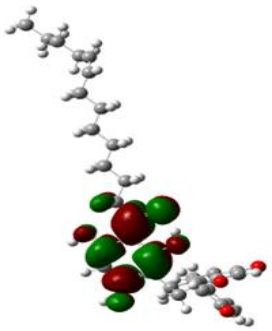	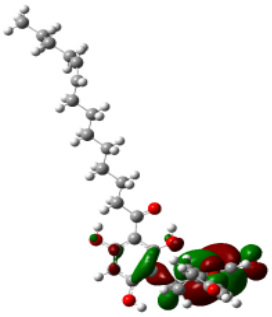 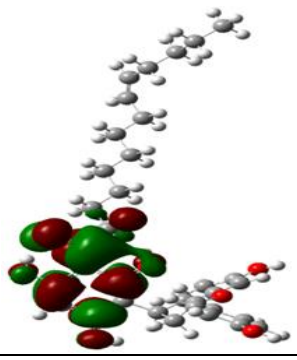
c-DBPO-d-w-q-a-f-j	c-DBPO-s-r-u-q-b-e-j
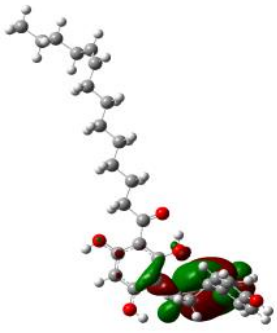 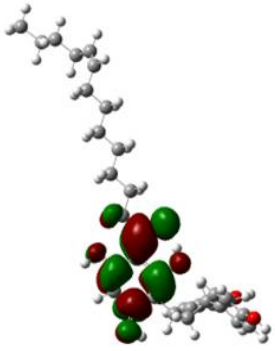	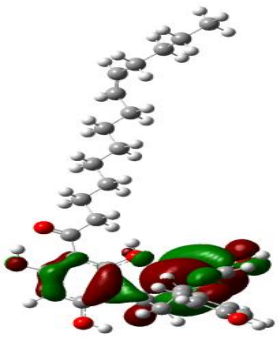 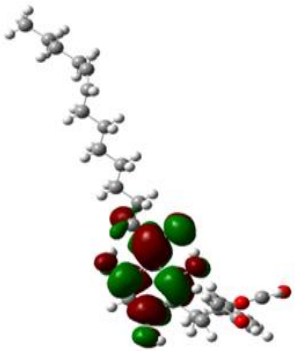
c-DBPO-d-r-q-a-e-j	c-DBPO-d-r-u-q-a-f-j
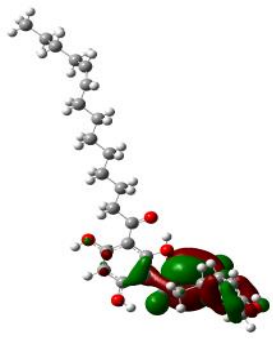 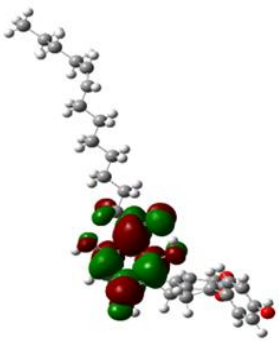	 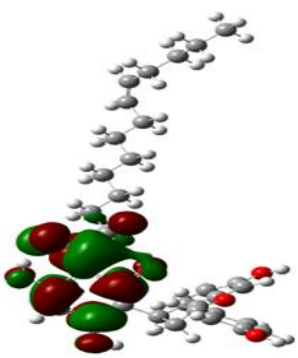
c-DBPO-d-r-q-b-e-k	c-DBPO-s-r-u-q-a-e-j

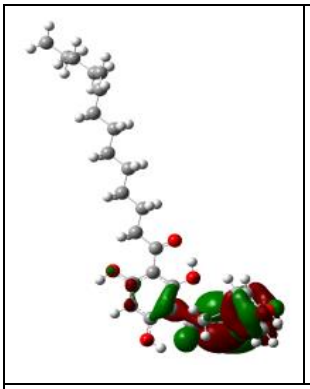 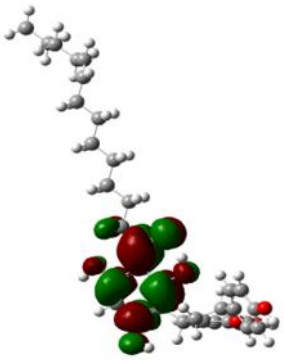	 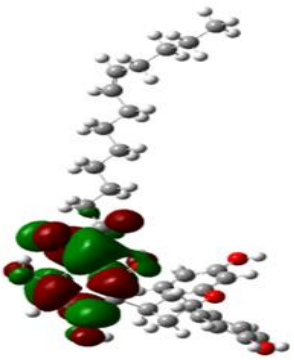
c-DBPO-d-r-q-b-e-j	c-DBPO-s-r-u-q-a-e-k
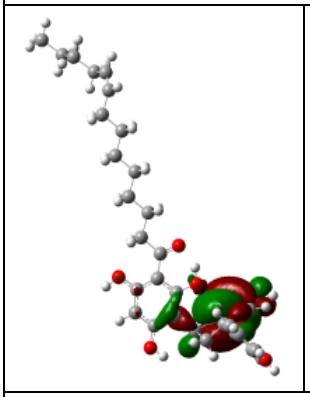 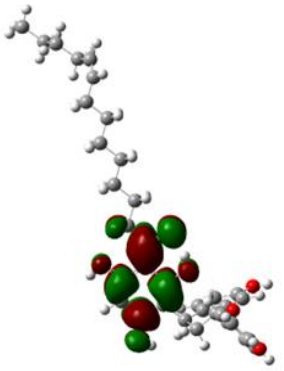	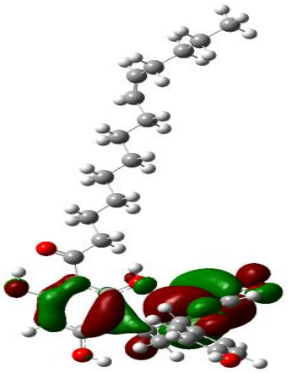 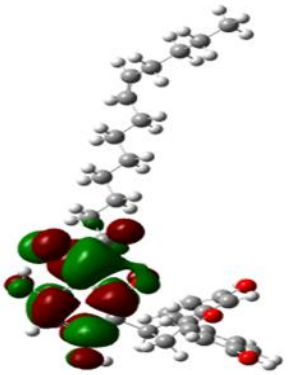
c-DBPO-d-r-q-a-e-k	c-DBPO-s-r-u-q-a-f-j
 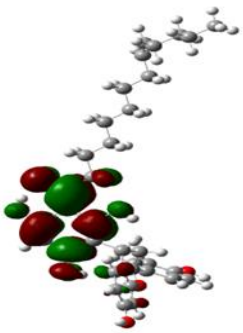	 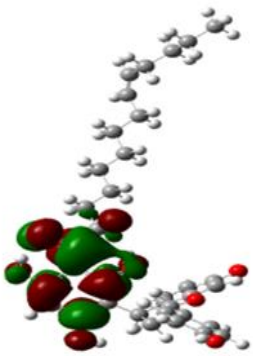
c-DBPO-s-r-η-p-a-f-j	c-DBPO-s-r-u-q-a-f-k
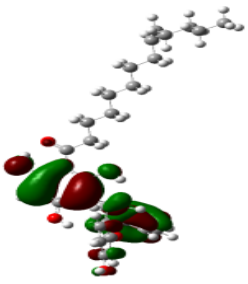 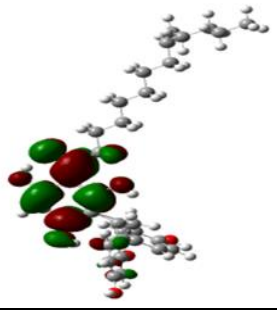	
c-DBPO-s-w-p-b-f-j	

Figure 6.4. Optimized conformers of the *cis*-DBPO isomer having different geometries of R and the same geometry of the ring system *in vacuo*.
HF/6-32G(d,p) results. Conformers are listed in order of increasing relative energy.

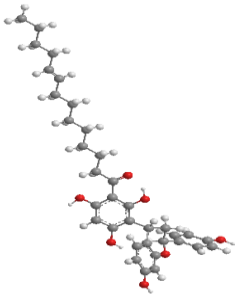
c-DBPO-d-r-η-p-a-e-j

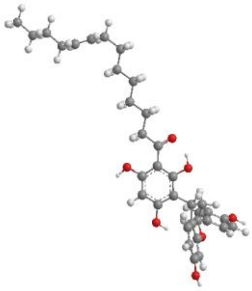
c-DBPO-d-r-η-p-a-e-j-8y

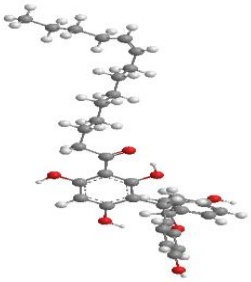
c-DBPO-d-r-η-p-a-e-j-3z

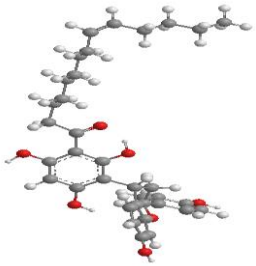
c-DBPO-d-r-η-p-a-e-j-3y

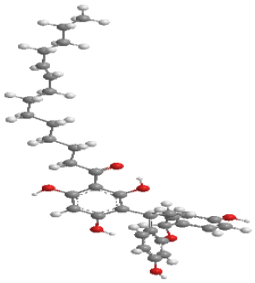
c-DBPO-d-r-η-p-a-e-j-7z

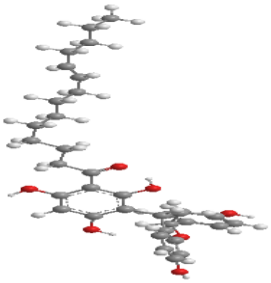
c-DBPO-d-r-η-p-a-e-j-5z


c-DBPO-d-r-η-p-a-e-j-5y

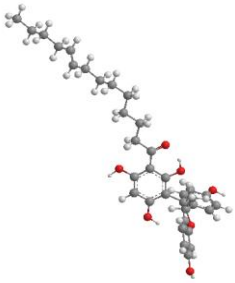
c-DBPO-d-r-η-p-a-e-j-6z

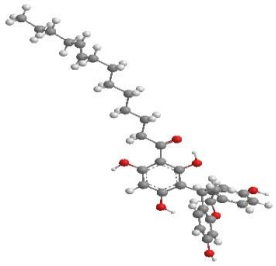
c-DBPO-d-r-η-p-a-e-j-8z

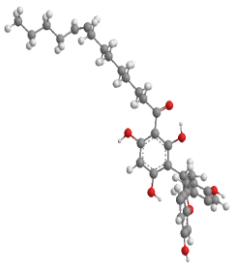
c-DBPO-d-r-η-p-a-e-j-2z

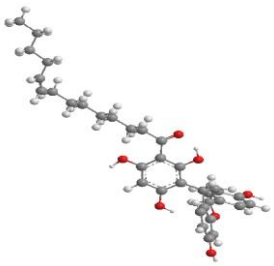
c-DBPO-d-r-η-p-a-e-j-2y

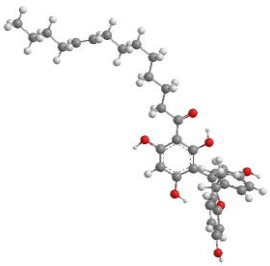
c-DBPO-d-r-η-p-a-e-j-6y

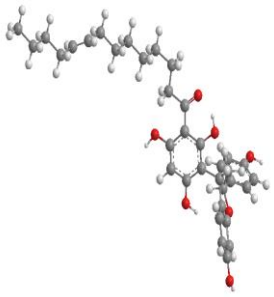
c-DBPO-d-r-η-p-a-e-j-4y

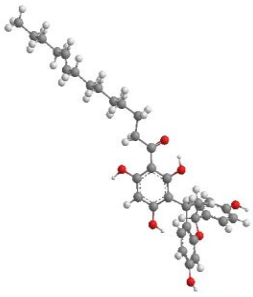
c-DBPO-d-r-η-p-a-e-j-4z

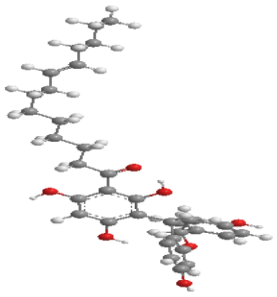
c-DBPO-d-r-η-p-a-e-j-7y

Table 6.6. Relative energies of the calculated conformers of *cis*-DBPO isomer having different geometries of R and the same geometry of the ring system *in vacuo*.
HF/6-31G(d,p) results from full optimisation. Conformers are listed in order of increasing relative energy in the HF results. The absolute energy of the lowest energy conformer is -1873.9714609 hartree.

Conformer	Relative energy (kcal/mol)	Conformer	Relative energy (kcal/mol)
c-DBPO-d-r-η-p-a-e-j	0.000	c-DBPO-d-r-η-p-a-e-j-8z	1.023
c-DBPO-d-r-η-p-a-e-j-8y	0.323	c-DBPO-d-r-η-p-a-e-j-2z	1.026
c-DBPO-d-r-η-p-a-e-j-3y	0.511	c-DBPO-d-r-η-p-a-e-j-2y	1.032
c-DBPO-d-r-η-p-a-e-j-3z	0.527	c-DBPO-d-r-η-p-a-e-j-6y	1.035
c-DBPO-d-r-η-p-a-e-j-7z	0.986	c-DBPO-d-r-η-p-a-e-j-4y	1.037
c-DBPO-d-r-η-p-a-e-j-5z	0.986	c-DBPO-d-r-η-p-a-e-j-4z	1.056
c-DBPO-d-r-η-p-a-e-j-5y	0.993	c-DBPO-d-r-η-p-a-e-j-7y	1.067
c-DBPO-d-r-η-p-a-e-j-6z	1.017		

Table 6.7. Relative energy corrected for ZPE (sum of electronic and zero-point energies, $\Delta E_{corrected}$, kcal/mol), ZPE correction to the electronic energy (ZPE_{corr}, kcal/mol), relative Gibbs free energies (sum of electronic and thermal free energy, $\Delta G_{corrected}$) and its thermal correction (G_{corr}), for the conformers of *cis*-DBPO having different geometries of R and the same geometry of the ring system *in vacuo*.
Results from HF/6-31G(d,p) frequency calculations. Conformers are listed in order of increasing relative energy in the HF results. HF/6-31G(d,p) results in vacuo. The corrected energies and corresponding corrections are from harmonic-approximation frequency calculations. The conformers are listed in order of increasing uncorrected relative energy. The absolute values for the lower energy conformer are -1873.211598 hartree ($\Delta E_{corrected}$) and -1873.292659 hartree ($\Delta G_{corrected}$).

Conformer	$\Delta E_{corrected}$	ZPE_{corr}	$\Delta G_{corrected}$	G_{corr}
c-DBPO-d-r-η-p-a-e-j	0.000	476.821	0.000	425.956
c-DBPO-d-r-η-p-a-e-j-8y	0.404	476.902	0.594	426.227
c-DBPO-d-r-η-p-a-e-j-3y	0.689	476.999	0.801	426.246
c-DBPO-d-r-η-p-a-e-j-3z	0.703	476.997	0.797	426.225
c-DBPO-d-r-η-p-a-e-j-7z	1.116	476.951	1.096	426.065
c-DBPO-d-r-η-p-a-e-j-5z	1.131	476.965	1.082	426.052
c-DBPO-d-r-η-p-a-e-j-5y	1.135	476.963	1.082	426.045
c-DBPO-d-r-η-p-a-e-j-6z	1.157	476.961	1.098	426.037
c-DBPO-d-r-η-p-a-e-j-8z	1.181	476.979	1.144	426.077
c-DBPO-d-r-η-p-a-e-j-2z	1.402	477.196	1.198	426.128
c-DBPO-d-r-η-p-a-e-j-2y	1.407	477.195	1.187	426.109
c-DBPO-d-r-η-p-a-e-j-6y	1.166	476.951	1.113	426.033
c-DBPO-d-r-η-p-a-e-j-4y	1.172	476.955	1.104	426.023
c-DBPO-d-r-η-p-a-e-j-4z	1.187	476.951	1.115	426.015
c-DBPO-d-r-η-p-a-e-j-7y	1.186	476.939	1.111	425.999

Table 6.8. Parameters of the first IHB and the distance between the H atom and the closest C atom in the acceptor aromatic ring for the O–H···η interactions of the selected calculated conformers of *cis*-DBPO having different geometries of R and the same geometry of the ring system.
HF/6-31G(d,p), DFT/B3LYP/B3LYP/6-31+G(d,p) and MP2/ 6-31G(d,p) results *in vacuo* denoted by the letter A, B and C respectively in the column headings 'Methods''. The first IHB is H15···O14. The results are from full optimisation calculations. Conformers are listed in order of increasing relative energy in the HF results.

Conformer	Parameters of the IHB		
	OH···O (Å)	O···O (Å)	OHO (°)
c-DBPO-d-r-η-p-a-e-j	1.652	2.508	146.4
c-DBPO-d-r-η-p-a-e-j-8y	1.644	2.506	147.2
c-DBPO-d-r-η-p-a-e-j-3y	1.649	2.509	147.0
c-DBPO-d-r-η-p-a-e-j-3z	1.647	2.507	147.0
c-DBPO-d-r-η-p-a-e-j-7z	1.644	2.506	147.2
c-DBPO-d-r-η-p-a-e-j-5z	1.645	2.507	147.1
c-DBPO-d-r-η-p-a-e-j-5y	1.643	2.505	147.2
c-DBPO-d-r-η-p-a-e-j-6z	1.645	2.506	147.2
c-DBPO-d-r-η-p-a-e-j-8z	1.644	2.506	147.2
c-DBPO-d-r-η-p-a-e-j-2z	1.638	2.502	147.4
c-DBPO-d-r-η-p-a-e-j-2y	1.638	2.502	147.4
c-DBPO-d-r-η-p-a-e-j-6y	1.652	2.508	146.4
c-DBPO-d-r-η-p-a-e-j-4y	1.645	2.506	147.1
c-DBPO-d-r-η-p-a-e-j-4z	1.644	2.505	147.2
c-DBPO-d-r-η-p-a-e-j-7y	1.645	2.506	147.2

Table 6.9. The distance between the H atom and the closest C atom in the acceptor aromatic ring for the O–H···π interactions of the selected calculated conformers of *cis*-DBPO having different geometries of R and the same geometry of the ring system *in vacuo*.
HF/6-31G(d,p) results are from full optimisation. Conformers are listed in order of increasing relative energy in the HF results.

Conformer	H16···C23 distance considered (Å)	Conformer	H16···C23 distance considered (Å)
c-DBPO-d-r-η-p-a-e-j	2.008	c-DBPO-d-r-η-p-a-e-j-8z	2.008
c-DBPO-d-r-η-p-a-e-j-8y	2.008	c-DBPO-d-r-η-p-a-e-j-2z	2.007
c-DBPO-d-r-η-p-a-e-j-3y	2.011	c-DBPO-d-r-η-p-a-e-j-2y	2.011
c-DBPO-d-r-η-p-a-e-j-3z	2.007	c-DBPO-d-r-η-p-a-e-j-6y	2.008
c-DBPO-d-r-η-p-a-e-j-7z	2.008	c-DBPO-d-r-η-p-a-e-j-4y	2.008
c-DBPO-d-r-η-p-a-e-j-5z	2.008	c-DBPO-d-r-η-p-a-e-j-4z	2.008
c-DBPO-d-r-η-p-a-e-j-5y	2.008	c-DBPO-d-r-η-p-a-e-j-7y	2.008
c-DBPO-d-r-η-p-a-e-j-6z	2.008		

Table 6.10. Vibrational frequency of the O–H bonds in the selected conformers of *cis*-DBPO having different geometries of R and the same geometry of the ring system *in vacuo*.
HF/6-31G(d,p) results. The frequency values have been scaled by 0.8992, as recommended for HF/6-31G(d,p) calculations [184]. Conformers are listed in order of increasing relative energy in the HF results.

Conformer	Vibrational frequencies (cm^{-1})				
	O8–H15	O10–H16	O12–H17	O44–H50	O51–H52
c-DBPO-d-r-η-p-a-e-j	3397.27	3704.30	3761.98	3769.56	3773.49
c-DBPO-d-r-η-p-a-e-j-8y	3396.62	3704.43	3762.01	3769.59	3773.51
c-DBPO-d-r-η-p-a-e-j-3y	3403.93	3704.04	3761.87	3769.55	3773.51
c-DBPO-d-r-η-p-a-e-j-3z	3404.14	3703.94	3761.83	3769.55	3773.49
c-DBPO-d-r-η-p-a-e-j-7z	3397.49	3704.25	3761.95	3769.57	3773.51
c-DBPO-d-r-η-p-a-e-j-5z	3397.38	3704.24	3761.96	3769.55	3773.51
c-DBPO-d-r-η-p-a-e-j-5y	3397.39	3704.25	3761.96	3769.56	3773.50
c-DBPO-d-r-η-p-a-e-j-6z	3397.01	3704.36	3761.98	3769.57	3773.51
c-DBPO-d-r-η-p-a-e-j-8z	3396.98	3704.37	3761.99	3769.57	3773.52
c-DBPO-d-r-η-p-a-e-j-2z	3375.58	3703.58	3763.08	3769.55	3773.51
c-DBPO-d-r-η-p-a-e-j-2y	3374.95	3703.52	3763.05	3769.55	3773.52
c-DBPO-d-r-η-p-a-e-j-6y	3397.09	3704.30	3761.97	3769.57	3773.51
c-DBPO-d-r-η-p-a-e-j-4y	3396.97	3704.30	3761.82	3769.58	3773.51
c-DBPO-d-r-η-p-a-e-j-4z	3397.10	3704.30	3761.92	3769.57	3773.52
c-DBPO-d-r-η-p-a-e-j-7y	3397.48	3704.26	3761.97	3769.56	3773.51

Table 6.11. Dipole moments of the calculated conformers of *cis*-DBPO having different geometries of R and the same geometry of the ring system *in vacuo*.
HF/6-31G(d,p) results are from full optimisation. Conformers are listed in order of increasing relative energy in the HF results.

Conformer	Dipole moments (Debye)	Conformer	Dipole moments (Debye)
c-DBPO-d-r-η-p-a-e-j	2.460	c-DBPO-d-r-η-p-a-e-j-8z	2.118
c-DBPO-d-r-η-p-a-e-j-8y	2.316	c-DBPO-d-r-η-p-a-e-j-2z	2.534
c-DBPO-d-r-η-p-a-e-j-3y	2.558	c-DBPO-d-r-η-p-a-e-j-2y	2.300
c-DBPO-d-r-η-p-a-e-j-3z	2.607	c-DBPO-d-r-η-p-a-e-j-6y	2.136
c-DBPO-d-r-η-p-a-e-j-7z	2.419	c-DBPO-d-r-η-p-a-e-j-4y	2.120
c-DBPO-d-r-η-p-a-e-j-5z	2.435	c-DBPO-d-r-η-p-a-e-j-4z	2.097
c-DBPO-d-r-η-p-a-e-j-5y	2.489	c-DBPO-d-r-η-p-a-e-j-7y	2.419
c-DBPO-d-r-η-p-a-e-j-6z	2.306		

Table 6.12. HOMO-LUMO energy gap of the calculated conformers of *cis*-DBPO having different geometries of R and the same geometry of the ring system *in vacuo.*
HF/6-31G(d,p) results are from full optimisation calculations. Conformers are listed in order of increasing relative energy in the HF results.

Conformer	HOMO-LUMO energy gap (kcal/mol)	Conformer	HOMO-LUMO energy gap (kcal/mol)
c-DBPO-d-r-η-p-a-e-j	257.410	c-DBPO-d-r-η-p-a-e-j-8z	257.448
c-DBPO-d-r-η-p-a-e-j-8y	257.511	c-DBPO-d-r-η-p-a-e-j-2z	255.359
c-DBPO-d-r-η-p-a-e-j-3y	256.890	c-DBPO-d-r-η-p-a-e-j-2y	255.396
c-DBPO-d-r-η-p-a-e-j-3z	256.934	c-DBPO-d-r-η-p-a-e-j-6y	257.429
c-DBPO-d-r-η-p-a-e-j-7z	257.367	c-DBPO-d-r-η-p-a-e-j-4y	257.448
c-DBPO-d-r-η-p-a-e-j-5z	257.367	c-DBPO-d-r-η-p-a-e-j-4z	257.410
c-DBPO-d-r-η-p-a-e-j-5y	257.354	c-DBPO-d-r-η-p-a-e-j-7y	257.379
c-DBPO-d-r-η-p-a-e-j-6z	257.442		

Table 6.13. Relative energies of the calculated conformers of *cis*-DBPO isomer having different geometries of R and the same geometry of the ring system *in vacuo.*
HF/6-31G(d,p), DFT/B3LYP/6-31+G(d,p) and MP2/6-31G(d,p) results *in vacuo*. The results are from full optimisation calculations. The conformers are listed in order of increasing relative energies in the HF results *in vacuo*. The absolute energies of the lowest-energy conformer is -1873.9714609, -1885.7347812 and -1879.9695879 hartree in the HF, DFT and MP2 results respectively.

Conformer	Relative energy (kcal/mol)		
	HF	DFT	MP2
c-DBPO-d-r-η-p-a-e-j	0.000	0.000	0.898
c-DBPO-d-r-η-p-a-e-j-8y	0.323	0.489	0.000
c-DBPO-d-r-η-p-a-e-j-3y	0.511	0.972	0.575
c-DBPO-d-r-η-p-a-e-j-3z	0.527	0.593	0.581
c-DBPO-d-r-η-p-a-e-j-7z	0.986	0.901	1.215
c-DBPO-d-r-η-p-a-e-j-5z	0.986	0.887	1.279
c-DBPO-d-r-η-p-a-e-j-5y	0.993	0.916	1.298
c-DBPO-d-r-η-p-a-e-j-6z	1.017	0.930	1.336
c-DBPO-d-r-η-p-a-e-j-8z	1.023	0.991	0.907
c-DBPO-d-r-η-p-a-e-j-2z	1.026	0.537	0.916
c-DBPO-d-r-η-p-a-e-j-2y	1.032	0.540	0.931
c-DBPO-d-r-η-p-a-e-j-6y	1.035	0.958	1.366
c-DBPO-d-r-η-p-a-e-j-4y	1.037	0.958	1.248
c-DBPO-d-r-η-p-a-e-j-4z	1.056	1.008	1.211
c-DBPO-d-r-η-p-a-e-j-7y	1.067	0.976	1.414

Table 6.14. Parameters of the first IHB of the selected calculated conformers of *cis*-DBPO having different geometries of R and the same geometry of the ring system.
HF/6-31G(d,p), DFT/B3LYP/6-31+G(d,p) and MP2/ 6-31G(d,p) results *in vacuo*. The first IHB is H15···O14. The results *in vacuo* are from full optimisation calculations. Conformers are listed in order of increasing relative energy in the HF results.

Conformer	Methods	Parameters of the IHB		
		OH···O (Å)	O···O (Å)	OHO (°)
c-DBPO-d-r-η-p-a-e-j	HF	1.652	2.508	146.4
	DFT	1.529	2.466	151.8
	MP2	1.583	2.505	151.4
c-DBPO-d-r-η-p-a-e-j-8y	HF	1.644	2.506	147.2
	DFT	1.530	2.467	151.7
	MP2	1.583	2.505	151.5
c-DBPO-d-r-η-p-a-e-j-3y	HF	1.649	2.509	147.0
	DFT	1.530	2.467	151.8
	MP2	1.585	2.505	151.3
c-DBPO-d-r-η-p-a-e-j-3z	HF	1.647	2.507	147.0
	DFT	1.531	2.467	151.7
	MP2	1.585	2.505	151.3
c-DBPO-d-r-η-p-a-e-j-7z	HF	1.644	2.506	147.2
	DFT	1.530	2.467	151.7
	MP2	1.584	2.505	151.4
c-DBPO-d-r-η-p-a-e-j-5z	HF	1.645	2.507	147.1
	DFT	1.529	2.466	151.8
	MP2	1.583	2.505	151.5
c-DBPO-d-r-η-p-a-e-j-5y	HF	1.643	2.505	147.2
	DFT	1.528	2.466	151.8
	MP2	1.583	2.505	151.5
c-DBPO-d-r-η-p-a-e-j-6z	HF	1.645	2.506	147.2
	DFT	1.529	2.466	151.8
	MP2	1.583	2.505	151.5
c-DBPO-d-r-η-p-a-e-j-8z	HF	1.644	2.506	147.2
	DFT	1.530	2.467	151.8
	MP2	1.583	2.505	151.5
c-DBPO-d-r-η-p-a-e-j-2z	HF	1.638	2.502	147.4
	DFT	1.516	2.458	152.1
	MP2	1.574	2.498	151.8
c-DBPO-d-r-η-p-a-e-j-2y	HF	1.638	2.502	147.4
	DFT	1.515	2.458	152.1
	MP2	1.574	2.499	151.8
c-DBPO-d-r-η-p-a-e-j-6y	HF	1.652	2.508	146.4
	DFT	1.530	2.467	151.7
	MP2	1.583	2.505	151.4
c-DBPO-d-r-η-p-a-e-j-4y	HF	1.645	2.506	147.1
	DFT	1.528	2.465	151.9
	MP2	1.583	2.504	151.5
c-DBPO-d-r-η-p-a-e-j-4z	HF	1.644	2.505	147.2

	DFT	1.530	2.467	151.8
	MP2	1.583	2.505	151.4
c-DBPO-d-r-η-p-a-e-j-7y	HF	1.645	2.506	147.2
	DFT	1.530	2.467	151.8
	MP2	1.583	2.505	151.5

Table 6.15. The distance between the H atom and the closest C atom in the acceptor aromatic ring for the O–H···π interactions of the selected calculated conformers of *cis*-DBPO having different geometries of R and the same geometry of the ring system *in vacuo*.
HF/6-31G(d,p), DFT/B3LYP/B3LYP/6-31+G(d,p) and MP2/ 6-31G(d,p) results. The results *in vacuo* are from full optimisation calculations. Conformers are listed in order of increasing relative energy in the HF results.

Conformer	H16···C23 distance considered (Å)		
	HF	DFT	MP2
c-DBPO-d-r-η-p-a-e-j	2.128	2.053	2.008
c-DBPO-d-r-η-p-a-e-j-8y	2.127	2.054	2.008
c-DBPO-d-r-η-p-a-e-j-3y	2.127	2.057	2.011
c-DBPO-d-r-η-p-a-e-j-3z	2.128	2.057	2.007
c-DBPO-d-r-η-p-a-e-j-7z	2.126	2.051	2.008
c-DBPO-d-r-η-p-a-e-j-5z	2.127	2.054	2.008
c-DBPO-d-r-η-p-a-e-j-5y	2.127	2.057	2.008
c-DBPO-d-r-η-p-a-e-j-6z	2.129	2.057	2.008
c-DBPO-d-r-η-p-a-e-j-8z	2.127	2.057	2.008
c-DBPO-d-r-η-p-a-e-j-2z	2.125	2.052	2.007
c-DBPO-d-r-η-p-a-e-j-2y	2.126	2.055	2.011
c-DBPO-d-r-η-p-a-e-j-6y	2.128	2.058	2.008
c-DBPO-d-r-η-p-a-e-j-4y	2.122	2.057	2.008
c-DBPO-d-r-η-p-a-e-j-4z	2.125	2.054	2.008
c-DBPO-d-r-η-p-a-e-j-7y	2.126	2.053	2.008

Table 6.16. Dipole moments of the calculated conformers of *cis*-DBPO having different geometries of R and the same geometry of the ring system *in vacuo*.
HF/6-31G(d,p), DFT/B3LYP/B3LYP/6-31+G(d,p) and MP2/6-31G(d,p) results. The results are from full optimisation calculations. Conformers are listed in order of increasing relative energy in the HF results.

Conformer	Dipole moments (Debye)		
	HF	DFT	MP2
c-DBPO-d-r-η-p-a-e-j	2.460	2.581	2.423
c-DBPO-d-r-η-p-a-e-j-8y	2.316	2.378	2.300
c-DBPO-d-r-η-p-a-e-j-3y	2.558	2.223	2.564
c-DBPO-d-r-η-p-a-e-j-3z	2.607	2.663	2.606
c-DBPO-d-r-η-p-a-e-j-7z	2.419	2.484	2.421
c-DBPO-d-r-η-p-a-e-j-5z	2.435	2.408	2.424
c-DBPO-d-r-η-p-a-e-j-5y	2.489	2.457	2.481
c-DBPO-d-r-η-p-a-e-j-6z	2.306	2.134	2.311
c-DBPO-d-r-η-p-a-e-j-8z	2.118	1.976	2.127
c-DBPO-d-r-η-p-a-e-j-2z	2.534	2.546	2.605
c-DBPO-d-r-η-p-a-e-j-2y	2.300	2.203	2.354
c-DBPO-d-r-η-p-a-e-j-6y	2.136	2.029	2.128
c-DBPO-d-r-η-p-a-e-j-4y	2.120	1.958	2.120
c-DBPO-d-r-η-p-a-e-j-4z	2.097	1.946	2.125
c-DBPO-d-r-η-p-a-e-j-7y	2.419	2.440	2.476

Table 6.17. HOMO-LUMO energy gap of the calculated conformers of *cis*-DBPO having different geometries of R and the same geometry of the ring system *in vacuo*.
HF/6-31G(d,p), DFT/B3LYP/B3LYP/6-31+G(d,p) and MP2/6-31G(d,p) results. The results are from full optimisation calculations. Conformers are listed in order of increasing relative energy in the HF results.

Conformer	HOMO-LUMO energy gap (kcal/mol)		
	HF	DFT	MP2
c-DBPO-d-r-η-p-a-e-j	257.410	105.133	248.996
c-DBPO-d-r-η-p-a-e-j-8y	257.511	105.246	249.083
c-DBPO-d-r-η-p-a-e-j-3y	256.890	105.214	248.356
c-DBPO-d-r-η-p-a-e-j-3z	256.934	104.731	248.274
c-DBPO-d-r-η-p-a-e-j-7z	257.367	105.139	248.908
c-DBPO-d-r-η-p-a-e-j-5z	257.367	105.139	248.920
c-DBPO-d-r-η-p-a-e-j-5y	257.354	105.007	248.920
c-DBPO-d-r-η-p-a-e-j-6z	257.442	105.158	249.021
c-DBPO-d-r-η-p-a-e-j-8z	257.448	105.196	249.071
c-DBPO-d-r-η-p-a-e-j-2z	255.359	103.401	247.565
c-DBPO-d-r-η-p-a-e-j-2y	255.396	103.263	247.665
c-DBPO-d-r-η-p-a-e-j-6y	257.429	105.145	249.027
c-DBPO-d-r-η-p-a-e-j-4y	257.448	105.214	249.071
c-DBPO-d-r-η-p-a-e-j-4z	257.410	105.202	249.021
c-DBPO-d-r-η-p-a-e-j-7y	257.379	105.227	248.939

Table 6.18. Relative energies of the calculated conformers of *cis*-DBPO having different geometries of R and the same geometry of the ring system *in vacuo* and in three solvents chloroform, acetonitrile and water (respectively denoted as vac, chlrf, actn, aq in the column headings.

HF/6-31G(d,p) results from full optimisation calculations. The conformers are listed in order of increasing relative energies in the HF results *in vacuo*. In the column headings, the media are denoted as vac, chlrf, actn and aq, respectively for vacuum, chloroform acetonitrile and water. The absolute energies of the lowest-energy conformer (hartree) are -1873.9714609, -1873.9904362, -1873.9953414 and -1873.9957572 in vacuo, chloroform, acetonitrile and water respectively.

Conformer	Relative energy (kcal/mol)			
	vac	chlrf	actn	aq
c-DBPO-d-r-η-p-a-e-j	0.000	0.000	0.000	0.000
c-DBPO-d-r-η-p-a-e-j-8y	0.323	0.378	0.392	0.393
c-DBPO-d-r-η-p-a-e-j-3y	0.511	0.734	0.793	0.798
c-DBPO-d-r-η-p-a-e-j-3z	0.527	0.763	0.821	0.826
c-DBPO-d-r-η-p-a-e-j-7z	0.986	0.989	0.995	0.996
c-DBPO-d-r-η-p-a-e-j-5z	0.987	1.013	1.021	1.022
c-DBPO-d-r-η-p-a-e-j-5y	0.993	1.044	1.059	1.060
c-DBPO-d-r-η-p-a-e-j-6z	1.017	1.038	1.044	1.045
c-DBPO-d-r-η-p-a-e-j-8z	1.023	1.055	1.064	1.065
c-DBPO-d-r-η-p-a-e-j-2z	1.026	0.950	0.925	0.923
c-DBPO-d-r-η-p-a-e-j-2y	1.033	0.977	0.955	0.953
c-DBPO-d-r-η-p-a-e-j-6y	1.035	1.035	1.034	1.033
c-DBPO-d-r-η-p-a-e-j-4y	1.037	1.065	1.069	1.069
c-DBPO-d-r-η-p-a-e-j-4z	1.056	1.076	1.080	1.081
c-DBPO-d-r-η-p-a-e-j-7y	1.068	1.091	1.100	1.101

Table 6.19. The solvation free energy (ΔG_{solv}) and its electrostatic component (G_{el}) of the calculated conformers of *cis*-DBPO having different geometries of R and the same geometry of the ring system *in vacuo* and in three solvents chloroform, acetonitrile and water (respectively denoted as vac, chlrf, actn, aq in the column headings.

HF/6-31G(d,p) results. The results *in vacuo* and in solution are from full optimisation calculations. Conformers are listed in order of increasing relative energy in the HF results *in vacuo*.

Conformer	(ΔG_{solv}) (kcal/mol)			(G_{el}) (kcal/mol)		
	chlrf	actn	aq	chlrf	actn	aq
c-DBPO-d-r-η-p-a-e-j	-2.22	6.21	-15.71	-8.21	-11.73	-27.43
c-DBPO-d-r-η-p-a-e-j-8y	-1.34	6.92	-15.49	-8.16	-11.68	-27.64
c-DBPO-d-r-η-p-a-e-j-3y	-1.59	6.78	-15.71	-8.04	-11.51	-27.49
c-DBPO-d-r-η-p-a-e-j-3z	-1.54	6.80	-15.63	-8.03	-11.51	-27.43
c-DBPO-d-r-η-p-a-e-j-7z	-1.71	6.62	-15.95	-8.17	-11.69	-27.74
c-DBPO-d-r-η-p-a-e-j-5z	-1.87	6.49	-16.14	-8.18	-11.70	-27.78
c-DBPO-d-r-η-p-a-e-j-5y	-1.94	6.43	-16.17	-8.18	-11.71	-27.75
c-DBPO-d-r-η-p-a-e-j-6z	-1.89	6.46	-16.11	-8.20	-11.73	-27.74
c-DBPO-d-r-η-p-a-e-j-8z	-1.92	6.43	-15.98	-8.16	-11.68	-27.64
c-DBPO-d-r-η-p-a-e-j-2z	-1.70	6.63	-15.79	-8.33	-11.89	-27.85
c-DBPO-d-r-η-p-a-e-j-2y	-1.64	6.73	-14.82	-8.34	-11.92	-26.25

c-DBPO-d-r-η-p-a-e-j-6y	-1.98	6.38	-16.16	-8.20	-11.75	-27.72
c-DBPO-d-r-η-p-a-e-j-4y	-1.85	6.51	-16.04	-8.19	-11.71	-27.74
c-DBPO-d-r-η-p-a-e-j-4z	-1.69	6.62	-15.85	-1.69	-11.72	-27.68
c-DBPO-d-r-η-p-a-e-j-7y	-2.01	6.37	-16.25	-8.19	-11.72	-27.78

Table 6.20. Parameters of the H17···O14 IHB of the calculated conformers of *cis*-DBPO having different geometries of R and the same geometry of the ring system. The IHB length refers to the H···O distance for the H17···O14, the donor-acceptor distance is O···O and the hydrogen bond angle is OĤO. HF/6-31G(d,p) results *in vacuo* and in three solvents chloroform, acetonitrile and water (respectively denoted as vac, chlrf, actn, aq in the column of media headings). The results *in vacuo* and in solution are from full optimisation calculations. Conformers are listed in order of increasing relative energy in the HF results *in vacuo*.

Conformer	Media	Parameters of the H17···O14 IHB		
		O···H (Å)	O···O (Å)	OĤO (°)
c-DBPO-d-r-η-p-a-e-j	vac	1.652	2.508	146.4
	chlrf	1.646	2.506	146.9
	actn	1.644	2.506	147.1
	aq	1.644	2.506	147.2
c-DBPO-d-r-η-p-a-e-j-8y	vac	1.644	2.506	147.2
	chlrf	1.646	2.506	146.9
	actn	1.644	2.506	147.1
	aq	1.644	2.506	147.2
	aq	1.645	2.506	147.2
c-DBPO-d-r-η-p-a-e-j-3y	vac	1.649	2.509	147.0
	chlrf	1.650	2.509	146.8
	actn	1.649	2.509	147.0
	aq	1.649	2.509	147.0
c-DBPO-d-r-η-p-a-e-j-3z	vac	1.647	2.507	147.0
	chlrf	1.649	2.508	146.8
	actn	1.647	2.507	147.0
	aq	1.647	2.507	147.0
c-DBPO-d-r-η-p-a-e-j-7z	vac	1.644	2.506	147.2
	chlrf	1.646	2.507	146.9
	actn	1.644	2.506	147.1
	aq	1.644	2.506	147.2
c-DBPO-d-r-η-p-a-e-j-5z	vac	1.644	2.505	147.2
	chlrf	1.646	2.506	146.9
	actn	1.644	2.505	147.1
	aq	1.644	2.505	147.2
c-DBPO-d-r-η-p-a-e-j-5y	vac	1.643	2.505	147.2
	chlrf	1.645	2.506	146.9
	actn	1.643	2.505	147.1
	aq	1.643	2.505	147.2
c-DBPO-d-r-η-p-a-e-j-6z	vac	1.645	2.506	147.2
	chlrf	1.647	2.507	146.9
	actn	1.645	2.506	147.1

	aq	1.645	2.506	147.2
c-DBPO-d-r-η-p-a-e-j-8z	vac	1.644	2.506	147.2
	chlrf	1.646	2.506	146.9
	actn	1.644	2.506	147.1
	aq	1.644	2.506	147.2
c-DBPO-d-r-η-p-a-e-j-2z	vac	1.638	2.502	147.4
	chlrf	1.640	2.502	147.2
	actn	1.638	2.502	147.4
	aq	1.638	2.502	147.4
c-DBPO-d-r-η-p-a-e-j-2y	vac	1.638	2.502	147.4
	chlrf	1.640	2.503	147.1
	actn	1.639	2.502	147.3
	aq	1.638	2.502	147.4
c-DBPO-d-r-η-p-a-e-j-6y	vac	1.652	2.508	146.4
	chlrf	1.646	2.506	146.9
	actn	1.644	2.506	147.1
	aq	1.644	2.506	147.1
c-DBPO-d-r-η-p-a-e-j-4y	vac	1.645	2.506	147.1
	chlrf	1.647	2.507	146.9
	actn	1.645	2.506	147.1
	aq	1.645	2.506	147.1
c-DBPO-d-r-η-p-a-e-j-4z	vac	1.644	2.505	147.2
	chlrf	1.646	2.506	146.9
	actn	1.644	2.505	147.1
	aq	1.644	2.505	147.2
c-DBPO-d-r-η-p-a-e-j-7y	vac	1.645	2.506	147.2
	chlrf	1.647	2.507	146.9
	actn	1.645	2.506	147.1
	aq	1.645	2.506	147.2

Table 6.21. Distance between the H atom and the closest C atom in the acceptor aromatic ring for the O–H···π interactions in selected conformers of *cis*-DBPO having different geometries of R and the same geometry of the ring system *in vacuo* and in three solvents chloroform, acetonitrile and water (respectively denoted as vac, chlrf, actn, aq in the column headings.
HF/6-31G(d,p) results. The results *in vacuo* and in solution are from full optimisation calculations. Conformers are listed in order of increasing relative energy in the HF results *in vacuo*.

Conformer	H16···C23 distance considered (Å)			
	vac	chlrf	actn	aq
c-DBPO-d-r-η-p-a-e-j	2.128	2.127	2.126	2.126
c-DBPO-d-r-η-p-a-e-j-8y	2.127	2.128	2.127	2.127
c-DBPO-d-r-η-p-a-e-j-3y	2.127	2.128	2.127	2.127
c-DBPO-d-r-η-p-a-e-j-3z	2.128	2.127	2.128	2.128
c-DBPO-d-r-η-p-a-e-j-7z	2.126	2.126	2.126	2.126
c-DBPO-d-r-η-p-a-e-j-5z	2.127	2.128	2.127	2.127
c-DBPO-d-r-η-p-a-e-j-5y	2.127	2.127	2.127	2.127
c-DBPO-d-r-η-p-a-e-j-6z	2.129	2.128	2.128	2.129
c-DBPO-d-r-η-p-a-e-j-8z	2.127	2.127	2.127	2.127
c-DBPO-d-r-η-p-a-e-j-2z	2.125	2.126	2.125	2.125
c-DBPO-d-r-η-p-a-e-j-2y	2.126	2.127	2.126	2.126
c-DBPO-d-r-η-p-a-e-j-6y	2.128	2.125	2.124	2.123
c-DBPO-d-r-η-p-a-e-j-4y	2.122	2.124	2.122	2.122
c-DBPO-d-r-η-p-a-e-j-4z	2.125	2.126	2.125	2.125
c-DBPO-d-r-η-p-a-e-j-7y	2.126	2.127	2.126	2.126

Table 6.22. Dipole moment of the calculated conformers of *cis*-DBPO having different geometries of R and the same geometry of the ring system *in vacuo* and in three solvents chloroform, acetonitrile and water (respectively denoted as vac, chlrf, actn, aq in the column headings. HF/6-31G(d,p) results. The results *in vacuo* and in solution are from full optimisation calculations. Conformers are listed in order of increasing relative energy in the HF results *in vacuo*.

Conformer	Dipole moment (Debye)			
	vac	chlrf	actn	aq
c-DBPO-d-r-η-p-a-e-j	2.460	2.926	3.098	3.114
c-DBPO-d-r-η-p-a-e-j-8y	2.316	2.764	2.947	2.964
c-DBPO-d-r-η-p-a-e-j-3y	2.558	2.879	3.009	3.021
c-DBPO-d-r-η-p-a-e-j-3z	2.607	3.009	3.151	3.164
c-DBPO-d-r-η-p-a-e-j-7z	2.419	2.849	3.020	3.036
c-DBPO-d-r-η-p-a-e-j-5z	2.435	2.796	2.946	2.960
c-DBPO-d-r-η-p-a-e-j-5y	2.489	2.895	3.060	3.076
c-DBPO-d-r-η-p-a-e-j-6z	2.306	2.737	2.901	2.916
c-DBPO-d-r-η-p-a-e-j-8z	2.118	2.483	2.621	2.635
c-DBPO-d-r-η-p-a-e-j-2z	2.534	3.051	3.253	3.272
c-DBPO-d-r-η-p-a-e-j-2y	2.300	2.728	2.903	2.919
c-DBPO-d-r-η-p-a-e-j-6y	2.136	2.731	2.673	2.687
c-DBPO-d-r-η-p-a-e-j-4y	2.120	2.539	2.692	2.705
c-DBPO-d-r-η-p-a-e-j-4z	2.097	2.463	2.596	2.609
c-DBPO-d-r-η-p-a-e-j-7y	2.419	2.980	3.163	3.179

Table 6.23. HOMO-LUMO energy gap of the calculated conformers of *cis*-DBPO having different geometries of R and the same geometry of the ring system *in vacuo* and in three solvents chloroform, acetonitrile and water (respectively denoted as vac, chlrf, actn, aq in the column headings.
HF/6-31G(d,p) results. The results *in vacuo* and in solution are from full optimisation calculations. Conformers are listed in order of increasing relative energy in the HF results *in vacuo*.

Conformer	HOMO-LUMO energy gap (kcal/mol)			
	vac	chlrf	actn	aq
c-DBPO-d-r-η-p-a-e-j	257.410	256.833	256.570	256.538
c-DBPO-d-r-η-p-a-e-j-8y	257.511	256.858	256.501	256.475
c-DBPO-d-r-η-p-a-e-j-3y	256.890	256.557	256.388	256.369
c-DBPO-d-r-η-p-a-e-j-3z	256.934	256.519	256.394	256.375
c-DBPO-d-r-η-p-a-e-j-7z	257.367	256.796	256.488	256.457
c-DBPO-d-r-η-p-a-e-j-5z	257.367	256.789	256.563	256.538
c-DBPO-d-r-η-p-a-e-j-5y	257.354	256.821	256.582	256.563
c-DBPO-d-r-η-p-a-e-j-6z	257.442	256.846	256.532	256.501
c-DBPO-d-r-η-p-a-e-j-8z	257.448	256.846	256.545	256.513
c-DBPO-d-r-η-p-a-e-j-2z	255.359	254.260	254.028	253.991
c-DBPO-d-r-η-p-a-e-j-2y	255.396	254.235	254.016	253.984
c-DBPO-d-r-η-p-a-e-j-6y	257.429	258.032	256.570	256.545
c-DBPO-d-r-η-p-a-e-j-4y	257.448	256.890	256.626	256.607
c-DBPO-d-r-η-p-a-e-j-4z	257.410	256.877	256.595	256.563
c-DBPO-d-r-η-p-a-e-j-7y	257.379	256.802	256.526	256.501

Table 6.24. Relative energies of all calculated conformers of *cis*- c-DBPO.
HF/6-31G(d,p) results *in vacuo*. The conformers are listed in order of increasing relative energy.

Conformer	Relative energy kcal/mol	Conformer	Relative energy kcal/mol
c-DBPO-d-r-η-p-a-e-j	0.000	c-DBPO-s-r-η-p-a-f-k	5.682
c-DBPO-d-r-η-p-a-e-k	0.014	c-DBPO-d-w-q-a-f-j	5.687
c-DBPO-d-r-η-p-a-e-j-8y	0.323	c-DBPO-d-r-q-a-e-j	5.718
c-DBPO-d-r-η-p-a-f-j	0.424	c-DBPO-d-r-q-b-e-k	5.719
c-DBPO-d-r-η-p-a-f-k	0.496	c-DBPO-d-r-q-b-e-j	5.736
c-DBPO-d-r-η-p-a-e-j-3y	0.511	c-DBPO-d-r-q-a-e-k	5.745
c-DBPO-d-r-η-p-a-e-j-3z	0.527	c-DBPO-s-r-η-p-a-f-j	5.754
c-DBPO-d-r-η-p-a-e-j-7z	0.986	c-DBPO-d-w-q-a-f-k	5.827
c-DBPO-d-r-η-p-a-e-j-5z	0.986	c-DBPO-d-w-q-b-f-j	5.853
c-DBPO-d-r-η-p-a-e-j-5y	0.993	c-DBPO-d-w-q-b-f-k	5.936
c-DBPO-d-r-η-p-a-e-j-6z	1.017	c-DBPO-d-r-q-b-f-j	6.116
c-DBPO-d-r-η-p-a-e-j-8z	1.023	c-DBPO-s-w-p-a-e-j	6.122
c-DBPO-d-r-η-p-b-e-k	1.023	c-DBPO-d-r-q-b-f-k	6.149
c-DBPO-d-r-η-p-a-e-j-2z	1.026	c-DBPO-d-r-q-a-f-j	6.158
c-DBPO-d-r-η-p-b-e-j	1.028	c-DBPO-d-r-q-a-f-k	6.228
c-DBPO-d-r-η-p-a-e-j-2y	1.032	c-DBPO-s-r-η-u-p-b-e-k	6.236
c-DBPO-d-r-η-p-a-e-j-6y	1.035	c-DBPO-s-r-η-u-p-a-e-j	6.281
c-DBPO-d-r-η-p-a-e-j-4y	1.037	c-DBPO-d-w-u-p-a-e-j	6.398

c-DBPO-d-r-η-p-a-e-j-4z	1.056	c-DBPO-s-w-p-a-f-j	6.429
c-DBPO-d-r-η-p-a-e-j-7y	1.067	c-DBPO-s-w-p-a-f-k	6.509
c-DBPO-s-w-ε-q-a-e-k	1.154	c-DBPO-s-w-u-p-b-f-j	6.615
c-DBPO-s-w-ε-q-a-e-j	1.200	c-DBPO-s-r-η-u-p-a-f-j	6.705
c-DBPO-d-r-η-p-b-f-j	1.231	c-DBPO-s-r-η-u-p-a-f-k	6.722
c-DBPO-d-r-η-p-b-f-k	1.264	c-DBPO-s-w-p-b-e-j	7.079
c-DBPO-s-w-ε-q-b-e-j	1.496	c-DBPO-s-w-p-e-a-k	7.159
c-DBPO-s-w-ε-q-a-f-j	1.636	c-DBPO-s-r-η-u-p-b-f-k	7.172
c-DBPO-s-w-ε-q-a-f-k	1.652	c-DBPO-s-r-η-p-b-f-k	7.459
c-DBPO-s-w-ε-q-b-f-k	1.976	c-DBPO-d-w-u-p-a-e-k	7.851
c-DBPO-d-w-p-a-e-j	4.323	c-DBPO-d-w-u-p-b-e-k	7.875
c-DBPO-d-w-p-a-e-k	4.459	c-DBPO-d-w-u-p-a-f-j	8.070
c-DBPO-d-w-p-a-f-j	4.658	c-DBPO-d-w-u-p-b-f-j	8.095
c-DBPO-d-w-p-b-f-j	4.678	c-DBPO-d-w-u-p-a-f-k	8.256
c-DBPO-d-r-η-u-p-a-e-j	4.696	c-DBPO-d-w-u-p-b-f-k	8.258
c-DBPO-d-r-η-u-p-a-e-k	4.684	c-DBPO-s-w-u-p-e-a-k	8.285
c-DBPO-s-r-ε-q-b-e-j	4.705	c-DBPO-d-w-u-q-a-e-j	8.391
c-DBPO-s-r-ε-q-b-f-j	4.833	c-DBPO-s-w-u-q-a-e-j	8.409
c-DBPO-d-w-p-a-f-k	4.853	c-DBPO-s-w-u-q-b-e-j	8.416
c-DBPO-s-r-ε-q-b-f-k	5.026	c-DBPO-d-w-u-q-b-e-j	8.459
c-DBPO-s-r-ε-q-a-e-k	5.031	c-DBPO-d-w-u-q-a-e-k	8.488
c-DBPO-s-r-η-p-b-e-j	5.046	c-DBPO-s-w-u-q-a-e-k	8.500
c-DBPO-d-r-η-u-p-a-f-j	5.096	c-DBPO-s-w-u-p-a-f-j	8.557
c-DBPO-s-r-ε-q-a-e-j	5.155	c-DBPO-s-w-u-p-b-e-k	8.572
c-DBPO-d-w-p-b-e-k	5.166	c-DBPO-s-w-u-p-a-f-k	8.702
c-DBPO-d-r-η-u-p-a-f-k	5.163	c-DBPO-d-w-u-q-a-f-j	8.850
c-DBPO-d-w-q-b-e-j	5.188	c-DBPO-s-w-u-p-b-f-k	8.867
c-DBPO-d-w-p-b-f-k	5.228	c-DBPO-s-w-u-q-a-f-k	8.884
c-DBPO-d-w-q-a-e-j	5.213	c-DBPO-d-w-u-q-a-f-k	9.008
c-DBPO-s-r-η-p-e-a-k	5.222	c-DBPO-d-w-u-q-b-f-k	9.239
c-DBPO-s-r-η-p-b-e-k	5.265	c-DBPO-d-r-u-q-a-e-j	10.163
c-DBPO-d-w-q-a-e-k	5.291	c-DBPO-s-r-u-q-b-e-j	10.283
c-DBPO-s-r-η-p-a-e-j	5.355	c-DBPO-d-r-u-q-a-f-j	10.563
c-DBPO-s-r-ε-q-a-f-k	5.505	c-DBPO-s-r-u-q-a-e-j	11.105
c-DBPO-d-w-q-b-e-k	5.559	c-DBPO-s-r-u-q-a-e-k	11.128
c-DBPO-s-r-ε-q-a-f-j	5.565	c-DBPO-s-r-u-q-a-f-j	11.402
c-DBPO-s-w-p-b-f-j	5.596	c-DBPO-s-r-u-q-a-f-k	11.487

Table 6.25. Parameters of the first IHB of all calculated conformers of *cis*- c-DBPO.
HF/6-31G(d,p) results *in vacuo*. For conformers of d type, the first IHB is H15···O14; for conformers of s type, the first IHB is H17···O14. The conformers are listed in order of increasing relative energy.

Conformer	Parameters of the first IHB		
	OH···O (Å)	OH···O (Å)	OH···O (°)
c-DBPO-d-r-η-p-a-e-j	1.652	2.508	146.4
c-DBPO-d-r-η-p-a-e-k	1.652	2.508	146.3
c-DBPO-d-r-η-p-a-e-j-8y	1.644	2.506	147.2
c-DBPO-d-r-η-p-a-f-j	1.652	2.508	146.4
c-DBPO-d-r-η-p-a-f-k	1.652	2.508	146.3
c-DBPO-d-r-η-p-a-e-j-3y	1.649	2.509	147.0
c-DBPO-d-r-η-p-a-e-j-3z	1.647	2.507	147.0
c-DBPO-d-r-η-p-a-e-j-7z	1.644	2.506	147.2
c-DBPO-d-r-η-p-a-e-j-5z	1.645	2.507	147.1
c-DBPO-d-r-η-p-a-e-j-5y	1.643	2.505	147.2
c-DBPO-d-r-η-p-a-e-j-6z	1.645	2.506	147.2
c-DBPO-d-r-η-p-a-e-j-8z	1.644	2.506	147.2
c-DBPO-d-r-η-p-b-e-k	1.651	2.508	146.6
c-DBPO-d-r-η-p-a-e-j-2z	1.638	2.502	147.4
c-DBPO-d-r-η-p-b-e-j	1.656	2.510	146.2
c-DBPO-d-r-η-p-a-e-j-2y	1.638	2.502	147.4
c-DBPO-d-r-η-p-a-e-j-6y	1.652	2.508	146.4
c-DBPO-d-r-η-p-a-e-j-4y	1.645	2.506	147.1
c-DBPO-d-r-η-p-a-e-j-4z	1.644	2.505	147.2
c-DBPO-d-r-η-p-a-e-j-7y	1.645	2.506	147.2
c-DBPO-s-w-ε-q-a-e-k	1.684	2.522	143.9
c-DBPO-s-w-ε-q-a-e-j	1.684	2.521	143.9
c-DBPO-d-r-η-p-b-f-j	1.656	2.510	146.2
c-DBPO-d-r-η-p-b-f-k	1.651	2.509	146.5
c-DBPO-s-w-ε-q-b-e-j	1.689	2.527	144.0
c-DBPO-s-w-ε-q-a-f-j	1.682	2.520	143.9
c-DBPO-s-w-ε-q-a-f-k	1.683	2.521	143.9
c-DBPO-s-w-ε-q-b-f-k	1.689	2.526	144.0
c-DBPO-d-w-p-a-e-j	1.656	2.511	146.2
c-DBPO-d-w-p-a-e-k	1.656	2.511	146.2
c-DBPO-d-w-p-a-f-j	1.656	2.511	146.2
c-DBPO-d-w-p-b-f-j	1.656	2.511	146.2
c-DBPO-d-r-η-u-p-a-e-j	1.676	2.523	145.4
c-DBPO-d-r-η-u-p-a-e-k	1.676	2.524	145.4
c-DBPO-s-r-ε-q-b-e-j	1.695	2.531	143.9
c-DBPO-s-r-ε-q-b-f-j	1.694	2.531	143.9
c-DBPO-d-w-p-a-f-k	1.656	2.511	146.2
c-DBPO-s-r-ε-q-b-f-k	1.694	2.531	143.9
c-DBPO-s-r-ε-q-a-e-k	1.692	2.527	143.8

c-DBPO-s-r-η-p-b-e-j	1.692	2.528	143.8
c-DBPO-d-r-η-u-p-a-f-j	1.675	2.522	145.4
c-DBPO-d-w-p-b-e-k	1.658	2.512	146.2
c-DBPO-d-r-η-u-p-a-f-k	1.676	2.523	145.4
c-DBPO-s-r-ε-q-a-e-j	1.690	2.526	143.8
c-DBPO-d-w-q-b-e-j	1.664	2.514	145.6
c-DBPO-d-w-p-b-f-k	1.659	2.513	146.1
c-DBPO-d-w-q-a-e-j	1.654	2.508	146.1
c-DBPO-s-r-η-p-e-a-k	1.697	2.532	143.7
c-DBPO-s-r-η-p-b-e-k	1.692	2.528	143.8
c-DBPO-d-w-q-a-e-k	1.654	2.508	146.1
c-DBPO-s-r-η-p-a-e-j	1.697	2.532	143.7
c-DBPO-s-r-ε-q-a-f-k	1.689	2.526	143.8
c-DBPO-d-w-q-b-e-k	1.664	2.514	145.6
c-DBPO-s-r-ε-q-a-f-j	1.688	2.524	143.9
c-DBPO-s-w-p-b-f-j	1.683	2.521	143.9
c-DBPO-s-r-η-p-a-f-k	1.697	2.532	143.7
c-DBPO-d-w-q-a-f-j	1.655	2.509	146.0
c-DBPO-d-r-q-a-e-j	1.646	2.503	146.4
c-DBPO-d-r-q-b-e-k	1.647	2.505	146.5
c-DBPO-d-r-q-b-e-j	1.647	2.504	146.4
c-DBPO-d-r-q-a-e-k	1.646	2.503	146.4
c-DBPO-s-r-η-p-a-f-j	1.696	2.531	143.7
c-DBPO-d-w-q-a-f-k	1.656	2.509	146.0
c-DBPO-d-w-q-b-f-j	1.657	2.510	145.9
c-DBPO-d-w-q-b-f-k	1.657	2.511	146.0
c-DBPO-d-r-q-b-f-j	1.649	2.506	146.3
c-DBPO-s-w-p-a-e-j	1.689	2.526	143.7
c-DBPO-d-r-q-b-f-k	1.649	2.506	146.3
c-DBPO-d-r-q-a-f-j	1.648	2.504	146.3
c-DBPO-d-r-q-a-f-k	1.648	2.504	146.3
c-DBPO-s-r-η-u-p-b-e-k	1.736	2.559	142.5
c-DBPO-s-r-η-u-p-a-e-j	1.737	2.560	142.4
c-DBPO-d-w-u-p-a-e-j	1.714	2.546	143.4
c-DBPO-s-w-p-a-f-j	1.689	2.526	143.8
c-DBPO-s-w-p-a-f-k	1.689	2.526	143.8
c-DBPO-s-w-u-p-b-f-j	1.739	2.562	142.5
c-DBPO-s-r-η-u-p-a-f-j	1.738	2.560	142.4
c-DBPO-s-r-η-u-p-a-f-k	1.737	2.560	142.4
c-DBPO-s-w-p-b-e-j	1.686	2.523	143.7
c-DBPO-s-w-p-e-a-k	1.686	2.523	143.8
c-DBPO-s-r-η-u-p-b-f-k	1.731	2.555	142.6
c-DBPO-s-r-η-p-b-f-k	1.686	2.523	143.8
c-DBPO-d-w-u-p-a-e-k	1.681	2.526	145.2
c-DBPO-d-w-u-p-b-e-k	1.681	2.526	145.2
c-DBPO-d-w-u-p-a-f-j	1.682	2.527	145.2
c-DBPO-d-w-u-p-b-f-j	1.682	2.527	145.3
c-DBPO-d-w-u-p-a-f-k	1.682	2.527	145.2
c-DBPO-d-w-u-p-b-f-k	1.682	2.528	145.3

c-DBPO-s-w-u-p-e-a-k	1.731	2.554	142.4
c-DBPO-d-w-u-q-a-e-j	1.685	2.530	145.2
c-DBPO-s-w-u-q-a-e-j	1.732	2.556	142.4
c-DBPO-s-w-u-q-b-e-j	1.730	2.555	142.6
c-DBPO-d-w-u-q-b-e-j	1.694	2.533	144.4
c-DBPO-d-w-u-q-a-e-k	1.686	2.530	145.2
c-DBPO-s-w-u-q-a-e-k	1.733	2.556	142.4
c-DBPO-s-w-u-p-a-f-j	1.731	2.554	142.4
c-DBPO-s-w-u-p-b-e-k	1.725	2.550	142.6
c-DBPO-s-w-u-p-a-f-k	1.731	2.554	142.4
c-DBPO-d-w-u-q-a-f-j	1.686	2.529	145.1
c-DBPO-s-w-u-p-b-f-k	1.726	2.551	142.6
c-DBPO-s-w-u-q-a-f-k	1.731	2.555	142.5
c-DBPO-d-w-u-q-a-f-k	1.687	2.530	145.1
c-DBPO-d-w-u-q-b-f-k	1.684	2.528	145.1
c-DBPO-d-r-u-q-a-e-j	1.676	2.520	145.0
c-DBPO-s-r-u-q-b-e-j	1.738	2.562	142.5
c-DBPO-d-r-u-q-a-f-j	1.679	2.522	144.8
c-DBPO-s-r-u-q-a-e-j	1.739	2.561	142.4
c-DBPO-s-r-u-q-a-e-k	1.740	2.562	142.4
c-DBPO-s-r-u-q-a-f-j	1.737	2.560	142.4
c-DBPO-s-r-u-q-a-f-k	1.738	2.561	142.4

Table 6.26. The distance between the H atom and the closest C atom in the acceptor aromatic ring for the O–H···π interactions of all calculated conformers of *cis*- c-DBPO.
HF/6-31G(d,p) results *in vacuo*. The conformers are arranged in order of increasing relative energy. For p-type conformers, the distance considered is H16···C23; for q-type conformers, the distance considered is H15···C23.

Conformer	H15···C23 or H16···C23 (Å)	Conformer	H15···C23 or H16···C23 (Å)
c-DBPO-d-r-η-p-a-e-j	2.128	c-DBPO-s-w-ε-q-b-e-j	2.185
c-DBPO-d-r-η-p-a-e-k	2.127	c-DBPO-s-w-ε-q-a-f-j	2.076
c-DBPO-d-r-η-p-a-e-j-8y	2.008	c-DBPO-s-w-ε-q-a-f-k	2.075
c-DBPO-d-r-η-p-a-f-j	2.131	c-DBPO-s-w-ε-q-b-f-k	2.187
c-DBPO-d-r-η-p-a-f-k	2.130	c-DBPO-d-r-η-u-p-a-e-j	2.128
c-DBPO-d-r-η-p-a-e-j-8y	2.008	c-DBPO-d-r-η-u-p-a-e-k	2.128
c-DBPO-d-r-η-p-a-e-j-3y	2.011	c-DBPO-s-r-ε-q-b-e-j	2.165
c-DBPO-d-r-η-p-a-e-j-3z	2.007	c-DBPO-s-r-ε-q-b-f-j	2.169
c-DBPO-d-r-η-p-a-e-j-7z	2.008	c-DBPO-s-r-ε-q-b-f-k	2.171
c-DBPO-d-r-η-p-a-e-j-5z	2.008	c-DBPO-s-r-η-p-b-e-j	2.216

c-DBPO-d-r-η-p-a-e-j-5y	2.008	c-DBPO-d-r-η-u-p-a-f-j	2.130
c-DBPO-d-r-η-p-a-e-j-6z	2.008	c-DBPO-d-r-η-u-p-a-f-k	2.130
c-DBPO-d-r-η-p-a-e-j-8z	2.008	c-DBPO-s-r-ε-q-a-e-j	2.058
c-DBPO-d-r-η-p-b-e-k	2.213	c-DBPO-s-r-η-p-e-a-k	2.109
c-DBPO-d-r-η-p-a-e-j-2z	2.007	c-DBPO-s-r-η-p-b-e-k	2.220
c-DBPO-d-r-η-p-b-e-j	2.236	c-DBPO-s-r-η-p-a-e-j	2.109
c-DBPO-d-r-η-p-a-e-j-2y	2.011	c-DBPO-s-r-ε-q-a-f-k	2.059
c-DBPO-d-r-η-p-a-e-j-6y	2.008	c-DBPO-s-r-ε-q-a-f-j	2.059
c-DBPO-d-r-η-p-a-e-j-4y	2.008	c-DBPO-s-r-η-p-a-f-k	2.111
c-DBPO-d-r-η-p-a-e-j-4z	2.008	c-DBPO-s-r-η-p-a-f-j	2.112
c-DBPO-d-r-η-p-a-e-j-7y	2.008	c-DBPO-s-r-η-u-p-b-e-k	2.121
c-DBPO-s-w-ε-q-a-e-k	2.074	c-DBPO-s-r-η-u-p-a-e-j	2.121
c-DBPO-s-w-ε-q-a-e-j	2.074	c-DBPO-s-r-η-u-p-a-f-j	2.123
c-DBPO-d-r-η-p-b-f-j	2.239	c-DBPO-s-r-η-u-p-a-f-k	2.123
c-DBPO-d-r-η-p-b-f-k	2.219	c-DBPO-s-r-η-u-p-b-f-k	2.240

Table 6.27. Dipole moments of all calculated conformers of *cis*-DBPO.
HF/6-31G(d,p) results *in vacuo*. The conformers are listed in order of increasing relative energy.

Conformer	Dipole moment (Debye)	Conformer	Dipole moment (Debye)
c-DBPO-d-r-η-p-a-e-j	2.460	c-DBPO-s-r-η-p-a-f-k	2.551
c-DBPO-d-r-η-p-a-e-k	3.834	c-DBPO-d-w-q-a-f-j	4.531
c-DBPO-d-r-η-p-a-e-j-8y	2.316	c-DBPO-d-r-q-a-e-j	8.205
c-DBPO-d-r-η-p-a-f-j	2.877	c-DBPO-d-r-q-b-e-k	4.035
c-DBPO-d-r-η-p-a-f-k	4.115	c-DBPO-d-r-q-b-e-j	3.641
c-DBPO-d-r-η-p-a-e-j-3y	2.558	c-DBPO-d-r-q-a-e-k	3.463
c-DBPO-d-r-η-p-a-e-j-3z	2.607	c-DBPO-s-r-η-p-a-f-j	4.755
c-DBPO-d-r-η-p-a-e-j-7z	2.419	c-DBPO-d-w-q-a-f-k	7.228
c-DBPO-d-r-η-p-a-e-j-5z	2.435	c-DBPO-d-w-q-b-f-j	0.892
c-DBPO-d-r-η-p-a-e-j-5y	2.489	c-DBPO-d-w-q-b-f-k	9.417
c-DBPO-d-r-η-p-a-e-j-6z	2.306	c-DBPO-d-r-q-b-f-j	5.606
c-DBPO-d-r-η-p-a-e-j-8z	2.118	c-DBPO-s-w-p-a-e-j	9.149
c-DBPO-d-r-η-p-b-e-k	2.597	c-DBPO-d-r-q-b-f-k	8.498
c-DBPO-d-r-η-p-a-e-j-2z	2.534	c-DBPO-d-r-q-a-f-j	4.731
c-DBPO-d-r-η-p-b-e-j	2.806	c-DBPO-d-r-q-a-f-k	4.463
c-DBPO-d-r-η-p-a-e-j-2y	2.300	c-DBPO-s-r-η-u-p-b-e-k	3.571
c-DBPO-d-r-η-p-a-e-j-6y	2.136	c-DBPO-s-r-η-u-p-a-e-j	6.137
c-DBPO-d-r-η-p-a-e-j-4y	2.120	c-DBPO-d-w-u-p-a-e-j	3.270
c-DBPO-d-r-η-p-a-e-j-4z	2.097	c-DBPO-s-w-p-a-f-j	5.700
c-DBPO-d-r-η-p-a-e-j-7y	2.419	c-DBPO-s-w-p-a-f-k	7.716
c-DBPO-s-w-ε-q-a-e-k	2.993	c-DBPO-s-w-u-p-b-f-j	4.223

c-DBPO-s-w-ε-q-a-e-j	5.279	c-DBPO-s-r-η-u-p-a-f-j	0.995
c-DBPO-d-r-η-p-b-f-j	3.489	c-DBPO-s-r-η-u-p-a-f-k	5.749
c-DBPO-d-r-η-p-b-f-k	3.723	c-DBPO-s-w-p-b-e-j	2.727
c-DBPO-s-w-ε-q-b-e-j	4.900	c-DBPO-s-w-p-e-a-k	4.389
c-DBPO-s-w-ε-q-a-f-j	5.068	c-DBPO-s-r-η-u-p-b-f-k	3.845
c-DBPO-s-w-ε-q-a-f-k	2.723	c-DBPO-s-r-η-p-b-f-k	7.838
c-DBPO-s-w-ε-q-b-f-k	2.780	c-DBPO-d-w-u-p-a-e-k	7.692
c-DBPO-d-w-p-a-e-j	6.642	c-DBPO-d-w-u-p-b-e-k	6.327
c-DBPO-d-w-p-a-e-k	3.062	c-DBPO-d-w-u-p-a-f-j	6.268
c-DBPO-d-w-p-a-f-j	7.227	c-DBPO-d-w-u-p-b-f-j	4.848
c-DBPO-d-w-p-b-f-j	5.408	c-DBPO-d-w-u-p-a-f-k	1.686
c-DBPO-d-r-η-u-p-a-e-j	5.472	c-DBPO-d-w-u-p-b-f-k	7.098
c-DBPO-d-r-η-u-p-a-e-k	0.648	c-DBPO-s-w-u-p-e-a-k	7.160
c-DBPO-s-r-ε-q-b-e-j	2.946	c-DBPO-d-w-u-q-a-e-j	4.116
c-DBPO-s-r-ε-q-b-f-j	7.759	c-DBPO-s-w-u-q-a-e-j	2.284
c-DBPO-d-w-p-a-f-k	6.184	c-DBPO-s-w-u-q-b-e-j	1.379
c-DBPO-s-r-ε-q-b-f-k	5.408	c-DBPO-d-w-u-q-b-e-j	1.363
c-DBPO-s-r-ε-q-a-e-k	4.480	c-DBPO-d-w-u-q-a-e-k	2.155
c-DBPO-s-r-η-p-b-e-j	3.536	c-DBPO-s-w-u-q-a-e-k	5.888
c-DBPO-d-r-η-u-p-a-f-j	5.494	c-DBPO-s-w-u-p-a-f-j	4.890
c-DBPO-d-w-p-b-e-k	2.573	c-DBPO-s-w-u-p-b-e-k	6.449
c-DBPO-d-r-η-u-p-a-f-k	6.559	c-DBPO-s-w-u-p-a-f-k	6.114
c-DBPO-s-r-ε-q-a-e-j	3.896	c-DBPO-d-w-u-q-a-f-j	3.390
c-DBPO-d-w-q-b-e-j	7.897	c-DBPO-s-w-u-p-b-f-k	3.661
c-DBPO-d-w-p-b-f-k	5.980	c-DBPO-s-w-u-q-a-f-k	6.114
c-DBPO-d-w-q-a-e-j	5.040	c-DBPO-d-w-u-q-a-f-k	2.491
c-DBPO-s-r-η-p-e-a-k	6.363	c-DBPO-d-w-u-q-b-f-k	7.871
c-DBPO-s-r-η-p-b-e-k	5.365	c-DBPO-d-r-u-q-a-e-j	7.985
c-DBPO-d-w-q-a-e-k	6.769	c-DBPO-s-r-u-q-b-e-j	1.061
c-DBPO-s-r-η-p-a-e-j	7.756	c-DBPO-d-r-u-q-a-f-j	5.163
c-DBPO-s-r-ε-q-a-f-k	5.723	c-DBPO-s-r-u-q-a-e-j	2.888
c-DBPO-d-w-q-b-e-k	4.350	c-DBPO-s-r-u-q-a-e-k	4.649
c-DBPO-s-r-ε-q-a-f-j	5.408	c-DBPO-s-r-u-q-a-f-j	3.273
c-DBPO-s-w-p-b-f-j	7.085	c-DBPO-s-r-u-q-a-f-k	3.566

Table 6.28. HOMO-LUMO energy gaps of all calculated conformers of *cis*-DBPO.
HF/6-31G(d,p) results *in vacuo*. The conformers are listed in order of increasing relative energy.

Conformer	HOMO-LUMO energy gap (kcal/mol)	Conformer	HOMO-LUMO energy gap (kcal/mol)
c-DBPO-d-r-η-p-a-e-j	257.410	c-DBPO-s-r-η-p-a-f-k	253.558
c-DBPO-d-r-η-p-a-e-k	257.517	c-DBPO-d-w-q-a-f-j	260.052
c-DBPO-d-r-η-p-a-e-j-8y	257.511	c-DBPO-d-r-q-a-e-j	242.206
c-DBPO-d-r-η-p-a-f-j	256.250	c-DBPO-d-r-q-b-e-k	250.928
c-DBPO-d-r-η-p-a-f-k	256.425	c-DBPO-d-r-q-b-e-j	247.075
c-DBPO-d-r-η-p-a-e-j-3y	256.890	c-DBPO-d-r-q-a-e-k	249.134
c-DBPO-d-r-η-p-a-e-j-3z	256.934	c-DBPO-s-r-η-p-a-f-j	246.529
c-DBPO-d-r-η-p-a-e-j-7z	257.367	c-DBPO-d-w-q-a-f-k	259.946
c-DBPO-d-r-η-p-a-e-j-5z	257.367	c-DBPO-d-w-q-b-f-j	253.125
c-DBPO-d-r-η-p-a-e-j-5y	257.354	c-DBPO-d-w-q-b-f-k	241.641
c-DBPO-d-r-η-p-a-e-j-6z	257.442	c-DBPO-d-r-q-b-f-j	242.457
c-DBPO-d-r-η-p-a-e-j-8z	257.448	c-DBPO-s-w-p-a-e-j	242.570
c-DBPO-d-r-η-p-b-e-k	254.612	c-DBPO-d-r-q-b-f-k	243.066
c-DBPO-d-r-η-p-a-e-j-2z	255.359	c-DBPO-d-r-q-a-f-j	246.523
c-DBPO-d-r-η-p-b-e-j	255.867	c-DBPO-d-r-q-a-f-k	252.158
c-DBPO-d-r-η-p-a-e-j-2y	255.396	c-DBPO-s-r-η-u-p-b-e-k	248.657
c-DBPO-d-r-η-p-a-e-j-6y	257.429	c-DBPO-s-r-η-u-p-a-e-j	247.728
c-DBPO-d-r-η-p-a-e-j-4y	257.448	c-DBPO-d-w-u-p-a-e-j	252.987
c-DBPO-d-r-η-p-a-e-j-4z	257.410	c-DBPO-s-w-p-a-f-j	251.493
c-DBPO-d-r-η-p-a-e-j-7y	257.379	c-DBPO-s-w-p-a-f-k	260.297
c-DBPO-s-w-ε-q-a-e-k	258.829	c-DBPO-s-w-u-p-b-f-j	236.100
c-DBPO-s-w-ε-q-a-e-j	258.785	c-DBPO-s-r-η-u-p-a-f-j	252.629
c-DBPO-d-r-η-p-b-f-j	255.992	c-DBPO-s-r-η-u-p-a-f-k	250.797
c-DBPO-d-r-η-p-b-f-k	256.049	c-DBPO-s-w-p-b-e-j	238.673
c-DBPO-s-w-ε-q-b-e-j	258.647	c-DBPO-s-w-p-e-a-k	251.085
c-DBPO-s-w-ε-q-a-f-j	258.069	c-DBPO-s-r-η-u-p-b-f-k	251.531
c-DBPO-s-w-ε-q-a-f-k	258.182	c-DBPO-s-r-η-p-b-f-k	260.404
c-DBPO-s-w-ε-q-b-f-k	239.796	c-DBPO-d-w-u-p-a-e-k	258.691
c-DBPO-d-w-p-a-e-j	243.844	c-DBPO-d-w-u-p-b-e-k	236.841
c-DBPO-d-w-p-a-e-k	258.276	c-DBPO-d-w-u-p-a-f-j	236.822
c-DBPO-d-w-p-a-f-j	242.739	c-DBPO-d-w-u-p-b-f-j	238.560
c-DBPO-d-w-p-b-f-j	244.427	c-DBPO-d-w-u-p-a-f-k	239.947
c-DBPO-d-r-η-u-p-a-e-j	244.415	c-DBPO-d-w-u-p-b-f-k	238.002
c-DBPO-d-r-η-u-p-a-e-k	251.581	c-DBPO-s-w-u-p-e-a-k	238.127
c-DBPO-s-r-ε-q-b-e-j	251.688	c-DBPO-d-w-u-q-a-e-j	237.111
c-DBPO-s-r-ε-q-b-f-j	260.855	c-DBPO-s-w-u-q-a-e-j	239.225
c-DBPO-d-w-p-a-f-k	260.743	c-DBPO-s-w-u-q-b-e-j	240.192
c-DBPO-s-r-ε-q-b-f-k	249.435	c-DBPO-d-w-u-q-b-e-j	240.267
c-DBPO-s-r-ε-q-a-e-k	260.680	c-DBPO-d-w-u-q-a-e-k	239.602

c-DBPO-s-r-η-p-b-e-j	253.099	c-DBPO-s-w-u-q-a-e-k	250.571
c-DBPO-d-r-η-u-p-a-f-j	261.025	c-DBPO-s-w-u-p-a-f-j	238.648
c-DBPO-d-w-p-b-e-k	250.527	c-DBPO-s-w-u-p-b-e-k	235.536
c-DBPO-d-r-η-u-p-a-f-k	242.338	c-DBPO-s-w-u-p-a-f-k	237.318
c-DBPO-s-r-ε-q-a-e-j	250.715	c-DBPO-d-w-u-q-a-f-j	240.236
c-DBPO-d-w-q-b-e-j	256.250	c-DBPO-s-w-u-p-b-f-k	239.796
c-DBPO-d-w-p-b-f-k	242.319	c-DBPO-s-w-u-q-a-f-k	237.318
c-DBPO-d-w-q-a-e-j	243.273	c-DBPO-d-w-u-q-a-f-k	240.775
c-DBPO-s-r-η-p-e-a-k	240.995	c-DBPO-d-w-u-q-b-f-k	236.747
c-DBPO-s-r-η-p-b-e-k	260.473	c-DBPO-d-r-u-q-a-e-j	237.424
c-DBPO-d-w-q-a-e-k	260.096	c-DBPO-s-r-u-q-b-e-j	241.961
c-DBPO-s-r-η-p-a-e-j	240.449	c-DBPO-d-r-u-q-a-f-j	248.312
c-DBPO-s-r-ε-q-a-f-k	249.096	c-DBPO-s-r-u-q-a-e-j	243.204
c-DBPO-d-w-q-b-e-k	260.561	c-DBPO-s-r-u-q-a-e-k	246.379
c-DBPO-s-r-ε-q-a-f-j	241.842	c-DBPO-s-r-u-q-a-f-j	245.858
c-DBPO-s-w-p-b-f-j	260.454	c-DBPO-s-r-u-q-a-f-k	247.345

Figure 6.5. Shapes of the HOMO and LUMO molecular orbitals of the calculated conformers of *cis*-DBPO having different geometries of R and the same geometry of the ring system *in vacuo*.
HF/6-31G(d,p) results. The conformers are listed in order of increasing relative energy.

HOMO	LUMO	HOMO	LUMO
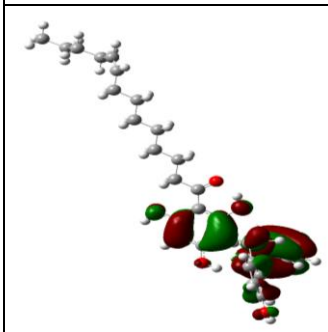	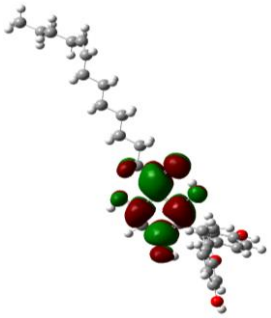		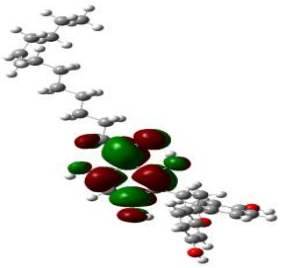
c-DBPO-d-r-η-p-a-e-j		c-DBPO-d-r-η-p-a-e-j-8z	
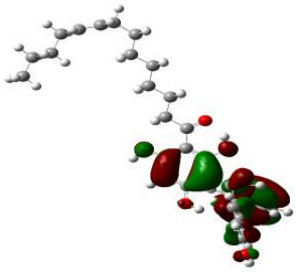	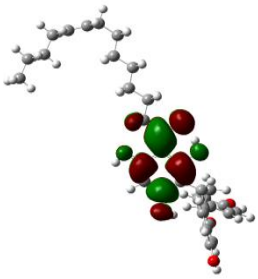	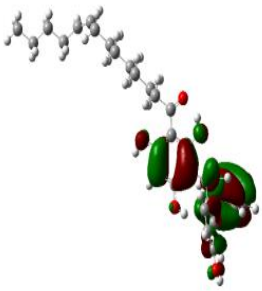	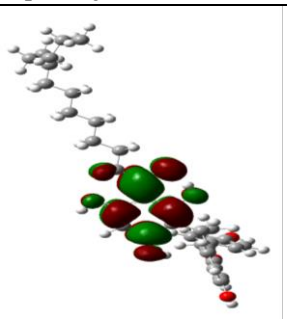
c-DBPO-d-r-η-p-a-e-j-8y		c-DBPO-d-r-η-p-a-e-j-2z	
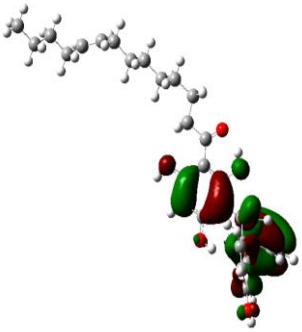	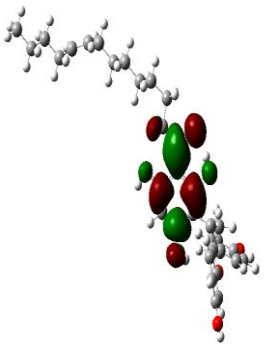	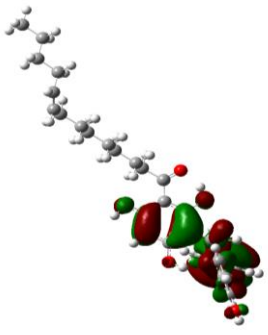	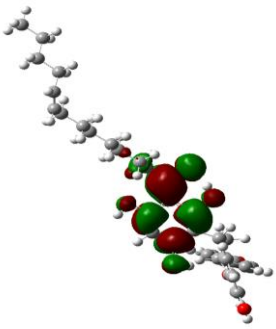
c-DBPO-d-r-η-p-a-e-j-3y		c-DBPO-d-r-η-p-a-e-j-2y	
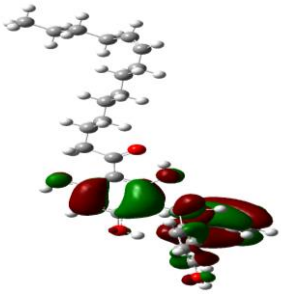	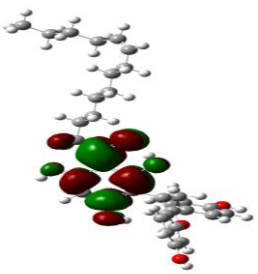		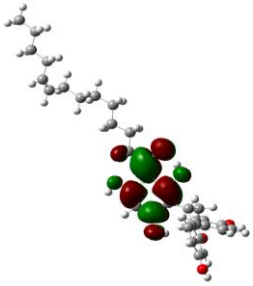
c-DBPO-d-r-η-p-a-e-j-3z		c-DBPO-d-r-η-p-a-e-j-6y	

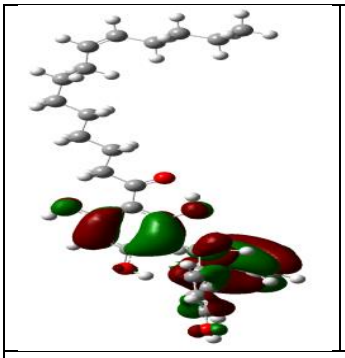	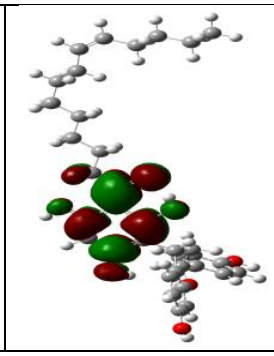
c-DBPO-d-r-η-p-a-e-j-7z	
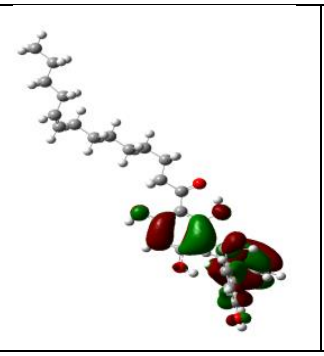	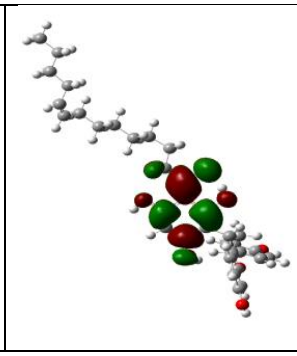
c-DBPO-d-r-η-p-a-e-j-4y	
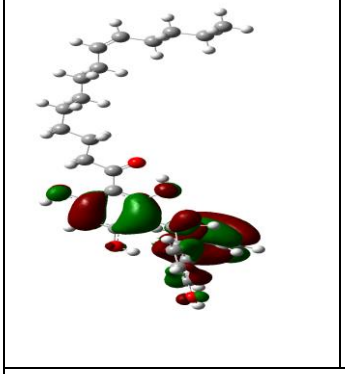	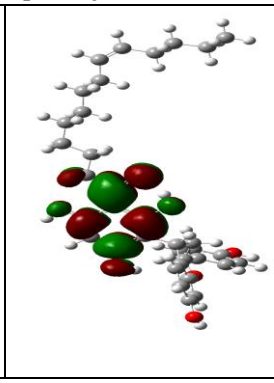
c-DBPO-d-r-η-p-a-e-j-5z	
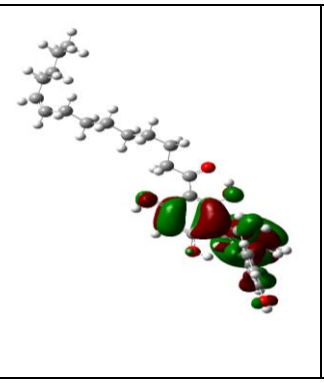	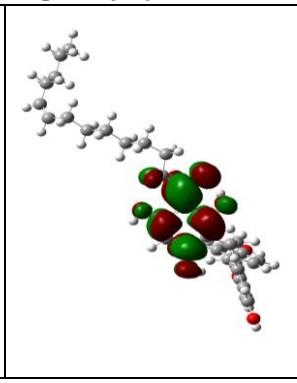
c-DBPO-d-r-η-p-a-e-j-4z	
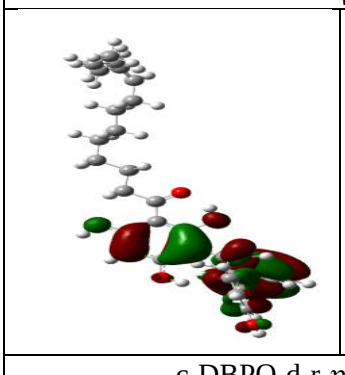	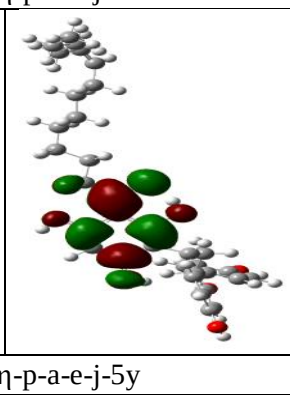
c-DBPO-d-r-η-p-a-e-j-5y	
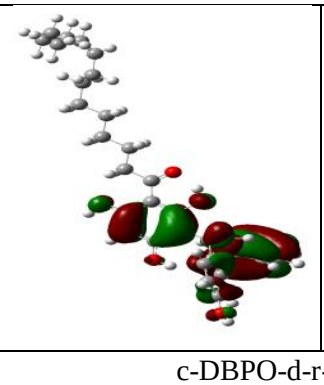	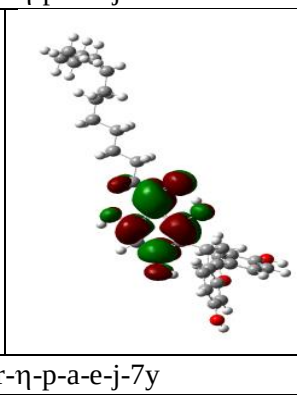
c-DBPO-d-r-η-p-a-e-j-7y	
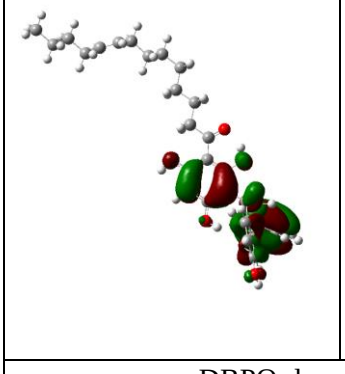	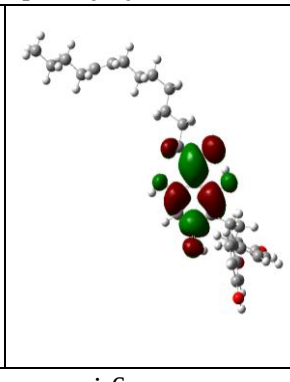
c-DBPO-d-r-η-p-a-e-j-6z	

CHAPTER 7

COMPUTATIONAL STUDY OF THE *TRANS*-DBPO ISOMER *IN VACUO* AND IN SOLUTION

This chapter presents the results of the conformational study of *trans*-DBPO isomer. The results are organised according to eh two types of study performed, as explained in section 4.4

7.1. Naming of conformers

Conformers are denoted with acronyms providing information on their characteristics. The same letters which are used to keep track of relevant geometry features of myristinin A (section 5.1) are also used for the conformers of *trans*-DBPO. Figure 7.1 shows the structure of *trans*-DBPO.

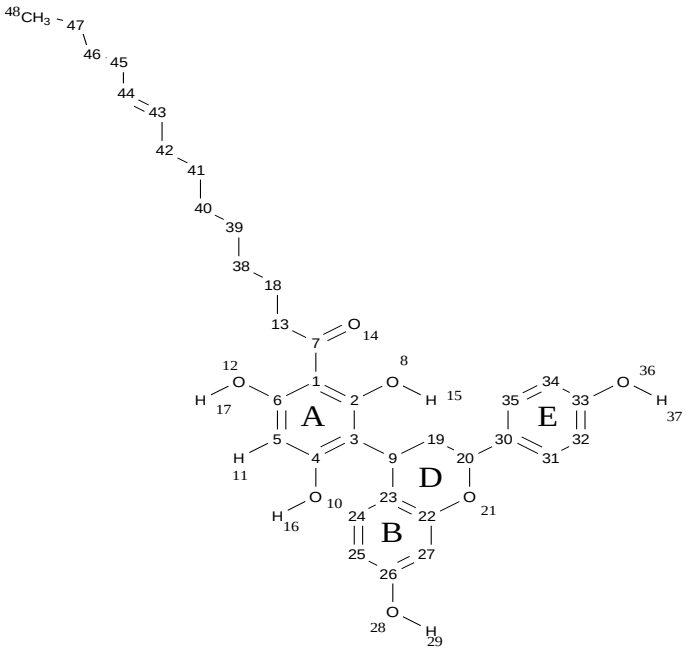

Figure 7.1. Structure of the *trans*-DBPO isomer and atom numbering utilised in this study.

The C atoms in the rings and in the acyl chain are represented by the numbers denoting their position (except one of the C atom at the end of the acyl chain) for better view of the structure. Only the H atoms attached to O atoms and to C5 atom are numbered individually while the other H atoms attached to the rest of the C atoms are given the same number as the C atom and are not shown in the structure. The rings are denoted by uppercase letters (A, B, D and E).

7.2. Results for conformers with the same geometry of R and different geometries of the ring system.

7.2.1. Results *in vacuo*

7.2.1.1. Relative energies of the conformers

This part of the study considered 95 conformers, each of them corresponding to one of the identified geometries of the ring systems [190] (fig.5.4). The geometries of the resulting conformers are shown in figure 7.2 and their relative energies are reported in table 7.1. The same conformational preferences identified in the study (part 1) of myristinin A and *cis*-DBPO still hold for *trans*-DBPO too.

The d conformers have lower energy than the s conformers; when there is O10–H16···π interaction between H16 and ring B, the r conformers have lower energy than the w conformers, and has higher energy than the w conformer when there is no O10–H16···π interaction between H16 and ring B; the u conformers always have higher energy than the corresponding non-u ones; the p conformer has lower energy than the q conformer when the q conformer does not have the O8–H15···π interaction between H15 and ring B and has higher energy than the q conformer when the q conformer has the O8–H15···π interaction between H15 and ring B. The following pairs of conformers, a/b, e/f and j/k shows no consistent pattern in the conformational preference.

7.2.1.2. Characteristics of intramolecular hydrogen bonds

Table 7.2 reports the parameters (H-O bond length, O···O distance, O$\hat{H}$O angle) of the first IHB of the calculated conformers of myristinin A. The trends identified from myristinin A hold for *trans*-DBPO. The comparison of the H···O length of pairs of conformers differing only by the position of the first IHB (H15···O14 or H17···O14) shows that the d conformers have shorter H···O length than the corresponding s conformers. Considering the distance between the two oxygen atoms, the O14···O8 distance in the d conformers is shorter than the O14···O12 distance in the s conformers. Considering the O$\hat{H}$O bond angles, d conformers have greater angle than the corresponding s conformers. All these values indicate that the H15···O14 first IHB is somewhat stronger than the H17···O14 first IHB.

It is also noted that non-u conformers have shorter H···O length than the u conformers. The orientation of O10–H16, O28–H29 and O36–H37, as well as the position of C19 in ring D do not influence the characteristics of the first IHB significantly.

As already mentioned earlier (section 5.2.1.2), in the case of the OH···π interaction, it is not possible to define an H-bond length, because the acceptor π system is not a single atom. However, it is interesting to consider the distance between the H atom and the closest C atoms in the acceptor ring B. Table 7.3 reports the distance (Å) between the H atom and the closest C atom in the acceptor aromatic ring, for the conformers in which the O–H···π interaction is present. The distance (2.059–2.240 Å) is in the shorter range for this type of interaction, suggesting that the OH···π interaction in this molecule are strong.

7.2.1.3. Dipole moments of the conformers

Table 7.4 reports the values of the dipole moments of the calculated conformers of *trans*-DBPO. The values of the dipole moments of the calculated conformers range between 0.855 and 9.417 Debye. The orientation of the phenol OHs has a significant influence on the dipole moment of the conformers of the *trans*-DBPO just like in case of myristinin A (section 5.2.1.3). The trends identified from myristinin A hold for *trans-DBPO*. The smallest dipole moment corresponds to the d-r-η-u-p-a-e-j conformer, in which the three OHs in the phloroglucinol moiety and the two OHs in the substituent ring system are oriented in a manner in which their contributions cancel. In this case, the orientation of the OHs in the phloroglucinol moiety is not uniform and, therefore, their total contribution to the dipole moment is not close to zero. On the other hand, O28–H29 and O36–H37 are oriented to the same side. Thus, it is reasonable to infer that the contributions from O28–H29 and O36–H37 and the contribution from the OH in the phloroglucinol moiety largely cancel each other. The highest dipole moment corresponds to the d-w-q-a-f-k conformer, where the OHs of the phloroglucinol moiety have non-uniform orientation and the contributions of O28–H29 and O36–H37 sum up to their contributions enhancing the dipole moment (O28–H29 and O36–H37 are both oriented towards the phloroglucinol moiety).

The u-conformers have smaller dipole moment that the corresponding non-u ones; d-r-u conformers have smaller dipole moment than d-r conformers; d-w-u conformers have smaller dipole moment than d-w conformers; s-r-u conformers have smaller dipole moment than s-r conformers; s-w-u conformers have smaller dipole moment than s-w conformers.

The d-r-e conformers have higher dipole moment than d-r-f conformers; d-w-e conformers have smaller dipole moment than d-w-f conformers; s-r-e conformers have smaller dipole moment than s-r-f conformers; s-w-e conformers have smaller dipole moment than s-w-f conformers. This suggests that the mutual orientation of O28–H29 and O10–H16 influence the dipole moment significantly.

The d-r-j conformers have higher dipole moment than d-r-k conformers; d-w-j conformers have smaller dipole moment than d-w-k conformers; s-r-j conformers have smaller dipole moment than s-r-k conformers; s-w-j conformers have smaller dipole moment than s-w-k conformers. Just like in the previous comparison the orientation of the O36–H37 with respect to the orientation of O10–H16 influence the dipole moment significantly.

The comparison of the dipole moments of conformers differing only by orientation of the B–D–E ring system with respect to the phloroglucinol moiety does not show a consistent pattern, because sometimes p conformer lower dipole moment than q conformer and other times they higher dipole moment. The difference is usually small. This suggests that the dipole moment of the conformers does not depend significantly on the orientation of the B–D–E ring system.

7.2.1.4. HOMO-LUMO energy gap of the conformers

Table 7.5 reports the energy difference between the frontier orbitals (HOMO, highest occupied molecular orbital, and LUMO, lowest unoccupied molecular orbital). The values of the HOMO-LUMO energy gap of the calculated conformers range between 235.536 and 261.025 kcal/mol. The trends observed in section 5.2.1.4 are similar to the ones observed in trans-BPO. The d conformers have smaller HOMO-LUMO energy gap than the corresponding s conformers. The non-u conformers have greater HOMO-LUMO energy gap than the corresponding u conformer. The conformers with O10–H16···π interaction have greater HOMO-LUMO energy gap than the corresponding conformers without O10–H16···π interaction. For d-type conformers, the p conformers have greater HOMO-LUMO energy than the corresponding q conformers. For s-type conformers, the p conformers have smaller HOMO-LUMO energy gap than the q conformer. The orientation of O28–H29 and O36–H37 do not influence the HOMO-LUMO energy difference significantly.

Figure 7.3 shows the shapes of the HOMO and LUMO frontier orbitals for the conformers listed in table 7.1. The shapes of HOMO orbitals show greater electron concentration density in the

phloroglucinol moiety and the other two ring system for all conformers with few exceptions for d-w, d-r-q and s-w-u conformers where the electron density in concentrated in the B–D rings. The shapes of LUMO orbitals show greater concentration of electrons in the phloroglucinol moiety.

7.3. Results for conformers with different geometries of R and the same geometries of the ring system.

7.3.1.1. Types of investigated conformers

This part consider the results of the study of conformers with different geometries of R associated with the best geometry of the phloroglucinol moiety and the B–D–E ring system identified from the study of a model structure considering of these units and R replaced by an ethyl (fig 5.4) [190]. The best identified geometry is d-r-η-p-a-e-j and its stabilising factors are already described in section 5.4.1.1.

Different geometries of the R chain were built by rotating each single bond in turn, as explained in section 4.4. This study involved 25 inputs and yielded 15 conformers, because all the inputs with the R chain bent by ±180° (remaining on the plane of the benzene ring A) optimized to conformers coinciding with those coming from inputs where R has been bent by -90° or +90°; for instance, the input where C13–C18 had been rotated by +180° (to the side of R′) as gave the same output geometry when it had been rotated by -90°.

7.3.1.2. Relative energies of the conformers

Conformers corresponding to the ±90° and ±180° rotations of all the single bonds in R were calculated at the HF/6-31G(d,p) level. The geometries of the optimized conformers are shown in figure 7.4 and their relative energies are reported in table 7.6. The lowest energy conformer is the same as for the first part of the study of *trans*-DBPO (table 7.1). When the R chain is bent, the energy of the conformers where the relevant bond has been rotated by +90 or -90 is the same as the energy of the conformers where the same bond has been rotated by +180 or -180, suggesting that the conformers where the R chain is bent out off the plane are the possible preferred ones than conformers with the R chain bent on the plane identified by the benzene ring A. When the R chain is bent, the energy of the conformers where the relevant bond is being rotated by +90 or -90 are nearly close, with some few exceptions, where the energies are not close, that is when the R chain is bent in the bond that is close to the double bond (C40–C41, C41–C42 and C42–C43). This suggests

that the double bond on the long acyl chain does slightly affect the optimisation of input with symmetrical R.

Table 7.7 reports the values of the relative energies corrected for ZPE and of the ZPE corrections as well as the relative Gibbs free energies ($\Delta G_{corrected}$, sum of electronic and thermal free energy) and its correction, G_{corr}, for the conformers listed in table 7.6 at HF level. The ZPE corrections for all the conformers are comparatively close. Their values range between 476,816 and 477,196 kcal/mol. The greater values of the ZPE corrections correspond to the conformers having higher energy. The relative energies corrected for ZPE and the uncorrected relative energies have the same trends, with only three exceptions (DBPO-d-r-η-p-a-e-j-8y, DBPO-d-r-η-p-a-e-j-2z and DBPO-d-r-η-p-a-e-j-2y). Conformers with lower relative energy have lower relative Gibbs free energies. The values of G_{corr} are comparatively close.

DFT/B3LYP/6-31+G(d,p) and MP2/ 6-31G(d,p) calculations were performed on the conformers of this part having lower energy in the HF results. Table 7.13 reports the relative energies obtained from these calculations and compares them with the HF results. The relative energy (kcal/mol) of the highest energy conformer of this set is 1.076 / HF, 1.013 /DFT and 0.896 /MP2, showing a narrowing of the energy range. Furthermore, the energy sequence of the conformers is not the same with the three methods. Thus, the lowest and highest energy conformers are not the same with the three methods, as it is, the lowest energy conformer at HF and DFT levels is DBPO d-r-η-p-a-e-j, and at MP2 level, is DBPO-d-r-η-p-a-e-j-8y. The highest energy conformer at HF and MP2 is DBPO-d-r-η-p-a-e-j-7z, and at DFT levels is DBPO-d-r-η-p-a-e-j-4z.

7.3.1.3. Characteristics of intramolecular hydrogen bonds

Table 7.14 reports the parameters of the first IHB in the lowest energy conformers of *trans*-DBPO listed in table 7.6 *in vacuo*, at HF/6-31G(d,p), DFT/B3LYP/B3LYP/6-31+G(d,p) and MP2/ 6-32G(d,p) levels of theory. HF gave the longest bond lengths, DFT gave the shortest and MP2 gave intermediate values. This is consistent with the fact that HF underestimates the strength of H-bonds, and DFT overestimates it; the MP2 results can be considered as those closer to the actual values. The ranges of the bond lengths (Å) of H15···O14 are 1.644–1.583 /HF, 1.518–1.530 /DFT and 1.573–1.585 /MP2. These values indicate that the first IHB is comparatively strong. The values of the O···O distance are nearly close to 2.5 Å for all results obtained (2.503–2.509 /HF, 2.459–2.468 /DFT and 2.498–2.505 /MP2.). The OĤO bond angles are estimated around 147° /HF, 151° /DFT and 151° MP2.

For the O–H···π interactions (table 7.15), the distance (Å) between the H atom and the closest C atom of the B aromatic ring is 127–2.129 /HF, 1.039–2.059 /DFT and 2.007–2.012 /MP2. By comparing the results of the three methods, one can see that MP2 optimizes to geometries with longer IHBs; this is consistent with the fact that it takes into account also dispersion contributions.

Table 7.10 reports the values of the calculated vibrational frequency of the O–H bonds in selected conformers of *trans*-DBPO *in vacuo* at the HF level. The values of the calculated vibrational frequency also show that the orientation of the R chain has a significant influence on the vibrational frequency of O8–H15 and O12–H17 and minor influence on the vibrational frequency of O51–H52, O28–H29 and O10–H16. When the R chain is bent at C13–C18 by +90° or -90°, the vibrational frequency of O8–H15 increases slightly and that of O12–H17 decreases slightly. When the R chain is bent at C7–C13 by +90° or -90°, the vibrational frequency of O8–H15 decreases slightly and that of O12–H17 increases slightly.

7.3.1.4. Dipole moments of the conformers

Table 7.16 reports the values of the dipole moments of the conformers calculated in this part, at HF/6-31G(d,p), DFT/B3LYP/B3LYP/6-31+G(d,p) and MP2/6-31G(d,p) levels of theory. There is no typical sequence in the values of the dipole moments in the results of the different methods utilised. Comparison of the values of the dipole moments obtained with the three different methods shows that DFT yields lower values with respect to other two methods. The values of the dipole moments range between 2.247 and 2.435 Debye in the HF results, between 2.181 and 2.497 Debye in the DFT results, and between 2.264 and 2.520 Debye in the MP2 results.

7.3.1.5. HOMO-LUMO energy gap of the conformers

Table 7.17 reports the values of the HOMO-LUMO energy gap of the calculated conformers of *trans*-DBPO *in vacuo,* at HF/6-31G(d,p), DFT/B3LYP/B3LYP/6-31+G(d,p) and MP2/6-31G(d,p) level of theory. The values of the HOMO-LUMO energy gap range between 255.396 and 257.561 kcal/mol in the HF results, between 1.989 and 3.075 kcal/mol in the DFT results, and 247.621 and 249.184 kcal/mol in the MP2 results.

Comparisons of the three methods show a huge difference between the values HOMO-LUMO energy gap of the DFT and the other two methods (HF and MP2). For analyses purpose, one can consider the values of the HOMO-LUMO energy gap from the MP2 results, because this method

gives the results which are close to the experimental ones. The highest values of HOMO-LUMO energy gap corresponds to the conformers which were obtained by bending the C38–C39, C40–C41 and C42–C43 bonds of the R chain by -90° or +90°. The smallest values of the HOMO-LUMO energy gap correspond to the conformers in which the bond that was rotated is closer to the sp^2 O of the acyl group (for instance, the C13–C18 bond).

Figure 7.5 shows the shapes of the HOMO and LUMO frontier orbitals for the conformers listed in table 7.6. The shapes of HOMO orbitals show a greater electron concentration density in the phloroglucinol moiety and B-D-E ring system. The shapes of LUMO orbitals show a greater electron concentration density in the phloroglucinol moiety.

7.3.2. Results in solution

7.3.2.1. Relative energies of the conformers

Calculations in solution were performed on the conformers listed in table 7.6, at the HF level. Table 7.18 reports the relative energy of these conformers in different media (vacuum, chloroform, acetonitrile and water). The relative energies of the conformers show that DBPO-d-r-η-p-a-e-j, remains the most stable conformer in solution. The values of the relative energy also show that the conformers have lower energy *in vacuo* than in solution. The relative energy of the conformers slightly increases with an increase in solvent polarity (taken as the chloroform–acetonitrile–water sequence), with only three exceptions (DBPO-d-r-η-p-a-e-j-2y, DBPO-d-r-η-p-a-e-j-2z and DBPO-d-r-η-p-a-e-j-6z) where the trend is reversed.

Table 7.19 reports the free energy of solvation (solvent effect, ΔG_{solv}) and its electrostatic component (G_{el}) for the conformers of *trans*-DBPO calculated in part two. ΔG_{solv} is positive in acetonitrile and negative in chloroform and water. The magnitude of ΔG_{solv} ranges between 1.97 to 2.55, 5.91 to 6.48 and 16.12 to 16.81 kcal/mol in chloroform, acetonitrile and water respectively. The magnitude of ΔG_{solv} increases with the solvent-polarity. The electrostatic component (G_{el}) has negative values in all three solvents and its magnitude is greater in water than in the other two solvents.

7.3.2.2. Characteristics of intramolecular hydrogen bonds

Table 7.20 reports the parameters of the first IHB *in vacuo* and in the three solvents, for the conformers that have been calculated in solution. The range of the bond lengths (Å) of the H15···O14 is 1.644–1.654, 1.640–1.651, 1.638–1.651 and 1. 1.638–1.651, respectively, *in vacuo*, chloroform acetonitrile and water. Thus, the value of the bond lengths of the H15···O14 decreases with an increase in the media polarity. The values of the O···O distance increases with an increase in the media polarity. The values of the OĤO bond angles increases with an increase in the media polarity.

Table 7.21 reports the distance (Å) between the H atom and the closest C atom (H16···C39) in the acceptor B aromatic ring for the O–H···π interactions of the calculated conformers of *trans*-DBPO in the media considered. There is no drastical change in the H16···C23 distance; however, there are some slight changes. The values of the H16···C23 distance range comparatively close to 2 in different media. Thus, the H16···C23 distance is smaller in chloroform than *in vacuo*, with only two exceptions (DBPO-d-r-η-p-a-e-j-7y and DBPO-d-r-η-p-a-e-j-4y), where the trend is reversed, and smaller in acetonitrile or water than in chloroform, with some few exceptions (DBPO-d-r-η-p-a-e-j-8y and DBPO-d-r-η-p-a-e-j-5y), where the distance remains the same.

7.3.2.3. Dipole moments and HOMO-LUMO energy gaps in different media

Table 7.22 reports the values of the dipole moments of the conformers of *trans*-DBPO calculated in different media. Dipole moment slightly increases as the medium polarity increases. The ranges of the values of the dipole moments are 2.097–2.607, 2.463–3.009, 2.596–3.253 and 2.609–3.272 Debye *in vacuo*, chloroform acetonitrile and water respectively.

Table 7.23 reports the values of the HOMO-LUMO energy gap of the conformers of *trans*-DBPO calculated in different media. The HOMO-LUMO energy gap slightly increases as the medium polarity increases. The ranges of the values of the HOMO-LUMO energy gaps are 255.359–257.511, 254.235–256.890, 254.016–256.626 and 253.984–256.607 kcal/mol *in vacuo*, chloroform acetonitrile and water respectively.

7.4. Overview of the results

The results have been analysed separately for part one and part two because of the different approaches in the preparation of the inputs and in the considering geometry aspects. Since the molecule is the same, it is important to have an overall view of all the results. Using the criteria explained in section 4.4, a total of 115 conformers of *trans*-DBPO was calculated.

Table 7.24 reports the values of the relative energies for all the conformers of *trans*-DBPO *in vacuo*, at the HF level. The relative energies of the conformers having different geometries of R and the same geometry of the ring system account for most of the lower energy conformers. This is to be expected because these conformers have the best geometry of the ring systems. Thus, these results show that the influence of the geometry of R on the overall energy of the molecule is smaller than the influence of the ring systems; this is understandable by considering that the ring system contains the most important stabilising factors such as the first IHB and O–H···π interaction. It is noticed that the acyl chain group and the ring systems somewhat do influence the conformational preferences and other molecular properties of *trans*-DBPO.

Table 7.25 reports the values of the parameters of the first IHB for all the conformers of *trans*-DBPO *in vacuo*, at the HF level. The values of the parameters of the first IHB of the conformers having different geometries of R and the same geometry of the ring system show that the influence of the geometry of R on the overall parameters of the first IHB of the molecule is smaller than the influence of the ring systems. Like for the energy, this is to be expected because these conformers have the best geometry for the ring systems as already mention in the previous comparison.

Table 7.26 reports the values of the distance between the H atom and the closest C atom in the acceptor aromatic B ring for all the conformers of *trans*-DBPO *in vacuo*, at the HF level. The values of the distance between the H atom and the closest C atom in the acceptor aromatic B ring of the conformers having different geometries of R and the same geometry of the ring system show that the geometry of R on the overall does influence the O–H···π interactions. Like for the energy, this is to be expected because these conformers have the best geometry for the ring systems as already mention in the previous comparison.

Table 7.27 reports the values of the dipole moments for all the conformers of *trans*-DBPO *in vacuo*, at the HF level. The values of the dipole moments of the conformers having different geometries of R and the same geometry of the ring system are all around 2 Debye; this is to be expected because

these conformers have the same geometry of the ring systems, all the OHs are oriented in the same way, and, therefore, it can be concluded that the orientation of the acyl chain does not significantly influence the values of the dipole moments.

Table 7.28 reports the values of the HOMO-LUMO energy gaps for all the conformers of *trans*-DBPO *in vacuo*, at the HF level. The HOMO-LUMO energy gaps of the conformers having different geometries of R and the same geometry of the ring system show that the influence of the geometry of R on the overall HOMO-LUMO energy gap of the molecule is smaller than the influence of the ring systems. Like for the energy, this is understandable by considering that the ring system contains the most important stabilising factors.

Figure 7.2. Optimized conformers of *trans*-DBPO having the same geometry of R and different geometries of the ring system *in vacuo*.
HF/6-31G(d,p) results. The conformers are listed in order of increasing relative energy.

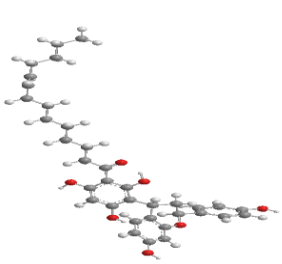

t-DBPO-d-r-η-p-a-e-j

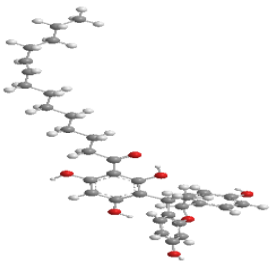

t-DBPO-d-r-η-p-a-e-k

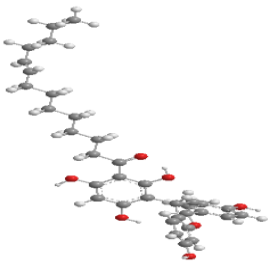

t-DBPO-d-r-η-p-a-f-j

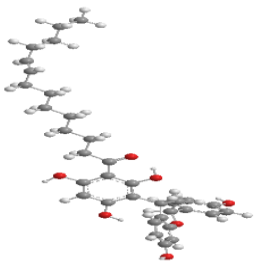

t-DBPO-d-r-η-p-a-f-k

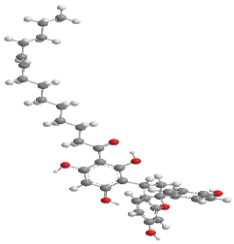

t-DBPO-d-r-η-p-b-e-k

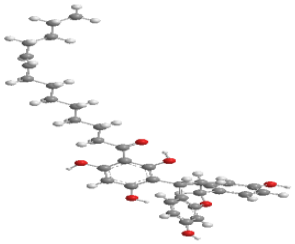

t-DBPO-d-r-η-p-b-e-j

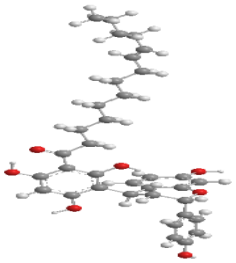

t-DBPO-s-w-ε-q-a-e-k

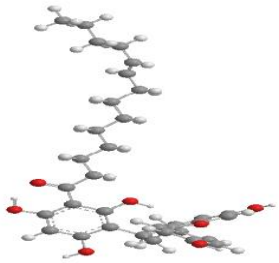

t-DBPO-s-w-ε-q-a-e-j

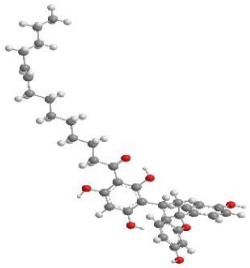

t-DBPO-d-r-η-p-b-f-j

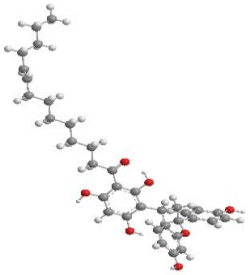

t-DBPO-d-r-η-p-b-f-k

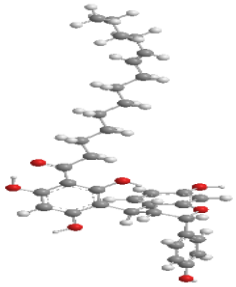

t-DBPO-s-w-ε-q-b-e-j

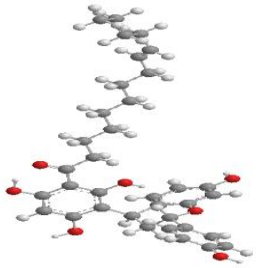

t-DBPO-s-w-ε-q-a-f-j

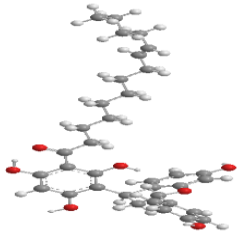

t-DBPO-s-w-ε-q-a-f-k

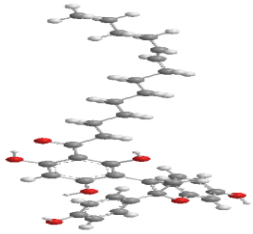

t-DBPO-s-w-u-q-b-e-k

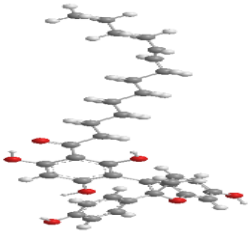

t-DBPO-s-w-ε-q-b-f-k

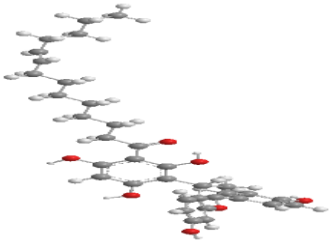

t-DBPO-d-w-p-a-e-k

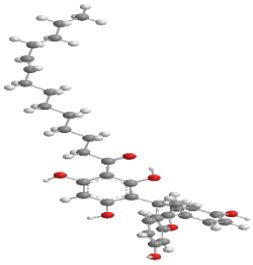

t-DBPO-d-w-p-a-f-j

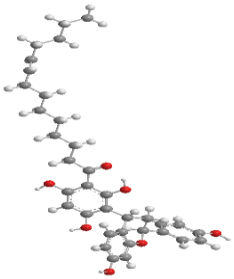

t-DBPO-d-w-p-b-f-j

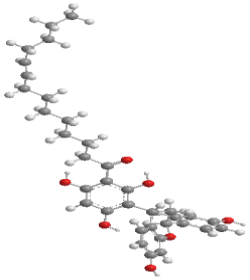

t-DBPO-d-r-η-u-p-a-e-j

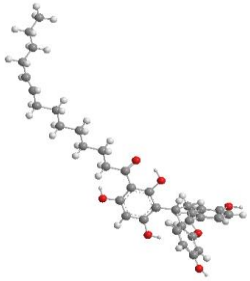

t-DBPO-d-r-η-u-p-a-e-k

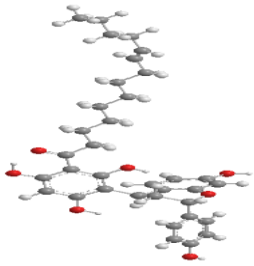

t-DBPO-s-r-ε-q-b-e-j

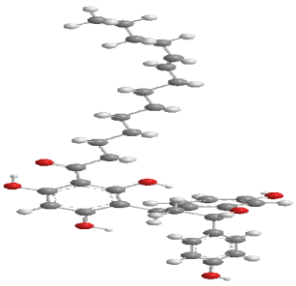

t-DBPO-s-r-ε-q-b-f-j

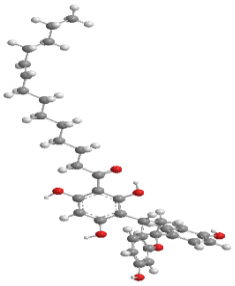

t-DBPO-d-w-p-a-f-k

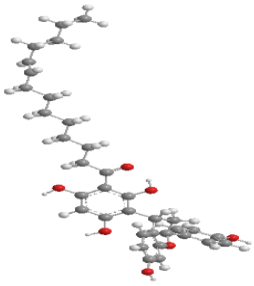

t-DBPO-d-w-p-b-e-j

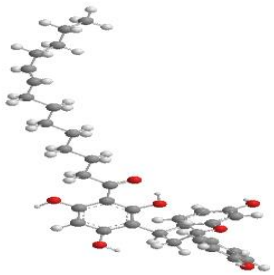

t-DBPO-d-r-q-b-f-j

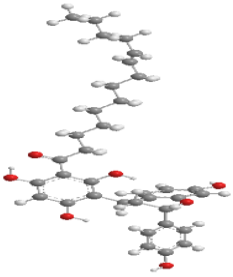

t-DBPO-s-r-ε-q-b-f-k

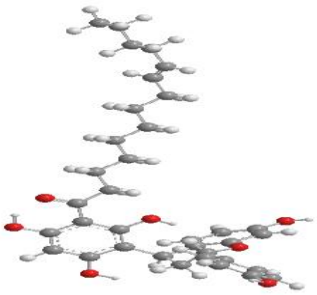

t-DBPO-s-r-ε-q-a-e-k

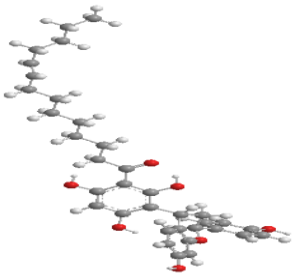

t-DBPO-d-r-η-u-p-a-f-j

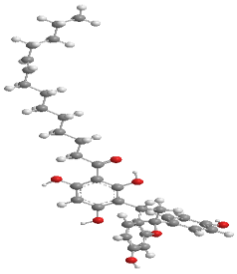

t-DBPO-d-w-p-b-e-k

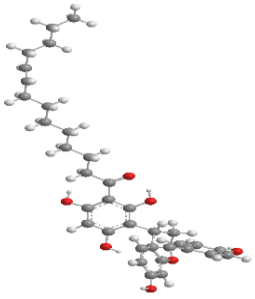

t-DBPO-d-r-η-u-p-a-f-k

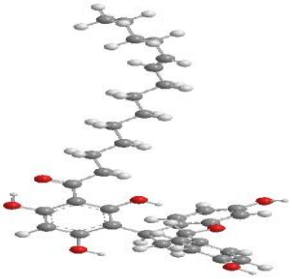

t-DBPO-s-r-ε-q-a-e-j

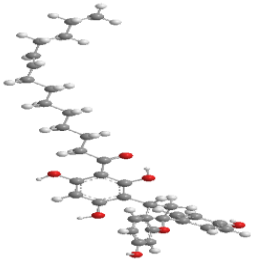

t-DBPO-d-w-q-b-e-j

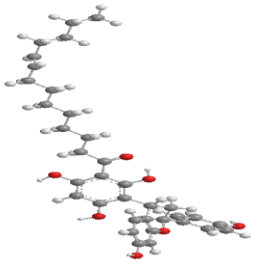

t-DBPO-d-w-p-b-f-k

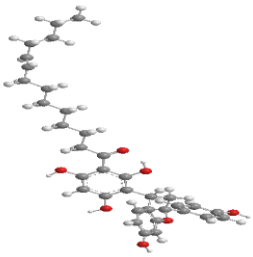

t-DBPO-d-w-p-a-e-j

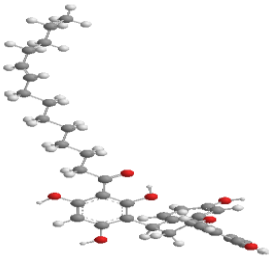

t-DBPO-d-w-q-a-e-j

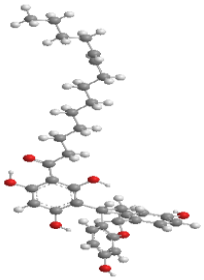

t-DBPO-s-r-η-p-e-a-k

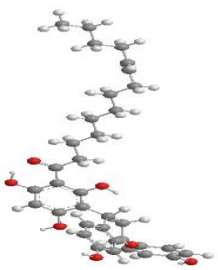

t-DBPO-s-r-η-p-b-e-k

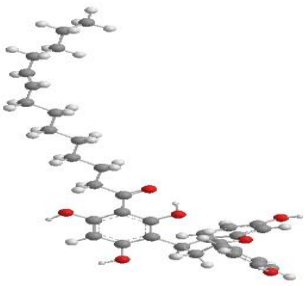

t-DBPO-d-w-q-a-e-k

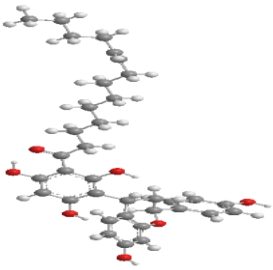

t-DBPO-s-r-η-p-a-e-j

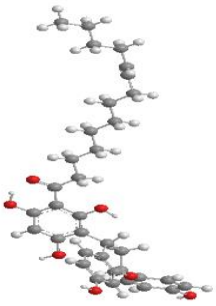

t-DBPO-s-r-η-p-b-f-k

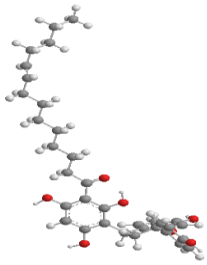

t-DBPO-d-w-q-b-f-j

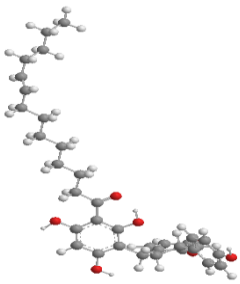

t-DBPO-d-r-q-b-f-k

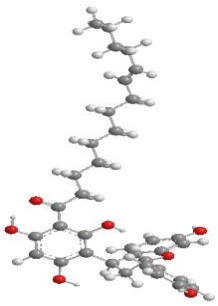

t-DBPO-s-r-ε-q-a-f-k

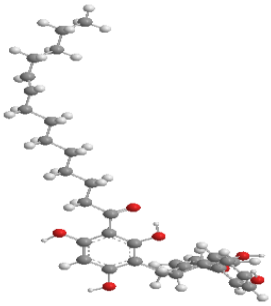

t-DBPO-d-w-q-b-e-k

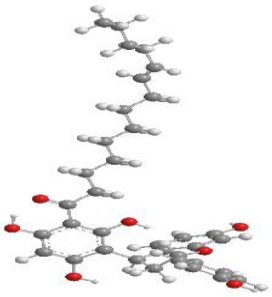

t-DBPO-s-r-ε-q-a-f-j

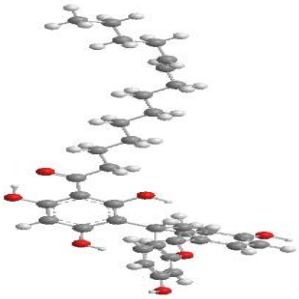

t-DBPO-s-w-p-b-f-j

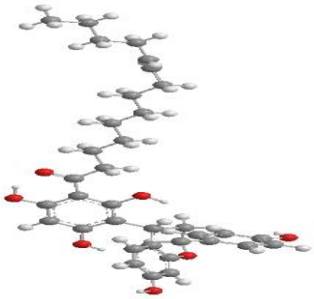

t-DBPO-s-r-η-p-a-f-k

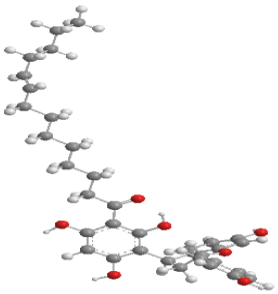

t-DBPO-d-w-q-a-f-j

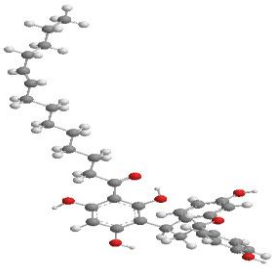

t-DBPO-d-r-q-a-e-j

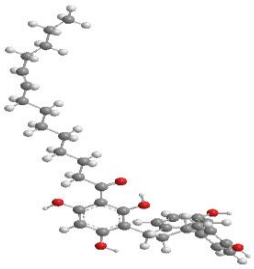

t-DBPO-d-r-q-b-e-j

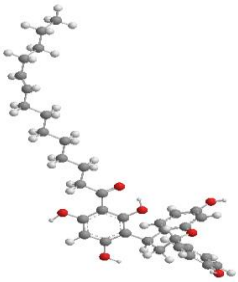

t-DBPO-d-r-q-a-e-k

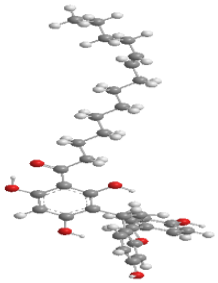

t-DBPO-s-r-η-p-a-f-j

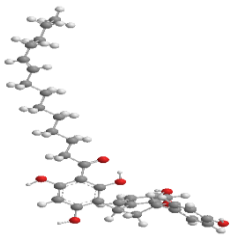

t-DBPO-d-w-q-a-f-k

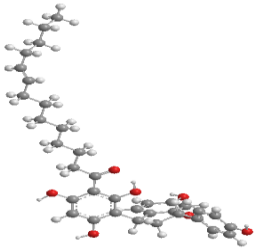

t-DBPO-d-w-q-b-f-k

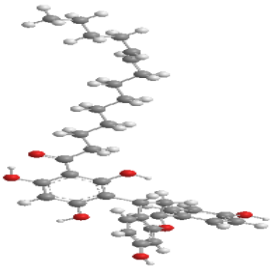

t-DBPO-s-w-p-a-e-j

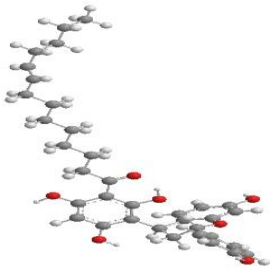

t-DBPO-d-r-q-a-f-k

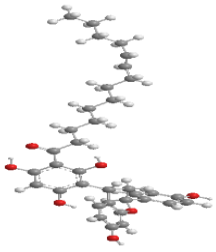

t-DBPO-s-r-η-u-p-a-e-j

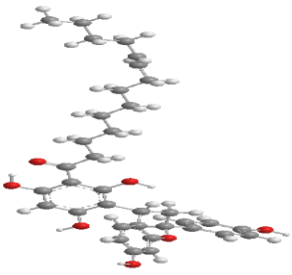

t-DBPO-s-w-p-a-f-j

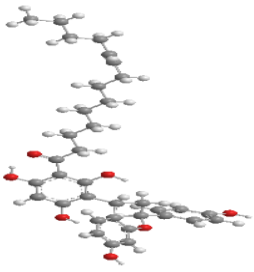

t-DBPO-s-r-η-p-b-e-j

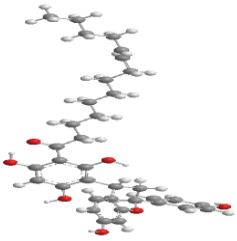

t-DBPO-s-w-p-a-f-k

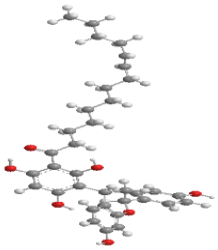

t-DBPO-s-r-η-u-p-a-f-j

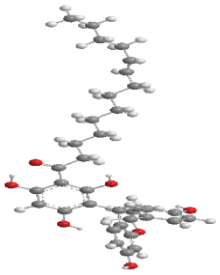

t-DBPO-s-r-η-u-p-a-f-k

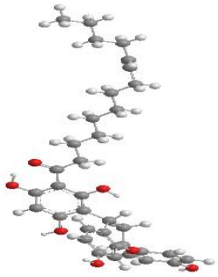

t-DBPO-d-r-q-b-e-k

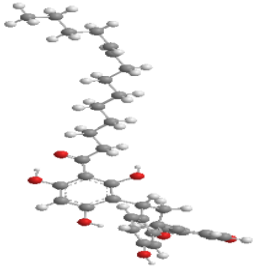

t-DBPO-s-r-η-u-p-b-e-k

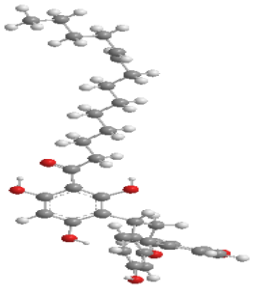

t-DBPO-s-r-η-u-p-b-f-k

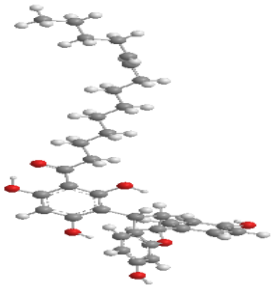

t-DBPO-s-w-p-e-a-k

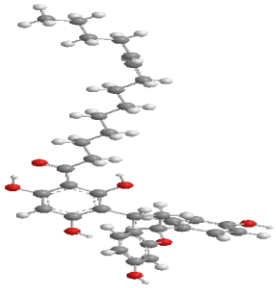

t-DBPO-d-w-u-p-a-e-j

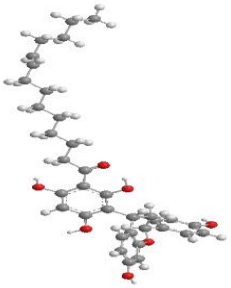

t-DBPO-d-w-u-p-a-e-k

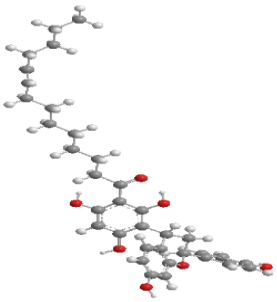

t-DBPO-d-w-u-p-b-e-k

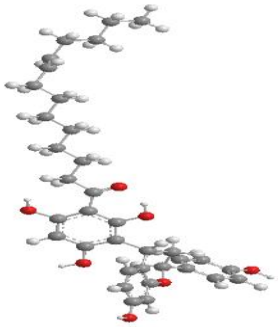

t-DBPO-d-w-u-p-a-f-j

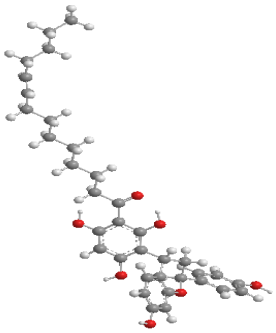

t-DBPO-d-w-u-p-b-f-j

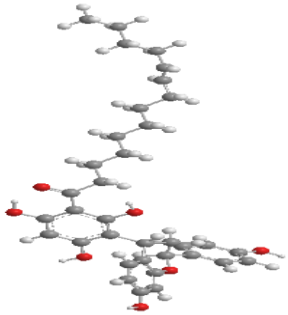

t-DBPO-s-w-u-p-a-f-j

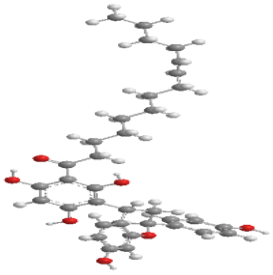

t-DBPO-s-w-u-p-b-e-j

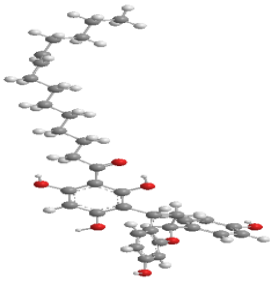

t-DBPO-d-w-u-p-a-f-k

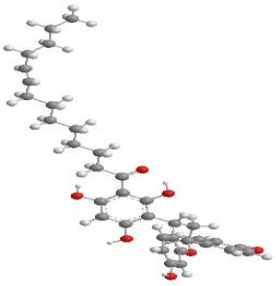

t-DBPO-d-w-u-p-b-f-k

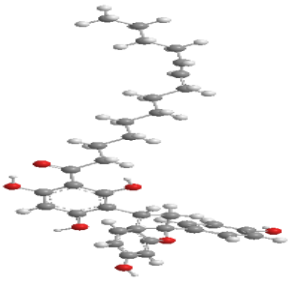

t-DBPO-s-w-u-p-e-a-k

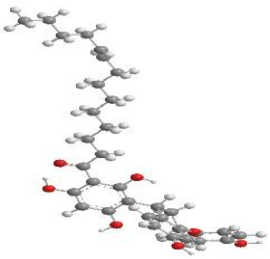

t-DBPO-s-w-p-b-e-j

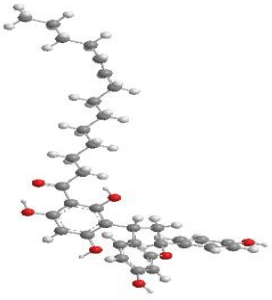

t-DBPO-s-w-u-p-a-e-j

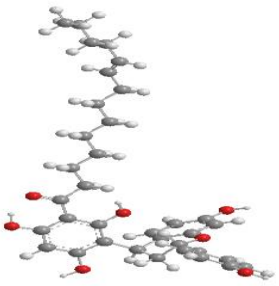

t-DBPO-s-w-u-q-a-e-j

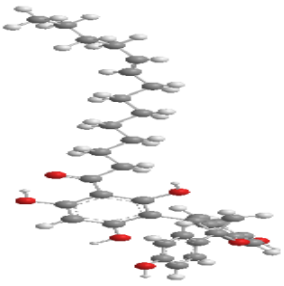

t-DBPO-s-w-u-q-b-e-j

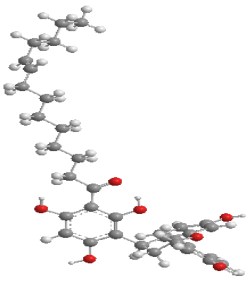

t-DBPO-d-w-u-q-b-e-j

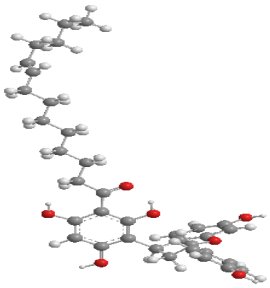

t-DBPO-d-w-u-q-a-e-j

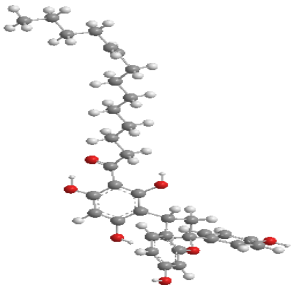

t-DBPO-s-w-u-p-b-f-j

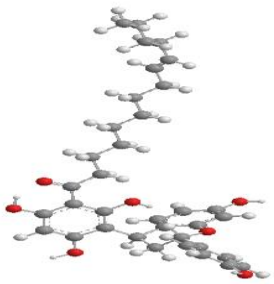

t-DBPO-s-w-u-q-a-e-k

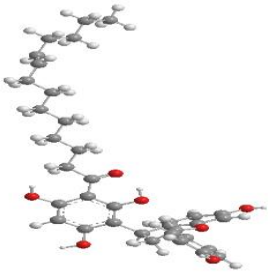

t-DBPO-d-w-u-q-a-e-k

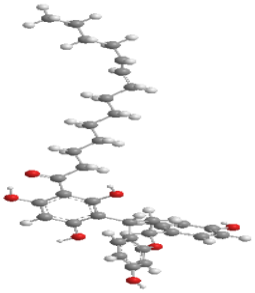

t-DBPO-s-w-u-p-b-e-k

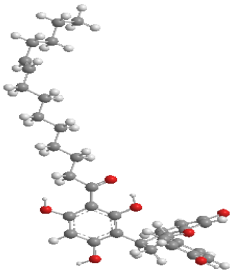

t-DBPO-d-w-u-q-b-f-j

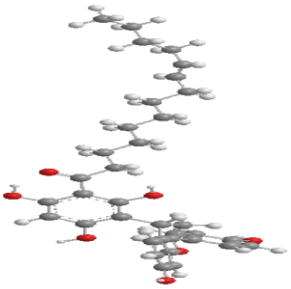

t-DBPO-s-w-u-p-a-f-k

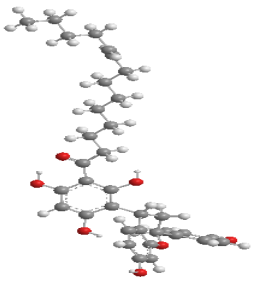

t-DBPO-s-w-u-p-b-f-k

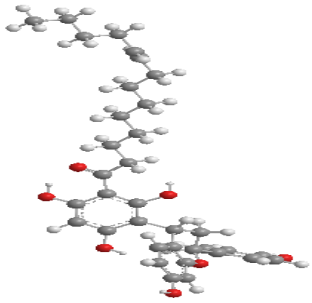

t-DBPO-d-w-u-q-a-f-j

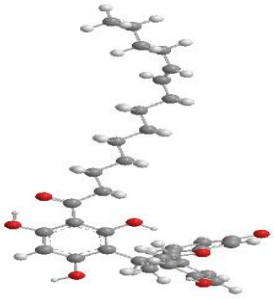

t-DBPO-s-w-u-q-a-f-k

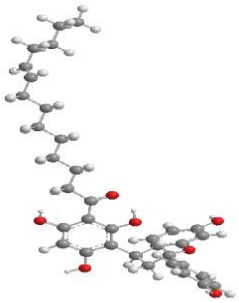

t-DBPO-d-w-u-q-a-f-k

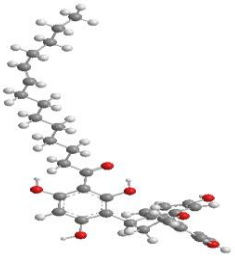

t-DBPO-d-w-u-q-b-f-k

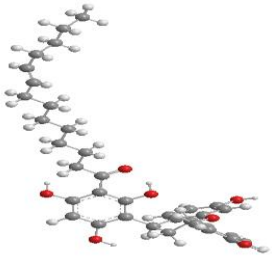

t-DBPO-d-r-u-q-a-e-j

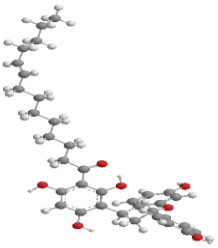

t-DBPO-s-r-u-q-b-e-j

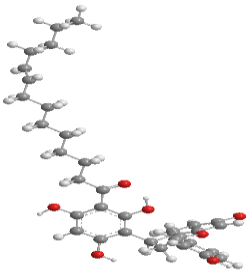

t-DBPO-d-r-q-a-f-

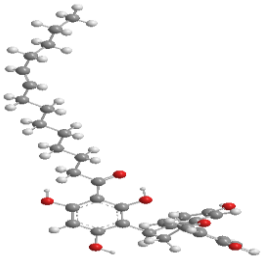

t-DBPO-d-r-u-q-a-f-j

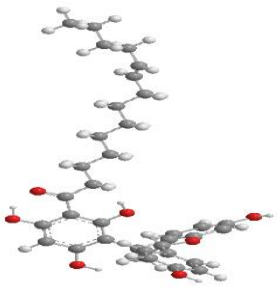

t-DBPO-s-r-u-q-a-e-j

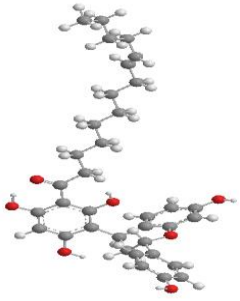

t-DBPO-s-r-u-q-a-e-k

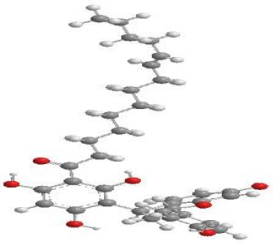

t-DBPO-s-r-u-q-a-f-j

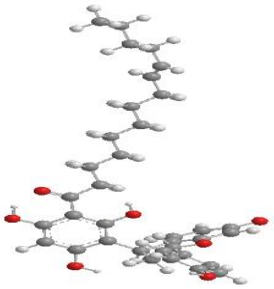

t-DBPO-s-r-u-q-a-f-k

Table 7.1. Relative energies of the calculated conformers of *trans*-DBPO having the same geometry of R and different geometries of the ring system.
HF/6-31G(d,p) results *in vacuo*. The conformers are listed in order of increasing relative energy. The absolute energy of the lowest energy conformer is -1885.7373341 hartree.

Conformer	Relative energy kcal/mol	Conformer	Relative energy kcal/mol
t-DBPO-d-r-η-p-a-e-j	0.000	t-DBPO-d-w-q-a-f-k	5.827
t-DBPO-d-r-η-p-a-e-k	0.014	t-DBPO-d-w-q-b-f-j	5.853
t-DBPO-d-r-η-p-a-f-j	0.424	t-DBPO-d-w-q-b-f-k	5.936
t-DBPO-d-r-η-p-a-f-k	0.496	t-DBPO-d-r-q-b-f-j	6.116
t-DBPO-d-r-η-p-b-e-k	1.023	t-DBPO-s-w-p-a-e-j	6.122
t-DBPO-d-r-η-p-b-e-j	1.028	t-DBPO-d-r-q-b-f-k	6.149
t-DBPO-s-w-ε-q-a-e-k	1.154	t-DBPO-d-r-q-a-f-j	6.158
t-DBPO-s-w-ε-q-a-e-j	1.200	t-DBPO-d-r-q-a-f-k	6.228
t-DBPO-d-r-η-p-b-f-j	1.231	t-DBPO-s-r-η-u-p-b-e-k	6.236
t-DBPO-d-r-η-p-b-f-k	1.264	t-DBPO-s-r-η-u-p-a-e-j	6.281
t-DBPO-s-w-ε-q-b-e-j	1.496	t-DBPO-d-w-u-p-a-e-j	6.398
t-DBPO-s-w-ε-q-a-f-j	1.636	t-DBPO-s-w-p-a-f-j	6.429
t-DBPO-s-w-ε-q-a-f-k	1.652	t-DBPO-s-w-p-a-f-k	6.509
t-DBPO-s-w-ε-q-b-f-k	1.976	t-DBPO-s-w-u-p-b-f-j	6.615
t-DBPO-d-w-p-a-e-j	4.323	t-DBPO-s-r-η-u-p-a-f-j	6.705
t-DBPO-d-w-p-a-e-k	4.459	t-DBPO-s-r-η-u-p-a-f-k	6.722
t-DBPO-d-w-p-a-f-j	4.658	t-DBPO-s-w-p-b-e-j	7.079
t-DBPO-d-w-p-b-f-j	4.678	t-DBPO-s-w-p-e-a-k	7.159
t-DBPO-d-r-η-u-p-a-e-j	4.696	t-DBPO-s-r-η-u-p-b-f-k	7.172
t-DBPO-d-r-η-u-p-a-e-k	4.684	t-DBPO-s-r-η-p-b-f-k	7.459
t-DBPO-s-r-ε-q-b-e-j	4.705	t-DBPO-d-w-u-p-a-e-k	7.851
t-DBPO-s-r-ε-q-b-f-j	4.833	t-DBPO-d-w-u-p-b-e-k	7.875
t-DBPO-d-w-p-a-f-k	4.853	t-DBPO-d-w-u-p-a-f-j	8.070
t-DBPO-s-r-ε-q-b-f-k	5.026	t-DBPO-d-w-u-p-b-f-j	8.095
t-DBPO-s-r-ε-q-a-e-k	5.031	t-DBPO-s-w-u-p-a-e-j	8.201
t-DBPO-s-r-η-p-b-e-j	5.046	t-DBPO-d-w-u-p-a-f-k	8.256
t-DBPO-d-r-η-u-p-a-f-j	5.096	t-DBPO-d-w-u-p-b-f-k	8.258
t-DBPO-s-r-ε-q-a-e-j	5.155	t-DBPO-s-w-u-p-e-a-k	8.285
t-DBPO-d-w-p-b-e-k	5.166	t-DBPO-d-w-u-q-a-e-j	8.391
t-DBPO-d-r-η-u-p-a-f-k	5.163	t-DBPO-s-w-u-q-a-e-j	8.409
t-DBPO-d-w-q-b-e-j	5.188	t-DBPO-d-w-u-q-a-e-k	8.488
t-DBPO-d-w-p-b-f-k	5.228	t-DBPO-s-w-u-q-a-e-k	8.500
t-DBPO-d-w-q-a-e-j	5.213	t-DBPO-s-w-u-p-a-f-j	8.557
t-DBPO-s-r-η-p-e-a-k	5.222	t-DBPO-s-w-u-p-a-f-k	8.702
t-DBPO-s-r ε-p-b-e-k	5.265	t-DBPO-s-w-u-q-b-e-k	8.739
t-DBPO-d-w-q-a-e-k	5.291	t-DBPO-d-w-u-q-a-f-j	8.850
t-DBPO-s-r-η-p-a-e-j	5.355	t-DBPO-s-w-u-p-b-f-k	8.867
t-DBPO-s-r-ε-q-a-f-k	5.505	t-DBPO-s-w-u-q-a-f-k	8.884
t-DBPO-d-w-q-b-e-k	5.559	t-DBPO-d-w-u-q-a-f-k	9.008
t-DBPO-s-r-ε-q-a-f-j	5.565	t-DBPO-d-w-u-q-b-f-k	9.239
t-DBPO-s-w-p-b-f-j	5.596	t-DBPO-d-r-u-q-a-e-j	10.163
t-DBPO-s-r-η-p-a-f-k	5.682	t-DBPO-s-r-u-q-b-e-j	10.283
t-DBPO-d-w-q-a-f-j	5.687	t-DBPO-d-r-u-q-a-f-j	10.563

t-DBPO-d-r-q-a-e-j	5.718	t-DBPO-s-r-u-q-a-e-j	11.105
t-DBPO-d-r-q-b-e-k	5.719	t-DBPO-s-r-u-q-a-e-k	11.128
t-DBPO-d-r-q-b-e-j	5.736	t-DBPO-s-r-u-q-a-f-j	11.402
t-DBPO-d-r-q-a-e-k	5.745	t-DBPO-s-r-u-q-a-f-k	11.487
t-DBPO-s-r-η-p-a-f-j	5.754		

Table 7.2. Parameters of the first IHB of the calculated conformers of *trans*-DBPO having the same geometry of R and different geometries of the ring system.
HF/6-31G(d,p) results *in vacuo*. For conformers of d type, the first IHB is H15···O14; for conformers of s type, the first IHB is H17···O14. The conformers are listed in order of increasing relative energy.

Conformer	OH···O (Å)	O···O (Å)	OHO (°)
t-DBPO-d-r-η-p-a-e-j	1.652	2.508	146.4
t-DBPO-d-r-η-p-a-e-k	1.652	2.508	146.3
t-DBPO-d-r-η-p-a-f-j-	1.652	2.508	146.4
t-DBPO-d-r-η-p-a-f-k	1.652	2.508	146.3
t-DBPO-d-r-η-p-b-e-k	1.651	2.508	146.6
t-DBPO-d-r-η-p-b-e-j	1.655	2.510	146.2
t-DBPO-s-w-ε-q-a-e-k	1.684	2.522	143.9
t-DBPO-s-w-ε-q-a-e-j	1.684	2.521	143.9
t-DBPO-d-r-η-p-b-f-j	1.655	2.510	146.2
t-DBPO-d-r-η-p-b-f-k	1.651	2.509	146.5
t-DBPO-s-w-ε-q-b-e-j	1.689	2.527	144.0
t-DBPO-s-w-ε-q-a-f-j	1.682	2.520	143.9
t-DBPO-s-w-ε-q-a-f-k	1.683	2.521	143.9
t-DBPO-s-w-ε-q-b-f-k	1.689	2.526	144.0
t-DBPO-d-w-p-a-e-j	1.656	2.511	146.2
t-DBPO-d-w-p-a-e-k	1.656	2.511	146.2
t-DBPO-d-w-p-a-f-j	1.656	2.511	146.2
t-DBPO-d-w-p-b-f-j	1.656	2.510	146.3
t-DBPO-d-r-η-u-p-a-e-j	1.675	2.523	145.4
t-DBPO-d-r-η-u-p-a-e-k	1.676	2.524	145.4
t-DBPO-s-r-ε-q-b-e-j	1.695	2.531	143.9
t-DBPO-s-r-ε-q-b-f-j	1.694	2.531	143.9
t-DBPO-d-w-p-a-f-k	1.656	2.511	146.2
t-DBPO-s-r-ε-q-b-f-k	1.694	2.531	143.9
t-DBPO-s-r-ε-q-a-e-k	1.692	2.527	143.8
t-DBPO-s-r-η-p-b-e-j	1.697	2.532	143.7
t-DBPO-d-r-η-u-p-a-f-j	1.675	2.522	145.4
t-DBPO-d-w-p-b-e-k	1.658	2.512	146.2
t-DBPO-d-r-η-u-p-a-f-k	1.676	2.523	145.4
t-DBPO-s-r-ε-q-a-e-j	1.690	2.526	143.8
t-DBPO-d-w-p-b-e-j	1.659	2.512	146.1
t-DBPO-d-w-q-b-e-j	1.664	2.514	145.6
t-DBPO-d-w-p-b-f-k	1.659	2.513	146.1

t-DBPO-d-r-q-b-f-j	1.649	2.506	146.3
t-DBPO-d-w-q-a-e-j	1.654	2.508	146.1
t-DBPO-s-r-η-p-e-a-k	1.697	2.532	143.7
t-DBPO-s-r-η-p-b-e-k	1.692	2.528	143.8
t-DBPO-d-w-q-a-e-k	1.654	2.508	146.1
t-DBPO-s-r-η-p-a-e-j	1.697	2.532	143.7
t-DBPO-s-r-ε-q-a-f-k	1.689	2.526	143.8
t-DBPO-d-w-q-b-e-k	1.664	2.514	145.6
t-DBPO-s-r-ε-q-a-f-j	1.688	2.524	143.9
t-DBPO-s-w-p-b-f-j	1.683	2.521	143.9
t-DBPO-s-r-η-p-a-f-k	1.697	2.532	143.7
t-DBPO-d-w-q-a-f-j	1.655	2.509	146.0
t-DBPO-d-r-q-a-e-j	1.646	2.503	146.4
t-DBPO-d-r-q-b-e-k	1.647	2.505	146.5
t-DBPO-d-r-q-b-e-j	1.647	2.504	146.4
t-DBPO-d-r-q-a-e-k	1.646	2.503	146.4
t-DBPO-s-r-η-p-a-f-j	1.696	2.531	143.7
t-DBPO-d-w-q-a-f-k	1.656	2.509	146.0
t-DBPO-d-w-q-b-f-k	1.657	2.511	146.0
t-DBPO-s-w-p-a-e-j	1.689	2.526	143.7
t-DBPO-d-r-q-b-f-k	1.649	2.506	146.3
t-DBPO-d-r-q-a-f-j	1.648	2.504	146.3
t-DBPO-d-r-q-a-f-k	1.648	2.504	146.3
t-DBPO-s-r-η-u-p-b-e-k	1.736	2.559	142.5
t-DBPO-s-r-η-u-p-a-e-j	1.737	2.560	142.4
t-DBPO-d-w-u-p-a-e-j	1.714	2.546	143.4
t-DBPO-s-w-p-a-f-j	1.689	2.526	143.8
t-DBPO-s-w-p-a-f-k	1.689	2.526	143.8
t-DBPO-s-w-u-p-b-f-j	1.739	2.562	142.5
t-DBPO-s-r-η-u-p-a-f-j	1.738	2.560	142.4
t-DBPO-s-r-η-u-p-a-f-k	1.737	2.560	142.4
t-DBPO-s-w-p-b-e-j	1.686	2.523	143.7
t-DBPO-s-w-p-e-a-k	1.686	2.522	143.8
t-DBPO-s-r-η-u-p-b-f-k	1.731	2.555	142.6
t-DBPO-s-r-η-p-b-f-k	1.686	2.523	143.8
t-DBPO-d-w-u-p-a-e-k	1.681	2.526	145.2
t-DBPO-d-w-u-p-b-e-k	1.681	2.526	145.2
t-DBPO-d-w-u-p-a-f-j	1.682	2.527	145.2
t-DBPO-d-w-u-p-b-f-j	1.682	2.527	145.3
t-DBPO-s-w-u-p-a-e-j	1.682	2.527	145.2
t-DBPO-d-w-u-p-a-f-k	1.682	2.527	145.2
t-DBPO-d-w-u-p-b-f-k	1.682	2.528	145.3
t-DBPO-s-w-u-p-e-a-k	1.731	2.554	142.4
t-DBPO-d-w-u-q-a-e-j	1.685	2.530	145.2
t-DBPO-s-w-u-q-a-e-j	1.732	2.555	142.4
t-DBPO-d-w-u-q-b-e-j	1.694	2.532	144.4
t-DBPO-d-w-u-q-a-e-k	1.686	2.530	145.2
t-DBPO-s-w-u-q-a-e-k	1.732	2.556	142.4
t-DBPO-s-w-u-p-a-f-j	1.731	2.554	142.4

t-DBPO-s-w-u-p-b-e-k	1.725	2.550	142.6
t-DBPO-s-w-u-p-a-f-k	1.731	2.554	142.4
t-DBPO-d-w-u-q-a-f-j	1.686	2.529	145.1
t-DBPO-s-w-u-p-b-f-k	1.725	2.551	142.6
t-DBPO-s-w-u-q-a-f-k	1.730	2.555	142.5
t-DBPO-d-w-u-q-a-f-k	1.687	2.530	145.1
t-DBPO-d-w-u-q-b-f-k	1.684	2.528	145.1
t-DBPO-d-r-u-q-a-e-j	1.676	2.520	145.0
t-DBPO-s-r-u-q-b-e-j	1.738	2.562	142.5
t-DBPO-d-r-u-q-a-f-j	1.679	2.522	144.8
t-DBPO-s-r-u-q-a-e-j	1.739	2.561	142.4
t-DBPO-s-r-u-q-a-e-k	1.740	2.562	142.4
t-DBPO-s-r-u-q-a-f-j	1.740	2.562	142.4
t-DBPO-s-r-u-q-a-f-k	1.738	2.560	142.4

Table 7.3. The distance between the H atom and the closest C atom in the acceptor aromatic ring for the O–H···π interactions of the calculated conformers of *trans*-DBPO having the same geometry of R and different geometries of the ring system.
HF/6-31G(d,p) results *in vacuo*. The conformers are arranged in order of increasing relative energy. For p-type conformers, the distance considered is H16···C23; for q-type conformers, the distance considered is H15···C23.

Conformer	H15···C23 or H16···C23 (Å)	Conformer	H15···C23 or H16···C23 (Å)
t-DBPO-d-r-η-p-a-e-j	2.128	t-DBPO-s-r-ε-q-a-e-k	2.058
t-DBPO-d-r-η-p-a-e-k	2.127	t-DBPO-s-r-η-p-b-e-j	2.109
t-DBPO-d-r-η-p-a-f-j	2.131	t-DBPO-d-r-η-u-p-a-f-j	2.130
t-DBPO-d-r-η-p-a-f-k	2.130	t-DBPO-d-r-η-u-p-a-f-k	2.130
t-DBPO-d-r-η-p-b-e-k	2.213	t-DBPO-s-r-ε-q-a-e-j	2.058
t-DBPO-d-r-η-p-b-e-j	2.236	t-DBPO-s-r-η-p-e-a-k	2.109
t-DBPO-s-w-ε-q-a-e-k	2.074	t-DBPO-s-r-ε-p-b-e-k	2.220
t-DBPO-s-w-ε-q-a-e-j	2.074	t-DBPO-s-r-η-p-a-e-j	2.109
t-DBPO-d-r-η-p-b-f-j	2.239	t-DBPO-s-r-ε-q-a-f-k	2.059
t-DBPO-d-r-η-p-b-f-k	2.219	t-DBPO-s-r-ε-q-a-f-j	2.059
t-DBPO-s-w-ε-q-b-e-j	2.185	t-DBPO-s-r-η-p-a-f-k	2.111
t-DBPO-s-w-ε-q-a-f-j	2.076	t-DBPO-s-r-η-p-a-f-j	2.112
t-DBPO-s-w-ε-q-a-f-k	2.075	t-DBPO-s-r-η-u-p-b-e-k	2.121
t-DBPO-s-w-ε-q-b-f-k	2.187	t-DBPO-s-r-η-u-p-a-e-j	2.121
t-DBPO-d-r-η-u-p-a-e-j	2.128	t-DBPO-s-r-η-u-p-a-f-j	2.123
t-DBPO-d-r-η-u-p-a-e-k	2.128	t-DBPO-s-r-η-u-p-a-f-k	2.123
t-DBPO-s-r-ε-q-b-e-j	2.165	t-DBPO-s-r-η-u-p-b-f-k	2.240
t-DBPO-s-r-ε-q-b-f-j	2.169		

Table 7.4. Dipole moment of the calculated conformers of *trans*-DBPO having the same geometry of R and different geometries of the ring system.
HF/6-31G(d,p) results *in vacuo*. The conformers are listed in order of increasing relative energy.

Conformer	Dipole moment (Debye)	Conformer	Dipole moment (Debye)
t-DBPO-d-r-η-p-a-e-j	2.460	t-DBPO-s-r-η-p-a-f-j	7.228
t-DBPO-d-r-η-p-a-e-k	3.834	t-DBPO-d-w-q-a-f-k	9.417
t-DBPO-d-r-η-p-a-f-j-	2.877	t-DBPO-d-w-q-b-f-j	8.498
t-DBPO-d-r-η-p-a-f-k	4.115	t-DBPO-s-w-p-a-e-j	4.463
t-DBPO-d-r-η-p-b-e-k	2.463	t-DBPO-d-r-q-b-f-k	5.723
t-DBPO-d-r-η-p-b-e-j	2.652	t-DBPO-d-r-q-a-f-j	5.049
t-DBPO-s-w-ε-q-a-e-k	2.993	t-DBPO-d-r-q-a-f-k	6.137
t-DBPO-s-w-ε-q-a-e-j	5.279	t-DBPO-s-r-η-u-p-b-e-k	3.845
t-DBPO-d-r-η-p-b-f-j	3.473	t-DBPO-s-r-η-u-p-a-e-j	5.700
t-DBPO-d-r-η-p-b-f-k	3.666	t-DBPO-d-w-u-p-a-e-j	7.692
t-DBPO-s-w-ε-q-b-e-j	4.900	t-DBPO-s-w-p-a-f-j	3.536
t-DBPO-s-w-ε-q-a-f-j	5.068	t-DBPO-s-w-p-a-f-k	0.995
t-DBPO-s-w-ε-q-a-f-k	2.723	t-DBPO-s-w-u-p-b-f-j	5.888
t-DBPO-s-w-ε-q-b-e-k	2.780	t-DBPO-s-r-η-u-p-a-f-j	5.749
t-DBPO-s-w-ε-q-b-f-k	3.062	t-DBPO-s-r-η-u-p-a-f-k	4.035
t-DBPO-d-w-p-a-e-j	5.040	t-DBPO-s-w-p-b-e-j	4.326
t-DBPO-d-w-p-a-e-k	7.227	t-DBPO-s-w-p-e-a-k	3.187
t-DBPO-d-w-p-a-f-j	5.408	t-DBPO-s-r-η-u-p-b-f-k	4.477
t-DBPO-d-w-p-b-f-j	5.348	t-DBPO-s-r-η-p-b-f-k	0.892
t-DBPO-d-r-η-u-p-a-e-j	0.855	t-DBPO-d-w-u-p-a-e-k	6.327
t-DBPO-d-r-η-u-p-a-e-k	2.946	t-DBPO-d-w-u-p-b-e-k	6.273
t-DBPO-s-r-ε-q-b-e-j	7.759	t-DBPO-d-w-u-p-a-f-j	4.848
t-DBPO-s-r-ε-q-b-f-j	6.184	t-DBPO-d-w-u-p-b-f-j	4.950
t-DBPO-d-w-p-a-f-k	7.432	t-DBPO-s-w-u-p-a-e-j	2.284
t-DBPO-s-r-ε-q-b-f-k	4.480	t-DBPO-d-w-u-p-a-f-k	7.098
t-DBPO-s-r-ε-q-a-e-k	5.494	t-DBPO-d-w-u-p-b-f-k	7.160
t-DBPO-s-r-η-p-b-e-j	7.838	t-DBPO-s-w-u-p-e-a-k	2.727
t-DBPO-d-r-η-u-p-a-f-j	2.573	t-DBPO-d-w-u-q-a-e-j	4.223
t-DBPO-d-w-p-b-e-k	6.530	t-DBPO-s-w-u-q-b-e-j	1.363
t-DBPO-d-r-η-u-p-a-f-k	3.896	t-DBPO-d-w-u-q-b-e-j	4.031
t-DBPO-s-r-ε-q-a-e-j	7.897	t-DBPO-d-w-u-q-a-e-k	6.449
t-DBPO-d-w-q-b-e-j	5.836	t-DBPO-s-w-u-q-a-e-k	2.061
t-DBPO-d-w-p-b-f-k	6.531	t-DBPO-s-w-u-p-a-f-j	3.271
t-DBPO-d-w-q-a-e-j	6.363	t-DBPO-s-w-u-p-b-e-k	3.384
t-DBPO-s-r-η-p-e-a-k	5.365	t-DBPO-s-w-u-p-a-f-k	3.661
t-DBPO-s-r-η-p-b-e-k	6.633	t-DBPO-d-w-u-q-a-f-j	6.114
t-DBPO-d-w-q-a-e-k	7.756	t-DBPO-s-w-u-p-b-f-k	3.533
t-DBPO-s-r-η-p-a-e-j	7.838	t-DBPO-s-w-u-q-a-f-k	2.661
t-DBPO-s-r-ε-q-a-f-k	4.350	t-DBPO-d-w-u-q-a-f-k	7.871
t-DBPO-d-w-q-b-e-k	7.438	t-DBPO-d-w-u-q-b-f-k	7.985
t-DBPO-s-r-ε-q-a-f-j	7.085	t-DBPO-d-r-u-q-a-e-j	1.061
t-DBPO-s-w-p-b-f-j	2.486	t-DBPO-s-r-u-q-b-e-j	4.605
t-DBPO-s-r-η-p-a-f-k	4.531	t-DBPO-d-r-u-q-a-f-j	2.888

t-DBPO-d-w-q-a-f-j	8.205	t-DBPO-s-r-u-q-a-e-j	4.507
t-DBPO-d-r-q-a-e-j	3.641	t-DBPO-s-r-u-q-a-e-k	3.117
t-DBPO-d-r-q-b-e-k	3.571	t-DBPO-s-r-u-q-a-f-j	7.085
t-DBPO-d-r-q-b-e-j	3.463	t-DBPO-s-r-u-q-a-f-k	1.315
t-DBPO-d-r-q-a-e-k	4.755		

Table 7.5. HOMO-LUMO energy gap of the calculated conformers of *trans*-DBPO having the same geometry of R and different geometries of the ring system *in vacuo*.

HF/6-31G(d,p) results The conformers are listed in order of increasing relative energy.

Conformer	HOMO-LUMO energy gap kcal/mol	Conformer	HOMO-LUMO energy gap kcal/mol
t-DBPO-d-r-η-p-a-e-j	257.410	t-DBPO-d-w-q-b-f-j	243.066
t-DBPO-d-r-η-p-a-e-k	257.517	t-DBPO-d-w-q-b-f-k	242.570
t-DBPO-d-r-η-p-a-f-j	256.250	t-DBPO-d-r-q-b-f-j	249.435
t-DBPO-d-r-η-p-a-f-k	256.425	t-DBPO-s-w-p-a-e-j	252.158
t-DBPO-d-r-η-p-b-e-k	254.649	t-DBPO-d-r-q-b-f-k	249.096
t-DBPO-d-r-η-p-b-e-j	255.904	t-DBPO-d-r-q-a-f-j	248.312
t-DBPO-s-w-ε-q-a-e-k	258.829	t-DBPO-d-r-q-a-f-k	247.728
t-DBPO-s-w-ε-q-a-e-j	258.785	t-DBPO-s-r-η-u-p-b-e-k	251.531
t-DBPO-d-r-η-p-b-f-j	256.042	t-DBPO-s-r-η-u-p-a-e-j	251.493
t-DBPO-d-r-η-p-b-f-k	255.126	t-DBPO-d-w-u-p-a-e-j	258.691
t-DBPO-s-w-ε-q-b-e-j	258.647	t-DBPO-s-w-p-a-f-j	253.099
t-DBPO-s-w-ε-q-a-f-j	258.069	t-DBPO-s-w-p-a-f-k	252.629
t-DBPO-s-w-ε-q-a-f-k	258.182	t-DBPO-s-w-u-p-b-f-j	250.571
t-DBPO-s-w-ε-q-b-f-k	258.276	t-DBPO-s-r-η-u-p-a-f-j	250.797
t-DBPO-d-w-p-a-e-j	243.273	t-DBPO-s-r-η-u-p-a-f-k	250.928
t-DBPO-d-w-p-a-e-k	242.739	t-DBPO-s-w-p-b-e-j	253.288
t-DBPO-d-w-p-a-f-j	244.427	t-DBPO-s-w-p-e-a-k	253.005
t-DBPO-d-w-p-b-f-j	244.452	t-DBPO-s-r-η-u-p-b-f-k	251.104
t-DBPO-d-r-η-u-p-a-e-j	251.619	t-DBPO-s-r-η-p-b-f-k	253.125
t-DBPO-d-r-η-u-p-a-e-k	251.688	t-DBPO-d-w-u-p-a-e-k	236.841
t-DBPO-s-r-ε-q-b-e-j	260.855	t-DBPO-d-w-u-p-b-e-k	236.866
t-DBPO-s-r-ε-q-b-f-j	260.743	t-DBPO-d-w-u-p-a-f-j	238.560
t-DBPO-d-w-p-a-f-k	243.888	t-DBPO-d-w-u-p-b-f-j	238.698
t-DBPO-s-r-ε-q-b-f-k	260.680	t-DBPO-s-w-u-p-a-e-j	239.225
t-DBPO-s-r-ε-q-a-e-k	261.025	t-DBPO-d-w-u-p-a-f-k	238.002
t-DBPO-s-r-η-p-b-e-j	260.404	t-DBPO-d-w-u-p-b-f-k	238.127
t-DBPO-d-r-η-u-p-a-f-j	250.527	t-DBPO-s-w-u-p-e-a-k	238.673
t-DBPO-d-w-p-b-e-k	242.375	t-DBPO-d-w-u-q-a-e-j	236.100
t-DBPO-d-r-η-u-p-a-f-k	250.715	t-DBPO-s-w-u-q-a-e-j	240.185
t-DBPO-s-r-ε-q-a-e-j	256.250	t-DBPO-s-w-u-q-b-e-j	240.267
t-DBPO-d-w-q-b-e-j	242.357	t-DBPO-d-w-u-q-b-e-j	237.154
t-DBPO-d-w-p-b-f-k	243.875	t-DBPO-d-w-u-q-a-e-k	235.536
t-DBPO-d-w-q-a-e-j	240.995	t-DBPO-s-w-u-q-a-e-k	239.621
t-DBPO-s-r-η-p-e-a-k	260.473	t-DBPO-s-w-u-p-a-f-j	240.355
t-DBPO-s-r-3-p-b-e-k	260.115	t-DBPO-s-w-u-p-b-e-k	239.395
t-DBPO-d-w-q-a-e-k	240.449	t-DBPO-s-w-u-p-a-f-k	239.796

t-DBPO-s-r-η-p-a-e-j	260.404	t-DBPO-d-w-u-q-a-f-j	237.318
t-DBPO-s-r-ε-q-a-f-k	260.561	t-DBPO-s-w-u-p-b-f-k	240.254
t-DBPO-d-w-q-b-e-k	241.880	t-DBPO-s-w-u-q-a-f-k	240.775
t-DBPO-s-r-ε-q-a-f-j	260.454	t-DBPO-d-w-u-q-a-f-k	236.747
t-DBPO-s-w-p-b-f-j	253.589	t-DBPO-d-w-u-q-b-f-k	237.424
t-DBPO-s-r-η-p-a-f-k	260.052	t-DBPO-d-r-u-q-a-e-j	241.961
t-DBPO-d-w-q-a-f-j	242.206	t-DBPO-s-r-u-q-b-e-j	246.523
t-DBPO-d-r-q-a-e-j	247.075	t-DBPO-d-r-u-q-a-f-j	243.204
t-DBPO-d-r-q-b-e-k	248.657	t-DBPO-s-r-u-q-a-e-j	246.366
t-DBPO-d-r-q-b-e-j	249.134	t-DBPO-s-r-u-q-a-e-k	245.852
t-DBPO-d-r-q-a-e-k	246.529	t-DBPO-s-r-u-q-a-f-j	260.454
t-DBPO-s-r-η-p-a-f-j	259.946	t-DBPO-s-r-u-q-a-f-k	246.862
t-DBPO-d-w-q-a-f-k	241.641		

Figure 7.3. Shapes of the HOMO and LUMO molecular orbitals of the calculated conformers of *trans*-DBPO having the same geometry of R and different geometries of the ring system *in vacuo***.**
HF/6-31G(d,p) results. The conformers are listed in order of increasing relative energy.

HOMO	LUMO	HOMO	LUMO
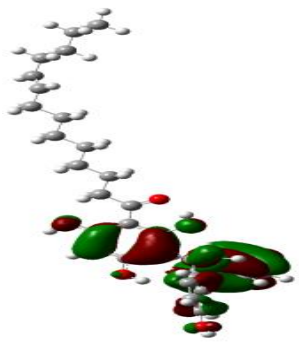	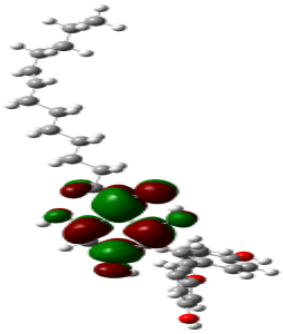	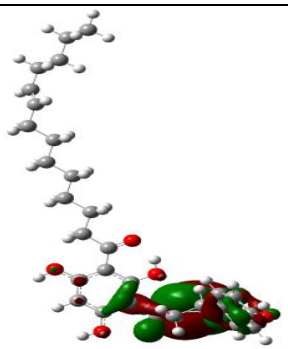	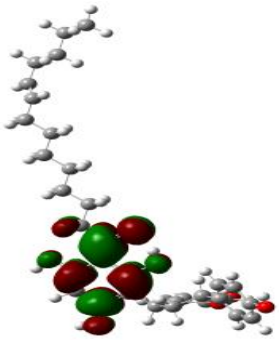
t-DBPO-d-r-η-p-a-e-j		t-DBPO-d-w-q-b-f-k	
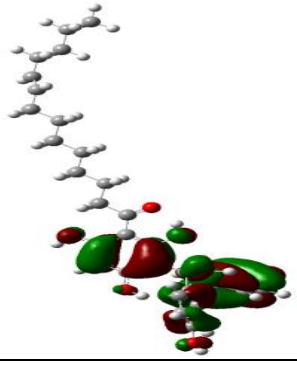	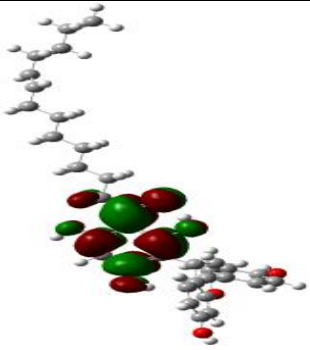		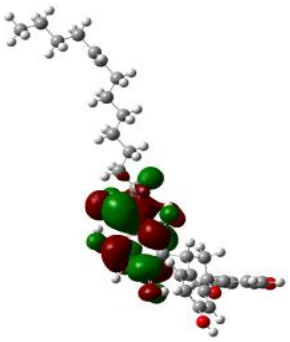
t-DBPO-d-r-η-p-a-e-k		t-DBPO-s-r-η-u-p-b-e-k	
	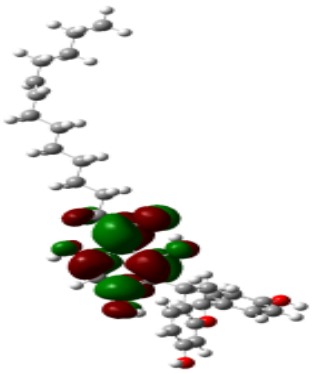	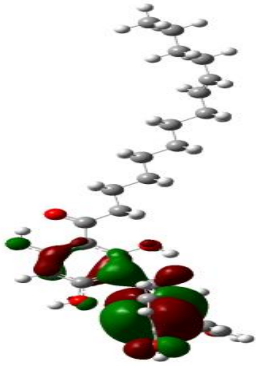	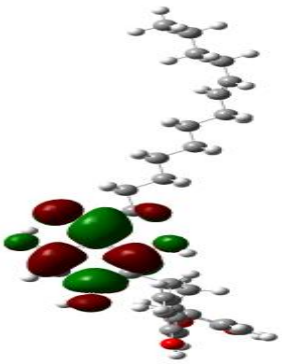
t-DBPO-d-r-η-p-a-f-j		t-DBPO-s-w-p-a-e-j	
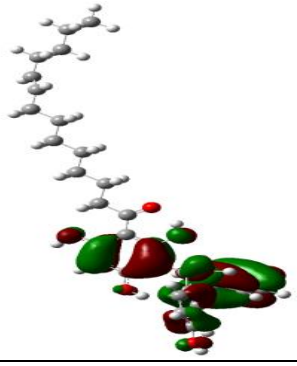	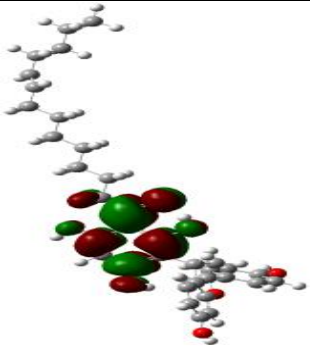	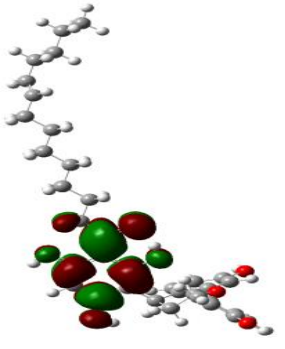	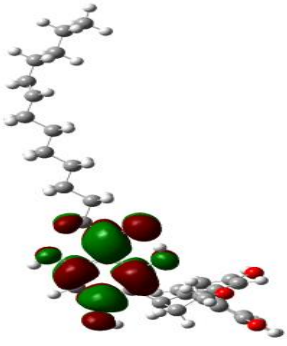
t-DBPO-d-r-η-p-b-e-k		t-DBPO-d-r-q-a-f-j	

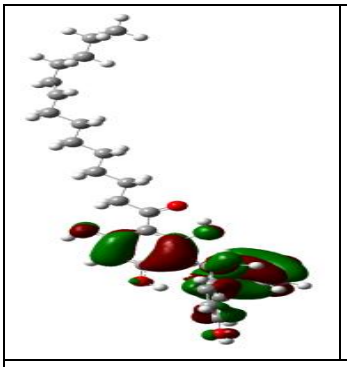	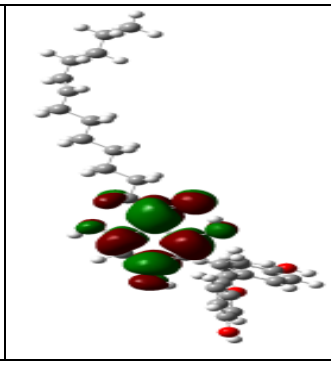
t-DBPO-d-r-η-p-b-e-j	t-DBPO-s-w-p-e-a-k
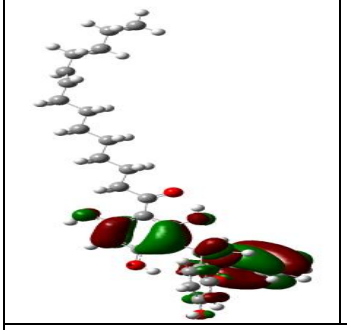	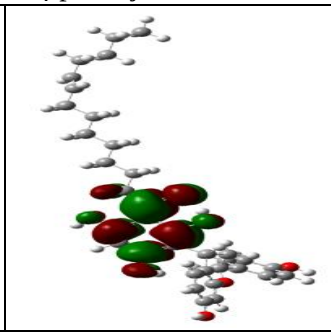
t-DBPO-d-r-η-p-b-f-j	t-DBPO-d-r-q-b-f-k
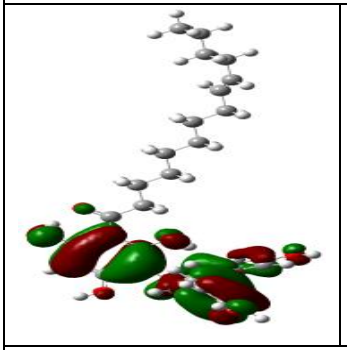	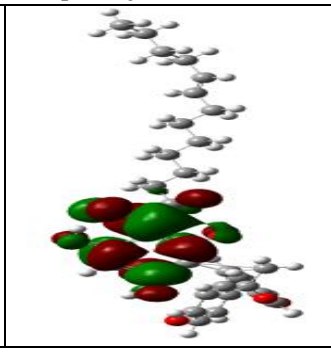
t-DBPO-s-w-e-q-a-e-k	t-DBPO-s-r-η-u-p-a-e-j
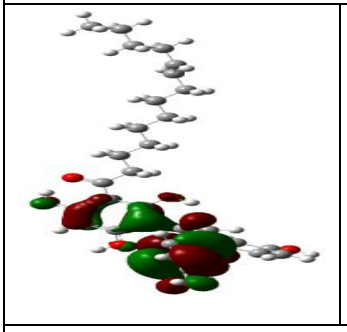	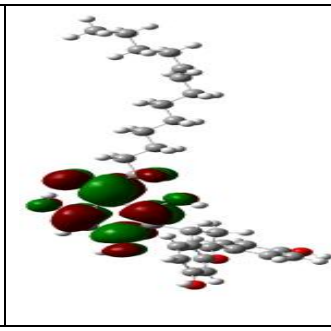
t-DBPO-s-w-ε-q-a-e-j	t-DBPO-s-w-p-a-f-j
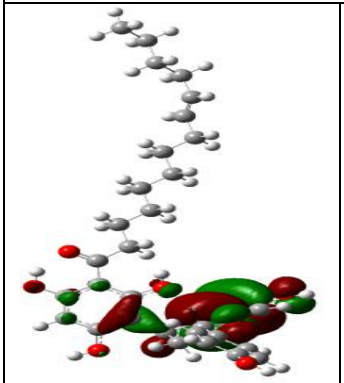	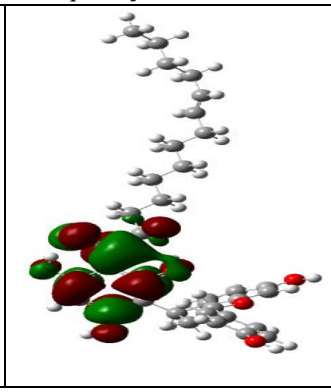
t-DBPO-s-w-u-q-a-e-j	t-DBPO-s-w-p-a-f-k

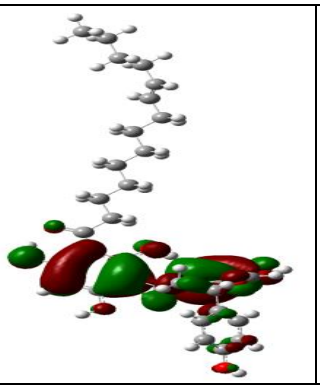	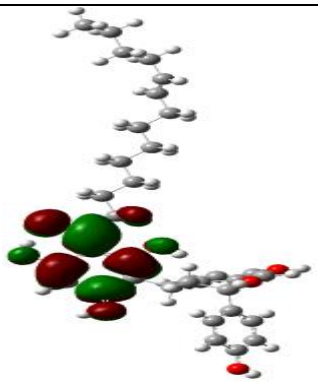
t-DBPO-s-w-ε-q-b-e-j	t-DBPO-s-r-η-u-p-b-f-k
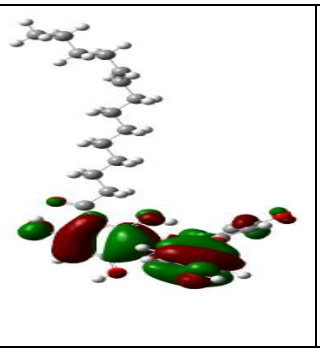	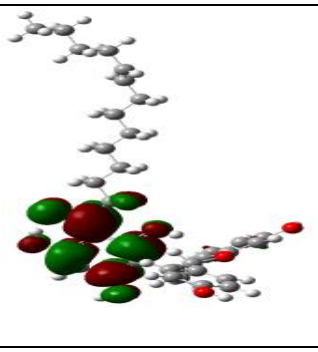
t-DBPO-s-w-ε-q-a-f-j	t-DBPO-s-w-u-p-b-f-k
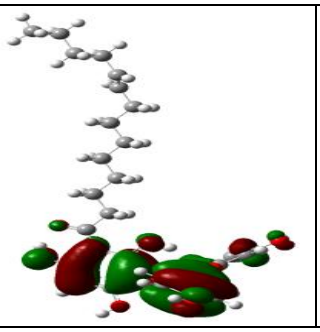	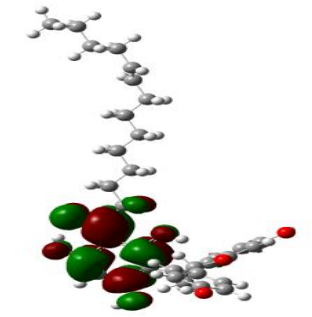
t-DBPO-s-w-ε-q-a-f-k	t-DBPO-s-w-u-p-b-f-j
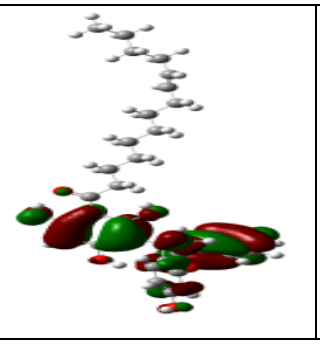	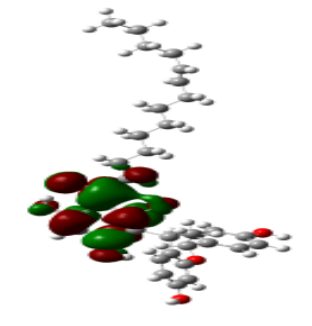
t-DBPO-s-w-u-q-a-f-k	t-DBPO-s-r-η-u-p-a-f-j
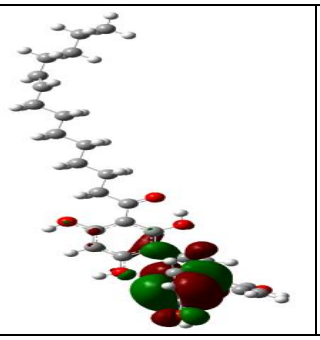	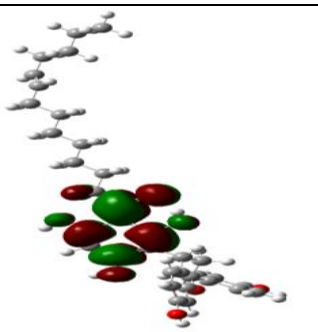
t-DBPO-d-w-p-a-e-j	t-DBPO-s-r-η-u-p-a-f-k

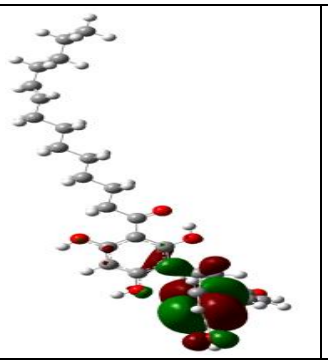	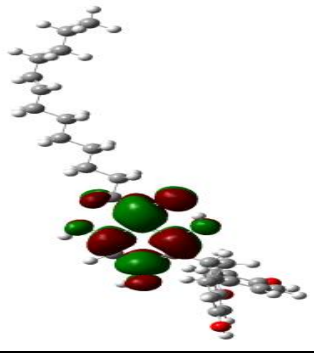
t-DBPO-d-w-p-b-e-j	t-DBPO-s-w-p-b-e-j
	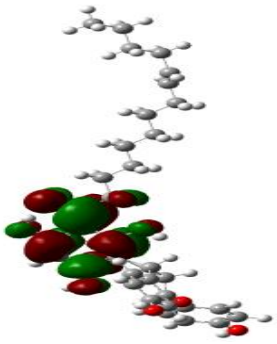
t-DBPO-d-w-p-a-e-k	t-DBPO-s-r-η-p-b-f-k
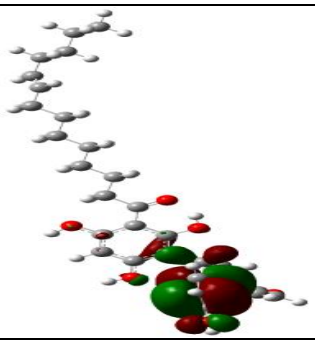	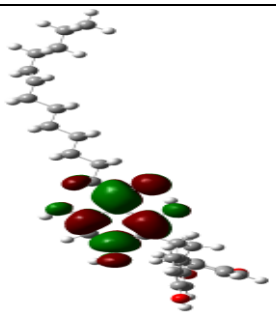
t-DBPO-d-w-p-b-e-k	t-DBPO-d-w-u-p-a-e-k
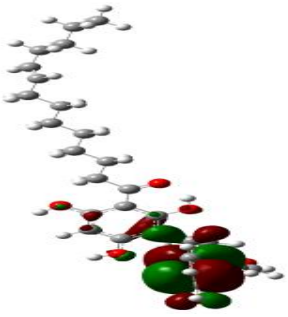	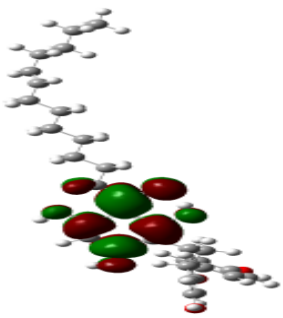
t-DBPO-d-w-p-a-f-j	t-DBPO-d-w-u-p-b-e-k
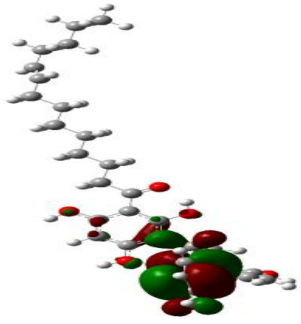	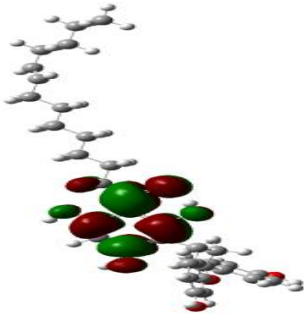
t-DBPO-d-w-p-b-f-j	t-DBPO-d-w-u-p-a-f-j

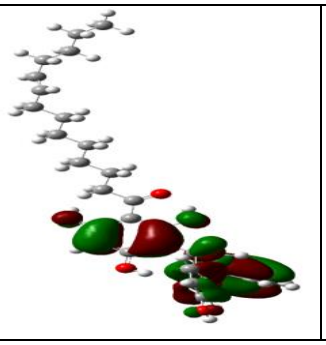 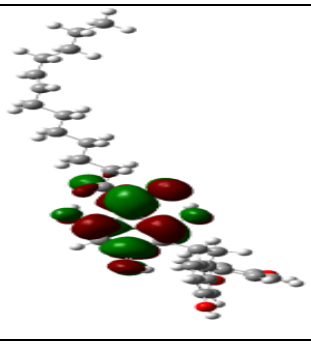	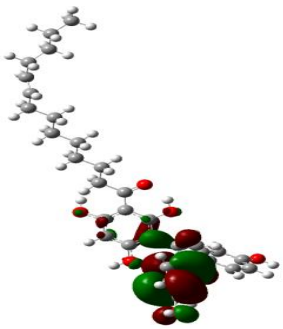 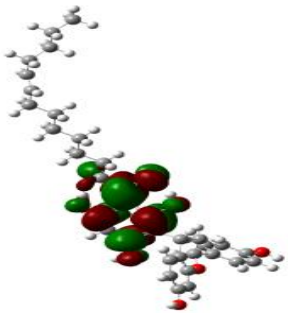
t-DBPO-d-r-η-u-p-a-e-j	t-DBPO-d-w-u-p-b-f-j
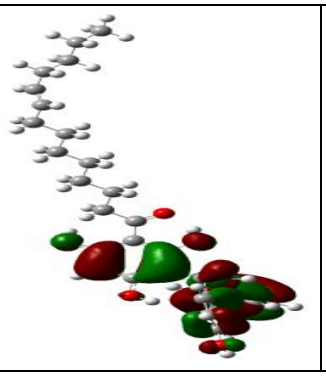 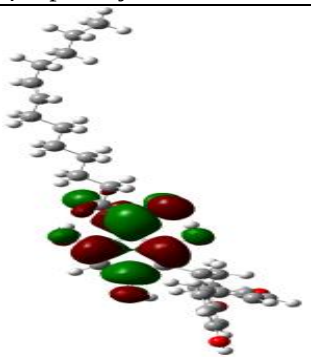	 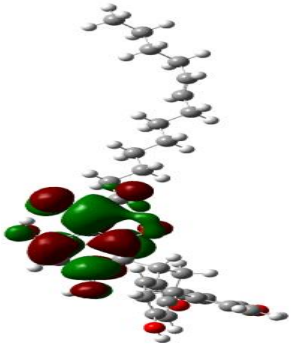
t-DBPO-d-r-η-u-p-a-e-k	t-DBPO-s-w-u-p-b-e-j
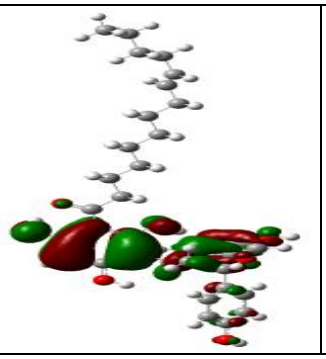 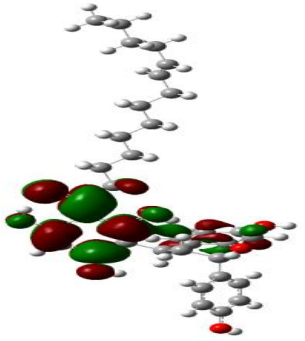	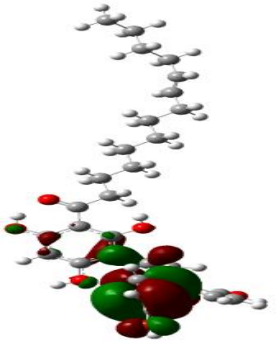 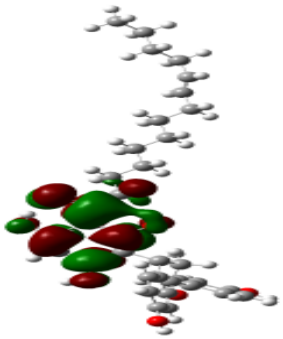
t-DBPO-s-r-ε-q-b-e-j	t-DBPO-s-w-u-p-a-e-j
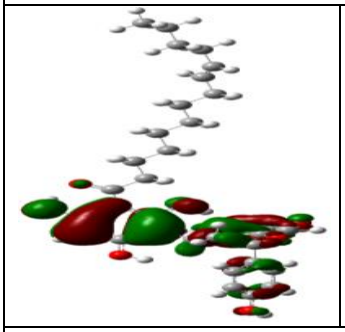 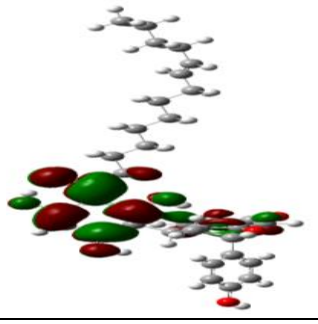	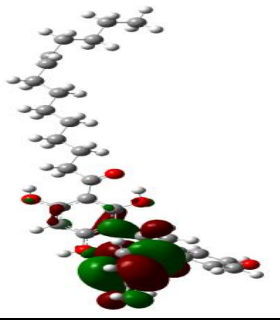 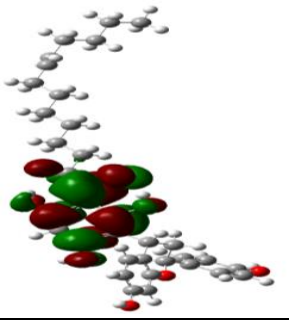
t-DBPO-s-r-ε-q-b-f-j	t-DBPO-d-w-u-p-a-f-k
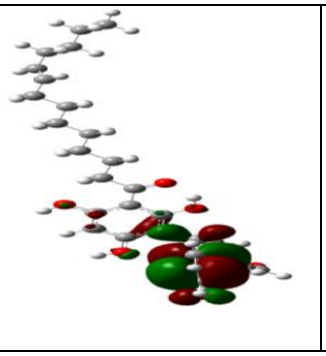 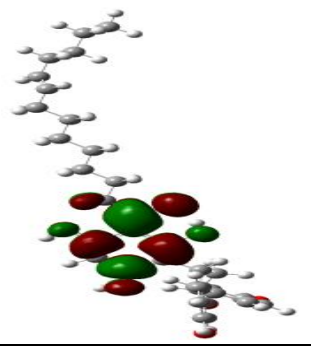	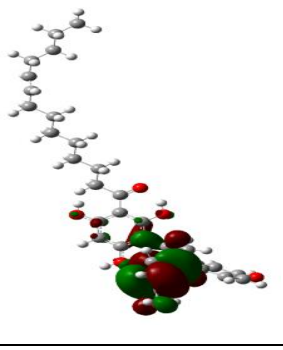 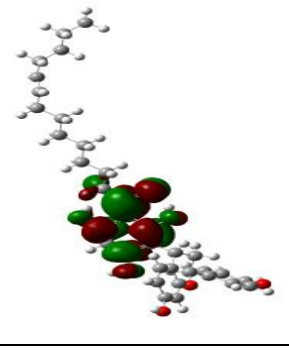
t-DBPO-d-w-p-a-f-k	t-DBPO-d-w-u-p-b-f-k

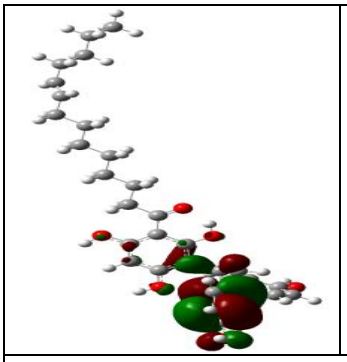	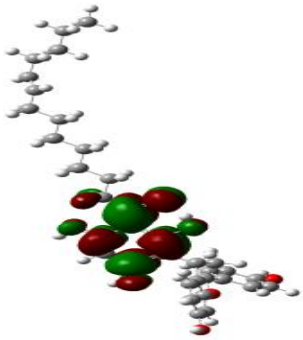
t-DBPO-d-w-p-b-f-k	t-DBPO-s-w-u-p-e-a-k
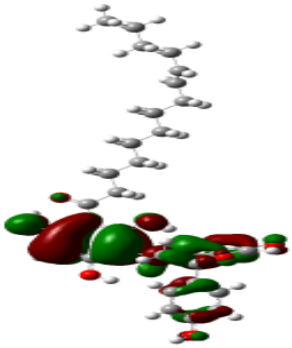	
t-DBPO-s-r-ε-q-b-f-k	t-DBPO-s-w-u-p-b-e-k
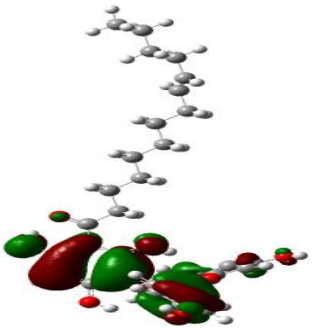	
t-DBPO-s-r-ε-q-a-e-k	t-DBPO-d-w-u-q-b-e-j
	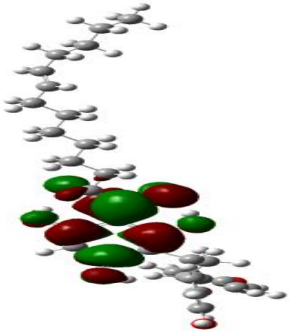
t-DBPO-d-r-η-u-p-a-f-j	t-DBPO-d-w-u-q-a-e-j
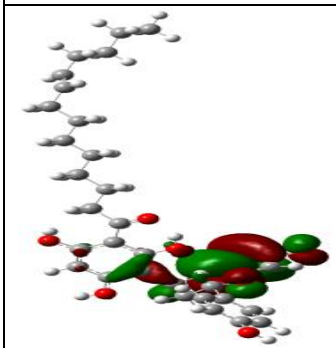	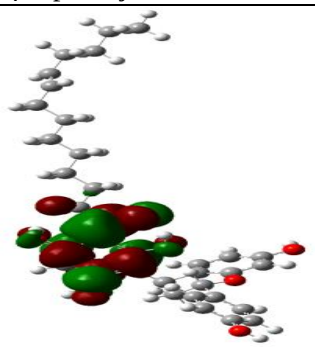
t-DBPO-s-r-ε-q-a-e-j	t-DBPO-d-w-u-q-a-e-k

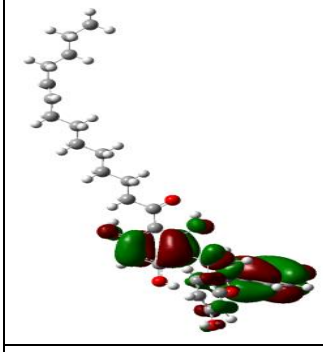 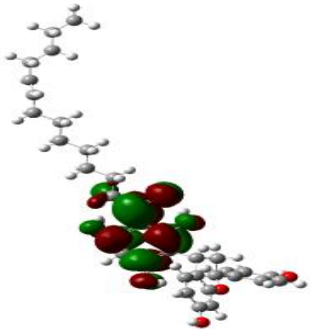	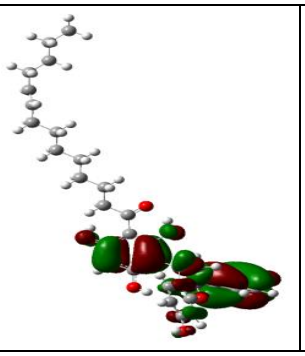 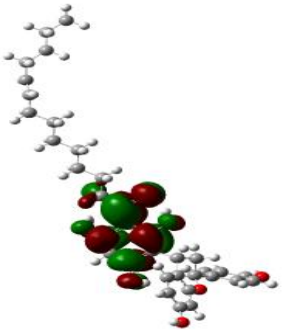
t-DBPO-d-r-η-u-p-a-f-k	t-DBPO-d-w-u-q-a-f-j
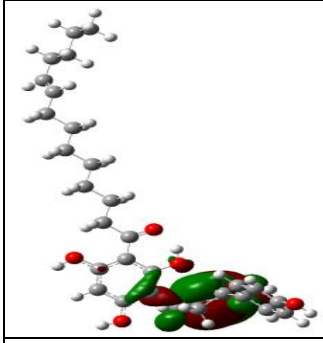 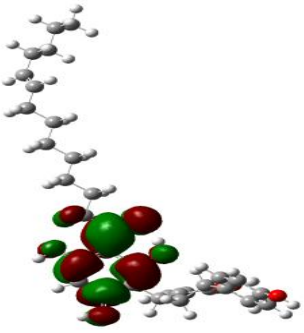	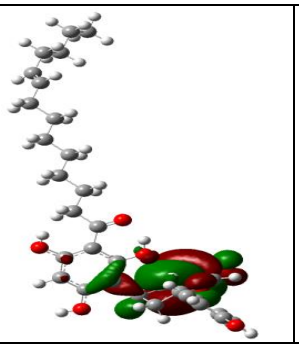 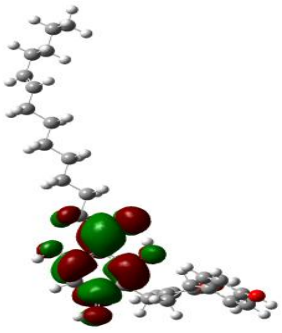
t-DBPO-d-w-q-a-e-j	t-DBPO-d-w-u-q-b-f-j
 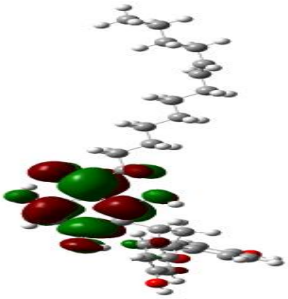	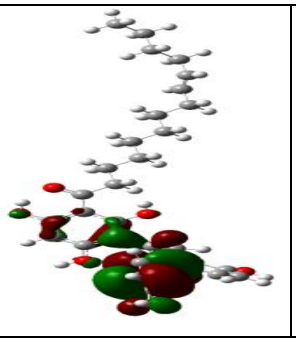 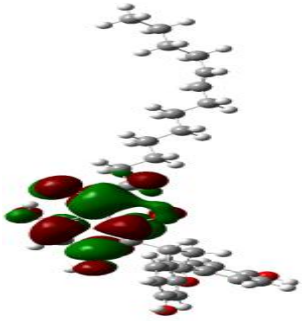
t-DBPO-s-r-η-p-e-a-k	t-DBPO-s-w-u-p-a-f-j
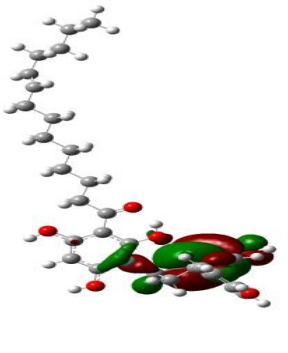 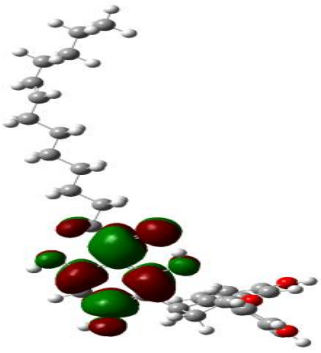	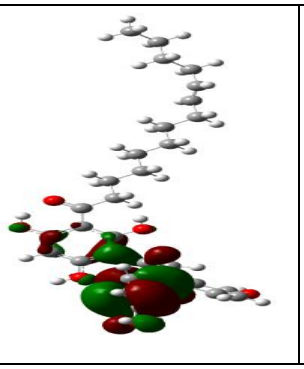 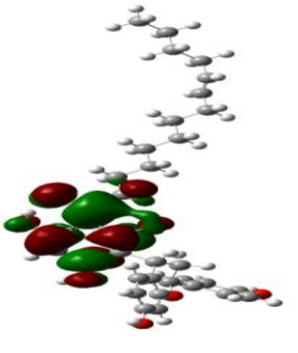
t-DBPO-d-w-q-a-e-k	t-DBPO-s-w-u-p-a-f-k
 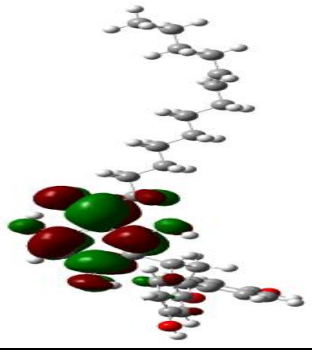	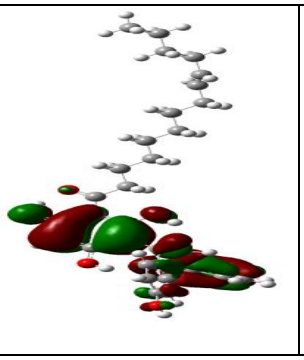 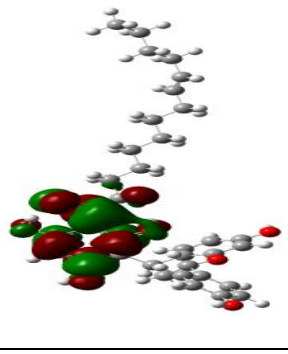
t-DBPO-s-r-η-p-a-e-j	t-DBPO-d-w-u-q-a-f-k

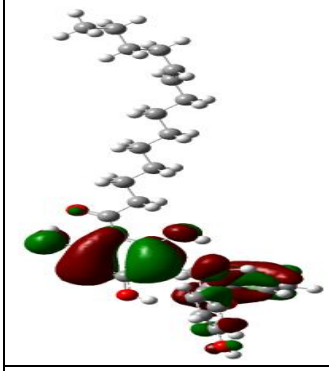	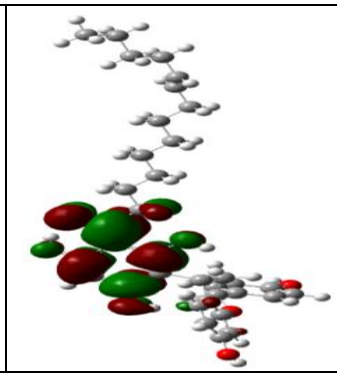
t-DBPO-s-r-η-p-b-e-j	t-DBPO-d-r-u-q-a-e-j
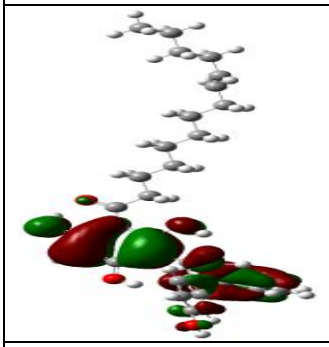	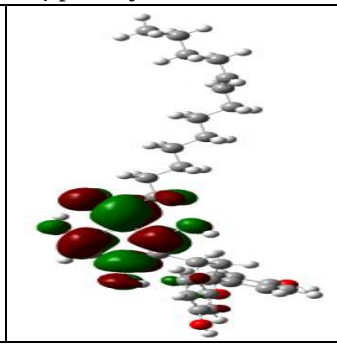
t-DBPO-d-w-u-p-a-e-j	t-DBPO-d-r-u-q-a-f-j
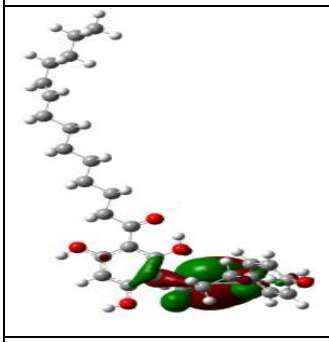	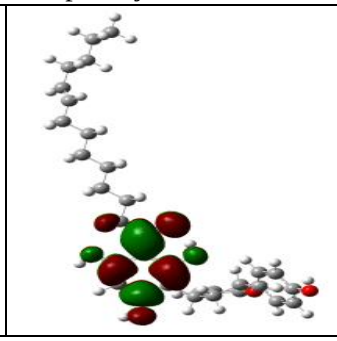
t-DBPO-d-w-q-b-e-k	t-DBPO-s-w-u-q-b-e-k
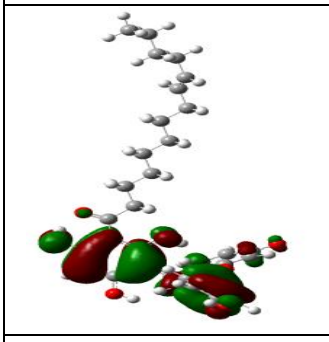	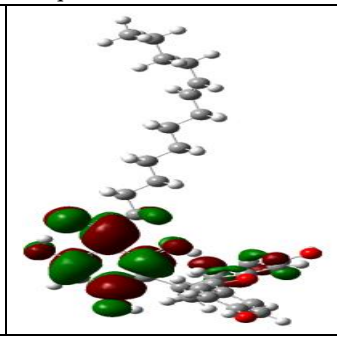
t-DBPO-s-r-ε-q-a-f-k	t-DBPO-s-w-ε-q-b-f-k
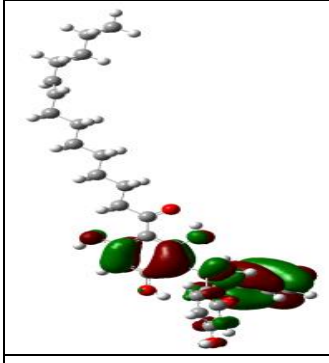	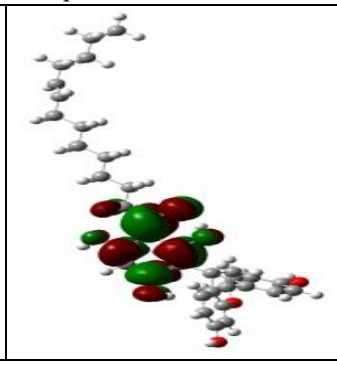
t-DBPO-s-r-ε-q-a-f-j	t-DBPO-d-r-η-p-b-f-k

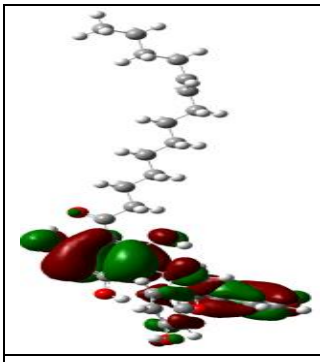	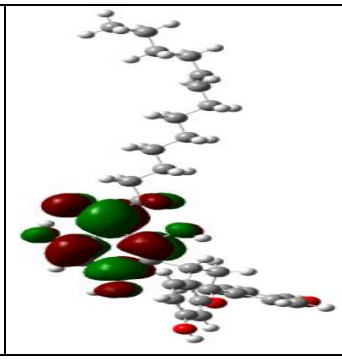
t-DBPO-s-r-η-p-a-f-k	t-DBPO-s-w-u-q-a-e-k
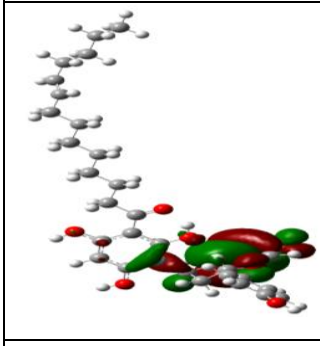	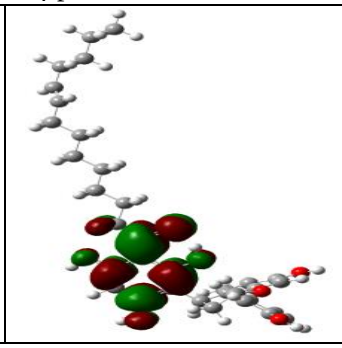
t-DBPO-d-w-q-a-f-j	t-DBPO-d-w-q-b-e-j
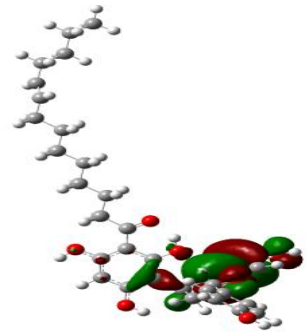	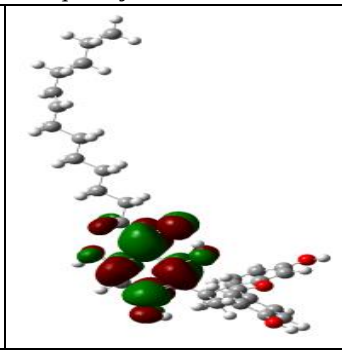
t-DBPO-d-r-q-a-e-j	t-DBPO-d-r-q-b-f-j
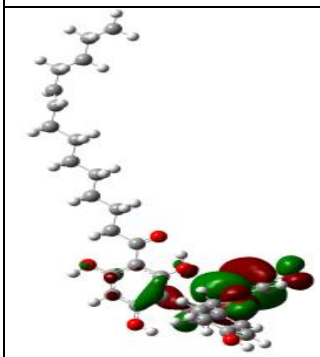	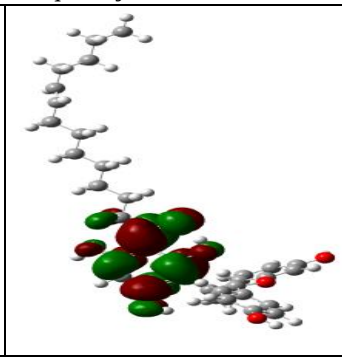
t-DBPO-d-r-q-b-e-j	t-DBPO-s-r-3-p-b-e-k
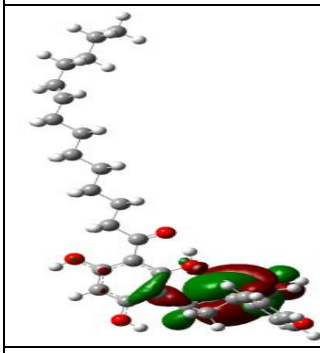	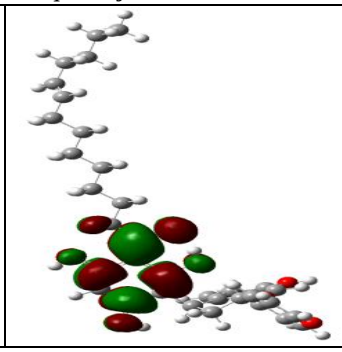
t-DBPO-d-r-q-a-e-k	t-DBPO-s-r-u-q-b-e-j

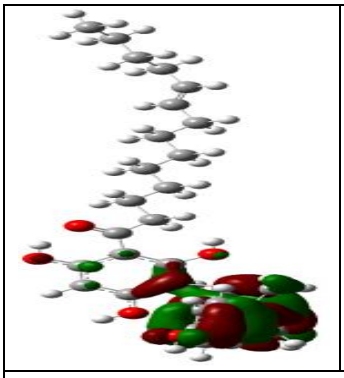 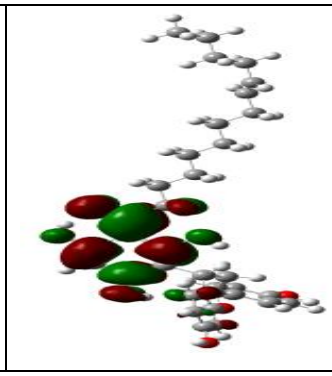	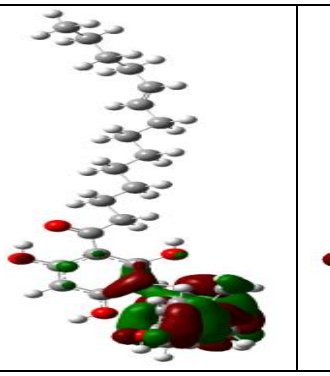 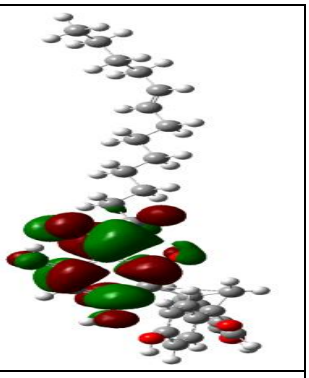
t-DBPO-s-r-η-p-a-f-j	t-DBPO-s-w-u-q-b-e-j
 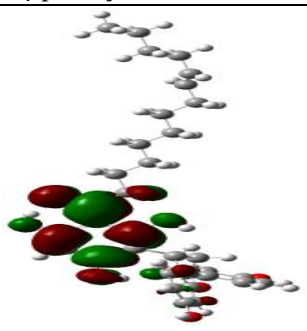	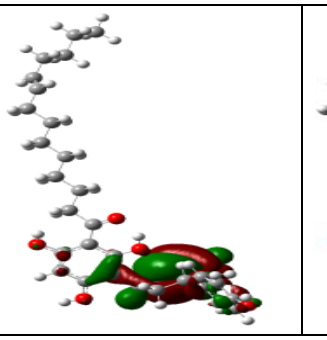 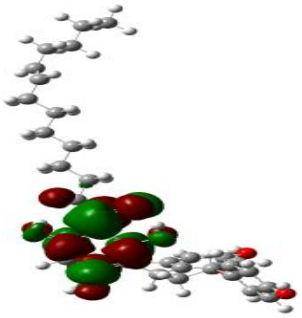
t-DBPO-s-w-p-b-f-j	t-DBPO-d-w-u-q-b-f-k
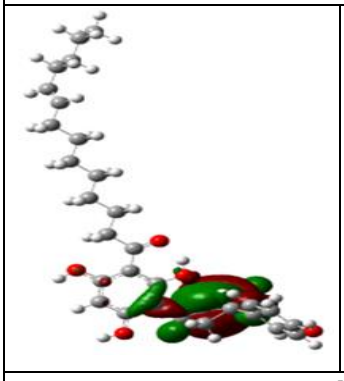 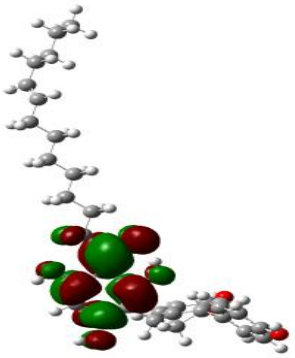	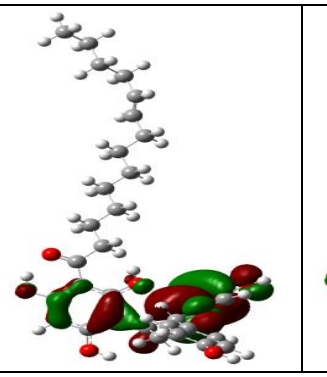 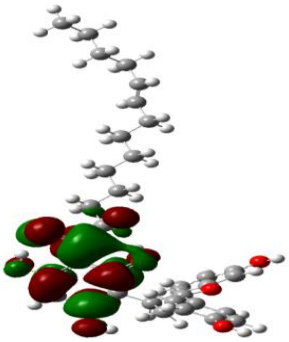
t-DBPO-d-w-q-a-f-k	t-DBPO-s-r-u-q-a-e-j
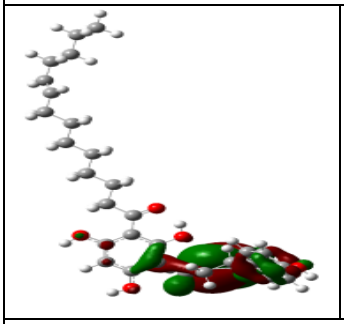 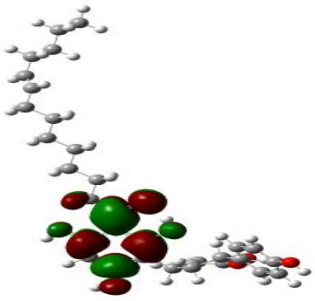	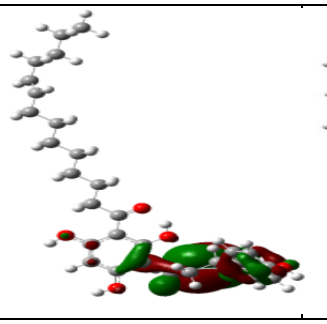 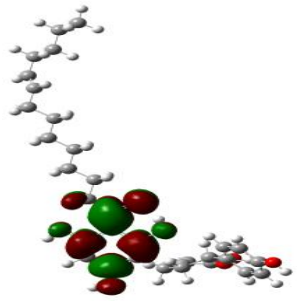
t-DBPO-d-w-q-b-f-j	t-DBPO-d-r-q-b-e-k
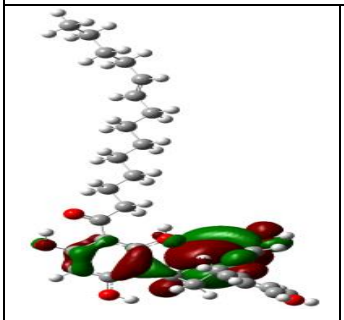 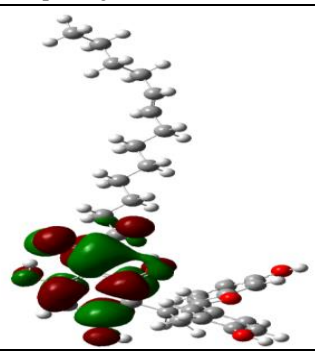	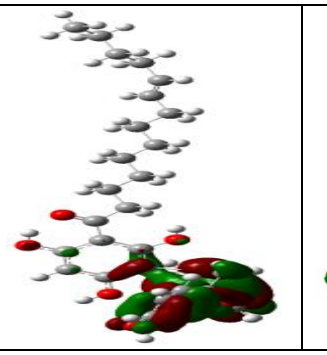 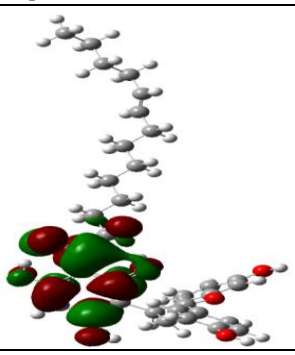
t-DBPO-s-r-u-q-a-e-k	t-DBPO-s-w-u-q-b-e-k

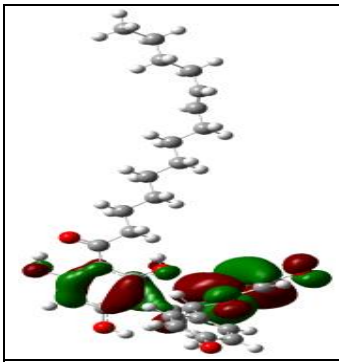	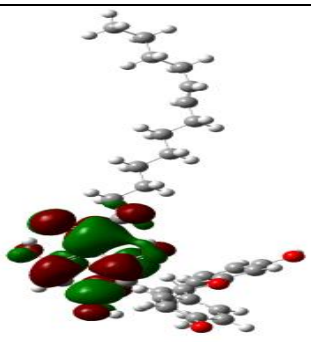		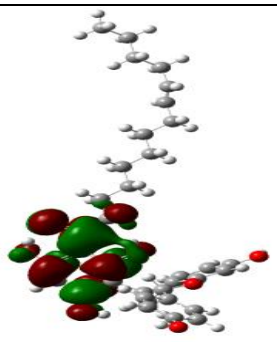
t-DBPO-s-r-u-q-a-f-j		t-DBPO-s-r-u-q-a-e-j	
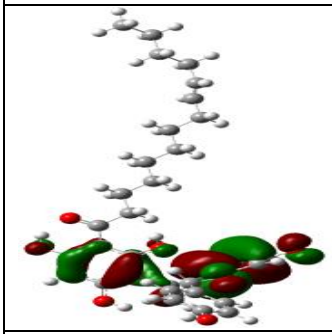	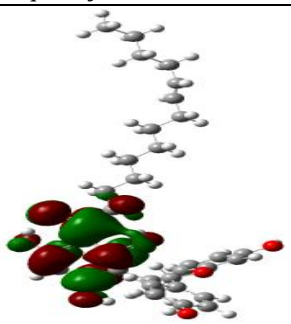		
t-DBPO-s-r-u-q-a-f-k			

Figure 7.4. Optimized conformers of *trans*-DBPO having different geometries of R and the same geometry of the ring system *in vacuo*.
HF/6-32G(d,p) results. The conformers are listed in order of increasing relative energy.

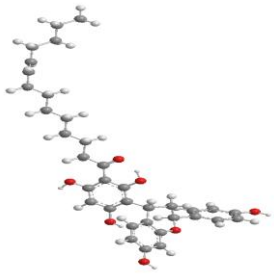

t-DBPO-d-r-η-p-a-e-j

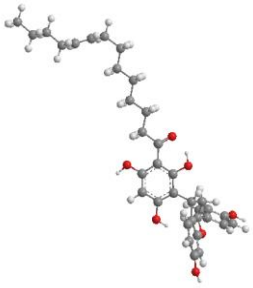

t-DBPO-d-r-η-p-a-e-j-8y

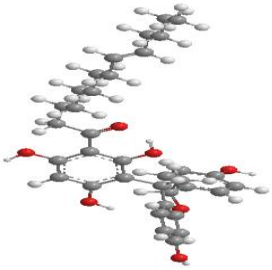

t-DBPO-d-r-1-p-a-e-j-3y

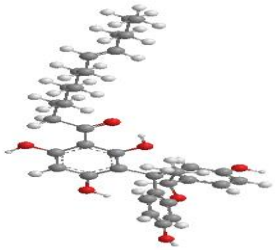

t-DBPO-d-r-1-p-a-e-j-3z

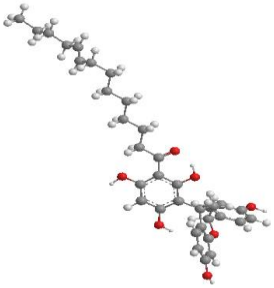

t-DBPO-d-r-η-p-a-e-j-8z

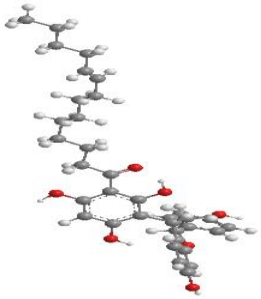

t-DBPO-d-r-η-p-a-e-j-5y

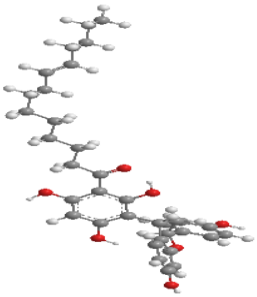

t-DBPO-d-r-η-p-a-e-j-7y

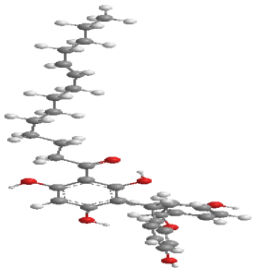

t-DBPO-d-r-η-p-a-e-j-5z

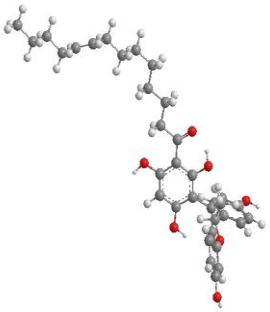

t-DBPO-d-r-η-p-a-e-j-6y

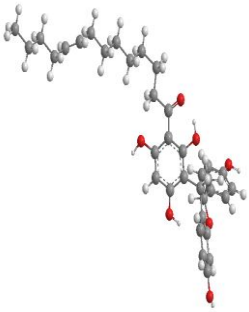

t-DBPO-d-r-1-p-a-e-j-4y

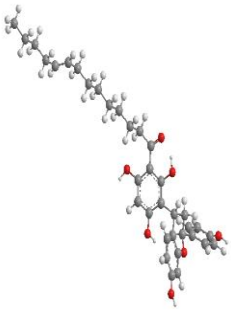

t-DBPO-d-r-1-p-a-e-j-2y

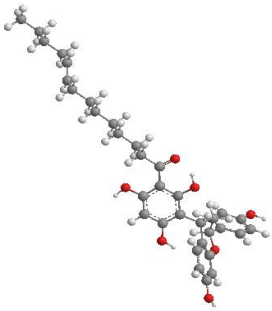

t-DBPO-d-r-1-p-a-e-j-2z

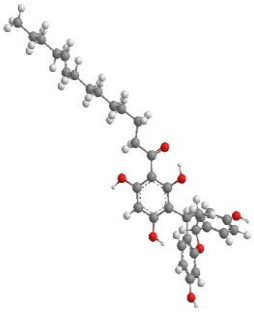

t-DBPO-d-r-1-p-a-e-j-4z

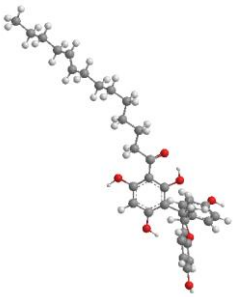

t-DBPO-d-r-η-p-a-e-j-6z

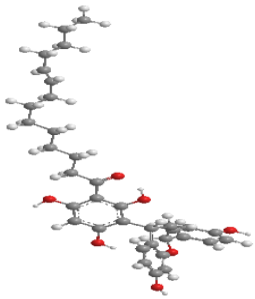

t-DBPO-d-r-η-p-a-e-j-7z

Table 7.6. Relative energies of the calculated conformers of *trans*-DBPO having different geometries of R and the same geometry of the ring system *in vacuo*.
HF/6-31G(d,p)) results. Conformers are listed in order of increasing relative energy in the HF results. The absolute energy of the lowest energy conformer is -1873.9743975 hartree.

Conformer	Relative energy (kcal/mol)	Conformer	Relative energy (kcal/mol)
t-DBPO-d-r-η-p-a-e-j	0.000	t-DBPO-d-r-η-p-a-e-j-6y	1.020
t-DBPO-d-r-η-p-a-e-j-8y	0.342	t-DBPO-d-r-η-p-a-e-j-4y	1.028
t-DBPO-d-r-η-p-a-e-j-3y	0.508	t-DBPO-d-r-η-p-a-e-j-2y	1.028
t-DBPO-d-r-η-p-a-e-j-3z	0.510	t-DBPO-d-r-η-p-a-e-j-2z	1.033
t-DBPO-d-r-η-p-a-e-j-8z	0.974	t-DBPO-d-r-η-p-a-e-j-4z	1.045
t-DBPO-d-r-η-p-a-e-j-5y	0.994	t-DBPO-d-r-η-p-a-e-j-6z	1.047
t-DBPO-d-r-η-p-a-e-j-7y	0.997	t-DBPO-d-r-η-p-a-e-j-7z	1.076
t-DBPO-d-r-η-p-a-e-j-5z	0.997		

Table 7.7. Relative energy corrected for ZPE (sum of electronic and zero-point energies, $\Delta E_{corrected}$, kcal/mol), ZPE correction to the electronic energy (ZPE_{corr}, kcal/mol), relative Gibbs free energies (sum of electronic and thermal free energy, $\Delta G_{corrected}$) and its thermal correction (G_{corr}), for the conformers of *trans*-DBPO having different geometries of R and the same geometry of the ring system *in vacuo*.
Results from HF/6-31G(d,p) frequency calculations. Conformers are listed in order of increasing relative energies in the HF results. The absolute values for the lower energy conformer are -1873.214981 hartree ($\Delta E_{corrected}$) and -1873.295407 hartree ($\Delta G_{corrected}$).

Conformer	$\Delta E_{corrected}$	ZPE_{corr}	$\Delta G_{corrected}$	G_{corr}
t-DBPO-d-r-η-p-a-e-j	0.000	476.541	0.000	426.072
t-DBPO-d-r-η-p-a-e-j-8y	0.449	476.648	0.463	426.194
t-DBPO-d-r-η-p-a-e-j-3y	0.693	476.725	0.812	426.376
t-DBPO-d-r-η-p-a-e-j-3z	0.695	476.725	0.796	426.359
t-DBPO-d-r-η-p-a-e-j-8z	1.136	476.702	1.063	426.161
t-DBPO-d-r-η-p-a-e-j-5y	1.157	476.704	1.081	426.159
t-DBPO-d-r-η-p-a-e-j-7y	1.133	476.677	1.102	426.178
t-DBPO-d-r-η-p-a-e-j-5z	1.141	476.685	1.086	426.162
t-DBPO-d-r-η-p-a-e-j-6y	1.165	476.687	1.101	426.153
t-DBPO-d-r-η-p-a-e-j-4y	1.169	476.682	1.104	426.150
t-DBPO-d-r-η-p-a-e-j-2y	1.405	476.918	1.188	426.232
t-DBPO-d-r-η-p-a-e-j-2z	1.409	476.918	1.203	426.243
t-DBPO-d-r-η-p-a-e-j-4z	1.184	476.680	1.115	426.143
t-DBPO-d-r-η-p-a-e-j-6z	1.189	476.682	1.123	426.148
t-DBPO-d-r-η-p-a-e-j-7z	1.197	476.661	1.123	426.120

Table 7.8. Parameters of the first IHB of the selected calculated conformers of *trans*-DBPO having different geometries of R and the same geometry of the ring system *in vacuo*.
HF/6-31G(d,p) results. Conformers are listed in order of increasing relative energy in the HF results. The first IHB is H15···O14.

Conformer	Parameters the first IHB		
	OH···O (Å)	O···O (Å)	OHO (°)
t-DBPO-d-r-η-p-a-e-j	1.652	2.508	146.4
t-DBPO-d-r-η-p-a-e-j-8y	1.651	2.508	146.4
t-DBPO-d-r-η-p-a-e-j-3y	1.654	2.509	146.3
t-DBPO-d-r-η-p-a-e-j-3z	1.654	2.509	146.3
t-DBPO-d-r-η-p-a-e-j-8z	1.652	2.508	146.4
t-DBPO-d-r-η-p-a-e-j-5y	1.652	2.508	146.4
t-DBPO-d-r-η-p-a-e-j-7y	1.652	2.508	146.4
t-DBPO-d-r-η-p-a-e-j-5z	1.652	2.508	146.4
t-DBPO-d-r-η-p-a-e-j-6y	1.652	2.508	146.4
t-DBPO-d-r-η-p-a-e-j-4y	1.651	2.508	146.4
t-DBPO-d-r-η-p-a-e-j-2y	1.644	2.503	146.6
t-DBPO-d-r-η-p-a-e-j-2z	1.644	2.503	146.6
t-DBPO-d-r-η-p-a-e-j-4z	1.651	2.508	146.4
t-DBPO-d-r-η-p-a-e-j-6z	1.652	2.508	146.4
t-DBPO-d-r-η-p-a-e-j-7z	1.652	2.508	146.4

Table 7.9. The distance between the H atom and the closest C atom in the acceptor aromatic ring for the O–H···π interactions of the selected calculated conformers of *trans*-DBPO having different geometries of R and the same geometry of the ring system *in vacuo*.
HF/6-31G(d,p) results. Conformers are listed in order of increasing relative energy in the HF results.

Conformer	H16···C23 distance considered (Å)	Conformer	H16···C23 distance considered (Å)
t-DBPO-d-r-η-p-a-e-j	2.128	t-DBPO-d-r-η-p-a-e-j-6y	2.128
t-DBPO-d-r-η-p-a-e-j-8y	2.128	t-DBPO-d-r-η-p-a-e-j-4y	2.128
t-DBPO-d-r-η-p-a-e-j-3y	2.129	t-DBPO-d-r-η-p-a-e-j-2y	2.128
t-DBPO-d-r-η-p-a-e-j-3z	2.127	t-DBPO-d-r-η-p-a-e-j-2z	2.129
t-DBPO-d-r-η-p-a-e-j-8z	2.128	t-DBPO-d-r-η-p-a-e-j-4z	2.128
t-DBPO-d-r-η-p-a-e-j-5y	2.128	t-DBPO-d-r-η-p-a-e-j-6z	2.128
t-DBPO-d-r-η-p-a-e-j-7y	2.128	t-DBPO-d-r-η-p-a-e-j-7z	2.128
t-DBPO-d-r-η-p-a-e-j-5z	2.128		

Table 7.10. Vibrational frequency of the O–H bonds in the selected conformers of *trans*-DBPO having different geometries of R and the same geometry of the ring system *in vacuo*.
HF/6-31G(d,p) results. The frequency values have been scaled by 0.8992, as recommended for HF/6-31G(d,p) calculations [184]. The conformers are arranged in order of increasing relative energy.

Conformer	Vibrational frequencies (cm^{-1})				
	O8–H15	O10–H16	O12–H17	O44–H50	O51–H52
t-DBPO-d-r-η-p-a-e-j	3397.11	3704.33	3761.97	3769.59	3773.51
t-DBPO-d-r-η-p-a-e-j-8y	3396.32	3704.53	3762.06	3769.59	3773.52
t-DBPO-d-r-η-p-a-e-j-3y	3403.37	3704.10	3770.89	3769.55	3773.51
t-DBPO-d-r-η-p-a-e-j-3z	3403.65	3704.03	3770.82	3769.55	3773.50
t-DBPO-d-r-η-p-a-e-j-8z	3397.04	3704.34	3762.00	3769.58	3773.51
t-DBPO-d-r-η-p-a-e-j-5y	3397.34	3704.28	3761.97	3769.58	3773.51
t-DBPO-d-r-η-p-a-e-j-7y	3397.20	3704.30	3761.98	3769.56	3773.51
t-DBPO-d-r-η-p-a-e-j-5z	3397.29	3704.30	3761.98	3769.57	3773.52
t-DBPO-d-r-η-p-a-e-j-6y	3396.90	3704.40	3761.99	3769.59	3773.52
t-DBPO-d-r-η-p-a-e-j-4y	3396.73	3704.33	3761.96	3769.58	3773.53
t-DBPO-d-r-η-p-a-e-j-2y	3374.72	3703.56	3763.05	3769.57	3773.52
t-DBPO-d-r-η-p-a-e-j-2z	3375.08	3703.62	3763.11	3769.56	3773.50
t-DBPO-d-r-η-p-a-e-j-4z	3396.86	3704.39	3761.89	3769.58	3773.50
t-DBPO-d-r-η-p-a-e-j-6z	3397.08	3704.34	3761.98	3769.56	3773.53
t-DBPO-d-r-η-p-a-e-j-7z	3397.31	3704.31	3762.22	3769.56	3773.50

Table 7.11. Dipole moments of the conformers of *trans*-DBPO having different geometries of R and the same geometry of the ring system *in vacuo*.
HF/6-31G(d,p) results. Conformers are listed in order of increasing relative energy in the HF results.

Conformer	Dipole moment (Debye)	Conformer	Dipole moment (Debye)
t-DBPO-d-r-η-p-a-e-j	2.288	t-DBPO-d-r-η-p-a-e-j-6y	2.288
t-DBPO-d-r-η-p-a-e-j-8y	2.247	t-DBPO-d-r-η-p-a-e-j-4y	2.280
t-DBPO-d-r-η-p-a-e-j-3y	2.424	t-DBPO-d-r-η-p-a-e-j-2y	2.418
t-DBPO-d-r-η-p-a-e-j-3z	2.424	t-DBPO-d-r-η-p-a-e-j-2z	2.435
t-DBPO-d-r-η-p-a-e-j-8z	2.293	t-DBPO-d-r-η-p-a-e-j-4z	2.276
t-DBPO-d-r-η-p-a-e-j-5y	2.350	t-DBPO-d-r-η-p-a-e-j-6z	2.290
t-DBPO-d-r-η-p-a-e-j-7y	2.316	t-DBPO-d-r-η-p-a-e-j-7z	2.326
t-DBPO-d-r-η-p-a-e-j-5z	2.331		

Table 7.12. HOMO-LUMO energy gap of the calculated conformers of *trans*-DBPO having different geometries of R and the same geometry of the ring system *in vacuo*.
HF/6-31G(d,p) results. Conformers are listed in order of increasing relative energy in the HF results.

Conformer	HOMO-LUMO energy gap (kcal/mol)	Conformer	HOMO-LUMO energy gap (kcal/mol)
t-DBPO-d-r-η-p-a-e-j	257.442	t-DBPO-d-r-η-p-a-e-j-6y	257.473
t-DBPO-d-r-η-p-a-e-j-8y	257.561	t-DBPO-d-r-η-p-a-e-j-4y	257.473
t-DBPO-d-r-η-p-a-e-j-3y	256.940	t-DBPO-d-r-η-p-a-e-j-2y	255.421
t-DBPO-d-r-η-p-a-e-j-3z	256.971	t-DBPO-d-r-η-p-a-e-j-2z	255.396
t-DBPO-d-r-η-p-a-e-j-8z	257.442	t-DBPO-d-r-η-p-a-e-j-4z	257.454
t-DBPO-d-r-η-p-a-e-j-5y	257.392	t-DBPO-d-r-η-p-a-e-j-6z	257.429
t-DBPO-d-r-η-p-a-e-j-7y	257.423	t-DBPO-d-r-η-p-a-e-j-7z	257.404
t-DBPO-d-r-η-p-a-e-j-5z	257.385		

Table 7.13. Relative energies of the calculated conformers of *trans*-DBPO having different geometries of R and the same geometry of the ring system *in vacuo*.
HF/6-31G(d,p), DFT/B3LYP/6-31+G(d,p) and MP2/6-31G(d,p) results *in vacuo*. The results are from full optimisation calculations. The conformers are listed in order of increasing relative energies in the HF results *in vacuo*. The absolute energies of the lowest-energy conformer is-1873.9743975, -1885.7373341 and -1879.9717771 hartree in the HF, DFT and MP2 results respectively.

Conformer	Relative energy (kcal/mol)		
	HF	DFT	MP2
t-DBPO-d-r-η-p-a-e-j	0.000	0.000	0.398
t-DBPO-d-r-η-p-a-e-j-8y	0.342	0.507	0.000
t-DBPO-d-r-η-p-a-e-j-3y	0.508	0.556	0.098
t-DBPO-d-r-η-p-a-e-j-3z	0.510	0.635	0.082
t-DBPO-d-r-η-p-a-e-j-8z	0.974	0.946	0.719
t-DBPO-d-r-η-p-a-e-j-5y	0.994	0.926	0.746
t-DBPO-d-r-η-p-a-e-j-7y	0.997	0.955	0.813
t-DBPO-d-r-η-p-a-e-j-5z	0.997	0.944	0.781
t-DBPO-d-r-η-p-a-e-j-6y	1.020	0.998	0.816
t-DBPO-d-r-η-p-a-e-j-4y	1.028	0.983	0.705
t-DBPO-d-r-η-p-a-e-j-2y	1.028	0.562	0.391
t-DBPO-d-r-η-p-a-e-j-2z	1.033	0.577	0.385
t-DBPO-d-r-η-p-a-e-j-4z	1.045	1.013	0.719
t-DBPO-d-r-η-p-a-e-j-6z	1.047	0.982	0.836
t-DBPO-d-r-η-p-a-e-j-7z	1.076	1.000	0.896

Table 7.14. Parameters of the first IHB of the selected calculated conformers of *trans*-DBPO having different geometries of R and the same geometry of the ring system *in vacuo*.
HF/6-31G(d,p) and DFT/B3LYP/B3LYP/6-31+G(d,p) and MP2/6-31G(d,p) results, are from full optimisation calculations. Conformers are listed in order of increasing relative energy in the HF results. The first IHB is H15···O14.

Conformer	Methods	Parameters the first IHB		
		OH···O (Å)	O···O (Å)	OHO (°)
t-DBPO-d-r-η-p-a-e-j	HF	1.652	2.508	146.4
	DFT	1.529	2.466	151.8
	MP2	1.583	2.505	151.5
t-DBPO-d-r-η-p-a-e-j-8y	HF	1.651	2.508	146.4
	DFT	1.530	2.467	151.7
	MP2	1.583	2.504	151.5
t-DBPO-d-r-η-p-a-e-j-3y	HF	1.654	2.509	146.3
	DFT	1.530	2.467	151.7
	MP2	1.585	2.505	151.3
t-DBPO-d-r-η-p-a-e-j-3z	HF	1.654	2.509	146.3
	DFT	1.529	2.466	151.7
	MP2	1.585	2.505	151.3
t-DBPO-d-r-η-p-a-e-j-8z	HF	1.652	2.508	146.4
	DFT	1.530	2.467	151.7
	MP2	1.583	2.505	151.5
t-DBPO-d-r-η-p-a-e-j-5y	HF	1.652	2.508	146.4
	DFT	1.529	2.467	151.5
	MP2	1.583	2.505	151.5
t-DBPO-d-r-η-p-a-e-j-7y	HF	1.652	2.508	146.4
	DFT	1.529	2.466	151.8
	MP2	1.583	2.505	151.5
t-DBPO-d-r-η-p-a-e-j-5z	HF	1.652	2.508	146.4
	DFT	1.529	2.467	151.8
	MP2	1.584	2.505	151.4
t-DBPO-d-r-η-p-a-e-j-6y	HF	1.652	2.508	146.4
	DFT	1.529	2.467	151.8
	MP2	1.583	2.505	151.5
t-DBPO-d-r-η-p-a-e-j-4y	HF	1.583	2.504	151.5
	DFT	1.530	2.467	151.7
	MP2	1.583	2.504	151.5
t-DBPO-d-r-η-p-a-e-j-2y	HF	1.644	2.503	146.6
	DFT	1.518	2.459	152.0
	MP2	1.574	2.498	151.8
t-DBPO-d-r-η-p-a-e-j-2z	HF	1.644	2.503	146.6
	DFT	1.518	2.459	152.0
	MP2	1.573	2.498	151.8
t-DBPO-d-r-η-p-a-e-j-4z	HF	1.651	2.508	146.4
	DFT	1.529	2.466	151.8
	MP2	1.583	2.504	151.5
t-DBPO-d-r-η-p-a-e-j-6z	HF	1.652	2.508	146.4
	DFT	1.530	2.467	151.8

	MP2	1.583	2.504	151.5
t-DBPO-d-r-η-p-a-e-j-7z	HF	1.652	2.508	146.4
	DFT	1.528	2.468	152.3
	MP2	1.584	2.505	151.5

Table 7.15. The distance between the H atom and the closest C atom in the acceptor aromatic ring for the O–H···π interactions of the selected calculated conformers of *trans*-DBPO having different geometries of R and the same geometry of the ring system *in vacuo*.
HF/6-31G(d,p), DFT/B3LYP/6-31+G(d,p) and MP2/ 6-31G(d,p) results are from full optimisation calculations. Conformers are listed in order of increasing relative energy in the HF results.

Conformer	H16···C23 distance considered (Å)		
	HF	DFT	MP2
t-DBPO-d-r-η-p-a-e-j	2.128	2.057	2.008
t-DBPO-d-r-η-p-a-e-j-8y	2.128	2.053	2.009
t-DBPO-d-r-η-p-a-e-j-3y	2.129	2.059	2.011
t-DBPO-d-r-η-p-a-e-j-3z	2.127	2.055	2.007
t-DBPO-d-r-η-p-a-e-j-8z	2.128	2.055	2.008
t-DBPO-d-r-η-p-a-e-j-5y	2.128	2.057	2.008
t-DBPO-d-r-η-p-a-e-j-7y	2.128	2.057	2.008
t-DBPO-d-r-η-p-a-e-j-5z	2.128	2.052	2.010
t-DBPO-d-r-η-p-a-e-j-6y	2.128	2.059	2.008
t-DBPO-d-r-η-p-a-e-j-4y	2.128	2.057	2.008
t-DBPO-d-r-η-p-a-e-j-2y	2.128	2.051	2.012
t-DBPO-d-r-η-p-a-e-j-2z	2.129	2.057	2.007
t-DBPO-d-r-η-p-a-e-j-4z	2.128	2.053	2.009
t-DBPO-d-r-η-p-a-e-j-6z	2.128	2.055	2.008
t-DBPO-d-r-η-p-a-e-j-7z	2.128	2.039	2.008

Table 7.16. Dipole moments of the calculated conformers of *trans*-DBPO having different geometries of R and the same geometry of the ring system *in vacuo*.
HF/6-31G(d,p), DFT/B3LYP/B3LYP/6-31+G(d,p) and MP2/6-31G(d,p) results are from full optimisation calculations. Conformers are listed in order of increasing relative energy in the HF results.

Conformer	Dipole moment (Debye)		
	HF	DFT	MP2
t-DBPO-d-r-η-p-a-e-j	2.288	2.193	2.277
t-DBPO-d-r-η-p-a-e-j-8y	2.247	2.216	2.264
t-DBPO-d-r-η-p-a-e-j-3y	2.424	2.341	2.434
t-DBPO-d-r-η-p-a-e-j-3z	2.424	2.308	2.432
t-DBPO-d-r-η-p-a-e-j-8z	2.293	2.266	2.285
t-DBPO-d-r-η-p-a-e-j-5y	2.350	2.262	2.356
t-DBPO-d-r-η-p-a-e-j-7y	2.316	2.181	2.306
t-DBPO-d-r-η-p-a-e-j-5z	2.331	2.274	2.330
t-DBPO-d-r-η-p-a-e-j-6y	2.288	2.183	2.289
t-DBPO-d-r-η-p-a-e-j-4y	2.280	2.190	2.296
t-DBPO-d-r-η-p-a-e-j-2y	2.418	2.323	2.504
t-DBPO-d-r-η-p-a-e-j-2z	2.435	2.497	2.520
t-DBPO-d-r-η-p-a-e-j-4z	2.276	2.216	2.288
t-DBPO-d-r-η-p-a-e-j-6z	2.290	2.217	2.285
t-DBPO-d-r-η-p-a-e-j-7z	2.326	2.197	2.329

Table 7.17. HOMO-LUMO energy gap of the calculated conformers of *trans*-DBPO having different geometries of R and the same geometry of the ring system *in vacuo*.
HF/6-31G(d,p), DFT/B3LYP/B3LYP/6-31+G(d,p) and MP2/6-31G(d,p) results are from full optimisation calculations. Conformers are listed in order of increasing relative energy in the HF results.

Conformer	HOMO-LUMO energy gap (kcal/mol)		
	HF	DFT	MP2
t-DBPO-d-r-η-p-a-e-j	257.442	105.177	249.020
t-DBPO-d-r-η-p-a-e-j-8y	257.561	105.277	249.184
t-DBPO-d-r-η-p-a-e-j-3y	256.940	104.744	248.431
t-DBPO-d-r-η-p-a-e-j-3z	256.971	104.800	248.330
t-DBPO-d-r-η-p-a-e-j-8z	257.442	105.164	249.039
t-DBPO-d-r-η-p-a-e-j-5y	257.392	105.101	248.964
t-DBPO-d-r-η-p-a-e-j-7y	257.423	105.064	249.002
t-DBPO-d-r-η-p-a-e-j-5z	257.385	105.139	249.065
t-DBPO-d-r-η-p-a-e-j-6y	257.473	105.158	249.071
t-DBPO-d-r-η-p-a-e-j-4y	257.473	105.233	249.102
t-DBPO-d-r-η-p-a-e-j-2y	255.421	103.332	247.703
t-DBPO-d-r-η-p-a-e-j-2z	255.396	103.326	247.621
t-DBPO-d-r-η-p-a-e-j-4z	257.454	105.271	249.058
t-DBPO-d-r-η-p-a-e-j-6z	257.429	105.158	249.002
t-DBPO-d-r-η-p-a-e-j-7z	257.404	105.854	248.970

Figure 7.5. Shapes of the HOMO and LUMO molecular orbitals of the calculated conformers of *trans*-DBPO having different geometries of R and the same geometry of the ring system *in vacuo*.
HF/6-31G(d,p) results. The conformers are listed in order of increasing relative energy.

HOMO	LUMO	HOMO	LUMO
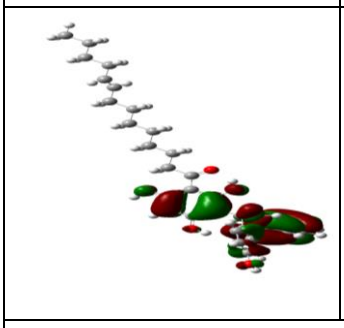	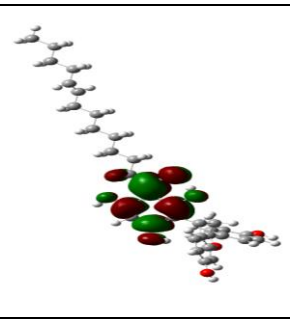	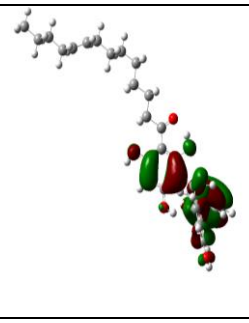	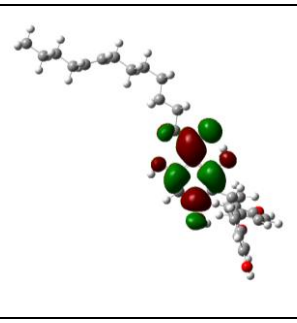
t-DBPO-d-r-η-p-a-e-j		t-DBPO-d-r-η-p-a-e-j-6y	
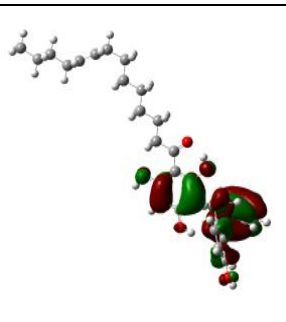	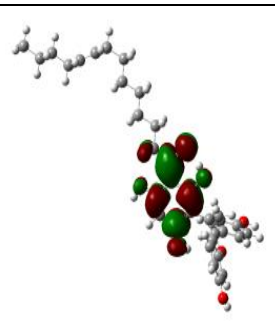	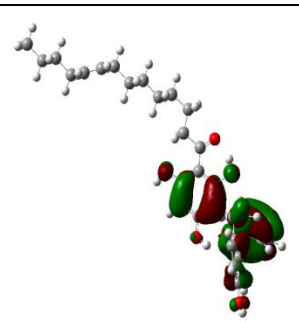	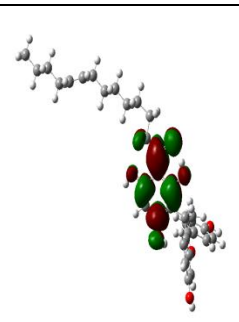
t-DBPO-d-r-η-p-a-e-j-8y		t-DBPO-d-r-η-p-a-e-j-4y	
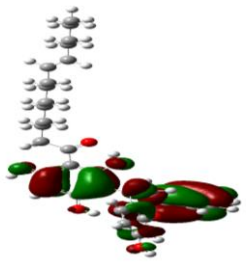	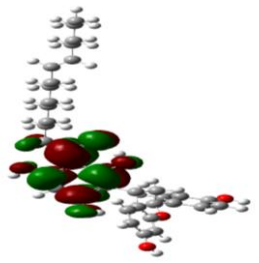	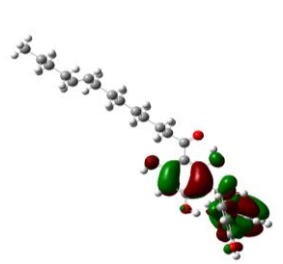	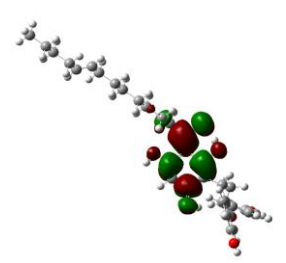
t-DBPO-d-r-η-p-a-e-j-3y		t-DBPO-d-r-η-p-a-e-j-2y	
	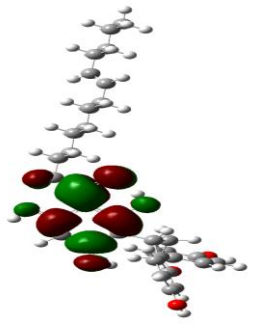	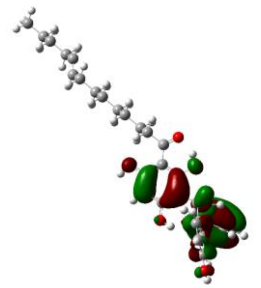	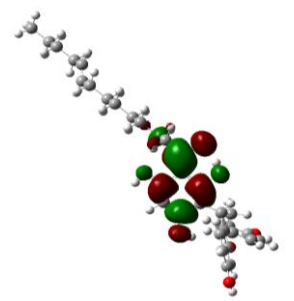
t-DBPO-d-r-η-p-a-e-j-3z		t-DBPO-d-r-η-p-a-e-j-2z	
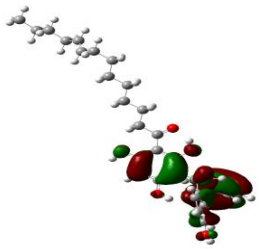	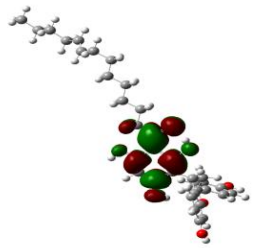	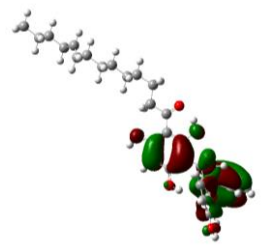	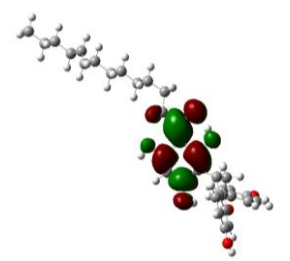

t-DBPO-d-r-η-p-a-e-j-8z		t-DBPO-d-r-η-p-a-e-j-4z	
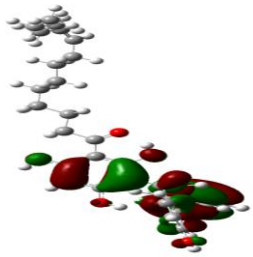	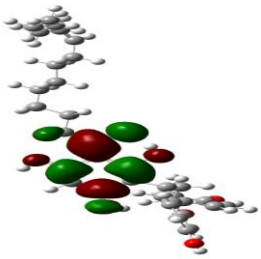	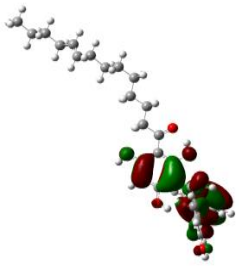	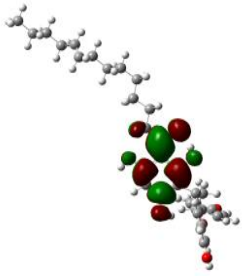
t-DBPO-d-r-η-p-a-e-j-5y		t-DBPO-d-r-η-p-a-e-j-6z	
	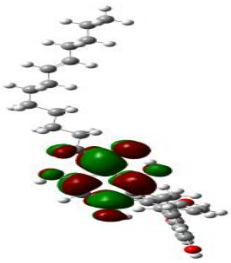		
t-DBPO-d-r-η-p-a-e-j-7y		t-DBPO-d-r-η-p-a-e-j-7z	
	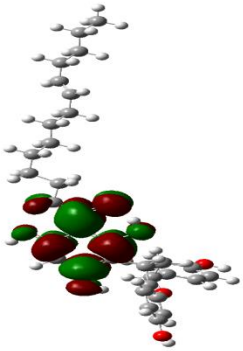		
t-DBPO-d-r-η-p-a-e-j-5z			

Table 7.18. Relative energies of the calculated conformers of *trans*-DBPO having different geometries of R and the same geometry of the ring system *in vacuo* and in three solvents chloroform, acetonitrile and water (respectively denoted as vac, chlrf, actn, aq in the column headings).
HF/6-31G(d,p) results from full optimisation calculations. The conformers are listed in order of increasing relative energies in the HF results *in vacuo*. In the column headings, the media are denoted as vac, chlrf, actn and aq, respectively for vacuum, chloroform acetonitrile and water. The absolute energies of the lowest-energy conformer (hartree) are -1885.7373341, -1873.9933068, -1873.9981978 and -1873.9986123 in vacuo, chloroform, acetonitrile and water respectively.

Conformer	Relative energy (kcal/mol)			
	vac	chlrf	actn	aq
t-DBPO-d-r-η-p-a-e-j	0.000	0.000	0.000	0.000
t-DBPO-d-r-η-p-a-e-j-8y	0.342	0.390	0.408	0.409
t-DBPO-d-r-η-p-a-e-j-3y	0.508	0.712	0.763	0.767
t-DBPO-d-r-η-p-a-e-j-3z	0.510	0.727	0.787	0.791
t-DBPO-d-r-η-p-a-e-j-8z	0.974	0.997	1.005	1.006
t-DBPO-d-r-η-p-a-e-j-5y	0.994	1.026	1.040	1.041
t-DBPO-d-r-η-p-a-e-j-7y	0.997	1.005	1.010	1.010
t-DBPO-d-r-η-p-a-e-j-5z	0.997	1.018	1.028	1.028
t-DBPO-d-r-η-p-a-e-j-6y	1.020	1.044	1.056	1.057
t-DBPO-d-r-η-p-a-e-j-4y	1.028	1.043	1.051	1.051
t-DBPO-d-r-η-p-a-e-j-2y	1.028	0.961	0.940	0.938
t-DBPO-d-r-η-p-a-e-j-2z	1.033	0.973	0.954	0.952
t-DBPO-d-r-η-p-a-e-j-4z	1.045	1.046	1.047	1.047
t-DBPO-d-r-η-p-a-e-j-6z	1.047	1.039	1.033	1.032
t-DBPO-d-r-η-p-a-e-j-7z	1.076	1.099	1.109	1.110

Table 7.19. The solvation free energy (ΔG_{solv}) and its electrostatic component (G_{el}) of the calculated conformers of *trans*-DBPO having different geometries of R and the same geometry of the ring system *in vacuo* and in three solvents chloroform, acetonitrile and water (respectively denoted as vac, chlrf, actn, aq in the column headings).
HF/6-31G(d,p) results. The results *in vacuo* and in solution are from full optimisation calculations.
Conformers are listed in order of increasing relative energy in the HF results *in vacuo*.

Conformer	(ΔG_{solv}) (kcal/mol)			(G_{el}) (kcal/mol)		
	chlrf	actn	aq	chlrf	actn	aq
t-DBPO-d-r-η-p-a-e-j	-2.55	5.91	-16.81	-8.21	-11.76	-27.79
t-DBPO-d-r-η-p-a-e-j-8y	-2.18	6.28	-16.24	-8.15	-11.64	-27.55
t-DBPO-d-r-η-p-a-e-j-3y	-2.12	6.37	-16.25	-8.05	-11.52	-27.53
t-DBPO-d-r-η-p-a-e-j-3z	-1.97	6.48	-16.12	-8.01	-11.49	-27.47
t-DBPO-d-r-η-p-a-e-j-8z	-2.36	6.07	-16.61	-8.18	-11.72	-27.75
t-DBPO-d-r-η-p-a-e-j-5y	-2.18	6.24	-16.41	-8.16	-11.68	-27.71
t-DBPO-d-r-η-p-a-e-j-7y	-2.34	6.12	-16.49	-8.20	-11.71	-27.68
t-DBPO-d-r-η-p-a-e-j-5z	-2.25	6.17	-16.47	-8.16	-11.70	-27.72
t-DBPO-d-r-η-p-a-e-j-6y	-2.26	6.17	-16.49	-8.19	-11.71	-27.74

t-DBPO-d-r-η-p-a-e-j-4y	-2.17	6.27	-16.37	-8.18	-11.68	-27.73
t-DBPO-d-r-η-p-a-e-j-2y	-2.15	6.29	-16.16	-8.35	-11.90	-27.81
t-DBPO-d-r-η-p-a-e-j-2z	-2.06	6.35	-16.21	-8.34	-11.89	-27.92
t-DBPO-d-r-η-p-a-e-j-4z	-2.17	6.27	-16.28	-8.18	-11.69	-27.64
t-DBPO-d-r-η-p-a-e-j-6z	-2.32	6.12	-16.56	-8.21	-11.74	-27.78
t-DBPO-d-r-η-p-a-e-j-7z	-2.37	6.08	-16.62	-8.18	-11.72	-27.77

Table 7.20. Parameters of the H17···O14 IHB of the calculated conformers of *cis*-t-DBPO having different geometries of R and the same geometry of the ring system *in vacuo* and in three solvents chloroform, acetonitrile and water (respectively denoted as vac, chlrf, actn, aq in the column of media headings).

HF/6-31G(d,p) results. The results *in vacuo* and in solution are from full optimisation calculations. Conformers are listed in order of increasing relative energy in the HF results *in vacuo*. The IHB length refers to the H···O distance for the H17···O14, the donor-acceptor distance is O8···O14 and the hydrogen bond angle is OĤO.

Conformer	Media	O···H (Å)	O···O (Å)	OĤO (°)
		1.652	2.508	146.4
	chlrf	1.647	2.507	146.9
	actn	1.645	2.506	147.1
	aq	1.645	2.506	147.1
t-DBPO-d-r-η-p-a-e-j-8y	vac	1.651	2.508	146.4
	chlrf	1.644	2.506	146.9
	actn	1.646	2.506	147.1
	aq	1.644	2.505	147.2
t-DBPO-d-r-η-p-a-e-j-3y	vac	1.654	2.509	146.3
	chlrf	1.651	2.509	146.8
	actn	1.649	2.509	147.0
	aq	1.649	2.509	147.0
t-DBPO-d-r-η-p-a-e-j-3z	vac	1.654	2.509	146.3
	chlrf	1.651	2.510	146.7
	actn	1.651	2.510	146.9
	aq	1.651	2.510	146.9
t-DBPO-d-r-η-p-a-e-j-8z	vac	1.652	2.508	146.4
	chlrf	1.646	2.506	146.9
	actn	1.644	2.506	147.1
	aq	1.644	2.506	147.2
t-DBPO-d-r-η-p-a-e-j-5y	vac	1.652	2.508	146.4
	chlrf	1.646	2.506	146.9
	actn	1.644	2.505	147.1
	aq	1.643	2.505	147.2
t-DBPO-d-r-η-p-a-e-j-7y	vac	1.652	2.508	146.4
	chlrf	1.646	2.506	146.9

	actn	1.644	2.505	147.1
	aq	1.644	2.505	147.2
t-DBPO-d-r-η-p-a-e-j-5z	vac	1.652	2.508	146.4
	chlrf	1.647	2.507	146.9
	actn	1.645	2.506	147.1
	aq	1.645	2.506	147.1
t-DBPO-d-r-η-p-a-e-j-6y	vac	1.652	2.508	146.4
	chlrf	1.646	2.506	146.9
	actn	1.644	2.505	147.1
	aq	1.644	2.505	147.2
t-DBPO-d-r-η-p-a-e-j-4y	vac	1.651	2.508	146.4
	chlrf	1.646	2.506	146.9
	actn	1.644	2.505	147.1
	aq	1.644	2.505	147.2
t-DBPO-d-r-η-p-a-e-j-2y	vac	1.644	2.503	146.6
	chlrf	1.642	2.504	147.1
	actn	1.641	2.504	147.3
	aq	1.640	2.503	147.3
t-DBPO-d-r-η-p-a-e-j-2z	vac	1.644	2.503	146.6
	chlrf	1.640	2.503	147.2
	actn	1.638	2.502	147.4
	aq	1.638	2.502	147.4
t-DBPO-d-r-η-p-a-e-j-4z	vac	1.651	2.508	146.4
	chlrf	1.646	2.506	146.9
	actn	1.644	2.505	147.1
	aq	1.644	2.505	147.2
t-DBPO-d-r-η-p-a-e-j-6z	vac	1.652	2.508	146.4
	chlrf	1.647	2.507	146.9
	actn	1.645	2.506	147.1
	aq	1.645	2.506	147.2
t-DBPO-d-r-η-p-a-e-j-7z	vac	1.652	2.508	146.4
	chlrf	1.647	2.507	146.9
	actn	1.645	2.506	147.1
	aq	1.644	2.506	147.1

Table 7.21. Distance between the H atom and the closest C atom in the acceptor aromatic ring for the O–H···π interactions in selected conformers of *trans*-DBPO having different geometries of R and the same geometry of the ring system *in vacuo* and in three solvents chloroform, acetonitrile and water (respectively denoted as vac, chlrf, actn, aq in the column headings.)
HF/6-31G(d,p) results. The results *in vacuo* and in solution are from full optimisation calculations. Conformers are listed in order of increasing relative energy in the HF results *in vacuo*.

Conformer	H16···C23 distance considered (Å)			
	vac	chlrf	actn	aq
t-DBPO-d-r-η-p-a-e-j	2.128	2.125	2.123	2.124
t-DBPO-d-r-η-p-a-e-j-8y	2.128	2.127	2.127	2.127
t-DBPO-d-r-η-p-a-e-j-3y	2.129	2.126	2.125	2.125
t-DBPO-d-r-η-p-a-e-j-3z	2.127	2.125	2.124	2.124
t-DBPO-d-r-η-p-a-e-j-8z	2.128	2.127	2.126	2.126
t-DBPO-d-r-η-p-a-e-j-5y	2.128	2.127	2.127	2.127
t-DBPO-d-r-η-p-a-e-j-7y	2.128	2.128	2.127	2.127
t-DBPO-d-r-η-p-a-e-j-5z	2.128	2.124	2.123	2.123
t-DBPO-d-r-η-p-a-e-j-6y	2.128	2.127	2.126	2.126
t-DBPO-d-r-η-p-a-e-j-4y	2.128	2.129	2.128	2.128
t-DBPO-d-r-η-p-a-e-j-2y	2.128	2.125	2.124	2.124
t-DBPO-d-r-η-p-a-e-j-2z	2.129	2.124	2.123	2.123
t-DBPO-d-r-η-p-a-e-j-4z	2.128	2.127	2.126	2.126
t-DBPO-d-r-η-p-a-e-j-6z	2.128	2.129	2.128	2.128
t-DBPO-d-r-η-p-a-e-j-7z	2.128	2.126	2.125	2.125

Table 7.22. Dipole moment of the calculated conformers of *trans*-DBPO having different geometries of R and the same geometry of the ring system *in vacuo* and in three solvents chloroform, acetonitrile and water (respectively denoted as vac, chlrf, actn, aq in the column headings).
HF/6-31G(d,p) results. The results *in vacuo* and in solution are from full optimisation calculations. Conformers are listed in order of increasing relative energy in the HF results *in vacuo*.

Conformer	Dipole moment (Debye)			
	vac	chlrf	actn	aq
t-DBPO-d-r-η-p-a-e-j	2.288	2.721	2.894	2.908
t-DBPO-d-r-η-p-a-e-j-8y	2.247	2.696	2.862	2.878
t-DBPO-d-r-η-p-a-e-j-3y	2.424	2.722	2.860	2.874
t-DBPO-d-r-η-p-a-e-j-3z	2.424	2.787	2.911	2.919
t-DBPO-d-r-η-p-a-e-j-8z	2.293	2.716	2.881	2.897
t-DBPO-d-r-η-p-a-e-j-5y	2.350	2.746	2.896	2.908
t-DBPO-d-r-η-p-a-e-j-7y	2.316	2.726	2.890	2.905
t-DBPO-d-r-η-p-a-e-j-5z	2.331	2.755	2.915	2.930
t-DBPO-d-r-η-p-a-e-j-6y	2.288	2.715	2.879	2.885
t-DBPO-d-r-η-p-a-e-j-4y	2.280	2.740	2.905	2.920
t-DBPO-d-r-η-p-a-e-j-2y	2.418	2.922	3.120	3.138
t-DBPO-d-r-η-p-a-e-j-2z	2.435	2.936	3.126	3.143
t-DBPO-d-r-η-p-a-e-j-4z	2.276	2.725	2.901	2.917
t-DBPO-d-r-η-p-a-e-j-6z	2.290	2.699	2.867	2.883
t-DBPO-d-r-η-p-a-e-j-7z	2.326	2.753	2.899	2.913

Table 7.23. HOMO-LUMO energy gap of the calculated conformers of *trans*-DBPO having different geometries of R and the same geometry of the ring system *in vacuo* and in three solvents chloroform, acetonitrile and water (respectively denoted as vac, chlrf, actn, aq in the column headings).
HF/6-31G(d,p) results. The results *in vacuo* and in solution are from full optimisation calculations. Conformers are listed in order of increasing relative energy in the HF results *in vacuo*.

Conformer	HOMO-LUMO energy gap (kcal/mol)			
	vac	chlrf	actn	aq
t-DBPO-d-r-η-p-a-e-j	257.442	256.846	256.576	256.551
t-DBPO-d-r-η-p-a-e-j-8y	257.561	256.827	256.532	256.501
t-DBPO-d-r-η-p-a-e-j-3y	256.940	256.626	256.406	256.381
t-DBPO-d-r-η-p-a-e-j-3z	256.971	256.526	256.344	256.337
t-DBPO-d-r-η-p-a-e-j-8z	257.442	256.802	256.519	256.488
t-DBPO-d-r-η-p-a-e-j-5y	257.392	256.777	256.513	256.488
t-DBPO-d-r-η-p-a-e-j-7y	257.423	256.789	256.501	256.475
t-DBPO-d-r-η-p-a-e-j-5z	257.385	256.839	256.570	256.551
t-DBPO-d-r-η-p-a-e-j-6y	257.473	256.827	256.545	256.526
t-DBPO-d-r-η-p-a-e-j-4y	257.473	256.783	256.501	256.475
t-DBPO-d-r-η-p-a-e-j-2y	255.421	254.405	253.991	253.953
t-DBPO-d-r-η-p-a-e-j-2z	255.396	254.424	254.034	253.997
t-DBPO-d-r-η-p-a-e-j-4z	257.454	256.846	256.563	256.538
t-DBPO-d-r-η-p-a-e-j-6z	257.429	256.833	256.545	256.519
t-DBPO-d-r-η-p-a-e-j-7z	257.404	256.814	256.570	256.551

Table 7.24. Relative energies of all calculated conformers of *trans*-DBPO.
HF/6-31G(d,p) results *in vacuo*. The conformers are listed in order of increasing relative energy.

Conformer	Relative energy kcal/mol	Conformer	Relative energy kcal/mol
t-DBPO-d-r-η-p-a-e-j	0.000	t-DBPO-d-r-q-b-e-k	5.719
t-DBPO-d-r-η-p-a-e-k	0.014	t-DBPO-d-r-q-b-e-j	5.736
t-DBPO-d-r-η-p-a-e-j-8y	0.342	t-DBPO-d-r-q-a-e-k	5.745
t-DBPO-d-r-η-p-a-f-j	0.424	t-DBPO-s-r-p-a-f-j	5.754
t-DBPO-d-r-η-p-a-f-k	0.496	t-DBPO-d-w-q-a-f-k	5.827
t-DBPO-d-r-η-p-a-e-j-3y	0.508	t-DBPO-d-w-q-b-f-j	5.853
t-DBPO-d-r-η-p-a-e-j-5z	0.997	t-DBPO-d-w-q-b-f-k	5.936
t-DBPO-d-r-η-p-a-e-j-6y	1.020	t-DBPO-d-r-q-b-f-j	6.116
t-DBPO-d-r-η-p-b-e-k	1.023	t-DBPO-s-w-p-a-e-j	6.122
t-DBPO-d-r-η-p-a-e-j-4y	1.028	t-DBPO-d-r-q-b-f-k	6.149
t-DBPO-d-r-η-p-a-e-j-2y	1.028	t-DBPO-d-r-q-a-f-j	6.158
t-DBPO-d-r-η-p-b-e-j	1.028	t-DBPO-d-r-q-a-f-k	6.228
t-DBPO-d-r-η-p-a-e-j-2z	1.033	t-DBPO-s-r-u-p-b-e-k	6.236
t-DBPO-d-r-η-p-a-e-j-4z	1.045	t-DBPO-s-r-u-p-a-e-j	6.281
t-DBPO-d-r-η-p-a-e-j-6z	1.047	t-DBPO-d-w-u-p-a-e-j	6.398
t-DBPO-d-r-η-p-a-e-j-7z	1.076	t-DBPO-s-w-p-a-f-j	6.429
t-DBPO-s-w-ε-q-a-e-k	1.154	t-DBPO-s-w-p-a-f-k	6.509

t-DBPO-s-w-ε-q-a-e-j	1.200	t-DBPO-s-w-u-p-b-f-j	6.615
t-DBPO-d-r-η-p-b-f-j	1.231	t-DBPO-s-r-u-p-a-f-j	6.705
t-DBPO-d-r-η-p-b-f-k	1.264	t-DBPO-s-r-u-p-a-f-k	6.722
t-DBPO-s-w-ε-q-b-e-j	1.496	t-DBPO-s-w-p-b-e-j	7.079
t-DBPO-s-w-ε-q-a-f-j	1.636	t-DBPO-s-w-p-e-a-k	7.159
t-DBPO-s-w-ε-q-a-f-k	1.652	t-DBPO-s-r-u-p-b-f-k	7.172
t-DBPO-s-w-ε-q-b-f-k	1.976	t-DBPO-s-r-p-b-f-k	7.459
t-DBPO-d-w-p-a-e-j	4.323	t-DBPO-d-w-u-p-a-e-k	7.851
t-DBPO-d-w-p-a-e-k	4.459	t-DBPO-d-w-u-p-b-e-k	7.875
t-DBPO-d-w-p-a-f-j	4.658	t-DBPO-d-w-u-p-a-f-j	8.070
t-DBPO-d-w-p-b-f-j	4.678	t-DBPO-d-w-u-p-b-f-j	8.095
t-DBPO-d-r-η-u-p-a-e-j	4.696	t-DBPO-s-w-u-p-a-e-j	8.201
t-DBPO-d-r-η-u-p-a-e-k	4.684	t-DBPO-d-w-u-p-a-f-k	8.256
t-DBPO-s-r-ε-q-b-e-j	4.705	t-DBPO-d-w-u-p-b-f-k	8.258
t-DBPO-s-r-ε-q-b-f-j	4.833	t-DBPO-s-w-u-p-e-a-k	8.285
t-DBPO-d-w-p-a-f-k	4.853	t-DBPO-d-w-u-q-a-e-j	8.391
t-DBPO-s-r-ε-q-b-f-k	5.026	t-DBPO-s-w-u-q-a-e-j	8.409
t-DBPO-s-r-ε-q-a-e-k	5.031	t-DBPO-d-w-u-q-b-e-j	8.459
t-DBPO-s-r-p-b-e-j	5.046	t-DBPO-d-w-u-q-a-e-k	8.488
t-DBPO-d-r-η-u-p-a-f-j	5.096	t-DBPO-s-w-u-q-a-e-k	8.500
t-DBPO-s-r-ε-q-a-e-j	5.155	t-DBPO-s-w-u-p-a-f-j	8.557
t-DBPO-d-w-p-b-e-k	5.166	t-DBPO-s-w-u-p-b-e-k	8.572
t-DBPO-d-r-η-u-p-a-f-k	5.163	t-DBPO-s-w-u-p-a-f-k	8.702
t-DBPO-d-w-q-b-e-j	5.188	t-DBPO-s-w-u-q-b-e-k	8.739
t-DBPO-d-w-p-b-f-k	5.228	t-DBPO-d-w-u-q-a-f-j	8.850
t-DBPO-d-w-q-a-e-j	5.213	t-DBPO-s-w-u-p-b-f-k	8.867
t-DBPO-s-r-p-e-a-k	5.222	t-DBPO-s-w-u-q-a-f-k	8.884
t-DBPO-s-r-3-p-b-e-k	5.265	t-DBPO-d-w-u-q-a-f-k	9.008
t-DBPO-d-w-q-a-e-k	5.291	t-DBPO-d-w-u-q-b-f-k	9.239
t-DBPO-s-r-p-a-e-j	5.355	t-DBPO-d-r-u-q-a-e-j	10.163
t-DBPO-s-r-ε-q-a-f-k	5.505	t-DBPO-s-r-u-q-b-e-j	10.283
t-DBPO-d-w-q-b-e-k	5.559	t-DBPO-d-r-u-q-a-f-j	10.563
t-DBPO-s-r-ε-q-a-f-j	5.565	t-DBPO-s-r-u-q-a-e-j	11.105
t-DBPO-s-w-p-b-f-j	5.596	t-DBPO-s-r-u-q-a-e-k	11.128
t-DBPO-s-r-p-a-f-k	5.682	t-DBPO-s-r-u-q-a-f-j	11.402
t-DBPO-d-w-q-a-f-j	5.687	t-DBPO-s-r-u-q-a-f-k	11.487
t-DBPO-d-r-q-a-e-j	5.718		

Table 7.25. Parameters of the first IHB of all calculated conformers of *trans*-DBPO.
HF/6-31G(d,p) results *in vacuo*. For conformers of d type, the first IHB is H15···O14; for conformers of s type, the first IHB is H17···O14. The conformers are listed in order of increasing relative energy.

Conformer	OH···O (Å)	O···O (Å)	OHO (°)
t-DBPO-d-r-η-p-a-e-j	1.652	2.508	146.4
t-DBPO-d-r-η-p-a-e-k	1.652	2.508	146.3
t-DBPO-d-r-η-p-a-e-j-8y	1.651	2.508	146.4
t-DBPO-d-r-η-p-a-f-j	1.652	2.508	146.4
t-DBPO-d-r-η-p-a-f-k	1.652	2.508	146.3
t-DBPO-d-r-η-p-a-e-j-3y	1.654	2.509	146.3
t-DBPO-d-r-η-p-a-e-j-3z	1.654	2.509	146.3
t-DBPO-d-r-η-p-a-e-j-8z	1.652	2.508	146.4
t-DBPO-d-r-η-p-a-e-j-5y	1.652	2.508	146.4
t-DBPO-d-r-η-p-a-e-j-7y	1.652	2.508	146.4
t-DBPO-d-r-η-p-a-e-j-5z	1.652	2.508	146.4
t-DBPO-d-r-η-p-a-e-j-6y	1.652	2.508	146.4
t-DBPO-d-r-η-p-b-e-k	1.651	2.508	146.6
t-DBPO-d-r-η-p-a-e-j-4y	1.651	2.508	146.4
t-DBPO-d-r-η-p-a-e-j-2y	1.644	2.503	146.6
t-DBPO-d-r-η-p-b-e-j	1.655	2.510	146.2
t-DBPO-d-r-η-p-a-e-j-2z	1.644	2.503	146.6
t-DBPO-d-r-η-p-a-e-j-4z	1.651	2.508	146.4
t-DBPO-d-r-η-p-a-e-j-6z	1.652	2.508	146.4
t-DBPO-d-r-η-p-a-e-j-7z	1.652	2.508	146.4
t-DBPO-s-w-ε-q-a-e-k	1.684	2.522	143.9
t-DBPO-s-w-ε-q-a-e-j	1.684	2.521	143.9
t-DBPO-d-r-η-p-b-f-j	1.655	2.510	146.2
t-DBPO-d-r-η-p-b-f-k	1.651	2.509	146.5
t-DBPO-s-w-ε-q-b-e-j	1.689	2.527	144.0
t-DBPO-s-w-ε-q-a-f-j	1.682	2.520	143.9
t-DBPO-s-w-ε-q-a-f-k	1.683	2.521	143.9
t-DBPO-s-w-ε-q-b-f-k	1.689	2.526	144.0
t-DBPO-d-w-p-a-e-j	1.656	2.511	146.2
t-DBPO-d-w-p-a-e-k	1.656	2.511	146.2
t-DBPO-d-w-p-a-f-j	1.656	2.511	146.2
t-DBPO-d-w-p-b-f-j	1.656	2.510	146.3
t-DBPO-d-r-η-u-p-a-e-j	1.675	2.523	145.4
t-DBPO-d-r-η-u-p-a-e-k	1.676	2.524	145.4
t-DBPO-s-r-ε-q-b-e-j	1.695	2.531	143.9
t-DBPO-s-r-ε-q-b-f-j	1.694	2.531	143.9
t-DBPO-d-w-p-a-f-k	1.656	2.511	146.2
t-DBPO-s-r-ε-q-b-f-k	1.694	2.531	143.9
t-DBPO-s-r-ε-q-a-e-k	1.692	2.527	143.8
t-DBPO-s-r-η-p-b-e-j	1.697	2.532	143.7
t-DBPO-d-r-η-u-p-a-f-j	1.675	2.522	145.4
t-DBPO-d-w-p-b-e-k	1.658	2.512	146.2
t-DBPO-d-r-η-u-p-a-f-k	1.676	2.523	145.4

t-DBPO-s-r-ε-q-a-e-j	1.690	2.526	143.8
t-DBPO-d-w-p-b-e-j	1.659	2.512	146.1
t-DBPO-d-w-q-b-e-j	1.664	2.514	145.6
t-DBPO-d-w-p-b-f-k	1.659	2.513	146.1
t-DBPO-d-r-q-b-f-j	1.649	2.506	146.3
t-DBPO-d-w-q-a-e-j	1.654	2.508	146.1
t-DBPO-s-r-η-p-e-a-k	1.697	2.532	143.7
t-DBPO-s-r-η-p-b-e-k	1.692	2.528	143.8
t-DBPO-d-w-q-a-e-k	1.654	2.508	146.1
t-DBPO-s-r-η-p-a-e-j	1.697	2.532	143.7
t-DBPO-s-r-ε-q-a-f-k	1.689	2.526	143.8
t-DBPO-d-w-q-b-e-k	1.664	2.514	145.6
t-DBPO-s-r-ε-q-a-f-j	1.688	2.524	143.9
t-DBPO-s-w-p-b-f-j	1.683	2.521	143.9
t-DBPO-s-r-η-p-a-f-k	1.697	2.532	143.7
t-DBPO-d-w-q-a-f-j	1.655	2.509	146.0
t-DBPO-d-r-q-a-e-j	1.646	2.503	146.4
t-DBPO-d-r-q-b-e-k	1.647	2.505	146.5
t-DBPO-d-r-q-b-e-j	1.647	2.504	146.4
t-DBPO-d-r-q-a-e-k	1.646	2.503	146.4
t-DBPO-s-r-η-p-a-f-j	1.696	2.531	143.7
t-DBPO-d-w-q-a-f-k	1.656	2.509	146.0
t-DBPO-d-w-q-b-f-k	1.657	2.511	146.0
t-DBPO-s-w-p-a-e-j	1.689	2.526	143.7
t-DBPO-d-r-q-b-f-k	1.649	2.506	146.3
t-DBPO-d-r-q-a-f-j	1.648	2.504	146.3
t-DBPO-d-r-q-a-f-k	1.648	2.504	146.3
t-DBPO-s-r-η-u-p-b-e-k	1.736	2.559	142.5
t-DBPO-s-r-η-u-p-a-e-j	1.737	2.560	142.4
t-DBPO-d-w-u-p-a-e-j	1.714	2.546	143.4
t-DBPO-s-w-p-a-f-j	1.689	2.526	143.8
t-DBPO-s-w-p-a-f-k	1.689	2.526	143.8
t-DBPO-s-w-u-p-b-f-j	1.739	2.562	142.5
t-DBPO-s-r-η-u-p-a-f-j	1.738	2.560	142.4
t-DBPO-s-r-η-u-p-a-f-k	1.737	2.560	142.4
t-DBPO-s-w-p-b-e-j	1.686	2.523	143.7
t-DBPO-s-w-p-e-a-k	1.686	2.522	143.8
t-DBPO-s-r-η-u-p-b-f-k	1.731	2.555	142.6
t-DBPO-s-r-η-p-b-f-k	1.686	2.523	143.8
t-DBPO-d-w-u-p-a-e-k	1.681	2.526	145.2
t-DBPO-d-w-u-p-b-e-k	1.681	2.526	145.2
t-DBPO-d-w-u-p-a-f-j	1.682	2.527	145.2
t-DBPO-d-w-u-p-b-f-j	1.682	2.527	145.3
t-DBPO-s-w-u-p-a-e-j	1.731	2.554	142.4
t-DBPO-d-w-u-p-a-f-k	1.682	2.527	145.2
t-DBPO-d-w-u-p-b-f-k	1.682	2.528	145.3
t-DBPO-s-w-u-p-e-a-k	1.731	2.554	142.4
t-DBPO-d-w-u-q-a-e-j	1.685	2.530	145.2
t-DBPO-s-w-u-q-a-e-j	1.732	2.555	142.4

t-DBPO-s-w-u-q-b-e-j	1.730	2.555	142.6
t-DBPO-d-w-u-q-b-e-j	1.694	2.532	144.4
t-DBPO-d-w-u-q-a-e-k	1.686	2.530	145.2
t-DBPO-s-w-u-q-a-e-k	1.732	2.556	142.4
t-DBPO-s-w-u-p-a-f-j	1.731	2.554	142.4
t-DBPO-s-w-u-p-b-e-k	1.725	2.550	142.6
t-DBPO-s-w-u-p-a-f-k	1.731	2.554	142.4
t-DBPO-d-w-u-q-a-f-j	1.686	2.529	145.1
t-DBPO-s-w-u-p-b-f-k	1.725	2.551	142.6
t-DBPO-s-w-u-q-a-f-k	1.730	2.555	142.5
t-DBPO-d-w-u-q-a-f-k	1.687	2.530	145.1
t-DBPO-d-w-u-q-b-f-k	1.684	2.528	145.1
t-DBPO-d-r-u-q-a-e-j	1.676	2.520	145.0
t-DBPO-s-r-u-q-b-e-j	1.738	2.562	142.5
t-DBPO-d-r-u-q-a-f-j	1.679	2.522	144.8
t-DBPO-s-r-u-q-a-e-j	1.739	2.561	142.4
t-DBPO-s-r-u-q-a-e-k	1.740	2.562	142.4
t-DBPO-s-r-u-q-a-f-j	1.740	2.562	142.4
t-DBPO-s-r-u-q-a-f-k	1.738	2.560	142.4

Table 7.26. The distance between the H atom and the closest C atom in the acceptor aromatic ring for the O–H···π interactions of all calculated conformers of *trans*-DBPO.
HF/6-31G(d,p) results *in vacuo*. The conformers are arranged in order of increasing relative energy. .For p-type conformers, the distance considered is H16···C23; for q-type conformers, the distance considered is H15···C23.

Conformer	H15···C23 or H16···C23 (Å)	Conformer	H15···C23 or H16···C23 (Å)
t-DBPO-d-r-η-p-a-e-j	2.128	t-DBPO-s-w-ε-q-a-f-j	2.076
t-DBPO-d-r-η-p-a-e-k	2.127	t-DBPO-s-w-ε-q-a-f-k	2.075
t-DBPO-d-r-η-p-a-e-j-8y	2.128	t-DBPO-s-w-ε-q-b-f-k	2.187
t-DBPO-d-r-η-p-a-f-j	2.131	t-DBPO-d-r-η-u-p-a-e-j	2.128
t-DBPO-d-r-η-p-a-f-k	2.130	t-DBPO-d-r-η-u-p-a-e-k	2.128
t-DBPO-d-r-η-p-a-e-j-3y	2.129	t-DBPO-s-r-ε-q-b-e-j	2.165
t-DBPO-d-r-η-p-a-e-j-3z	2.127	t-DBPO-s-r-ε-q-b-f-j	2.169
t-DBPO-d-r-η-p-a-e-j-8z	2.128	t-DBPO-s-r-ε-q-a-e-k	2.109
t-DBPO-d-r-η-p-a-e-j-5y	2.128	t-DBPO-s-r-η-p-b-e-j	2.109
t-DBPO-d-r-η-p-a-e-j-7y	2.128	t-DBPO-d-r-η-u-p-a-f-j	2.130
t-DBPO-d-r-η-p-a-e-j-5z	2.128	t-DBPO-d-r-η-u-p-a-f-k	2.130
t-DBPO-d-r-η-p-a-e-j-6y	2.128	t-DBPO-s-r-ε-q-a-e-j	2.058
t-DBPO-d-r-η-p-b-e-k	2.213	t-DBPO-s-r-η-p-e-a-k	2.109
t-DBPO-d-r-η-p-a-e-j-4y	2.128	t-DBPO-s-r-η-p-b-e-k	2.220
t-DBPO-d-r-η-p-a-e-j-2y	2.128	t-DBPO-s-r-η-p -a-e-j	2.109
t-DBPO-d-r-η-p-b-e-j	2.236	t-DBPO-s-r-ε-q-a-f-k	2.059

t-DBPO-d-r-η-p-a-e-j-2z	2.129	t-DBPO-s-r-ε-q-a-f-j	2.059
t-DBPO-d-r-η-p-a-e-j-4z	2.128	t-DBPO-s-r-η-p-a-f-k	2.111
t-DBPO-d-r-η-p-a-e-j-6z	2.128	t-DBPO-s-r-η-p-a-f-j	2.112
t-DBPO-d-r-η-p-a-e-j-7z	2.128	t-DBPO-s-r-η-u-p-b-e-k	2.121
t-DBPO-s-w-ε-q-a-e-k	2.074	t-DBPO-s-r-η-u-p-a-e-j	2.121
t-DBPO-s-w-ε-q-a-e-j	2.074	t-DBPO-s-r-η-u-p-a-f-j	2.123
t-DBPO-d-r-η-p-b-f-j	2.239	t-DBPO-s-r-η-u-p-a-f-k	2.123
t-DBPO-d-r-η-p-b-f-k	2.219	t-DBPO-s-r-η-u-p-b-f-k	2.240
t-DBPO-s-w-ε-q-b-e-j	2.185		

Table 7.27. Dipole moment of all calculated conformers of *trans*-DBPO.
HF/6-31G(d,p) results *in vacuo*. The conformers are listed in order of increasing relative energy.

Conformer	Dipole moment (Debye)	Conformer	Dipole moment (Debye)
t-DBPO-d-r-η-p-a-e-j	2.460	t-DBPO-s-w-p-b-f-j	2.486
t-DBPO-d-r-η-p-a-e-k	3.834	t-DBPO-s-r-η-p-a-f-k	4.531
t-DBPO-d-r-η-p-a-e-j-8y	2.247	t-DBPO-d-w-q-a-f-j	8.205
t-DBPO-d-r-η-p-a-f-j	2.877	t-DBPO-d-r-q-a-e-j	3.641
t-DBPO-d-r-η-p-a-f-k	4.115	t-DBPO-d-r-q-b-e-k	3.571
t-DBPO-d-r-η-p-a-e-j-3y	2.424	t-DBPO-d-r-q-b-e-j	3.463
t-DBPO-d-r-η-p-a-e-j-3z	2.424	t-DBPO-d-r-q-a-e-k	4.755
t-DBPO-d-r-η-p-a-e-j-8z	2.293	t-DBPO-s-r-η-p-a-f-j	7.228
t-DBPO-d-r-η-p-a-e-j-5y	2.350	t-DBPO-d-w-q-a-f-k	9.417
t-DBPO-d-r-η-p-a-e-j-7y	2.316	t-DBPO-d-w-q-b-f-j	8.498
t-DBPO-d-r-η-p-a-e-j-5z	2.331	t-DBPO-s-w-p-a-e-j	4.463
t-DBPO-d-r-η-p-a-e-j-6y	2.288	t-DBPO-d-r-q-b-f-k	5.723
t-DBPO-d-r-η-p-b-e-k	2.463	t-DBPO-d-r-q-a-f-j	5.049
t-DBPO-d-r-η-p-a-e-j-4y	2.280	t-DBPO-d-r-q-a-f-k	6.137
t-DBPO-d-r-η-p-a-e-j-2y	2.418	t-DBPO-s-r-η-u-p-b-e-k	3.845
t-DBPO-d-r-η-p-b-e-j	2.652	t-DBPO-s-r-η-u-p-a-e-j	5.700
t-DBPO-d-r-η-p-a-e-j-2z	2.435	t-DBPO-d-w-u-p-a-e-j	7.692
t-DBPO-d-r-η-p-a-e-j-4z	2.276	t-DBPO-s-w-p-a-f-j	3.536
t-DBPO-d-r-η-p-a-e-j-6z	2.290	t-DBPO-s-w-p-a-f-k	0.995
t-DBPO-d-r-η-p-a-e-j-7z	2.326	t-DBPO-s-w-u-p-b-f-j	5.888
t-DBPO-s-w-ε-q-a-e-k	2.993	t-DBPO-s-r-η-u-p-a-f-j	5.749
t-DBPO-s-w-ε-q-a-e-j	5.279	t-DBPO-s-r-η-u-p-a-f-k	4.035
t-DBPO-d-r-η-p-b-f-j	3.473	t-DBPO-s-w-p-b-e-j	4.326
t-DBPO-d-r-η-p-b-f-k	3.666	t-DBPO-s-w-p-e-a-k	3.187
t-DBPO-s-w-ε-q-b-e-j	4.900	t-DBPO-s-r-η-u-p-b-f-k	4.477
t-DBPO-s-w-ε-q-a-f-j	5.068	t-DBPO-s-r-η-p-b-f-k	0.892
t-DBPO-s-w-ε-q-a-f-k	2.723	t-DBPO-d-w-u-p-a-e-k	6.327
t-DBPO-s-w-u-q-b-e-k	2.780	t-DBPO-d-w-u-p-b-e-k	6.273
t-DBPO-s-w-ε-q-b-f-k	3.062	t-DBPO-d-w-u-p-a-f-j	4.848

t-DBPO-d-w-p-a-e-j	5.040	t-DBPO-d-w-u-p-b-f-j	4.950
t-DBPO-d-w-p-a-e-k	7.227	t-DBPO-s-w-u-p-a-e-j	2.284
t-DBPO-d-w-p-a-f-j	5.408	t-DBPO-d-w-u-p-a-f-k	7.098
t-DBPO-d-w-p-b-f-j	5.348	t-DBPO-d-w-u-p-b-f-k	7.160
t-DBPO-d-r-η-u-p-a-e-j	0.855	t-DBPO-s-w-u-p-e-a-k	2.727
t-DBPO-d-r-η-u-p-a-e-k	2.946	t-DBPO-d-w-u-q-a-e-j	4.223
t-DBPO-s-r-ε-q-b-e-j	7.759	t-DBPO-s-w-u-q-b-e-j	1.363
t-DBPO-s-r-ε-q-b-f-j	6.184	t-DBPO-d-w-u-q-b-e-j	4.031
t-DBPO-d-w-p-a-f-k	7.432	t-DBPO-d-w-u-q-a-e-k	6.449
t-DBPO-s-r-ε-q-b-f-k	4.480	t-DBPO-s-w-u-q-a-e-k	2.061
t-DBPO-s-r-ε-q-a-e-k	5.494	t-DBPO-s-w-u-p-a-f-j	3.271
t-DBPO-s-r-η-p-b-e-j	7.838	t-DBPO-s-w-u-p-b-e-k	3.384
t-DBPO-d-r-η-u-p-a-f-j	2.573	t-DBPO-s-w-u-p-a-f-k	3.661
t-DBPO-d-w-p-b-e-k	6.530	t-DBPO-d-w-u-q-a-f-j	6.114
t-DBPO-d-r-η-u-p-a-f-k	3.896	t-DBPO-s-w-u-p-b-f-k	3.533
t-DBPO-s-r-ε-q-a-e-j	7.897	t-DBPO-s-w-u-q-a-f-k	2.661
t-DBPO-d-w-q-b-e-j	5.836	t-DBPO-d-w-u-q-a-f-k	7.871
t-DBPO-d-w-p-b-f-k	6.531	t-DBPO-d-w-u-q-b-f-k	7.985
t-DBPO-d-w-q-a-e-j	6.363	t-DBPO-d-r-u-q-a-e-j	1.061
t-DBPO-s-r-η-p-e-a-k	5.365	t-DBPO-s-r-u-q-b-e-j	4.605
t-DBPO-s-r-η-p-b-e-k	6.633	t-DBPO-d-r-u-q-a-f-j	2.888
t-DBPO-d-w-q-a-e-k	7.756	t-DBPO-s-r-u-q-a-e-j	4.507
t-DBPO-s-r-η-p-a-e-j	7.838	t-DBPO-s-r-u-q-a-e-k	3.117
t-DBPO-s-r-ε-q-a-f-k	4.350	t-DBPO-s-r-u-q-a-f-j	7.085
t-DBPO-d-w-q-b-e-k	7.438	t-DBPO-s-r-u-q-a-f-k	1.315
t-DBPO-s-r-ε-q-a-f-j	7.085		

Table 7.28. HOMO-LUMO energy gaps of all calculated conformers of *trans*-DBPO.
HF/6-31G(d,p) results *in vacuo*. The conformers are listed in order of increasing relative energy.

Conformer	HOMO-LUMO energy gap kcal/mol	Conformer	HOMO-LUMO energy gap kcal/mol
t-DBPO-d-r-η-p-a-e-j	257.410	t-DBPO-d-w-q-a-f-j	242.206
t-DBPO-d-r-η-p-a-e-k	257.517	t-DBPO-d-r-q-a-e-j	247.075
t-DBPO-d-r-η-p-a-e-j-8y	257.561	t-DBPO-d-r-q-b-e-k	248.657
t-DBPO-d-r-η-p-a-f-j	256.250	t-DBPO-d-r-q-b-e-j	249.134
t-DBPO-d-r-η-p-a-f-k	256.425	t-DBPO-d-r-q-a-e-k	246.529
t-DBPO-d-r-η-p-a-e-j-3y	256.940	t-DBPO-s-r-η-p-a-f-j	259.946
t-DBPO-d-r-η-p-a-e-j-3z	256.971	t-DBPO-d-w-q-a-f-k	241.641
t-DBPO-d-r-η-p-a-e-j-8z	257.442	t-DBPO-d-w-q-b-f-j	243.066
t-DBPO-d-r-η-p-a-e-j-5y	257.392	t-DBPO-d-w-q-b-f-k	242.570
t-DBPO-d-r-η-p-a-e-j-7y	257.423	t-DBPO-d-r-q-b-f-j	249.435
t-DBPO-d-r-η-p-a-e-j-5z	257.385	t-DBPO-s-w-p-a-e-j	252.158
t-DBPO-d-r-η-p-a-e-j-6y	257.473	t-DBPO-d-r-q-b-f-k	249.096
t-DBPO-d-r-η-p-b-e-k	254.649	t-DBPO-d-r-q-a-f-j	248.312

t-DBPO-d-r-η-p-a-e-j-4y	257.473	t-DBPO-d-r-q-a-f-k	247.728
t-DBPO-d-r-η-p-a-e-j-2y	255.421	t-DBPO-s-r-η-u-p-b-e-k	251.531
t-DBPO-d-r-η-p-b-e-j	255.904	t-DBPO-s-r-η-u-p-a-e-j	251.493
t-DBPO-d-r-η-p-a-e-j-2z	255.396	t-DBPO-d-w-u-p-a-e-j	258.691
t-DBPO-d-r-η-p-a-e-j-4z	257.454	t-DBPO-s-w-p-a-f-j	253.099
t-DBPO-d-r-η-p-a-e-j-6z	257.429	t-DBPO-s-w-p-a-f-k	252.629
t-DBPO-d-r-η-p-a-e-j-7z	257.404	t-DBPO-s-w-u-p-b-f-j	250.571
t-DBPO-s-w-ε-q-a-e-k	258.829	t-DBPO-s-r-η-u-p-a-f-j	250.797
t-DBPO-s-w-ε-q-a-e-j	258.785	t-DBPO-s-r-η-u-p-a-f-k	250.928
t-DBPO-d-r-η-p-b-f-j	256.042	t-DBPO-s-w-p-b-e-j	253.288
t-DBPO-d-r-η-p-b-f-k	255.126	t-DBPO-s-w-p-e-a-k	253.005
t-DBPO-s-w-ε-q-b-e-j	258.647	t-DBPO-s-r-η-u-p-b-f-k	251.104
t-DBPO-s-w-ε-q-a-f-j	258.069	t-DBPO-s-r-η-p-b-f-k	253.125
t-DBPO-s-w-ε-q-a-f-k	258.182	t-DBPO-d-w-u-p-a-e-k	236.841
t-DBPO-s-w-ε-q-b-f-k	258.276	t-DBPO-d-w-u-p-b-e-k	236.866
t-DBPO-d-w-p-a-e-j	243.273	t-DBPO-d-w-u-p-a-f-j	238.560
t-DBPO-d-w-p-a-e-k	242.739	t-DBPO-d-w-u-p-b-f-j	238.698
t-DBPO-d-w-p-a-f-j	244.427	t-DBPO-s-w-u-p-a-e-j	239.225
t-DBPO-d-w-p-b-f-j	244.452	t-DBPO-d-w-u-p-a-f-k	238.002
t-DBPO-d-r-η-u-p-a-e-j	251.619	t-DBPO-d-w-u-p-b-f-k	238.127
t-DBPO-d-r-η-u-p-a-e-k	251.688	t-DBPO-s-w-u-p-e-a-k	238.673
t-DBPO-s-r-ε-q-b-e-j	260.855	t-DBPO-d-w-u-q-a-e-j	236.100
t-DBPO-s-r-ε-q-b-f-j	260.743	t-DBPO-s-w-u-q-a-e-j	240.185
t-DBPO-d-w-p-a-f-k	243.888	t-DBPO-s-w-u-q-b-e-j	240.267
t-DBPO-s-r-ε-q-b-f-k	260.680	t-DBPO-d-w-u-q-b-e-j	237.154
t-DBPO-s-r-ε-q-a-e-k	261.025	t-DBPO-d-w-u-q-a-e-k	235.536
t-DBPO-s-r-η-p-b-e-j	260.404	t-DBPO-s-w-u-q-a-e-k	239.621
t-DBPO-d-r-η-u-p-a-f-j	250.527	t-DBPO-s-w-u-p-a-f-j	240.355
t-DBPO-d-w-p-b-e-k	242.375	t-DBPO-s-w-u-p-b-e-k	239.395
t-DBPO-d-r-η-u-p-a-f-k	250.715	t-DBPO-s-w-u-p-a-f-k	239.796
t-DBPO-s-r-ε-q-a-e-j	256.250	t-DBPO-d-w-u-q-a-f-j	237.318
t-DBPO-d-w-q-b-e-j	242.357	t-DBPO-s-w-u-p-b-f-k	240.254
t-DBPO-d-w-p-b-f-k	243.875	t-DBPO-s-w-u-q-a-f-k	240.775
t-DBPO-d-w-q-a-e-j	240.995	t-DBPO-d-w-u-q-a-f-k	236.747
t-DBPO-s-r-η-p-e-a-k	260.473	t-DBPO-d-w-u-q-b-f-k	237.424
t-DBPO-s-r-η-p-b-e-k	260.115	t-DBPO-d-r-u-q-a-e-j	241.961
t-DBPO-d-w-q-a-e-k	240.449	t-DBPO-s-r-u-q-b-e-j	246.523
t-DBPO-s-r-η-p-a-e-j	260.404	t-DBPO-d-r-u-q-a-f-j	243.204
t-DBPO-s-r-ε-q-a-f-k	260.561	t-DBPO-s-r-u-q-a-e-j	246.366
t-DBPO-d-w-q-b-e-k	241.880	t-DBPO-s-r-u-q-a-e-k	245.852
t-DBPO-s-r-ε-q-a-f-j	260.454	t-DBPO-s-r-u-q-a-f-j	260.454
t-DBPO-s-w-p-b-f-j	253.589	t-DBPO-s-r-u-q-a-f-k	246.862
t-DBPO-s-r-η-p-a-f-k	260.052		

CHAPTER 8

8. DISCUSSION AND CONCLUSIONS

This chapter will consider a comparison of all the molecules studied in the current work and a comparison of the results of each molecule with the results of the model structure. Tables comparing all the values of the three molecules and the model structure are prepared and are utilised for both sections.

8.1. Comparison of the results for the three molecules considered in this study

The computational study of myristinin A, *cis*-DBPO isomer and *trans*-DBPO isomer *in vacuo* and in solution has considered a number of aspects that are relevant for understanding of the properties of these molecules. The study *in vacuo* focused mainly on the identification of informative conformers following two approaches; keeping the same geometry of the R chain as in the lowest energy conformer and changing the geometry of the ring systems or keeping the same geometry of the ring system as in the lowest energy and changing the geometry of the R chain. These two options were important because they enabled meaningful selection out of the huge number of conformers that can be obtained if one couples each possible geometry of the R chain with each possible geometry of the ring systems. As a result, 123 conformers were calculated for myristinin A, and 115 conformers for each of the two DBPO isomers.

In all the considered molecules, the conformational preferences and other molecular properties are majorly influenced by the presence and position of the first IHB (dominant factor) and of the O–H···π interaction between a phenol H and ring B of the substituent. Other factors which have a significant influence on conformational preferences include the orientation of the ring system at C3; the orientation of the OHs in ring A; and the orientation of the R chain. The orientation of the OHs in ring B and E have minor influence on the conformational preferences.

In all the considered molecules, the analysis of the characteristics of the first IHBs shows that the type of R chain does not influence the parameters of the first IHB. Thus, in all cases, O14···H15 and H17···O14 are the same for the same type of conformers in the three molecules. Thus, it can be concluded that the type of R chain in these molecules does not influence the first IHB. It is noted that the O14···H15 distance is slightly shorter than the H17···O14 distances; the O14···O8 distance

is slightly shorter than the O14···O12 distance, and the d conformers have greater OĤO bond angle than the s conformers. The values of the bond length of O14···H15 and H17···O14 suggested a moderate-to-strong IHB, in all of these molecules, and the red shift for the vibrational frequencies of the donor also confirm this inferred strength of the first IHBs and show that the O–H···π interaction is somewhat weaker.

The HOMO-LUMO energy difference in all the considered molecules is mostly influenced by the presence of the O–H···π interaction. The orientation of the B-D-E ring system and the orientation of the OH *ortho* to the acyl group and not engaged in the first IHB also have a significant influence. The position of the first IHB has minor influence and the rest of other factors such as the orientation of the OHs in rings B and E have no significant influence. The shapes of the HOMO frontier orbitals for the conformers show a greater electron concentration density in the phloroglucinol moiety and the B-D-E ring system for all conformers, with few exceptions for d-w, d-r-q and s-w-u conformers, where the electron density in concentrated in the B-D-E ring system only. The shapes of LUMO orbitals show a greater electron concentration density in the phloroglucinol moiety.

In all the molecules, the dipole moment of the conformers is greatly influenced by the orientation of all OHs. When more OHs are oriented in the same direction, the dipole moment becomes greater. The type of R chain of the considered molecules does not influence the dipole moment significantly.

The solvent effect in all the considered conformers is positive in acetonitrile and negative in chloroform and water for all the molecules considered in this study. Thus, the magnitude of ΔG_{solv} increases with solvent-polarity and it is greatest in water.

8.2. Comparison of the results obtained in this study with the results of the model structure

As already mentioned (section 4.4), a preliminary study of a model structure considering the geometry of the phloroglucinol moiety and the B–D–E ring system, and with R replaced by an ethyl, had been performed [190]. It is therefore relevant to compare the results for the model structure and for the molecules considered in the current study, to check how good the model structure was.

It is more interesting to focus the comparison on low-energy conformers, since conformers of higher energy do not influence the biological activity of a molecule. Therefore, comparisons of the results of the model structure and the molecules considered here are carried out for conformers with relative energy <5.7 kcal/mol. The comparison has a meaning for the conformers of part one for each of these molecules, because those are the conformers where the geometry of the overall ring systems changes, like in the study of the model structure.

Table 8.1 shows the comparison of the relative energies for the conformers of the model structure and the molecules considered in this work. The values of the relative energies of the molecules considered follow the same trends as from the model structure, with some few exceptions for higher energy conformers, which might be due to the presence of the long R chain. This suggests that the model was good enough to determine the conformational preferences of the phloroglucinol moiety and the B–D–E ring system, above all for lower energy conformers

Table 8.2 compares the parameters of the first IHBs for the conformers of the model structure and the molecules considered in this work. The values of the H···O length and of the O···O distance are comparatively close for the conformers of the model structure and the corresponding conformers of the molecules considered. However, the values of the H···O length and of the O···O distance of the model structure are slightly greater than in the molecules considered (with ≤0.002 difference). This suggests that the R chain has some influence, although minor, on the H···O length and the O···O distance. The values of the O$\hat{H}$O bond angles are the same for the conformers of the model structure and the corresponding conformers of the molecules considered, with some few exceptions.

Table 8.3 compares the distance between the H atom and the closest C atom in the acceptor aromatic B ring for the O–H···π interactions for the conformers of the model structure and the molecules considered in this work. The values of this distance are the same for the conformers of the model structure and the corresponding conformers of the molecules considered. This implies that the model structure was good in the estimation of the O–H···π interaction.

Table 8.4 compares the dipole moments for the conformers of the model structure and the molecules considered in this work. The values of the dipole moments of these molecules follow the same trend as the model structure. This confirms that the dipole moments of the conformers are majorly influenced by the orientation of the OHs, than by the R chain. It is noted that the values of the dipole moments of myristinin A are slightly smaller than those of the model structure, while

those of the two isomers of DBPO are comparatively close to the ones of the model structure. This also confirms that the type of R chain has only minor influence on the dipole moment.

The HOMO-LUMO energy gaps for the conformers of the model structure and the corresponding conformers of the molecules considered in this work (table 8.5) are comparatively close. This suggests that the R chain has minor influence on the HOMO-LUMO energy gaps.

The comparisons of the results of model structure and molecules considered in this work show that the model structure is good enough to be used to investigate other derivatives of this kind of molecules.

Table 8.1. Comparison of the relative energies of the conformers of the model structure and the molecules considered in the current study.

Conformers	Relative energy (kcal/mol)			
	Model structure	Myristinin A	*cis*-DBPO	*trans*-DBPO
d-r-η-p-a-e-j	0.000	0.000	0.000	0.000
d-r-η-p-a-e-k	0.013	0.013	0.014	0.007
d-r-η-p-a-f-j	0.423	0.423	0.424	0.418
d-r-η-p-a-f-k	0.494	0.495	0.496	0.489
d-r-η-p-b-e-k	1.003	1.004	1.023	1.003
d-r-η-p-b-e-j	1.007	1.010	1.028	1.010
s-w-ε-q-a-e-k	1.140	1.160	1.154	1.158
s-w-ε-q-a-e-j	1.188	1.207	1.200	1.196
d-r-η-p-b-f-j	1.209	1.212	1.231	1.212
d-r-η-p-b-f-k	1.243	1.244	1.264	1.238
s-w-ε-q-b-e-j	1.486	1.501	1.496	1.491
s-w-ε-q-a-f-j	1.619	1.646	1.636	1.636
s-w-ε-q-a-f-k	1.633	1.661	1.652	1.651
s-w-ε-q-b-f-k	1.962	1.984	1.974	1.972
d-w-p-a-e-k	4.463	4.452	4.459	4.449
d-w-p-a-f-j	4.663	4.652	4.658	4.650
s-r-ε-q-b-e-j	4.693	4.707	4.705	4.698
s-r-ε-q-b-f-j	4.815	4.837	4.833	4.829
d-r-η-u-p-a-e-j	4.848	4.659	4.696	4.667
d-r-q-a-e-j	4.848	5.716	5.718	5.711
d-w-p-a-f-k	4.857	4.846	4.853	4.843
d-r-η-u-p-a-e-k	4.857	4.666	4.684	4.674
d-w-p-b-e-j	4.928	4.921	4.323	4.917
d-r-1-q-b-f-k	4.981	5.485	6.149	6.142
d-r-1-q-b-f-j	4.981	4.981	6.116	6.123
s-r-ε-q-a-e-k	5.016	5.034	5.031	5.024
s-r-ε-q-a-e-j	5.141	5.158	5.155	5.148
d-w-p-b-e-k	5.149	5.143	5.166	5.138
d-w-q-b-f-k	5.210	5.868	5.936	5.926
s-r-η-p-a-e-k	5.214	5.220	5.222	5.214
d-w-q-b-e-j	5.216	5.165	5.188	5.198
d-w-q-a-e-j	5.216	5.206	5.213	5.203
d-r-η-u-p-a-f-j	5.266	5.080	5.096	5.088
d-w-q-a-e-k	5.293	5.284	5.687	5.282
d-r-η-u-p-a-f-k	5.334	5.145	5.163	5.154
s-r-η-p-a-e-j	5.349	5.353	5.355	5.347
s-r-η-p-b-f-k	5.372	5.383	7.459	7.453
d-w-q-b-f-j	5.469	5.461	5.853	5.842
s-r-ε-q-a-f-k	5.484	5.511	5.505	5.501
d-w-q-b-e-k	5.543	5.536	5.559	5.532
s-r-ε-q-a-f-j	5.545	5.572	5.565	5.562
s-w-p-b-f-j	5.566	5.581	5.596	5.744
s-r-η-p-a-f-k	5.672	5.679	5.682	5.673
d-r-q-b-e-k	5.722	6.761	5.719	5.721
d-r-q-b-e-j	5.741	5.733	5.736	5.729
d-r-q-a-e-k	5.745	5.743	5.745	5.739

s-r-η-p-a-f-j	5.745	5.751	5.754	5.744
d-w-p-b-f-k	5.876	5.203	5.228	5.200
d-w-q-a-f-k	5.827	5.819	5.827	5.816
d-w-q-a-f-j	5.689	5.679	5.291	5.676

Table 8.2. Comparison of the parameters of the first IHBs of the conformers of the model structure and the molecules considered in the current study.

Conformers	Structure considered	Parameters of the first IHB		
		OH···O (Å)	O···O (Å)	OHO (°)
d-r-η-p-a-e-j	Model structure	1.653	2.509	146.3
	Myristinin A	1.652	2.508	146.4
	cis-DBPO	1.652	2.508	146.4
	trans-DBPO	1.652	2.508	146.4
d-r-η-p-a-e-k	Model structure	1.654	2.510	146.3
	Myristinin A	1.652	2.508	146.3
	cis-DBPO	1.652	2.508	146.3
	trans-DBPO	1.652	2.508	146.3
d-r-η-p-a-f-j	Model structure	1.653	2.509	146.3
	Myristinin A	1.652	2.508	146.4
	cis-DBPO	1.652	2.508	146.4
	trans-DBPO	1.652	2.508	146.4
d-r-η-p-a-f-k	Model structure	1.653	2.510	146.3
	Myristinin A	1.652	2.508	146.4
	cis-DBPO	1.652	2.508	146.3
	trans-DBPO	1.652	2.508	146.3
d-r-η-p-b-e-k	Model structure	1.652	2.510	146.5
	Myristinin A	1.651	2.508	146.6
	cis-DBPO	1.651	2.508	146.6
	trans-DBPO	1.651	2.508	146.6
d-r-η-p-b-e-j	Model structure	1.657	2.511	146.2
	Myristinin A	1.655	2.510	146.2
	cis-DBPO	1.656	2.510	146.2
	trans-DBPO	1.655	2.510	146.2
s-w-ε-q-a-e-k	Model structure	1.685	2.523	143.9
	Myristinin A	1.684	2.522	143.9
	cis-DBPO	1.684	2.522	143.9
	trans-DBPO	1.684	2.522	143.9
s-w-ε-q-a-e-j	Model structure	1.685	2.522	143.9
	Myristinin A	1.683	2.521	143.9
	cis-DBPO	1.684	2.521	143.9
	trans-DBPO	1.684	2.521	143.9
d-r-η-p-b-f-j	Model structure	1.657	2.512	146.2
	Myristinin A	1.655	2.510	146.2
	cis-DBPO	1.656	2.510	146.2
	trans-DBPO	1.655	2.510	146.2

d-r-η-p-b-f-k	Model structure	1.653	2.510	146.5
	Myristinin A	1.651	2.508	146.5
	cis-DBPO	1.651	2.509	146.5
	trans-DBPO	1.651	2.509	146.5
s-w-ε-q-b-e-j	Model structure	1.690	2.528	144.0
	Myristinin A	1.689	2.527	144.0
	cis-DBPO	1.689	2.527	144.0
	trans-DBPO	1.689	2.527	144.0
s-w-ε-q-a-f-j	Model structure	1.684	2.521	143.9
	Myristinin A	1.682	2.520	143.9
	cis-DBPO	1.682	2.520	143.9
	trans-DBPO	1.682	2.520	143.9
s-w-ε-q-a-f-k	Model structure	1.684	2.522	143.9
	Myristinin A	1.683	2.521	143.9
	cis-DBPO	1.683	2.521	143.9
	trans-DBPO	1.683	2.521	143.9
s-w-ε-q-b-f-k	Model structure	1.690	2.528	144.0
	Myristinin A	1.689	2.526	144.0
	cis-DBPO	1.689	2.526	144.0
	trans-DBPO	1.689	2.526	144.0
d-w-p-a-e-k	Model structure	1.658	2.512	146.2
	Myristinin A	1.656	2.511	146.2
	cis-DBPO	1.656	2.511	146.2
	trans-DBPO	1.656	2.511	146.2
d-w-p-a-f-j	Model structure	1.657	2.512	146.2
	Myristinin A	1.656	2.511	146.3
	cis-DBPO	1.656	2.511	146.2
	trans-DBPO	1.656	2.511	146.2
s-r-ε-q-b-e-j	Model structure	1.696	2.532	143.9
	Myristinin A	1.695	2.531	143.9
	cis-DBPO	1.695	2.531	143.9
	trans-DBPO	1.695	2.531	143.9
s-r-ε-q-b-f-j	Model structure	1.696	2.532	143.9
	Myristinin A	1.694	2.531	143.9
	cis-DBPO	1.694	2.531	143.9
	trans-DBPO	1.694	2.531	143.9
d-r-η-u-p-a-e-j	Model structure	1.675	2.523	145.4
	Myristinin A	1.675	2.523	145.4
	cis-DBPO	1.676	2.523	145.4
	trans-DBPO	1.675	2.523	145.4
d-r-q-a-e-j	Model structure	1.675	2.523	145.5
	Myristinin A	1.646	2.503	146.4
	cis-DBPO	1.646	2.503	146.4
	trans-DBPO	1.646	2.503	146.4
d-w-p-a-f-k	Model structure	1.658	2.512	146.2
	Myristinin A	1.656	2.511	146.2
	cis-DBPO	1.656	2.511	146.2
	trans-DBPO	1.656	2.511	146.2
d-r-η-u-p-a-e-k	Model structure	1.676	2.523	145.4
	Myristinin A	1.676	2.524	145.4
	cis-DBPO	1.676	2.524	145.4
	trans-DBPO	1.676	2.524	145.4

d-w-p-b-e-j	Model structure	1.660	2.514	146.1
	Myristinin A	1.659	2.512	146.1
	cis-DBPO	1.658	2.512	146.2
	trans-DBPO	1.658	2.512	146.2
d-r-1-q-b-f-k	Model structure	1.658	2.511	145.9
	Myristinin A	1.659	2.511	145.8
	cis-DBPO	1.649	2.506	146.3
	trans-DBPO	1.649	2.506	146.3
d-r-1-q-b-f-j	Model structure	1.658	2.511	145.9
	Myristinin A	1.657	2.510	145.9
	cis-DBPO	1.649	2.506	146.3
	trans-DBPO	1.649	2.506	146.3
s-r-ε-q-a-e-k	Model structure	1.691	2.527	143.8
	Myristinin A	1.692	2.527	143.8
	cis-DBPO	1.692	2.527	143.8
	trans-DBPO	1.692	2.527	143.8
s-r-ε-q-a-e-j	Model structure	1.690	2.526	143.8
	Myristinin A	1.690	2.526	143.8
	cis-DBPO	1.690	2.526	143.8
	trans-DBPO	1.690	2.526	143.8
d-w-p-b-e-k	Model structure	1.660	2.514	146.2
	Myristinin A	1.658	2.512	146.2
	cis-DBPO	1.658	2.512	146.2
	trans-DBPO	1.658	2.512	146.2
d-w-q-b-f-k	Model structure	1.666	2.516	145.6
	Myristinin A	1.665	2.515	145.6
	cis-DBPO	1.657	2.511	146.0
	trans-DBPO	1.657	2.511	146.0
s-r-η-p-a-e-k	Model structure	1.698	2.533	143.7
	Myristinin A	1.697	2.532	143.8
	cis-DBPO	1.697	2.532	143.7
	trans-DBPO	1.697	2.532	143.7
d-w-q-b-e-j	Model structure	1.655	2.509	146.1
	Myristinin A	1.664	2.514	145.6
	cis-DBPO	1.664	2.514	145.6
	trans-DBPO	1.664	2.514	145.6
d-w-q-a-e-j	Model structure	1.655	2.509	146.1
	Myristinin A	1.654	2.508	146.1
	cis-DBPO	1.654	2.508	146.1
	trans-DBPO	1.654	2.508	146.1
d-r-η-u-p-a-f-j	Model structure	1.675	2.522	145.4
	Myristinin A	1.675	2.522	145.4
	cis-DBPO	1.675	2.522	145.4
	trans-DBPO	1.675	2.522	145.4
d-w-q-a-e-k	Model structure	1.655	2.509	146.1
	Myristinin A	1.654	2.508	146.1
	cis-DBPO	1.654	2.508	146.1
	trans-DBPO	1.654	2.508	146.1
d-r-η-u-p-a-f-k	Model structure	1.675	2.523	145.4
	Myristinin A	1.676	2.523	145.4
	cis-DBPO	1.676	2.523	145.4
	trans-DBPO	1.676	2.523	145.4

s-r-η-p-a-e-j	Model structure	1.698	2.532	143.7
	Myristinin A	1.697	2.532	143.8
	cis-DBPO	1.697	2.532	143.7
	trans-DBPO	1.697	2.532	143.7
s-r-η-p-b-f-k	Model structure	1.692	2.528	143.8
	Myristinin A	1.691	2.527	143.8
	cis-DBPO	1.686	2.523	143.8
	trans-DBPO	1.686	2.523	143.8
d-w-q-b-f-j	Model structure	1.667	2.516	145.5
	Myristinin A	1.665	2.515	145.6
	cis-DBPO	1.657	2.510	145.9
	trans-DBPO	1.657	2.510	145.9
s-r-ε-q-a-f-k	Model structure	1.689	2.526	143.9
	Myristinin A	1.689	2.526	143.8
	cis-DBPO	1.689	2.526	143.8
	trans-DBPO	1.689	2.526	143.8
d-w-q-b-e-k	Model structure	1.660	2.514	146.2
	Myristinin A	1.664	2.514	145.6
	cis-DBPO	1.664	2.514	145.6
	trans-DBPO	1.664	2.514	145.6
s-r-ε-q-a-f-j	Model structure	1.689	2.525	143.9
	Myristinin A	1.688	2.524	143.9
	cis-DBPO	1.688	2.524	143.9
	trans-DBPO	1.688	2.524	143.9
s-w-p-b-f-j	Model structure	1.685	2.522	143.9
	Myristinin A	1.683	2.521	143.9
	cis-DBPO	1.683	2.521	143.9
	trans-DBPO	1.683	2.521	143.9
s-r-η-p-a-f-k	Model structure	1.698	2.532	143.7
	Myristinin A	1.696	2.532	143.8
	cis-DBPO	1.697	2.532	143.7
	trans-DBPO	1.697	2.532	143.7
d-r-q-b-e-k	Model structure	1.648	2.506	146.5
	Myristinin A	1.646	2.504	146.5
	cis-DBPO	1.647	2.505	146.5
	trans-DBPO	1.647	2.505	146.5
d-r-q-b-e-j	Model structure	1.648	2.506	146.4
	Myristinin A	1.646	2.504	146.5
	cis-DBPO	1.647	2.504	146.4
	trans-DBPO	1.647	2.504	146.4
d-r-q-a-e-k	Model structure	1.648	2.505	146.4
	Myristinin A	1.646	2.503	146.4
	cis-DBPO	1.646	2.503	146.4
	trans-DBPO	1.646	2.503	146.4
s-r-η-p-a-f-j	Model structure	1.697	2.532	143.7
	Myristinin A	1.696	2.531	143.8
	cis-DBPO	1.696	2.531	143.7
	trans-DBPO	1.696	2.531	143.7
d-w-p-b-f-k	Model structure	1.661	2.514	146.1
	Myristinin A	1.659	2.513	146.1
	cis-DBPO	1.659	2.513	146.1
	trans-DBPO	1.659	2.513	146.1

d-w-q-a-f-k	Model structure	1.657	2.510	146.0
	Myristinin A	1.656	2.509	146.0
	cis-DBPO	1.656	2.509	146.0
	trans-DBPO	1.656	2.509	146.0
d-w-q-a-f-j	Model structure	1.657	2.510	146.0
	Myristinin A	1.655	2.508	146.0
	cis-DBPO	1.655	2.509	146.0
	trans-DBPO	1.655	2.509	146.0

Table 8.3. Comparison of the distance between the H atom and the closest C atom in the acceptor B aromatic ring for the O–H···π interactions of the conformers of the model structure and the molecules considered in the current study.

Conformers	Structure considered	H15···C23 or H16···C23 (Å)
d-r-η-p-a-e-j	Model structure	2.128
	Myristinin A	2.128
	cis-DBPO	2.128
	trans-DBPO	2.128
d-r-η-p-a-e-k	Model structure	2.127
	Myristinin A	2.127
	cis-DBPO	2.127
	trans-DBPO	2.127
d-r-η-p-a-f-j	Model structure	2.131
	Myristinin A	2.131
	cis-DBPO	2.131
	trans-DBPO	2.131
d-r-η-p-a-f-k	Model structure	2.130
	Myristinin A	2.130
	cis-DBPO	2.130
	trans-DBPO	2.130
d-r-η-p-b-e-k	Model structure	2.213
	Myristinin A	2.213
	cis-DBPO	2.213
	trans-DBPO	2.213
d-r-η-p-b-e-j	Model structure	2.236
	Myristinin A	2.236
	cis-DBPO	2.236
	trans-DBPO	2.236
s-w-ε-q-a-e-k	Model structure	2.074
	Myristinin A	2.074
	cis-DBPO	2.074
	trans-DBPO	2.074
s-w-ε-q-a-e-j	Model structure	2.074
	Myristinin A	2.074

	cis-DBPO	2.074
	trans-DBPO	2.074
d-r-η-p-b-f-j	Model structure	2.239
	Myristinin A	2.239
	cis-DBPO	2.239
	trans-DBPO	2.239
d-r-η-p-b-f-k	Model structure	2.219
	Myristinin A	2.219
	cis-DBPO	2.219
	trans-DBPO	2.219
s-w-ε-q-b-e-j	Model structure	2.185
	Myristinin A	2.185
	cis-DBPO	2.185
	trans-DBPO	2.185
s-w-ε-q-a-f-j	Model structure	2.076
	Myristinin A	2.076
	cis-DBPO	2.076
	trans-DBPO	2.076
s-w-ε-q-a-f-k	Model structure	2.075
	Myristinin A	2.075
	cis-DBPO	2.075
	trans-DBPO	2.075
s-w-ε-q-b-f-k	Model structure	2.187
	Myristinin A	2.187
	cis-DBPO	2.187
	trans-DBPO	2.187
s-r-ε-q-b-e-j	Model structure	2.165
	Myristinin A	2.165
	cis-DBPO	2.165
	trans-DBPO	2.165
s-r-ε-q-b-f-j	Model structure	2.169
	Myristinin A	2.169
	cis-DBPO	2.169
	trans-DBPO	2.169
d-r-η-u-p-a-e-j	Model structure	2.128
	Myristinin A	2.128
	cis-DBPO	2.128
	trans-DBPO	2.128
d-r-η-u-p-a-e-k	Model structure	2.127
	Myristinin A	2.128
	cis-DBPO	2.128
	trans-DBPO	2.128
s-r-ε-q-a-e-k	Model structure	2.056
	Myristinin A	2.056
	cis-DBPO	2.056
	trans-DBPO	2.056
s-r-ε-q-a-e-j	Model structure	2.058
	Myristinin A	2.058
	cis-DBPO	2.058
	trans-DBPO	2.058
s-r-η-p-a-e-k	Model structure	2.109
	Myristinin A	2.109

	cis-DBPO	2.109
	trans-DBPO	2.109
d-r-η-u-p-a-f-j	Model structure	2.130
	Myristinin A	2.130
	cis-DBPO	2.130
	trans-DBPO	2.130
d-r-η-u-p-a-f-k	Model structure	2.130
	Myristinin A	2.130
	cis-DBPO	2.130
	trans-DBPO	2.130
s-r-η-p-a-e-j	Model structure	2.109
	Myristinin A	2.109
	cis-DBPO	2.109
	trans-DBPO	2.109
s-r-η-p-b-f-k	Model structure	2.222
	Myristinin A	2.222
	cis-DBPO	2.222
	trans-DBPO	2.222
s-r-ε-q-a-f-k	Model structure	2.058
	Myristinin A	2.059
	cis-DBPO	2.059
	trans-DBPO	2.059
s-r-ε-q-a-f-j	Model structure	2.059
	Myristinin A	2.059
	cis-DBPO	2.059
	trans-DBPO	2.059
s-r-η-p-a-f-k	Model structure	2.111
	Myristinin A	2.111
	cis-DBPO	2.111
	trans-DBPO	2.111
s-r-η-p-a-f-j	Model structure	2.112
	Myristinin A	2.112
	cis-DBPO	2.112
	trans-DBPO	2.112

Table 8.4. Comparison of the dipole moments of the conformers of the model structure and the molecules considered in the current study.

Conformers	Dipole moment (Debye)			
	Model structure	Myristinin A	*cis*-DBPO	*trans*-DBPO
d-r-η-p-a-e-j	2.412	2.278	2.460	2.460
d-r-η-p-a-e-k	3.867	3.695	3.834	3.834
d-r-η-p-a-f-j	2.962	2.873	2.877	2.877
d-r-η-p-a-f-k	4.174	4.092	4.115	4.115
d-r-η-p-b-e-k	2.556	2.468	2.597	2.463
d-r-η-p-b-e-j	2.777	2.643	2.806	2.652
s-w-ε-q-a-e-k	2.909	2.792	2.993	2.993
s-w-ε-q-a-e-j	5.234	5.111	5.279	5.279
d-r-η-p-b-f-j	3.577	3.475	3.489	3.473
d-r-η-p-b-f-k	3.738	3.697	3.723	3.666
s-w-ε-q-b-e-j	4.872	4.746	4.900	4.900
s-w-ε-q-a-f-j	5.058	4.964	5.068	5.068
s-w-ε-q-a-f-k	2.694	2.640	2.723	2.723
s-w-ε-q-b-f-k	2.969	2.906	2.780	3.062
d-w-p-a-e-k	7.221	7.121	7.227	7.227
d-w-p-a-f-j	5.467	5.378	5.408	5.408
s-r-ε-q-b-e-j	7.777	7.629	7.759	7.759
s-r-ε-q-b-f-j	6.228	6.089	6.184	6.184
d-r-η-u-p-a-e-j	0.773	0.860	0.648	0.855
d-r-q-a-e-j	1.238	3.511	3.511	3.641
d-w-p-a-f-k	7.462	7.395	7.432	7.432
d-r-η-u-p-a-e-k	2.783	2.852	2.946	2.946
d-w-p-b-e-j	5.646	5.510	5.510	5.510
d-r-1-q-b-f-k	4.846	4.738	4.480	5.7234
d-r-1-q-b-f-j	4.845	4.715	3.896	3.896
s-r-ε-q-a-e-k	5.494	5.339	5.494	5.494
s-r-ε-q-a-e-j	7.909	7.754	7.897	7.897
d-w-p-b-e-k	6.649	6.548	6.363	6.530
d-w-q-b-f-k	9.142	9.019	9.417	9.149
s-r-η-p-a-e-k	5.428	5.269	5.040	5.365
d-w-q-b-e-j	6.397	5.856	5.494	5.836
d-r-η-u-p-a-f-j	2.419	2.759	2.573	2.7407
d-r-η-u-p-a-f-k	3.675	2.759	3.896	3.896
s-r-η-p-a-e-j	4.697	7.703	7.756	7.756
s-r-η-p-b-f-k	5.013	4.877	3.896	3.896
d-w-q-b-f-j	7.962	7.718	5.723	7.838
s-r-ε-q-a-f-k	4.370	4.877	4.350	5.723
d-w-q-b-e-k	7.590	7.831	6.559	4.350
s-r-ε-q-a-f-j	7.111	4.240	7.085	4.350
s-w-p-b-f-j	2.606	7.463	2.551	7.438
s-r-η-p-a-f-k	4.545	6.978	4.035	7.085
d-r-q-b-e-k	3.629	2.483	3.641	2.486
d-r-q-b-e-j	3.479	4.414	3.463	4.531
d-r-q-a-e-k	4.828	3.609	4.755	3.571
s-r-η-p-a-f-j	7.235	3.340	7.228	3.463

d-w-p-b-f-k	6.662	4.715	6.642	4.755
d-w-q-a-e-k	7.820	7.092	7.756	7.228
d-w-q-a-e-j	6.397	6.559	6.363	6.531
d-w-q-a-f-k	9.448	9.326	9.417	9.417
d-w-q-a-f-j	8.212	8.066	8.205	8.205

Table 8.5. Comparison of the HOMO-LUMO energy gaps of the conformers of the model structure and the molecules considered in the current study

Conformers	HOMO-LUMO energy gaps of gap (kcal/mol)			
	Model structure	Myristinin A	*cis*-DBPO	*trans*-DBPO
d-r-η-p-a-e-j	257.323	257.479	257.410	257.410
d-r-η-p-a-e-k	257.423	257.574	257.517	257.517
d-r-η-p-a-f-j	256.143	256.319	256.250	256.250
d-r-η-p-a-f-k	256.312	256.494	256.425	256.425
d-r-η-p-b-e-k	254.543	254.693	254.612	254.649
d-r-η-p-b-e-j	255.791	255.942	255.867	255.904
s-w-ε-q-a-e-k	258.791	258.854	258.829	258.829
s-w-ε-q-a-e-j	258.741	258.816	258.785	258.785
d-r-η-p-b-f-j	255.898	256.099	255.992	256.042
d-r-η-p-b-f-k	255.026	255.170	256.049	255.126
s-w-ε-q-b-e-j	258.609	258.678	258.647	258.647
s-w-ε-q-a-f-j	258.013	258.101	258.069	258.069
s-w-ε-q-a-f-k	258.126	258.207	258.182	258.182
s-w-ε-q-b-f-k	258.239	258.308	258.276	258.276
d-w-p-a-e-k	242.608	242.815	242.739	242.739
d-w-p-a-f-j	244.302	244.503	244.427	244.427
s-r-ε-q-b-e-j	260.855	260.868	260.855	260.855
s-r-ε-q-b-f-j	260.743	260.768	260.743	260.743
d-r-η-u-p-a-e-j	251.424	251.650	251.581	251.619
d-r-q-a-e-j	241.892	247.144	247.075	247.075
d-w-p-a-f-k	243.762	243.963	243.066	243.888
d-r-η-u-p-a-e-k	251.518	251.732	251.688	251.688
d-w-p-b-e-j	242.902	243.091	242.457	243.091
d-r-q-b-f-k	249.742	249.504	249.096	249.096
d-r-q-b-f-j	249.736	249.918	249.435	249.918
s-r-ε-q-a-e-k	261.006	261.056	261.025	261.025
s-r-ε-q-a-e-j	260.899	260.975	256.250	256.250
d-w-p-b-e-k	242.225	242.426	242.338	242.375
d-w-q-b-f-k	243.731	242.846	243.273	242.570
s-r-η-p-a-e-k	260.454	260.498	261.025	260.473
d-w-q-b-e-j	240.869	242.413	242.319	242.357
d-r-η-u-p-a-f-j	250.313	241.070	250.527	240.995
d-r-η-u-p-a-f-k	250.502	250.589	250.715	250.527
s-r-η-p-a-e-j	260.391	260.435	260.404	240.449
s-r-η-p-b-f-k	260.096	260.128	253.125	250.715

d-w-q-b-f-j	243.135	243.323	243.066	260.404
s-r-ε-q-a-f-k	260.535	260.128	260.561	260.128
d-w-q-b-e-k	241.735	241.936	241.842	243.323
s-r-ε-q-a-f-j	260.435	260.586	260.454	260.561
s-w-p-b-f-j	253.482	253.620	253.558	253.620
s-r-η-p-a-f-k	260.021	260.473	260.052	260.454
d-r-q-b-e-k	248.531	248.751	247.075	253.589
d-r-q-b-e-j	249.008	249.203	249.134	260.052
d-r-q-a-e-k	246.404	248.751	246.529	248.657
s-r-η-p-a-f-j	259.927	249.203	259.946	249.134
d-w-p-b-f-k	243.731	246.592	243.844	246.529
d-w-q-a-e-k	240.311	259.977	240.449	259.946
d-w-q-a-e-j	240.863	243.932	240.995	243.875
d-w-q-a-f-k	241.516	241.710	241.641	241.641
d-w-q-a-f-j	242.080	242.275	242.206	242.206

REFERENCES

1. Osteoarthritis Medications List: Opioids, NSAIDs, and More – Healthline, https://www.healthline.com/health/osteoarthritis/medications-list, 15/02/2017.
2. NON-STEROIDAL ANTIINFLAMMATORY DRUGS (NSAIDS), http://www.auburn.edu/~deruija/nsaids_2002.pdf, 16/02/2017.
3. I. P. Singh, S. B. Bharate, Phloroglucinol Compound of Natural Origin, *Natural Product Reports*, **23**, 591, 2006.
4. M. M. Kabanda, Computational study of the caespitate molecule. M. Sc. Thesis at the University of Venda, 2007.
5. L. Mammino, M.M. Kabanda, Model structures for the study of acylated phloroglucinols and computational study of the caespitate molecule. *Journal of Molecular Structure* (Theochem), **805**, 52, 2007.
6. L. Mammino, M. M. Kabanda, Computational study of nodifloridin A and nodifloridin B *in vacuo* and in water solution. *WSEAS Transactions on Biology and Biomedicine*, **6**, 88, 2009.
7. L. Mammino, M.M. Kabanda, A computational study of the interactions of the phloroglucinol molecule with water, *Journal of Molecular Structure (Theochem)*, **852**, 45, 2008.
8. L. Mammino, M. M. Kabanda, A study of the intramolecular hydrogen bond in acylphloroglucinols, *Journal of Molecular Structure (Theochem)*, **901**, 219, 2009.
9. L. Mammino, M. M. Kabanda, A computational study of the effects of different solvents on the characteristics of the intramolecular hydrogen bond in acylphloroglucinols, *The Journal of Physical Chemistry A*, **113**, 15077, 2009.
10. L. Mammino, M. M. Kabanda, Adducts of acylphloroglucinols with explicit water molecules: Similarities and differences across a sufficiently representative number of structures, *International Journal of Quantum Chemistry*, **110**, 2390, 2010.
11. L. Mammino, M. M. Kabanda, Comparison of possible conformations and conformational preferences of the Z and E isomers of caespitate. In: Niola V, Ka-Lok Ng (Eds.), *Recent Researches in Chemistry, Biology, Environment and Culture*, WSEAS Press, 124, 2011.
12. M. M. Kabanda, *Computational study of the molecules of selected acylated phloroglucinols in vacuo and in solution*. Ph.D. Thesis at the University of Venda, 2011.
13. L. Mammino, M. M. Kabanda, The geometric isomers of caespitate: a computational study *in vacuo* and in solution. *International Journal of Biology and Biomedical Engineering*, **1**, 133, 2012.

14. L. Mammino, Results accuracy versus computational costs: Indications on the performance of different levels of theory from an extensive computational study of acylphloroglucinols. In: S. Oprisan, A. Zaharim, S. Eslamian, M. S. Jian, C. A. F. Ajub, A. Azami (Eds), *Advances in Environment, Computational Chemistry and Bioscience, WSEAS Press*, 42, 2012.
15. M. M. Kabanda, L. Mammino, The conformational preferences of acylphloroglucinols – a promising class of biologically active compounds, *International Journal of Quantum Chemistry*, **112**, 3702, 2012.
16. L. Mammino, M. M. Kabanda, Computational study of the patterns of weaker intramolecular hydrogen bonds stabilizing acylphloroglucinols, *International Journal of Quantum* Chemistry, **112**, 2658, 2012.
17. L. Mammino, Kabanda M. M. The role of additional O–H···O intramolecular hydrogen bonds for acylphloroglucinols' conformational preferences *in vacuo* and in solution, *Molecular Simulation*, **39**, 13, 2013.
18. L. Mammino, Computational Study of Arzanol – an antioxidant compound of natural origin, international journal of biology and biomedical engineering, **7**(3), 125, 2013.
19. L. Mammino, A computational study of euglobal G1 – an acylphloroglucinol with anticancer activity. *Current Bioactive Compounds*, **10**, 180, 2014.
20. L. Mammino, *Ab initio* and DFT study of chinesin I and chinesin II. *Current Physical Chemistr*y **5**, 293, 2015.
21. IUPAC, (2006). Compendium of chemical terminology (2nd ed.). The "Gold Book". Online corrected version: "Molecule".
22. D. D. Ebbin, (1990). General chemistry (3rd ed.). Boston: Houghton Mifflin Co.
23. T. L. Brown, C. K. Kenneth, Theodore L. Brown; Harold Eugene LeMay; Bruce Edward Bursten, (2003). Chemistry – the Central Science (9th ed.). New Jersey: Prentice Hall. R.
24. S. S. Zumdahl, (1997). Chemistry (4th ed.). Boston: Houghton Mifflin.
25. Chirality and Stereoisomers - Chemistry LibreTexts, https://chem.libretexts.org/Bookshelves/Organic_Chemistry/Supplemental_Modules_(Organic_Chemistry)/Chirality/Chirality_and_Stereoisomers, 15/03/2018.
26. E. G. Lewars . The concept of the potential energy surface, Chapter from book Computational Chemistry, 49, 2016.
27. Computational chemistry and molecular modeling MidTerm, https://slideplayer.com/slide/4913912/, 15/03/2018.
28. J. P. Crocombette, F. Willaime, 1.08. *Ab initio* electronic structure calculations for nuclear materials, *Comprehensive Nuclear Materials*, **1**, 248, 2012.

29. J. N. Murrell, The potential energy surface of polyatomic molecules, Structure and Bonding, **32**, 146, 1977.
30. E. Schrödinger, Quantisierung als eigenwertproblem, *Erste Mitteilung*, **79**, 376, 1926.
31. E. Schrödinger, Quantisierung als eigenwertproblem, *Zweiter Mitteilung*, **79**, 527, 1926.
32. Ward-B-2016-PhD-Thesis.pdf
33. M. Born, R. Oppenheimer, Zur quantentheorie der molekeln, *Annalen der Physik*, **84**, 484, 1927.
34. A. Szabo, N. S. Ostlund, Modern quantum chemistry, introduction to advanced electronic structure theory, Dover Publishing, New York, 1996.
35. G. I. Kerley, On corrections to the Born-Oppenheimer approximation, A Kerley Technical Services Research Report, Consultant, 2011.
36. E. Fermi, Eine statistische methode zur bestimmung einiger eigenschaften des atoms und ihre anwendung auf die theorie des periodischen systems der elemente, *Zeitschrift für Physik*, **48**, 73, 1928.
37. Exchange, antisymmetry and Pauli repulsion - Theory of Condensed http://www.tcm.phy.cam.ac.uk/~mdt26/PWT/lectures/towler_pauli.pdf, 15/03/2018.
38. C. J. Cramer, (2004). Essentials of computational chemistry, John Wiley and Sons Ltd., Hoboken, NJ, USA.
39. T. Engel, Quantum chemistry and spectroscopy, Pearson education, Inc., 344, 2006.
40. F. Jensen, (2007). Introduction to computational chemistry. Second edition, John Willey and sons.
41. H. Dorsett, A. White, (2000). Overview of molecular modeling and *ab initio* molecular orbital methods suitable for use with energetic materials. Salisbury, South Australia, Australia; DSTO Aeronautical and Marine Research Laboratory.
42. A. Leach, (2001). Molecular Modelling: Principles and Applications (2nd ed.). Harlow: Prentice Hall.
43. E. G. Lewars, (2016). Computational chemistry: Introduction to the theory and applications of molecular and quantum mechanics (3rd ed.). Springer.
44. F. F. Charlotte, General Hartree-Fock program'', *Computer Physics Communications*, **43**, 365, 1987.
45. J. B. Foresman, A. Frisch, Exploring chemistry with electronic structure methods, Gaussian, Inc., Pittsburg, PA (USA), 59, 1995.
46. Jensen Chpt. 4, http://www.pitt.edu/~jordan/chem3430/chapter4.pdf, 15/03/2018.

47. Theoretical investigation of the potential energy, dipole moment and polarizability surfaces of the CH4-N2 and C2H4-C2H4 van der Waals complexes. https://www.theses.fr/2010DIJOS063.pdf
48. Introduction to Electron Correlation C. David Sherrill School of Chemistry and Biochemistry Georgia Institute of Technology, http://vergil.chemistry.gatech.edu/courses/chem6485/pdf/intro-e-correlation.pdf, 15/03/2018.
49. J. C. Slater, Note on Hartree's method, *Physical Review*, **35**, 211, 1930.
50. J. Lennard-Jones, The electronic of some diatomic molecules, *Transactions of the Faraday Society*, **25**, 686, 1929.
51. J. Yves, F. Volatron, (1993). An introduction to molecular orbitals, Ed, Budett. J., oxford university press. New York.
52. K. V. Berezin, V. V. Nechaev, Comparison of theoretical methods and basis sets for *ab initio* and DFT calculations of the structure and frequency of normal vibrations of polyatomic molecules, *Journal of Applied Spectroscopy*, **71**, 164, 2004.
53. R. M. Balabin, Communications: Intramolecular basis set superposition error as a measure of basis set incompleteness: can one reach the basis set limit without extrapolation*?*, *The Journal of Chemical Physics*, **132**, 211103, 2010.
54. R. D. Ernest, D. Feller, Basis set selection for molecular calculations, *Chemical Reviews*, **86**, 696, 1988.
55. K. Butler, K. Jelfs, W. Gren, An introduction to computational methods, 25, 2008.
56. E. Valeev, Basis Sets in Quantum Chemistry, 13, 2015.
57. U. Burkert, N. L. Allinger, Molecular mechanics, ACS Monograph no. 177, American Chemical Society, Washington D.C, 1982.
58. J. A. Pople, R. K. Nesbet, chemistry and physics of energetic materials, *Journal Chemistry and Physics*, **22**, 571, 1954.
59. J. H. Warren, *A Guide to Molecular Mechanics and Quantum Chemical Calculations*, 35, 2003
60. C. Møller, M. S. Plesset, Note on an approximation treatment for many-electron system, J*ournal of Physical Review*, **46**, 618–622, 1934.
61. R. J. Bartlett, Many-Body perturbution theory and coupled cluster theory for electron correlation in molecules, *Annual Review of Physical Chemistry*, **32**, 401, 1981.
62. A. Tkatchenko, R. A. J. Distasio, M. Head-Gordon, M. Scheffler. Dispersion-corrected Møller– Plesset second order perturbation theory, *The Journal of Chemical Physics*, **131**, 6, 2009.

63. A. Leach, (2001) Molecular modelling principles and applications, 2nd Ed., Prentice Hall: Harlow.
64. A. D. Becke, Density functional thermochemistry. III. The role of exact exchange, *The Journal of Chemical Physics*, **98**, 5652, 1993.
65. A. E. Taylor, Advanced calculus, Blaidsell Publishing Company, New York, 371, 1955.
66. Density Functional Theory for Emergents - cond-mat.de, https://www.cond-mat.de/events/correl13/manuscripts/jones.pdf, 11/05/2017.
67. Density Functional Theory, https://www.southampton.ac.uk/assets/centresresearch/documents/compchem/DFT_L9.pdf, 13/05/2017.
68. A. D. Becke, Density-functional exchange-energy approximation with correct asymptotic behaviour, *Physical Review A*, **38**, 3098, 1988.
69. Density Functionals (XC) — ADF 2018 documentation - SCM.com, https://www.scm.com/doc/ADF/Input/Density_Functional.html, 15/03/2018.
70. R. G. Parr, W. Yang, Density functional theory of atoms and molecules. Oxford University Press, New York, 174, 1989.
71. P. Gori-Giorgi, A. Savin, Degeneracy and size consistency in electronic density functional theory, *Journal of Physics*: Conference Series, **117**, 012017, 2008.
72. A. Savin, Is size-consistency possible with density functional approximations?, *Chemical Physic*, 7, 2008.
73. M. J. S. Dewar, E. G. Zoebisch, E. F. Healy, J. J. P. Stewart, Development and use of quantum mechanical molecular models. 76. AM1: a new general purpose quantum mechanical molecular model, *Journal of the American Chemical Society*, **107**, 3909, 1985.
74. T. Clark, A handbook of computational chemistry: A practical guide to chemical structure and energy calculations, John Wiley, New York, 332, 1985.
75. J. P. S. James, Optimization of parameters for semiempirical methods I. Method, *Journal of Computational Chemistry*, **10**, 220, 1989.
76. J. J. P. Stewart, Optimization of parameters for semiempirical methods V: modification of NDDO approximations and application to 70 elements, *Journal of Molecular Modeling*, **13**, 1123, 2007.
77. C. Cohen-Tannoudji, B. Diu, F. Lalo?, "Quantum Mechanics," Hermann and Wiley, Paris, 1977.
78. M. Drees, Introduction to computational chemistry for Experimetanl cheimsts (Part 1/2), 11th PhD seminar, Grching, September 12th 2008.

79. HyperChem Computational Chemistry: Part 1: Practical Guide, Part 2: Theory and Methods, Hypercube, Inc., 1996.
80. M. Walther, P. Plochocka, B. Fischer, H. Helm, P. Uhd Jepsen, "Collective vibrational modes in biological molecules investigated by THz Time-Domain spectroscopy" *Biopolymers* (Biospectroscopy), **67**, 313, 2002.
81. I. N. Levine, Quantum chemistry, 5th Ed, Prentice Hall, Upper Saddle River, NJ, 65, 2000.
82. Morse potential – Wikipedia, https://en.wikipedia.org/wiki/Morse_potential, 13/05/2017.
83. F. Ian, Frontier orbitals and organic chemical reactions, London: Wiley. 109, 1978.
84. R. B. Woodward, R. Hoffmann, Stereochemistry of electrocyclic reactions, *Journal of the American Chemical Society*, **87**, 397, **1965.**
85. F.Kenichi, Y. Teijiro; S, Haruo "A Molecular orbital theory of reactivity in aromatic hydrocarbons", *The Journal of Chemical Physics*, **20,** 722, 1952.
86. L. Salem, intermolecular orbital theory of the interaction between conjugated systems. I. General theory, *Journal of the American Chemical Society*, **90**, 552, 1968.
87. Density functional study of molecular orbitals of cobaltocene and nickelocene molecules, http://www.imedpub.com/articles/density-functional-study-of-molecular-orbitals-of-cobaltocene-and-nickelocene-molecules.php?aid=17921, 13/05/2017.
88. H. M. Langoor, H. J. van der Maas, On the competitive intramolecular H-bonding in alcohols with two accepting sites, *Journal of Molecular Structure*, **403,** 229, 1997.
89. X. Meng-Xia, L. Yuan, Studies on the hydrogen bonding of aniline's derivatives by FT-IR, *Spectrochimica Acta Part A*, **58**, 2826, 2002.
90. S. Schlucker, K. S. Ranjan, B. P. Asthana, J. Popp, W. Kiefer, Hydrogen-bonded pyridine–water complexes studied by density functional theory and Raman spectroscopy, *The Journal of Physical Chemistry A*, **105**, 9989, 2001.
91. D. D. Gadade, S. S. Pekamwar, Pharmaceutical cocrystals: Regulatory and strategic aspects, design and development, *Advanced Pharmaceutical Bulletin*, **6**, 494, 2016.
92. H. H. J. Ter, P. W. Cains, Co-Crystal polymorphs from a solvent-mediated transformation, *Crystal Growth & Design*, **8**, 2542, 2008.
93. What is hydrogen bonding? What are its types? – Quora, https://www.quora.com/What-is-hydrogen-bonding-What-are-its-types., 15/06/2017.
94. G. Gilli, Hydrogen bonding and other molecular interactions, IUPAC workshop, Pisa, Italy, 2005.
95. P. Gilli, G. Gilli, Hydrogen bond models and theories: The dual hydrogen bond model and its consequences, *Journal of Molecular Structure*, **972**, 10, 2010.

96. J. Poater, X. Fradera, M. Sola, M. Duran, S. Simon, On the electron-pair of the hydrogen bond in the framework of the atoms in molecules theory, *Chemical Physics Letters*, **369**, 255, 2003.
97. G. A. Jeffrey, An introduction to hydrogen bonding, Oxford University Press, Oxford, 1997.
98. L. Sobczyk, S. J. Grabowski, T. M. Krygowski, Interrelation between in H-Bond and Pi-electron delocalization, *Chemical Reviews*, **105**, 3560, 2005.
99. A. I. Kitaigorodskii, Molecular crystals and molecules; academic press: New York, 1973.
100. H. M. Langoor, H. J. van der Maas, On the competitive intramolecular h—bonding in alcohols with two accepting sites, *Journal of Molecular Structure*, **403**, 229, 1997.
101. Electric charge – MIT, http://web.mit.edu/8.02t/www/802TEAL3D/visualizations/coursenotes/modules/guide02.pdf, 15/03/2018.
102. Biology: The hydrophobic effect and properties of small polyatomic molecules, https://chem.libretexts.org/Bookshelves/General_Chemistry/Book%3A_ChemPRIME_(Moore_et_al.)/07Further_Aspects_of_Covalent_Bonding/7.11%3A_Polarity_in_Polyatomic_Molecules/Biology%3A_The_Hydrophobic_Effect_and_Properties_of_Small_Polyatomic_Molecules, 12/08/2017.
103. Dipole Moment, https://ch301.cm.utexas.edu/section2.php?target=imfs/polar/dipole-moment.html, 12/08/2017.
104. L. Mammino, M. K. Bilonda,T. Tshiwawa, *Ab-Initio* and DFT study of the Muchimangin-B molecule, Frontiers in Quantum Methods and Applications in Chemistry and Physics, **29**, 114, 2015.
105. N. Ree, M. Harring Hansen, A. S. Gertsen, K. V. Mikkelsen, Density functional theory study of the solvent effects on systematically substituted dihydroazulene/vinylheptafulvene systems: Improving the capability of molecular energy storage, *The Journal of Physical Chemistry A*, 121, 8865. 2017.
106. Solvent effects and conformation searching, https://about.illinoisstate.edu/standard/Documents/CHE%20380.37/Handouts/380.37confsearch3.pdf, 11/06/2017.
107. H. A. Alvarez , C. Llerena Suster, A. N. McCarthy, Consistent acetonitrile molecular models for both standard and computationally efficient molecular dynamics studies, *Asian Journal of Computer and Information Systems*, **2**, 5658, 2014.
108. T. Dziembowska, Z. Malarski, B. Szczodrowska, Solvent effect on the intramolecular hydrogen bond in 8-quinolinol N-oxide, *Journal of Solution Chemistry*, **25**, 189, 1996.

109. M. Z. Yakupov, N. K. Lyapina, V. V. Shereshovets, U. B. Imashev, The Solvent effect on the rate of reaction between propanethiol and chlorine dioxide, *Kinetics and Catalysis*, **42**, 612, 2001.

110. P. K. Chattaraj, chemical reactivity theory: a density functional view, CRC Press, Boca Raton, 2009.

111. K. B. Wiberg, Properties of some condensed aromatic systems, *Journal of Organic Chemistry*, **62**, 5727, 1997.

112. S. Miertus, J. Tomasi, Approximate evaluations of the electrostatic free energy and internal energy changes in solution processes, *Chemical Physics*, **65**, 245, 1982.

113. V. Barone, M. Cossi, A New definition of cavities for the computation of solvation free energy by the polarizable continuum model, *The Journal of Chemical Physics*, **107**, 3221, 1997.

114. J. Tomas, B. Mennucci, R. Cammi, Quantum mechanical continuum solvation models, *Chemical Reviews*, **105**, 3093, 2005.

115. V. Barone, M. Cossi, J. Tomas, Geometry optimization of molecular structures in solution by the polarizable continuum model, *Journal of Computational Chemistry*, **19**, 417, 1998.

116. M. Cossi, G. Scalmani, N. Rega, V. Barone, New Developments in the polarizable continuum model for quantum mechanical and classical calculations on molecules in solution, *The Journal of Chemical Physics*, **107**, 3041, 1997.

117. E. Cancès, B. Mennucci, J. Tomas, A new integral equation formalism for the polarizable continuum model: theoretical background and applications to isotropic and anisotropic dielectrics, *The Journal of Chemical Physics*, **107**, 3041, 1997.

118. J. Tomas, B. Mennucci, E. Cancès, The IEF version of the PCM solvation method: an overview of a new method addressed to study molecular solutes at the QM ab initio level, *Journal of Molecular Structure*. (Theochem), **464**, 211, 1999.

119. M. Cossi, Continuum solvation model for infinite, *Chemical Physics Letters*, **384**, 179, 2004.

120. L. Frediani, R. Cammi, S. Corni, J. Tomas, A polarizable continuum model for molecules at diffuse interfaces, *The Journal of Chemical Physics*, **120**, 3893, 2004.

121. M. Cossi, N. Rega, G. Scalman, V. Barone, Energies, structures, and electronic properties of molecules in solutions with C-PCM solvation model, *Journal of Computational Chemistry*, **24**, 681, 2003.

122. C. Csaszar, P. Pulay, Geometry optimization by direct invention in the iterative subspace, *Journal of Molecular Structure*, **114**, 34, 1984.

123. J. B. Foresman, T. A. Keith, K. B. Wiberg, J. Snoonian, M. J. Frisch, Solvent Effect. 5. Influence of cavity shape, truncation of electrostatics, and electron correlation on ab initio reaction field calculations, *The Journal of Physical Chemistry*, **100**, 16098, 1996.

124. R. M. Balabin, ''Enthalpy difference between conformations of normal alkenes: intramolecular basis set superposition error (BSSE) in the case of n-butane and n-hexane'', *The Journal of Chemical Physics*, **129**, 164101, 2008.

125. P, Hobza, K. Muller-Dethlefs, Non-covalent interactions: Theory and experiment (PDF). Cambridge, England: *Royal Society of chemistry*, 13, 2010.

126. I. Mayer, P. Valiron, '' Second order Moller–Plesset perturbation theory without basis set superposition error'', *The Journal of Chemical Physics*, **109**, 3373, 1998.

127. F. B. Van Duijneveldt, J. G. C. M. Van Duijneveldt-van de Rijdt, J. P. Van Lenthe, ''state of the art in counterpoise theory'', *Chemical Reviews*, **94**, 1885, 1994.

128. Biologically active compounds, https://senr.osu.edu/sites/senr/files/imce/files/course_materials/enr6610/Section09_Graphics.pdf, 16/09/2017.

129. I. N. Okeke, O. A. Aboderin, D. K. Byarugaba, K. K. Ojo, J. A. Opintan, Growing Problem of Multidrug Resistant Enteric Pathogens in Africa, *Emerging Infectious Diseases·www.cgc.gov/eid*, **13**, 1645, 2007.

130. L. Verotta, Are acylphloroglucinols lead structures for the treatment of degenerative diseases?, *Phytochemistry Reviews*, **1**, 407, 2002.

131. Horsfieldia amygdalina - Useful Tropical Plants, http://tropical.theferns.info/viewtropical.php?id=Horsfieldia+amygdalina, 18/04/2017.

132. C. Wiart, (2006) Medicinal Plant of Asia-Pacific-Drugs for the Future. World Scientific Publishing Co. Pte. Ltd., British Library Cataloguing-in-Publication Data, 380.

133. L. M. Perry, Medicinal plants of east and Southeast Asia: Attributed properties and uses, MIT Press, Cambridge, 279, 1980.

134. N. Rangkaew, R. Suttisri, M. Moriyasu, K. Kawanishi, A New Acyclic Diterpene Acid and Bioactive Compounds from Knema glauca, *Archives of Pharmacal Research*, **32**, 692, 2009.

135. S. Sawadjoon, P. Kittakoop, K. Kirtikara, V. Vichai, M. Tanticharoen, Y. Thebtaranonth, Atropisomeric Myristinins: Selective COX-2 Inhibitors and Antifungal Agents from Myristica cinnamomea, *Journal of Organic Chemistry*, **67**, 5475, 2002.

136. J. Z Deng, S. R. Starck, S. Li, S. M Hecht, (+)-Myristinins A and D from *Knema elegans*, which inhibit DNA polymerase β and cleave DNA. *Journal of Natural Products*, **68**, 1628, 2005.

137. D. J. Maloney, J. Deng, S. R. Starck, Z. Gao, S. M. Hecht, (+)-Myristinin A, Naturally Occurring DNA Polymerase β Inhibitor and Potent DNA-Damaging Agent, *Journal of the American Chemical Society*, **127**, 4141, 2005.

138. Inflammation-MCCC, http://www.mccc.edu/~behrensb/documents/documents/2011Inflammation.pdf, 11/03/2018.

139. J. R. Vane, R. Botting, Mechanism of action of anti-inflammatory drugs, *The FASEB Journal*, **1**, 96, 1987

140. I. Morita, Distinct functions of COX-1 and COX-2, *Prostaglandins & other lipid mediators*, **75**, 69, 2002.

141. J. Clària, Cyclooxygenase-2 biology, *Current Pharmaceutical Design*, **9**, 2003.

142. W. G, Derek, L. Toby, P. Mauro, G. R. Adriano, inflammatory resolution: new opportunities for drug discovery, *Nature Reviews Drug Discovery*, **3**, 416, 2004.

143. K. Sagini, E. Costanz, C. Emiliani, S. Buratta, L. Urbanelli, Extracellular Vesicles as Conveyors of Membrane-Derived Bioactive Lipids in Immune System, *International Journal of Molecular Sciences*, **19**, 1227, 2018.

144. Zarghi, S. Arfaei, Selective COX-2 Inhibitors: A review of their structure-activity relationships, *Iranian Journal of Pharmaceutical Research*, **10**, 683, 2011.

145. L. J. Mengle-Gaw, B. D. Schwartz, Cyclooxygenase-2 inhibitors: Promise or peril?, *Mediators of Inflammation*, **11**, 286, 2002.

146. A validated molecular docking study of lipid–protein interactions, http://vuir.vu.edu.au/29731/1/Rajyalakshmi%20Gaddipati%20.pdf, 15/03/2018.

147. S. D. Oniga, L. Pacureanu, C. I. Stoica, M. D. Palage, A. Crăciun, L. R. Rusu, E. Crisan, C. Araniciu, COX Inhibition Profile and Molecular Docking Studies of Some 2-(Trimethoxyphenyl)-Thiazoles, *Molecules*, **22**, 1507, 2017.

148. Structure of cox-2 active site solved - BioProcess Online, https://www.bioprocessonline.com/doc/structure-of-cox-2-active-site-solved-0001, 15/03/2018.

149. N. S. Yarla, K. Satyakumar, D. Srinivasu, K. DSVGK, G. Aliev, G. Dharmapuri, G. Raju, S. P. Swathi Putta, S. Jagarlapoodi, V. Bheeram, S. P. Sadu, G. R. Duddukuri, Phospholipase A2: A potential therapeutic target in inflammation and cancer (In silico, In vitro, In vivo and Clinical Approach), *Journal of Cancer Science & Therapy*, **7**, 252, 2015.

150. J. Y. Hayashi, F. Tamanoi, Chapter seven - Exploiting enzyme alterations in cancer for drug activation, drug delivery, and nanotherapy, *The Enzymes*, **42**, 172, 2017.

151. J. E. Burke, E. A. Dennis, Phospholipase A2 structure/function, mechanism, and signaling[1], *Journal of Lipid Research*, 50, S242, 2009.

152. N. D. Quach, R. D. Arnold, B. S. Cummings, Secretory phospholipase A2 enzymes as pharmacological targets for treatment of disease, *Biochemical pharmacology*, **90**, 348, 2014.

153. The involvement of phospholipase A2 (PLA2) in Acylation Stimulating Protein (ASP) signalling, http://digitool.library.mcgill.ca/webclient/StreamGate?folder_id=0&dvs=1548762620458~840, 15/03/2018.

154. Rheumatoid Arthritis (RA) diet, treatment, symptoms, causes & pictures, https://www.medicinenet.com/rheumatoid_arthritis/article.htm, 20/03/2018.

155. S. Masuda, M. Murakami, K. Komiyama, M. Ishihara, Y. Ishikawa, T. Ishii, I. Kudo, Various secretory phospholipase A2 enzymes are expressed in rheumatoid arthritis and augment prostaglandin production in cultured synovial cells, *The FASEB Journal*, **272**, 672, 2005.

156. S. Mebarek, A. Abousalham, D. Magne, L. D. D. J. Bandorowicz-Pikula, S. Pikula, R. Buchet, Phospholipases of mineralization competent cells and matrix vesicles: Roles in physiological and pathological mineralizations, *International Journal of Molecular Sciences*, **14**, 5129; 2013.

157. Phospholipase A2 as a therapeutic target for atherosclerosis, http://www.tandfonline.com/doi/pdf/10.2217/clp.09.74, 20/03/2018.

158. Z. Dong, J. Meller, P. Succop, J. Wang, k. Wikenheiser-Brokamp, S. Starnes, S. Lu, Secretory phospholipase A2-IIa upregulates HER/HER2-elicited signalling in lung cancer cells, *International Journal of Oncology*, **45** , 984, 2014.

159. D. Y. Hui, Phospholipase A_2 enzymes in metabolic and cardiovascular diseases, *Current Opinion In Lipidology*, **23**, 240, 2012.

160. N. Kumar, S. Drabu, S. C. Mondal, NSAID's and selectively COX-2 inhibitors as potential chemoprotective agents against cancer, *Arabian Journal of Chemistry*, **6**, 23, 2013.

161. N. S. Yarla, A. Bishayee, L. Vadlakonda, R. Chintala, G. R. Duddukuri1, P. Reddanna, K. S.V.G.K. Dowluru, Phospholipase a_2 isoforms as novel targets for prevention and treatment of inflammatory and oncologic diseases, *Current Drug Targets*, **17**, 2016.

162. R. M. Botting, inhibitors of cyclooxygenases: mechanisms, selectivity and uses, *Journal of Physiology and Pharmacology*, **57**, 124, 2006.

163. A. S. Kalgutkar, B. C. Crews, S. W. Rowlinson, A. B. Marnett, K. R. Kozak, R. P. Remmel, L. J. Marnett, Biochemically based design of cyclooxygenase-2 (COX-2) inhibitors: Facile conversion of nonsteroidal antiinflammatory drugs to potent and highly selective COX-2 inhibitors, *Proceedings of the National Academy of Sciences of the United States of America*, **97**, 930, 2000.

164. L. J. Crofford, Use of NSAIDs in treating patients with arthritis, Arthritis Research & Therapy, **15**, S2, 2013.
165. R. T. Mendes, C. P. Stanczyk, R. Sordi, M. F. Otuki, F. A. d. Santos, D. Fernandes, Selective inhibition of cyclooxygenase-2: risks and benefits, *Revista Brasileira de Reumatologia*, **52**, 2012.
166. L. G. Howes, Selective COX-2 inhibitors, NSAIDs and cardiovascular events – is celecoxib the safest choice?, *Therapeutics and Clinical Risk Management*, **3**, 845, 2007.
167. E. Fosslien, Review: Cardiovascular Complications of Non-Steroidal Anti-Inflammatory Drugs, *Annals of Clinical & Laboratory Science*, **35**, 385, 2005.
168. W. Ericson-Neilsen, A. D. Kaye, Steroids: Pharmacology, Complications, and Practice Delivery Issues, *Ochsner Journal*, **14**, 207, 2014.
169. Glucocorticoids - HOPES Huntington's disease Information, http://web.stanford.edu/group/hopes/cgi-bin/hopes_test/glucocorticoids/, 15/03/2018.
170. A REVIEW OF NATURAL STEROIDS AND THEIR APPLICATIONS, http://ijpsr.com/bft-article/a-review-of-natural-steroids-and-their-applications/?view=fulltext
171. An Overview of the Adrenal Glands - Beyond Fight or Flight, https://www.endocrineweb.com/endocrinology/overview-adrenal-glands, 15/03/2018.
172. Glucocorticoids [TUSOM | Pharmwiki] - TMedWeb. http://tmedweb.tulane.edu/pharmwiki/doku.php/glucocorticoids, 11/04/2018.
173. D. H. van Raalte, M. Diamant, Steroid diabetes: from mechanism to treatment?, *Netherland Journal of Medicine*, february, **72**, 2014.
174. Adrenocorticosteroids & adrenocortical antagonists, https://accessmedicine.mhmedical.com/content.aspx?bookid=1193&sectionid=69109924&jumpsectionID=69109986&Resultclick=2, 14/05/2018.
175. Holland-Frei Cancer Medicine. 6th edition. D.W. Kufe, R.E. Pollock, R.R. Weichselbaum, et al., editors. Hamilton (ON): BC Decker; 2003. Physiologic and Pharmacologic Effects of Corticosteroids, Lorraine I. McKay, PhD and John A. Cidlowski, PhD.
176. J. A. Falk, O. A. Minai, Z. Mosenifar, Inhaled and systemic corticosteroids in chronic obstructive pulmonary disease, *Proceedings of the American Thoracic Society*, **5**, 512, 2008.
177. A. Ahluwalia, Topical glucocorticoids and the skin–mechanisms of action: an update, Mediators of Inflammation, **7**, 193, 1998.
178. G. Ruiz-Irastorza, A. Danza, M. Khamashta, Glucocorticoid use and abuse in SLE, *Rheumatology*, **51**, 1153, 2012.
179. Corticosteroids Pharmacology | All the Facts in One Place!, https://pharmafactz.com/corticosteroids-pharmacology/, 18/05/2018.

180. Y. Shen, S. Huang, J. Kang, J. Lin, K. Lai, Y. Sun, W. Xiao, L. Yang, W. Yao, S. Cai, K Huang, F. Wen, Management of airway mucus hypersecretion in chronic airway inflammatory disease: Chinese expert consensus (English edition), *International Journal of Chronic Obstructive Pulmonary Disease*, **13**, 407, 2018.

181. S. Dhar, J. Seth, D. Parikh, Systemic side-effects of topical corticosteroids, *Indian Journal of Dermatology*, **59**, 464, 2014.

182. J. J. W. McDoual, Computational quantum chemistry: molecular structure and properties *in silico*, RSC Theoretical and Computational Chemistry Series No 5, 2013.

183. J. P. Merrick, D. Moran, L. Radom, An evaluation of harmonic vibrational frequency scale factors, *The Journal of Physical Chemistry A*, **111**, 11700, 2007.

184. G. A. A. Saracino, R, Improta, V. Barone, Absolute pKa determination for carboxylic acids using density functional theory and the polarizable continuum model, *Chemical Physics Letters*, **373**, 415, 2003.

185. M. J. Frisch, G. W. Trucks, H. B. Schlegel, G. E. Scuseria, M. A. Rob, J. R. Cheeseman, J. A. Montgomery Jr., T. Vreven, K. N. Kudin, J. C. Burant, J. M. Millam, S. S. Iyengar, J. Tomasi, V. Barone, B. Mennucci, M. Cossi, G. Scalmani, N. Rega, G. A. Petersson, H. Nakatsuji, M. Hada, M. Ehara, K. Toyota, R. Fukuda, J. Hasegawa, M. Ishida, T. Nakajima, Y. Honda, O. Kitao, H. Nakai, M. Klene, X. Li, J. E. Knox, H. P. Hratchian, J. B. Cross, V. Bakken, C. Adamo, J. Jaramillo, R. Gomperts, R. E. Stratmann, O. Yazyev, A. J. Austin, R. Cammi, C. Pomelli, J. W. Ochterski, P. Y. Ayala, K. Morokuma, G. A. Voth, P. Salvador, J. J. Dannenberg, V. G. Zakrzewski, S. Dapprich, A. D. Daniels, M. C. Strain, O. Farkas, D. K. Malick, A. D. Rabuck, K. Raghavachari, J. B. Foresman, J. V. Ortiz, Q. Cui, A. G. Baboul, S. Clifford, J. Cioslowski, B. B. Stefanov, G. Liu, A. Liashenko, P. Piskorz, I. Komaromi, R. L. Martin, D. J. Fox, T. Keith, M. A. Al-Laham, C. Y. Peng, A. Nanayakkara, M. Challacombe, P. M. W. Gill, B. Johnson, W. Chen, M. W. Wong, C. Gonzalez, J. A. Pople, *Gaussian 03* (Gaussian, Inc., Wallingford, CT, 2003).

186. M. J. Frisch, G. W. Trucks, H. B. Schlegel, G. E. Scuseria, M. A. Robb, J. R. Cheeseman, G. Scalmani, V. Barone, B. Mennucci, G. A. Petersson, H. Nakatsuji, M. Caricato, X. Li, H. P. Hratchian, A. F. Izmaylov, J. Bloino, G. Zheng, J. L. Sonnenberg, M. Hada, M. Ehara, K. Toyota, R. Fukuda, J. Hasegawa, M. Ishida, T. Nakajima, Y. Honda, O. Kitao, H. Nakai, T. Vreven, J. A. Montgomery, Jr., J. E. Peralta, F. Ogliaro, M. Bearpark, J. J. Heyd, E. Brothers, K. N. Kudin, V. N. Staroverov, R. Kobayashi, J. Normand, K. Raghavachari, A. Rendell, J. C. Burant, S. S. Iyengar, J. Tomasi, M. Cossi, N. Rega, J. M. Millam, M. Klene, J. E. Knox, J. B. Cross, V. Bakken, C. Adamo, J. Jaramillo, R. Gomperts, R. E. Stratmann, O. Yazyev, A. J. Austin, R. Cammi, C. Pomelli, J. W. Ochterski, R. L. Martin, K.

Morokuma, V. G. Zakrzewski, G. A. Voth, P. Salvador, J. J. Dannenberg, S. Dapprich, A. D. Daniels, Ö. Farkas, J. B. Foresman, J. V. Ortiz, J. Cioslowski, and D. J. Fox, *Gaussian 09* (Gaussian, Inc., Wallingford CT, 2009).

187. R. Dennington, T. Keith, J. Millam, Gauss View, Version 4.1.2. Semichem Inc., Shawnee Mission, 2007.

188. L. D. Mendelsohn. ChemDraw 8 Ultra, windows and macintosh versions, *Journal of Chemical Information and Modeling*, **44**, 2226. 2004.

189. M. Tshilande, Ab initio conformational study of a model structure for Myristinin A and other phloroglucinol molecules differing only by the R chain in the acyl group. Bachelor Of Science Honours In Chemistry, Thesis at University of Venda, 2016.